Department of Organic Chemistry

Faculty of Sciences

Polymer & Biomaterials Research Group (PBM)

2012

# The development and characterisation of multifunctional polymers as delivery systems for gene therapy

Thesis submitted in fulfillment of the requirements

for the degree of Doctor of Science: Chemistry

**Vincent Vermeersch**

Promotors: Prof. P. Dubruel

Prof. E. Schacht

## Dankwoord

Completing this doctoral thesis would not have been possible without the support, trust and help of a large of group of people.

First of all I want to thank my promoters, Prof. Em. E. Schacht and Prof. P. Dubruel for the chances of carrying out the Ph.D in an established laboratory with an international renown character. In combination with funding granted by European union (PolExGene), I got the pleasure of working together with distinguished European academic partner and the opportunity to meet new, interesting people. Also the numerous meetings in European capitals as well as the many chances to participate in international conferences, have helped in developing my life experience. For that and several other chances I might forget, I would like to express my gratitude.

Furthermore, within the PolExGene project, I would like to thank my colleagues, Dr. Veska Toncheva and Dr. Sandra Van Vlierberghe, working in close collaboration on the various research topics as well as for the exchange of information & data that have helped in shaping this doctoral thesis. Also the master students, Ina, Jan, Inki, Arne and Lies, that I have guided throughout those 4 years and who's efforts and results were of high value for my research deserve a more than honourable citation!

Additionally, I would like to express my gratitude to Dr. A. Joliot & Dr. L. Tibaldi (Collège de France, Paris) for performing the many transfection and viability screening experiments on cells. Also. Dr. H. Bueth and Dr. H. Thielecke (Fraunhofer Institute, Stuttgart) , I would like to thank for the FCS and Impedance measurements.

Finally, I would also like to thank Jo Vandervoort (UA) for the possibility to carry out the Zeta-potential measurements.

Naast de professionele contacten, wil ik ook graag de mensen van het PBM labo danken, zowel deze van de huidige generatie die nu de gangen bevolken als deze van de 'oude' generatie. Een special woordje van dank gaat u naar mijn thesis begeleider Ives, de man die mij talen leerde spreken Servinho, mijn partner in chinese food Tim VG, mijn psycholoog Tim D, mijn vrouwenadviseurs Sandra en Kristin VDT en de poker god Jorgski! Ook de nieuwe generatie aan doctoraatstudenten, Thomas, Valerie, Mieke, Stijnie, Arnie, Maria en Elke VDW alsook onze charmante labomanager Veerle, allen bedankt voor de fijne tijden.

Also, the international connection i want to thank for the cultural diversity and the ability to improve my Dutch… Kenny, Ana (and her many last names), Olga, Jordi and Monika. An

special thanks goes out to my favorite Spanish connection, Ana JG, it was truly a pleasure to have met you and to have experienced the close friendship we have formed.

Verder wil ik ook graag de andere mensen uit de S4 bedanken zoals Maarten, Sam, Joris Dierck en de collega's uit de werkplaats alsook de andere ondersteunende diensten (Tom P, Ingird, Freddy, Hector) maar ook mensen uit het verleden zoals Roeland.

Ook de vele collega's vanuit Bekaert die met vaste regelmaat naar het doctoraat zijn blijven vragen om mij zodoende te motiveren, bedankt voor de steun!

Uiteindelijk zijn er ook mensen die ik wil bedanken die een bron van inspiratie zijn geweest en dit om diverse redenen. Eerst en vooral wil ik Dr. Baekelandt en Dr. Callewaert danken voor de vruchteloze pogingen die ze ondernomen hebben (en nog steeds) om mij iets bij te brengen over de dinges des levens (zoals der zijn chemie, vrouwen en het uitgangsleven). Gelieve te blijven proberen! Ook Ko en Matthias, partners in crime tijdens de studies, de daaropvolgende doctoraat periode en hopelijk nog lang nadien, de tijden waren onvergetelijk! Daarnaast wil ik ook graag nog eens Els bedanken voor de speciale band die tijdens deze periode in de S4 ontstond (en die het dagelijkse doctoraatsleven sterk beïnvloed heeft).

Ook een aantal andere mensen buiten het kader van de universiteit wil ik graag danken zoals Yves, Dens, Karel om mij te vermaken en te helpen de zinnen te verzetten op dagen dat het labo wat te veel werd. Ook de mannen van de voetbal, Mario, de Goeteyns, de Lipskes en Filip! Ook Fabienne wens ik te bedanken voor de steun in de finale periode van het doctoraat, dit was ten zeerste geapprecieerd! Verder mag ik vooral een van de belangrijkste personen niet vergeten, namelijk Tim, jouw grapjes waren altijd om te gieren en daardoor ideaal als tussendoortje tijdens het schrijven!

Last but not least, zijn er natuurlijk de mensen die rondom mij geweest zijn van kinds been af, familie en vrienden (die ik misschien vergat te vermelden) maar vooral mijn zus Julie en mijn ouders. Uiteraard was dit niet mogelijk zonder jullie maar dat is nog veel te licht uitgedrukt als ik bedenk hoeveel jullie over al die jaren al gedaan hebben en wat jullie al allemaal hebben moeten verduren. Uit de grond van mijn hart bedankt!

## Table of contents

## Chapter 1 - Introduction & Objective


**1 The promising rise of gene therapy ..... 1**

**2 Gene Delivery systems ..... 4**

2.1 Physical methods ..... 7
2.1.1 Direct gene delivery using plasmid DNA ..... 7
2.1.2 Gene gun ..... 8
2.1.3 Electroporation ..... 8
2.1.4 Gene transfer by ultrasound radiation ..... 9
2.2 Viral vectors ..... 10
2.2.1 Adenovirus ..... 11
2.2.2 Adeno-associated virus ..... 12
2.2.3 Retrovirus ..... 12
2.2.4 Herpes simplex virus ..... 13
2.2.5 The viral future? ..... 14
2.3 Non-viral vectors ..... 15
2.3.1 Inorganic based delivery systems ..... 15
2.3.2 Liposomal based delivery systems ..... 16
2.3.3 Delivery systems based on peptides ..... 19
2.3.4 Polymer based delivery systems ..... 21
2.3.4.1 Polymers ..... 21
2.3.4.2 Application of biomaterials as gene delivery platforms ..... 26
2.3.4.3 Scaffold encapsulation ..... 28
2.3.4.4 Surface immobilization ..... 29

**3 Overcoming general limitations in human gene delivery ..... 30**

3.1 DNA interaction and packaging ..... 31
3.2 Cell internalisation (endocytosis) ..... 32
3.3 Cytoplasmatic release (DNA release) ..... 34
3.4 Polyplex dissociation and intracellular trafficking ..... 35
3.5 Nuclear uptake & gene expression ..... 37

**4 Objective of the doctoral thesis ..... 38**

4.1 Treatment of age-related macula degeneration (ARMD) ..... 39
4.2 Development of biodegradable, synthetic vectors ..... 40
4.3 Development of non-biodegradable, synthetic vectors ..... 42
4.4 Biological evaluation of multifunctional vectors ..... 43
4.5 Optimisation of vectors by the incorporation of cell-penetrating peptides ..... 43

**5 References ..... 44**


## Chapter 2 - Synthesis of biodegradable polymer vectors


**1 Introduction ..... 61**

**2 Synthesis of poly-L-glutamine derivatives ..... 63**

2.1 Synthesis of protected L-glutamic acid (γ-benzyl-L-glutamate) ..... 63
2.2 Monomer synthesis (γ-benzyl-L-glutamate-N-carboxyanhydride) ..... 64
2.3 Polymerisation ..... 67
2.3.1 Reaction mechanism ..... 67
2.3.2 Synthesis of poly-γ-benzyl-L-glutamate ..... 70
2.3.2.1 Application of primary amines as initiator ..... 70
2.3.2.2 Application of tertiary amines as initiators ..... 72
2.3.2.3 Viscosimetry ..... 72
2.3.2.4 Set-up of a mastercurve (ratio M/I) for MW determination of poly-&-amino acids ..... 73
2.4 Aminolysis ..... 75
2.4.1 Aminolysis reaction mechanism ..... 76
2.4.2 Synthesis of poly(dimethylaminoethyl)-L-glutamine (pDMAEG) ..... 77
2.4.3 Synthesis of poly(dimethylaminoethyl-co-aminoethyl)-L-glutamine (p(DMAEG-AEG)) ..... 79
2.4.4 Synthesis of poly(dimethylaminoethyl-co-hydroxyethyl)-L-glutamine (p(DMAEG-HEG)) ..... 80
2.4.5 Synthesis of poly(aminoethyl-co-hydroxyethyl-co-imidazolethyl)-L-glutamine (p(AEG-HEG-ImEG)) ..... 81
2.4.6 Synthesis of poly(hydroxyethyl-co-guanidylethyl)-L-glutamine (p(HEG-GuAEG)) ..... 82
2.4.7 Synthesis of multifunctional poly-L-glutamines ..... 84

**3 Synthesis of poly-L-arginine derivatives ..... 86**

3.1 N-carboxyanhydride derivative of $N^{\delta}$-benzyloxy-L-ornithine (ZO) ..... 86
3.2 Polymerisation: synthesis of poly($^{\delta}$N-CBZ)-L-ornithine ..... 87
3.3 Deprotection: synthesis of poly-L-ornithine ..... 87
3.4 Guanidine conversion: synthesis poly-L-arginine ..... 88

**4 Synthesis of L-glutamine and L-arginine copolymers ..... 91**

**5 Biodegradable graft-copolymers ..... 91**

**6 Conclusion ..... 93**

**7 References ..... 94**

## Chapter 3 - Synthesis of non-biodegradable polymer vectors

**1 Introduction ..... 97**

**2 Free radical polymerisation of methacrylates ..... 97**

**3 Polymethacrylate derivatives as synthetic vectors ..... 99**

3.1 Description of a free-radical polymerisation ..... 99
3.2 Chain transfer agents regulate polymerisation for low MW's ..... 100
3.3 Synthesis of poly(dimethylaminoethyl)methacrylate (pDMAEMA) ..... 101
3.4 Amine-containing methacrylates ..... 103
3.4.1 Synthesis of (N-tert-butoxycarbonyl)aminoethylmethacrylate ..... 104
3.4.2 Synthesis of poly(aminoethyl)methacrylate (pAEMA) ..... 105
3.4.3 Synthesis of poly(guanidylethyl)methacrylate (pGuAEMA) ..... 105

3.4.4 Synthesis of poly(aminoethyl-co-dimethylaminoethyl)methacrylate (p(DMAEMA-AEMA)) ..... 106
3.5 Hydroxyl containing polymethacrylates ..... 107
3.5.1 Synthesis of poly(dimethylaminoethyl-co-hydroxyethyl)methacrylate (p(DMAEMA-HEMA)) ..... 108
3.5.2 Synthesis of poly(guanidylethyl-co-hydroxyethyl)methacrylate (p(GuAEMA-HEMA)) ..... 109

**4 Conclusion ..... 110**

**5 References ..... 111**

**Chapter 4 - Physico-chemical characterisation of multifunctional synthetic vectors**

**1 Introduction ..... 113**

**2 Polyelectrolyte complex formation theory ..... 114**

2.1 The concept of mass per charge and the calculation of polyplex composition ..... 114
2.2 Standardised protocol ..... 115
2.3 One-step versus multi-step polymer addition ..... 115
2.4 Polyplex mixing sequence ..... 116

**3 Characterisation of polyplex formation properties ..... 119**

3.1 Ethidium Bromide Fluorescence ..... 119
3.1.1 One-step versus multi-step polyplex formation ..... 121
3.1.2 Polyplex formation: kinetics and stability in time ..... 122
3.1.3 Biodegradable polymers ..... 123
3.1.3.1 p(DMAEG) ..... 123
3.1.3.2 The main effect of functional group replacement ..... 124
3.1.3.3 p(HEG-GuAEG) ..... 124
3.1.3.4 Imidazole-containing polymers ..... 125
3.1.3.5 The effect of charge on the overall condensation ability ..... 126
3.1.3.6 Arginine-based polymers ..... 128
3.1.4 Non-biodegradable polymers ..... 129
3.1.4.1 p(DMAEMA) ..... 129
3.1.4.2 The effect of functional group replacement ..... 130
3.1.4.3 The impact of type of functional group ..... 132
3.1.5 PEI & PEI-derivatives ..... 132
3.1.6 Conclusion ..... 134
3.2 Agarose Gel-electrophoresis ..... 136
3.2.1 DNA-condensation by cationic biodegradable polymers ..... 136
3.2.2 Gel-electrophoresis results of non-biodegradable polymers ..... 139
3.2.3 Influence of DNA concentration on polyplex formation ..... 141

**4 Polyplex size and distribution ..... 142**

4.1 Dynamic light scattering (DLS) ..... 142
4.2 PEI and modified PEI derivatives ..... 144
4.3 Polyplexes based on biodegradable polymers ..... 145

4.4 Size & distribution of polymethacrylate-DNA complexes ..... 148
4.5 Parameters that influence particle size ..... 150
4.5.1 Time (stability) ..... 150
4.5.2 Temperature ..... 151
4.5.3 Buffer medium ..... 151
4.5.4 DNA concentration ..... 152

**5 Polyplex stability ..... 153**

5.1 Zeta-potential ..... 153
5.2 Colloidal stability of biodegradable polyplexes ..... 155

**6 Influence of charge: geometrical orientation on a polymer ..... 158**

**7 Summary ..... 161**

**8 References ..... 162**

**Chapter 5 - Optimisation & modification of multifunctional vectors**

**1 Introduction ..... 165**

**2 Development of fluorescently labelled polymer carriers ..... 166**

2.1 Visualising polyplexes ..... 166
2.2 Covalent coupling of fluorescent tags ..... 168
2.3 Influence of fluorescent tags on the polyplex physico-chemical properties ..... 169
2.4 Formation kinetics of polyplexes ..... 172
2.4.1 FCS analysis ..... 172
2.4.2 UV/VIS absorption tests of fluorescent active polyplexes ..... 174

**3 Application of Cell Penetrating Peptides in polymeric gene delivery ..... 176**

3.1 Synthesis of polymer-CPP conjugates ..... 176
3.1.1 Coupling strategies ..... 176
3.1.2 Coupling protocol ..... 176
3.2 Overview of the developed polymer-CPP conjugates ..... 178
3.2.1 Penetratine (PEN) containing conjugates ..... 178
3.2.2 Octa-Arginine (Arg8) ..... 179
3.2.3 Influence of spacer on CPP activity ..... 179
3.3 Physico-chemical characterisation ..... 181
3.3.1 Polyplex formation ..... 181
3.3.2 Agarose gel-electrophoresis (AGE) ..... 183
3.3.3 Polyplex size and distribution ..... 184
3.3.4 Stability of polyplexes in aqueous environment ..... 186
3.3.5 Cell membrane interaction ..... 187

**4 Comparison of physical versus chemical CPP mixing ..... 192**

**5 Conclusion ..... 194**

**6 References ..... 195**

**Chapter 6 - Biological evaluation of polymer-DNA complexes**

**1 Introduction ..... 199**

**2 Efficiency of polyplexes as in-vitro gene delivery systems ..... 200**

2.1 Principle of cell toxicity - viability ..... 200
2.2 Transfection efficiency: protein production of modified DNA ..... 201
2.3 Results ..... 202
2.3.1 PEI & CPP-coupled PEI-derivatives ..... 202
2.3.2 Vector efficiency of poly-L-glutamines ..... 204
2.3.3 Guanidylated PEI and other reference polymers ..... 211
2.3.4 Polymethacrylates ..... 213
2.3.5 Summary: activity of vectors compared to PEI ..... 216
2.4 Physical mixing of CPP's with vector systems: sequence of addition ..... 218

**3 DNA-protection ability ..... 219**

3.1 Principle of enzymatic DNA degradation ..... 219
3.2 Experimental set-up ..... 221
3.3 Results ..... 221
3.3.1 PEI ..... 222
3.3.2 Poly-L-glutamine derivatives ..... 223
3.3.3 Polymethracylate derivatives ..... 227

**4 In vitro degradation ..... 230**

4.1 Principle of enzymatic polymer degradation ..... 230
4.2 Experimental set-up ..... 231
4.3 Results ..... 232

**5 Blood compatibility ..... 234**

5.1 Haemolysis ..... 235
5.1.1 Description of haemolytic effect ..... 235
5.1.2 Experimental part ..... 236
5.1.3 Results ..... 236
5.1.3.1 Vectors based on poly-$\alpha$-aminoacids ..... 236
5.1.3.2 Vectors based on polymethacrylates ..... 239
5.2 Haemo-agglutination ..... 241
5.2.1 Description & experimental set-up ..... 241
5.2.2 Results for poly-$\alpha$-amino acids ..... 242
5.2.3 Results of polymethacrylates ..... 246
5.3 Histologocial data ..... 248

**6 Confocal microscopy ..... 250**

**7 Conclusion ..... 257**

**8 References ..... 258**

## Chapter 7 - Final Conclusions

**1 Synthesis of suitable vectors for gene delivery ..... 261**

**2 Physico-chemical properties of developed polymers ..... 262**

3 Optimising polymeric vectors ..... 263
4 Biological success of improved vector systems ..... 265
5 Epilogue. ..... 266

Chapter 8 - Experimental part ..... 268

Chapter 9 - Nederlandse samenvatting ..... 291

Appendix 1 - CV ..... 307

## List of abbreviations

DNA = deoxyribonucleic acid

RNA = ribonucleic acid

AIDS = acquired immune-defficiency syndrome

Ad = adenovirus

AdAv = adeno-associated virus

HSV = herpes simplex virus

kb = kilobases

CPP = cell-penetrating peptide

CIP = cell-interacting peptide

RGD = arginine(R) - glycine(G) - aspartic acid(D)

MM = molecular mass

MW = molecular weight

PAMAM = polyamidoamine

PDMAEMA = poly(dimethyalaminoethyl)methacrylate

pNIPAAm = poly(*N*-isopropylacrylamide)

pEI = polyethyleneimine

PLL = poly-L-lysine

PEG = polyethyleneglycol

PLGA = poly(lactic-co-glycolic acid)

LCST = lower critical solution temperature

UCST = upper critical solution temperature

ECM = extra-cellular matrix

GAM = gene-activated matrix

IPEC = inter-polyelectrolyte complex

NLS = nuclear localization signal

NPC = nuclear pore complex

ARMD = age-related macular degeneration

pDMAEG = poly(dimethylaminoethyl)-L-glutamine

pBG = poly-$\gamma$-benzyl-L-glutamate

pZO = poly-δ-benzyloxycarbonyl-L-ornithine

NCA = N-carboxyanhydride

GFP = green fluorescent protein

ROP = ring-opening polymerisation

AIBN = azo-bisisobutyronitrile

2-HP = 2-hydroxypyridine

DMAEA = dimethylaminoethylamine

TrAEA = tritylaminoethylamine

AE = aminoethanol

DMF = dimethylformamide

DCM = dichloromethane (= methylenechloride)

EtOAc = ethylacetate

APS = ammonium persulphate

TFA = trifluoroacetic acid

DLS = dynamic light scattering

CR = charge ratio

ARPE19 (or RPE) = A retinal pigment epithelium 19

HEK cells = human endothelial kidney cells

COS cells (acronym) = "**C**ytomegalus Virus-1 in **O**rigin carrying the **S**V40 genetic material" cells

TB = tryphan blue

HEPES = (4-(2-hydroxyethyl)-1-piperazineethanesulfonic acid

EtBr = ethidiumbromide

GPC = gel-permeation chromatography

## Note: Chemical structure – stereochemistry

Inside this doctoral thesis, various chemical compounds are presented and depicted in the form of molecular or condensed structures. As many of these structures contain stereogenic centres, stereochemistry (information on the asymmetry of molecule) is an important aspect of the correct representation of these molecules. Especially when focusing on biochemical and biomedical relevant applications, as intended within this doctoral research, the use of specific compounds with the proper chirality (L, levorotatory or D, dextrorotatory) is of the utmost importance. Naturally occurring proteins and other structures composed of amino acids (except glycine which has no stereogenic centre) bear stereogenic centres characterized by the L-form.

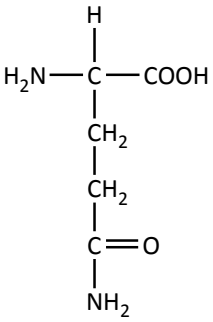

**glutamine**

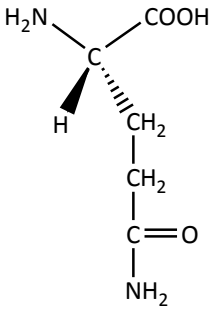

**L-glutamine**

Therefore, within this thesis, the aim was to synthesise also L-based polymers (e.g. poly-L-glutamine). To simplify the representation, specifically when condensed polymer formulas are in order, the exact nature of the stereogenic centre is not specified when depicting the R-group of the poly-L-amino acid (oriented away from the reader). Nevertheless, when talking about the polymer and more specifically polymer structure further on, the L-form and it's corresponding representation is always implied.

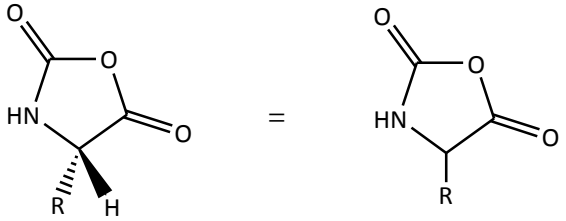

**L-NCA**

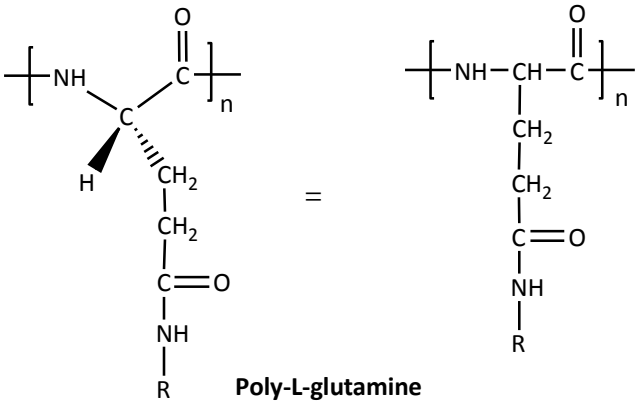

**Poly-L-glutamine**

# Chapter 1

# Introduction & objective

# 1 The promising rise of gene therapy

Gene therapy or gene delivery is an approach towards healing a person who is suffering from a genetic anomaly. The strength of this application lies in its basic concept, being the repair of malfunctioning DNA, the root cause of the illness. To understand this idea, it is necessary to comprehend the importance and role of DNA within the body. As many people are aware of the fact that DNA consists of the basic building blocks relevant for functioning of the body, few know in what way this is achieved. DNA is the carrier of hereditary information (a 'blueprint'), consisting of nucleotides that have a specific sequence which is typical for a certain characteristic of the body, often referred to as a gene sequence (e.g. brown eyes, the production of insulin, etc.). Each nucleotide consists of a nucleobase attached to a sugar (deoxyribose) and phosphate unit, that build up rigidity to form polymer strains. There are 4 nucleobases,i.e adenine, guanine (purines), thymine and cytosine (pyrimidines) that are endlessly repeated in a specific order, forming the total genetic information. Every cell within the body, possesses a complete copy of all the genes, which are appearing as chromosomes (densely packed, long coils of DNA). Cells differ in function because they use different parts of the chromosomes to produce their typical proteins. This is done by a specific process that requires several intermediate agents (Fig. 1.1).

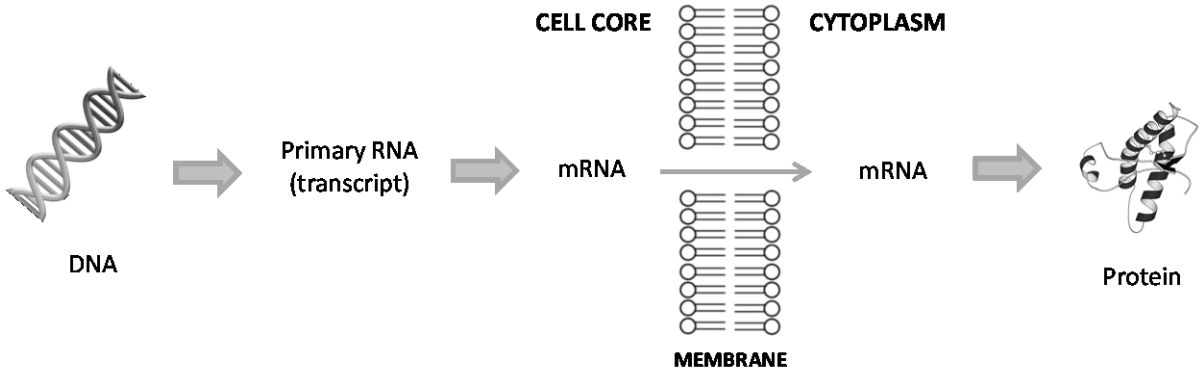


**Figure 1.1 – Simplified scheme for the synthesis of a protein.**

In some cases (e.g. genetic mutation) certain gene sequences can become erroneous, resulting in defective DNA and might lead to the insufficient or incorrect production of proteins which could induce disease patterns. Currently, treatments for these conditions are focused on symptoms whereas the ideal cure should address the source of the problem.

Gene therapy could be an answer to a huge amount of diseases that are affected by defective DNA like for instance schizophrenia, cystic fibrosis or age related macular degeneration. This way of working could be expanded to the treatment of other diseases like AIDS or cancer. The alteration of genes in order to cure diseases was already postulated by E. Tatum (1958)[1] but since insufficient knowledge on the human genome was available at

that time, successful practical experiments could only be executed in the early 1990's[2]. With increasing biological and medical understanding of genetic mechanisms, this has lead to recent applications in clinical trials for cancer[3], blindness[4] and deafness[5].
Theoretically, the replacement of a faulty gene within the chromosome, is physically possible but very challenging and so far not fully understood. The lack of understanding gene replacement is not really a drawback since in the majority of therapies, an easier solution can be found in the plain addition of a specific gene to the cell. In this way the need for a certain protein can be compensated[6]. Nevertheless, introducing foreign substances into the body remains a tricky endeavour since the immune system of mammals has increasingly evolved through time. This phenomenon is also applicable for gene therapy and comprises the main difficulty this research encounters. DNA is a highly negative molecule (due to phosphate residues) which is often very large in size. Together with obvious immunological implications, the introduction of DNA to a cell requires consideration on the use of a delivery system that could prevent rapid DNA clearance or destruction before reaching its target[7]. Moreover, a carrier would ideally facilitate the cell internalisation by encompassing the cell membrane barrier.

At current, gene delivery can be classified in 3 categories.

> ***Ex vivo:*** Prior to incubation with DNA and a delivery system, cells are removed from the body, after which the cells are readministered. This is mainly applied for blood cells (due to the ease of withdrawal and subsequent administration).
> ***In situ:*** A delivery system containing DNA is put directly into the target tissue.
> ***In vivo:*** The delivery system is brought into the bloodstream and is presented throughout the body (systemically).

One of the main application domains for gene therapy is obviously hereditary diseases. To treat these disorders, the insertion of a correct version of a defective gene into the genome of stem cells is attempted. These methods primarily target easily accessible tissue[8] (muscle, lung, blood) and also make use of delivery systems[9]. Another area of interest, on which a huge amount of genetic research is focussed, is cancer. Since this is the number two cause of death in the world, it is not surprising that the highest amount of clinical tests in gene therapy are aimed at curing cancer or cancer related issues[10]. Cancer therapy can be addressed in several ways:

> ***Immunotherapy:*** using this approach, the immunogenicity towards tumours is increased by locally producing immune-stimulating substances (interleukins, lymphokines) so that the body is prompted to take action against the malignant

tumours. In this way the immune system can reach tumour cells that were not covered by the initial therapy (systemic advantage)[11,12].

***Repair of original cell function:*** to treat cancer there is generally a need to affect genes that are involved in the cell cycle. Therefore, the oncogenes should be deactivated and tumour suppressor genes activated. Upon oncogene mutation, the gene that causes proliferation of tumour cells is rendered useless by antisense therapy (introduction of single stranded RNA that caps a part of the mRNA, coding for the mutated protein). The activation of suppressor genes is achieved by bringing genes into the cell that recover the tumour suppressing ability of the cell[13,14].

***Use of suicide genes:*** via this dual therapy, an enzyme-coding gene is introduced, followed by the administration of a harmless pro-drug. The added enzyme is capable of converting this pro-drug into a highly cytotoxic drug that destroys the tumour cells (for instance, brain tumour cells)[15].

***Anti-angiogenesis therapy:*** tumours induce blood vessel growth (angiogenesis) by secreting various growth factors (VEGF) and basic fibroblast growth factor (bFGF). To disrupt nutrient supply and metabolite activity, the suppression of angiogenic factors or the reinforcement of angiogenic inhibitors (endostatin, angiostatin) is the start of tumour isolation and eventually death[16,17].

Furthermore, gene therapy can be employed to treat AIDS[18]. There are two main strategies used for this, avoiding that the HIV replicates or preventing the infection of healthy cells. The first strategy is achieved by introducing genes that code for ribozymes, capable of destroying the viral DNA whereas in the second approach genes are added to healthy cells that consider HIV as a foreign entity and which is followed by antibody production[19,20,21]. Many of these investigations already reached clinical trials[22,23]. Recently, a new intervention strategy has surfaced enabling the treatment of AIDS related diseases based on genetically engineered hematopoietic stem cells that possess the capacity for prolonged self-renewal and which are able to continuously produce protected immune cells to fight against HIV[24,25]. Finally, one of the other appealing applications of gene therapy is the recovery of bone defects[26]. Instead of stabilising the defect and minimalising the pain, genes are added to the cells that code for specific cytokines or hormones that are implicated in the remineralisation (bone morphogenic proteins, BMP-4 or growth factors).

Besides DNA, alternative approaches were developed over the last 20 years making use of RNA interfering strategies[27] (RNAi, a cellular mechanism). RNAi is a potent and specific gene silencing event in which small interfering RNA (siRNA) degrades target mRNA by mediation at the posttranscriptional level, for instance in the case of HIV-1 virus-related

conditions[28,29]. The first clinical trials were reported to use lentiviral gene therapy[30] and has rapidly grown[31].

Despite the tremendous advances in antiretroviral combination therapy over the last decade, eradication of HIV from the infected organism is still an elusive goal. Lifelong therapy is associated with potential long-term toxicity, adherence problems, and development of drug resistance. Current approaches were mainly limited by a low number of transduced cells and genotoxicity[32]. The use of new vector systems and the right choice of target cells and improved transduction protocols may overcome these obstacles. Over the last decade, the emphasis of gene delivery research has been on finding these suitable delivery systems that can aid in targeting the proper tissue, protecting the DNA from destruction and promoting the transport to the nucleus once inside the cell. In combination with significant advances in molecular understanding of bioactive processes, it is believed that gene therapy holds a considerable promise for treating thousands of human genetic diseases for which there is no adequate treatment at present[33]. Because of that, the rise of gene therapy could very well become a milestone in medical history enabling higher life quality and reducing costs for extravagant treatments that up to now, have only focussed on symptoms.

## 2 Gene Delivery systems

There are different types of delivery systems that can be divided in two groups, the viral and the non-viral delivery systems. Each of these has certain advantages and drawbacks. Viral systems generally show the highest activity but most are more prone to mutation and secondary toxicity (inflammatory response) whereas the non-viral systems appear to be less potent but display better biocompatibility. Additionally, there are also methods for introducing DNA into the body using physical techniques. Only a limited amount of delivery systems express properties that are sufficient to continue the investigation up to the level of clinical trials. In figure 1.2, the number of delivery systems that was used in clinical trials so far is listed and confirms the superior importance of viral research which accounts for almost 70% of the total amount of delivery systems applied in clinical trials[25]. Not counting the use of naked (plasmid) DNA, the application of non-viral systems, both synthetic and natural, barely exceeds 10% of the total amount used in clinical trials. When looking at the different phases, the amount of trials in phase III is < 1% of the total[34]. Below, a table with a list of examples of both viral vectors (including plasmids) (table 1.1) and non-viral vectors (table 1.2) that reached clinical trials is shown. The number of clinical trials using polymeric synthetic vectors is at this moment very low, yet it's use for clinical trials is strongly increasing during the last years[35].

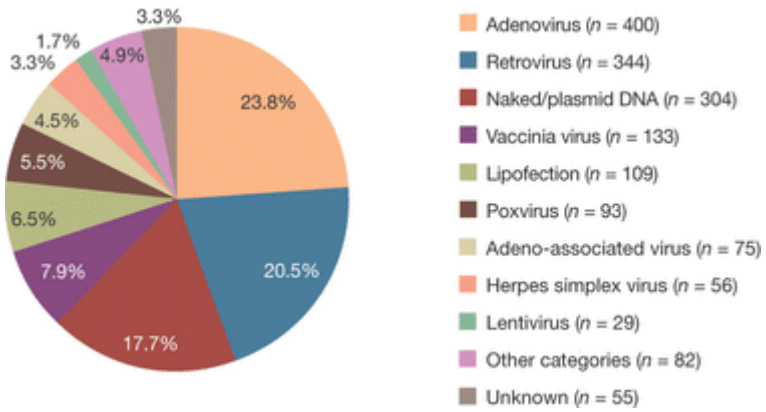


**Figure 1.2 – breakdown of delivery systems used in clinical trials[25,36].**

| Non-viral vector | Disease | Status |
|---|---|---|
| DMRIE:DOPE (1:1) | i. Melanoma<br>ii. Melanoma and renal cell cancer | i. Phase III<br>ii. Phase II |
| DOPSA:DOPE (3:1) | Solid tumours | Phase I |
| DC-Chol:DOPE (1.5:1) | i. Head and neck cancer<br>ii. Ovarian cancer<br>iii. Cystic fibrosis | i. Phase II<br>ii. Phase I<br>iii. Phase I |
| DC-Chol:DOPE (3:7) | Glioblastoma multiforme | Phase II |
| DOTAP | Cystic fibrosis | Phase I |
| GL-67:DOPE (1:2) | Cystic fibrosis | Phase I |
| *In vivo jet* PEI | Bladder cancer | Phase IIb |
| PEG-PEI-Chol | Ovarian cancer by radiation induced promoter | Phase I |
| PEI mannose and dextrose | HIV | Phase II |
| PEGylated 30mer PLL | Cystic fibrosis | Phase II |
| Cyclodextrin based polymer | Solid tumours | Phase I |
| Naked DNA | Liver, breast and colorectal cancers, leukemia | Phase I/II |
| Electroporation | Melanoma, glioma, renal cell cancer | Phase I |

**Table 1.1 – Overview of non-viral vectors used for clinical trials[35].**

| Type of virus | Therapy | Indication | Phase |
|---|---|---|---|
| Retrovirus | ADA-SCID GT: $CD34^+$ cells transduced with Moloney murine leukemia virus carrying ADA gene | Primary immunodeficiencies | 1/2 |
| | $CD34^+$ cells transduced with retrovirus vector with multiple ribozymes | Non-Hodgkin's lymphoma, HIV/AIDS | 2 |
| | Toca-511: replication-competent retrovirus with prodrug activator cytosine deamidase gene injected into tumor | Glioma | 1/2 |
| Lentivirus | LentiGlobin: introduces globin gene into patient hematopoietic stem cells | β-thalassemia and sickle cell anemiaPhase 1/2 | 1/2 |
| | LG-740: T cells treated *ex vivo* with lentivirus with chimeric T-cell receptor gene | 740: T cells treated *ex vivo* with lentivirus with chimeric T | 1 |
| | ProSavin: lentivirus with three genes required for dopamine biosynthesis injected into striatum of brain | Parkinson's disease | 1/2 |
| Adenovirus | Adenoviral mediated interferon-β | Pleural mesothelioma<br>Colon cancer, glioma | 1<br>1/2 |
| | TNFerade: replication deficient adenovirus with TNF-a controlled | Esophageal cancer | 2 |
| | rAd-p53: replication deficient adenovirus encoding hu recombinant p53 | Advanced thyroid tumors, oral, maxillofacial tumors | 4 |
| Adeno-associated virus | AMT-101: AAV with human lipoprotein lipase (LPL) gene | LPL deficiency | 3 |
| | AAV2-sFLT01: AAV with anti-VEGF | Wet macular degeneration | 1 |
| | tgAAC94: AAV2 with TNF-α-IgG1 | Arthritis | 2 |
| Plasmids | Allovectin-7: plasmid with gene for HLA-B7 and β-2 microglobulin genes, injected into tumors | Melanoma | 3 |
| | Hepatocyte growth factor plasmid | Arterial disease | 2 |

**Table 1.2 – Examples of viral vectors used in clinical trials[35].**

## 2.1 Physical methods

### *2.1.1 Direct gene delivery using plasmid DNA*

The simplest and safest approach of delivering DNA is transfection using naked plasmid DNA. Transfection is referred to as the total process of introducing DNA into a host cell and its consequent expression of a protein. In 1990, it was first demonstrated that upon intramuscular injection, naked plasmid DNA was efficiently expressed in myofibers[37]. This observation is due to, on one hand the slow turn-over of myofiber nuclei and on the other hand the unusual high access of DNA into the nucleus of myocytes. This muscle transfection ability opened doors for DNA vaccines[38,39,34]. Later on, it was shown that the efficiency of this gene transfer was improved by using precursors of delivery systems with polymers such as polyvinyl pyrrolidone (PVP) that weakly interact with DNA[40,41]. It is assumed that these polymers protect DNA from enzymatic degradation and that they provide a sort of storage system allowing DNA to be released over a prolonged period. In addition to muscles, the skin, some tumours and certain immune cells are also susceptible to naked DNA-mediated gene transfer. However, it should be noted that the levels of expression after intra-tumoural injection are much lower compared to intramuscular injection.

Intravascular injection of plasmid DNA generally results in limited gene expression in all major organs[42,43]. Research has been performed to discover the causes of this observation. It was observed that the hepatic clearance of naked DNA was very close to the plasma flow rate through the liver and decomposition traces were found in the skin and intestine due to the possible binding to serum components like albumin[44]. In addition, it was also found that DNA is rapidly degraded by plasma nucleases[45]. The incorporation of polysaccharides into non-viral gene delivery systems, on the other hand demonstrated a reduced toxicity and greater stability into biological fluids[46]. Furthermore, it has been demonstrated that intravascular injection may result in high levels of gene expression when the injection occurs under high hydrostatic pressure[47]. It is believed that this pressure enhances expression by facilitating the passage of the plasmid DNA out of the blood vessels[48].

Introduction of plasmid via microinjection has led to successful delivery of genes including GFP, interleukin (IL)18, Flt23k, endostatin, MMP14, and vasohibin into various cells of the cornea (ocular applications)[49,50,51] by targeting different layers performed at various anatomic locations including intrastromal, subconjunctival, and directly into the anterior chamber. For example, successful transgene delivery in the cornea *in vivo* was reached using intrastromal lamellar implantation of a partially dried p-bFGFeSAINT-18 complex composed of SAINT-18 (non-liposomal delivery device[52]) and plasmid vector encoding reporter or FGF2 gene.

Intra-nuclear injection results in a high efficiency of DNA transfer into the nucleus. This procedure which can only be used *in vitro* and *ex vivo*, however, is laborious because each cell needs to be treated separately but is able to overcome some drawbacks associated with naked DNA delivery to tissue, such as the size and negative charge density of the plasmid that can prevent the crossing of cellular boundaries[53].

### *2.1.2 Gene gun*

This particle-mediated gene transfer is achieved by a physical force. A gene gun accelerates DNA coated gold particles to high speeds by means of a high pressure (5-8 bar) stream of helium gas. This force is sufficient to allow the penetration of physical barriers such as plant cell walls and cell membranes. An improved transfection efficiency is obtained due to the induction of micro-traumas within the treated tissue[54], which increases DNA uptake. The introduction of foreign particles (gold) on the other hand, is a disadvantage as well as the depth that can be reached by the particles. This technology has been widely used for gene transfer to the skin[55].

For ocular applications, the use of a gene gun reported successful delivery in the cornea for genes such as IL4 and IL10 plasmid DNA and opioid growth factor receptor, introduced into the corneal epithelium[56,57,58.]

### *2.1.3 Electroporation*

Electroporation is a technique in which cells are exposed to intense electric fields that induce a transmembrane potential[59]. A sufficiently high potential will trigger a dielectric breakdown of the membrane which results in formation of transient breaks (e.g. pores in the plasma membrane) allowing DNA and other molecules to enter the cytoplasm. Both *in vitro* as well as *in vivo* gene delivery using electroporation have been reported[60]. In the latter case, cell electro-permeabilisation is achieved by means of electrodes for example in electro-chemotherapy, to facilitate cellular entry of anticancer agents. However, several drawbacks are associated with this method. To begin, it's effective range within the tissue is limited which results in reduced transfection efficiency for large tissue areas. Secondly, a surgical procedure is needed to place the electrodes into the organ of interest. Finally, the thermal heating generated by the high voltage applied may irreversibly damage tissue[61]. For *In vitro* applications, cells and DNA are combined in a recipient which is placed between electrodes. When voltage is applied, a small incubation time is needed to allow the membrane passage. Hereafter, the cells are restored to normal culture conditions[62]. Compared to *in vivo*, higher charges can be applied which results in the cell-crossing of larger DNA molecules (larger membrane breaches). Most reports show a 10 to 1000-fold increase in transfection when DNA injection was followed by electroporation[63]. It should be noted that different tissues may

respond differently to electroporation due to biological differentiation. Amongst the key parameters to optimise this technique are the electric field strength and the pulse length[64]. An advantage of this technique is also the large DNA constructs that can be transported into cells, although specialized equipment is necessary[65].

Few studies have been performed during last years which target ocular applications. Electrically assisted gene delivery to the endothelium of *ex vivo* human corneas was recently described[66].

### *2.1.4 Gene transfer by ultrasound radiation*

Another physical method used to enhance tissue penetration is via ultrasound (US) radiation[67]. US waves render the membrane permeable by creating small cavitations that allow the delivery of DNA into the cytoplasm through passive diffusion. This is in contrast to electroporation where the DNA is moved along the electric field. The transfection efficiency is determined by several factors such as the frequency, the output strength, the irradiation time and the DNA dose. The efficiency can be enhanced by using contrast agents like air-filled micro-bubbles that readily expand or shrink under ultrasound treatment or by combining DNA with cationic liposomes[68]. In the first approach, local shock waves are generated to induce transient corridors that permeate the cell membranes in close proximity[69]. It was shown that US could enhance transfection efficiency of DNA both *in vitro* and *in vivo*[70]. The benefit of US assisted technique was proven for both viral and non-viral vectors in tissue like cardiac muscle[71], the pancreas[72] or even tumours[73].

Also for the cornea, ultrasonic radiation waves enhance transfection efficiency of several vectors applied (e.g. liposomal gold particles[74]). For a specific type of adeno-associated viruses; efficient transfection was achieved *in vitro* for human RPE cells and even *in vivo* for rat retina[75].

Combining plasmid DNA with cationic lipids (lipoplexes) or cationic polymers (polyplexes) may overcome problems associated with the previously mentioned methods. The subsequent particle formation effectively reduces the size of DNA and creates a less negative surface charge. Additionally it protects the DNA against degradation and facilitates intracellular trafficking. Furthermore, the cationic lipids and polymers that form the DNA complexes can be designed to target specific processes such as receptor binding, nuclear localization or modulation of immune response[76]. As a final note, the use of the above mentioned techniques can be combined and even extended with other newly emerging methods (e.g. combining US microbubbles and magnetic particles[77]).

## 2.2 Viral vectors

Due to natural invading mechanisms, viruses are suitable candidates for delivery of DNA into targeted cells. Currently the use of viral vectors is the most efficient method known for gene transfer *in vivo*. The process that introduces a gene of interest into a host cell is referred to as viral transduction. Viral particles are composed of a nucleic acid genome surrounded by a capsid of proteins. They efficiently gain access to host cells where the genetic information is replicated by the host's machinery. In the ideal case, these viral vectors utilise the viral infection pathway but avoid the subsequent expression of viral genes as this may lead to self-replication and potential toxic effects. Optimally, the gene must be incorporated into a virus that is replication-deficient[78]. This is achieved by deleting all of the coding regions from the viral genome except for sequences that provide functions such as packaging of the therapeutic gene into the virus capsid or the integration into the host's genome. The previously mentioned deletion of the coding regions creates space for the incorporation of the therapeutic gene into the viral backbone. The deleted genes are subsequently utilised in a separate packaging construct to provide helper functions. This construct contains viral genes derived from the parental virus that encode structural proteins and proteins that are required for vector genome replication. Finally, packaging cells are transfected with the vector genome and the packaging construct, which results in production of recombinant vector particles (Fig. 1.3)[79].

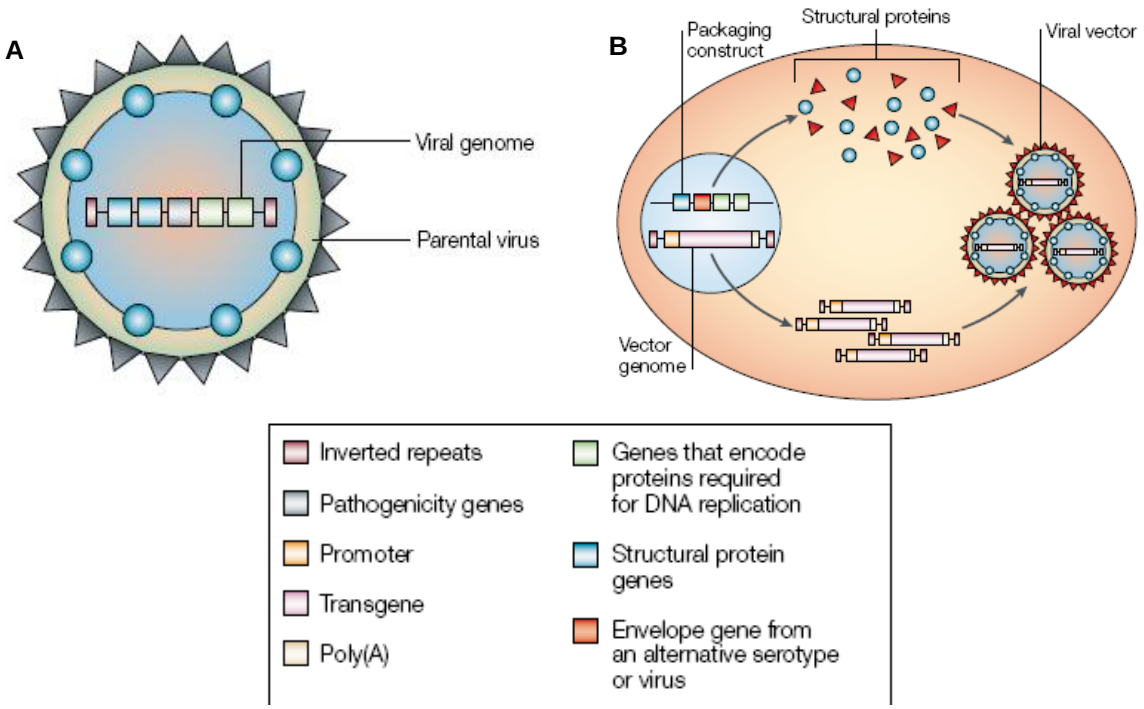


**(A) a generic viral vector including structural proteins, (B) a packaging cell construct with vector genome that contains the therapeutic gene flanked by inverted terminal repeats and *cis*-acting sequences required for genome encapsulation**

**Figure 1.3 - Viral vector modification[54].**

The most frequently used viruses as gene delivery vectors include adenoviruses, adeno-associated viruses, retroviruses (incl. Lentivirus) and herpes simplex viruses.

### *2.2.1 Adenovirus*

This type of virus was one of the first viruses to be investigated[80]. More than 50 human serotypes from six different groups are known (Fig. 1.4). Their genetic material consists of double stranded DNA and they are divided in two groups dependent on the time of genetic expression (early and late)[81]. Generally, certain genes are deleted in order to render the virus replication deficient. Adenoviruses (Ad) are able to transfect both dividing and non-dividing cells. The mechanism of cell-entry is well known and initiation of the cell binding usually occurs through the coxsackie- and adenovirus-receptor[82]. Subsequent interaction with cell integrins allows internalization of the virus through clathrin-mediated endocytosis[83]. Inside the endosomes, a part of the virus particle is removed, followed by transport to the nucleus. The virus replicates episomal (outside the chromosomes) in the nucleus and is consequently not inserted in the hosts genome[84].

As a result, adenoviruses are only used when temporarily expression is sufficient to obtain the desired therapeutic effect. On the other hand, these vectors have a large loading capacity (up to 36 kb) for insertion of therapeutic DNA and are very efficient in transducing cells[85]. One of the main side-effects is (mild) flue and occurs in healthy persons which means that a large amount of the population possesses antibodies against Ad. This implies neutralisation of the infection in the long run and limits the time of expression. Because of that, extensive research was performed to design vectors that combine Ad with non-viral vectors[86]. In 1999, a 18-year-old patient died in of the first clinical trials due to direct administration of an adenoviral vector into the liver through the hepatic artery[87]. An autopsy, however, showed that substantial amounts of this vector were distributed into the circulation and had accumulated in the spleen, lymph nodes and bone marrow.

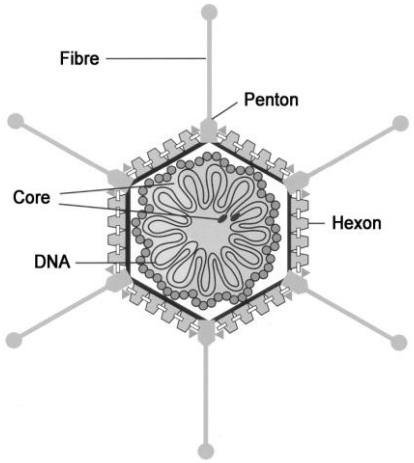


**Figure 1.4 - Adenovirus composition[86].**

The systemic delivery of the vector triggered a massive inflammatory response which resulted in death within 4 days. Subsequent studies in monkeys demonstrated that the adenoviral capsid proteins were responsible for the cause of an early inflammatory cytokine cascade. To avoid these safety issues, recent research has been focussed on gutless viruses[88], a type of Ad of which large parts of the viral genome are removed. When these viruses are used, the expression in the transduced cells lasts longer because of the lack of immune response. Due to the rise of other viral research domains, the investigation of Ad viruses has drastically decreased, yet focus on hybrid Ad systems remains[89].

### *2.2.2 Adeno-associated virus*

An adeno-associated virus (AdAV) is non-pathogenic when applied in humans but requires co-infection of a helper virus (Ad or herpes virus) to be efficient[90]. There are more than 8 serotypes available of which AdAV serotype 2 is commonly used. The viral genome is composed of single stranded DNA that codes for two genes (rep and cap). This first gene is known to code for proteins that control the viral replication and promote integration into the host genome. The other one codes for structural proteins that form the capsid and is usually replaced by the therapeutic gene, but restricts the length of the gene to 4.7 kb. A huge advantage of AdAV is the ability to offer permanent expression of the delivered genes and its capability of infecting dividing as well as non-dividing cells. Additionally, there's a minimal immunogenic response related to AdAV use and this virus also doesn't produce viral proteins, allowing repeated administration[91]. Limitations of AdAV include their small packaging capacity and possible production issues due to increased chances of contamination. The AdAV has been one of the most studies viral vectors and resulted in over a 100 models explored, yet very few actually reached clinical phase trials[92]. Recent advances with clinical application were made using AdAV in the treatment of lipoprotein lipase deficiency[93], muscle desease[94] or rheumatoid arthritis[95].
Ocular approaches focussing on Leber congenital amaurosis have confirmed the potential of AdAV's for retinal[96] and corneal[97] applications

### *2.2.3 Retrovirus*

Another type of frequently investigated viruses are retroviruses. Most of them are mainly based on the murine leukemia virus, a cancer inducing virus for mice. Their genetic material appears as single stranded RNA that replicates by reverse transcriptase via a DNA intermediate. The retroviral genome contains three regions, 'gag', 'pol' and 'env', which encode for the capsid proteins, the viral enzymes (reverse transcriptase, integrase and protease) and the envelope proteins, respectively[98]. Given removal to avoid replication, they create space for the loading of therapeutic genes[99]. Notable is that genome integration

occurs and this establishes a sustained gene expression[100]. Unfortunately, the integration in the genome of the host cell is only possible in dividing cells because the nuclear membrane has to be fragmented to allow entry into the nucleus. This drawback on the other hand could play a major role in transduction of tumour cells, which are located between slowly dividing tissues such as brain tissue. Other drawbacks include the random insertion into the host genome, which can result in activation or inactivation of a host gene. Finally the capacity for insertion of therapeutic DNA is limited to 8,5 kb which is rather small for elaborate applications. Several types of retroviruses have been developed for gene therapy including lentiviruses such as HIV-1[101,102,103] (Fig. 1.5). Moreover, they are currently the focus of considerable other viral gene therapy research like for instance in Parkinsons disease[104], treatment of melanoma[105] or retinal disorders[106,107].

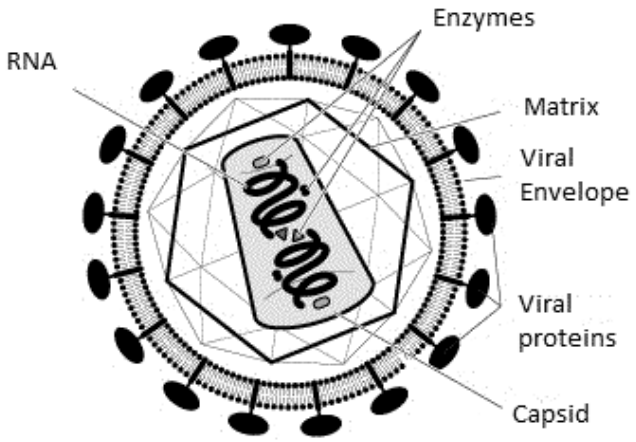


**Figure 1.5 – Structural formation of a lentivirus (HIV-1)[98].**

### *2.2.4 Herpes simplex virus*

A final, major group of viruses widely investigated in gene therapy research are herpes simplex viruses (HSV). As main advantage they have the ability to infect a broad range of dividing as well as non-dividing cells. Replication-defective HSV-type 1 vectors are produced by deleting all, or a combination of, five immediate-early genes (ICP 0, 4, 22, 27 and 47), which are required for infection and expression of all other viral proteins coded by dsDNA. Despite the ICP0 gene product is cytotoxic, it is required for high levels of sustained transgene expression. Recent research solved this problem by substituting ICP0 by a protein which facilitates efficient transgene expression without cytotoxicity[51]. Moreover, due to its large genome, about 30-50 kb of therapeutic gene can be introduced into the vector. Furthermore, HSV's do not insert their DNA into the host's genome thus avoiding the deleterious effects that may occur by random integration[7]. HSV replicates in epithelial cells and establishes a life-long latent infection in neuronal cell bodies within the sensory ganglia, where the latent viral genome is maintained in an episomal state[50,54]. This has led to quite a

lot of studies and clinical trials in the field of tumours (e.g. melanoma[108], carcinoma[109], etc.) but in many cases clinical trials are not progressing due to the possibility of adverse effects[110].

### *2.2.5 The viral future?*

Viral vectors derived from natural viruses are still actively investigated and used in clinical gene therapy due to their inherent high transduction capabilities. It has been demonstrated that one viral particle is already sufficient to induce a measurable effect[36]. These high efficiencies are to a large extent due to the excellent cell-membrane rupture mechanisms[111]. However, several limitations have reduced their use in clinical settings, such as the induction of cancer by insertional mutagenesis. Because of random transgenic insertion into the host's chromosome, the normal expression of a critical gene that regulates cell growth and division gets often disrupted[112]. The lack of cell or tissue specificity of these vectors is also a major drawback. Another adverse factor is the pre-existing or acquired immune responses that are experienced when viral vectors are applied. With these immune responses neutralising antibodies will quickly clear viral vectors from circulation and this results in a reduced efficacy and hampered repeated administration. Finally, various viral vectors fail to transfer high levels of genes which are required to achieve therapeutic effects in several cell types.

These issues along with devastating results of viral gene therapy induced death of patients have motivated the exploration for safer, less pathogenic and less immunogenic gene delivery alternatives including genetically modified viruses and lipid or polymer based delivery systems[113]. Extensive research has been performed in the field of combining viruses and polymers to overcome the aforesaid drawbacks. In this approach, the role of the polymer is passive. It facilitates the delivery of the virus, whereas the active gene transfer function is carried out by the viral part[114]. Polymers are very well suited for this task since macromolecules are composed of multiple active sites which enable interaction with the virus. This results in an efficient protection and can additionally allow controlled release when biodegradable polymers are used. In these polymer-based viral gene delivery approaches four categories can be distinguished[30]. At first method, a polymer matrix encapsulates viral vectors to allow delivery into the body through surgical implantation or injection. Polymers used for this approach can be natural as well as synthetic. Secondly, positively charged polymers (polycations) can form complexes with negative viral vectors resulting in viral complexation. Additionally, polycations such as polylysine and polyethylenimine also neutralize the negatively charged cell. A third series of polymers are hydrophobic, biodegradable polyesters that form microspheres that entrap viruses and

release the virus continuously when degrading. In the last approach, the polymer is anchored chemically to the surface of the virus[34].

From the information given above, it is safe to state that viruses form very potent and attractive delivery systems for genetic, therapeutic purposes. Nevertheless, since the inherent toxic effects of the viral pathway still comprise too much danger, alternatives are imposed on gene therapy research. Because the incubation of a viral vector can provoke a cascade of replications within the host cells (Fig. 1.6) and as long as the understanding of viral vector methods is not adequate, the need for non-viral systems will exist and gain increasingly more interest.

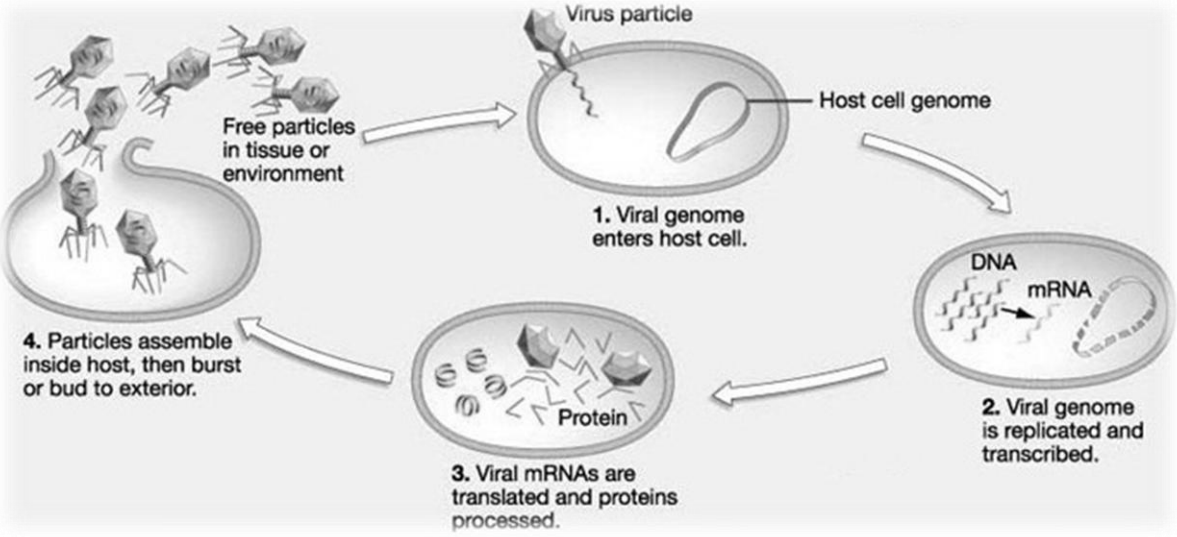


**Figure 1.6 - The viral pathway[115].**

## 2.3 Non-viral vectors

### *2.3.1 Inorganic based delivery systems*

In the beginning, research on inorganic materials that could aid in the delivery of genes into tissue and cells was focused on the use of divalent cations like calcium. This method was precedingly used for bacterial transformation and a similar strategy was reasoned to enhance the uptake of DNA into mammalian cells far before the time of gene therapy started[116]. A frequently used material is $Ca_3(PO_4)_2$ which has an excellent biocompatibility due to its chemical similarity to human hard tissue (bone). In nano-particle dispersed form, it can be used as a carrier in biological systems[117]. This is basically achieved by allowing co-precipitation of a diluted DNA solution in the presence of a low concentration of phosphate ions. In subsequent steps, $Ca^{2+}$ ions $(CaCl_2)$, are graduately added to the solution until precipitation of DNA occurs[118]. The formed calcium phosphates protect DNA from nucleases such as those present in serum. Finally, the precipitated DNA is taken up by cells by means

of endocytosis[23]. Some of the benefits include a stable and sustained expression of the gene, ease of use and a low cost. However precise control over the pH is required and large amounts of DNA are needed to obtain efficient precipitate formation. Unfortunately, the sustained expression is often low and difficult to apply in vivo[60].

Recent research is for a large part focused on magnetic based materials like hydroxyapatite[119] or iron(oxide) containing compounds[120,121,122]. Additional to packing DNA, these structures are susceptible to magnetic force. This benefit is exploited by applying a magnetic field after injection in order to facilitate tissue and cell entry. Other natural minerals that are increasingly evaluated as biomaterials to be applied as delivery systems are layered double hydroxides, a family of anionic clay materials, exemplified by the natural mineral hydrotalcite [$Mg_6Al_2(OH)_{16}CO_3x4H_2O$]. They were found to be efficient in the delivery of siRNA to cells (HEK293T)[123]. Also in combination with organic systems, inorganic based materials such as silica containing bioceramics or alginate hydrogels loaded with $Ca_3(PO_4)_2$ nanoparticles are successfully applied[124,125]. Finally, quite some research is emerging in the domain of gold nanoparticles due to good biocompatibility, monodispersity and ready functionalisation[126,127].

### *2.3.2 Liposomal based delivery systems*

Many different systems based on lipids have been developed as vectors for gene therapy *in vitro* and *in vivo*. Early studies made use of neutral and anionic liposomes because they are less toxic and better compatible with biological fluids and therefore more appropriate for systemic gene delivery[128] (Fig. 1.7). However due to the previously mentioned characteristics of DNA, such as the large hydrodynamic diameter and the negative charge, the encapsulation efficiency was limited. Other drawbacks of these anionic and neutral liposomes include insufficient cell interaction and lack of endosome disruption. Therefore, at present, most of the research is performed in the field of cationic lipids[27,54].

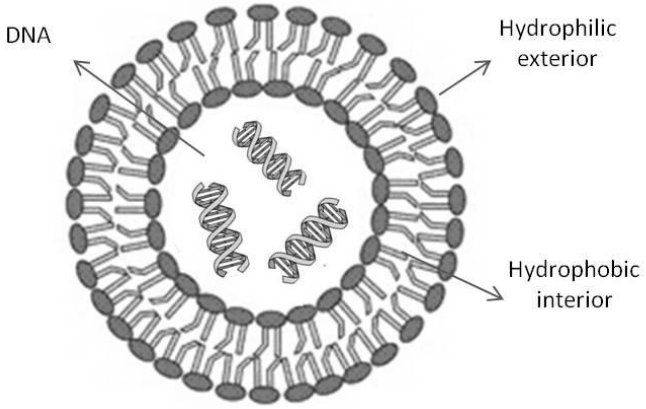


**Figure 1.7 - DNA-encapsulated (neutral) liposome[128].**

All cationic lipids possess a hydrophobic group, which is often one or two alkyl-containing $C_{12-18}$ chains or a cholesterol unit, as well as a charged group like an amine or phosphate group[67]. In some cases, this amphiphilic molecule contains also a linker group (e.g. ether or ester). Single chain hydrocarbon-anchored lipids, such as cetyltrimethyl-ammonium bromide (CTAB), tetradecyl-trimethylammonium bromide (TTAB) and dodecyltrimethylammonium bromide (DTAB) form micelles and can be classified as detergents. Lipids with a double chain like 1,2-dioleoyl-3-trimethylammoniumpropane (DOTAP) and *N*-(1-(2,3-dioleoyloxy)propyl)-*N,N,N*-trimethylammonium chloride (DOTMA) are more efficient in transfection compared to the single chain lipids[27] (Fig. 1.9). The presence of cholesterol in the lipoplex results in an increased stability. The hydrophobic moiety of these compounds is of a slightly different nature since it contains cyclic groups. An example of such a lipid, is 3b-[*N*-(*N,N*-dimethylaminoethane)-carbamoyl]cholesterol hydrochloride (DC-Chol.HCl)[6,27,63] (Fig. 1.8).

Above a certain concentration and when dispersed in an aqueous environment, hydrophobic moieties are responsible for the rearrangement of cationic lipids into bilayer vesicles. This assembling process effectively shields the hydrophobic portion of the molecule and exposes the charged heads to the aqueous medium. Cationic groups are required for the electrostatic interaction with DNA and its subsequent, spontaneous condensation. This results in a considerable, reduced size of the anionic DNA which is residing within those liposomes or is often trapped between individual liposomes, referred to as lipoplexes[61]. Lipoplexes have sizes that can cover a range from 50 nm to over 1 µm[67] and it has been demonstrated that there is no size limitation in the complexation of DNA[129]. Additionally, depending on the $pK_a$ of the used lipid (charged group), the pH can also affect the interaction of cationic lipids with DNA and the structures of the complexes[27]**.** Lipoplexes are prepared in such a way that a residual positive charge remains to allow interaction with the negatively charged cell membrane. The main property of the charged groups is to complex with DNA. This phenomenon occurs continuously by liposomes in order to stabilize the cationic charge. Unfortunately, this process renders lipoplexes limitedly usable since continuous aggregation forms aggregates that become too large for cellular uptake. Other structural parameters that influence the transfection efficiency are the length of the aliphatic chain, the degree of saturation and the addition of neutral lipids. Neutral lipids induce a conformational change from double-layer to hexagonal structure when applied and promote endosomal escape[130].

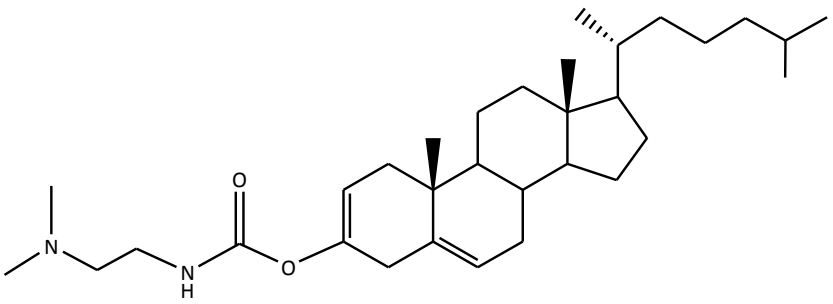


**Figure 1.8 - Structure of DC-Chol.**

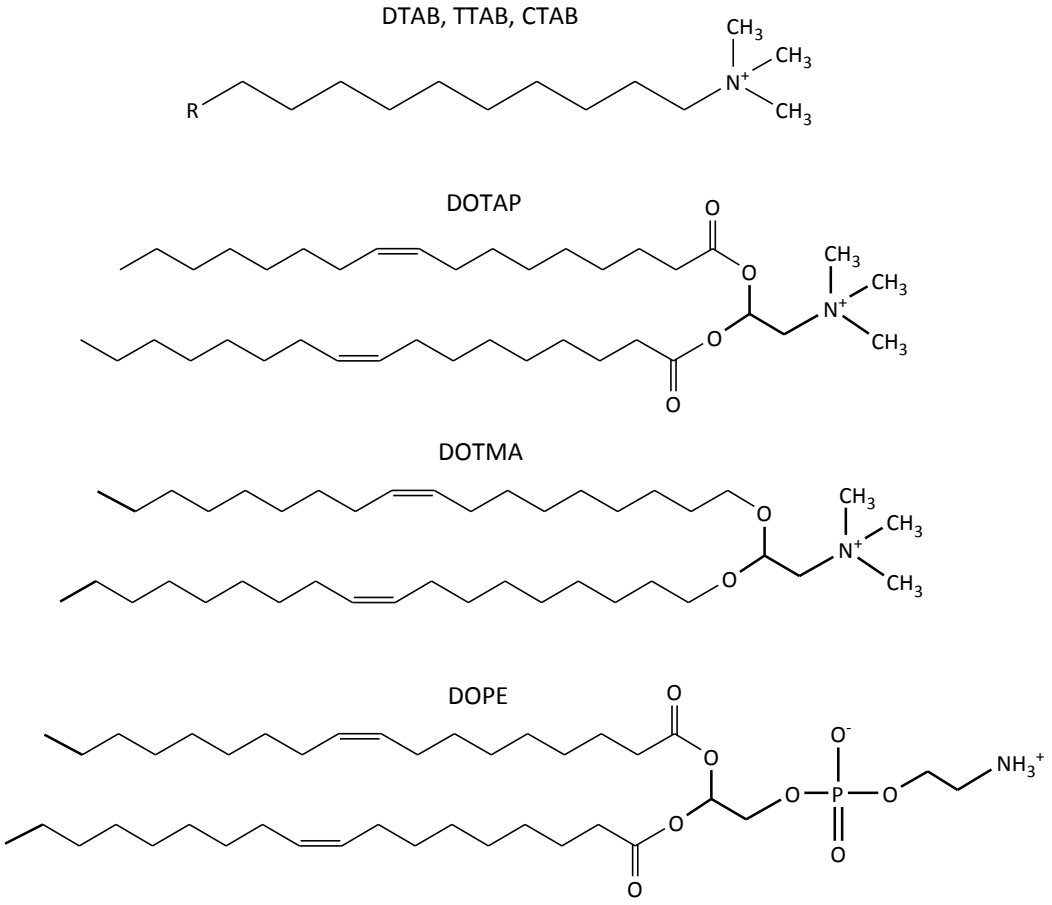


**R = H (DTAB), R = $CH_3CH_2$ (TTAB) and $CH_3(CH_2)_3$ (CTAB)**

**Figure 1.9 - Structure of liposome forming compounds.**

For a long time spontaneous fusion of the liposome with the cell membrane was accepted as main route for the uptake of lipoplexes in the cell[19]. The advantage of this fusion would have been the introduction of DNA into the cytoplasm instead of the endosomal uptake, where DNA is more prone to degradation[24]. However, recent studies, demonstrated that this way of internalization only accounts for a minor percentage and that generally cationic liposomes bind to the cell surface via ionic interactions and are taken up by non-receptor mediated endocytosis[7,72]. Proteoglycans (PG) present on the cell membrane seem to play an essential role in these interactions as cells deficient in PG synthesis are more difficult to transfect[27].

When lipoplexes are taken up via endocytosis they are introduced in the endosomal pathway but need to be effectively liberated ('endosomal escape') to deliver their contents into the cytoplasm. This endosomal release is thought to occur by interaction and following fusion of the lipid layer with the membrane layer of the endosome vesicle. In turn, this fusion creates membrane destabilization and release of DNA into the cytoplasm[131]. This assumption was supported by the observed enhancement of transgene expression when 1,2-dioleoylphosphatidyl-ethanolamine (DOPE) was included within the complexes. DOPE can be catalogued under the group of neutral lipids that promote transfection efficiency by enhancing the endosomal escape due to membrane fusion and disruption. This molecule is neutral, yet internally charged, containing a dipolar head (one positive and one negative charge) and two bulky fatty acyl chains[67]. The fusion of lipid bilayers is often pH-dependent, a quality that is eagerly exploited inside the late endosomes where the pH drop catalyses the fusion of the lipid bilayers of liposome and endosome.

In recent approaches, more attention is given to the incorporation of fusogenic agents in lipoplexes with the intent of further destabilising the endosomal membrane. Successfully utilised fusogens include adenoviral particles, peptides of viral origin and subunits of toxins[132,133].

The use of lipids as gene delivery systems offers some advantages, such as their lack of immunogenicity which makes repeated delivery *in vivo* possible[134]. Another advantage is the ability to deliver large amounts of DNA while ensuring sufficient protection of DNA against physical forces and enzymatic degradation. Even so, certain limitations like degree and duration of expression remain[79]. Present studies demonstrate higher transfection efficiencies when lipid gene delivery systems are combined with cationic polymers[50,135,136]. Gene delivery in cultured human epithelial cells and in rabbit corneal epithelium in vivo has also been reported with DOTAP/DOPE transfection mixture[137]. Recently, a new domain of lipid-based materials is explored, making use of combinatorial methods to create large family's of lipids, termed lipipoids[127]. Studies deploying such a strategy proved successful in the treatment of ovarian cancer with siRNA[138] or could be even used for liver gene silencing by one single shot addition[139].

### *2.3.3 Delivery systems based on peptides*

The discovery that certain molecular structures have the ability to readily move across the cell-membrane (translocation) was made already in the late 1980's[140]. In that experiment, a living cell could easily internalise a peptide consisting of 86 amino acid units (part of the HIV-1 Tat protein). Some years later, a similar compound was identified derived from the Drosophilia Antennapedia protein, capable of translocating along the cellular boundary[141].

Further research uncovered that small parts of these sequences (often 10-30 amino acid residues) were responsible for these excellent translocation properties and because of that were categorised as cell-penetrating-peptides (CPP). This opened possibilities for the introduction of the model amphiphilic peptide MAP[142] and other well known peptides like Penetratin[143] and Tat[144] (Fig. 1.10). Up to now, a limited number of CPP's is known and they consist of different primary and secondary structures[145].

**Penetratin** **$NH_2$-lys-lys-trp-lys-met-arg-arg-asp-gln-phe-trp-ile-lys-ile-gln-arg-OH**

**TAT** **$NH_2$-arg-arg-arg-gln-arg-arg-lys-lys-arg-gly-tyr-OH**

**Figure 1.10 – Amino acid sequence of two known cell-penetrating peptides.**

One important feature of CPP's is their amphiphilic nature. Both hydrophilic/cationic and hydrophobic amino acids are incorporated in a peptide sequence. It is this combination that facilitates cell-internalisation and the transport of active molecules like for instance DNA. This groups of peptides is also referred to as protein transduction domains (PTD's).

The mechanism of cell-internalisation consists of two steps[146]. Initially, interaction is established between the CPP and the cell surface based on electrostatic forces. This process induces already to a certain extent, membrane de-stabilisation (due to a conformational transition) but complete translocation only occurs after membrane disruption by both hydrophobic and hydrophilic units (often present in an $\alpha$-helical structure)[147]. A thorough or precise idea of the internalisation mechanism is still the topic of many discussions but generally it is believed that most of the CPP's are internalised by different forms of endocytosis[148]. The fact that different forms of endocytosis are applicable can be correlated with the composition of the peptide. Sequences containing a number of guanidine functional groups for instance are inclined towards receptor mediated endocytosis since guanidine is a bidentate ligand that can form two adjacent H-bridge connections with proteoglycanes[149]. An example of a prominent proteoglycan is heparin sulphate which is capable of binding the Tat sequence by its whole length and initiate translocation[89]. A considerable disadvantage of CPP's is noticeable once the peptide and cargo are internalised and reside inside an endosome. Release from the vesicle seems restricted since CPP's do not possess qualities that provoke cell-rupture, hence eventual degradation inside the lysosome is likely to occur (including its cargo)[90].

Delivering DNA can in principal be achieved by CPP's in two ways[150]. Utilising the cationic charges and hydrophobic groups present on CPP's, a complex could be formed with DNA (co-incubation method). Additionally, the DNA and CPP could be covalently linked to each other. This latter method however, is difficult to execute since it requires certain purification

steps that endanger the DNA integrity but on the other hand creates well-defined structures. Moreover, larger amounts of DNA seem to be needed to obtain significant results. Although CPP's transport macromolecules through the cell-membrane in an excellent way *in vitro*, the *in vivo* translocation is limited by a low cell-specificity[151]. Certain studies showed that if Tat-β-galactosidase was introduced in mice, the produced peptide was recovered all over the body (including the brain)[152]. Because of this, higher doses are required which could evoke secondary, adverse effects (random insertion). Therefore, recent investigation is devoted to CPP's that address specific cells and tissue to minimise side-effects[153]. This was achieved by for instance a drug or a vector[154].

An accepted solution is found in the use of cell-interactive peptides (CIP's)[155]. These peptides are similar to CPP's (specific sequences of amino-acids that perfectly match chemical structures on the outside of particular cells) but have a strong affinity for a fixed cell-type. In combination with CPP's, this leads to a considerable higher and clear expressed gene delivery. One of the best known CIP's is the RGD-peptide (arginine – glycine – aspartic acid) that interacts with integrin receptors ($\alpha_V\beta_3$) which play a major role in angiogenesis of tumours, hence the active investigation in cancer treatment in recent years[87,156,157]. Its affinity towards these receptors is even increased when cyclisation or multimerisation is applied, mainly because the conformation of the cyclic RGD peptide is spatially better suitable for interaction with receptors than the linear counterpart[158].

Combining CPP's and CIP's is promising yet not all problems are addressed. Endosomal escape and DNA shielding for *in vivo* applications remain weak links. A better approach would consist of the combination of CPP's (and CIP's) with a suitable polymer carrier.

### *2.3.4 Polymer based delivery systems*

#### *2.3.4.1 Polymers*

A final group of delivery systems that is gaining increasingly more attention during the last decade are polymers. Vectors based on polymer systems have the advantage that they can be tailored to address specific needs in for instance DNA protection, cell internalisation and nuclear transduction. This is achieved by synthesizing multifunctional polymers containing particular functional groups and ligands that enhance the transfection efficiency. The interaction between cationic polymers and DNA was already known in the 60's because of research on condensation methods for genetic material[159]. The outcome of this investigation led to the rational selection of histone-like materials (e.g. poly-L-lysine or poly-L-arginine) but its potential use as delivery system was not successfully exploited at that time[160,161]. Polysaccharides like dimethylaminoethyl-modified dextran[162] or chitosan[163] (Fig. 1.11) where the real first type of polymers that were explored as gene delivery systems.

Parallel with an improved understanding of cellular processes over the last two decades, a wide variety of polymers has been studied as synthetic vector. Up to now, one of the polymers which displays the highest potential in transfecting cells is polyethyleneimine (PEI)[164,165]. Extensive research of this polymer has elucidated the importance of certain structural parameters on the success cell transfection and research on modified versions is still ongoing, like coupling to chitosan[166] or other ligands (e.g. RGD[167] or albumin[168]). A first parameter is the pH-dependence. Dependent on the type of functional groups ($pK_a$) present, polymers bear charges when dissolved in a physiological environment (pH ≈ 7.2). This is necessary for DNA complexation, cell-membrane interaction and buffering of the endosome. One of the unique properties of comblike (branched) PEI is its buffering capacity[169]. The optimal range of buffering is situated between pH 4-11 which is due to the combination of primary, secondary and tertiary amines, the 3D-structure as well as the proton-neighbouring effect[170]. Furthermore, the importance of molecular weight and spatial rearrangement (branching) was determined in the case of PEI (Fig. 1.11). Branched PEI has an apparent advantage over linear chains in transfection efficiency[171]. Moreover, for linear derivatives the transfection efficiency was proportional to the molecular weight whereas the cell-viability on the other hand was inversely related. This problem was partially solved by introducing biodegradable crosslinks (disulfides) between low MW PEI units[172,173]. Chemically modifying PEI with polyethyleneglycol[174,175] (PEG) chains or lactose units[176] also improves both *in vitro* and *in vivo* transfection. Tuning the chemical structure of polymeric vectors with PEG (Fig. 1.11) is a general trend for improving *in vivo* application since PEG is known for its excellent biocompatibility[177]. Additionally, it shields the negative presence of high amounts of charge that lead to membrane stabilization of cell-organelles[178,179,180]. PEI was successfully used in *in vivo* gene delivery for human corneal epithelium tissue[181].

Other types of polymers that have been subjected to frequent examination are poly-α-aminoacids (Fig. 1.11 – polylysine or polyarginine). Considering the discovery of efficient complexation of DNA and histone-like polymers, the use of poly-L-lysine was straightforward[182]. Other polymers within this class are often based on amino acids, for instance, L-aspartamide[183,184] or L-glutamic acid[185]. One of the notable downsides is the clear lack of buffering capacity when compared to PEI[86]. In some case, the use of imidazole was suggested as a possible solution since this molecule exhibits buffering properties which are suitable for endosomal escape ($pK_a$ of conjugated acid ≈ 7)[186,187]. Additionally, the excessive presence of charges demonstrated high toxicity. Again, attempts to circumvent this disadvantage were found in the coupling of PEG[188]. On the other hand, poly-α-amino acids (as well as other polyamides or polyesters) have the huge advantage of being readily

metabolised (degraded) by the cell (peptidase enzymes), a beneficiary effect when acceptable cytotoxicity is desired[189,190].

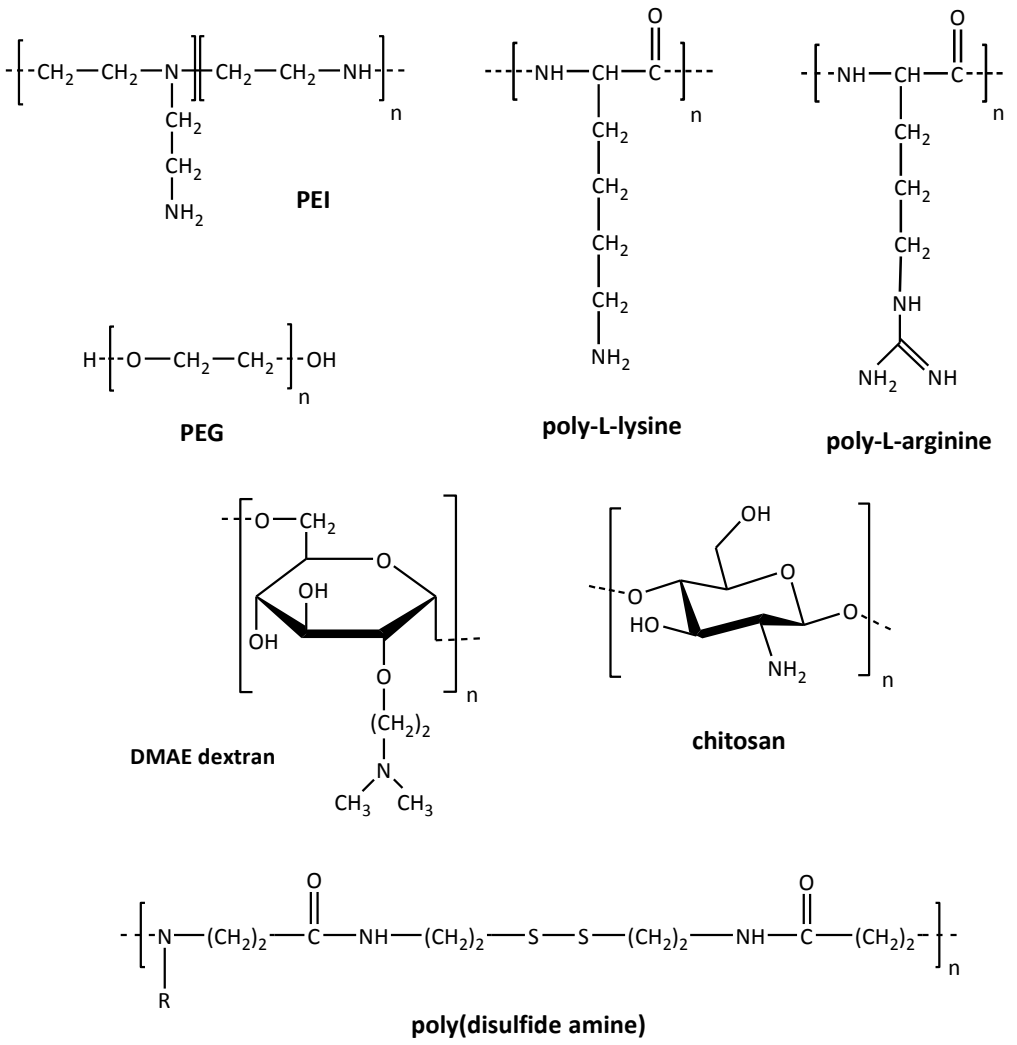


**Figure 1.11 - Polymers for gene delivery.**

In combining two of the above mentioned advantages, branching and biodegradability, a series of dendrimers, of which the most widely studied is based on polyamidoamine (PAMAM)[191,192], were explored as potential delivery system. Dendrimers are synthetic[193], hyperbranched polymers that are produced via a so called 'diverging' strategy in which by stepwise addition more functionality (higher number of functional end-groups) and branching is introduced to the system (Fig. 1.12). The end-groups of these branches are covered with primary amines that allow complexation with DNA (high density of primary amines provokes a strong interaction). Internal amine groups are largely shielded from interacting with large anionic molecules and contribute only to the buffering ability of the polymer. Dendrimers are ideally used for their high solubility and ability to release their cargo constantly[85]. Additionally, dendrimers demonstrate good shielding properties for enzymatic attack of DNA. Regrettably, few polyplexes based on dendrimers are able to transfect DNA and most exhibit

a substantial toxicity (due to considerable haemolysis and high charge densities)[194]. To improve the transfection efficiency and to reduce the cytotoxicity, several modifications were attempted. For instance, coupling to the amphiphilic 'GALA'-peptide (30-units long peptide with EALA repeats)[195], to PEG or by introducing disulfide bonds in individual PAMAM units[196,197]. Also arginine modification of PAMAM was proven to have a positive effect[198,199]. Some PAMAM derivatives (4$^{th}$ generation) proved to possess anti-tumour regulating properties when combined with oligodeoxynucleotide complexes, applicable in breast cancer treatments (*in vitro* & *in vivo*)[200].

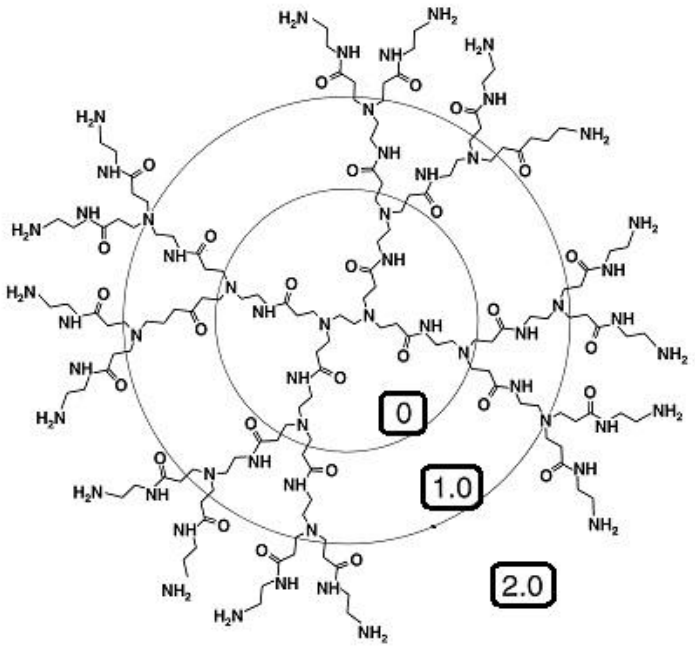


**Figure 1.12 - PAMAM dendrimer (2.0 = Generation 2 = 2$^{nd}$ expansion addition).**

Within the group of polymer gene delivery systems, an important class are methacrylate based polymers. Due to their simple (often one-pot) synthesis and commercial availability of monomers, these systems have been the subject of extensive research[201,202]. A commonly accepted transfection-efficient vector is poly(dimethylaminoethyl)methacrylate (pDMAEMA) which contains tertiary amines for DNA interaction and appears to have sufficient buffering properties for endosomal escape[174,203,204]. To reduce the inherent cytotoxicity and protein-interaction, coupling to PEG or internal modification (copolymerisation) with ethoxytriethyleneglycol or *N*-vinylpyrrolidon was successfully carried out[205,206]. Upon *in vivo* application in nude mice, pDMAEMA showed even better transfection results than PEI[207]. Many copolymer derivatives (also block copolymers) containing DMAEMA were as a result investigated and reported interesting properties when combined with poly-ε-caprolacton (PCL) for cancer treatment[208,209] or SiRNA delivery[210]. Other types of interaction between DNA and the polymeric carrier were explored such as hydrophobic (coupling to *N*-

vinylpyrrolidon[204], butylmethacrylate[211], methylmethacrylate[233], etc.) or primary amine coupling, introduced as an intermediate for ligand coupling[212]. This family of methacrylate-based polymers was even expanded with thermo- and pH-sensitive derivatives. Copolymerisation with respectively pNIPAAm[233,213] and monomers containing imidazole or pyridine functional groups[214,215] expressed such properties. More recently, polymethacrylates were adopted as gel-based materials for matrix-based gene delivery[216,217] (see paragraph 2.3.4.2) which becomes an increasingly more potent research field.

Finally, there are also delivery systems known that react to external stimuli like temperature or pH[218,219,220]. Dependent on the external environment, these polymers undergo a reversible transition from random coil to DNA-complexed globule. In the case of thermo-responsive polymers, a critical solution temperature (and concentration) can induce this transition[221]. With regard to the nature of the material this temperature provokes a rearrangement of the material from two to one phase (LCST, lower critical solution temperature) or the other way around, from one to two phases (UCST, upper critical solution temperature)[222]. When DNA and polymer are randomly dissolved (relaxed, hydrophilic, coil conformation), this is seen as a two-phase system whereas the DNA-associated particle (collapsed, less soluble or hydrophobic globules) is considered as the one-phase stage (Fig. 1.13). The driving force for this phenomenon can be either thermodynamic or entropic ($\Delta G = \Delta H - T.\Delta S$). Given this information, materials possessing LCST behaviour close to the body temperature possess unique characteristics that can be used in gene delivery since polymer-DNA complexes could be formed above LCST, remain as a particle inside the body but become unstable upon local temperature decrease and dissociate[223,224].

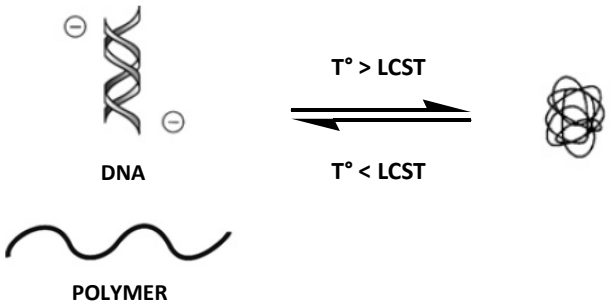


**Figure 1.13 - Thermo-responsive behaviour of pNIPAAm.**

Poly(*N*-isopropylacrylamide) (pNIPAAm) is a clear example of a thermo-responsive polymer with an LCST value just below body-temperature (± 32 °C)[225,226]. They can be used to deliver tightly condensed DNA complexes to cells (globule complexes at 37 °C)[227,228,229]. Once inside the cells, an externally applied temperature reduction to below the LCST induces the relaxed, extended-chain conformation (DNA dissociation)[230]. Other benefits of pNIPAAm in biomedical applications include its simple chemical structure and sharp phase-transition

behaviour, necessary to prevent extreme temperature reduction[231,232]. The LCST of pNIPAAm (Fig. 1.14) can be altered by copolymerization with hydrophilic monomers like acrylamide (LCST increase) and hydrophobic monomers, such as n-butyl acrylamide (LCST decrease)[233].

Adding hydrophilic, charged monomers such as DMAEMA into the polymeric structure can make the resulting copolymer both temperature and pH responsive[188,234]. In general, a pH-sensitive material consists of both hydrophilic and hydrophobic moieties. Changes in pH and therefore also in net charge cause certain phase-transitions which are induced by protonated functional groups[235]. Copolymers of methylmethacrylate and methacrylic acid can undergo phase transition at low pH since carboxylic groups become protonated and render the total polymer highly hydrophobic. Dependent on the environment, this can result in precipitation or solubilisation or the loss or gain of interaction with other solutes. A similar result can be obtained with copolymers of methylmethacrylate and DMAEMA (Fig. 1.14), where the use of a high pH can turn a hydrophilic polymer into a hydrophobic one[108].

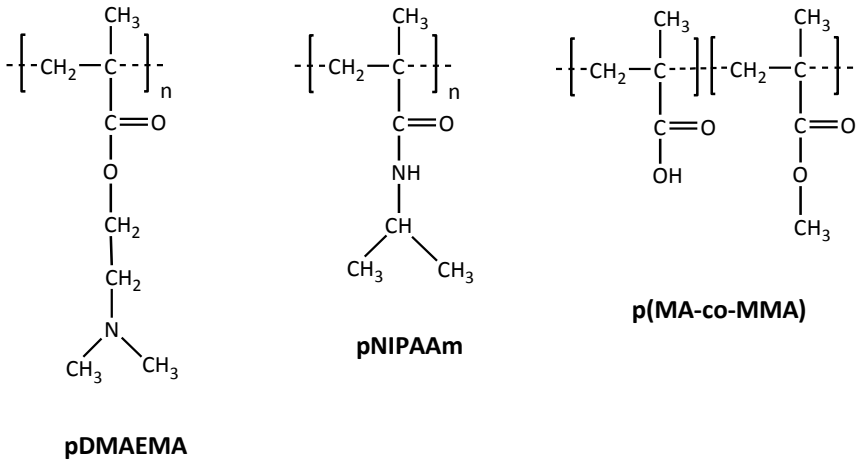


**Figure 1.14 - Structure of methacrylate-based compounds for gene delivery.**

*2.3.4.2 Application of biomaterials as gene delivery platforms*

An alternative strategy to delivering DNA to tissue or cells via polymer carriers is the use of 3-dimensional structures that can encapsulate or immobilise DNA and polymer-DNA complexes[236]. These biomaterials (or tissue engineering scaffolds) should ideally mimic the extracellular matrix (ECM) and are therefore mostly composed of highly biocompatible materials (often naturally occurring polymers). This concept gave rise to the use of gene activated matrices (GAM) for therapeutic purposes[64]. To satisfy fundamental requirements of the ECM, the scaffolds should meet certain design criteria such as mechanical strength, cell adhesion, infiltration and migration[140,237]. Especially these last requirements turn out to be somehow complex in attaining due to the need for a construct of a vascular and metabolite

network, essential for cell proliferation. It is important that cells from the surrounding tissue are capable of infiltrating the engineered scaffold to allow integration as well as development of a vascular network to supply necessary metabolites for continued cell proliferation[238]. Gene delivery from those scaffolds may represent a versatile approach to manipulating the local environment for directing cell function[239]. Using this technique, several approaches can be employed to increase the expression of tissue inductive factors or block the expression of factors that would inhibit tissue formation[240]. Utilising gene therapy enables localised expression due to site-specific implantation. Additionally the scaffold can protect the vector (when applied) from degradation by serum nucleases, increase the residence time and minimise the inflammatory response[241]. Furthermore, a major advantage of scaffold-based delivery is the sustained release of the vector, which enhances gene transfer[242].

In most cases natural materials like gelatin, collagen and chitosan are applied but also synthetic materials like PEG or Pluronics® are promising candidates or can assist in fine-tuning the properties of natural compounds[202]. Naturally occurring materials have been widely used in tissue engineering for their innate cellular interactions and cell mediated degradation. Biodegradable polymers are developed to avoid a second surgical procedure. The release pattern can be controlled by influencing the biodegradable part of the polymers (in time). GAM's are categorised according to the mechanism by which DNA is incorporated, via scaffold encapsulation or surface immobilization[88] (Fig. 1.15).

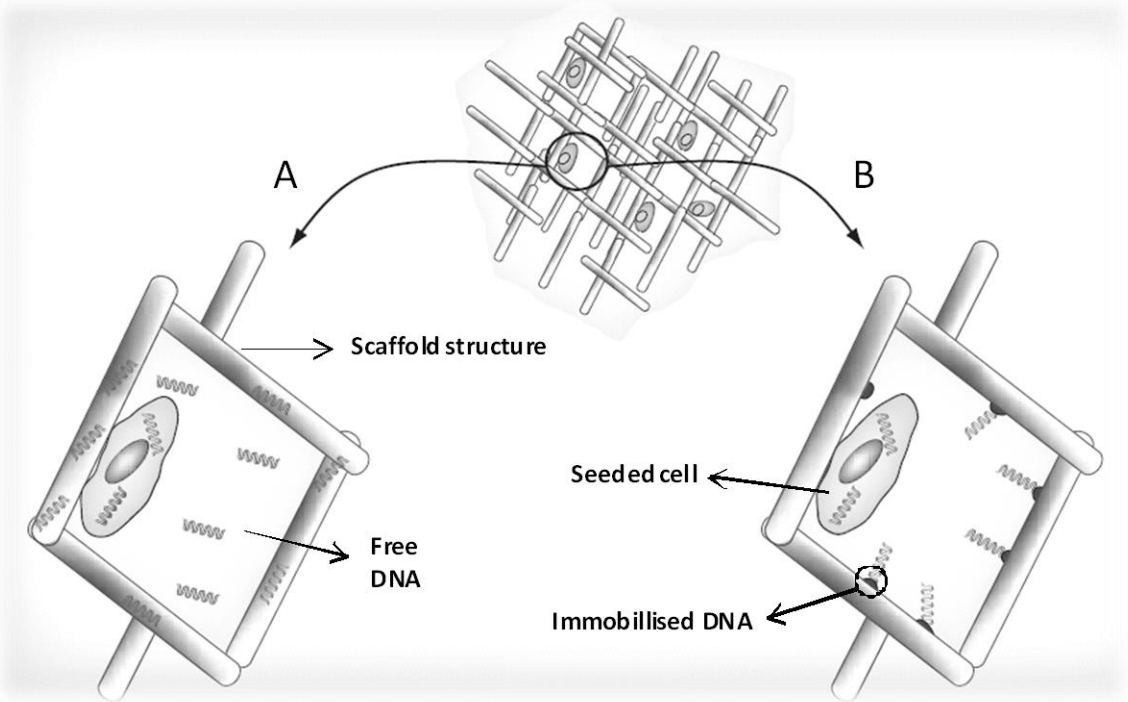


**Figure 1.15 – GAM for DNA delivery: (A) Scaffold encapsulation; (B) Surface immobillisation[88].**

*2.3.4.3 Scaffold encapsulation*

In the case of scaffold encapsulation, the main attention is focused on scaffold fabrication. Critically in the design is the presence of DNA that could be easily affected by external stimuli[243.] Even when the DNA is enveloped by a vector, high temperature, the use of organic solvents, the presence of free radicals and the occurrence of shear stresses could readily affect DNA integrity. There are two types of scaffolds that are frequently described, being hydrogels and some hydrophobic polymer structures[244].

Hydrogels are highly hydrophilic polymeric networks that can absorb a huge amount of water (up to 99%). In the formation of these structures, mild processing conditions are applied, favourable for encapsulated vectors. The hydrogels can be constructed ex vivo before implantation or in situ245 and are divided into natural and synthetic polymers. Early work in the field of gene therapy explored natural polysaccharides like pullulan[246], chitosan[247,248] or collagen[249,250,251] often in combination with hyaluronic acid (HA)[252]. Also agarose[253] and alginates[254] are successfully used as base polymers in the design of scaffolds. They can possess different morphologies and geometrical structures ranging from films over sponges to pellets and microtubular networks[2451].

Soon focus was also put on synthetic polymers because of their ease of production and versatility in structure modificiation. One of the most studied polymers is poly(lactic-co-glycolic acid) (PLGA) which was used as polyplex reservoir. The importance of the scaffolds geometries receives increasingly more attention (scaffolds presented as films[251], microspheres[255], fibrous scaffolds[256] or even foams[257]). Varying the process parameters of these structures allows the scaffold to be uniquely designed for each required purpose, e.g. degradation rate, pore size and mechanical stiffness. In vivo trials have revealed the potential of such delivery devices for bone regeneration in nude mice[258,259] and for tumours in rats[260,261]. Other studied polymers which contain biodegradable ester links are for instance poly(D,L-lactide) (PDLLA) and derivatives thereof but just as for PLGA, acidic scaffold waste products may provoke an inflammatory response[262]. Hydrogels composed of PEG[100,263] or pegylated polymers[264] are also of high interest as they are highly biocompatible and produce very flexbile geometries. Block-copolymers containing PEG/PEO (e.g. Pluronics[265,266,267]) or PEO in combination with other synthetic polymers like PLA[268] or PCL[269,] prove to be versatile delivery devices (many are characterised by thermo- and pH responsive properties). Within the group of polyesters also the use of PET[270] and PCL[271] for designing degradable constructs was reported.

Finally, combining natural and synthetic polymers seems logical in cumulating the advantageous properties (maximising biocompatibility and degradability[272,273]) of both groups yet, limited research has appeared in literature[274]. Mainly PEG based copolymers were

retrieved (e.g. with HA and Chitosan[275] or for pluronics with cyclodextrins[276]) but also matrices composed of collagen and PGA[277] or GAM's formed by crosslinked dextran-glycidyl methacrylate polymers[278.]

The release of the vector and subsequently DNA occurs through diffusion and in the case of biodegradable polymers, also by structural disintegration[279]. Hydrophobic polymers don't possess the quality of attracting water[280] but can be interesting as gene delivery device due to the facile release of weakly surface-bound DNA-vector complexes. Nevertheless, diffusion of these complexes in a non-hydrophilic environment is somehow hampered. This process can be sped up by introducing hydrophilic, biodegradable linkages (e.g.PLGA) that are prone to enzymatic hydrolysis[281,282]. Alternatively, in non-biodegradable materials (e.g. poly(ethylene-co-vinylacetate), water-penetration can be increased by incorporating a pre-existing network of pores through which diffusion can be facilitated[283].

#### *2.3.4.4 Surface immobilization*

Another approach to deliver DNA via matrices makes use of coupling DNA or polyplexes covalently to the scaffold surface structure. In this way, immobilized vector DNA can be transfected if target cells adhere to the substrate which averts the limitations related to mass transport. The coupling of the polyplex is achieved post scaffold fabrication. Cells cultured on the substrate can internalise DNA either directly from the surface or by degrading the linkage between the vector and the biomaterial[284]. Alternatively, specific interactions between the cell and the vector/scaffold can be introduced by using complementary functional groups, such as antigen/antibody reactions. On the other hand, the integrity of the DNA is more susceptible to surrounding interaction when it's not protected within a matrix, therefore the proposed approach consists of coupling of vector/DNA complexes rather than DNA as such[285].

In this way, localised gene delivery can be obtained, for instance in gene-eluting stents for vascular applications making use of polyallylamine bisphosphonate matrix[286] or gelatine/collagen impregnated with PEI[287,290]. VEGF and angiopoietin-coupled collagen scaffolds proved to exhibit advantageous properties for revascularisation purposes. For bone regeneration, suitable scaffold candidates were found in poly(lactide-co-glycolide) derivatives immobilised with viral vectors[288]. In general, similar scaffold structures (and materials) as for encapsulation are used but with an extra coupling step in the total design that allows attachment of the DNA/vector to the polymer network, either through traditional chemical coupling strategies (e.g. EDC coupling or disulfide linkage[289] or by means of a bio-relevant couple (e.g. avidin/biotine[290]).

## 3 Overcoming general limitations in human gene delivery

Up to now, gene therapy could not redeem the expectations that were initially considered as revolutionary. Considering that the concepts that were put forward are well engineered and supported by substantial *in vitro* and *ex vivo* evidence, the limited success for *in vivo* applications should be mainly attributed to the body and its natural defence system. This is especially the case for non-viral delivery systems that encounter numerous barriers between administration and nuclear activity. Since it's very unlikely that therapeutic DNA passes these hurdles passively, vectors with an optimised design are needed to meet the criteria for DNA interaction, protection and cell-internalisation. In an ideal scenario, vector-associated DNA complexes target specific cells or tissue, become internalised and escort the DNA to the cell-nucleus where transcription can result in the production of a therapeutic molecule (protein)[100]. The transfection process can be divided in several subcategories (Fig. 1.16):

- ► DNA interaction (condensation) and protection stage I
- ► Cell-interaction and internalisation stage II
- ► Cytoplasmic release stage III
- ► Polyplex dissociation stage IV
- ► Nuclear translocation and entry stage V
- ► Gene-expression (protein production) stage VI

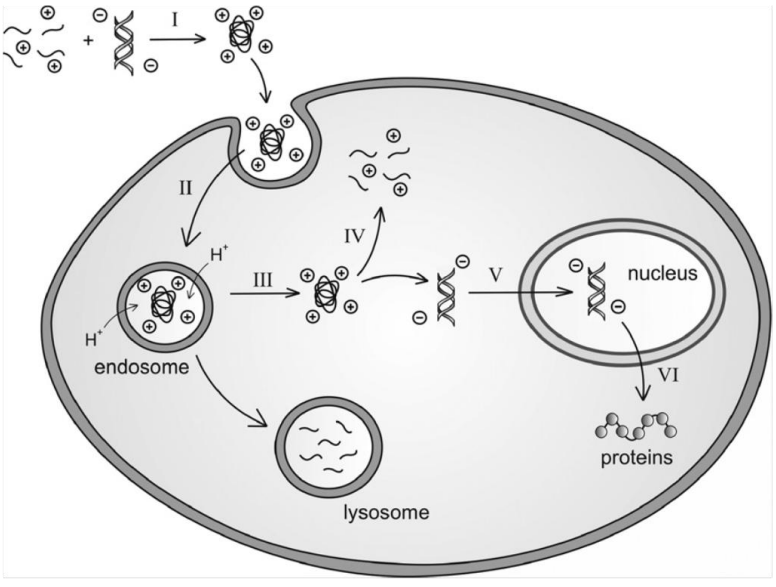


**Figure 1.16 - Overview of the transfection process[202].**

### 3.1 DNA interaction and packaging

At the start of the transfection process, carefully selected therapeutic DNA plasmids need to be protected by synthetic vectors. Non-condensed DNA is a vast molecule that is unable to cross the nuclear membrane. The dimensions of plasmids of just a few kbase easily reach several hundred nanometers which implies the need for a condensed state to ensure swift uptake[291]. Similarly to natural DNA condensation into chromosomes by cellular proteins like histones, synthetic vectors can undergo an electrostatic interaction with cationic polymers which yields an inter polyelectrolyte complex (IPEC) also referred to as polyplex. This self-assembly is the result of charge neutralisation and polyelectrolyte bridging followed by hydrophobic condensation[292] (Fig. 1.17).

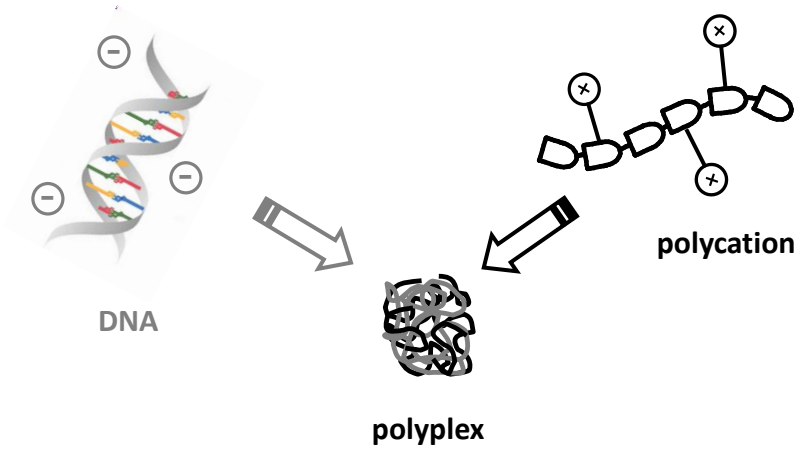


**Figure 1.17 - Self-assembly of IPEC's (polyplex).**

The extent to which polyelectrolytes adhere, is not only dependent on the charge. Many other facets like chain length, chain stiffness, ionic salt concentration and surface charge density have been recognised as being key parameters for IPEC formation[293]. Charge by itself can be imputed to the structure of the polyion and is mostly pH-dependent (for weak polyelectrolytes)[294]. The key parameters of theories that reveal the mechanism of charge-mediated forces for polyelectrolytes become overwhelmingly large so that usually simplifications are required[295]. Geometrical constrains of the different polyelectrolytes involved in complexation highly affect the spatial arrangement of the complex which in turn can influence the cell-interaction and internalisation behavior (Fig. 1.18)[296]. Complexes with DNA occur most often as geometrical form C and F or a combination (but this is subject to the rigidity of the DNA).

Because of the need for cationic vectors, polymers are equipped with functional groups that bear positive charges in a physiological environment (pH ≈ 7.2). That is why for instance amine functional groups (and derivatives) are frequently used ($pK_a$ of $R\text{-}NH_3^+$ ≈ 10).

Besides electrostatic interaction, the packaging shields DNA from nucleases and other blood components. An excess of vector on the other hand implies the presence of a surplus of

cationic charges which is often correlated with increased cytotoxic effects. A beneficial consequence of excess charge is the prevention of aggregation. The strength of the electrostatic bond is also important for the polyplex stability but can hamper the dissociation of polyplexes inside the cytoplasm.

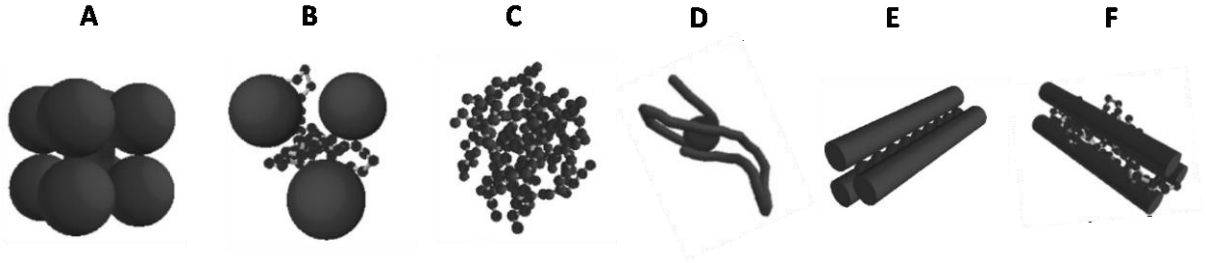


**Figure 1.18 - Various combinations of macroion complexes: (A) globular + globular, (B) flexible linear + globular, (C) flexible linear + flexible linear, (D) semi-flexible linear, (E) rodlike linear + globular, (F) rodlike linear + flexible linear[296].**

### 3.2 Cell internalisation (endocytosis)

If small DNA-containing particles are available, they have to get past the first physical barrier which is the cell membrane. Firstly, targeting specific cells and initiating the interaction with the cellular exterior is a requirement that partially can be met by the vector. Predominantly positively charged particles can be attracted by negatively charged glycoaminoglycans to start negotiating possible entry mechanisms. Moreover the vector can be embedded with certain cell-specific sequences (peptides for integrin receptors) that target well-defined tissues. Passive diffusion is not possible due to size restrictions of regular transmembrane pores (1-5 nm). Strategies used to surmount this physical barrier are based upon processes by which cells naturally internalise macromolecules like nutrients and bacteria from the extracellular space, a process better known as endocytosis[297]. This cellular entry is tightly regulated to avoid uptake of undesirable or unnecessary particles and can occur by at least 5 pathways (clathrin-mediated endocytosis, caveolae-mediated endocytosis, phagocytosis, macropinocytosis and clathrin- and caveolae-independent endocytosis) of which the first two represent the most plausible entry mechanism for linear polymers with side-chain charges[298].

The internalisation of polyplexes may occur by means of a clathrin-mediated endocytosis pathway. This is the best characterised and kinetically most effective route for various polyplexes[299]. The first step in this pathway is the binding of certain molecules to clathrin related structures on the plasma membrane. After binding to the plasma membrane, a clathrin coated pit is formed at the basolateral side of the cell membrane. This pit ensures the formation of a membrane invagination which is pinched off from the plasma membrane by dynamin to form intracellular clathrin-coated vesicles with diameters ranging from 100-

150 nm. Hereafter, the clathrin coat is rapidly depolymerised and individual vesicles fuse to form the early endosome[291]. During this internalisation pathway, the polymer-gene construct undergoes a pH drop from 7.4 at the cell surface to approximately 5.5 in the lumen of the endosome. When the endosome fuses with the lysosomes the pH is further decreased to 4.5 and the DNA becomes susceptible to degradation by hydrolytic enzymes present in the lysosome which emphasises the need for endosomal escape. Caveolae-mediated endocytosis is similar to its clathrin counterpart and starts with the formation of invaginations on the cell surface which are lined by caveolin-1[300]. The buds are formed from hydrophobic membrane micro-domains rich in cholesterol and sphingolipids (lipid rafts). Once internalised the polyplex resides inside caveosomes that in a later stage may fuse with the early endosomes but avoid direct trafficking to the more acidic late endosomes and lysosomes[301,302]. Determining which internalisation mechanism will be involved, depends on various factors like polymer structure, polyplex composition and size, cell type and cell stage. Since caveosomes do not always experience a significant pH-drop this could explain why some polycations with considerable proton buffering capacities are not effective in gene transfection.

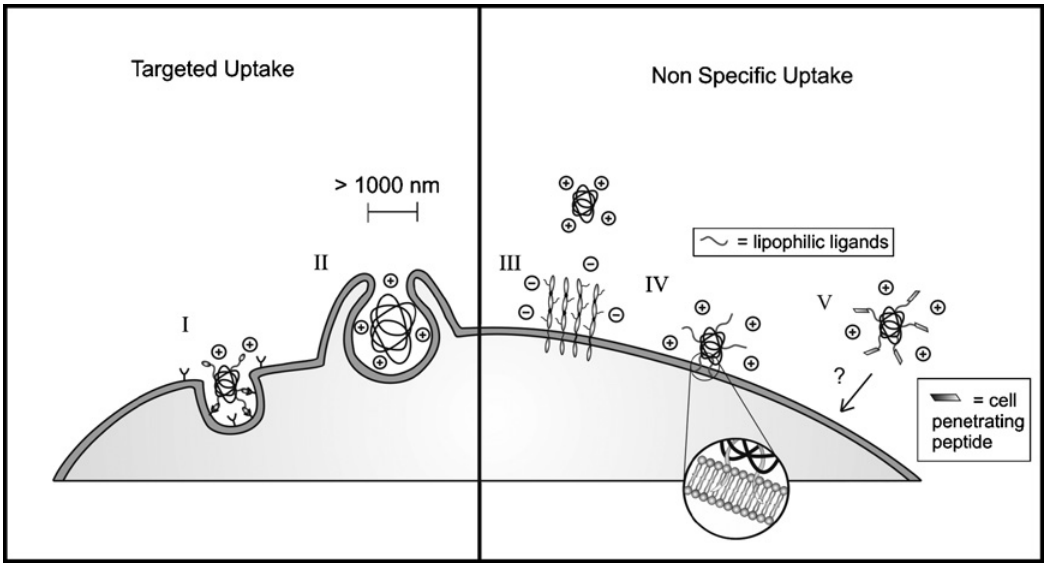


**Figure 1.19 - Illustrations of targeted and non-specific uptake[186]: I – pinocytotic uptake (endocytosis), II – polyplex internalisation via phagocytosis, III – interaction of cationic polyplexes and proteoglycans , IV – internalisation via lipophilic ligand coupling, V – CPP mediated internalisation[202].**

The formerly discussed entry mechanisms are classified as forms of pinocytosis, processes that internalise mostly particles up to 200 nm (although in some cases particles up to 500 nm were reported)[303]. Larger particles, in general, are internalised via phagocytosis, a process in which extra-cellular particles are engulfed by membrane segments that get detached from

the membrane to form a phagosome. Via this method molecular structures up to 1 µm can be taken up by the cell. Besides forms of targeted uptake, there are also several non-specific internalisation mechanisms. These occur through interaction with negatively charged proteoglycans, present within the membrane or by the coupling of lipophilic ligands and cell-penetrating peptides. This latter method is the topic of much recent work, yet the internalisation mechanism is not fully known (Fig. 1.19).

### 3.3 Cytoplasmatic release (DNA release)

When polyplexes are internalised (using a variety of entry-mechanisms), they most likely reside within a vesicle. Several subsequent processes can follow the vesicular internalisation. The vesicle can be recycled at the cell-surface or can be delivered to cell-organelles like the Golgi-apparatus. The most feasible follow-up action however is the fusion with lysosomes[188]. These cellular entities are responsible for cellular waste and destruction of foreign material since they contain a wide range of hydrolytic enzymes (sulfatases, phosphatases, nucleases, etc.) situated in a acidic environment (pH ≈ 4.5). Obviously, the polyplex needs to escape from the endosome before fusion with the lysosome occurs. Different theories exist on how polyplexes can be released from the endosome but the most widely accepted theory is the proton-sponge theory as stated by J.P Behr[304]. This theory suggests that high concentrations of protonable groups effectively buffer the endosomal pH drop which occurs when endosomes mature. If carefully selected polymers with suitable buffering properties are presented to such an environment, the resulting protonation of the polymer will destabilise the endosomal pH. Endosomal ATPases however, try to keep the endosomal pH constant by coupling the proton influx to the influx of the counter anion chloride[33,159]. This causes a huge increase in ionic concentration within the endosome resulting in osmotic swelling and finally bursting of the vesicle with release of its contents[188] (Fig. 1.20). Moreover, it is also believed that protonation of the polymers increases the dimensions of the polyplexes, thereby putting more pressure on the endosomal membrane while also inducing increased interaction with the endosomal membrane. To cover the continuous pH decrease during maturation of the endosome, polymeric vectors are equipped with considerable buffering functional groups (like imidazole and pyridine of which the conjugated acids have $pK_a$ values around 7 and 5 respectively). Also amine and to a lesser extent, guanidine groups, can be used for this when present in a polymer chain due to the proton-neighbouring effect. In general, synthetic vectors that should be capable of escaping the endosomal pathway have to buffer efficiently between a pH of 5.5-7.5. When expanding the buffering capacity of vectors, there's a higher chance for endosomal escape since the time before reaching the lysosomal stage is extended[305].

Although this hypothesis is still being contested, it is backed up by the fact that viruses, such as the influenza virus, make use of a similar mechanism. They efficiently use the previously described decrease in pH, to induce a conformational change in proteins[306]. These proteins, called endosomal release proteins, undergo a structural transformation from a random coil at neutral pH to an α-helical conformation at lower pH. The α-helical conformation is believed to induce membrane interaction and disruption, leading to release of the endosomal content into the cytosol[307]. Examples of such release proteins are melitin, influenza virus hemagglutin, diphtheria toxin, GALA, KALA and JTS-1[188]. Specific for these compounds, is the presence of both carboxyl functional groups (for pH control) and hydrophobic alkyl chains (for membrane disruption)[308].

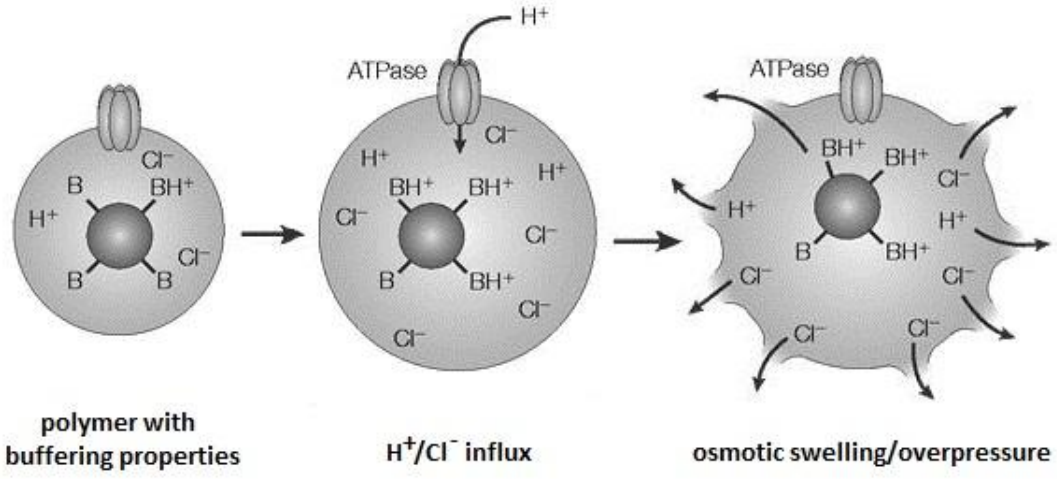


**Figure 1.20 - Mechanism of the 'Proton Sponge' theory[304].**

### 3.4 Polyplex dissociation and intracellular trafficking

Following endosomal escape, polyplexes are exposed to the cellular environment (cytosol). One final barrier remains before replication of the genetically engineered protein can be attained, which is the directing of the polyplex to the nucleus where it should be taken up. It is not fully clear weather the polyplex should dissociate before nuclear internalisation or when present within the cell core[299]. There is evidence that migration of polyplexes (or DNA) to the nucleus periphery through the cytoplasm is an active (not diffusive) transport process mediated by the microtubule network[309,310]. This process is typically not a rate-limiting step in intracellular trafficking of polyplexes (or DNA). However, the entry of polyplexes (or DNA) into the nucleus typically imposes a huge barrier to transgene expression because of the small functional size of the nuclear pore complex in the nucleus (≈ 10 nm or about 30 nm even under the inclusion of a nuclear localization signal/sequence[311]) of a non-dividing ("postmitotic") cell. Therefore, the association of DNA and its vector remain beneficiary[312].

Polyplexes entering the cytosol, either directly or upon escaping the endo-lysosomal pathway are faced with a hostile environment containing nucleases that are able to degrade unprotected nucleic acids. It was demonstrated that microinjection of DNA into the cytoplasm resulted in degradation of DNA with a half-life of 50 to 90 minutes[313]. These enzymes are interspersed in a dense network of microtubules, intermediate filaments and microfilaments which form the cytoskeleton that maintains cell shape and enables cellular motion as well as intracellular transport[314] (Fig. 1.21). The microtubuli network impedes the passive diffusion of naked DNA greater than 80 nm thus imposing an active transport mechanism on polyplexes (50 - 150 nm), using molecular motors associated with the microtubule network or actin microfilaments[315]. Movement is mediated by two classes of motor proteins, namely kinesins (outward direction) and dyneins (inward direction). Therefore, kinesins are linked to the secretory pathway while dyneins regulate perinuclear transport[316]. It is worth to mention that the polyplex may not escape the endosomes too early as this may prevent the arrival at deeper regions of the cell (the nucleus). Directing a polyplex to the nucleus may also be performed by an appropriate ligand (nuclear localisation signals, NLS)[317]. Also this aspect can to some extent be fulfilled by the delivery system as NLS contain several cationic sequences that can be mimicked by the carrier (e.g. arginine or lysine containing). Established NLS-containing compounds are for instance histone[318] and protamine[319] (proteins) as well as viral compounds like the SV40-large tumour antigen[320].

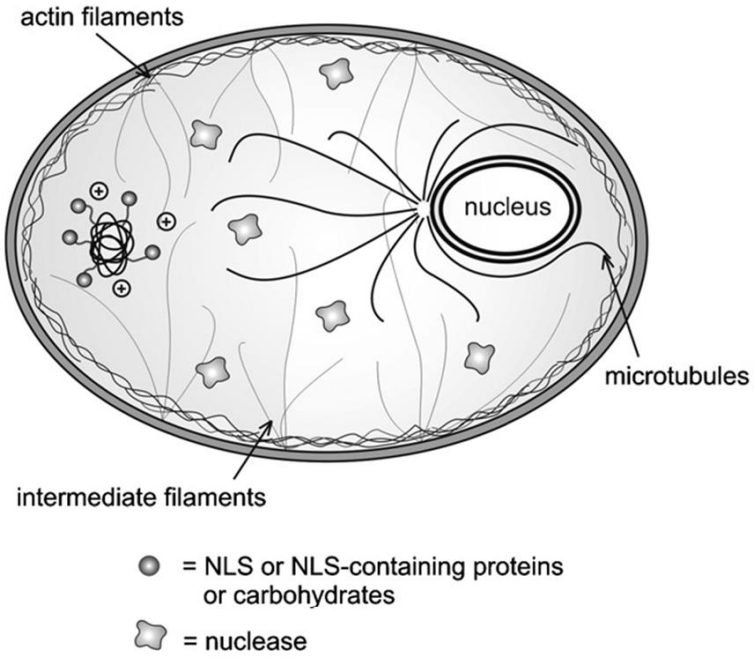


**Figure 1.21 - Intracellular trafficking of polyplexes/DNA[202].**

In order to initiate the delivery of DNA cargo for transcription and gene expression, the vector/DNA complex should dissociate safely and effectively. This phenomenon however, is

in contrast with the previously described complex formation needed to allow cell uptake. Ideally, a polyplex strongly interacts with DNA before cell-internalisation after which the attraction graduately diminishes under influence of environmental stimuli (pH, temperature, ionic concentration or electric fields) until dissociation occurs at nuclear entry. Intelligent polymers are able to exhibit large changes in their physical state or properties due to small changes in environmental stimuli. Structural adaptions for vectors often comprise of cleavable disulfide bonds (via glutathione) or hydrolysable groups like esters. Typically, the strength of the polyplex is related to the amount of charge present on a vector. Replacing by or adding other types of attractive forces like Van der Waals and H-bonding can initially create a similar binding pattern to DNA but in a later stage facilitate the intracellular dissociation of the polyplex. Once the DNA cargo is released, the polymeric carrier has served its purpose and is considered a 'waste' product of the gene delivery cycle. Ideally, the carrier is fully biodegradable and can be metabolized by the cell.

### 3.5 Nuclear uptake & gene expression

The nuclear membrane is a barrier that prevents uptake of the majority of macromolecules into the nucleus, unless they are able to interact with the nuclear active transport system. This system consists of nuclear membrane proteins that form the nuclear pore complex (NPC) as well as soluble proteins present in the cytoplasm. These NPCs are gateways for export and import of proteins and nucleic acids. Each NPC is an assembly of at least 30 distinct proteins, is cylindrical in shape and has pores that span the inner and outer nuclear membrane with a diameter of about 125 nm. These channels allow free movement of molecules (< 10 nm)[321]. It has been demonstrated that although the pore occupies a diameter larger than 10 nm, passive movement is restricted to that size due to the presence of a central granule[322]. This granule is able to change conformation when a suitable NLS is coupled to the relevant particles. Cytosolic import of large molecules is therefore regulated by import proteins (e.g. importunes) which actively transport them through the NPC.

A second method by which DNA may gain access to the nucleus is during mitosis, when the nuclear envelope is disintegrated. It has been proven that DNA is localised in the perinuclear region of the cell where it remains until breakdown of the nuclear membrane. Therefore, gene expression may be considerably enhanced if transfection occurs shortly before cell division[323]. This method however is clinically limited as most cells in the body are in postmitotic state.

After dissociation and upon arrival into the nucleus the genes must be transcribed into mRNA before they can be translated into therapeutic proteins, produced in the cytosol (Fig.

1.22). As mentioned earlier, the expression of these proteins can be sustained or transient. Ideally, DNA is permanently inserted into the genome by means of DNA transposons. This renders the use of additional DNA administrations obsolete but has the main drawback that the integration could be random and lead to gene disruption with undesired side-effects. Dependent on the desired therapeutic effect, specific plasmid DNA (or sequences) can be developed and delivered via a vector in order to cure illnesses and genetic disorders.

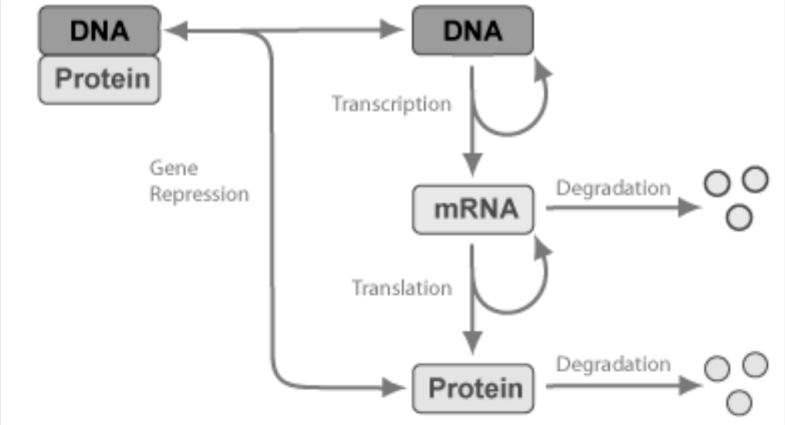


**Figure 1.22 - DNA transcription into mRNA and translation of a protein.**

## 4 Objective of the doctoral thesis

In order to meet the current needs on finding suitable synthetic vectors for gene delivery, this thesis has the aim to synthesise and characterise biodegradable and non-biodegradable vectors for ocular and cardiovascular applications. Biodegradable compounds are derived from poly-α-amino acids (polyamides) whereas the non-biodegradable compounds are derived from methacrylate-based polymers. The properties of the synthetic vectors will be evaluated both at a physico-chemical level as well as for biological applications. In addition, the advantage of coupling cell-penetrating peptides to cationic polymers in terms of transfection enhancement will be examined for several peptides. Furthermore, a selection of polymer compounds are provided with fluorescent molecules to enable mechanistic elucidation of the intra-cellular trafficking and inter-polyelectrolyte formation. Moreover, immunological and haemo-compatible considerations towards *in vivo* uses will be monitored. Finally, the activity and toxicity will be assessed for most vectors on relevant cells such as ARPE19, HEK 293 or COS cells.

Within the polymer & biomaterials research group (PBM – Ugent), earlier work was performed on (cationic) polymers for gene delivery/therapy on which this doctoral thesis continues. In the work of Luc Dekie[185,324], the use of poly-L-glutamine derivatives containing

amine, pyridine and carboxylic acid functional groups was investigated as potential gene carriers. The multifunctional polymers were further derivatised with reagents such as agmatine and fluoresceine. Transfection efficiency studies elucidated that only the agmatine-containing polymers expressed biological activity. Analogue research was done for polymethacrylate compounds by Peter Dubruel[201,206,325], in which specific functional groups like amines, pyridine and carboxylic acids were evaluated as gene carriers. The most optimal transfection results were obtained for pDMAEMA with a high MM. Furthermore, there was also research performed by Kathleen de Winnie on pHEG-PAMAM dendrimers which confirmed the positive effect on the cell viability compared to regular PAMAM while maintaining the high DNA load possible (due to the high surface charge density)[326].

### 4.1 Treatment of age-related macula degeneration (ARMD)

In the framework of a European project (EU-STREP, PolExGene – Nr. 019114), the synthetic vectors, developed in this doctoral thesis, will amongst others have the aim to deliver therapeutic DNA for the treatment of ophthalmological disorders. An important syndrome that is expressed in up to 30 % of the older adults (> 60 years), is age-related macular degeneration (ARMD)[327]. In the US alone, 200.000 new cases are discovered every year[328]. This is a medical condition that results in the loss of vision in the center of the vision field (macula) due to retinal damage. It occurs in 'dry' and 'wet' form, dependent on the cause of the deficiency (Fig. 1.23). Dry ARMD results from atrophy to the retinal pigment epithelial layer (natural abrasion of photoreceptors) and cannot be treated at current while wet ARMD is caused by unregulated, abnormal blood vessel growth (choroidal neovascularisation). Eventual blood and protein leakage can damage the photoreceptors which rapidly causes fading of vision quality. For wet ARMD, there are certain treatments available like photodynamic therapy (stops blood vessel growth) or laser therapy (destroys leaking blood vessels) but they inflict surrounding tissue with scarring as a result (Fig. 1.24). Recenlty also commercially available drugs (antibodies, Ranibizumab[329] or Bevacizumab) have emerged in this field which act on VEGF suppression. Gene therapy is one of the promising alternative approaches[330] and solutions can be found in the use of DNA that encodes for anti-angiogenesis or anti-VEGF[331] proteins that should prevent the proliferation of blood vessels and as a result induce a reduction of the unregulated blood vessel growth[332]. Ocular applications are ideally suited for gene therapy. One obvious advantage is that therapy on the genetic level addresses the source of the problem, not just the symptoms, and the option for local delivery may improve effectiveness without systemic toxicity. Animal models containing loss-of-function and gain-of-function mutations are available, as are models containing mutations in structural, functional, and developmental genes, and models for testing the effects of genetic therapies on wound healing and surgical

interventions enabling researchers to test therapies designed to target a variety of disease categories[333,334].

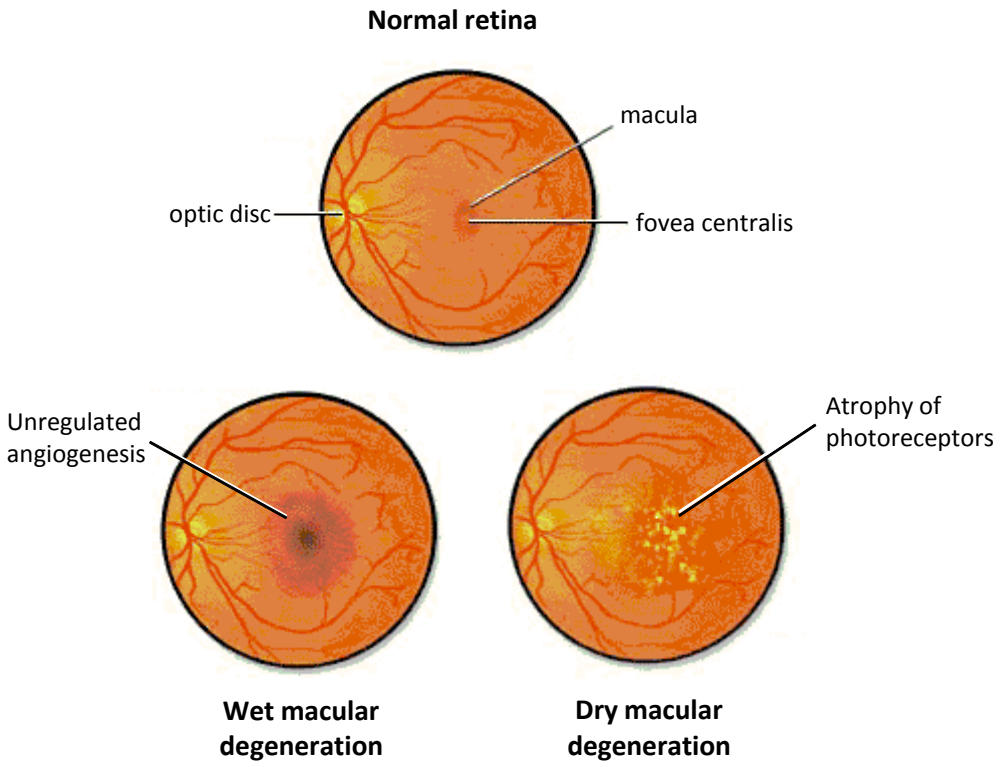


**Figure 1.23 - ARMD disorders: dry and wet macular degeneration[332].**

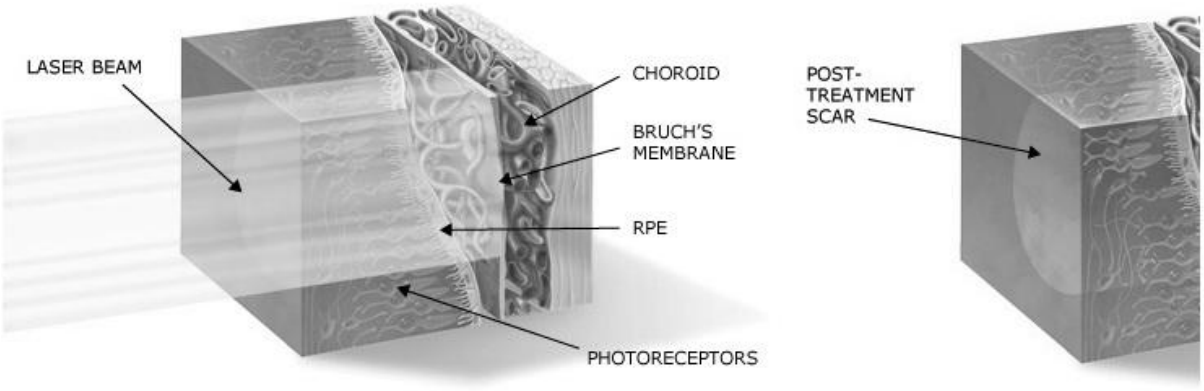


**Figure 1.24 – Laser therapy for wet ARMD: destruction of leaking blood vessels and the occurrence of scarring as a result[332].**

## 4.2 Development of biodegradable, synthetic vectors

The production of biodegradable poly-α-amino acids, applicable as synthetic vector starts with the synthesis of the base polymer. For poly-γ-benzyl-L-glutamate (pBG) or poly-δ-benzyloxycarbonyl-L-ornithine (pZO), the corresponding N-carboxyanhydride (NCA)

derivative of γ-benzylglutamate and δ-benzyloxycarbonyl-ornithine is polymerised with a primary or tertiary amine as initiator, dependent on the desired molecular mass (MM). Therefore, the ratio of monomer to initiator is varied to obtain polymers with a broad range of MM's (Fig. 1.25). The MM of these polymers will be investigated with viscometry ($M_v$).

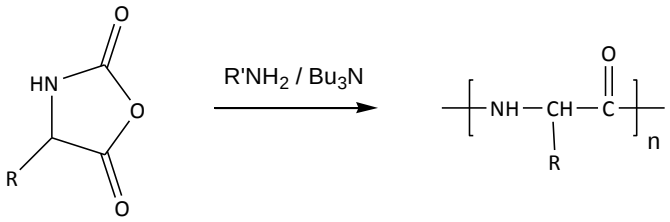


**Figure 1.25 - Synthesis of base polymers (L-derivative).**

In order to acquire multifunctional vectors, the base polymers will be converted to cationic polymers (amine or guanidine side-groups). For pBG this will be done by means of an aminolysis reaction with bifunctional reagents that possess a primary amine on one side and the desired functional group on the other side (hydroxyl, protected primary amine, tertiary amine, imidazole, etc.), each with specific properties in DNA complexation (Fig. 1.26). In case of pZO, an intermediate polycation (poly-L-ornithine) is initially generated after deprotection of the Z-group. Afterwards, the primary amine side-groups can be (partially) converted into a guanidine functional group via a specific reagent (Fig. 1.27).

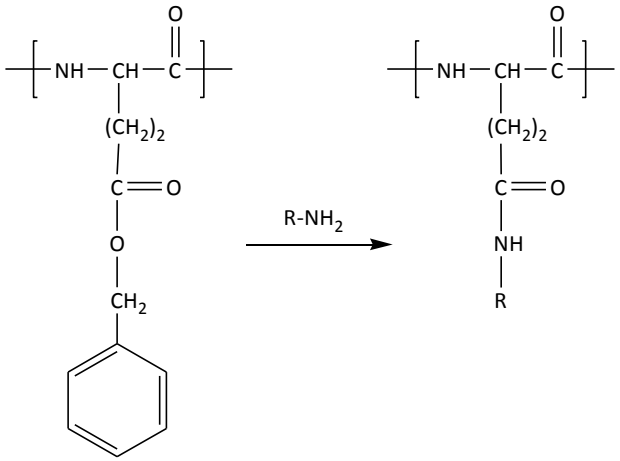


**Figure 1.26 – Synthesis of multifunctional poly-L-glutamine derivatives.**

All chemical structures of the polymers will be verified for the degree of purity and the MM will be regulated by the initiator type and quantity. The properties and behaviour of these polymers in DNA-complexation will be extensively studied using ethidiumbromide fluorescence measurements, agarose gel-electrophoresis tests, zeta(ζ)-potential and dynamic light scattering experiments in order to obtain a more complete insight on the interaction with DNA.

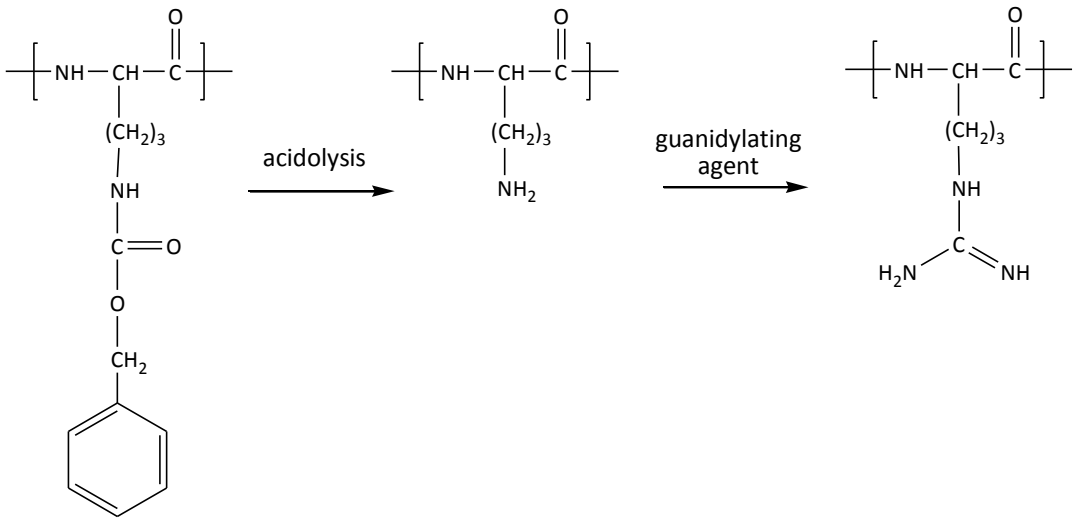


**Figure 1.27 – Synthesis of L-arginine based vectors.**

### 4.3 Development of non-biodegradable, synthetic vectors

Genetic vectors based on non-degradable methacrylates (MA) will be produced by radical polymerisation using thermal initiators (AIBN or APS). Various monomers, both commercially available, as well as modified compounds, will be combined to yield multifunctional polymers with various MM. Certain monomers require protective groups before polymerisation can occur. Hence, additional protection and deprotection steps will be required. The polymer composition and MM will be validated and the physico-chemical properties of the polymers related to DNA interaction will be assessed using analogue methods as before mentioned.

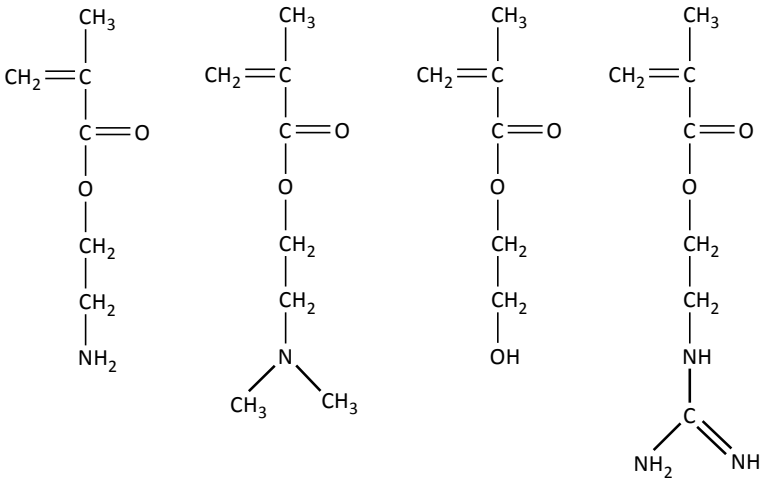

**Figure 1.27 – Monomers for non-biodegradable vectors (AEMA, DMAEMA, HEMA, GuAEMA).**

## 4.4 Biological evaluation of multifunctional vectors

The final step in the development of suitable synthetic vectors includes the investigation of the biocompatibility and the efficiency of delivering DNA, including transfection of the cell. From a range of synthetic vectors of which the physico-chemical properties were screened, candidates that show the most promising results will be selected to undergo different biological tests. In a first test, the ability to protect its DNA cargo from degradable enzymes, will be tested using a model nuclease (DNAse I). The interaction of the polymer and polyplex with blood can be derived from haemolysis and haemo-agglutination studies using human erythrocytes. In the case of biodegradable polymers, their property to degrade inside the body can be tested using protease like enzymes (papaine). Furthermore, polyplexes will be subjected to cytotoxicity tests. More importantly, the efficiency to transfect cells will be tested using a RucHA model plasmid (Renilla Luciferase coding for green fluorescent protein, GFP) on COS and ARPE19 cells[335,336].

## 4.5 Optimisation of vectors by the incorporation of cell-penetrating peptides

Given the added value of incorporating CPP's into a delivery system in terms of enhanced cell-internalisation, synthetic vectors are expected to show an increased transfection efficiency when combined with a CPP (penetratin or octa-arginine). Therefore, certain polymers will be covalently coupled to CPP's. Additionally, modified CPP's with variable spacer lengths and composition will be tested. Finally, CPP's will be physically combined with polyplexes by mixing them in an attempt to compare the influence of CPP and polyplex formulations. These optimised compounds are also examined on both their physico-chemical and biological properties. Mechanistic studies on the preferred internalisation route will be established for a selection of relevant polyplexes by providing the polymers with fluorescent tags to enable detailed investigation by confocal microscopy.

# 5 References


[1] Tatum, E.L., (1966). “Molecular biology nucleic acids and future of medicine”. Perspectives in Biology and Medicine **10**(1): p. 19.

[2] Anderson, W.F., (1992) “Human Gene Therapy”. Science. **256**(5058): p. 808-813.

[3] Schatzlein, A., (2009). “Delivering on a promise? Synthetic vectors for the genetic therapy of cancer”. Journal of Pharmacy and Pharmacology, **61**: p. 233.

[4] Bainbridge, J.W.B., et al., (2008). “Effect of gene therapy on visual function in Leber's congenital amaurosis.” New England Journal of Medicine, **358**(21): p. 2231-2239.

[5] Hendricks, J.L., et al., (2008). “Localized cell and drug delivery for auditory prostheses”. Hearing Research, **242**(1-2): p. 117-131

[6] Wiethoff, C.M. and C.R. Middaugh, (2002). “Barriers to nonviral gene delivery”. Journal of Pharmaceutical Sciences. **92**: p. 203-217

[7] Bleiziffer, et al., (2007). “Gene transfer strategies in tissue engineering”. Journal of cellular and molecular medicine, **11**(2): p. 206-223

[8] Velu, T., V. Cool, and D. Spindler, (1996). “Centers for producing gene therapy reagents: Belgium, in Eurocancer 96” , Proceedings of the Ninth Congress p. 71-72

[9] Alton, E., et al., (1992) “New treatments for cystic fibrosis”. British Medical Bulletin, **48**(4): p. 785-804.

[10] http://www.genetherapynet.com/clinical-trials.html

[11] Boulikas, T., (1996). “Gene therapy to human diseases: Ex vivo and in vivo studies (Review)”. International Journal of Oncology, **9**(6): p. 1239-1251.

[12] Cao, S., A. Cripps, and M.Q. Wei, (2010). “New strategies for cancer gene therapy: Progress and Opportunities”. Clinical and Experimental Pharmacology and Physiology, **37**: p. 108-114.

[13] Roth, J.A., (1996). “Retrovirus-mediated p53 gene therapy – Reply”. Nature Medicine, **2**(11): p. 1163-1163.

[14] Poppe, B., (2009). “Human genetics and genetic diseases”. Course book

[15] Ram, Z., et al., (1997). “Therapy of malignant brain tumors by intratumoral implantation of retroviral vector-producing cell”. Nature Medicine, **3**(12): p. 1354-1361

[16] Niu, G. and X. Chen (2007). "Vascular Endothelial Growth Factor as an Anti-Angiogenic Target for Cancer Therapy." Current Drug Targets **11**(8): 1000-1017

[17] Gardlik, R., M. Behuliak, et al. (2008). "Gene therapy for cancer: bacteria-mediated anti-angiogenesis therapy." Gene Ther **18**(5): 425-431.

[18] Wolkowicz, R. and G. P. Nolan (2005). "Gene therapy progress and prospects: Novel gene therapy approaches for AIDS." Gene Ther **12**(6): 467-476.

[19] Riddell, S.R., et al., (1992) “Phase I Study of Cellular Adoptive Immunotherapy Using Genetically Modified CD8+ HIV-Specific T Cells for HIV Seropositive Patients Undergoing Allogeneic Bone Marrow Transplant. Fred Hutchinson Cancer Research Center and the University of Washington”. Human Gene Therapy, **3**(3): p. 319-338.

[20] Symonds, G., H. Johnstone, et al (2010). "The use of cell-delivered gene therapy for the treatment of HIV/AIDS." Immunologic Research **48**(1): 84-98

[21] Jayakumar, R., K. P. Chennazhi, et al (2009). "Chitosan conjugated DNA nanoparticles in gene therapy." Carbohydrate Polymers **79**(1): 1-8.

[22] Mitsuyasu, R. T., J. A. Zack, et al. (2011). "Phase I/II Clinical Trials Using Gene-Modified Adult Hematopoietic Stem Cells for HIV: Lessons Learnt.", Stem Cells International

[23] Mitsuyasu, R. T., T. C. Merigan, et al. (2009). "Phase 2 gene therapy trial of an anti-HIV ribozyme in autologous CD34+ cells." Nat Med **15**(3): 285-292

[24] Kitchen, S. G., S. Shimizu, et al. (2011) "Stem cell-based anti-HIV gene therapy." Virology **411**(2): 260-272.

[25] Sheridan, C. (2011). "Gene therapy finds its niche." Nat Biotech **29**(2): 121-128.

[26] Park, J., et al.,(2008), "Bone regeneration in critical size defects by cell-mediated BMP-2 gene transfer: a comparison of adenoviral vectors and liposomes". Gene Ther. **10**(13): p. 1089-1098

[27] Chetverin, A. B. and A. S. Spirin (1995). "Replicable RNA vectors – propstects for cell-free gene amplification expression and cloning." Progress in Nucleic Acid Research and Molecular Biology, Vol 51 **51**: 225-270.

[28] Eekels, J. J. M., B. Berkhout, et al (2011). "Toward a Durable Treatment of HIV-1 Infection Using RNA Interference". Progress in Molecular Biology and Translational Science, **102:** 141-163.

[29] Thiel, V., N. Karl, et al. (2003). "Multigene RNA Vector Based on Coronavirus Transcription." Journal of Virology **77**(18): 9790-9798

[30] Schambach, A. and C. Baum (2008). "Clinical Application of Lentiviral Vectors -- Concepts and Practice". Current gene therapy, Bentham Science Publishers Ltd. **8:** 474-482.

[31] Vaishnaw, A. et al. *(*2010). "A status report on RNAi therapeutics". Silence **1**:14

[32] van Lunzen, J., B. Fehse, et al. (2010). "Gene Therapy Strategies: Can We Eradicate HIV?" Current HIV/AIDS Reports **8**(2): 78-84.

[33] Williams, P. D., P. Ranjzad, et al. "Development of Viral Vectors for Use in Cardiovascular Gene Therapy." Viruses-Basel **2**(2): 334-371.

[34] Kutzler, M. A. and D. B. Weiner (2008). "DNA vaccines: ready for prime time?" Nat Rev Genet **9**(10): 776-788.

[35] Pathak, A., S. Patnaik, et al. (2009). "Recent trends in non-viral vector-mediated gene delivery." Biotechnology Journal **4**(11): 1559-1572.

[36] http://www.wiley.com//legacy/wileychi/genmed/clinical/

[37] Li, S. and Z. Ma, (2001) "Nonviral gene therapy", Current gene therapy, **1**: p. 201-226

[38] Dupuis, M., K. Denis-Mize, et al. (2000). "Distribution of DNA Vaccines Determines Their Immunogenicity After Intramuscular Injection in Mice." The Journal of Immunology **165**(5): 2850-2858.

[39] Fynan, E. F., R. G. Webster, et al. (1993). "DNA vaccines: protective immunizations by parenteral, mucosal, and gene-gun inoculations." Proceedings of the National Academy of Sciences **90**(24): 11478-11482.

[40] Ledley, F. D. (1996). "Pharmaceutical Approach to Somatic Gene Therapy." Pharmaceutical Research **13**(11): 1595-1614.

[41] Mahato, R. I., L. C. Smith, et al. (1999). "4 Pharmaceutical Perspectives of Nonviral Gene Therapy". Advances in Genetics, Academic Press. **Volume 41:** 95-156.

[42] Lewis, D. L., J. A. Wolff, et al. (2005). "Delivery of siRNA and siRNA Expression Constructs to Adult Mammals by Hydrodynamic Intravascular Injection". Methods in Enzymology, Academic Press. **Volume 392:** 336-350.

[43] Herweijer, H. and J. A. Wolff (2007) "Progress and prospects: naked DNA gene transfer and therapy." Gene Ther **10**(6): 453-458.

[44] Guofeng Zhang, Vladimir Budker, and Jon A. Wolff. Human Gene Therapy. July 1999, 10(10): 1735-1737

[45] Fath, A., P. C. Bethke, et al. (1999). "Barley aleurone cell death is not apoptotic: characterization of nuclease activities and DNA degradation." The Plant Journal **20**(3): 305-315.

[46] Janes, K. A., P. Calvo, et al. (2001). "Polysaccharide colloidal particles as delivery systems for macromolecules." Advanced Drug Delivery Reviews **47**(1): 83-97.

[47] Lewis, D. L. and J. A. Wolff (2007). "Systemic siRNA delivery via hydrodynamic intravascular injection." Advanced Drug Delivery Reviews **59**(23): 115-123.

[48] Andre, F. M., C. Cournil-Henrionnet, et al. (2006). "Variability of naked DNA expression after direct local injection: the influence of the injection speed." Gene Therapy **13**(23): 1619-1627.

[49] Kim, B., S. Lee, et al. (2005). "Application of Plasmid DNA Encoding IL-18 Diminishes Development of Herpetic Stromal Keratitis by Antiangiogenic Effects." The Journal of Immunology **175**(1): 509-516.

[50] Galiacy, S. D., P. Fournie, et al. "Matrix metalloproteinase 14 overexpression reduces corneal scarring." Gene Ther **18**(5): 462-468.

[51] Zhou, R. and D. A. Dean (2007). "Gene Transfer of Interleukin 10 to the Murine Cornea Using Electroporation." Experimental Biology and Medicine **232**(3): 362-369.

[52] http://lifesciences.sourcebioscience.com/applications/additional-content/transfection/saint-18.aspx

[53] Wolff, J. A., V. Budker, et al. (2005). The Mechanism of Naked DNA Uptake and Expression. Advances in Genetics, Academic Press. **Volume 54:** 1-20.

[54] Fensterle, J., L. Grode, et al. (1999). "Effective DNA Vaccination Against Listeriosis by Prime/Boost Inoculation with the Gene Gun." The Journal of Immunology **163**(8): 4510-4518.

[55] Geerts, N. and E. Eiser, (2008) "DNA-functionalized colloids: Physical properties and applications". Soft Matter. **6**(19): p. 4647-4660.

[56] Hao, J., S. K. Li, et al. (2010). "Gene delivery to cornea." Brain Research Bulletin **81**(23): 256-261.

[57] Bauer, D., M. Lu, et al. (2006). "Immunomodulation by topical particle-mediated administration of cytokine plasmid DNA suppresses herpetic stromal keratitis without impairment of antiviral defense." Graefe's Archive for Clinical and Experimental Ophthalmology **244**(2): 216-225.

[58] Zagon, I. S., J. W. Sassani, et al. (2006). "Regulation of Corneal Repair by Particle-Mediated Gene Transfer of Opioid Growth Factor Receptor Complementary DNA." Arch Ophthalmol **124**(11): 1620-1624.

[59] Aihara, H. and J.-i. Miyazaki (1998). "Gene transfer into muscle by electroporation in vivo." Nat Biotech **16**(9): 867-870.

[60] Golzio, M., M. P. Rols, et al. (2004). "In vitro and in vivo electric field-mediated permeabilization, gene transfer, and expression." Methods **33**(2): 126-135.

[61] Sun, X.-D. and L. I.-S. (2006). "Gene technology in tissue engineering." American Journal of Biochemistry and Biotechnology **2**: 66-72.

[62] Makrides, S. C. (2003). "Gene transfer and expression in mammalian cells." New Comprehensive Biochemistry - Elsevier **38**: 265-277.

[63] Rizzuto, G., M. Cappelletti, et al. (1999). "Efficient and regulated erythropoietin production by naked DNA injection and muscle electroporation." Proceedings of the National Academy of Sciences **96**(11): 6417-6422.

[64] Schellekens, H., P. H. van Bragt, et al. (2001). "Medische biotechnologie." Elsevier: 409-413.

[65] Williams, K. A. and D. J. Coster (2009) "Gene therapy for diseases of the cornea – a review." Clinical & Experimental Ophthalmology **38**(2): 93-103.

[66] He, Z., A. Pipparelli, et al. (2009). "Ex vivo Gene Electrotransfer to the Endothelium of Organ Cultured Human Corneas." Ophthalmic Research **43**(1): 43-55.

[67] Taniyama, Y., K. Tachibana, et al. (2002). "Development of safe and efficient novel nonviral gene transfer using ultrasound: enhancement of transfection efficiency of naked plasmid DNA in skeletal muscle." Gene Therapy **9**(6): 372-80.

[68] Wells, D. (2009) "Electroporation and ultrasound enhanced non-viral gene delivery in vitro and in vivo." Cell Biology and Toxicology **26**(1): 21-28.

[69] Gao, X., K.-S. Kim, et al. (2007). "Nonviral gene delivery: what we know and what is next." American Association of Pharmaceutical Scientists **9**: E92-E104.

[70] Yamamoto, M. and Y. Tabata (2006). "Tissue engineering by modulated gene delivery." Advanced Drug Delivery Reviews **58**: 535-554.

[71] Alter, J., C. A. Sennoga, et al. (2009). "Microbubble Stability is a Major Determinant of the Efficiency of Ultrasound and Microbubble Mediated in vivo Gene Transfer." Ultrasound in Medicine & Biology **35**(6): 976-984.

[72] Chen, K.-H., C.-H. Wu, et al. (2008). "Intrathecal coelectrotransfer of a tetracycline-inducible, three-plasmid-based system to achieve tightly regulated antinociceptive gene therapy for mononeuropathic rats." The Journal of Gene Medicine **10**(2): 208-216.

[73] Nie, F., H.-X. Xu, et al. (2008). "Anti-angiogenic gene therapy for hepatocellular carcinoma mediated by microbubble-enhanced ultrasound exposure: An in vivo experimental study." Journal of Drug Targeting **16**(5): 389-395.

[74] Li, D., P. Li, et al. (2009). "The effect of nocodazole on the transfection efficiency of lipid-bilayer coated gold nanoparticles." Biomaterials **30**(7): 1382-1388.

[75] Li, H. L., X. Z. Zheng, et al. (2009). "Ultrasound-targeted microbubble destruction enhances AAV-mediated gene transfection in human RPE cells in vitro and rat retina in vivo." Gene Ther **16**(9): 1146-1153.

[76] Jang, J.-H., T. L. Houchin, et al. (2004). "Gene delivery from polymer scaffolds for tissue engineering." Expert Review of Medical devices **1**(1): 127-136.

[77] Stride, E., C. Porter, et al. (2009). "Enhancement of Microbubble Mediated Gene Delivery by Simultaneous Exposure to Ultrasonic and Magnetic Fields." Ultrasound in Medicine & Biology **35**(5): 861-868.

[78] Bronzino, J. D. (2006). "Tissue engineering and artificial organs." CRC press Taylor and Francis Ed. 3: 43/1-43/15.

[79] Thomas, C. E., A. Ehrhardt, et al. (2003). "Progress and problems with the use of viral vectors for gene therapy." Nature **4**: 346-358.

[80] Schellekens, H. et al. (2001) “Medische biotechnologie.” Elsevier: 409-413

[81] Mittereder, N., K. L. March, et al. (1996). "Evaluation of the concentration and bioactivity of adenovirus vectors for gene therapy." Journal of Virology **70**(11): 7498-509.

[82] Okegawa, T., Y. Li, et al. (2000). "The Dual Impact of Coxsackie and Adenovirus Receptor Expression on Human Prostate Cancer Gene Therapy." Cancer Research **60**(18): 5031-5036.

[83] Wang, C. and P.-T. Pham (2008). "Polymers for viral gene delivery." Expert Opinion on Drug Delivery **5**: 386-401.

[84] Emery, D. W. (2004). "Gene therapy for genetic diseases: on the horizon." Clinical and Applied Immunology Reviews **4**: 411-422.

[85] Mhashilkar, A., S. Chada, et al. (2001). "Gene therapy: Therapeutic approaches and implications." Biotechnology Advances **19**(4): 279-297.

[86] Hermens, W. and J. Verhaagen (1998). "Viral vectors, tools for gene transfer in the nervous system." Progress in Neurobiology **55**(4): 399-432.

[87] http://blog.bioethics.net/2008/01/on-gene-therapy-and-informed-consent/#comments

[88] Alba, R., A. Bosch, et al. (2009), "Gutless adenovirus: last-generation adenovirus for gene therapy." Gene Ther **12**(S1): S18-S27

[89] Kang, E.A. (2010). “Mini Review : Current advances in adenovirus nanocomplexes: more specificity and Less immunogenicity.” Biochemistry and Molecurar Biology Reports 43(12): 781-788

[90] Asokan, A., J. C. Conway, et al. (2009) "Reengineering a receptor footprint of adeno-associated virus enables selective and systemic gene transfer to muscle." Nat Biotech **28**(1): 79-82.

[91] Van Tendeloo, V. F. I., C. Van Broeckhoven, et al. (2001). "Gene therapy: principles and applications to hematopoietic cells." Leukemia **15**(4): 523-544.

[92] Aalbers, C., Tak, P., et al. (2011). "Advancements in adeno-associated viral gene therapy approaches: exploring a new horizon". F1000 Med Reports2011, **3**:17

[93] Stroes, E. S., M. C. Nierman, et al. (2008). "Intramuscular Administration of AAV1-Lipoprotein Lipase(S447X) Lowers Triglycerides in Lipoprotein Lipase-Deficient Patients." Arteriosclerosis Thrombosis and Vascular Biology **28**(12): 2303-U264.

[94] DiPrimio, N., S. W. J. McPhee, et al. (2010) "Adeno-associated virus for the treatment of muscle diseases: Toward clinical trials." Current Opinion in Molecular Therapeutics **12**(5): 553-560.

[95] Mease, P. J., N. Wei, et al. (2008), "Safety, Tolerability, and Clinical Outcomes after Intraarticular Injection of a Recombinant Adeno-associated Vector Containing a Tumor Necrosis Factor Antagonist Gene: Results of a Phase 1/2 Study." Journal of Rheumatology **37**(4): 692-703.

[96] Surace, E. M. and A. Auricchio (2008). "Versatility of AAV vectors for retinal gene transfer." Vision Research **48**(3): 353-359.

[97] Maguire, A. M., K. A. High, et al. (2009). "Age-dependent effects of RPE65 gene therapy for Leber's congenital amaurosis: a phase 1 dose-escalation trial." The Lancet **374**(9701): 1597-1605.

[98] El-Aneed, A. (2004). "An overview of current delivery systems in cancer gene therapy." Journal of Controlled Release **94**(1): 1-14.

[99] Palù, G., C. Parolin, et al. (2000). "Progress with retroviral gene vectors." Reviews in Medical Virology **10**: 185-202.

[100] De Laporte, L. and L. D. Shea (2007). "Matrices and scaffolds for DNA delivery in tissue engineering." Advanced Drug Delivery Reviews **59**: 292-307.

[101] Escors, D. and K. Breckpot, (2006), "Lentiviral Vectors in Gene Therapy: Their Current Status and Future Potential." Archivum Immunologiae et Therapiae Experimentalis **58**(2): 107-119.

[102] Corey, L., G. J. Nabel, et al. (2010). "HIV-1 Vaccines and Adaptive Trial Designs." Science Translational Medicine **3**(79): 79ps13.

[103] Levine, B. L., L. M. Humeau, et al. (2006). "Gene transfer in humans using a conditionally replicating lentiviral vector." Proceedings of the National Academy of Sciences of the United States of America **103**(46): 17372-17377.

[104] Lewis, T. B. and D. G. Standaert (2008). "Design of clinical trials of gene therapy in Parkinson disease." Experimental Neurology **209**(1): 41-47.

[105] Coccoris, M., T. Straetemans, et al. (2010). "T cell receptor (TCR) gene therapy to treat melanoma: lessons from clinical and preclinical studies." Expert Opinion on Biological Therapy **10**(4): 547-562.

[106] Liu, M. M., J. Tuo, et al. (2010). "Gene therapy for ocular diseases." British Journal of Ophthalmology **95**(5): 604-612.

[107] Bemelmans, A. P., Y. Arsenijevic, et al. (2009). "Efficient lentiviral gene transfer into corneal stroma cells using a femtosecond laser." Gene Ther **16**(7): 933-938.

[108] Kaufman, H. L. and S. D. Bines. (2010). "OPTIM trial: a Phase III trial of an oncolytic herpes virus encoding GM-CSF for unresectable stage III or IV melanoma." Future Oncology **6**(6): 941-949.

[109] Sangro, B., G. Mazzolini, et al. (2010). "A phase I clinical trial of thymidine kinase-based gene therapy in advanced hepatocellular carcinoma." Cancer Gene Ther **17**(12): 837-843.

[110] Manservigi, R., Argnani, R., et. al. (2010). “HSV Recombinant Vectors for Gene Therapy.” Open Virology Journal; **4**: 123–156

[111] Behr, J. P. (1997). "The proton sponge: a trick to enter cells the viruses did not exploit." Chimia **51**: 34-36.

[112] Lin, C. and J. F. J. Engbersen (2008). "Effect of chemical functionalities in poly(amido amine)s for non-viral gene transfection." Journal of Controlled Release **132**: 267-272.

[113] Brown, M. D., A. G. Schätzlein, et al. (2001). "Gene delivery with synthetic (non viral) carriers." International Journal of Pharmaceutics **229**: 1-21.

[114] Toyoda, K., H. Ooboshi, et al. (1998). "Cationic polymer and lipids enhance adenovirus-mediated gene transfer to rabbit carotid artery." Stroke **29**(10): 2181-2187.

[115] http://www.informahealthcare.com

[116] Graham, F. L. and A. J. Van der Eb (1973). "A new technique for the assay of infectivity of adenovirus 5 DNA." Virology **52**: 456-467.

[117] Epple, M., K. Ganesan, et al.(2008), "Application of calcium phosphate nanoparticles in biomedicine." Journal of Materials Chemistry **20**(1): 18-23.

[118] Roy, I., S. Mitra, et al. (2003). "Calcium phosphate nanoparticles as novel non-viral vectors for targeted gene delivery." International Journal of Pharmaceutics **250**(1): 25-33.

[119] Wu, H. C. and F. H. Lin, (2007) "Evaluation of magnetic-hydroxyapatite nanoparticles for gene delivery carrier." Biomedical Engineering-Applications Basis Communications **22**(1): 33-39.

[120] Mahmoudi, M., A. Simchi, et al (2006). "Recent Advances in Surface Engineering of Superparamagnetic Iron Oxide Nanoparticles for Biomedical Applications." Journal of the Iranian Chemical Society **7**: S1-S27.

[121] Figuerola, A., R. Di Corato, et al. (2009) "From iron oxide nanoparticles towards advanced iron-based inorganic materials designed for biomedical applications." Pharmacological Research **62**(2): 126-143.

[122] Mahmoudi, M., H. Hosseinkhani, et al. (2011). "Magnetic Resonance Imaging Tracking of Stem Cells in Vivo Using Iron Oxide Nanoparticles as a Tool for the Advancement of Clinical Regenerative Medicine." Chemical Reviews **111**(2): 253-280.

[123] Ladewig, K., M. Niebert, et al. (2009), "Efficient siRNA delivery to mammalian cells using layered double hydroxide nanoparticles." Biomaterials **31**(7): 1821-1829.

[124] Vallet-Regi, M., M. Colilla, et al. (2010), "Medical applications of organic-inorganic hybrid materials within the field of silica-based bioceramics." Chemical Society Reviews **40**(2).

[125] Krebs, M. D., E. Salter, et al. (2009), "Calcium phosphate-DNA nanoparticle gene delivery from alginate hydrogels induces in vivo osteogenesis." Journal of Biomedical Materials Research Part A **92A**(3): 1131-1138.

[126] Zhang, S., Y. Zhao, et al. (2011). "Non-viral vectors for the mediation of RNAi." Bioorganic Chemistry **40**(0): 10-18.

[127] Giljohann, D. A., D. S. Seferos, et al. (2009). "Gene Regulation with Polyvalent siRNAâˆ'Nanoparticle Conjugates." Journal of the American Chemical Society **131**(6): 2072-2073.

[128] Felgner, P. L., T. R. Gadek, et al. (1987). "Lipofection – a highly efficient lipid-mediated DNA-transfection procedure." Proceedings of the National Academy of Sciences of the United States of America **84**(21): 7413-7417.

[129] Zhdanov, R. I., O. V. Podobed, et al. (2002). "Cationic lipid-DNA complexes-lipoplexes-for gene transfer and therapy." Bioelectrochemistry **58**: 53-64.

[130] Giordano, C., F. Causa, et al. (2006). "Gene therapy: The state of the art and future directions." Journal of applied Biomaterials & Biomechanics **4**(2): 73-79.

[131] Lechardeur, D., A. S. Verkman, et al. (2005). "Intracellular routing of plasmid DNA during non-viral gene transfer." Advanced Drug Delivery Reviews **57**: 755-767.

[132] Zabner, J., A. J. Fasbender, et al. (1995). "Cellular and molecular barriers to gene transfer by a cationic lipid." Journal of Biological Chemistry **270**(32): 18997-19007.

[133] Kamiya, H., H. Tsuchiya, et al. (2001). "Intracellular trafficking and transgene expression of viral and non-viral gene vectors." Advanced Drug Delivery Reviews **52**: 153-164.

[134] Hyde, S. C., K. W. Southern, et al. (2000). "Repeat administration of DNA/liposomes to the nasal epithelium of patients with cystic fibrosis." Gene Therapy **7**(13): 1156-1165.

[135] Tros de Ilarduya, C., Y. Sun, et al. (2009) "Gene delivery by lipoplexes and polyplexes." European Journal of Pharmaceutical Sciences **40**(3): 159-170.

[136] SchÃfer, J., S. HÃbel, et al, (2010), "Liposome-polyethylenimine complexes for enhanced DNA and siRNA delivery." Biomaterials **31**(26): 6892-6900.

[137] Toropainen, E., M. Hornof, et al. (2007). "Corneal epithelium as a platform for secretion of transgene products after transfection with liposomal gene eyedrops." The Journal of Gene Medicine **9**(3): 208-216.

[138] Huang, Y.-H., Y. Bao, et al. (2009). "Claudin-3 gene silencing with siRNA suppresses ovarian tumor growth and metastasis." Proceedings of the National Academy of Sciences **106**(9): 3426-3430.

[139] Love, K. T., K. P. Mahon, et al. (2010), "Lipid-like materials for low-dose, in vivo gene silencing." Proceedings of the National Academy of Sciences **107**(5): 1864-1869.

[140] Green, M. and P. M. Loewenstein (1988). "AUTONOMOUS FUNCTIONAL DOMAINS OF CHEMICALLY SYNTHESIZED HUMAN IMMUNODEFICIENCY VIRUS TAT TRANS-ACTIVATOR PROTEIN." Cell **55**(6): 1179-1188.

[141] Derossi, D., A. H. Joliot, et al. (1994). "THE 3RD HELIX OF THE ANTENNAPEDIA HOMEODOMAIN TRANSLOCATES THROUGH BIOLOGICAL-MEMBRANES." Journal of Biological Chemistry **269**(14): 10444-10450.

[142] Oehlke, J., E. Krause, et al. (1997). "Extensive cellular-uptake into endothelial cells of an amphipathic beta-sheet forming peptide." Febs Letters **415**(2): 196-199.

[143] Lundberg, P. and U. Langel (2003). "A brief introduction to cell-penetrating peptides." Journal of Molecular Recognition **16**(5): 227-233.

[144] Vives, E., P. Brodin, et al. (1997). "A truncated HIV-1 Tat protein basic domain rapidly translocates through the plasma membrane and accumulates in the cell nucleus." Journal of Biological Chemistry **272**(25): 16010-16017.

[145] Kerkis, A., M. A. F. Hayashi, et al. (2006). "Properties of cell penetrating peptides (CPPs)." Iubmb Life **58**(1): 7-13.

[146] Joliot, A. and A. Prochiantz (2004). "Transduction peptides: from technology to physiology." Nat Cell Biol **6**(3): 189-196.

[147] Scheller, A., J. Oehlke, et al. (1999). "Structural requirements for cellular uptake of alpha-helical amphipathic peptides." Journal of Peptide Science **5**(4): 185-194.

[148] Mae, M., S. El Andaloussi, et al. (2009). "Chemically modified cell-penetrating peptides for the delivery of nucleic acids." Expert Opinion on Drug Delivery **6**(11): 1195-1205.

[149] Duchardt, F., M. Fotin-Mleczek, et al. (2007). "A comprehensive model for the cellular uptake of cationic cell-penetrating peptides." Traffic **8**(7): 848-866.

[150] Johnson, L. N., S. M. Cashman, et al. (2008). "Cell-penetrating peptide for enhanced delivery of nucleic acids and drugs to ocular tissues including retina and cornea." Molecular Therapy **16**(1): 107-114.

[151] Martin, I. M., M. Teixido, et al. (2011), "Towards a new anionic Cell-Penetrating Peptide: SAP(E)." Journal of Peptide Science **16**: 147-148.

[152] Patel, L. N., J. L. Zaro, et al. (2007). "Cell penetrating peptides: Intracellular pathways and pharmaceutical perspectives." Pharmaceutical Research **24**(11): 1977-1992.

[153] JÃrver, P., I. MÃger, et al. (2010). "In vivo biodistribution and efficacy of peptide mediated delivery." Trends in Pharmacological Sciences **31**(11): 528-535.

[154] Martín, I.; Teixidó, M.; Giralt, E. (2010), "Building Cell Selectivity into CPP-Mediated Strategies". Pharmaceuticals **3,** 1456-1490

[155] Kubas, H., M. SchÃ¤fer, et al. (2010). "Multivalent cyclic RGD ligands: influence of linker lengths on receptor binding." Nuclear medicine and biology **37**(8): 885-891.

[156] Dijkgraaf, I., J. A. W. Kruijtzer, et al. (2007). "Improved targeting of the alpha(v)beta(3) integrin by multimerisation of RGD peptides." European Journal of Nuclear Medicine and Molecular Imaging **34**(2): 267-273.

[157] Dal Pozzo, A., M.-H. Ni, et al. (2010). "Novel tumor-targeted RGD peptideâ€"camptothecin conjugates: Synthesis and biological evaluation." Bioorganic & Medicinal Chemistry **18**(1): 64-72.

[158] Haubner, R., D. Finsinger, et al. (1997). "Stereoisomeric peptide libraries and peptidomimetics for designing selective inhibitors of the alpha(V)beta(3) integrin for a new cancer therapy." Angewandte Chemie-International Edition **36**(13-14): 1375-1389.

[159] Olins, D. E., A. L. Olins, et al. (1967). "MODEL NUCLEOPROTEIN COMPLEXES - STUDIES ON INTERACTION OF CATIONIC HOMOPOLYPEPTIDES WITH DNA." Journal of Molecular Biology **24**(2): 157-176.

[160] Vonhippe.Ph and J. D. McGhee (1972). "DNA-PROTEIN INTERACTIONS." Annual Review of Biochemistry **41**: 231-300.

[161] Shapiro, J. T., M. Leng, et al. (1969). "DEOXYRIBONUCLEIC ACID-POLYLYSINE COMPLEXES . STRUCTURE AND NUCLEOTIDE SPECIFICITY." Biochemistry **8**(8): 3219-3234.

[162] Vaheri, A. and J. S. Pagano (1965). "INFECTIOUS POLIOVIRUS RNA - A SENSITIVE METHOD OF ASSAY." Virology **27**(3): 434-&.

[163] Kawai, S. and M. Nishizawa (1984). "New procedure for DNA transfection with polycation and dimethyl sulfoxide." Mol. Cell. Biol. **4**(6): 1172-1174.

[164] Erbacher, P., T. Bettinger, et al. (2004). "Genuine DNA/polyethylenimine (PEI) complexes improve transfection properties and cell survival." Journal of Drug Targeting **12**(4): 223-236.

[165] Boussif, O., F. Lezoualch, et al. (1995). "A VERSATILE VECTOR FOR GENE AND OLIGONUCLEOTIDE TRANSFER INTO CELLS IN CULTURE AND IN-VIVO - POLYETHYLENIMINE." Proceedings of the National Academy of Sciences of the United States of America **92**(16): 7297-7301

[166] Zhao, Q.-Q., J.-L. Chen, et al. (2008). "Combination of poly(ethylenimine) and chitosan induces high gene transfection efficiency and low cytotoxicity." Journal of Bioscience and Bioengineering **105**(1): 65-68.

[167] Kichler, A. (2004). "Gene transfer with modified polyethylenimines." The Journal of Gene Medicine **6**(S1): S3-S10.

[168] Sakae, M., T. Ito, et al. (2008). "Highly efficient in vivo gene transfection by plasmid/PEI complexes coated by anionic PEG derivatives bearing carboxyl groups and RGD peptide." Biomedicine & Pharmacotherapy **62**(7): 448-453.

[169] Nagaya, J., M. Homma, et al. (1996). "Relationship between protonation and ion condensation for branched poly(ethylenimine)." Biophysical Chemistry **60**: 45-51.

[170] Koper, G. J. M., R. C. van Duijvenbode, et al. (2003). "Synthesis and protonation behavior of comblike poly(ethyleneimine)." Macromolecules **36**(7): 2500-2507.

[171] Fischer, D., T. Bieber, et al. (1999). "A novel non-viral vector for DNA delivery based on low molecular weight, branched polyethylenimine: Effect of molecular weight on transfection efficiency and cytotoxicity." Pharmaceutical Research **16**(8): 1273-1279.

[172] Thomas, M., Q. Ge, et al. (2005). "Cross-linked small polyethylenimines: While still nontoxic, deliver DNA efficiently to mammalian cells in vitro and in vivo." Pharmaceutical Research **22**(3): 373-380.

[173] Merdan, T., K. Kunath, et al. (2002). "Intracellular processing of poly(ethylene imine)/ribozyme complexes can be observed in living cells by using confocal laser scanning microscopy and inhibitor experiments." Pharmaceutical Research **19**(2): 140-146.

[174] Koyama, Y., T. Ito, et al. (2003). "Novel poly(ethylene glycol) derivatives with carboxylic acid pendant groups: synthesis and their protection and enhancing effect on non-viral gene transfection systems." Journal of Biomaterials Science-Polymer Edition **14**(6): 515-531.

[175] Merdan, T., K. Kunath, et al. (2005). "PEGylation of Poly(ethylene imine) Affects Stability of Complexes with Plasmid DNA under in Vivo Conditions in a Dose-Dependent Manner after Intravenous Injection into Mice." Bioconjugate Chemistry **16**(4): 785-792.

[176] Grosse, S. p., G. ThÃ©venot, et al. (2008). "In vivo gene delivery in the mouse lung with lactosylated polyethylenimine, questioning the relevance of in vitro experiments." Journal of Controlled Release **132**(2): 105-112.

[177] Peeters, L., N. N. Sanders, et al. (2007). "Post-pegylated lipoplexes are promising vehicles for gene delivery in RPE cells." Journal of Controlled Release **121**: 208-217.

[178] Merdan, T., J. Kopecek, et al. (2002). "Prospects for cationic polymers in gene and oligonucleotide therapy against cancer." Advanced Drug Delivery Reviews **54**(5): 715-758.

[179] Forrest, M. L., G. E. Meister, et al. (2004). "Partial acetylation of polyethylenimine enhances in vitro gene delivery." Pharmaceutical Research **21**(2): 365-371.

[180] Iida, T., T. Mori, et al. (2007). "Overall interaction of cytosolic proteins with the PEI/DNA complex." Journal of Controlled Release **118**(3): 364-369.

[181] Hornof, M., M. de la Fuente, et al. (2008). "Low molecular weight hyaluronan shielding of DNA/PEI polyplexes facilitates CD44 receptor mediated uptake in human corneal epithelial cells." The Journal of Gene Medicine **10**(1): 70-80.

[182] Katayose, S. and K. Kataoka (1997). "Water-soluble polyion complex associates of DNA and poly(ethylene glycol)-poly(L-lysine) block copolymer." Bioconjugate Chemistry **8**(5): 702-707.

[183] Xue, W. H., H. J. Diao, et al. (2007). "An efficient vector for gene delivery: alpha,beta-poly(3-dimethylaminopropyl-D,L-aspartamide)." European Journal of Pharmaceutics and Biopharmaceutics **66**(3): 327-333.

[184] Itaka, K., T. Ishii, et al. (2010) "Biodegradable polyamino acid-based polycations as safe and effective gene carrier minimizing cumulative toxicity." Biomaterials **31**(13): 3707-3714.

[185] Dekie, L., V. Toncheva, et al. (2000). "Poly-L-glutamic acid derivatives as vectors for gene therapy." Journal of Controlled Release **65**(1-2): 187-202.

[186] Putnam, D., C. A. Gentry, et al. (2001). "Polymer-based gene delivery with low cytotoxicity by a unique balance of side-chain termini." Proceedings of the National Academy of Sciences of the United States of America **98**(3): 1200-1211.

[187] Toncheva, V., M. A. Wolfert, et al. (1998). "Novel Vectors for gene delivery formed by self-assembly of DNA with poly(L-lysine) grafted with hydrophilic polymers." Biochimica Et Biophysica Acta-General Subjects **1380**(3): 354-368.

[188] Hoste, K. (1999). “studie van poly(ethyleenglycol)-geënte polyglutamines als dragermolecule voor de bereiding van macromoleculaire geneesmiddelderivaten”. Gent, Universiteit Gent.

[189] Chiu, H.-C., P. Kopečková, et al. (1997). "Lysosomal degradability of poly(α-amino acids)." Journal of Biomedical Materials Research **34**(3): 381-392.

[190] Obst, M. and A. Steinbachel (2004). "Microbial Degradation of Poly(amino acid)s." Biomacromolecules **5**(4): 1166-1176.

[191] Ke, W., K. Shao, et al. (2009). "Gene delivery targeted to the brain using an Angiopep-conjugated polyethyleneglycol-modified polyamidoamine dendrimer." Biomaterials **30**(36): 6976-6985.

[192] Mei, M., Y. Ren, et al. (2009). "Suppression of breast cancer cells in vitro by polyamidoamine-dendrimer-mediated 5-fluorouracil chemotherapy combined with antisense micro-RNA 21 gene therapy." Journal of Applied Polymer Science **114**(6): 3760-3766.

[193] Qin, L., *et al.* (1998). “Efficient transfer of genes into murine cardiac grafts by Starburst polyamidoamine dendrimers.” Human Gene Therapy **9:** 553–560.

[194] Yellepeddi, V. K., A. Kumar, et al. (2009). "Surface modified poly(amido)amine dendrimers as diverse nanomolecules for biomedical applications." Expert Opinion on Drug Delivery **6**(8): 835-850.

[195] Li, W., F. o. Nicol, et al. (2004). "GALA: a designed synthetic pH-responsive amphipathic peptide with applications in drug and gene delivery." Advanced Drug Delivery Reviews **56**(7): 967-985.

[196] Tiera, M. J., F. M. Winnik, et al. (2006). "Synthetic and natural polycations for gene therapy: State of the art and new perspectives." Current Gene Therapy **6**(1): 59-71.

[197] Lin, C. and J. F. J. Engbersen (2009). "The role of the disulfide group in disulfide-based polymeric gene carriers." Expert Opinion on Drug Delivery **6**(4): 421-439.

[198] Nam, H. Y., H. J. Hahn, et al. (2008). "Evaluation of generations 2, 3 and 4 arginine modified PAMAM dendrimers for gene delivery." International Journal of Pharmaceutics **363**(1-2): 199-205.

[199] Choi, J. S., K. Nam, et al. (2004). "Enhanced transfection efficiency of PAMAM dendrimer by surface modification with l-arginine." Journal of Controlled Release **99**(3): 445-456.

[200] Guohong Xin, Xinhan Zhao, et al. (2012). “Antitumor Effect of a Generation 4 Polyamidoamine Dendrimer/Cyclooxygenase-2 Antisense Oligodeoxynucleotide Complex on Breast Cancer *In Vitro* and *In Vivo* .“ Cancer Biotherapy & Radiopharmaceuticals **27**(1): 77-87.

[201] Dubruel, P. and E. Schacht (2006). "Vinyl polymers as non-viral gene delivery carriers: Current status and prospects." Macromolecular Bioscience **6**(10): 789-810.

[202] Wong, S. Y., J. M. Pelet, et al. (2007). "Polymer systems for gene delivery-Past, present, and future." Progress in Polymer Science **32**: 799-837.

[203] Liu, Z., Z. Zhang, et al. (2010), "Hydrophobic modifications of cationic polymers for gene delivery." Progress in Polymer Science **35**(9): 1144-1162.

[204] van de Wetering, P., J.-Y. Cherng, et al. (1998). "2-(dimethylamino)ethyl methacrylate based (co)polymers as gene transfer agents." Journal of Controlled Release **53**: 145-153.

[205] Cherng, J. Y., P. vandeWetering, et al. (1996). "Effect of size and serum proteins on transfection efficiency of poly((2-dimethylamino)ethyl methacrylate)-plasmid nanoparticles." Pharmaceutical Research **13**(7): 1038-1042.

[206] Dubruel, P. and E. H. Schacht (2000). "Effect of polyethylene oxide blocks or grafts on the physicochemical properties of poly(2-N-(dimethylaminoethyl) methacrylate) DNA complexes." Journal of Bioactive and Compatible Polymers **15**(4): 279-296.

[207] Verbaan, F. J., G. W. Bos, et al. (2004). "A comparative study of different cationic transfection agents for in vivo gene delivery after intravenous administration." Journal of Drug Delivery Science and Technology **14**(2): 105-111.

[208] Zhu, C., S. Jung, et al. (2010), "Co-delivery of siRNA and paclitaxel into cancer cells by biodegradable cationic micelles based on PDMAEMA-PCL-PDMAEMA triblock copolymers." Biomaterials **31**(8): 2408-2416.

[209] Zhu, C., S. Jung, et al. "Reduction-responsive cationic biodegradable micelles based on PDMAEMA-SS-PCL-SS-PDMAEMA triblock copolymers for gene delivery." Journal of Controlled Release **152, Supplement 1**(0): e188-e190.

[210] Convertine, A. J., D. S. W. Benoit, et al. (2009). "Development of a novel endosomolytic diblock copolymer for siRNA delivery." Journal of Controlled Release **133**(3): 221-229.

[211] Manganiello, M. J., C. Cheng, et al. "Diblock copolymers with tunable pH transitions for gene delivery." Biomaterials **33**(7): 2301-2309.

[212] van Steenis, J. H., E. M. van Maarseveen, et al. (2003). "Preparation and characterization of folate-targeted pEG-coated pDMAEMA-based polyplexes." Journal of Controlled Release **87**(13): 167-176.

[213] Hinrichs, W. L. J., N. M. E. Schuurmans-Nieuwenbroek, et al. (1999). "Thermosensitive polymers as carriers for DNA delivery." Journal of Controlled Release **60**(2â€“3): 249-259.

[214] Dubruel, P., V. Toncheva, et al. (2000). "pH sensitive vinyl copolymers as vectors for gene therapy." Journal of Bioactive and Compatible Polymers **15**(3): 191-213.

[215] Vuillaume, P. Y., M. Brunelle, et al. (2009). "Tail-end amphiphilic dimethylaminopyridinium-containing polymethacrylates for gene delivery." New Journal of Chemistry **33**(9).

[216] Kabanov, A. V. and S. V. Vinogradov (2009). "Nanogels as Pharmaceutical Carriers: Finite Networks of Infinite Capabilities." Angewandte Chemie International Edition **48**(30): 5418-5429.

[217] Lin, S. et al. (2011). "A pH Responsive Ternary **Gene** Carrier based on Branched-Poly(ethylenimine) and Poly(2-ethyl-2-oxazoline)-block- Poly(methacrylic acid)." J Biotechnol Biomaterial **1**:4.

[218] Yang, X., J. J. Grailer, et al. (2010). "Tumor-Targeting, pH-Responsive, and Stable Unimolecular Micelles as Drug Nanocarriers for Targeted Cancer Therapy." Bioconjugate Chemistry **21**(3): 496-504.

[219] Gao, W., J. M. Chan, et al. (2010) "pH-Responsive Nanoparticles for Drug Delivery." Molecular Pharmaceutics **7**(6): 1913-1920.

[220] Ma, Y., S. Hou, et al. (2010). "A Novel Temperature-Responsive Polymer as a Gene Vector." Macromolecular Bioscience **10**(2): 202-210

[221] A.S. Hoffman *et al.* Polym. Gels, 268 (1991), p. 82

[222] Dirk, S. (2006). "Thermo- and pH-responsive polymers in drug delivery." Advanced Drug Delivery Reviews **58**(15): 1655-1670.

[223] Kabanov, A., J. Zhu, et al. (2005). Pluronic Block Copolymers for Gene Delivery. Advances in Genetics, Academic Press. **53:** 231-261.

[224] Twaites, B. R., C. de las Heras Alarcón, et al. (2004). "Thermo and pH responsive polymers as gene delivery vectors: effect of polymer architecture on DNA complexation in vitro." Journal of Controlled Release **97**(3): 551-566.

[225] Dong, L. C. and A. S. Hoffman (1987). "THERMALLY REVERSIBLE HYDROGELS - SWELLING CHARACTERISTICS AND ACTIVITIES OF COPOLY(N-ISOPROPYLACRYLAMIDE-ACRYLAMIDE) GELS CONTAINING IMMOBILIZED ASPARAGINASE." Acs Symposium Series **350**: 236-244.

[226] Hoffman, A. S. and A. Afrassiabi (1986). "REVERSIBLE SWELLING AND DESWELLING OF HYDROGELS." Abstracts of Papers of the American Chemical Society **191**: 204-POLY.

[227] Dincer, S., M. Turk, et al. (2005). "Intelligent polymers as nonviral vectors." Gene Therapy **12**: S139-S145.

[228] Afrassiabi, A., A. S. Hoffman, et al. (1987). "EFFECT OF TEMPERATURE ON THE RELEASE RATE OF BIOMOLECULES FROM THERMALLY REVERSIBLE HYDROGELS." Journal of Membrane Science **33**(2): 191-200.

[229] Allan S, H. (1987). "Applications of thermally reversible polymers and hydrogels in therapeutics and diagnostics." Journal of Controlled Release **6**(1): 297-305.

[230] Li, Z., X. Guo, et al. (2011), "Differentiation of cardiosphere-derived cells into a mature cardiac lineage using biodegradable poly(N-isopropylacrylamide) hydrogels." Biomaterials **32**(12): 3220-3232.

[231] Yokoyama, M. (2005). "Non-viral Gene Therapy: Controlled release of DNA using thermoresponsive polymers." Springer Tokyo: 165-175.

[232] Wu, X. S., A. S. Hoffman, et al. (1992). "Synthesis and characterization of thermally reversible macroporous poly(N-isopropylacrylamide) hydrogels." Journal of Polymer Science Part A: Polymer Chemistry **30**(10): 2121-2129.

[233] Kurisawa, M., M. Yokoyama, et al. (2000). "Gene expression control by temperature with thermo-responsive polymeric gene carriers." Journal of Controlled Release **69**: 127-137.

[234] Tamai, Y., H. Tanaka, et al. (1996). "Molecular dynamics study of polymer-water interaction in hydrogels .1. Hydrogen-bond structure." Macromolecules **29**(21): 6750-6760.

[235] Zhang, X.-Z., D.-Q. Wu, et al. (2004). "Synthesis, characterization and controlled drug release of thermosensitive IPNâ€“PNIPAAm hydrogels." Biomaterials **25**(17): 3793-3805.

[236] He, C.-X., Y. Tabata, et al. "Non-viral gene delivery carrier and its three-dimensional transfection system." International Journal of Pharmaceutics **386**(1â€“2): 232-242.

[237] Van Blitterswijk, C. (2008). "Tissue Engineering." Elsevier: 255-278.

[238] Orsi, S., A. De Capua, et al. (2010), "Cell recruitment and transfection in gene activated collagen matrix." Biomaterials **31**(3): 570-576.

[239] Kulkarni, M., U. Greiser, et al. (2010). "Liposomal gene delivery mediated by tissue-engineered scaffolds." Trends in Biotechnology **28**(1): 28-36.

[240] Peng, L., X. R. Cheng, et al. (2009). "Novel gene-activated matrix with embedded chitosan/plasmid DNA nanoparticles encoding PDGF for periodontal tissue engineering." Journal of Biomedical aterials Research Part A **90A**(2): 564-576.

[241] Jang, J.-H., D. V. Schaffer, et al. (2011), "Engineering Biomaterial Systems to Enhance Viral Vector Gene Delivery." Mol Ther **19**(8): 1407-1415.

[242] Holladay, C., M. Keeney, et al. (2009). "A matrix reservoir for improved control of non-viral gene delivery." Journal of Controlled Release **136**(3): 220-225.

[243] Jang, J.-H., C. B. Rives, et al. (2005). "Plasmid Delivery in Vivo from Porous Tissue-Engineering Scaffolds: Transgene Expression and Cellular Transfection." Mol Ther **12**(3): 475-483.

[244] Hamidi, M., M.-A. Shahbazi, et al. (2011), "Copolymers: Efficient Carriers for Intelligent Nanoparticulate Drug Targeting and Gene Therapy." Macromolecular Bioscience **12**(2): 144-164.

[245] O'Rorke, S., M. Keeney, et al. (2010) "Non-viral polyplexes: Scaffold mediated delivery for gene therapy." Progress in Polymer Science **35**(4): 441-458.

[246] Gupta, M. and A. K. Gupta (2004). "Hydrogel pullulan nanoparticles encapsulating pBUDLacZ plasmid as an efficient gene delivery carrier." Journal of Controlled Release **99**(1): 157-166.

[247] Kim, I.-Y., S.-J. Seo, et al. (2008). "Chitosan and its derivatives for tissue engineering applications." Biotechnology Advances **26**(1): 1-21.

[248] Jayakumar, R., D. Menon, et al. (2010). "Biomedical applications of chitin and chitosan based nanomaterials: A short review." Carbohydrate Polymers **82**(2): 227-232.

[249] Masaki Endo, Shinji Kuroda, Hisatomo Kondo, Yutaka Maruoka, Keiichi Ohya, and Shohei Kasugai. (2006) Tissue Engineering., 12(3): 489-497. doi:10.1089/ten.2006.12.489.

[250] Chevallay, B. and D. Herbage (2000). "Collagen-based biomaterials as 3D scaffold for cell cultures: applications for tissue engineering and gene therapy." Medical and Biological Engineering and Computing **38**(2): 211-218.

[251] Bielinska, A. U., A. Yen, et al. (2000). "Application of membrane-based dendrimer/DNA complexes for solid phase transfection in vitro and in vivo." Biomaterials **21**(9): 877-887.

[252] Malafaya, P. c. B., G. A. Silva, et al. (2007). "Natural origin polymers as carriers and scaffolds for biomolecules and cell delivery in tissue engineering applications." Advanced Drug Delivery Reviews **59**(45): 207-233.

[253] Meilander, N. J., M. K. Pasumarthy, et al. (2003). "Sustained release of plasmid DNA using lipid microtubules and agarose hydrogel." Journal of Controlled Release **88**(2): 321-331.

[254] Lim, S. H., I. C. Liao, et al. (2006). "Nonviral Gene Delivery from Nonwoven Fibrous Scaffolds Fabricated by Interfacial Complexation of Polyelectrolytes." Mol Ther **13**(6): 1163-1172.

[255] Bengali, Z., A. K. Pannier, et al. (2005). "Gene delivery through cell culture substrate adsorbed DNA complexes." Biotechnology and Bioengineering **90**(3): 290-302.

[256] Jang, J.-H., Z. Bengali, et al. (2006). "Surface adsorption of DNA to tissue engineering scaffolds for efficient gene delivery." Journal of Biomedical Materials Research Part A **77A**(1): 50-58.

[257] Capan, Y., B. H. Woo, et al. (1999). "Influence of formulation parameters on the characteristics of poly(d,l-lactide-co-glycolide) microspheres containing poly(l-lysine) complexed plasmid DNA." Journal of Controlled Release **60**(23): 279-286

[258] Nie, H., M.-L. Ho, et al. (2009). "BMP-2 plasmid loaded PLGA/HAp composite scaffolds for treatment of bone defects in nude mice." Biomaterials **30**(5): 892-901.

[259] Fu, Y.-C., H. Nie, et al. (2008). "Optimized bone regeneration based on sustained release from three-dimensional fibrous PLGA/HAp composite scaffolds loaded with BMP-2." Biotechnology and Bioengineering **99**(4): 996-1006.

[260] Yen-Chen Huang, Kathryn Riddle, et al. (2005). "Long-Term *In Vivo* Gene Expression via Delivery of PEI–DNA Condensates from Porous Polymer Scaffolds". Human Gene Therapy **16**(5): 609-617.

[261] Chumakova, O. V., A. V. Liopo, et al. (2008). "Composition of PLGA and PEI/DNA nanoparticles improves ultrasound-mediated gene delivery in solid tumors in vivo." Cancer Letters **261**(2): 215-225.

[262] Lee, S.-H. and H. Shin (2007). "Matrices and scaffolds for delivery of bioactive molecules in bone and cartilage tissue engineering." Advanced Drug Delivery Reviews **59**(45): 339-359.

[263] Micic, M., Y. Zheng, et al. (2003). "Comparative studies of surface topography and mechanical properties of a new, photo-switchable PEG-based hydrogel." Colloids and Surfaces B: Biointerfaces **27**(2â€“3): 147-158.

[264] Joralemon, M. J., S. McRae, et al. "PEGylated polymers for medicine: from conjugation to self-assembled systems." Chemical Communications **46**(9).

[265] Chen, Y.-C., L.-P. Jiang, et al. (2011). "Enhanced Gene Transduction into Skeletal Muscle of Mice In Vivo with Pluronic Block Copolymers and Ultrasound Exposure." Cell Biochemistry and Biophysics **60**(3): 267-273.

[266] Xiong, X.-B., A. Falamarzian, et al. (2011). "Engineering of amphiphilic block copolymers for polymeric micellar drug and gene delivery." Journal of Controlled Release **155**(2): 248-261.

[267] Lai, T. C., K. Kataoka, et al. (2011). "Pluronic-based cationic block copolymer for forming pDNA polyplexes with enhanced cellular uptake and improved transfection efficiency." Biomaterials **32**(20): 4594-4603.

[268] Quick, D. J. and K. S. Anseth (2003). "Gene Delivery in Tissue Engineering: A Photopolymer Platform to Coencapsulate Cells and Plasmid DNA." Pharmaceutical Research **20**(11): 1730-1737.

[269] Park, J. S., D. G. Woo, et al. (2007). "In vitro and in vivo test of PEG/PCL-based hydrogel scaffold for cell delivery application." Journal of Controlled Release **124**(12): 51-59.

[270] Yubing Xie, S.T. Yang, et. al. (2001). "Three-Dimensional Cell-Scaffold Constructs Promote Efficient Gene Transfection: Implications for Cell-Based Gene Therapy." Tissue Engineering 7(5): 585-598.

[271] Roosa, S. M. M., J. M. Kemppainen, et al. (2010). "The pore size of polycaprolactone scaffolds has limited influence on bone regeneration in an in vivo model." Journal of Biomedical Materials Research Part A **92A**(1): 359-368.

[272] Dang, J. M. and K. W. Leong (2006). "Natural polymers for gene delivery and tissue engineering." Advanced Drug Delivery Reviews **58**(4): 487-499.

[273] Yang, F., S.-W. Cho, et al. (2009), "Genetic engineering of human stem cells for enhanced angiogenesis using biodegradable polymeric nanoparticles." Proceedings of the National Academy of Sciences **107**(8): 3317-3322.

[274] Kim, S. and K. Park Tailor-Made Hydrogels for Tumor Delivery. Drug Delivery in Oncology, Wiley-VCH Verlag GmbH & Co. KGaA**:** 1071-1097.

[275] Raviña, M., E. Cubillo, et al. (2010). "Hyaluronic Acid/Chitosan-g-Poly(ethylene glycol) Nanoparticles for Gene Therapy: An Application for pDNA and siRNA Delivery." Pharmaceutical Research **27**(12): 2544-2555.

[276] Fan, M.-M., X. Zhang, et al. (2011), "Self-Assembly Pluronic and β-Cyclodextrin to Hollow Nanospheres for Enhanced Gene Delivery." Macromolecular Rapid Communications **32**(19): 1533-1538.

[277] Hosseinkhani, H., M. Hosseinkhani, et al. (2008). "DNA nanoparticles encapsulated in 3D tissue-engineered scaffolds enhance osteogenic differentiation of mesenchymal stem cells." Journal of Biomedical Materials Research Part A **85A**(1): 47-60.

[278] Lo, C.-W. and H. Jiang. (2010). "Photopatterning and degradation study of dextran-glycidyl methacrylate hydrogels." Polymer Engineering & Science **50**(2): 232-239.

[279] Fukunaka, Y., K. Iwanaga, et al. (2002). "Controlled release of plasmid DNA from cationized gelatin hydrogels based on hydrogel degradatio." Journal of Controlled Release **80**(1-3): 333-343.

[280] Lo, C.-W. and H. Jiang, (2010) "Photopatterning and degradation study of dextran-glycidyl methacrylate hydrogels." Polymer Engineering & Science **50**(2): 232-239.

[281] Huang, Y. C., C. Simmons, et al. (2005). "Bone regeneration in a rat cranial defect with delivery of PEI-condensed plasmid DNA encoding for bone morphogenetic protein-4 (BMP-4)." Gene Therapy **12**(5): 418-426.

[282] Liang, D. H., Y. K. Luu, et al. (2005). "In vitro non-viral gene delivery with nanofibrous scaffolds." Nucleic Acids Research **33**(19).

[283] Jong, Y. S., J. S. Jacob, et al. (1997). "Controlled release of plasmid DNA." Journal of Controlled Release **47**(2): 123-134.

[284] Salvay, D. M., M. Zelivyanskaya, et al. (2010). "Gene delivery by surface immobilization of plasmid to tissue-engineering scaffolds." Gene Ther **17**(9): 1134-1141.

[285] Li, C. Y., W. Yuan, et al. (2011) "PCL Film Surfaces Conjugated with P(DMAEMA)/Gelatin Complexes for Improving Cell Immobilization and Gene Transfection." Bioconjugate Chemistry **22**(9): 1842-1851.

[286] Lai, T. C., K. Kataoka, et al. (2011), "Pluronic-based cationic block copolymer for forming pDNA polyplexes with enhanced cellular uptake and improved transfection efficiency." Biomaterials **32**(20): 4594-4603.

[287] Nolte, A., T. Walker, et al. (2011), "Small-Interfering RNA-Eluting Surfaces as a Novel Concept for Intravascular Local Gene Silencing." Molecular Medicine **17**(11-12): 1213-1222.

[288] Shin, S., D. M. Salvay, et al. (2010), "Lentivirus delivery by adsorption to tissue engineering scaffolds." Journal of Biomedical Materials Research Part A **93A**(4): 1252-1259

[289] Singh, A. N., S. Singh, et al. (2011). "Glutaraldehyde-Activated Chitosan Matrix for Immobilization of a Novel Cysteine Protease, Procerain B." Journal of Agricultural and Food Chemistry **59**(11): 6256-6262.

[290] Orsi, S., A. De Capua, et al. (2011). "Cell recruitment and transfection in gene activated collagen matrix." Biomaterials **31**(3): 570-576.

[291] Chaffey, N. (2003). "Alberts, B., Johnson, A., Lewis, J., Raff, M., Roberts, K. and Walter, P. Molecular biology of the cell. 4th edn." Annals of Botany **91**(3): 401.

[292] Kabanov, A. V. and V. A. Kabanov (1995). "DNA Complexes with Polycations for the Delivery of Genetic Material into Cells." Bioconjugate Chemistry **6**(1): 7-20.

[293] Ulrich, S., M. Seijo, et al. (2006). "The many facets of polyelectrolytes and oppositely charged macroions complex formation." Current Opinion in Colloid & Interface Science **11**(5): 268-272.

[294] Borkovec, M., G. J. M. Koper, et al. (2006). "Ion binding to polyelectrolytes." Current Opinion in Colloid & Interface Science **11**(5): 280-289.

[295] Forsman, J. (2006). "Polyelectrolyte mediated forces between macromolecules." Current Opinion in Colloid & Interface Science **11**(5): 290-294.

[296] de Vries, R. and M. Cohen Stuart (2006). "Theory and simulations of macroion complexation." Current Opinion in Colloid & Interface Science **11**(5): 295-301.

[297] Ziello, J. E., Y. Huang, et al. (2011), "Cellular Endocytosis and Gene Delivery." Molecular Medicine **16**(5-6): 222-229.

[298] Midoux, P., et al. (2008), "Polymer-based gene delivery: a current review on the uptake and intracellular trafficking of polyplexe", Current gene therapy, **8**(5): p. 335-352.

[299] Won, Y.-Y., R. Sharma, et al. (2009). "Missing pieces in understanding the intracellular trafficking of polycation/DNA complexes." Journal of Controlled Release **139**: 88-93.

[300] Pelkmans, L., J. Kartenbeck, and A. Helenius, (2001). "Caveolar endocytosis of simian virus 40 reveals a new two-step esicularтransport pathway to the ER.". Nature Cell Biology **3**: p. 473-483.

[301] Gabrielson, N. P. and D. W. Pack (2009). "Efficient polyethylenimine-mediated gene delivery proceeds via a caveolar pathway in HeLa cells." Journal of Controlled Release **136**: 54-61.

[302] Ferrari, A., V. Pellegrini, et al. (2003). "Caveolae-Mediated internalization of extracellular HIV-1 Tat fusion proteins visualized in real time." Molecular Therapy **8**(2): 284-294.

[303] Rejman, J. Oberle, V. et al. (2004). "Size-dependent internalization of particles via the pathways of clathrin- and caveolae-mediated endocytosis." Biochemistry Journal. 1; 377(Pt 1):159-69

[304] Belguise-Valladier, P. and J. P. Behr (2001). "Nonviral gene delivery: Towards artificial viruses." Cytotechnology **35**(3): 197-201.

[305] Reschel, T., C. Konak, et al. (2002). "Physical properties and in vitro transfection efficiency of gene delivery vectors based on complexes of DNA with synthetic polycations." Journal of Controlled Release **81**(1-2): 201-217.

[306] Klasse, P. J., R. Bron, et al. (1998). "Mechanisms of enveloped virus entry into animal cells." Advanced Drug Delivery Reviews **34**(1): 65-91.

[307] Li, W., F. Nicol, et al. (2004). "GALA: a designed synthetic pH-responsive amphipathic peptide with applications in drug and gene delivery." Advanced Drug Delivery Reviews **56**: 967-985.

[308] Bieber, T., W. Meissner, et al. (2002). "Intracellular route and transcriptional competence of polyethylenimine–DNA complexes." Journal of Controlled Release **82**: 441-454.

[309] Suh, J., D. Wirtz, et al. (2003). "Efficient active transport of gene nanocarriers to the cell nucleus." Proceedings of the National Academy of Sciences of the United States of America **100**(7): 3878-3882.

[310] Bausinger, R., K. von Gersdorff, et al. (2006). "The Transport of Nanosized Gene Carriers Unraveled by Live-Cell Imaging." Angewandte Chemie **118**(10): 1598-1602.

[311] Dworetzky, S. I., R. E. Lanford, et al. (1988). "THE EFFECTS OF VARIATIONS IN THE NUMBER AND SEQUENCE OF TARGETING SIGNALS ON NUCLEAR UPTAKE." Journal of Cell Biology **107**(4): 1279-1287.

[312] Pollard, H., J. S. Remy, et al. (1998). "Polyethylenimine but not cationic lipids promotes transgene delivery to the nucleus in mammalian cells." Journal of Biological Chemistry **273**(13): 7507-7511.

[313] Pollard, H., G. Toumaniantz, et al. (2001). "$Ca_2$-Sensitive cytosolic nucleases prevent efficient delivery to the nucleus of injected plasmids." Journal of Gene Medicine **3**(2): 153-164.

[314] Lechardeur, D. and G. L. Lukacs (2006). "Nucleocytoplasmic transport of plasmid DNA: A perilous journey from the cytoplasm to the nucleus." Human Gene Therapy **17**: 882-889.

[315] Hamm-Alvarez, S. F. (1998). "Molecular motors and their role in membrane traffic." Advanced Drug Delivery Reviews **29**: 229-242.

[316] Dauty, E. and A. S. Verkman (2005). "Actin cytoskeleton as the principal determinant of size-dependent DNA mobility in cytoplasm." Journal of Biological Chemistry **280**(9): 7823-7828.

[317] Kalderon, D., et al.,(1984), "A SHORT AMINO-ACID SEQUENCE ABLE TO SPECIFY NUCLEAR LOCATION". Cell, 1984. **39**(3): p. 499-509.

[318] Chen, J. Stickles, R. et al. (1994). Human Gene Therapy 5(4): 429-435.

[319] Sorgi, F. L., S. Bhattacharya, et al. (1997). "Protamine sulfate enhances lipid-mediated gene transfer." Gene Therapy **4**(9): 961-8.

[320] Moffatt, S., S. Wiehle, et al. (2006). "A multifunctional PEI-based cationic polyplex for enhanced systemic p53-mediated gene therapy." Gene Ther **13**(21): 1512-1523.

[321] Zanta, M. A., P. Belguise-Valladier, et al. (1999). "Gene delivery: A single nuclear localization signal peptide is sufficient to carry DNA to the cell nucleus." Proceedings of the National Academy of Sciences **96**: 91-96.

[322] Pouton, C. W. (1998). "Nuclear import of polypeptides, polynucleotides and supramolecular complexes." Advanced Drug Delivery Reviews **34**: 51-64.

[323] Brunner, S., T. Sauer, et al. (2000). "Cell cycle dependence of gene transfer by lipoplex, polyplex and recombinant adenovirus." Gene Therapy **7**(5): 401-407.

[324] Dekie, L. (2001). "Synthese en evaluatie van poly-L-glutaminezuurderivaten als vectoren voor gentherapie". Ph.D Thesis, PBM research group, Ugent, Gent.

[325] Dubruel, P. (2003). "Studie van synthetische polymeren als vectoren voor gentherapie." Ph.D Thesis, PBM research group, Ugent, Gent

[326] de Winne, K., S. Vanderkerken, et al. (2004). "Dendritic Poly-[N-(2-Hydroxyethyl)-L-Glutamine] as Potential Drug Carrier." Journal of Bioactive and Compatible Polymers **19**(5): 367-382.

[327] Marano, R. J., N. Wimmer, et al. (2004). "Inhibition of in vitro VEGF expression and choroidal neovascularization by synthetic dendrimer peptide mediated delivery of a sense oligonucleotide." Experimental Eye Research **79**(4): 525-535.

[328] Kaufman SR. (2009). “Developments in age-related macular degeneration: Diagnosis and treatment.” Geriatrics **64**(3):16-9

[329] Brown, D. M., P. K. Kaiser, et al. (2006). "Ranibizumab versus Verteporfin for Neovascular Age-Related Macular Degeneration." New England Journal of Medicine **355**(14): 1432-1444.

[330] Zarbin, M. A. and P. J. Rosenfeld, (2010), "PATHWAY-BASED THERAPIES FOR AGE-RELATED MACULAR DEGENERATION: An Integrated Survey of Emerging Treatment Alternatives." RETINA **30**(9): 1350-1367

[331] Immonen, I., S. Seitsonen, et al. (2010), "Vascular Endothelial Growth Factor Gene Variation and the Response to Photodynamic Therapy in Age-Related Macular Degeneration." Ophthalmology **117**(1): 103-108

[332] Sharma, K., Prabhakar, S., et al. (2009). “ARMD: advances and trends.” Annals of neuroscience 16(2): 62-71

[333] den Hollander, A. I., R. Roepman, et al. (2008). "Leber congenital amaurosis: Genes, proteins and disease mechanisms." Progress in Retinal and Eye Research **27**(4): 391-419.

[334] Baehr, W. and J. M. Frederick (2009). "Naturally occurring animal models with outer retina phenotypes." Vision Research **49**(22): 2636-2652.

[335] Bhaumik, S. and S. S. Gambhir (2002). "Optical imaging of Renilla luciferase reporter gene expression in living mice." Proceedings of the National Academy of Sciences **99**(1): 377-382.

[336] Greer, L. F. and A. A. Szalay (2002). "Imaging of light emission from the expression of luciferases in living cells and organisms: a review." Luminescence **17**(1): 43-74.

# Chapter 2

# Synthesis of biodegradable polymer vectors

# 1 Introduction

For polymers, considered as possible delivery systems for DNA into a cell or cellular structure, a whole range of qualifications needs to be met. As was mentioned in the introduction, polymer structures can be tailored to fulfil these requirements. This starts with the selection of a base polymer that has a specific composition and structure. From literature, several polymer systems are known to be suitable for gene delivery including polysaccharides[1], vinyl-based polymers[2], poly(β-amino esters)[3] or polyphosphoric ester derivatives[3]. One of the most actively studied polymers in gene delivery is (branched) pEI[4], a highly active polymer that unfortunately expresses a high degree of cytotoxicity[5]. In many cases, toxicity issues result from non-biodegradable properties, preventing for instance intracellular degradation. Repeated administration can result in accumulation within the lysosome, a condition labelled as lysosomal storage disease[6]. Keeping these considerations in mind, this work has the aim to synthesise and apply biodegradable polymers with superior DNA interaction and protection properties as well as minimal cytotoxic implications or haemolytic effects while being highly efficient in transfecting the cell. A class of synthetic polymers that has high potential for these applications is poly-α-aminoacids. Due to their natural occurrence, excellent biocompatibility is presumable as well as their ability to be degraded within the body (enzymatic degradation of amide bonds). Furthermore, there are numerous approaches that allow control of the composition and the MM (by introducing or modifying functional groups located on the side chains).

Derivatives of poly-L-lysine have been explored before as gene delivery system because of their presence in histones, the natural packaging material for DNA and chromosomes. However unsuccessful results were obtained by severe toxicity[7,8]. Also L-arginine, which is substantially present in the histones, was proposed but only a few actual try-outs were achieved[9]. In some cases, arginine residues were incorporated into or combined with other structures like pNIPAAm[10] or poly-L-leucine[11] to reduce its toxic behaviour. A similar approach was applied for poly-L-lysine, such as the coupling to PEG[12] or with poly-L-ornitine[13] in order to improve the cell-viability. Alternative strategies were found in the use of polyaspartamide[14,15] and L-glutamic acid derivatives[16]. Based on this latter research, initial promising results (e.g. positive transfection for polyagmatine-containing derivatives) suggested further exploration of this starting material using new synthesis approaches. Preparing multifunctional polymers based on L-glutamine is a multistep process in which starting polymers (poly-γ-benzyl-L-glutamate, pBG) are prepared from L-glutamic acid and its corresponding NCA. After that, various functional groups can be introduced during the subsequent modification steps in order to yield synthetic vectors with desired properties for gene delivery (e.g. buffering, DNA complexation, charge separation), as shown in fig. 2.1.

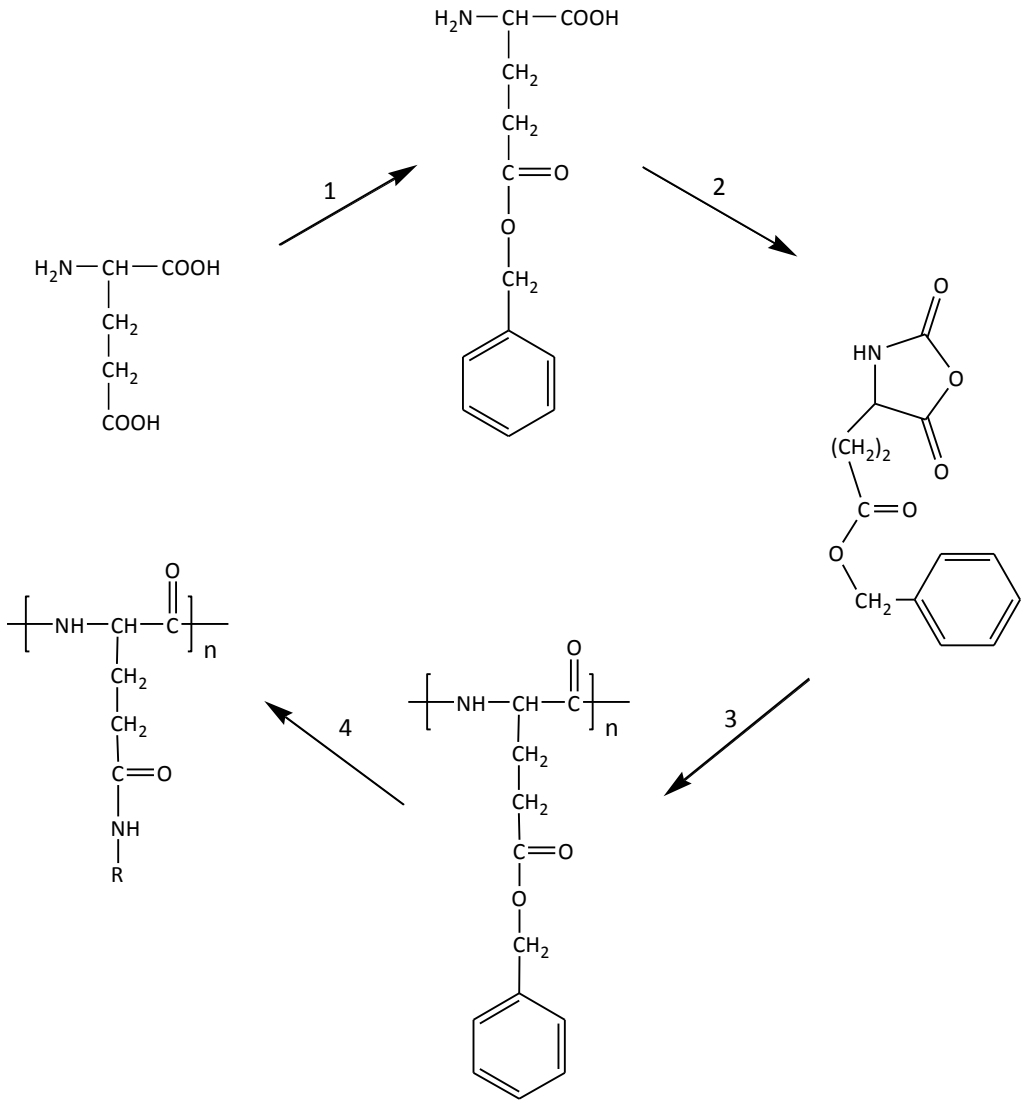


**Figure 2.1 – Different steps in the synthesis of poly-L-glutamine derivatives.**
**1. Protection ; 2. Cyclisation ; 3. Polymerisation ; 4. Aminolysis**

Additionally, poly-L-arginine is selected to be combined with poly-L-glutamines in an attempt to mimic the biological behaviour of DNA condensation in the cell. Poly-L-arginine and derivatives can be synthesised via a similar strategy. The formation of a cyclic arginine compound is not straightforward due to the nucleophilic nature of the side-group[17] and because of that, the use of a precursor (L-ornithine) is chosen. In an subsequent step, poly-L-ornithine can be converted into poly-L-arginine by using an appropriate reagent ('guanidylating agent'). Moreover, a protected derivative of this precursor ($N^{\delta}$-carbobenzyloxy-L-ornithine) is commercially available, eliminating the need for a preceding protection step. The total process for poly-L-arginine is shown in figure 2.2.

All individual reaction steps influence different aspects of the total synthetic pathway and will be discussed accordingly.

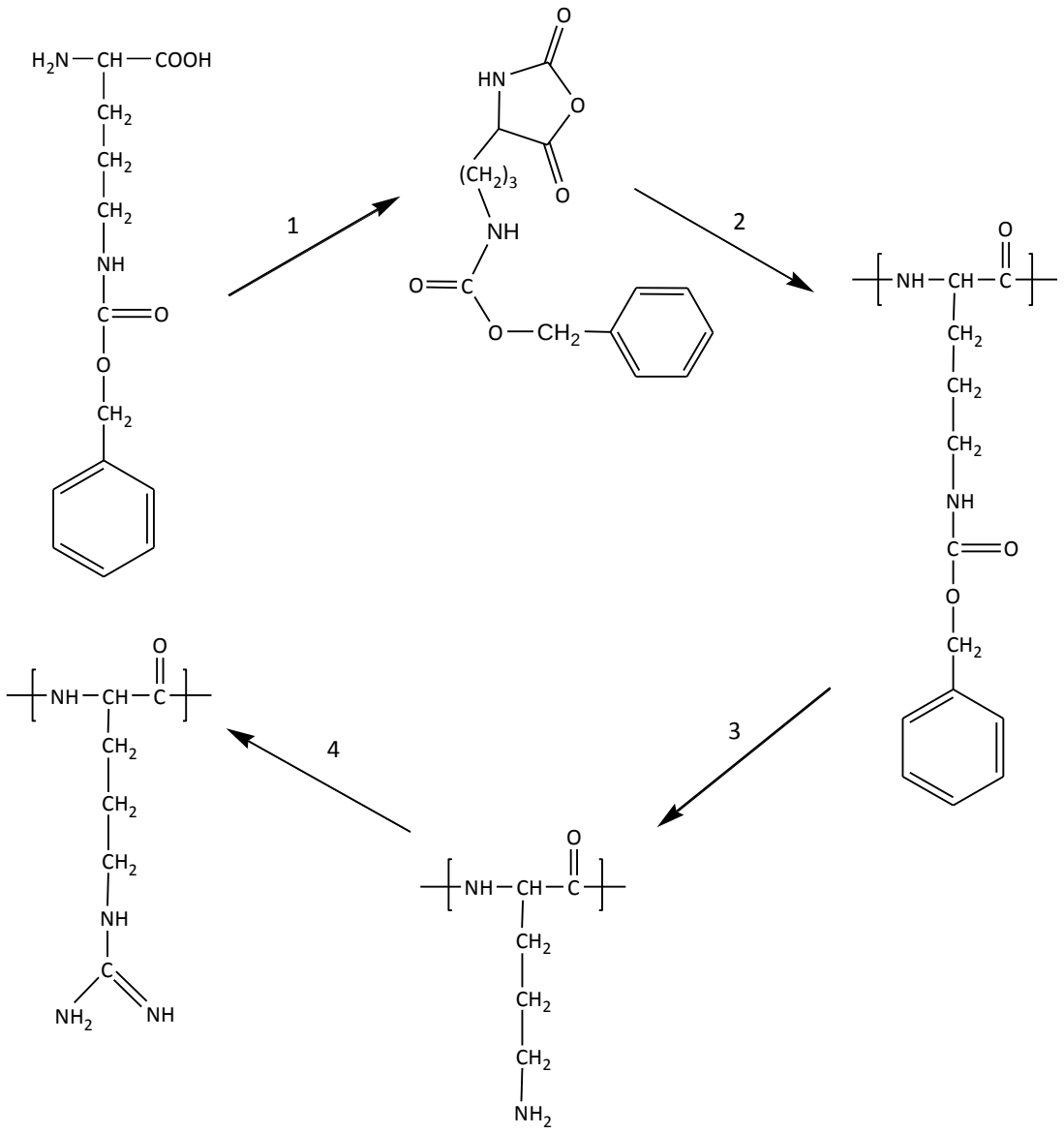


**Figure 2.2 – Different steps in the synthesis of poly-L-arginine derivatives.**
**1. Cyclisation ; 2. Polymerisation ; 3. Acidolysis ; 4. Guanidylation**

## 2 Synthesis of poly-L-glutamine derivatives

### 2.1 Synthesis of protected L-glutamic acid (γ-benzyl-L-glutamate)

To be able to form a cyclic monomer, required for subsequent ring-opening polymerisation of the intermediate pBG, the functional group located on the side chain of L-glutamic acid needs to be protected[18]. If not, side products (6-membered NCA derivative) can hamper the cyclisation of the correct NCA molecule[17]. The starting reagent, L-glutamic acid is selectively esterified by reaction with benzylalchohol in diethylether catalysed by sulphuric acid at room temperature (as was described before by R. Vercauteren[19]). The final product γ-benzyl-L-glutamate (BG) was obtained in a moderate yield (50-60%) as shown in fig. 2.3.

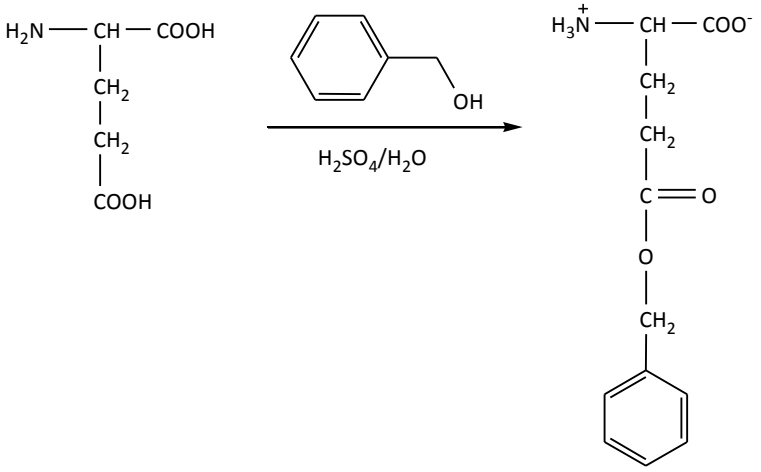


**Figure 2.3 - Synthesis of γ-benzyl-L-glutamate.**

## 2.2 Monomer synthesis (γ-benzyl-L-glutamate-*N*-carboxyanhydride)

Cyclic derivatives of amino acids (*N*-carboxy-α-anhydride or NCA) have already been described long time ago and are often referred to as 'Leuchs' anhydrides[20]. They have the significant advantage that neither the synthesis nor the polymerisation induce racemisation if conducted under appropriate conditions[21]. The versatility of their polymerisation reactions, in particular the ability to incorporate a large variety of amino acid monomers, both natural and synthetic, results in unprecedented flexibility of molecular design (giving rise to the formation of homo, co, block or graft-polypeptides)[18,22,23].

The simplest way of achieving ring formation is the reaction of an amino acid and phosgene[21]. Via this reaction, *N*-chloroformyl-L-glutamic acid is formed which undergoes intramolecular cyclisation to form its corresponding NCA (Fig. 2.4). An excess of HCl is produced during this reaction and needs to be readily removed from the reaction mixture since the presence of HCl can cause side reactions like the reverse ring opening that can subsequently be phosgenated into an α-isocyanate acid chloride (Fig. 2.5).

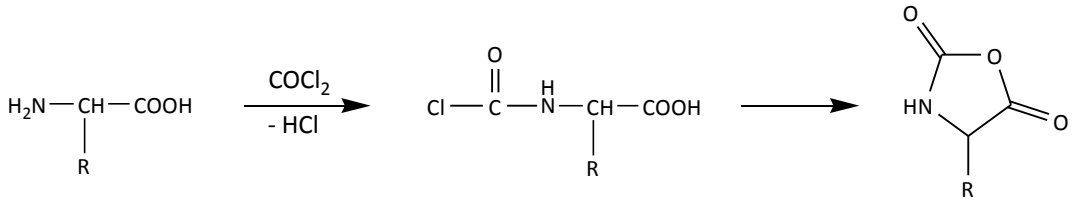


**Figure 2.4 - NCA formation by phosgene mediated cyclisation.**

The use of phosgene represents hazardous implications due to its toxic nature. Therefore, alternative reagents can be applied by using phosgene precursors like trichloromethylcarbonate [22] (diphosgene) or di-(trichloromethyl)carbonate [23] (triphosgene)

which naturally occur in a liquid and solid state respectively at room temperature. Because residual triphosgene is difficult to remove from the reaction mixture (can eventually decompose with new HCl production as a result), priority is given to the use of diphosgene which demonstrates better handling properties and can be more easily removed (although HCl production is still possible).

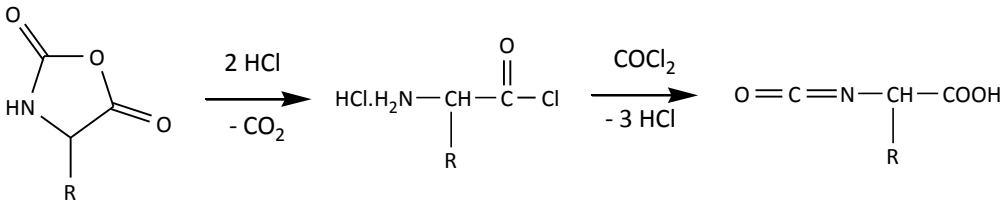


**Figure 2.5 – Unwanted side reaction during NCA synthesis.**

Despite the use of diphosgene, several recrystallisations of the final product remain necessary to achieve a sufficient level of purity[24]. An important aspect of this purity is the amount of free chlorine present, generated by the production of HCl and can be checked using an $AgNO_3$ test which results in precipitation of insoluble AgCl (due to the extremely low solubility, $K_s$ = 1.77x10$^{-10}$), followed by visual comparison to standardised solutions. In this case, pure tapwater is put forward as a sufficiently 'chloride free' solution (10-100 mg/l).

The reaction is carried out by heating a suspension of γ-benzyl-L-glutamate in dry ethylacetate (EtOAc) to 60 °C. A portion of diphosgene, dissolved in EtOAc (15 v/v %), is added dropwise to the mixture and allowed to react for 20 minutes. After that, Ar is used to degas the mixture in order to remove any formed HCl and prevent the occurrence of side reactions. This portionwise addition and degassing is repeated until all diphosgene has been consumed (visible by the transition of suspension to solution). At that moment no additional diphosgene should be added (to limit side reactions) and the mixture is thoroughly degassed (using He or $N_2$) for about 1 hour at elevated temperature and additionally for 30 minutes at room temperature. Subsequently, the product is precipitated in cooled pentane and recrystallised in EtOAc until the amount of free chlorine is acceptable according to the $AgNO_3$ test. Generally, yields up to 80-90 % can be obtained via this method. The final product, γ-benzyl-L-glutamate-N-carboxyanhydride (BG-NCA) is verified using $^1$H-NMR ($CDCl_3$) and FTIR spectroscopy (Fig. 2.6 & 2.7).

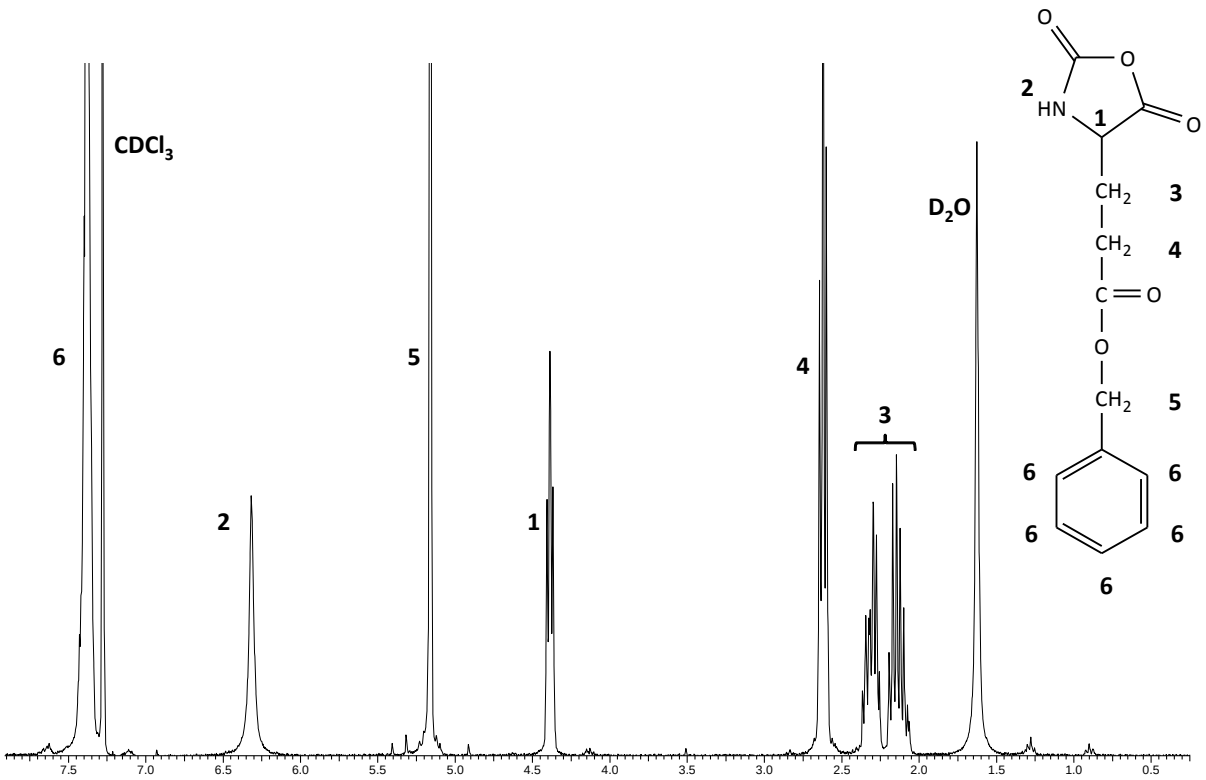


**Figure 2.6 - $^{1}$H-NMR of BG-NCA (with peak assignment).**

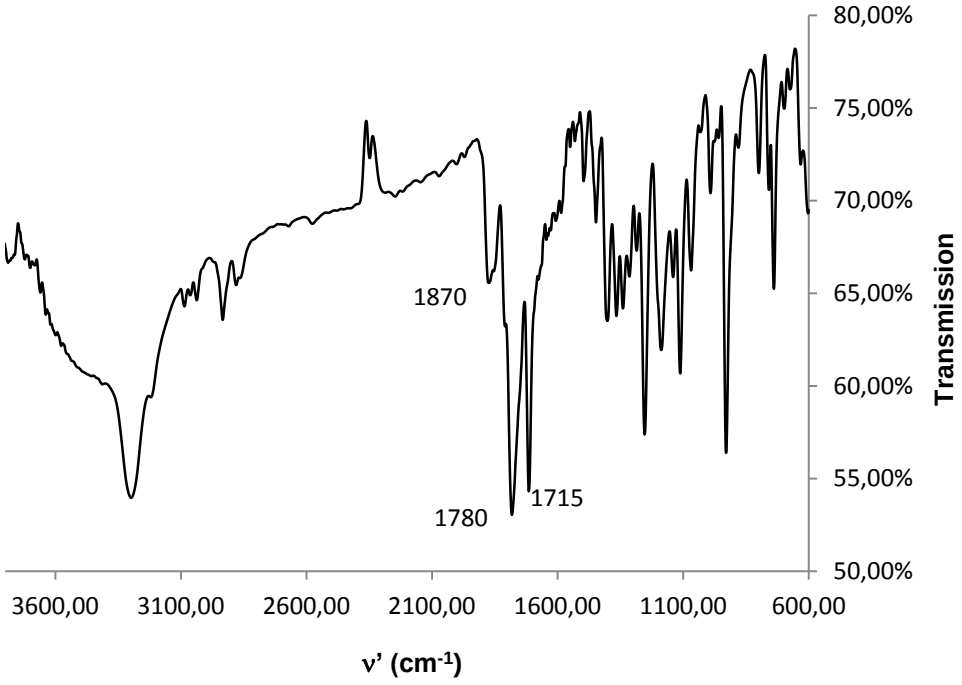


**Figure 2.7 – FTIR spectrum (KBr) of BG-NCA with characteristic peaks: ester (1715 cm$^{-1}$), anhydride peak 1 (1780 cm$^{-1}$) and anhydride peak 2 (1870 cm$^{-1}$).**

## 2.3 Polymerisation

In order to synthesise a long peptide chain, one of the most convenient methods, both practical and economical, is a ring-opening polymerisation (ROP) of NCA (BG-NCA). Five-membered α-NCA rings possess 3 reactive centers that can be employed (Fig. 2.8), 2 carboxyl groups and an NH-group. Due to the presence of the nitrogen atom, the C2 carboxyl is less electrophilic than carboxyl C5. Both the NH-group as well as the α-CH don't exhibit nucleophilic behaviour but can form strong nucleophilic anions upon deprotonation. Since the NH-group is distinctly more acidic than the α-CH, the latter will only be deprotonated if the NH-group is substituted[25].

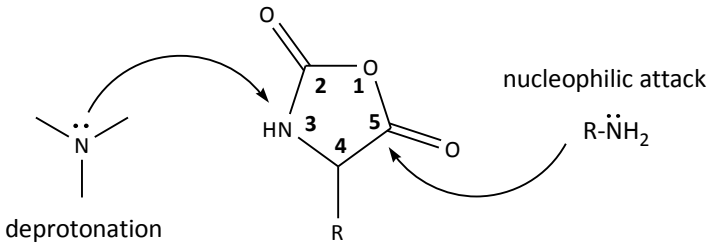


**Figure 2.8 - Reactive centres & initiation of an α-NCA.**

### *2.3.1 Reaction mechanism*

Because of the availability of different reaction centres the initiation of the ROP can be classified in two groups (Fig. 2.8), a nucleophilic attack on the C5-carbonyl and the deprotonation of the nitrogen (N3) referred to as the activated monomer mechanism. The extent to which a certain initiation will be preferred is dependent on several parameters like solvent, ionic strength[26], nature of the R-group, monomer concentration and most importantly the type of initiator used[27]. The most important aspect of an initiator is its ratio of nucleophilicity/basicity which is determined by the electrondensity, polarisibility of the the free electron pair and steric hindrance. Initiators can be divided into protic and aprotic systems and subjected to the choice of initiator, their corresponding propagation mechanisms are variable (activated monomer mechanism[28], amine mechanism or carbamate mechanisme[24]). Two major groups of initiators are used in nearly all polymerisations used, amines and alcohols/alkoxides of which only the first group was employed herein.

*Initiation by use of primary amines*

Primary amines demonstrate a high nucleophilicity/basicity ratio and because of that the polymerisation occurs nearly exclusively by nucleophilic attack on the C5-carbonyl. Unstable, intermediate carbamic acids are formed due to the ring-opening reaction but a stable peptide compound is rapidly generated by spontaneous decarboxylation. The resulting molecule

retains a free amine that is able to start a new ring-opening reaction. This procedure lasts until all reactive monomer is consumed and polypeptides are formed (Fig. 2.9)[29].

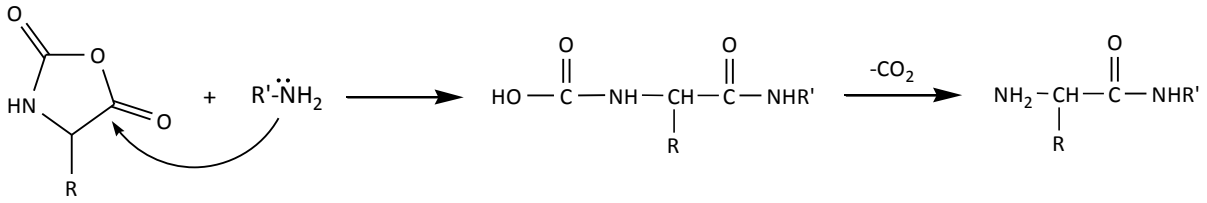

**Figure 2.9 – "NCA-polymerisation" cycle using primary amines as initiator.**

The course of polymerisation is determined by the nucleophilic character of the initiator and the monomer to initiator ratio. Because both the initiator as the formed peptide contain a free amine that can induce ROP, control over the molecular weight can only be established if the initiator is considerably more nucleophilic than the active chain-end (amine). This implies that the initiation is faster than the propagation and because of that the amount of active chains can be directly related to the initiator concentration (every initiator molecule is the start of an active chain). The degree of polymerisation (DP) can be calculated from the following equation:

$$DP = \frac{M}{I} \cdot \frac{\%\ conversion}{100}$$

This formula is applicable for a living polymerisation. In practice, small deviations of this value are observed due to decreased solubility (and increased viscosity) of large polymer chains that invoke a physical 'death'. Alternatively, intra-molecular termination is possible when free amine react with a benzyl ester to form undesired and non-reactive pyrrolidon-rings[30] (Fig. 2.10). These termination reactions are mainly noticed for high NCA/initiator concentrations and are responsible for a MW limitation of about 40.000 Da when using primary amines as initiating systems while maintaining sufficient polydispersity control.

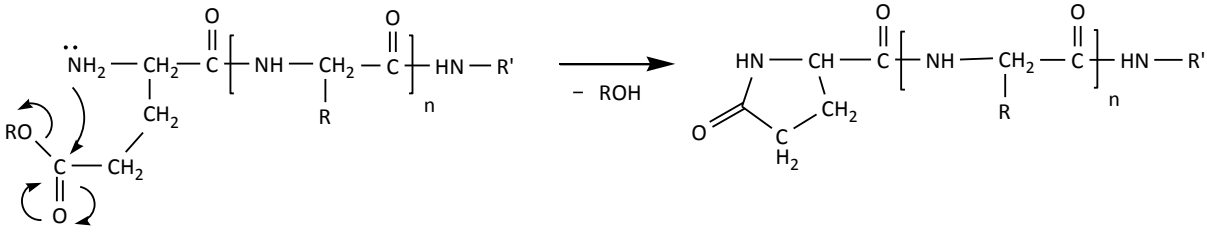

**Figure 2.10 - Intramolecular termination (pyrrolidone formation).**

When the propagation is faster than the initiation, polymers with a DP higher than calculated are obtained, hence the loss of control as a side-effect.

*Initiation by use of tertiary amines*

Tertiary amines display much lower nucleophilic behaviour than primary amines, especially when alkyl chains with a considerable length are used (e.g. tributylamine). Consequently, a tertiary amine will deprotonate the NH-group of the NCA molecule and form a highly reactive anion that will attack a second NCA molecule yielding a dimer with an *N*-acyl-NCA part and a carbamate anion. Since the *N*-acyl-NCA is more electrophilic than a non-substituted NCA, chain growth is achieved by reaction of anions with *N*-acyl-NCA chain ends. Moreover, nucleophilic attack will predominantly be carried out by the charged anion rather than the intermediate primary amine. This process is labelled as activated monomer mechanism[27] (Fig. 2.11).

The polymerisation of an NCA by a tertiary amine occurs seemingly through a living-like reaction since the propagation speed is much higher than the initiation speed[31]. Additionally, termination or chain transfer processes were not abundantly reported. This allows for the production of polymers with a very high MW (up to 300.000 Da)[17].

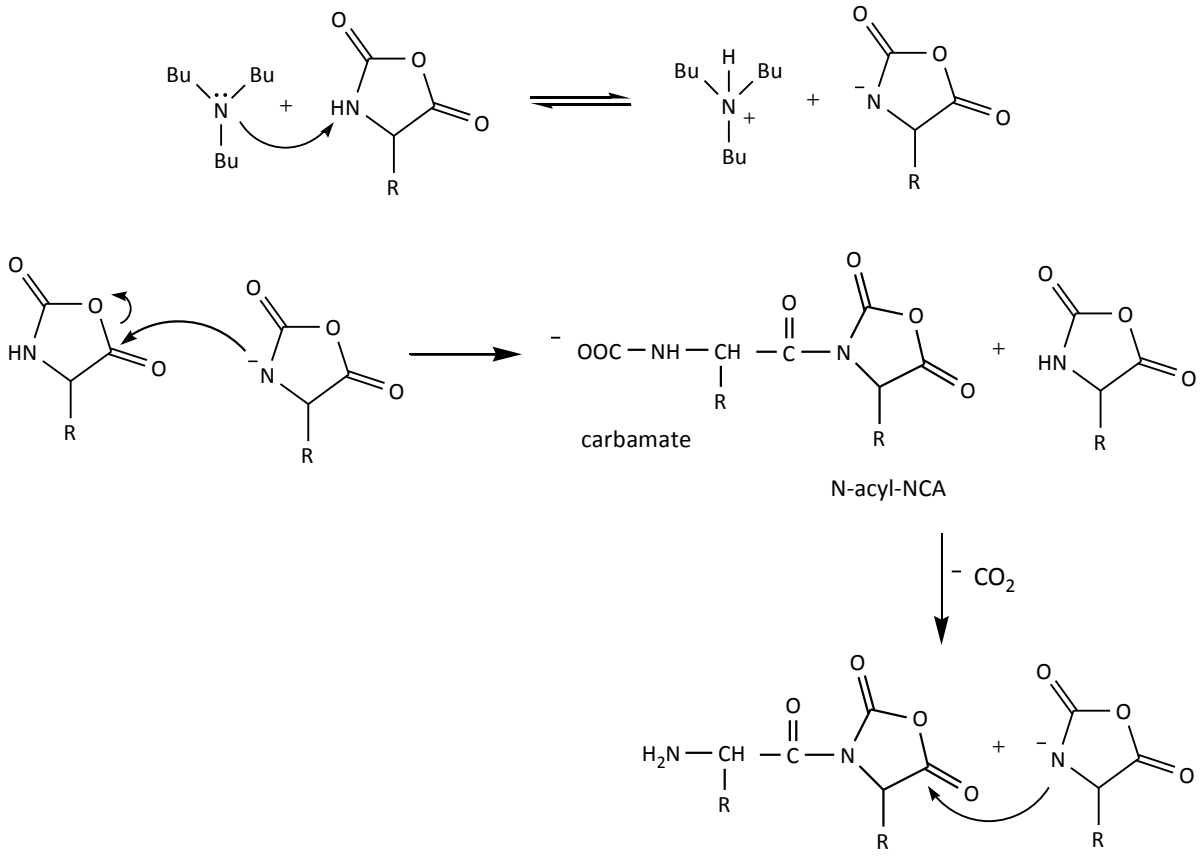


**Figure 2.11 - Activated monomer mechanism: initiation and propagation steps.**

Polymerisations using alkoxides or alcohols make use of similar initiation steps (deprotonation and activated monomer mechanism respectively) and propagation mechanisms (mainly carbamate).

### *2.3.2 Synthesis of poly-γ-benzyl-L-glutamate*

#### *2.3.2.1 Application of primary amines as initiator*

The polymerisation of BG-NCA using an appropriate initiator yields poly-γ-benzyl-L-glutamate (pBG) after 40 hours of stirring at room temperature in a mixture of DCM/EtOAc (6/1 v/v)[32]. The polymer is purified by precipitation in a methanol/diethylether mixture (2/1 v/v). In the case of high MW pBG, the mixture is diluted with DCM prior to precipitation. This is due to the molecular association of pBG in non-hydrogen bonding solvents like DCM which greatly enhances the viscosity (end-to-end associations). For low MW compounds, the portion of methanol in the non-solvent is reduced to 1/1 or 1/2 to decrease the polarity of the mixture in order to preferentially keep oligomeric peptides and low MW pBG dissolved while precipitating the high MW compounds (Fig. 2.12).

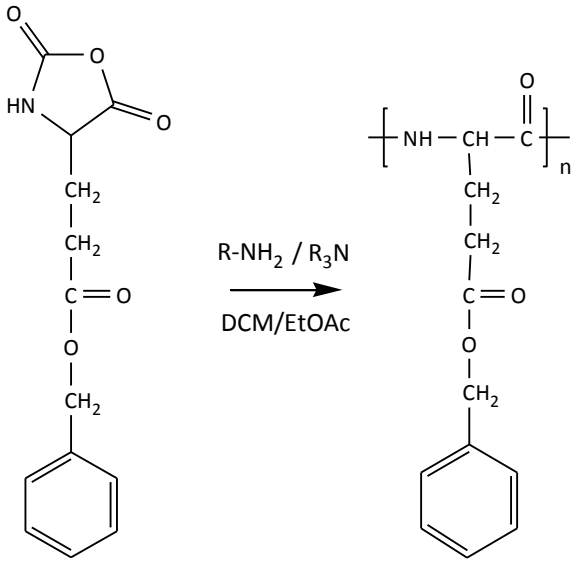


**Figure 2.12 - Synthesis of pBG.**

The reaction can be followed by FTIR since specific peaks disappear (NCA, C=O stretch vibrations at 1780 and 1870 $cm^{-1}$) and new peaks arise (formation of the amide bond, 1650 and 1550 $cm^{-1}$) during polymerisation (Fig. 2.13 & table 2.1). The values of the amide I and II peak are indicative for the formation of an ordered α-helical structure (H-bonding of the amide backbone) in solution, which was proven prior in literature[33]. In dipolar, aprotic solvents like DMF, the α-helix end can be dissolved by the solvent and there's no resulting molecular association. To prove the helicity, circular dichroism measurements were executed as was reported by Reinaudo et al[38].

| Peak value ($cm^{-1}$) | Corresponding structure |
|---|---|
| 3.300 | Amide N-H stretch |
| 2.800-2.950 | C-H stretch ($-CH_2$/$-CH_3$) |
| 1.730 | O=C-O (carbonyl) stretch |
| 1.650 / 1.550 | Amide I + II bend |

**Table 2.1 – Peak assignment of the FTIR spectrum of pBG (KBr).**

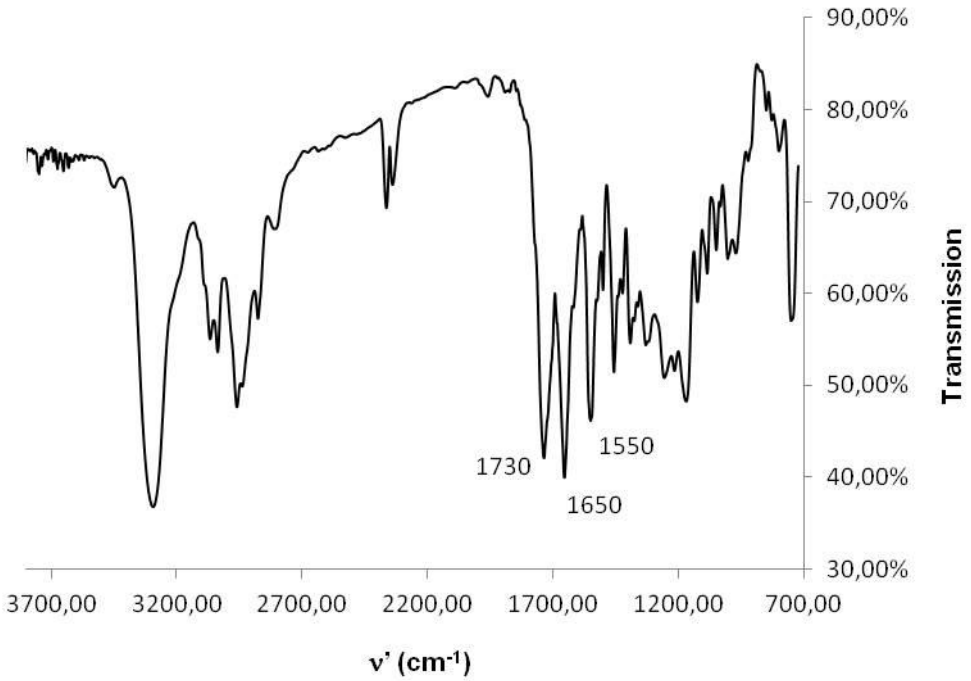


**Figure 2.13 – FTIR spectrum (KBr) of pBG with characteristic peaks (table 2.1).**

The use of n-butylamine as an initiator generated pBG of a rather low MW (determined by the monomer to initiator ratio). Additionally, the $\delta$-$CH_3$ unit of n-butylamine can easily be observed in the $^1$H-NMR spectrum and can also be used to calculate the MW (Fig. 2.14). The number of repeat units can be derived by integrating the surface of this peak and comparing to the integration value of the $\alpha$-CH peak of pBG. From NMR analysis, it could be concluded that excellent control over the MW was possible (table 2.2).

| Calculated MW (Da) | Experimental MW (Da) |
|---|---|
| 5.000 | 5.700 |
| 10.000 | 9.900 |
| 20.000 | 19.700 |
| 30.000 | 29.600 |

**Table 2.2 – MW of pBG produced via primary amine initiaton.**

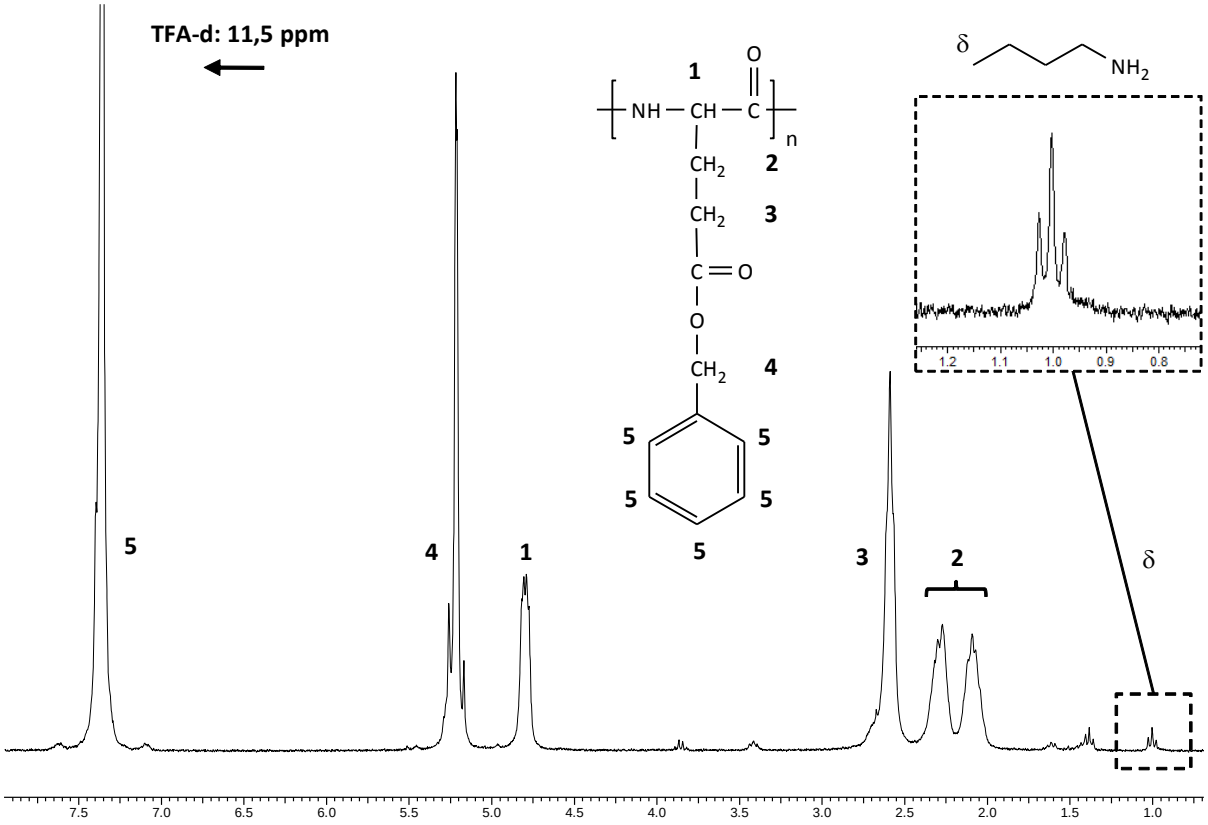


**Figure 2.14 - $^{1}$H-NMR spectrum of pBG - 10.000 Da in TFA-d as a solvent.**

### *2.3.2.2 Application of tertiary amines as initiators*

When tributylamine is applied as initiator system, pBG with high MW can be achieved. Since in this case the initiator is not covalently linked to the polymer, it can not be traced in the $^{1}$H-NMR spectrum and used for calculation of the MW (Fig. 2.14). The initiator is removed during purification and because of that the MW can only be determined using traditional methods like viscosimetry (Ubbelohde apparatus) and is therefore difficult to compare with other MW-determination techniques (e.g. light scattering).

### *2.3.2.3 Viscosimetry*

Viscosimetry was used to determine the molecular mass of polymers ($M_v$) based on the viscosity of polymer solutions. With increasing length of polymer chains, an increase in viscosity can be detected (while concentration and temperature are given and kept constant). The molecular weight can be acquired by approximation using the following formula:

$$[\eta] = KM_w^{\alpha} \qquad \text{(Mark-Houwink relation)} \qquad (1)$$

With $\eta$ being the intrinsic viscosity, $M_w$ the molecular weight and $K$ and $\alpha$ Mark-Houwink parameters, specific for a certain polymer dissolved in a known solvent at a given temperature (25 °C).

The intrinsic viscosity can be derived using an approximation method for polymers at low concentration (0.1-0.2 w/w%)[34]. In practice, this comes down to a measurement of the time, a polymer solution (*t*) or a blank (pure solvent, $t_0$) needs to flow through a predetermined volume. From these results the specific and relative viscosity can be calculated:

$$\eta_{sp} = \frac{t - t_0}{t_0} \qquad n_{rel} = \frac{t}{t_0}$$

Using these parameters, the intrinsic viscosity is given by the equation:

$$[\eta] = \frac{\sqrt{2}}{c}\sqrt{(\eta_{sp} - \ln \eta_{rel})} \tag{2}$$

Combining both formula's allows for the molecular weight to be determined. Determination of the $M_v$ by viscosimetry gives rise to a specific molecular mass that is situated in between $M_w$ and $M_n$. This is due to the higher importance of long polymer chains in the contribution to the total viscosity (Fig. 2.15). Dependent on the method to analyse the MM of a polymer, the resulting value is given as either $M_n$ (number-average molecular mass), $M_p$ (peak-value molecular mass), $M_v$ (viscosity-based molecular mass) or $M_w$ (weight-averaged molecular mass). The ratio of $M_w/M_n$ is described as the polydispersity ($\delta$ or PD) of the polymer.

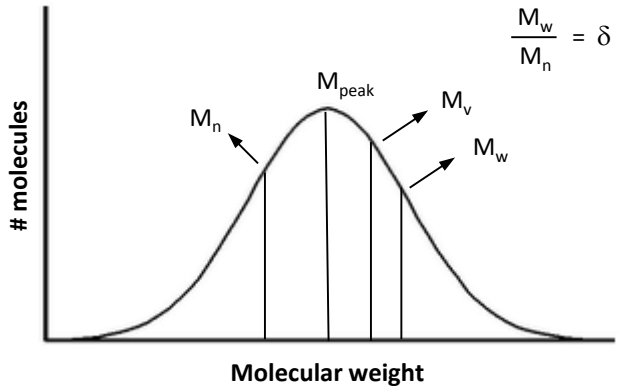


**Figure 2.15 - Molecular weight as a function of the polymer distribution.**

*2.3.2.4 Set-up of a mastercurve (ratio M/I) for MW determination of poly-$\alpha$-amino acids*

In general, the amount of initiator (in case of deprotonation) added to start a polymerisation, is expressed in terms of M/I ratio. As the polymerisation appears to have an upper limit in MM, a deviation of the living polymerisation course is to be anticipated. Because of that, prediction of the final obtained MM was difficult. For that reason, a series of pBG's with various MM was synthesised and analysed for MM via viscosimetry in an attempt to determine a relation between the initiator amount (M/I) and the obtained $M_v$.

The polymers were measured in a solution of dichloroacetic acid ($CHCl_2COOH$) at a temperature of 25 °C and a concentration of 0.2 % (w/w). This solvent was chosen due to the unusually strong secondary bonding with pBG allowing full dissolution and a random coil configuration[33]. The Mark-Houwink parameters, $\alpha$ and K for pBG in $CHCl_2COOH$ (25 °C) are 0.87 & $2.78.10^{-3}$ g/ml respectively[35]. Because the polymerisation of tertiary amines occurs via the highly reactive activated monomer mechanism, polymers with a high MM can easily be obtained but control of the propagation is limited and can cause an increase in polydispersity (PD)[36]. Theoretically, termination reactions are not readily expected, nonetheless, a decline in MW is observed with increasing M/I ratios. When the initiation step is fast, compared to the propagation, the concentration of active centres is equal to the initiator concentration, hence the simultaneous propagation of the polymer chains. The degree of polymerisation should therefore augment proportionally with the degree of conversion:

$$DP \sim \frac{[M_0]}{[I]}$$

This relation was not found for the ROP of BG-NCA which implies that termination reactions still occur. They can be attributed to the increased viscosity and lack of surrounding monomer needed for further propagation[37]. Intra or intermolecular cyclisation reactions are rather limited and mainly regulated by the geometrical arrangement of the polymer, that forms $\alpha$-helices (starting at lengths of 10 structure units) which puts a considerable restraint on the chain mobility (macromolecular stiffness) and propagation capability[38]. From the viscosity measurement, the $M_v$ (and DP) and the M/I ratio prove to be logarithmically connected (Fig. 2.16).

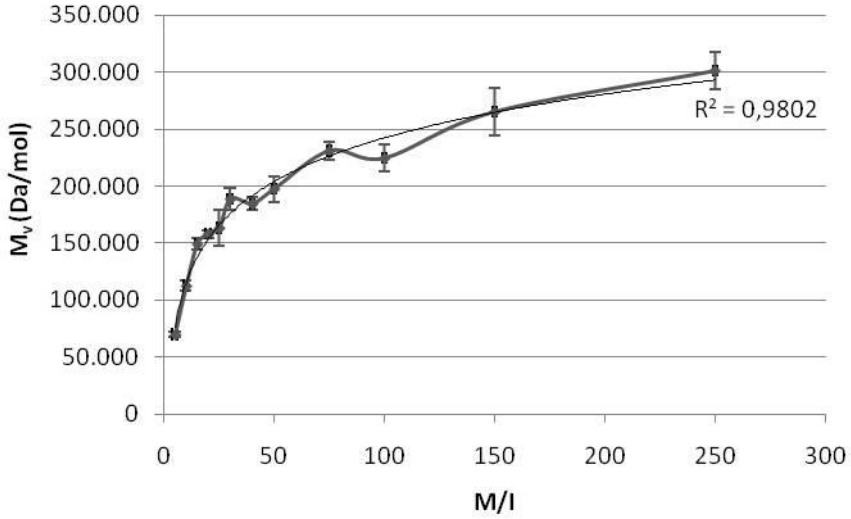


**Figure 2.16 - Mastercurve for pBG (using $Bu_3N$ as initiator) as obtained by viscosimetry.**

At first, for low DP's, the relation appeared linear but was graduately deviating from this relation with increasing M/I ratio. A living polymerisation displays first-order kinetics which

implies that the monomer concentration is decreasing linear in time. Due to the logarithmical relation observed, this value was more inclined towards a second-order kinetic approach (especially for higher M/I ratios).

$$M_v = 55.300 \,.\ln\left(\frac{M}{I}\right) - \ 12.400$$

High MW pBG was synthesised in a range from 70.000 – 300.000 Da.

## 2.4 Aminolysis

During the polymerisation of pBG, the MM of the compound is determined. These polymers need to be further derivatised if they need to exhibit DNA-interacting functional groups (for complexation, buffering, etc.). This can be achieved by modifying the functional group of the side chain while preserving the integrity of the backbone (and its correlated MM). By selecting a suitable reagent, the desired functional groups can be introduced and at the same time, the protective benzyl ester can be removed. This modification is carried out by an aminolysis reaction (carbonyl substitution) in which an ester is transformed into a thermodynamically stronger amide-bond by an amine-containing reagent. To extend the length of the side chain in order to optimise flexibility towards interaction, reagents with a spacer length of two $CH_2$-moieties were chosen (Fig. 2.17).

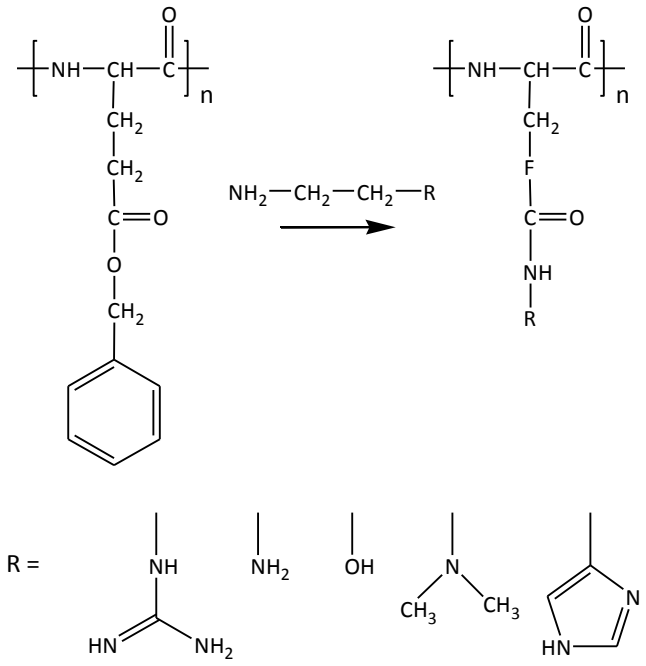


**Figure 2.17 - Synthesis of multifunctional cationic polymers via aminolysis.**

### *2.4.1 Aminolysis reaction mechanism*

Initial modificiation experiments of pBG revealed that the MM of the polymer after aminolysis reached maximum 70% of the original weight and that the polydispersity was substantially increased[39]. This drop in MM can be attributed to transamidation or chain cleavage of the amide backbone. Hence these reactions complicate the development of well-defined polymers. Optimisation procedures (e.g. solvent and temperature[40]) for this modification were carried out but were not deemed successful until the use of a bifunctional catalyst was proposed[41] (previous investigation performed in the research group by K. Hoste). The addition of an excess of 2-hydroxypyridine was able to speed up the reaction time and simultaneously prevent chain scission at the same time[42].

2-hydroxypyridine (Fig. 2.18) contains a nucleophilic (pyridine) and electrophilic group (phenol), oriented in such a way that they can provoke the selective elimination of benzylalcohol from the substrate, pBG. Substitution was reported to occur through a concerted mechanism in which a cyclic transition state favours the reaction on the side chain rather than on the polymer backbone (with the assistance of H-bonding)[43,44]. However, this 8-membered-ring transition state (Fig. 2.18) can only be achieved by have 3 molecules interacting simultaneously, an entropically unfavourable state. An alternative strategy could exist in the consecutive reaction of 2-HP with pBG forming a reactive ester that subsequently can be transformed in the amide by means of the amine reagent. The catalyst is present as one of 2 tautomeric forms of which the N-protonated form (lactam derivative) is the most likely one in polar solutions (like DMF), yet the energy difference between both is low (theoretically 8.9 kJ/mol)[45]. Dimerisation can take place and would imply that higher concentration of the product are required to reach the same level of efficiency as without the presence of dimerisation but this effect is mainly predominant in non-polar solvents[46]. To optimise the speed of conversion and to limit backbone scissoring, the amount of catalyst added, was set to 5 equivalents (relative to the # moles benzylester)[41].

Besides the obvious importance of temperature, also the solvent was found to exhibit a distinct influence on the reaction. When pBG is dissolved in dichloroacetic acid or trifluoroacetic acid (TFA), polymer chains are present as random coils (parameters similar to $\theta$-solvent) which is the reason for using this solvent in viscosimetry. Most organic solvents (DCM, THF, etc.) induce the formation of $\alpha$-helices as secondary structures, followed by the aggregation of these structures. In dipolar aprotic solvents (DAS) like DMF or DMSO, $\alpha$-helix formation still occurs but aggregation is prevented due to the H-bonding with the solvent instead. On the other hand, the presence of a solvatation layer inhibits aminolysis at the start but when a few side groups are modified, the layer is fragmented and the reaction speed drastically increases.

The final products were verified using FTIR and $^{1}$H-NMR. Due to the solubility of these compounds in water, the molecular weight was determined by gel-permeation chromatography (GPC) in a $NaH_2PO_4/CH_3CN$ buffer (pH = 4) using dextran standards.

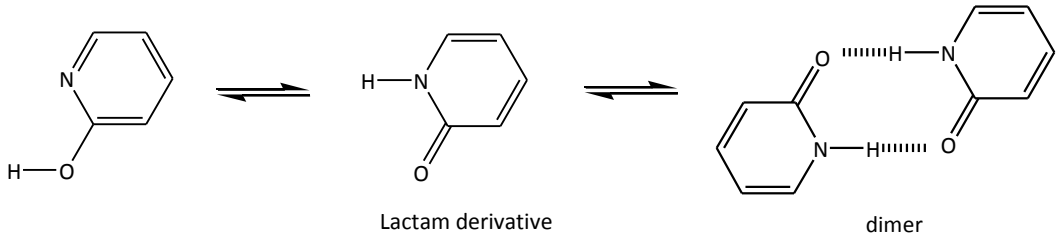


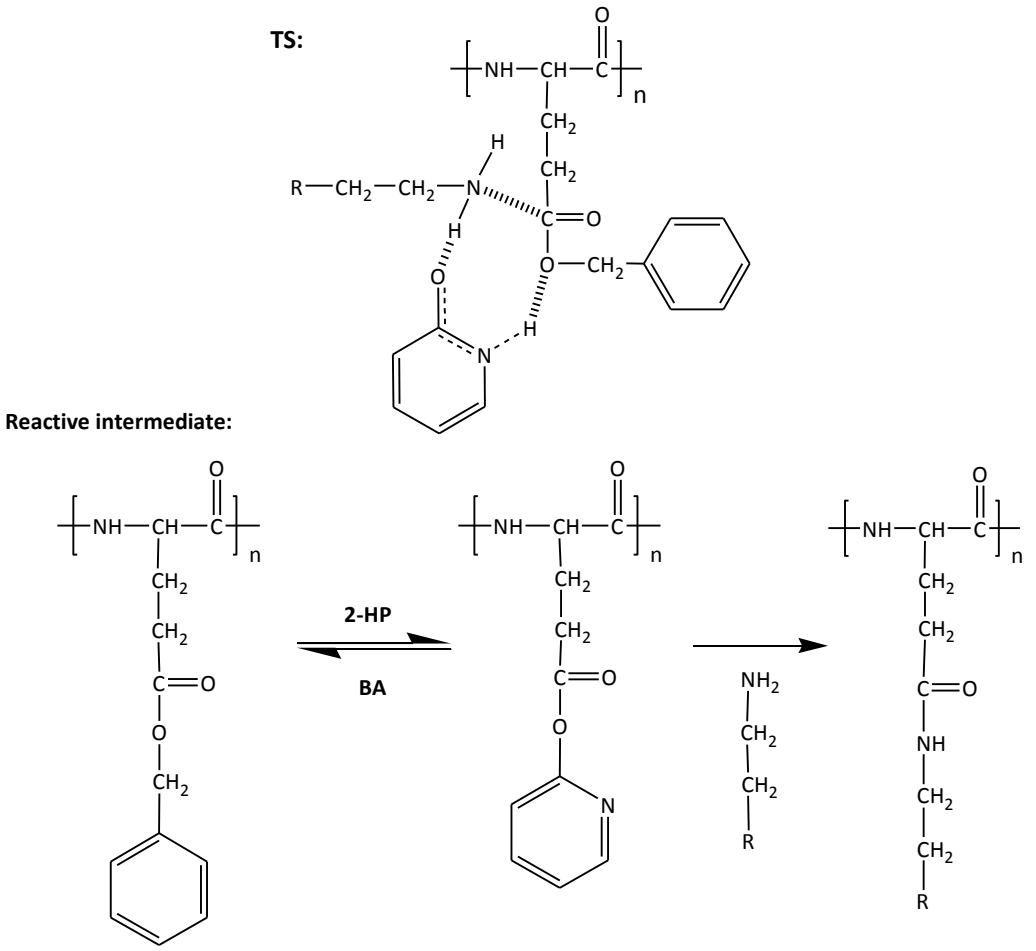


**Figure 2.18 – Tautomeric forms of the bifunctional catalyst 2-hydroxypyridine and the representation of the possible TS-mechanism versus the reactive intermediate compound strategy during aminolysis reaction of pBG & reagent[42].**

### *2.4.2 Synthesis of poly(dimethylaminoethyl)-L-glutamine (pDMAEG)*

Similar to well-studied polymers like pEI and pLL, the presence of charged groups in L-glutamine derivatives is a necessity for obtaining DNA packing into small, well-defined structures. For that reason, the incorporation of tertiary amines was applied and expected to yield polymers which possess functional groups with proper $pK_a$ behaviour (≈ 10.5)[16,47]. The

reaction was carried out in DMF (pBG concentration of 10 w/v %) at a temperature of 50 °C. Five equivalents of 2-HP were added to prevent transamidation of the backbone as well as a 20-fold excess of dimethylaminoethylamine (DMAEA) to ensure complete conversion of the benzylester. The amount of amine reagent added, is determining for the conversion rate. Too few product can only reach partial conversion, too much equivalents can enhance backbone scissoring. The conversion was followed via FTIR. After 48 hours, another five equivalents of DMAEA were added and allowed to react for 2 hours to ensure complete conversion. The final product was purified and isolated by precipitation in cooled diethylether and subsequently dialysed. The product was verified by $^{1}$H-NMR ($D_2O$) as shown Fig. 2.19.

Several polymers with different MW were prepared (Table 2.3). For pDMAEG based on low MW pBG, the polydispersity was not determined experimentally but is expected to be close to one (like its base polymer pBG) as the backbone cutting is minimised by the catalyst.

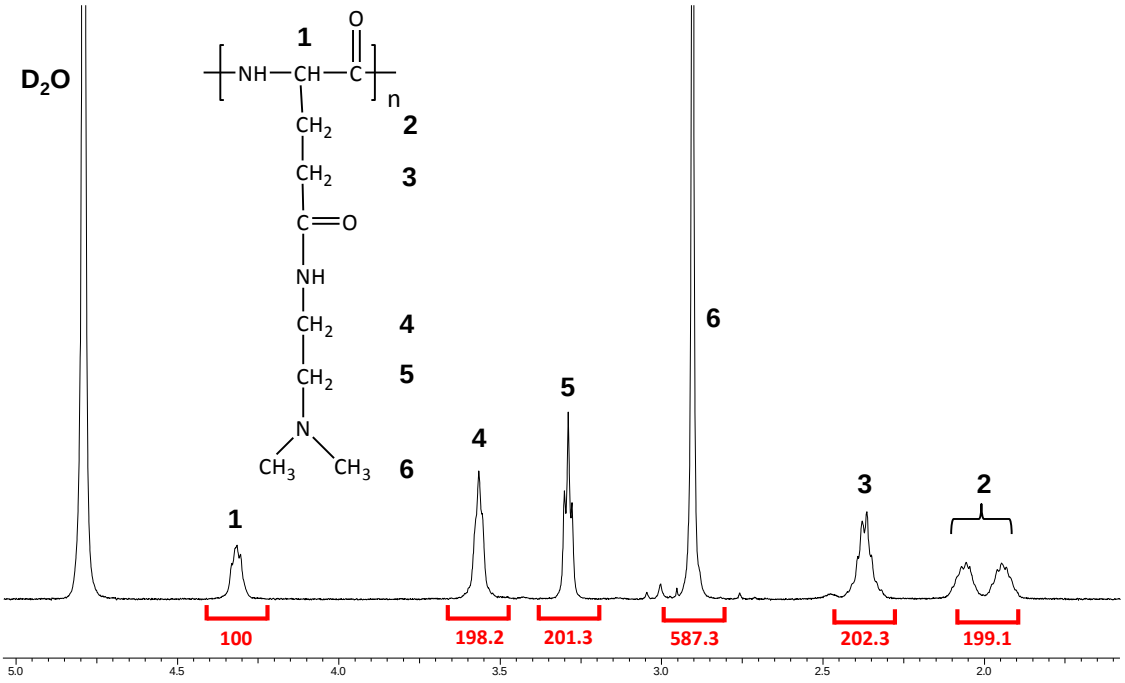


**Figure 2.19 - $^{1}$H-NMR of pDMAEG (obtained in $D_2O$).**

| MW (Da) | polydispersity (λ) |
|---|---|
| 10.000 | - |
| 29.000 | - |
| 80.000 | 1,24 |
| 242.000 | 1,36 |

**Table 2.3 – Overview of the MW of various pDMAEG prepared**

### *2.4.3 Synthesis of poly(dimethylaminoethyl-co-aminoethyl)-L-glutamine (p(DMAEG-AEG))*

For certain applications, polymers need to be functionalised using bioactive molecules (cell-penetrating peptides, glycoaminoglycans, etc.). Coupling to a tertiary amine, present in pDMAEG, is not straightforward due to the limited nucleophilic properties for coupling reactions. Therefore, primary amines were introduced as an extra functional group. Since a small quantity of active molecules is traditionally sufficient to induce an obvious effect, a low amount of primary amines was built-in during aminolysis (in combination with tertiary amines). To a solution of pBG in DMF (10 w/v %), both DMAEA (15 equivalents) as well as mono-protected diamine, *N*-tritylaminoethylamine (TrAEA, 5 equivalents) and 2-HP (5 equivalents) were added and reacted for 48 hours at 50 °C. Another 5 equivalents of DMAEA was reacted for 2 more hours to ensure full conversion. The resulting product was isolated in cooled diethylether, dried and redissolved in pure TFA in order to cleave the trityl protective group. The final product was again precipitated in diethylether, dried and dissolved in water to be purified finally by dialysis. Confirmation of the polymer structure and purity was proven by $^{1}$H-NMR (Fig 2.20 – detail, other peaks equal to the $^{1}$H-NMR of pDMAEG, Fig. 2.19).

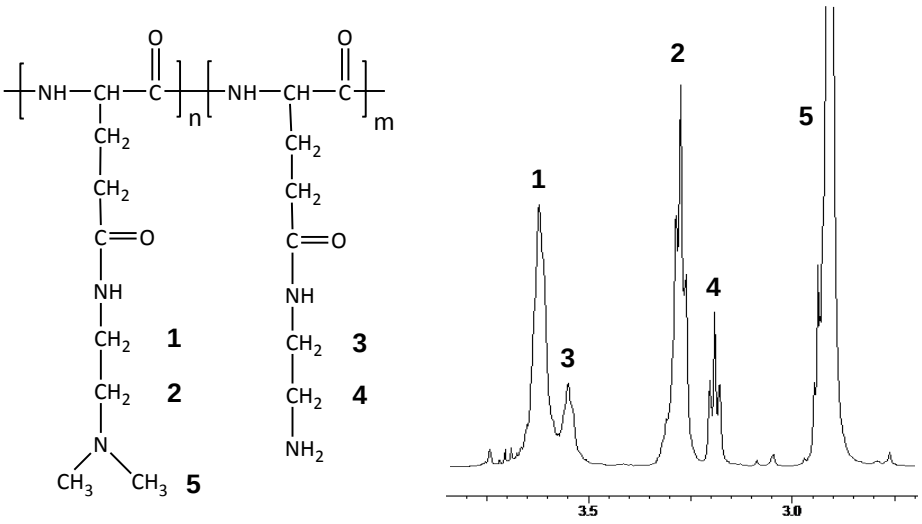


**Figure 2.20 - Structure of p(DMAEG-AEG) as determined by $^{1}$H-NMR.**

Regarding the amount of primary amines required, consideration was given to the lower reactivity of the voluminous trityl (triphenylmethyl-) group and the equivalents used for the aminolysis reaction. Preliminary experiments showed that a degree of 15 % primary amines could be obtained with a ratio of 15/5 equivalents DMAEA/TrAEA. Continued synthesis led to the conclusion that for shorter polymer chains, the degree of primary amines was slightly reduced (to 10 %) using the same ratio of reagents. Several compounds of various MW were produced with a nearly constant degree of primary amines (10-15 %) (Table 2.4).

| MW (Da) | Composition ($NMe_2/NH_2$) | polydispersity ($\lambda$) |
|---|---|---|
| 5.500 | 90 / 10 % | - |
| 27.000 | 90 / 10 % | - |
| 91.000 | 85 / 15 % | 1,51 |
| 242.000 | 85 / 15 % | 1,43 |

**Table 2.4 - Overview of the MW of the various p(DMAEG-AEG).**

### *2.4.4 Synthesis of poly(dimethylaminoethyl-co-hydroxyethyl)-L-glutamine (p(DMAEG-HEG))*

Besides the evident interaction properties with DNA, a synthetic vector must also be able to introduce DNA into the cytoplasm of a cell. Therefore it is believed that DNA should dissociate from the vector when it has escaped the endosomal pathway. Polyplexes which exhibit attractive forces that are too strong, can experience difficulties in releasing the DNA and accordingly hamper the transfection process. To anticipate this problem, a series of polymers was developed using neutral groups (hydroxyl groups) that are not charged at physiological pH. These functional groups can easily be incorporated during the final aminolysis step by applying a suitable reagent (2-aminoethanol, AE). To synthesise an L-glutamine derivative with both neutral and charged groups, pBG is dissolved in DMF and heated to 50 °C. Five equivalents of 2-HP, together with a combined amount of DMAEA and AE (relative ratio equal to the desired polymer composition and considering the difference in reactivity, see 2.4.7) totalling a 20-fold excess were added and the mixture was stirred for 48 hours followed by the addition of another 2 equivalents (reaction of 2 hours). The reaction was purified by precipitation in cooled diethylether, filtered off, washed and redissolved in water for purification by dialysis. The formed compounds are displayed in table 2.5. Compared to TrAEA, the reactivity of the AE reagent was higher and resulted in polymers composed of less tertiary amines.

| MW (Da) | Composition ($NMe_2$/OH) | polydispersity ($\lambda$) |
|---|---|---|
| 11.100 | 40 / 60 % | - |
| 11.900 | 61 / 39 % | - |
| 179.000 | 62 / 38 % | 1,19 |

**Table 2.5 - Overview of the MW of various p(DMAEG-HEG) prepared.**

Structure elucidation and composition was obtained via $^1$H-NMR analysis (Fig 2.21 – detail other peaks equal to pDMAEG, Fig. 2.19).

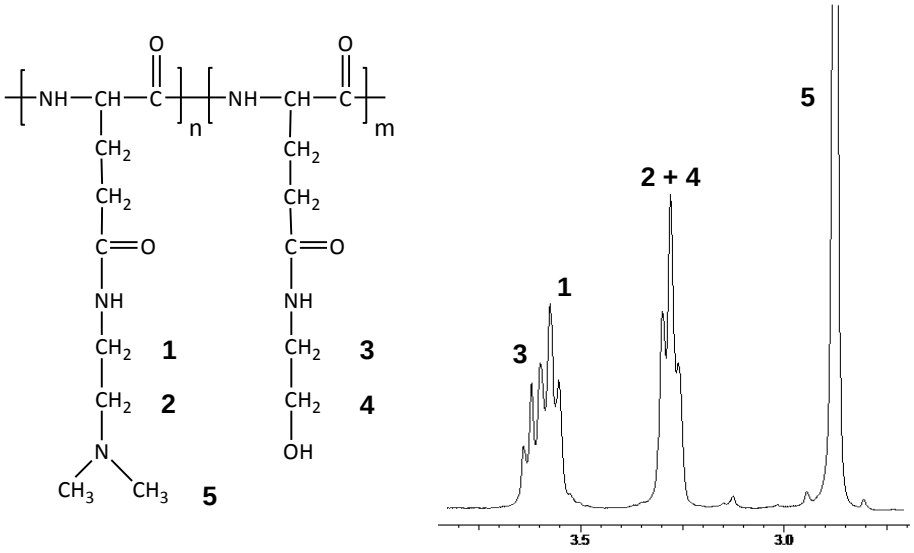


**Figure 2.21 - Structure of p(DMAEG-HEG) as obtained by $^1$H-NMR ($D_2O$).**

### *2.4.5 Synthesis of poly(aminoethyl-co-hydroxyethyl-co-imidazolethyl)-L-glutamine (p(AEG-HEG-ImEG))*

Another crucial aspect of the transfection process lies in the ability of a polyplex to be released from endosome vesicles, once internalised in the cell. As mentioned before, the generally accepted mechanism for this escape, is the proton sponge theory. Consequently, the use of functional groups that can buffer during this endosomal stay, increase the chance for release. One of the chemical structures that displays acid-base properties in the range of the endosomal pH is imidazole ($pK_a$ of conjugated acid ≈ 7). Also pyridine could be selected for this task ($pK_a$ conjugated acid ≈ 5) but priority was given to the more natural resembling imidazole moieties (e.g. histidine). These functional groups can be introduced by using histamine ($NH_2$-$CH_2$-$CH_2$-Imidazole) as an aminolysis reagent (in combination with other aminolysis reagents in a relative ratio corresponding with the desired polymer composition and considering the reactivity properties). Dependent on the amount of imidazole required, an excess is used. A similar reaction course and purification method as before was carried out. The composition of the polymer was determined using $^1$H-NMR of which the structure and corresponding distinct peaks are displayed in Fig. 2.22. The synthesised compounds are given in table 2.6.

| MW (Da) | Composition ($NH_2$/OH/Im) | polydispersity ($\lambda$) |
|---|---|---|
| 26.000 | 12 / 79 / 9 % | - |
| 9.900 | 15 / 49 / 36 % | - |

**Table 2.6 - Overview of the MW of the various p(AEG-HEG-ImEG): MW & composition.**

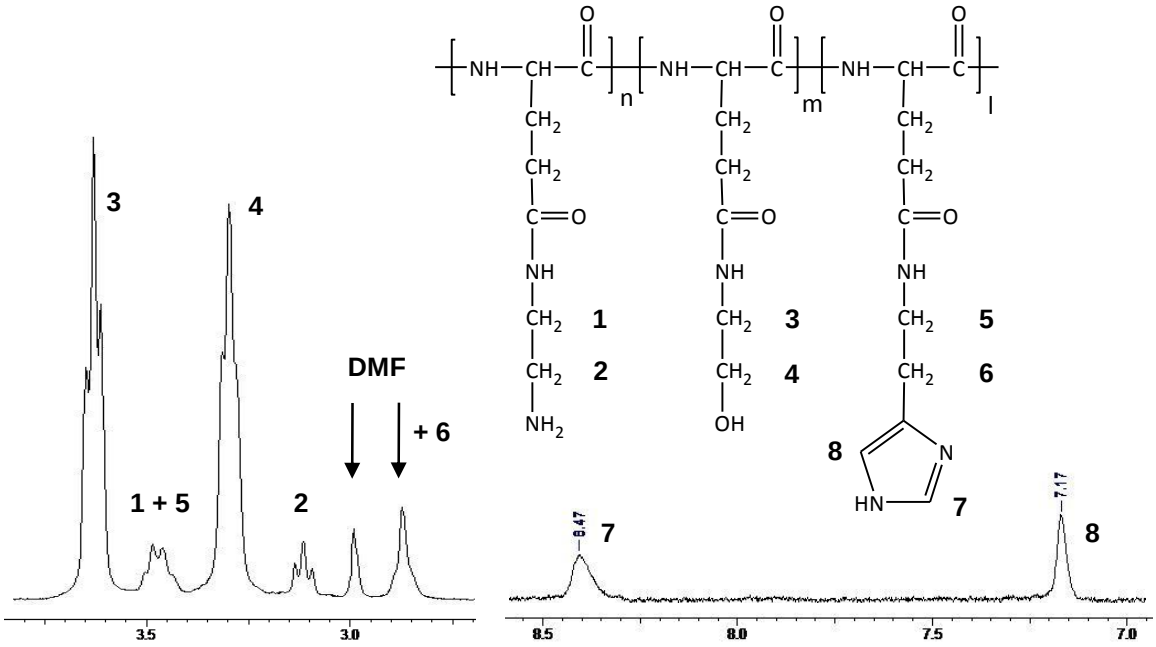


**Figure 2.22 - Structure of p(AEG-HEG-ImEG) as obtained by $^{1}$H-NMR ($D_2O$).**

### *2.4.6 Synthesis of poly(hydroxyethyl-co-guanidylethyl)-L-glutamine (p(HEG-GuAEG))*

In an attempt to produce synthetic vectors which display optimal, biocompatible properties, an alternative functional group for DNA interaction was considered. Due to the natural resemblance with histones, guanidine functional groups are believed to interact strongly with DNA and can additionally assist in the cellular uptake (see chapter 1 – 3.2)[16]. The distribution of the charge for a guanidine group is more diffuse than for a tertiary or primary amine which results in a different interaction behaviour and the ability to target different types of anionic ligands present on the cell surface (e.g. glycoaminoglycans) via bidentate bridges (Fig. 2.23).

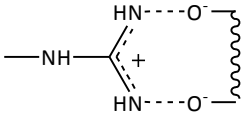

**Figure 2.23 – bidentate bridging for a guanidine functional group.**

Because of the nucleophilic nature of guanidine ($pK_a$ conjugated acid ≈ 12.5), the functional group needs to be protected or introduced during a separate modification step. Two pathways were compared and achieved equal final products (Fig. 2.24).

> *Guanidine conversion:* in a first approach, the polymers are functionalised with primary amines (including other functional groups) during aminolysis. After deprotection, the primary amine can be converted into a guanidine using 3,5-dimethyl-1-guanylpyrrazole (DMGP) via a nucleophilic substitution reaction[50,51].

*Protected guanidine:* commercially available, BOC-protected derivatives of guanidinethylamine are used during aminolysis. In a next step the BOC group is removed via acidolysis (TFA/$CH_2Cl_2$).

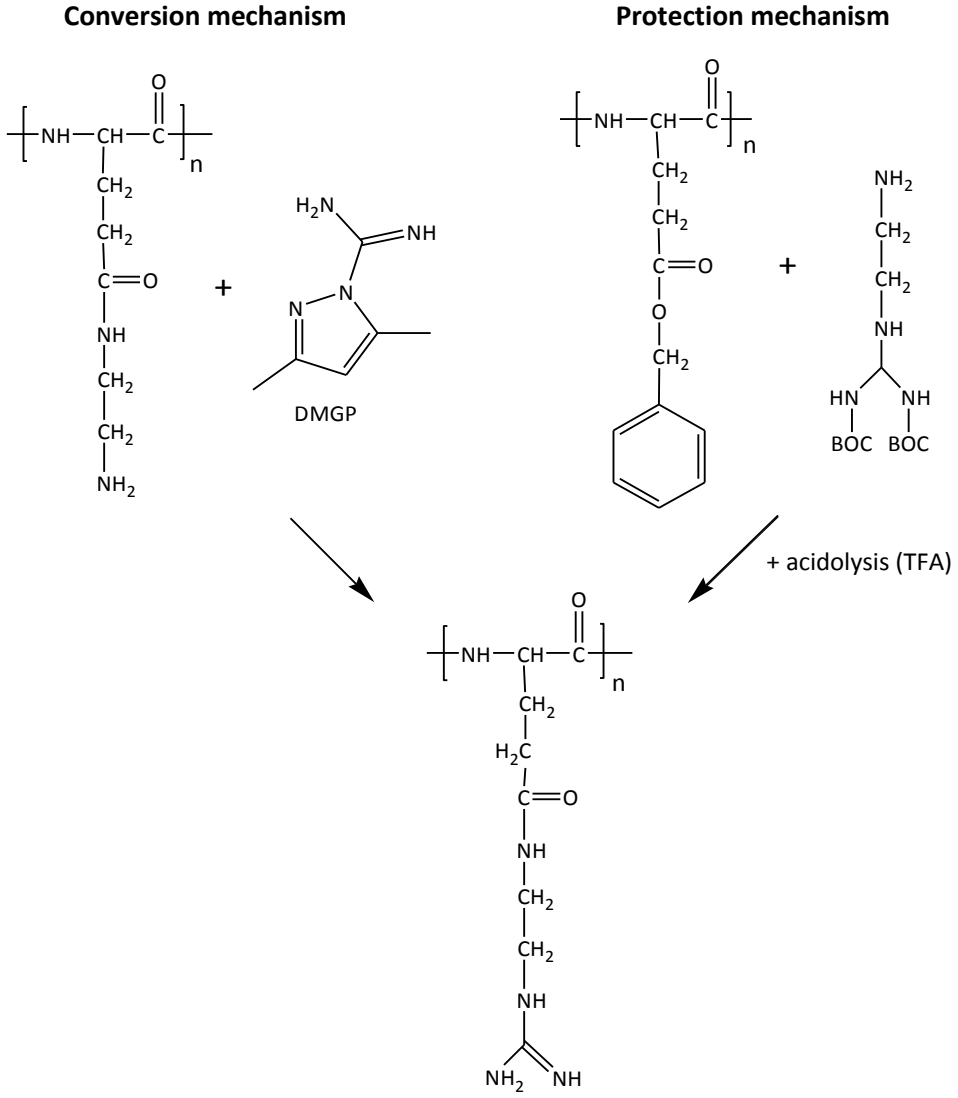


**Figure 2.24 – Overview of two alternative reaction strategies for the introduction of guanidine functional groups: conversion or protection strategy.**

The practical synthesis of p(HEG-GuAEG) using the protection strategy is similar to the aminolysis and acidolysis of p(DMAEG-AEG). For the use of the conversion method, an additional reaction step is required. Once the production of p(HEG-AEG) is completed (post dialysis), the polymer is dissolved in $H_2O$ (5 w/w %) and KI is added to a total concentration of 6 M. In a separate recipient, 16 equivalents (relative to corresponding # of moles $–NH_2$) of DMGP are dissolved in $H_2O$ and the pH is adjusted to 9.5 using KOH (4 M). The 2 mixtures are combined and allowed to react overnight. Next, neutral pH is restored and the solution is dialysed against pure water. The side product, 3,5-dimethylpyrazole, is poorly soluble in an

acidic environment and needs to be removed prior to protonation of the guanidylated polymer (achieved via acidic dialysis, 0.1 M HCl). The composition was again confirmed by $^{1}$H-NMR (Fig. 2.25).

Since guanidine-containing compounds are expected to yield promising results in biological testing, a series of polymers was produced (table 2.7).

| MW (Da) | Composition (OH/Gua) | polydispersity (λ) |
|---|---|---|
| 9.600 | 63 / 37 % | - |
| 10.200 | 75 / 25 % | - |
| 11.400 | 85 / 15 % | - |
| 26.900 | 87 / 13 % | - |
| 146.000 | 87 / 13 % | 1,79 |

**Table 2.7 – Overview of the MW of the various p(HEG-GuAEG).**

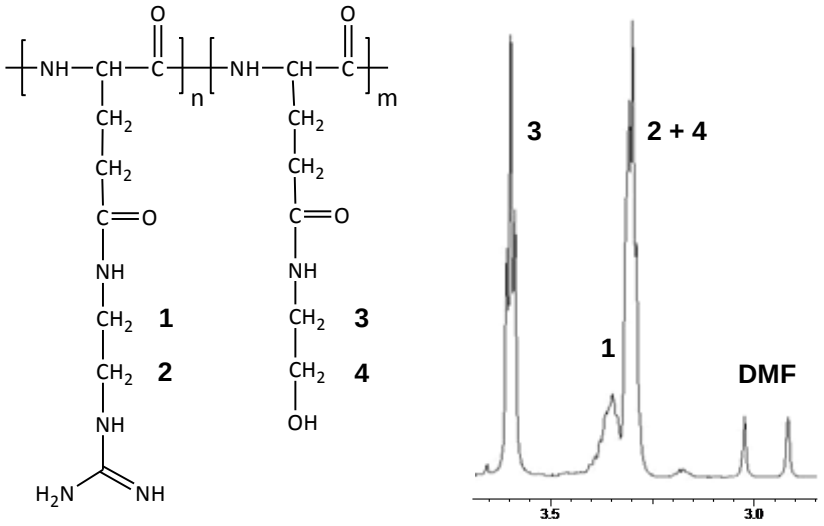


**Figure 2.25 - Structure of p(HEG-GuAEG) as obtained by $^{1}$H-NMR.**

### *2.4.7 Synthesis of multifunctional poly-L-glutamines*

As was already mentioned during the introduction, diverse functional groups are required to form a synthetic vector which possesses all the properties that ensure the appropriate functioning as a delivery device. In the previous sections, the synthesis of polymers with different types of functional groups was reported and by combining one or more of these modification reactions, poly-L-glutamine derivatives with multifunctional properties were prepared. Table 2.8 gives an overview of the composition (% molar ratio) and MW (Da) of these compounds .

| MW (Da) | -guanidine | -$NMe_2$ | -$NH_2$ | -OH | -imidazole | polydispersity ($\delta$) |
|---|---|---|---|---|---|---|
| 59.700 | 11 % | 13 % | - | 76 % | - | 1.37 |
| 9.300 | 27 % | 23 % | - | 50 % | - | - |
| 63.200 | - | 13 % | 11 % | 76 % | - | 1.40 |
| 50.400 | - | 23 % | 21 % | 56 % | - | 1.24 |
| 23.000 | 21 % | - | 16 % | 63 % | - | - |
| 23.000 | 32 % | - | 5 % | 63 % | - | - |
| 12.000 | 50 % | - | 7 % | 43 % | - | - |
| 9.700 | 26 % | - | 32 % | 42 % | - | - |
| 9.600 | 11 % | - | - | 32 % | 57 % | - |
| 12.800 | 20 % | - | - | - | 80 % | - |
| 13.000 | 35 % | - | - | - | 65 % | - |

**Table 2.8 - Overview of multifunctional vectors: composition (% molar ratio) and MW (Da).**

In all cases, polymers containing a substantial amount of neutral functional groups (non-charged) were synthesised. Furthermore, a combination of charged moieties was incorporated as well as primary amines that allowed subsequent coupling. All polymers were verified by $^{1}$H-NMR analysis. The presence of two or more functional groups gave rise to overlapping signals but did not hamper the identification since one reference signal always remained.

The numerous modification reactions (aminolysis) allowed the subdivision of the reagents in terms of reactivity. The trend could be fully attributed to the degree of spatial volume of the reagent and the steric hindrance. A qualitative ordering is given in Fig. 2.26.

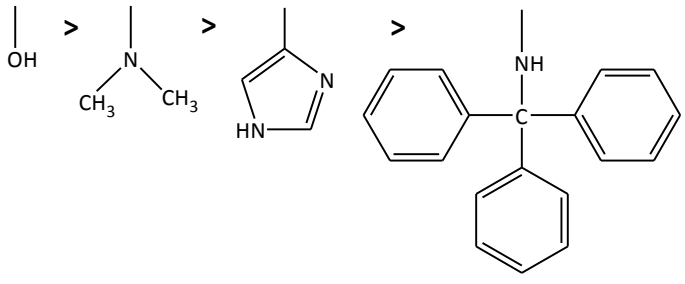


**Figure 2.26 - subdivision of reagent reactivity.**

## 3 Synthesis of poly-L-arginine derivatives

The synthesis of poly-L-arginine is not straightforward due to the high basicity of the guanidinium group that exhibits specific nucleophilic properties. To circumvent the laborious methods of protecting all nitrogen containing functional groups so that cyclisation of an NCA becomes feasible[48], the use of a precursor polymer was considered (poly-L-ornithine). Moreover, the use of protected L-arginine derivatives does not ensure success since the cyclisation of such a compound is seriously hampered by the competing intra-molecular δ-lactam formation[49]. The use of this precursor requires an additional modification step but on the other side, initial protection is not required since this compound is commercially available.

### 3.1 N-carboxyanhydride derivative of $N^{\delta}$-benzyloxy-L-ornithine (ZO)

Producing the α-NCA derivative of protected $N^{\delta}$-benzyloxy-L-ornithine (ZO) occurs in the same way as for BG-NCA (mentioned in section 2.2). The reaction is carried out by reacting with diphosgene in EtOAc at elevated temperature until the suspension becomes a solution. Thorough degassing remains a crucial step to prevent side-reactions and to minimise the presence of chloride ions inside the final product. The product is recrystallised from EtOAc and precipitated in cooled pentane. The product was again confirmed by $^{1}$H-NMR and FTIR (Table 2.9). Seeing that the R-specific group of the NCA has no influence on the carbonyl stretches of the anhydride, the absorption peaks have the same value. Only the urethane carbonyl stretch is slightly different. Characteristic peaks of the $^{1}$H-NMR are shown in the image below (Fig. 2.27). A slight contamination of EtOAC can be observed (peaks a, b, c).

| Peak value ($cm^{-1}$) | Corresponding structure |
|---|---|
| 3.300 | amide N-H stretch |
| 3.020 | C-H stretch (benzyl) |
| 2.800-2.950 | C-H stretch (-$CH_2$/-$CH_3$) |
| 1.870 | anhydride I (-N-**C=O**) stretch |
| 1.780 | anhydride II (-C-**C=O**) stretch |
| 1.740 | **O=C**-NH (carbonyl) stretch |
| 1.520 | O=C-**NH** (amide II) bend |
| 730 | C-H bend (benzyl) |

**Table 2.9 – Diagnostic FTIR signals for ZO-NCA (KBr).**

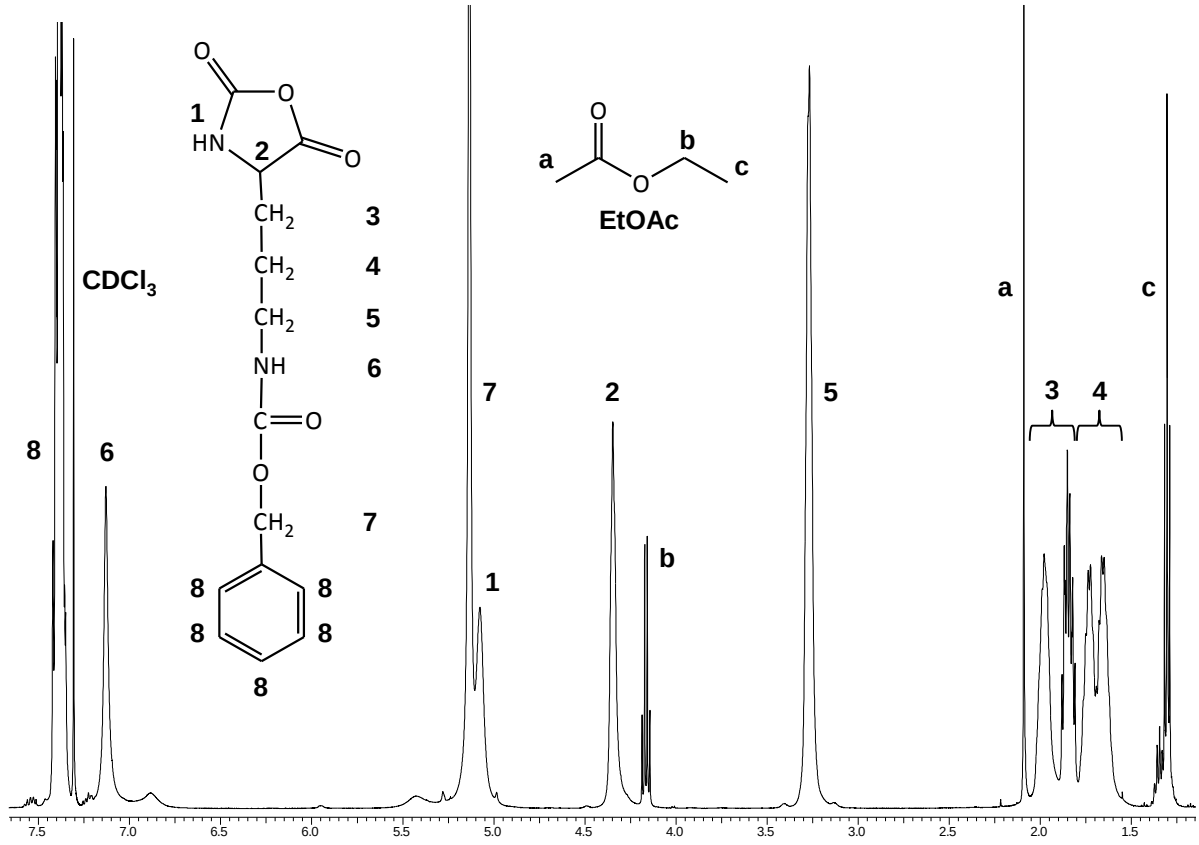


**Figure 2.27 – Structure of ZO-NCA as obtained by $^{1}$H-NMR (in $CDCl_3$).**

### 3.2 Polymerisation: synthesis of poly($^{\delta}$N-CBZ)-L-ornithine

In a corresponding way to the previous ring-opening-polymerisation of BG-NCA (section 2.3.), the formation of poly($^{\delta}$N-carbobenzyloxy)-L-ornithine (pZO) occurs through a similar reaction mechanism. Dependent on the type of initiator used, different propagation mechanisms are realised. Also the MW is controlled by the amount of initiator added (low MW polymers via R-$NH_2$ and high MW polymers by the use of $R_3N$). Viscosimetry (in $CHCl_2COOH$) was used to determine the MW of the intermediate compound.

### 3.3 Deprotection: synthesis of poly-L-ornithine

Following polymerisation, the intermediate poly($^{\delta}$N-CBZ)-L-ornithine is immediately converted into poly-L-ornithine by removal (cleavage) of the protective group (acidolysis in HBr). Poly($^{\delta}$N-CBZ)-L-ornithine is first dissolved in $CHCl_3$ (20 w/v%) and 10 ml of HBr (33 % in $CH_3COOH$) is gently added. The mixture is allowed to react for 1 hour and is subsequently precipitated in cooled diethylether and filtered off. The final product, poly-L-ornithine (pORN) is neutralised in $NaHCO_3$-containing water (4 w/v %) and further purified by liquid extraction with diethylether. The water phase, containing the polymer is isolated and dialysed against NaCl (0.5 M) followed by HCl (0.1 M) and ultrapure water (analysis via $^{1}$H-NMR, Fig. 2.28).

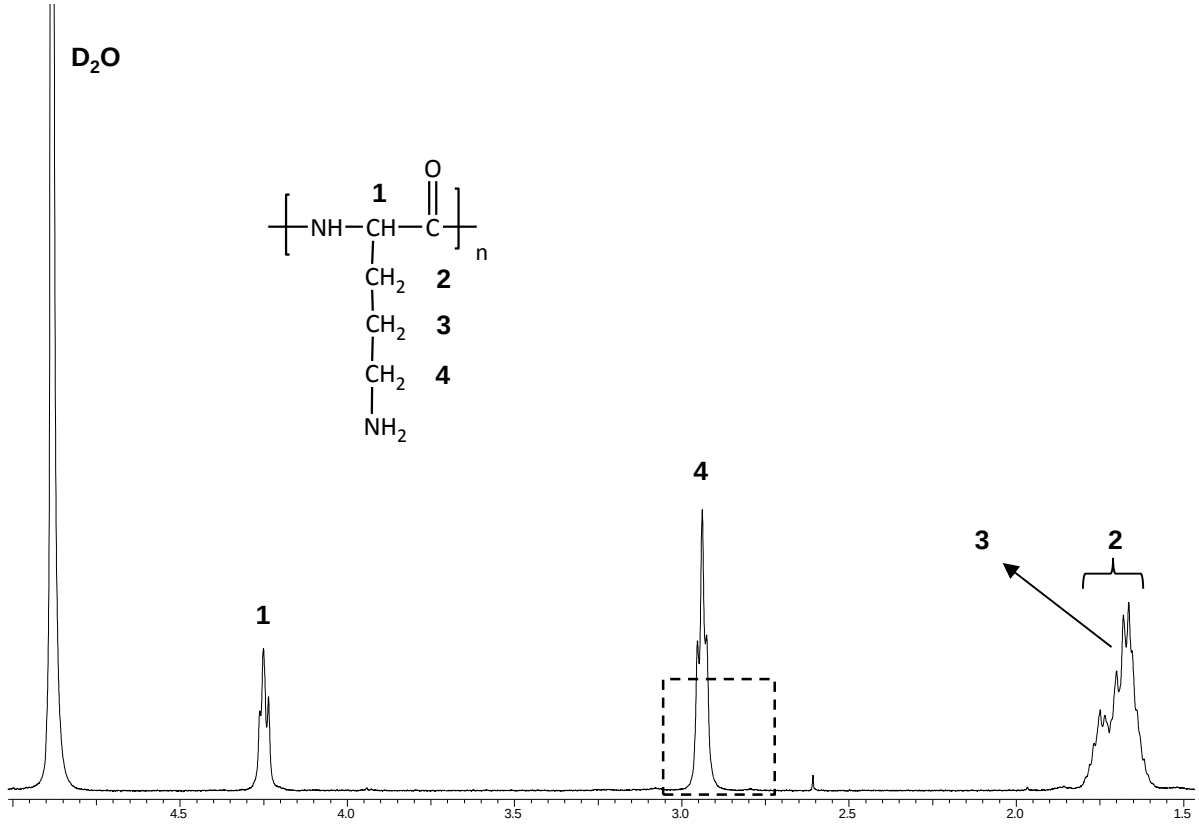


**Figure 2.28 – Structure of pORN as obtained by $^{1}$H-NMR.**

### 3.4 Guanidine conversion: synthesis poly-L-arginine

Once the precursor (pORN) is available, poly-L-arginine (pARG) can be obtained via a guanidine modification. To realise this, a guanidylating agent (3,5-dimethyl-1-guanylpyrazole or DMGP) was allowed to react with a solution of pORN.HCl in water (at pH = 9.5)[50]. The conversion of an amine into a guanidine functional group is a straightforward reaction but converting all functional groups located on side-chains of (high MW) polymers has sterical implications[51]. As a first measure, a substantial excess of guanidylating agent is added (15 equivalents). Additionally, initial testing has pointed out that no more than 70 % of the amines were converted using this method. To improve this modification, the use of high ionic concentrations was suggested and was tested for KI (6M)[52]. It appears that the addition of these ions was able to increase the conversion to nearly quantitative yields (Fig. 2.29). Since the addition of KI to the conversion reaction of L-ornithine into L-arginine has no apparent influence, it is believed that the effect is exclusively macromolecular (conformational), most likely due to the large atomic ratio and corresponding lower surface charge of the iodine anion which is able to interact better with the macromolecule (which is at that time deprotonated and can undergo only hydrophobic/hydrophilic interactions rather than dispersion forces)[53]. As a result, the degree of conversion can be controlled in time which was confirmed by the observed decrease when the MW of pORN was lowered (table 2.10).

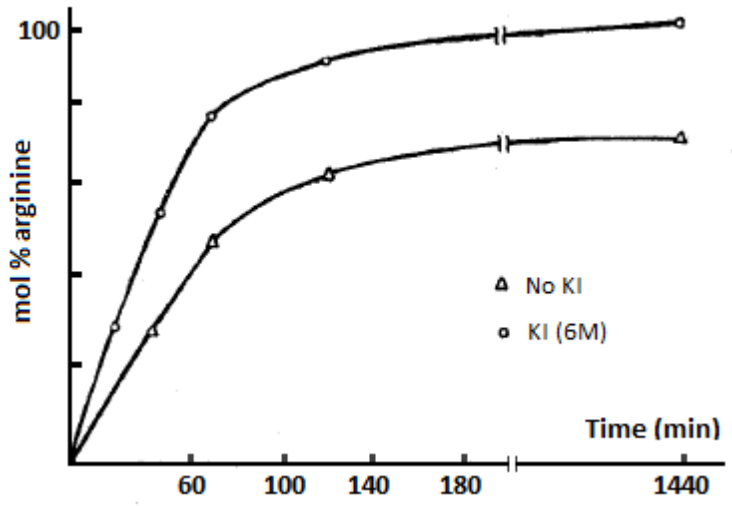


**Figure 2.29 – Influence of KI (6M) on the conversion of pORN in pARG.**

Given this information, it is possible to select the degree of conversion by adjusting the reaction time. In this way, the pARG derivative still contains primary amines available for subsequent coupling reactions.

Practically, pORN is dissolved in water (5 w/w %). A solution of 15 equivalents DMGP, dissolved in water and adjusted to a pH of 9.5, is added to the polymer solution. Finally, KI is mixed in to attain a total concentration of 6M. The reaction is allowed to continue overnight after which the pH is neutralised using 0.1 M HCl and dialysed against ultrapure water. After 24 hours, the polymer solution is acidified (pH ≈ 5) and further dialysed against ultratpure water.

Confirmation of the product was obtained by $^{1}$H-NMR (Fig. 2.30). In the past, the presence of guanidine functional groups was predominantly demonstrated by the Sakaguchi reaction[54]. In this reaction, the specific and exclusive coloration interaction between the guanidine group and $\alpha$-napthol/NaOBr was determined using VIS-spectroscopy (and a calibration curve)[55]. Because of the extensive procedure and time-consuming nature in combination with the relative error margin that is inherent to coloration methods, this experiment was only applied as a proof of principle. More reliable results can nowadays be obtained by improved NMR techniques with high magnetic fields (e.g. 700 MHz)[56]. The chemical structure of pORN and pARG is very similar and the conversion can only be determined by comparing the $\delta$-$CH_2$ peak of both components which displays triplet-coupling at 2.9 ppm for pORN that undergoes a shift to 3.1 ppm in the case of pARG. The detailed part of the spectrum indicates that the remaining amine signal is not higher than 1 %.

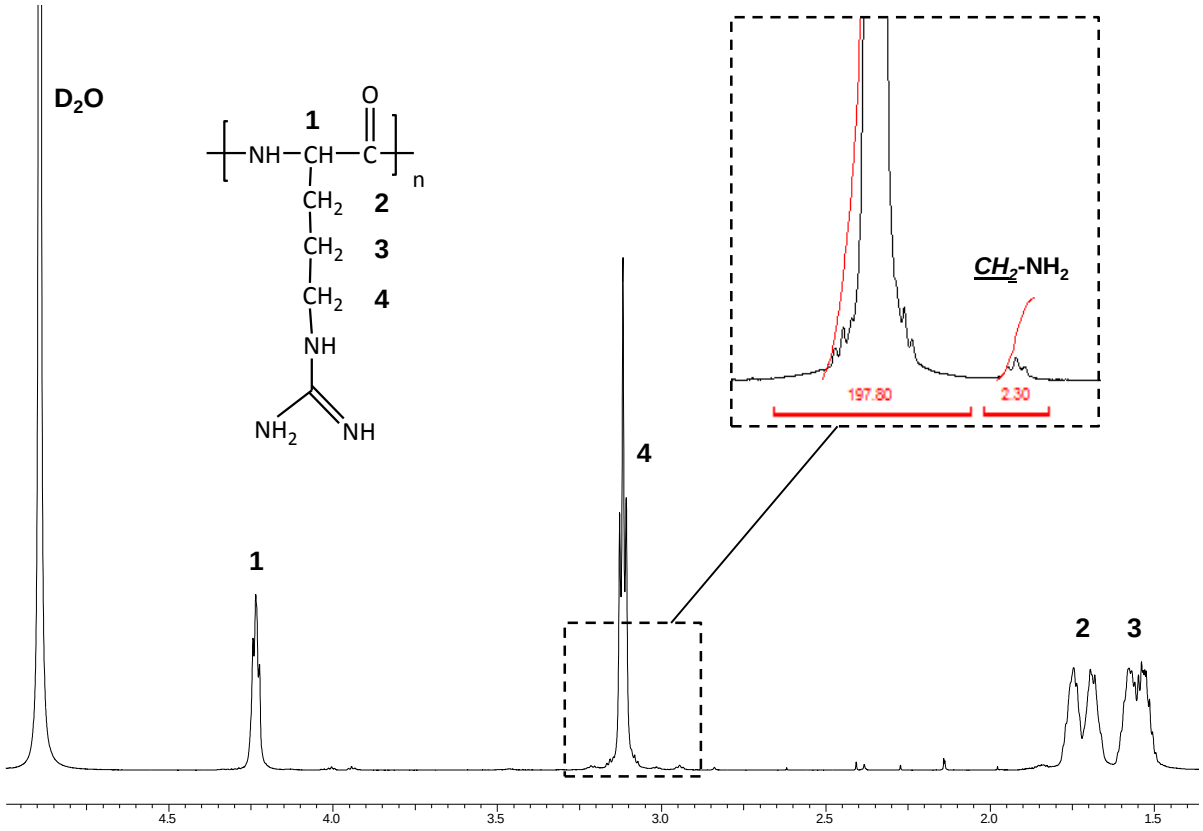


**Figure 2.30 – Structure of pARG as obtained by $^{1}$H-NMR (in D2O)**

As was performed for poly-L-glutamines, pARG derivatives with a broad range of MW were synthesised as well as polymers still possessing primary amines (pORN-ARG). Gel permeation chromatography experiments (relative to dextran standards) also confirmed the lower degree of conversion for low MW compounds (less quantitative) up to 90-95% suggesting the macromolecular effect of KI addition.

| MW (Da) | Presence of $-NH_2$ | polydispersity ($\lambda$) |
|---|---|---|
| 6.000 | 7 % | - |
| 13.000 | 5 % | - |
| 22.800 | 3 % | - |
| 78.800 | 1 % | 1,16 |
| 187.000 | 1 % | 1,49 |
| 71.100 | 18 % | 1,63 |

**Table 2.10 - Overview of pARG and p(ORN-ARG) compounds prepared.**

## 4 Synthesis of L-glutamine and L-arginine copolymers

Seeing that the polymerisation conditions of both BG-NCA as ZO-NCA are nearly identical, initial tests to form copolymers of L-(hydroxyethyl)glutamine (HEG) and L-arginine were applied. Synthesising pBG-pZO was readily achieved by ROP of a mixture of the corresponding NCA's in DCM/EtOAc. To prevent intra-molecular coupling, the primary amine of pZO needed to remain protected during aminolysis. Carbobenzyloxy (Z) is reported to be a stable protective group under nucleophilic conditions[57]. Hence, aminolysis can be performed prior to Z-deprotection (by acidolysis). Finally, guanidine conversion can be easily carried out without compromising the L-glutamine side-chains (both the amide bonds as well as the chain-end functional groups) followed by purification via dialysis. Two compounds were produced to verify the feasibility of the reaction (using a primary amine and tertiary amine respectively) as shown in table 2.11. The identical composition moreover, validates the precise practical execution of the reaction as well as the highly controllable nature of the aminolysis reaction.

| MW (Da) | % HEG | % ARG |
|---|---|---|
| 11.200 | 58 % | 42 % |
| 56.000 | 58 % | 42 % |

**Table 2.11 – Overview of p(HEG-ARG) compounds.**

## 5 Biodegradable graft-copolymers

It is generally accepted that cationic charges are important for DNA interaction and delivery. Besides the fact that the amount of charges and the combination with other functional groups needs to be controlled, there's also a substantial influence of the spatial arrangement of those charged units. Since the guanidinium group is believed to yield optimal interaction properties, several orientations of this functional group were examined. Charged groups can for instance be located on the backbone, within side chains, at the end of a side chain or on grafts starting from side chains (Fig. 2.31). The way charges are positioned within a polymer has an influence on the formation of polyplexes and the interaction with cellular entities. Finding the most advantageous charge orientation is relevant in order to minimise the amount of charge and the related toxicity.

Examples of polymers with charged guanidine groups present in side chains were shown in afore mentioned paragraphs. A special type of polymer, which bears charges in its backbone structure is pEI. Via commercial synthetic pathways, branched pEI is obtained with a ratio of primary, secondary and tertiary amines equal to about 1-2-1. Grafted (co)polymers can be produced by specific coupling reactions or by using a pre-polymer as an initiator for graft

polymerisation. Such a graft-copolymerisation was carried out using an amine-containing pre-polymer and a particular NCA (Fig. 2.32). Since primary amines are used, nearly perfect control over the MW of the grafts (living-like polymerisation) can be achieved. Unlike previous polymerizations of R-NCA, the reaction is performed in DMF which is one of the few solvents suitable for dissolving both reagents. Because the H-bonding influences the dissolution and molecular association of the formed polymers, small deviations of the MW (higher) are observed as well as a change in polydispersity[58].

Prior to the grafting process, polymers containing primary amines need to be available. Because the polymers are isolated as hydrochloride salts ($-NH_3^+Cl^-$), they need to be deprotonated. Therefore, an equivalent of KOtBu is added to a solution of the pre-polymer in DMF and reacted for 15 minutes. Next, an NCA of choice is added, followed by the standard reaction pathway required for the synthesis of multifunctional polymers as described above. Different types of pre-polymer were tested (Fig. 2.32). Glutamine (GLN) derivatives were provided with ARG-grafts whereas for PEI, grafts composed of GLN-derivatives (hydroxyethyl, HEG and guanidine-ethyl, GuAEG) were used. A large number of neutral hydroxyl groups was introduced since it is expected to be advantageous for the cytotoxicity (sufficient charge remains due to the secondary and tertiary amines present on branched PEI (table 9)). Moreover, as a result of the re-orientation of charged groups towards the outer environment, an enhanced interaction with DNA is expected.

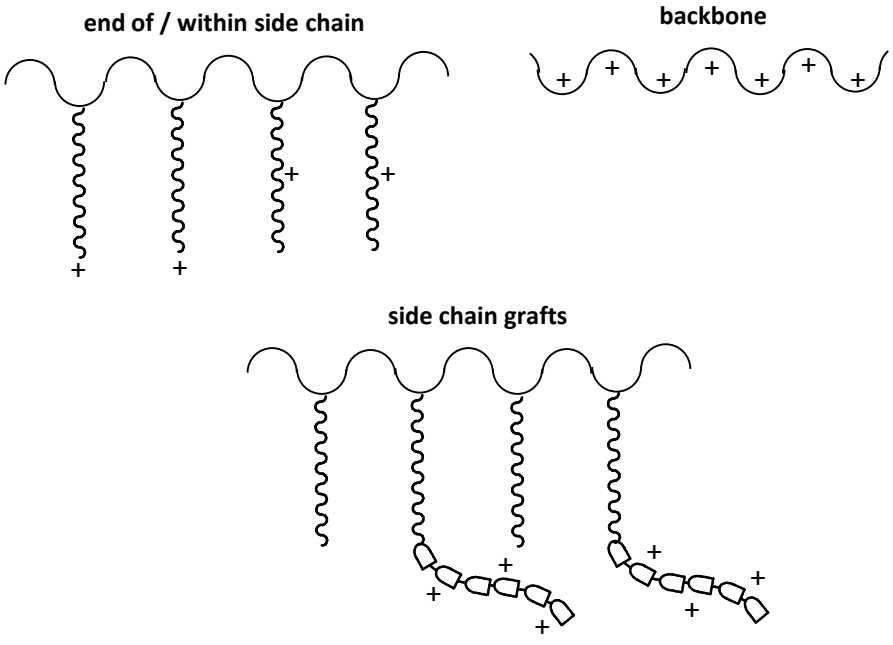


**Figure 2.31 - Position of cationic charges within a polymer**

It is also possible to incorporate guanidine groups onto branched PEI by converting the primary amines of PEI in a similar reaction as for the guanidine modification of pORN (Fig.

2.32). The degree of modification (up to 25 %) can be controlled in time and verified by a ninhydrine test or Sakaguchi test. By controlling the quantity of reagent or the reaction time, PEI-Guanidine derivatives containing 14 and 20 % of guanidine groups were prepared.

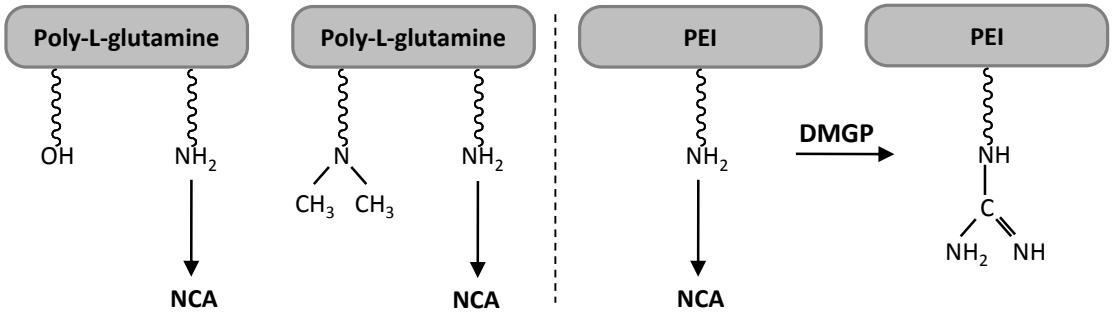


**Figure 2.32 – Schematic representation of the structure of grafted-NCA (using -$NH_2$ pre-polymer); PEI modification via NCA grafting or guanidine conversion.**

| Pre-polymer | MW (Da) | Graft type | Graft MW |
|---|---|---|---|
| p(DMAEG-AEG) | 91.000 | pARG | 5000 (± 25 units) |
| p(HEG-AEG) | 27.700 | pARG | 1500 (± 8 units) |
| pEI | 25.000 | pGLN ($OH_{63\%}$, $Gua_{37\%}$) | 3500 (± 17 units) |

**Table 2.12 – Overview of graft copolymers (composition determined by $^1$H-NMR).**

## 6 Conclusion

In this chapter, several methods were discussed that led to the synthesis of an elaborate series of multifunctional, biodegradable polymers. Various linear polymers based on L-glutamine and L-arginine, composed of different functional groups and with MW's ranging from 5.000 to 250.000 were obtained. Every different functional group is relevant for certain properties related to the vector requirements. Additionally, a well-established polymer (PEI) was subjected to guanidine conversion to assess if the positive effect of guanidine functional groups in terms of reduced toxicity and increased DNA interaction could be extended to other polymer families. Finally, also graft copolymers were produced to allow the study on charge orientation within a polymer and the implications towards polymer-DNA formation.

# 7 References


[1] Lee, K. Y., I. C. Kwon, et al. (1998). "Preparation of chitosan self-aggregates as a gene delivery system." Journal of Controlled Release **51**(2-3): 213-220.

[2] Cherng, J. Y., P. vandeWetering, et al. (1996). "Effect of size and serum proteins on transfection efficiency of poly((2-dimethylamino)ethyl methacrylate)-plasmid nanoparticles." Pharmaceutical Research **13**(7): 1038-1042.

[3] Jeong, J. H., S. W. Kim, et al. (2007). "Molecular design of functional polymers for gene therapy." Progress in Polymer Science **32**(11): 1239-1274.

[4] Nichol, C. A., D. Yang, et al. (1999). "Biodistribution and imaging of polyethyleneimine - A gene delivery agent." Drug Delivery **6**(3): 187-194.

[5] Bashford, C. L., G. M. Alder, et al. (1986). "Membrane damage by hemolytic viruses, toxings, complement and other cytotoxic agents – a common mechanism blocked by divalent-cations." Journal of Biological Chemistry **261**(20): 9300-9308.

[6] Wraith, J. E. (2001). "Advances in the treatment of lysosomal storage disease." Developmental Medicine and Child Neurology **43**(9): 639-646.

[7] Bouri, K., W. G. Feero, et al. (1999). "Polylysine modification of adenoviral fiber protein enhances muscle cell transduction." Human Gene Therapy **10**(10): 1633-1640.

[8] Chan, C. K. and D. A. Jans (1999). "Enhancement of polylysine-mediated transferrinfection by nuclear localization sequences: Polylysine does not function as a nuclear localization sequence." Human Gene Therapy **10**(10): 1695-1702.

[9] Matsui, H., K. Tomizawa, et al. (2003). "Protein therapy: In vivo protein transduction by polyarginine (11R) PTD and subcellular targeting delivery." Current Protein & Peptide Science **4**(2): 151-157.

[10] Cheng, N., W. G. Liu, et al. (2006). "A study of thermoresponsive poly(N-isopropylacrylamide)/polyarginine bioconjugate non-viral transgene vectors." Biomaterials **27**(28): 4984-4992.

[11] Holowka, E. P., V. Z. Sun, et al. (2007). "Polyarginine segments in block copolypeptides drive both vesicular assembly and intracellular delivery." Nature Materials **6**(1): 52-57.

[12] Lee, H., J. H. Jeong, et al. (2002). "PEG grafted polylysine with fusogenic peptide for gene delivery: high transfection efficiency with low cytotoxicity." Journal of Controlled Release **79**(1-3): 283-291.

[13] Ramsay, E. and M. Gumbleton (2002). "Polylysine and polyornithine gene transfer complexes: A study of complex stability and cellular uptake as a basis for their differential in-vitro transfection efficiency." Journal of Drug Targeting **10**(1): 1-9.

[14] Xue, W. H., H. J. Diao, et al. (2007). "An efficient vector for gene delivery: α,β-poly(3-dimethylaminopropyl-D,L-aspartamide)." European Journal of Pharmaceutics and Biopharmaceutics **66**(3): 327-333.

[15] Itaka, K., T. Ishii, et al. (2010), "Biodegradable polyamino acid-based polycations as safe and effective gene carrier minimizing cumulative toxicity." Biomaterials **31**(13): 3707-3714.

[16] Doctoral research: L. Dekie (2003). Ghent University.

[17] Liang, K., R. Jie, et al. (2009). "6-membered ring derivatives in polymerization of N-carboxyanhydride-L-a-arginine in H2O." Science in China series B: Chemistry **52**(8): 1220-1226

[18] Blout, E. R. and R. H. Karlson (1956). "POLYPEPTIDES .3. THE SYNTHESIS OF HIGH MOLECULAR WEIGHT POLY-GAMMA-BENZYL-L-GLUTAMATES." Journal of the American Chemical Society **78**(5): 941-946.

[19] Doctoral research: Vercauteren R. (1992). Ghent University.

[20] Leuchs, H. (1906). "Ueber die Glycin-carbonsäure." Berichte der deutschen chemischen Gesellschaft **39**(1): 857–861,

[21] Farthing, A. (1950). Journal of the American Chemical Society: 3213

[22] Katakai, R., K. Uno, et al. (1972). "STEPWISE SYNTHESIS OF OLIGOPEPTIDES WITH N-CARBOXY-ALPHA AMINO ACID ANHYDRIDES .4. GLYCINE NCA." Journal of Organic Chemistry **37**(2): 327-&.

[23] Oya, M., R. Katakai, et al. (1973). "NOVEL SYNTHESIS OF N-CARBOXY-ALPHA-AMINO ACID ANHYDRIDE." Chemistry Letters(11): 1143-1144.

[24] Fuller, W. D., M. S. Verlander, et al. (1976). "PROCEDURE FOR FACILE SYNTHESIS OF AMINO-ACID N-CARBOXYANHYDRIDES." Biopolymers **15**(9): 1869-1871.

[25] Kricheldorf, K. (1987). alfa-Aminoacid-N-Carboxyanhydrides and Related Heterocycles. B. Heidelberg. NY.

[26] Mori, H., M. Iwata, et al. (2007). "Ring-opening polymerization of gamma-benzyl-L-glutamate-N-carboxyanhydride in ionic liquids." Polymer **48**(20): 5867-5877.

[27] Deming, T. J. (2000). "Living polymerization of alpha-amino acid-N-carboxyanhydrides." Journal of Polymer Science Part a-Polymer Chemistry **38**(17): 3011-3018.

[28] Bamford, C. H., A. C. P. Pugh, et al. (1961). "POLYMERIZATION OF 3-SUBSTITUTED OXAZOLIDINE-2,5-DIONES." Journal of the Chemical Society(MAY): 2057-2059.

[29] Deming, T. J. (1997). "Polypeptide Materials: New synthetic methods and applications." Advanced Materials **9**(4): 299-311.

[30] Lundberg, R. D. and P. Doty (1957). "POLYPEPTIDES .17. A STUDY OF THE KINETICS OF THE PRIMARY AMINE-INITIATED POLYMERIZATION OF N-CARBOXY-ANHYDRIDES WITH SPECIAL REFERENCE TO CONFIGURATIONAL AND STEREOCHEMICAL EFFECTS." Journal of the American Chemical Society **79**(15): 3961-3972.

[31] Scoffone, E., E. Peggion, et al. (1965). "Molecular weight distribution of polymers of gama-benzyl L glutamate." biopolymers **3**(5): 535-543.

[32] Doctoral Research: Soyez, H. (1997), Ghent University.

[33] Doty, P., J. H. Bradbury, et al. (1956). "Polypeptides. IV. The Molecular Weight, Configuration and Association of Poly-Î³-benzyl-L-glutamate in Various Solvents." Journal of the American Chemical Society **78**(5): 947-954.

[34] O. F. Solomon, I. Z. C. and acaron (1962). "Détermination de la viscosité intrinsèque de solutions de polymères par une simple détermination de la viscosité." Journal of Applied Polymer Science **6**(24): 683-686.

[35] Brandrup, J.; Immergut, et al. (1999; 2005). Polymer Handbook (4th Edition). John Wiley & Sons.

[36] Gibson, M. I. and N. R. Cameron (2009). "Experimentally Facile Controlled Polymerization of N-Carboxyan hydrides (NCAs), Including O-Benzyl-L-threonine NCA." Journal of Polymer Science Part a-Polymer Chemistry **47**(11): 2882-2891.

[37] Rinaudo, M. and A. Domard (1975). "Preparation and characterization of α-L-glutamic acid oligomers." biopolymers **14**(10): 2035-2048.

[38] Ravanat, G. and M. Rinaudo (1980). "Investigation on oligo- and polygalacturonic acids by potentiometry and circular dichroism." biopolymers **19**(12): 2209-2222.

[39] Lupulota.N, A. Yaron, et al. (1965). "CONFORMATION CHANGES IN NONIONIZABLE WATER-SOLUBLE SYNTHTIC POLYPEPTIDE POLY-N5-(3-HYDROXYPROPYL) -L-GLUTAMINE." Biopolymers **3**(6): 625.

[40] Noskova, D., R. Kotva, et al. (1988). "POLY(N-5-HYDROXYALKYL GLUTAMINES) .2. THE EFFECT OF CONFORMATION AND SOLVENT ON THE KINETICS OF POLY(GAMMA-ALKYL GLUTAMATE) AMINOLYSIS." Polymer **29**(11): 2072-2075.

[41] De Marre, A., H. Soyez, et al. (1994). "Improved method for the preparation of poly[N5-(2-hydroxyethyl)-l-glutamine] by aminolysis of poly([gamma]-benzyl-l-glutamate)." Polymer **35**(11): 2443-2446.

[42] deMarre, A., K. Hoste, et al. (1996). "Synthesis, characterization, and in vitro biodegradation of poly(ethylene glycol) modified poly[N-5-(2-hydroxyethyl-L-glutamine]." Journal of Bioactive and Compatible Polymers **11**(2): 85-99.

[43] Swain, C. G. and J. F. Brown (1952). "Concerted Displacement Reactions. VIII. Polyfunctional Catalysis1." Journal of the American Chemical Society **74**(10): 2538-2543.

[44] H. Beyerman, van den Brink W. Maassen, Proc. Chem. Soc. (1963), p. 266

[45] Brown, R. S., A. Tse, et al. (1980). "Photoelectron-determined core binding energies and predicted gas-phase basicities for the 2-hydroxypyridine .dblarw. 2-pyridone system." Journal of the American Chemical Society **102**(3): 1174-1176.

[46] Hammes, G. G. and P. J. Lillford (1970). "Kinetic and equilibrium study of the hydrogen bond dimerization of 2-pyridone in hydrogen bonding solvents." Journal of the American Chemical Society **92**(26): 7578-7585.

[47] Dekie, L., B. Calisle, et al. (2001). "New vectors for gene delivery based on poly-alpha-amino acids." Journal of Controlled Release **72**(1-3): 246-247.

[48] Hayakawa T, Kondo Y, et al. (1969). "The synthesis of poly-L-arginine hydrobromide and copolymers of L-arginine and other amino acids." Bulletin of the Chemical Society of Japan 42(2): 479-482

[49] Seo, J. and R. B. Silverman (2006). "Synthesis of arginine-containing hydroxamate dipeptidomimetics." Tetrahedron Letters **47**(24): 4069-4073.

[50] Bannard, R. A. B., A. A. Casselman, et al. (1958). "GUANIDINE COMPOUNDS .2. PREPARATION OF MONO-ALKYLGUANIDINES AND N,N-DI-ALKYLGUANIDINES." Canadian Journal of Chemistry-Revue Canadienne De Chimie **36**(11): 1541-1549.

[51] Habeeb, F. (1959). "A new reagent for the guanidination of proteins." Biochimica & Biophysica acta. **34**(6): 294-296.

[52] V.G Debabov, V. D. D., Yu.N. Kosaganov (1966). "Synthesis of poly-L-arginine and the statistical copolymer of L-arginin, L-lysine, and neutral amino acids." Khimiya Prirodnykh Soedinenii **2**(3): 195-200.

[53] Lund, M., R. Vacha, et al. (2008). "Specific Ion Binding to Macromolecules: Effects of Hydrophobicity and Ion Pairing." Langmuir **24**(7): 3387-3391.

[54] SAKAGUCHI, S. (1950). "A NEW METHOD FOR THE COLORIMETRIC DETERMINATION OF ARGININE." Journal of Biochemistry **37**(2): 231-236.

[55] Gilboe, D. D. and J. N. Williams (1956). "EVALUATION OF THE SAKAGUCHI REACTION FOR QUANTITATIVE DETERMINATION OF ARGININE." Proceedings of the Society for Experimental Biology and Medicine **91**(4): 535-536.

[56] Pauli, G. F., B. U. Jaki, et al. (2004). "Quantitative 1H NMR: Development and Potential of a Method for Natural Products Analysis." Journal of Natural Products **68**(1): 133-149.

[57] Bergmann, M. and L. Zervas (1932). "Über ein allgemeines Verfahren der Peptid-Synthese." Berichte der deutschen chemischen Gesellschaft (A and B Series) **65**(7): 1192-1201.

[58] Habraken, G. J. M., M. Peeters, et al. (2009). "How controlled and versatile is N-carboxy anhydride (NCA) polymerization at 0 [degree]C? Effect of temperature on homo-, block- and graft (co)polymerization." Polymer Chemistry **1**(4).

# Chapter 3

# Synthesis of non-biodegradable polymer vectors

# 1 Introduction

In the previous chapter, the synthesis of biodegradable systems was discussed. It is believed that these compounds would ideally be non-toxic because of their biodegradable backbone (polyamide) which can be digested by enzymes within the body and are therefore put forward as outstanding delivery systems. As could be noticed before, the total synthesis of such a polymeric vector can be quite comprehensive (up to 6 individual synthesis steps).

In literature, many non-biodegradable based delivery systems were already positively evaluated[1]. An important class of synthetic vectors explored for genetic delivery is based on methacrylate derivatives[2,3]. The presence of an aliphatic backbone renders these polymers more hydrophobic and excludes the process of enzymatic degradation[4]. In addition, corresponding polymers can be easily produced in one-pot reactions given the availability of suitable monomers.

A possible solution for the requirement of a straightforward reaction when possible industrial applications are kept in mind as well as for the validated use in terms of transfection efficiency, methacrylate-based synthetic polymers were also explored as potential delivery systems. Moreover, specific trends and correlations (for the MW or composition of functional groups) that are existing for biodegradable compounds could consequently be compared to non-biodegradable systems (or vice-versa). In this chapter, polymethacrylates will be synthesised with functional groups similar to poly-L-glutamine and poly-L-arginine derivates discussed before. Comparing the MW proved to be less simple since one of the main drawbacks of polymethacrylate synthesis is the limited control over the MW due to the unregulated nature of free radical polymerisations.

# 2 Free radical polymerisation of methacrylates

Unlike the nucleophilic ring-opening-polymerisation of NCA, the polymerisation of methacrylates occurs most conveniently via a radical mechanism. The double bond ($\pi$-bond) of a monomer can be disrupted by radicals originating from initiators which are capable of forming new C-C bonds. If this process is continuously repeated, long polymer chains (aliphatic) are developed. Traditionally, this mechanism occurs in three steps (Fig. 3.1).

*Initiation:* generally, an initiator molecule (In) is required to produce radicals needed for the homolytic cleavage of the double bond. In a first step, the initiator is split in several parts, yielding one or more radicals that are transferred to the monomer in a next step.

*Propagation:* once a radical containing monomer is generated, new monomers can be consecutively adhered. This process can be continuous until all monomer is consumed or interference reactions arise.

*Termination:* Several mechanisms can restrict or end polymerisation. The most frequently occurring reactions are transfer of the radical onto a non-reactive species (transfer agent), disproportionation and combination between two active chains.

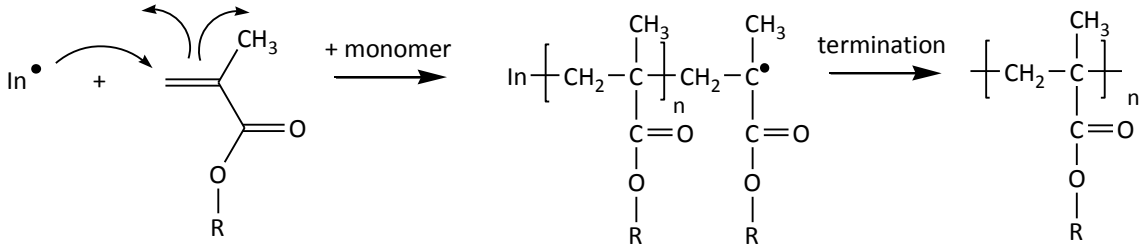


**Figure 3.1 - Schematic stepwise process of a free radical polymerisation.**

It is obvious that the synthesis of these materials needs to be carried out in clean conditions in order to limit termination reactions and accordingly have as much control as possible over the polymerisation process. A frequently encountered inhibition phenomenon is the presence of $O_2$ within the monomer solution. Oxygen is a unique molecule since it's one of the few molecules which has a triplet di-radical as ground state due to its electronic structure[5] (Fig. 3.2).

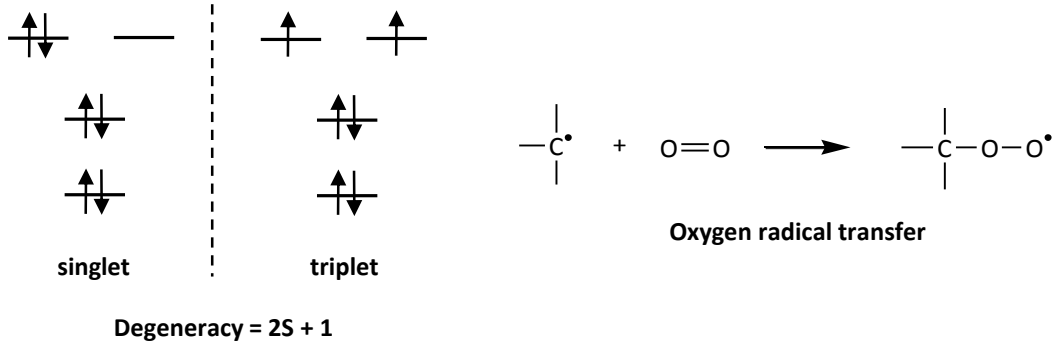


**Figure 3.2 - Oxygen inhibition: electronic & chemical structure.**

If the radical required for propagation is transferred to oxygen, the resulting peroxide (Fig. 3.2) intermediate is much less reactive towards the coupling of additional monomers. Moreover, when making use of photo-initiators, the excited state of the sensitizer can be transferred to oxygen (which induces triplet → singlet transition) thereby decelerating the polymerisation[6]. Due to the omnipresence of this molecule, most radical polymerisation reactions undergo one or more degassing steps. This can involve the set-up of a vacuum or the extensive bubbling through of inert gasses (Ar/He/$N_2$).

Free radical polymerisations are difficult to control and because of that, regulating the MW is difficult and reproducibility moderate. This limited control is often expressed in a high polydispersity ($\lambda$). The occurrence of transfer and termination reactions is numerous and can only be minimised by working in clean conditions with pure reagents and solvents while carrying out thorough degassing procedures. To determine the MW, certain approximations are carried out. To simplify the calculation, the appearance of chain transfer (to reagent, solvent, etc.) is disregarded. Furthermore, termination of the propagation chain is believed to occur via disproportionation rather than by combination. Finally, a steady-state (dynamic equilibrium) is put forward which claims an equal rate of initiation and termination. The equation for relating the MW (degree of polymerisation = DP) to the amount of initiator and monomer required is as follows:

$$DP = \frac{k_p.[M]}{2.\sqrt{f.k_d.k_t.[I]}}$$

With $k_p$, $k_d$ and $k_t$ being the propagation, dissociation and termination constants respectively, f being the initiator efficiency, [M] = monomer concentration and [I] = initiator concentration. Other important aspects that influence the outcome of a radical polymerisation are related to viscosity (e.g. Trommsdorff effect), the temperature, the solvent and type of initiator used.

## 3 Polymethacrylate derivatives as synthetic vectors

Just like for biodegradable synthetic vectors (chapter 2), a whole list of requirements and conditions are to be considered for the synthesis of non-biodegradable polymeric vectors. In order to compare both classes of polymers, methacrylates possessing similar types and amounts of functional groups are prepared with a MW of comparable size according to methods from literature[1,2,7,8,9,10]. Dependent on the desired polymer structures, polymerisations were carried out in aqueous or organic environments using correspondingly soluble initiators.

### 3.1 Description of a free-radical polymerisation

As is traditionally used for free radical polymerisations, thermal initiators were adopted as radical producing compounds. Upon heating, generally to temperatures of about 60-80 °C, the initiator dissociates (with a dissociation constant, $k_d$) in one or more radicals. For polymerisations carried out in organic solvents, 2,2′-Azobis(2-methylpropionitrile) (AIBN) was used whereas for polymerisations in the aqueous phase, ammoniumpersulfate (APS) was applied (Fig. 3.3). Both compounds undergo a homolytic cleavage of the weakest bond when

energy is provided whereby two identical radicals are produced (optionally with a by-product, $N_2$ in the case of AIBN)[11]. The dissociation speed of APS is also pH-dependent.

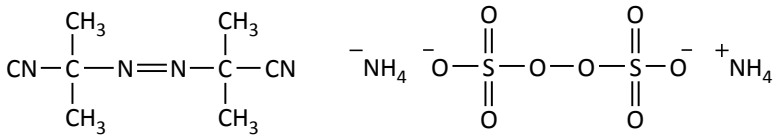


**Figure 3.3 - Chemical structure of initiators: AIBN and APS.**

To set up a polymerisation, a two-neck flask is equipped with a septum and a reflux cooler with a tap. Via this tap, the whole set-up can be put under vacuum with a pump. A degassing procedure then consists of repeated steps of stirring under vacuum to remove air from the solution with the introduction of an inert $N_2$ atmosphere afterwards. This action is repeated three times after which the initiator (from a stock solution) is added through the septum and degassing is carried out for the last time in order to allow start of the polymerisation by temperature increase.

## 3.2 Chain transfer agents regulate polymerisation for low MW's

In some cases, very small polymers are required but given the highly reactive nature of a radical polymerisation, short polymer chains are difficult to obtain. By using AIBN, it appeared to be difficult to produce polymers with a MW smaller than 40.000 Da without the use of a chain transfer agent (CTA or regulator). A well known regulator is 2-mercaptoethanol (EtSH), which can absorb the active chain radicals and accordingly lower the expected MW. The decrease in obtained MW is due to the higher stability of the radical $EtS^{\bullet}$ and the corresponding lower reactivity towards radical combination (Fig. 3.4). With a decreasing M/CTA ratio (or increasing CTA concentration), shorter polymer chains were obtained while keeping the amount of initiator constant (typically 1-10% of the monomer concentration)[12].

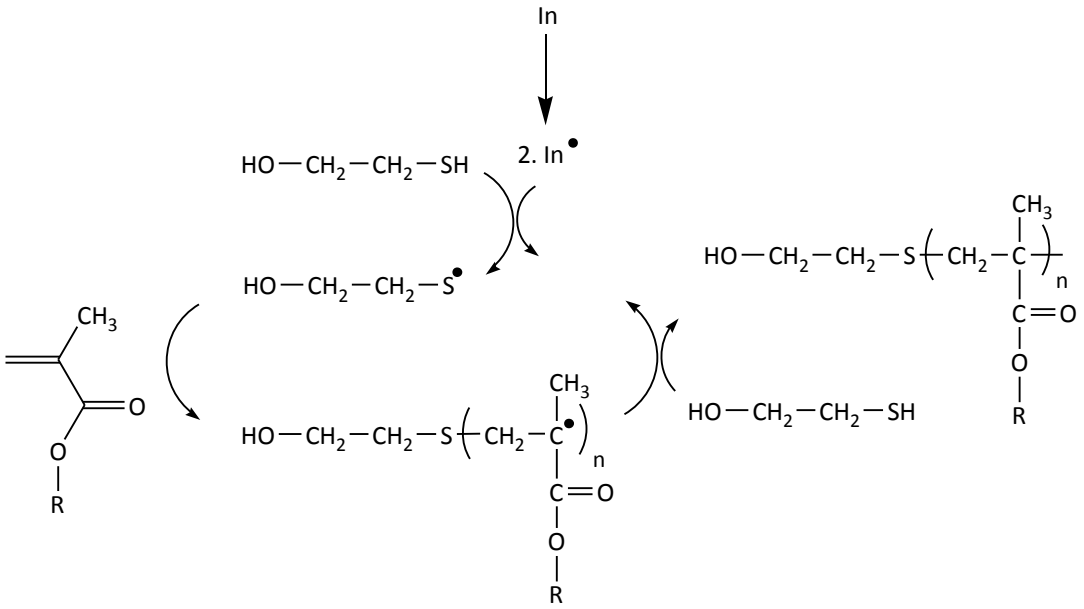


**Figure 3.4 - Chain transfer mechanism for the production of low MW methacrylate compounds.**

### 3.3 Synthesis of poly(dimethylaminoethyl)methacrylate (pDMAEMA)

In accordance with its biodegradable counterpart, a polymethacrylate homopolymer containing only tertiary amine functional groups (located on the side chain) was synthesised. Poly(dimethylaminoethyl)methacrylate (pDMAEMA) could be readily obtained in a one-step synthesis from its commercially available monomer, dimethylaminoethylmethacrylate. Polymerisation is carried out in solution with monomer concentrations of 10-20 % (v/v) at elevated temperature (75 °C) and is allowed to react overnight to increase the degree of conversion. The purification and isolation is subject to the type of initiator and solvent used.

In the case of AIBN, the polymerisation is performed in toluene. After the reaction, the polymer is isolated by precipitation in ice-cooled pentane, filtered off, washed and re-dissolved in water to be further purified by dialysis. When APS is used (typically 0.1-4 mol%), the polymerisation is carried out in water (pH ≈ 5) and precipitated in ice-cooled acetone, filtered off, washed and re-dissolved in water to be further purified by dialysis. For AIBN, MW's up to 300.000 Da could be achieved while the use of APS yielded polymers up to 1.000.000 Da[13]. As the results in table 3.1 confirm, the polydispersity of APS initiated polymers is lower (compared to AIBN) due to the precipitation in more polar non-solvents that are able to retain low MW fractions better and artificially improve polydispersity (closer to 1). This effect is also more pronounced for low MW compounds (AIBN initiation). The MW of these compounds was checked via GPC measurements using an aqueous buffer (5 % $NaH_2PO_4$, 3 % $CH_3CN$, pH = 4) whereas the degree of purity (disappearance of vinyl protons) and confirmation of the structure was given by $^1$H-NMR (Fig. 3.5).

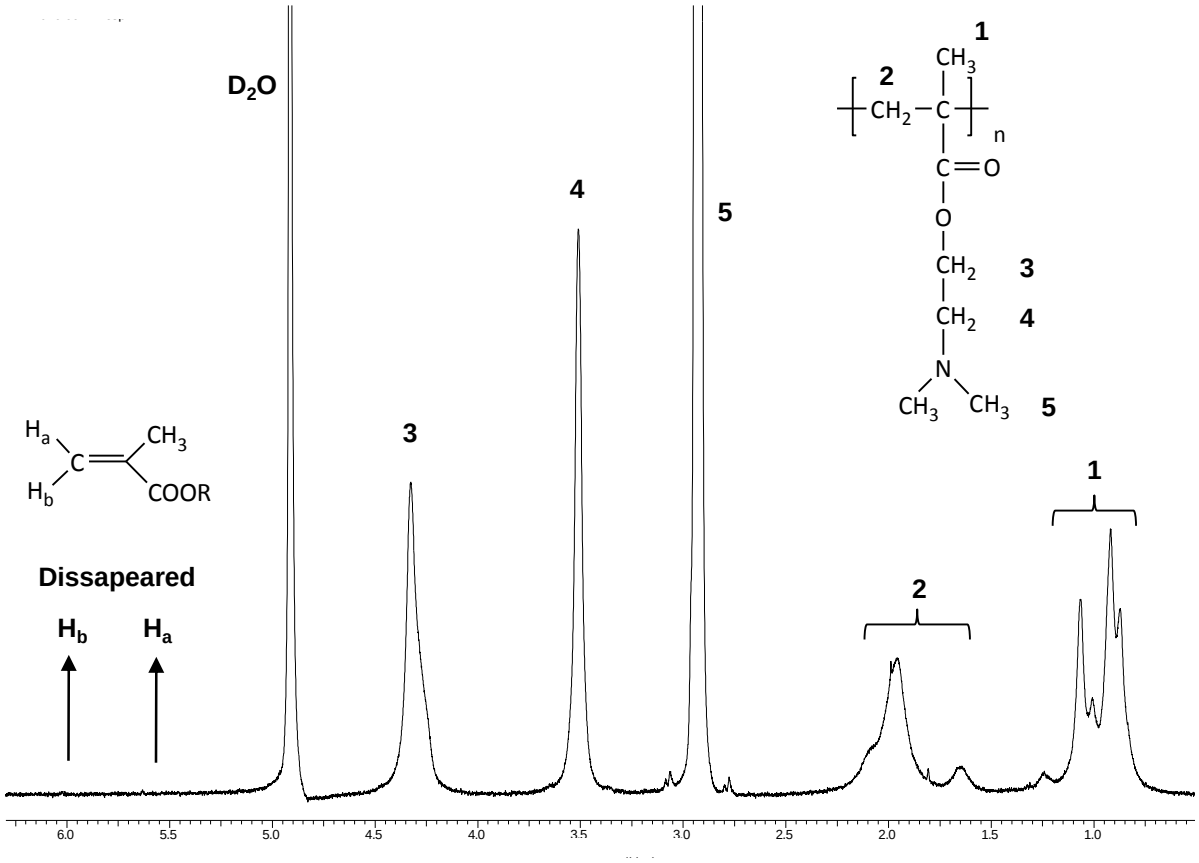


**Figure 3.5 – Structure of pDMAEMA as obtained by $^{1}$H-NMR ($D_2O$).**

Several homopolymers with different MW were produced to investigate the relation between the MW and the properties related to the delivery of DNA (table 3.1).

| MW (Da) | Initiator | M/CTA | polydispersity (λ) |
|---|---|---|---|
| 11.900 | AIBN | 9/1 | 1.54 |
| 29.200 | AIBN | 20/1 | 1.61 |
| 62.900 | AIBN | - | 2.01 |
| 121.000 | AIBN | - | 1.90 |
| 310.000 | APS | - | 1.38 |
| 658.000 | APS | - | 1.49 |

**Table 3.1 – Overview of various pDMAEMA compounds.**

The polydispersity of the final products was susceptible to the type of initiator system used. Polymers with a low MW showed tendency for having a correspondent lower polydispersity compared to high MW compounds. In contrast, the use of APS generally yielded final products with a considerable narrower polydispersity (range = 1.3 – 1.7) than for AIBN.

### 3.4 Amine-containing methacrylates

Having a polymer at its disposal that contains numerous functional groups for both complexation and continued coupling is of high interest to obtain multifunctional polymers. The production of poly(aminoethyl)methacrylate (pAEMA) can be used as such but can also be utilised for coupling to peptides or as a precursor for the formation of guanidylated compounds. The polymerisation of the corresponding monomer (aminoethylmethacrylate hydrochloride) is complicated due to the high occurrence of side-reactions (Fig. 3.6).

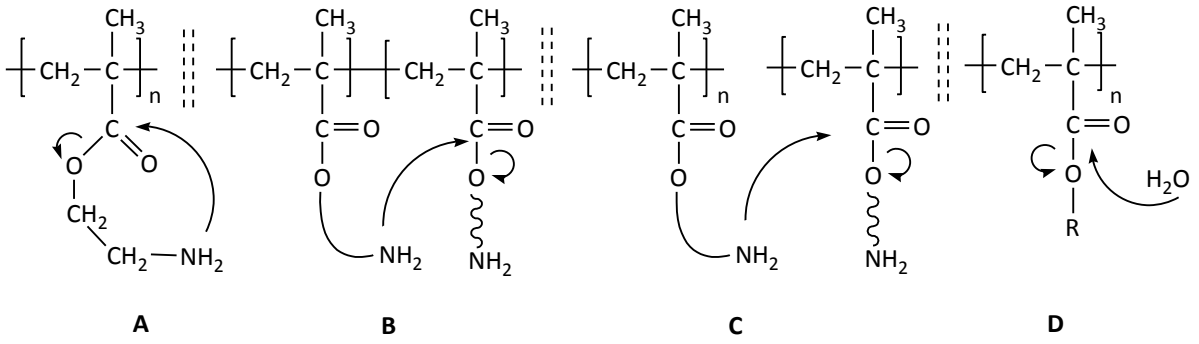


**(A) Intra-molecular amidation I ; (B) Intra-molecular amidation II ; (C) Intermolecular amidation ; (D) Hydrolysis**

**Figure 3.6 – Overview of possible side reactions during the polymerisation of AEMA.**

The occurrence of these side reactions can alter the final products completely. The presence of hydrolysed methacrylic esters (D) can turn solutions into hydrogels (high polarity and water absorption) or even worse in the case of intermolecular amidation (C), initiate the formation of covalently crosslinked networks. The chances of intra-molecular amidation II (B) happening are rather low due to the entropically unfavourable formation of 9-membered rings (or larger if the ester bond is not positioned on the adjacent unit). Because of the exclusive solubility in water, copolymerisation with other monomers is limited. Therefore the monomer needs to be protected during polymerisation. This can be achieved in two ways. By applying the proper pH, the amine functional group can be protonated, thereby eliminating its nucleophilic property. Fine-tuning the pH is of the utmost importance given the need for a pH that can quantitatively protonate primary amines ($pK_a \approx 9.5$) while at the same time prevents the hydrolysis of the ester[14]. A pH close to 5 proved to fulfil both requirements. An alternative solution for this problem is the use of a protected amine derivative. A urethane protection (tert-butoxycarbonyl - BOC) was proposed to reduce the nucleophilic capacity through its electron withdrawing ability as well as the sterical hindrance[15]. Additionally, the synthesis of BOC-AEMA rendered the monomer less polar, allowing the subsequent dissolution in organic solvents and the correspondent copolymerisation with other monomers. Recovering the original functional group can be achieved by swift cleavage

under strongly acidic conditions (TFA or HF). The application of polymethacrylamides could solve this problem due to its thermo-dynamical stability but forms a drawback towards degradability of the chemical bond (esters degrade better via enzymatic hydrolysis) although the polymer backbone remains non-degradable for both. Its use was not further considered.

### *3.4.1 Synthesis of (N-tert-butoxycarbonyl)aminoethylmethacrylate*

The production of BOC-AEMA was achieved by reacting a cooled suspension of AEMA.HCl in DCM (0.3 M) which was mixed with 1.1 equivalent of triethylamine (TEA) with a solution of bis(*tert*-butyl)dicarbonate (1.1 eq) in DCM. The reaction was acclimatised to room temperature and stirred overnight. Purification of the formed BOC-AEMA was carried out by liquid extraction, firstly with 0.5 M HCl (repeated 2x) to remove remaining AEMA.HCl and TEA.HCl, followed by 0.5 M $NaHCO_3$ to remove remaining tert-butoxycarboxylic acid and finalised by extraction with 0.1 M NaCl. The organic phase was collected an dried over $MgSO_4$ and filtered after which it was concentrated by rotary evaporation. The solution was then crystallised in a cold mixture of pentane/diethylether (1/1 v/v). The final product was isolated by decantation and dried *in vacuo*. Structure validation was obtained via $^1$H-NMR (Fig. 3.7) and FTIR. The overall yield proved to be around 75 %.

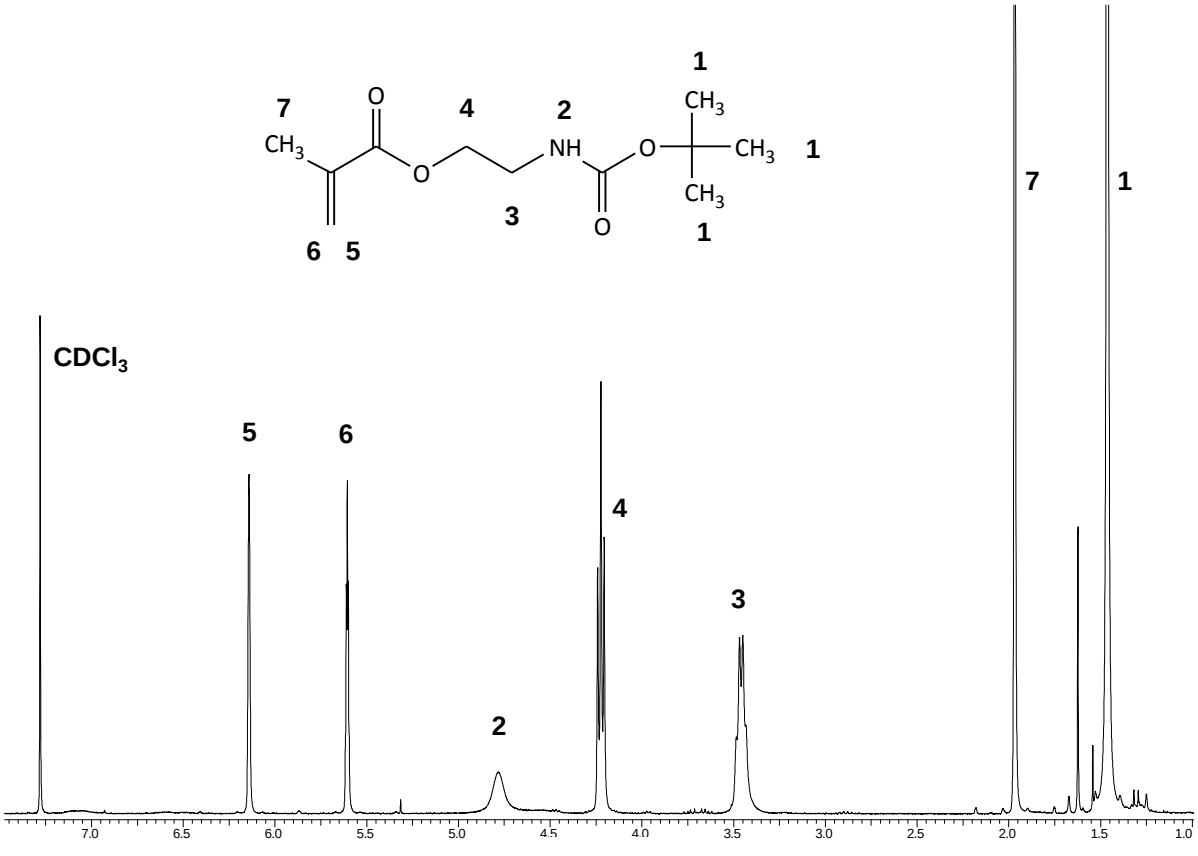


**Figure 3.7 – Structure of BOC-AEMA as obtained by $^1$H-NMR ($CDCl_3$).**

### *3.4.2 Synthesis of poly(aminoethyl)methacrylate (pAEMA)*

In order to obtain guanidine-containing polymethacrylates, primary amine-containing derivatives are required. Since the protection of AEMA is a time-consuming step, BOC-AEMA was only used for copolymerisation using different monomers. The production of homopolymers was performed using AEMA.HCl. Therefore AEMA.HCl was dissolved in water and adjusted to pH = 5 after which it was thoroughly degassed. Ammoniumpersulfate was added as an initiator (10 mg/ml stock) in concentrations ranging from 0.1 to 4 mol %. The final product was purified by dialysis and isolated by freeze-drying followed by structure confirmation via $^{1}$H-NMR (Fig. 3.8).

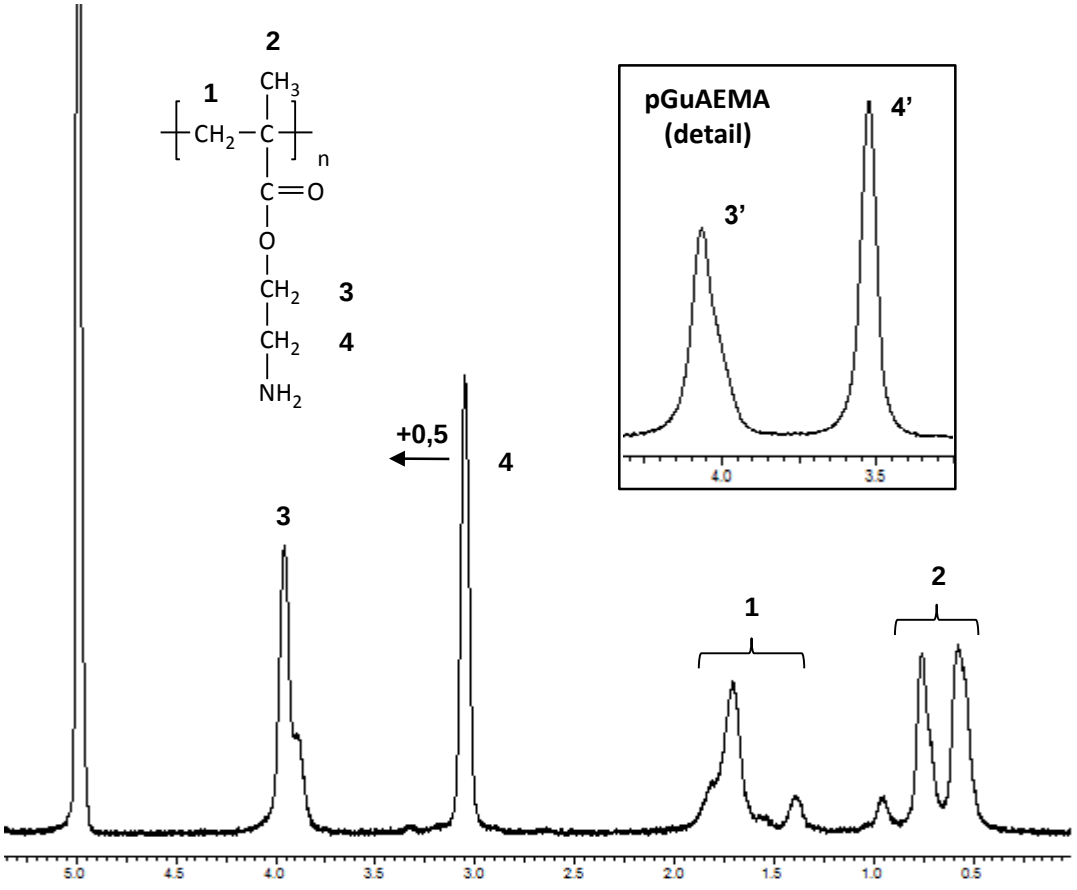


**Figure 3.8 – Structure of pAEMA and pGuAEMA (detail) as obtained by $^{1}$H-NMR ($D_2O$).**

### *3.4.3 Synthesis of poly(guanidylethyl)methacrylate (pGuAEMA)*

In accordance with previously described guanidine conversion reactions (section 2.3.4) pAEMA was converted into pGuAEMA during a one-step reaction. Nearly quantitative modification was observed from $^{1}$H-NMR (Fig. 3.8 – peaks 3' and 4'). A detailed spectrum of the guanidine derivative revealed a peak shift of 0.5 ppm for $C_4$-H and 0.1 ppm for $C_3$-H. An overview of the synthesised pAEMA and pGuAEMA compounds is given in table 3.2. The

low MW pAEMA was used for the guanidine conversion, hence the modest increase in MW and polydispersity. The GPC analysis of pGuAEMA was next to the phosphate buffer also performed in a 0.5 M NaCl buffer to see the possible effect of elution retardation (due to sticking or blocking of the GPC column pores) but the resulting MW proved to be in the same MW range.

| Polymer | MW (Da) | polydispersity (λ) |
|---|---|---|
| pAEMA | 61.200 | 1.34 |
| pAEMA | 176.300 | 1.83 |
| pAEMA | 841.200 | 1.54 |
| pGuAEMA | 63.000 | 1.49 |

**Table 3.2 - pAEMA & pGuAEMA overview.**

### *3.4.4 Synthesis of poly(aminoethyl-co-dimethylaminoethyl)methacrylate (p(DMAEMA-AEMA))*

To allow additional coupling reactions (e.g. fluorescent tags), primary amines are required to enable straightforward coupling to a methacrylate polymer. Moreover, the addition of primary amines is expected to influence the complexation in a different way as for L-glutamine containing polymers since H-bonding with the polymer backbone is not possible. To prepare this polymer, the reaction can be performed in both organic and aqueous environments but due to the additional practical work caused by AEMA protection, all polymerisations were carried out in water (pH ≈ 5) using reaction parameters described above (section 3.1 & 3.4.2). APS was used as initiating system in high concentrations (2-4 wt %) to yield polymers with sufficiently low MW. The composition was verified by $^{1}$H-NMR and is shown below in figure 3.9 and table 3.3.

| MW (Da) | -$NMe_2$/-$NH_2$ | polydispersity (PD) |
|---|---|---|
| 51.000 | 79 / 21 | 1.69 |
| 191.000 | 82 / 18 | 1.44 |
| 135.000 | 54 / 46 | 1.42 |
| 132.000 | 23 / 77 | 1.29 |

**Table 3.3 - overview of p(DMAEMA-AEMA) compounds.**

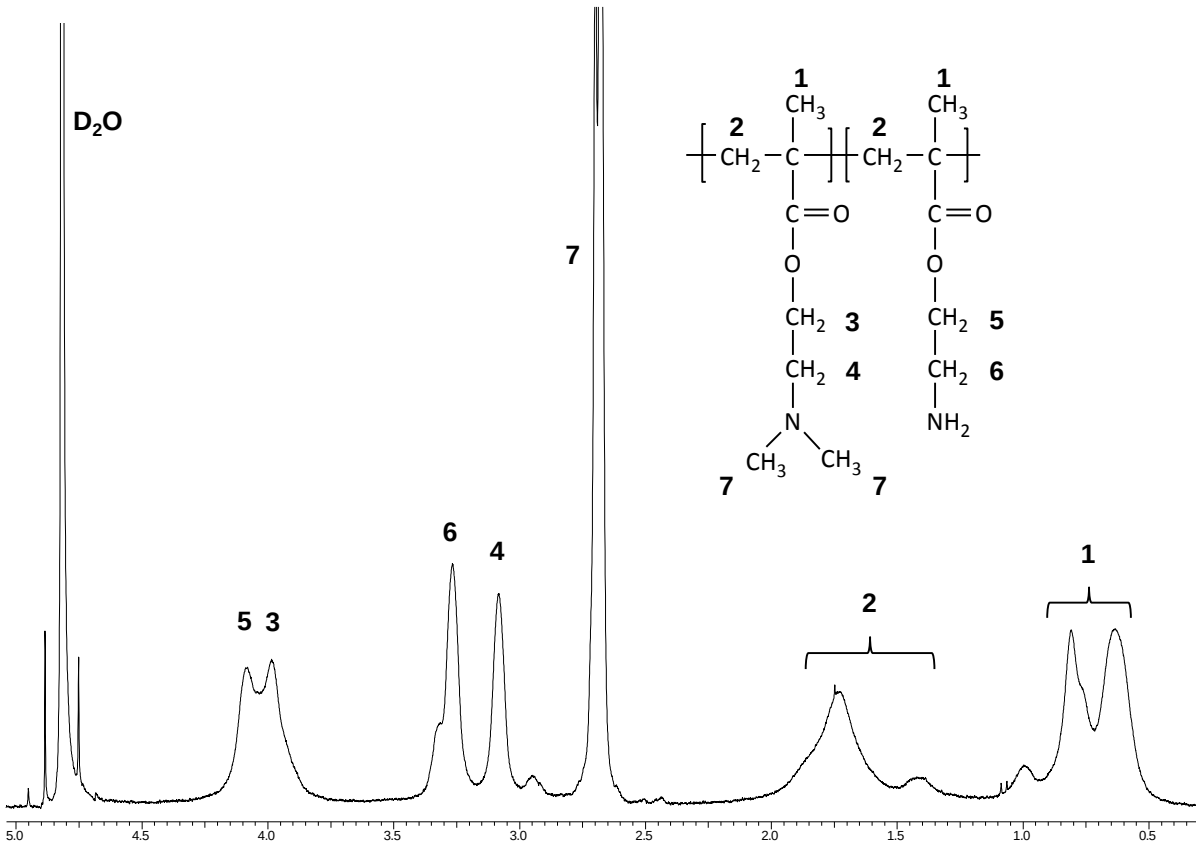


**Figure 3.9 – Structure of p(DMAEMA-AEMA) as obtained by $^{1}$H-NMR ($D_2O$).**

## 3.5 Hydroxyl containing polymethacrylates

Similar to biodegradable synthetic vectors, also polymethacrylates were assumed to experience a positive effect when incorporating neutral hydroxyl groups into the structure since these functional groups can dissipate the excess of cationic charge and consequently improve cell-viability. Making use of the generally-known and commercially available hydroxyethylmethacrylate (HEMA) would be natural but side-reactions of the same nature as for pAEMA derivatives are inhibiting its use (intermolecular trans-esterification which can result in crosslinking, Fig. 3.10). For that reason and also to minimise to occurrence of chain transfer reactions by the free hydroxyl group, an alternate form of this monomer containing the trimethylsilyloxy (TMS) protective group is used[16]. Due to the presence of TMS, polymerisation can only proceed in organic solvents and additional deprotection (acidic cleavage) was required (Fig. 3.9). This latter step was completed under cooled conditions (0 °C) to prevent intermolecular transesterification of the cleaved hydroxyl groups (which is increased at elevated temperature). The possibility of crosslinking for HEMA-containing compounds (e.g. into ethyleneglycoldimethacrylate type of compounds) always remains and should therefore be contained by keeping temperatures low and limit the time in solution.

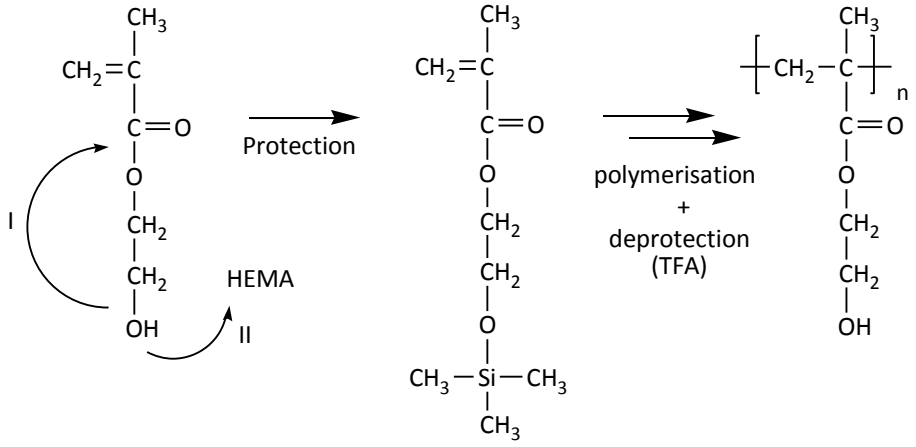


**Figure 3.10 – Side-reactions related to the use of non-protected HEMA and structure of the protected TMS-HEMA and final pHEMA.**

### *3.5.1 Synthesis of poly(dimethylaminoethyl-co-hydroxyethyl)methacrylate (p(DMAEMA-HEMA))*

Creating a polymer with only hydroxyl functional groups was not expected to yield a vector capable of sufficient DNA interaction and complexation. Therefore, TMS-HEMA was only used in combination with charged monomers like DMAEMA. The production of these copolymers was carried out in toluene and their composition and MW were chosen to be similar to their biodegradable equivalents (chapter 2). Both monomers were dissolved in toluene (20 wt % monomer combined) and according to the desired MW, initiator (AIBN) was added while performing the required degassing steps. The reaction was accomplished overnight at elevated temperature (75 °C) and was finished by precipitation in cold pentane/diethylether (1/1 v/v) and dried *in vacuo*. Next, the intermediate polymer (containing TMS-protected HEMA) was dissolved in $CHCl_3$ (20 w/v %) and TFA was added to remove the TMS-group. After precipitation in cold pentane, the product was re-dissolved in water (0.1 M HCl) for further purification by dialysis. The composition and purity of the polymers was checked by $^1$H-NMR (Fig. 3.10). Polymer compounds with a desired number of charged groups, around 25, 50 and 75 % respectively, were calculated prior to polymerisation. An overview of the produced polymers is given in table 3.4.

| MW (Da) | -OH/$NMe_2$ | polydispersity ($\lambda$) | MW (Da) | -OH/$NMe_2$ | polydispersity ($\lambda$) |
|---|---|---|---|---|---|
| 9.800 | 45 / 55 | 1.60 | 187.500 | 20 / 80 | 1.43 |
| 218.000 | 44 / 56 | 2.26 | 14.900 | 69 / 31 | 2.46 |
| 22.800 | 23 / 77 | 1.69 | 241.900 | 66 / 34 | 2.85 |

**Table 3.4 – overview of p(DMAEMA-HEMA) compounds.**

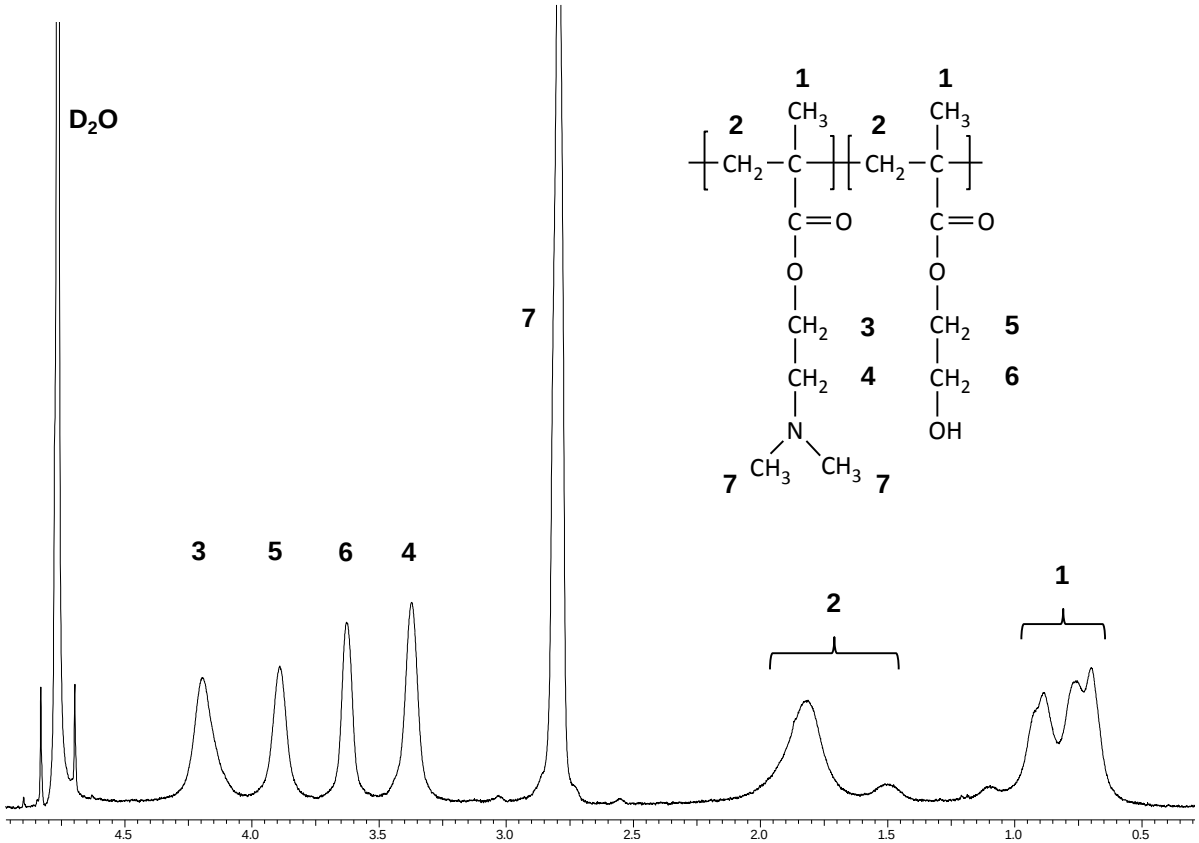


**Figure 3.11 – Structure of p(DMAEMA-HEMA) as obtained by $^{1}$H-NMR ($D_2O$).**

### *3.5.2 Synthesis of poly(guanidylethyl-co-hydroxyethyl)methacrylate (p(GuAEMA-HEMA))*

In order to produce a polymer with both primary amines (the precursor of guanidine) and hydroxyl functional groups, protected derivatives of the respective monomers are to be used. In this way, polymers containing a hydrophobic backbone and also a biologically highly relevant guanidine group can be compared to biodegradable vectors of similar composition and MW. Because of solubility reasons, polymerisation of such monomers can only be carried out in toluene using identical parameters as described above (20 wt % monomer concentration). Post precipitation, both protective groups can be removed using TFA. After purification and isolation, the primary amines can be converted into guanidine groups (as specified above, section 2.1.6). The composition and structure are verified by $^{1}$H-NMR (Fig. 3.11 & table 3.4).

| MW (Da) | -OH/Gua | polydispersity (λ) |
|---|---|---|
| 29.500 | 60/40 | 1,54 |

**Table 3.5 - Composition and MW of p(GuAEMA-HEMA).**

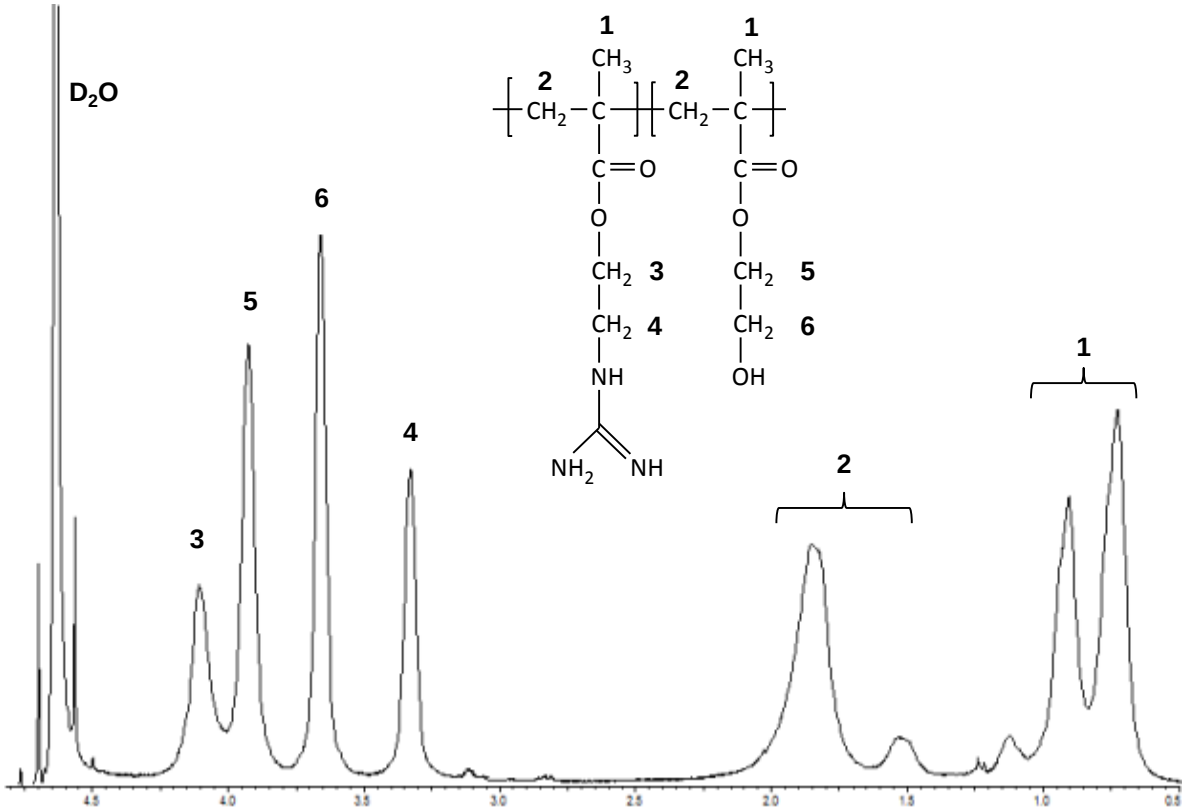


**Figure 3.12 – Structure of p(GuAEMA-HEMA) as obtained by $^{1}$H-NMR ($D_2O$).**

## 4 Conclusion

In this chapter, the production of non-biodegradable polymers based on methacrylate monomers that bear different functional groups was discussed. Similar to the biodegradable counterparts, every functional group was introduced to possess specific physico-chemical properties. The composition and MW was controlled in such a way that trends related to the more hydrophobic polymethacrylates could be compared and if necessary implemented in biodegradable derivatives without carrying out its corresponding complexer synthesis. Synthetic vectors of a desired composition (functional groups) were accordingly produced. Due to the different nature of polymerisation (free radical versus controlled living-like), anticipated lower control of the MW was observed. Moreover, the copolymerisation of monomers with variable functional groups seemed to have almost no effect on the acquired polymer composition which suggested that the reaction kinetics are nearly equal. The conversion degree of the polymerisations revealed that in most cases yields up to 50% were possible. Despite the more hydrophobic nature of these polymers, the solubility in water was still high (although not always confirmed in NMR spectra because of the broad peaks observed with lack of coupling identification, a result of the average shift value of the different repeating units).

# 5 References


[1] Dubruel, P. and E. Schacht (2006). "Vinyl polymers as non-viral gene delivery carriers: Current status and prospects." Macromolecular Bioscience **6**(10): 789-810.

[2] van de Wetering, P., J.-Y. Cherng, et al. (1998). "2-(dimethylamino)ethyl methacrylate based (co)polymers as gene transfer agents." Journal of Controlled Release **53**: 145-153.

[3] P. Dubruel, (2003) "Studie van synthetische polymeren als vectoren voor gentherapie", Ghent University, Doctoral research

[4] Verbaan, F. J., G. W. Bos, et al. (2004). "A comparative study of different cationic transfection agents for in vivo gene delivery after intravenous administration." Journal of Drug Delivery Science and Technology **14**(2): 105-111.

[5] Hanrahan, M. J. (1992). "Overcoming the effects of oxygen on cured and uncured UV formulations." Journal of Radiation Curing **19** (40).

[6] Wight, F.R. and Numez, I.M. (1989). ""Oxygen inhibition of acrylate photopolymerisation." Journal of Radiation Curing **16**(1): 3-7..

[7] Dubruel, P. and E. H. Schacht (2000). "Effect of polyethylene oxide blocks or grafts on the physicochemical properties of poly(2-N-(dimethylaminoethyl) methacrylate) DNA complexes." Journal of Bioactive and Compatible Polymers **15**(4): 279-296.

[8] Dubruel, P., V. Toncheva, et al. (2000). "pH sensitive vinyl copolymers as vectors for gene therapy." Journal of Bioactive and Compatible Polymers **15**(3): 191-213.

[9] van de Wetering, P., J.-Y. Cherng, et al. (1997). "Relation between transfection efficiency and cytotoxicity of poly(2-(dimethylamino)ethyl methacrylate)/plasmid complexes." Journal of Controlled Release **49**(1): 59-69.

[10] Cherng, J. Y., H. Talsma, et al. (1999). "Long term stability of poly((2-dimethylamino)ethyl methacrylate)-based gene delivery systems." Pharmaceutical Research **16**(9): 1417-1423.

[11] Vorsina, I. A. and Y. I. Mikhailov (1996). "Kinetics of thermal decomposition of ammonium persulfate." Russian Chemical Bulletin **45**(3): 539-542.

[12] Boyer, C., G. Boutevin, et al. (2004). "Study of the telomerization of dimethylaminoethyl methacrylate (DMAEMA) with mercaptoethanol. Application to the synthesis of a new macromonomer." Polymer **45**(23): 7863-7876.

[13] Layman, J. M., S. M. Ramirez, et al. (2009). "Influence of polycation molecular weight on poly(2-dimethylaminoethyl methacrylate)-mediated DNA delivery in vitro." Biomacromolecules **10**(5): 1244-1252.

[14] Thompson, K. L., E. S. Read, et al. (2008). "Chemical degradation of poly(2-aminoethyl methacrylate)." Polymer Degradation and Stability **93**(8): 1460-1466.

[15] Dufresne, M.-H. and J.-C. Leroux (2004). "Study of the micellization behavior of different order amino block copolymers with heparin." Pharmaceutical Research **21**(1): 160-169.

[16] Hirao, A., H. Kato, et al. (1986). "Polymerization of monomers containing functional groups protected by trialkylsilyl groups." Macromolecules **19**: 1294-1299.

# Chapter 4

# Physico-chemical characterisation of multifunctional synthetic vectors

# 1 Introduction

One of the primary requirements of a synthetic polymer that needs to be applied as a vector for gene delivery, is the ability to engage in an associative way with DNA, RNA or a sequence of nucleotides. As was mentioned earlier, this can be achieved in the most straightforward way by electrostatic attractions, hence cationic polymers were synthesised. Regarding restrictions of the body on a cellular and systemic level, certain aspects of the polymer-DNA interaction are considered essential for the proper functioning as a delivery device. Among these critical conditions are the size of the formed particles, their ability to be taken up by the cell and the capacity to protect the DNA from external stimuli. Moreover, the interaction between DNA and the vector should be stable (in time and in saline buffered environments) to allow prolonged results and the delivery system should ideally be non-toxic afterwards, in other words: be metabolised by the body down to basic structures.

A whole range of analytical techniques exists, allowing the investigation of certain physical and chemical properties that can be correlated with the conditions described above. In this chapter, several properties and conclusions derived from every individual characterisation method will be discussed. The focus of the physico-chemical analysis of polymer-DNA complexes is therefore on the formation of these particles, their size and size-distribution and their stability in solution. The capacity of delivery systems to protect its DNA cargo from enzymatic degradation as well as the extent to which the polymer can be degraded after dissociation was investigated as well. Throughout the characterisation, structure-related properties of polymers were interpreted to result in the discovery of specific trends. One important quality that is not covered by these characterisation tests but which should be mentioned as an additional parameter in the total evaluation of a vector, is the buffering capacity of the polymers. From previous doctoral research[1,2], the buffering range of polymers with similar functional groups (and compositions) was found to be in the range of pH = 5.5-7.5, which is in good correspondence with the pH-drop that is realised during cell-internalisation using the endocytotic pathway (endosomes).

In order to fully comprehend the way polyplexes are prepared, the theory of polyelectrolytes (mutual association) will be clarified first as will their method of preparation. Before polymers can be used as synthetic vectors they need to be completely, chemically characterised (structure, composition and MW).

## 2 Polyelectrolyte complex formation theory

It is imperative for polymers that have to interact with DNA, to posses cationic charges that can induce an electrostatic interaction with the negatively charged sugar-phosphate backbone of DNA (polyanion). Therefore, during synthesis the polymers were provided with functional groups that are positively charged in a physiological environment (to become polycations). Upon physical mixing, these two macro-ions form self-assembling inter-polyelectrolyte complexes (IPEC's or polyplexes) that drastically change the properties of the individual components (Fig. 4.1). A polyplex is thus composed of a certain ratio of polymer to DNA (cation to anion), which is better known as the charge ratio (CR). Many facets influence this formation, such as charge density, salt concentration, order of mixing and polymer chain flexibility[3]. In order to have a reproducible way of forming these polymer-DNA complexes, it is essential to have a well established protocol.

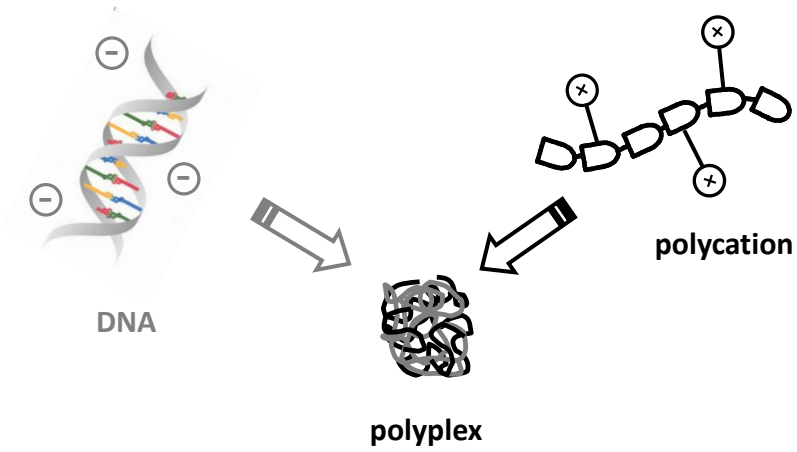


**Figure 4.1 – Simplified representation of the IPEC formation between DNA and a polymer.**

### 2.1 The concept of mass per charge and the calculation of polyplex composition

The charge of a macro-ion at physiological pH depends on its structure (type and amount of functional groups). Every charge on the polymer, corresponds with a certain molecule mass, defined as the mass per charge (M/C). This value is often the molecular mass of one structure unit (in case of fully charged polymers) and is needed for all macro-ions involved in the formation of the polyplex. For DNA, this value is fixed since it consists of a sugar unit (deoxyribose), a phosphate group and the average weight of nucleic acids according to the Chargaff rule[4,5]. It is of great importance that the calculated M/C of polyelectrolytes can be mutually compared so that uniform conclusions can be drawn from experimental analysis between polyplexes composed of different vectors. Because of that, the M/C was put forward as the value corresponding with 100% of the polyelectrolyte being charged. This definition is specifically relevant for polymers with neutral groups since a correction needs to

be made for the lack of cationic charges. Even though the assumption that a polymer is fully charged, is not entirely correct (proton neighbouring effect), it allows for a simple and swift way of calculating the M/C. The M/C of a cationic polymer is calculated by determining the mean molecular weight of the different structure units of the polymer (including counter-ion if present) and dividing it by the relative amount of charged structure units (in %).

In a polymer-DNA complex, the CR is defined using the mutual relation of mass/charge between the macro-ions, expressed in the following equation:

$$x = z \,.\left(\frac{X}{Y} \,.\, y\right)$$

$X$ = mass/charge of polycation (g/mol)

$Y$ = mass/charge of polyanion (g/mol)

$y$ = amount of polyanion added (g)

$x$ = amount of polycation added (g)

$z$ = integer multiple of the excess of polycation over polyanion (where z equals 1 for a charge ratio of 1/1).

Given these parameters, polyplexes at different CR can be calculated from the amount of DNA that needs to be effectively delivered. In typical characterisation experiments, concentrations of 20 µg/ml DNA are used. The order of compound addition and mixing is critical as will be demonstrated later. Firstly DNA is added to water and subsequently polymer is added, followed by briefly vortexing the entire mixture.

### 2.2 Standardised protocol

For reasons of uniform experimental testing (standardisation) as well as to respect the need for harmony within a partner-based project, a standard protocol was established that describes the preparation of polyplexes in solution. Prior to practical execution, the desired CR of the polyplex is calculated using the formula given above and a polymer (1 mg/ml) and DNA stock (2.5 mg/ml) are prepared. All polyplexes were prepared in a total volume of 2 ml and need to be dissolved in ultrapure water to prevent precipitation. Mixing with a buffer can only be carried out after polyplex formation in water (via dilution). Calf Thymus DNA (sodium salt) of about 23,000 basepairs was used as standard DNA (Sigma). Polyplexes based on plasmid DNA (pDNA) were in certain cases also applied. It is imperative that the order of mixing is carried out as described. It appeared that the vortex time and speed play a big role in the size and distribution of the particles (determined by DLS).

*Practical execution*

- 16 µl of a DNA stock solution (= 40 µg) is brought into a vial
- Water is added after which the solution is gently shaken (manually).
- An amount of polymer, corresponding with the desired CR is added (µl range)
- The mixture is vortexed for 5 seconds at medium speed (≈ 1500 rpm)

## 2.3 One-step versus multi-step polymer addition

Dependent on the method of characterisation applied, polyplexes with the same CR can be achieved in a different way, that is by single-shot addition or by multi-step addition. For EtBr displacement assays, a CR of 2/1 is reached by repeated additions of 0.2 CR units (multi-step) in order to determine the condensation point of the polyplex. On the other hand, when the size of a 2/1 polyplex needs to be measured, a single addition of polymer to DNA is performed to get to the desired CR (single-shot addition). Therefore, these two methods of polyplex formation were compared to verify weather similar conclusions could be drawn from different characterisation techniques. The use of small polymer additions to a DNA solution (including a vortexing step of two seconds between each addition) allows a better orientation of polymer around DNA so that the most optimal interaction can be achieved (thermodynamically favourable). Adding the total required amount of polymer at once, induces polyplex formation which is largely kinetically driven. The extent to which the way of polymer addition has an influence on the final polyplex formation was investigated by UV spectrometry for p(DMAEG) 80 kDa (Fig. 4.2 & 4.3).

In figure 4.2, the UV absorbance as a function of polymer addition (stepwise / multishot increase of CR) displays a sudden increase in UV intensity until a maximum value is reached (CR 0.8/1) which corresponds with the CR for polyplex formation. The conformational change from free dissolved DNA to collapsed complex (particle) induces a absorbance increase which is most likely due to attenuation (scattering) as the UV absorption of DNA is shielded by the polymer. Afterwards, the absorbance declines (only limitedly) as a result of the larger amount of polymer which is gradually added around the preformed polyplex (adding up to the shielding effect). A clear difference between uncomplexed DNA and complexed DNA remains and the observed difference pre- and post-polyplex formation confirms the use of UV spectrometry as an alternative in case EtBr fluorescence measurements would be excluded. Additionally, UV analysis is able to produce smaller standard deviations compared to EtBr fluorescence (< 1%, the standard deviation is not shown when < 0.1%). When the formation of a polyplex based on pDMAEG is subjected to a single shot addition (i.e. all polymer is added at once), the maximum value measured, is situated close to the value for a multishot addition (A = 0.4356 instead of 0.4203) which is a

negligible difference (Fig. 4.3). Moreover, the discrepancy between free DNA and complexed DNA is also here apparent and remains clear as the CR is further increased (here shown up to a CR of 6/1).

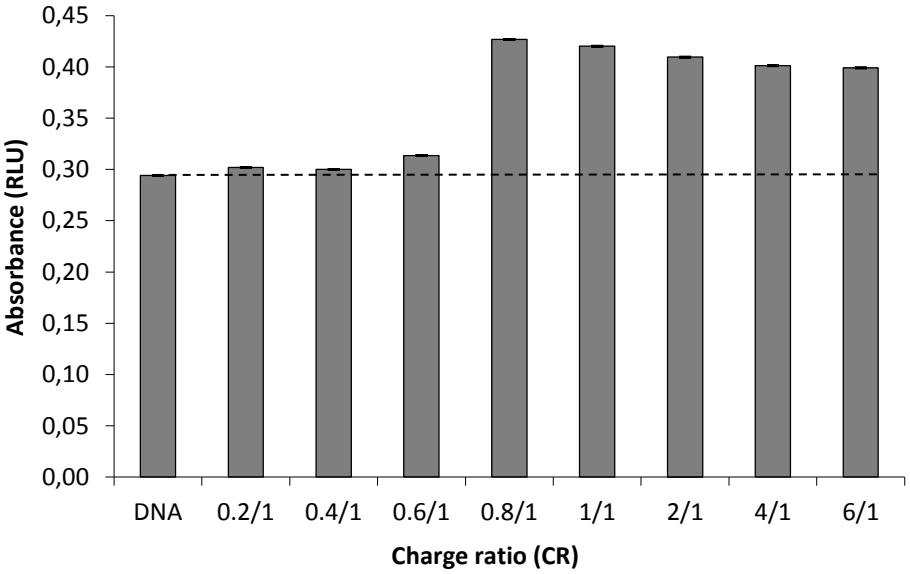


**Figure 4.2 - UV absorbance profile (λ = 260 nm) for polyplex formation using p(DMAEG) 80 kDa (formed by multishot addition).**

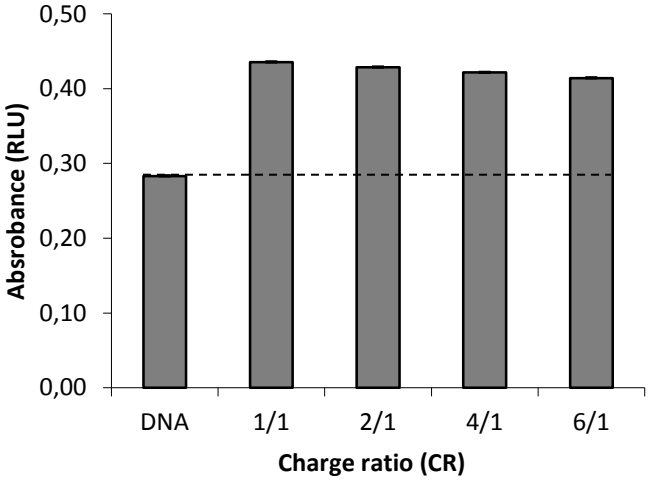


**Figure 4.3 – UV absorbance profile (λ = 260 nm) for polyplex formation using p(DMAEG) 80 kDa (formed by single-shot addition).**

## 2.4 Polyplex mixing sequence

A final topic that needs to be dealt with in order to attain a comprehensive understanding of polyplex formation is the order of mixing. As was stated in the standard protocol, the sequence in which polyelectrolytes are added and the capacity in which they are present (in solution, solid, etc.) can have far-reaching consequences on the polyplex composition. Principally, DNA is dissolved in water prior to the addition of polymer. This method was

mainly chosen for arbitrary reasons, more specifically because the dose of DNA used in polyplex formation is kept constant (20 µg/ml) while the polymer content is varied. Working in reversed order for instance, that is adding DNA to a polymer solution, should theoretically result in equal polyplex formation if both components are thoroughly dissolved and if the mixing process could stimulate optimal polyelectrolyte contact and arrangement. This is practically not always applicable due to the nature of the polyelectrolytes involved (e.g. the dimensions of the polymer coils). If these components possess sufficient flexibility and mobility the order of mixing is assumed to be irrelevant but when the structural integrity limits one of these properties, exceptions are observed. When using plasmid DNA (pDNA), an obvious difference between the two sequences of addition was noticed as was determined by fluorescence fluctuation spectroscopy based on EtBr intercalation (see also chapter 5, section 2.4). Plasmid DNA (pDNA) is a specific, mostly circular type of DNA (with different variants in configuration) of over a 1000 base pairs long and double stranded. Regular (or lineair) double stranded DNA on the other hand, is not expressed as a supra-molecular structure (e.g. circle). Figure 4.4 demonstrates that mixing sequence I (addition of polymer to dissolved pDNA) exhibits slightly less fluorescence, which indicates a somewhat stronger polyplex interaction but with clear spikes at random times observed. Mixing sequence II (addition of pDNA to a polymer solution) displays a little higher fluorescence than sequence I but is far more constant (no spikes visible).

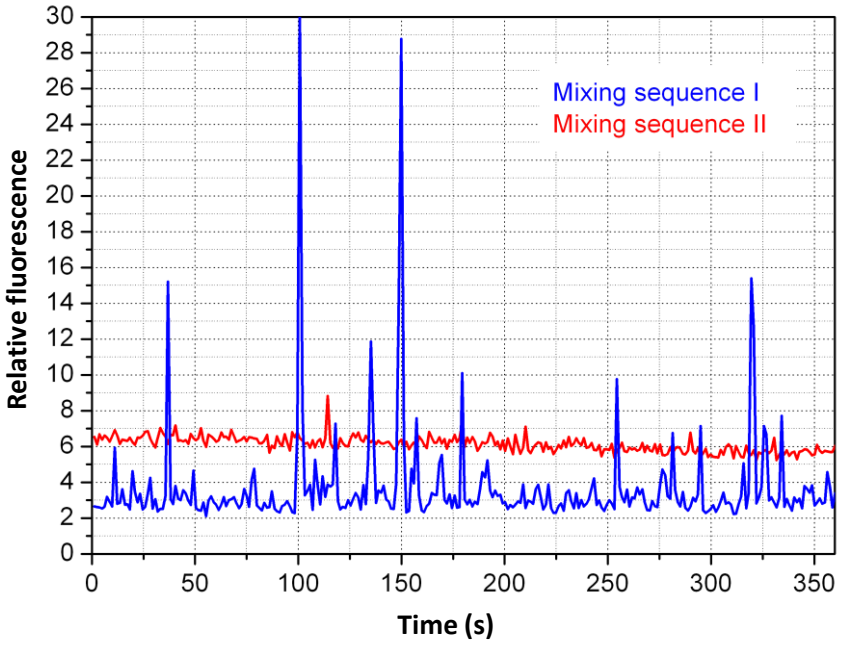


**Figure 4.4 - Fluorescence yield as a function of time for 2 mixing sequences (addition of polymer to DNA (I) and DNA to polymer (II)).**

A hypothesis was proposed on what happens on a molecular level when both components are mixed (Fig. 4.5). If polymer was added to a solution of pDNA, the initially concentrated polymer drop blends into the medium (solvent), thereby searching possible interactions with oppositely charged entities. As the first molecules they encounter and associate with, not readily disperse away from the more concentrated polymer area (due to their lower mobility or reduced Brownian motion), they keep on attracting additional polymer and form even tighter complexes. In this way, most of the polymer is consumed before reaching other parts of the solution, hence a significant part of the pDNA remains weakly bound or simply uncomplexed. The solution is then composed of a combination of heavily interacting polyplexes, medium interacting polyplexes and free DNA, which explains the variable fluorescence values which exhibit a considerable amount of spikes. These spikes should probably be attributed to weak or non-complexed DNA that passes the laser when measuring the fluorescence (by EtBr intercalation).

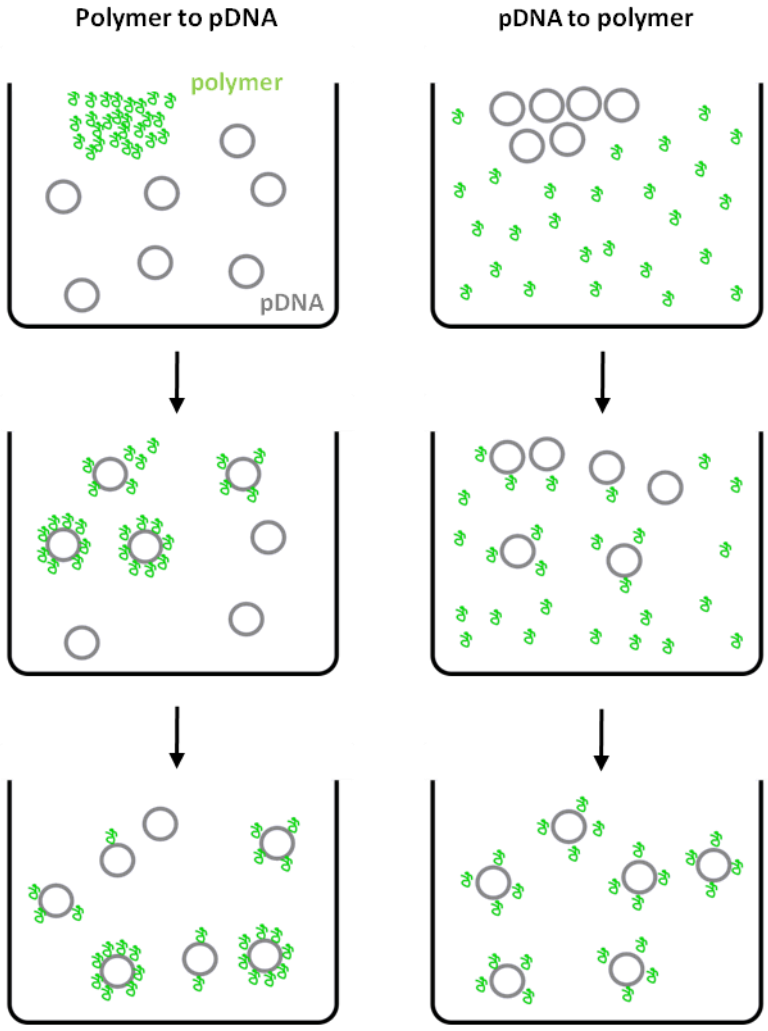


**Figure 4.5 – Hypothetical model of the interaction between polymer and DNA related to the difference in mixing-order.**

To confirm this latter statement, fluorescence measurements of highly diluted DNA (in an EtBr solution) should be carried out to verify the occurrence of random peak spikes (data not available).

On the other hand, when pDNA was combined with a polymer solution, a more evenly distributed appearance of equally tight polyplexes can be observed. Since the polymer is now homogenously spread, no excess is present when the first molecules of pDNA start interacting. Gaining additional cationic charges, can only occur when the pDNA moves on through the solution, gradually taking up more polymer, consequently generating a more equal distribution of polyplex composition.

Although the polymer-to-DNA method could generate less homogenously composed polyplexes this problem is only of importance when the DNA or polymer (or both) are voluminous (less mobile), poorly soluble or too much or less concentrated.

## 3 Characterisation of polyplex formation properties

To start with the development of a full, physico-chemical profile of a polymer that can be adopted as vector for gene delivery, the ability to associate with DNA is the first parameter to be investigated. If a polymer does not fulfil this basic condition, further experimental analysis is rendered useless. As an important result from these tests, the amount of polymer required to obtain a stable and well defined polymer-DNA complex, can be deduced. The amount of positively charged polymer is a crucial factor for the toxicity of the polyplex which, in case of toxicity, generally rises with an increased amount of polymer (and positive charge, e.g. higher CR). It is therefore recommended to develop synthetic polymers that require small quantities to ensure full interaction with DNA into an associated complex.

There are two characterisation methods that are often used for facile screening of the polymer's DNA-interactive properties. The first one, fluorescence spectroscopy based on EtBr intercalation, makes use of light to distinguish complexed and free DNA. A frequently used alternative to this method is gel-electrophoresis based on agarose. Differentiation between a polyplex and uncomplexed DNA is here based on the migration of free DNA through a gel matrix stimulated by an electric field.

### 3.1 Ethidium Bromide Fluorescence

Ethidium Bromide (EtBr) is a planar, aromatic molecule with a particular tendency to specifically interact with DNA. This process is called intercalation and can be described as the realization of non-specific bonding (VDW and $\pi$-$\pi$ stacking) between the bases of the DNA and the EtBr molecule. In other words, the EtBr molecule slides in between the base-

pairs of the minor groove part of the helix and causes a deformation of the DNA strand which is countered by the rigidity of the phosphate-sugar backbone [6]. The intercalation phenomenon can be detected by fluorescence measurements originating from the EtBr molecule. Upon irradiation, the EtBr molecule absorbs light (UV or VIS, see excitation curve Fig. 4.6) and emits correspondingly light of 590 nm by means of fluorescence. When DNA is brought into a solution of EtBr, abundant intercalation will cause a considerable increase in fluorescence (> 20 times). If polymer is added to this solution, intercalation is inhibited because the electrostatic attraction forces between DNA and the polymer are multiple times stronger which is accompanied by a loss in fluorescence, hence the use of the term EtBr displacement assay[7]. The stepwise addition of polymer to an EtBr-intercalated DNA solution enables the set-up of a condensation profile (in which the fluorescence yield is correlated with the amount of polymer added, expressed in CR).

Since EtBr intercalation substantially stabilizes the DNA, the concentration of EtBr used should be carefully selected. An optimum is to be reached between opposite needs that on one hand require a sufficient amount of EtBr present in order to detect a clear signal whereas on the other hand the quantity of EtBr should be kept as low as possible to allow inhibition of the intercalation process by cationic polyplex formation. From literature, this value was found to function best within the range of 0.2-0.4 µg/ml[8]. The spectrum of EtBr (excitation and emission pattern) as well as the structure are shown below (Fig. 4.6).

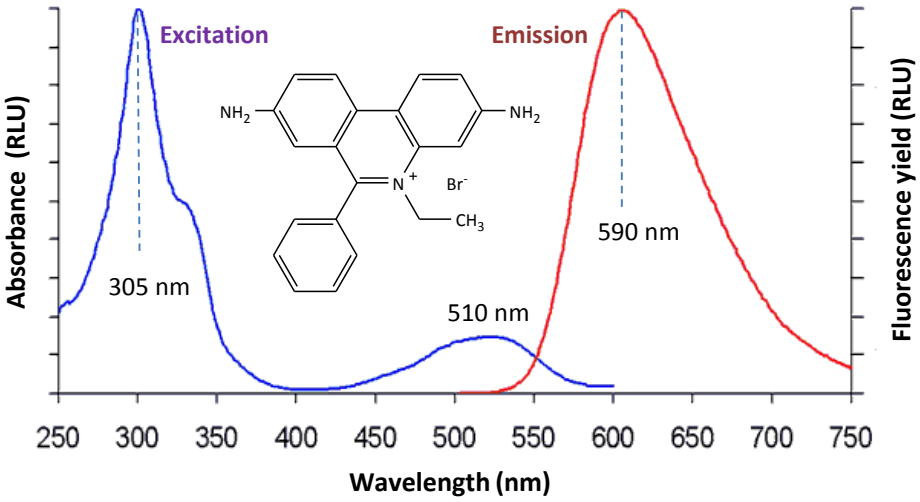


**Figure 4.6 - Fluorescence wavelength spectrum of EtBr and its structure**

Throughout these experiments, polymer was added to a DNA/EtBr solution (20 µg/ml DNA and 400 ng/ml EtBr) in portions representing a CR of 0.2 and the fluorescence signal was repeatedly measured until a total CR of 2/1 was reached. Initially, the DNA/EtBr was calibrated as 100% relative fluorescence. The addition of a critical amount of polymer induces a sudden and steep drop in fluorescence which corresponds with the formation of a

polyplex. Prior to this collapse, the fluorescence signal generally increases modestly, a phenomenon which can explained by the presence of small quantities of polymer that promote the stability of DNA and allow an even higher level of intercalation. Polymers can be mutually compared by plotting the fluorescence as a function of polymer added. Several interpretations are given to these graphs of which the $Min_F$ (relative fluorescence at a CR of 2/1) and the $CR_{minF}$ (lowest CR that represents the steepest fluorescence drop), derived from the intersection of the tangent and the X-axis, are considered the most relevant. This latter value is often referred to as the complexation or condensation point.

### *3.1.1 One-step versus multi-step polyplex formation*

Conform the data presented in section 2.3 of this chapter, the use of EtBr fluorescence spectroscopy was likewise applied to confirm the similarity in polyplex formation between one-step and multi-step polymer addition. A comparison between these two methods (up to polyplexes with a CR of 2/1) led to the conclusion that after 30 minutes of stabilisation, $Min_F$ fluorescence values did not differ more than 5 % (Fig. 4.7). Unlike for UV analysis, the decrease in fluorescence yield is a measure for the formation of a polyplex and corresponds with a loss of EtBr intercalation (described in section 3.1) rather than being the result of higher level of shield (and DNA absorbance decrease). These results validate the possibility to apply both methods, yet preference is given to the more sensitive fluorescence analysis.

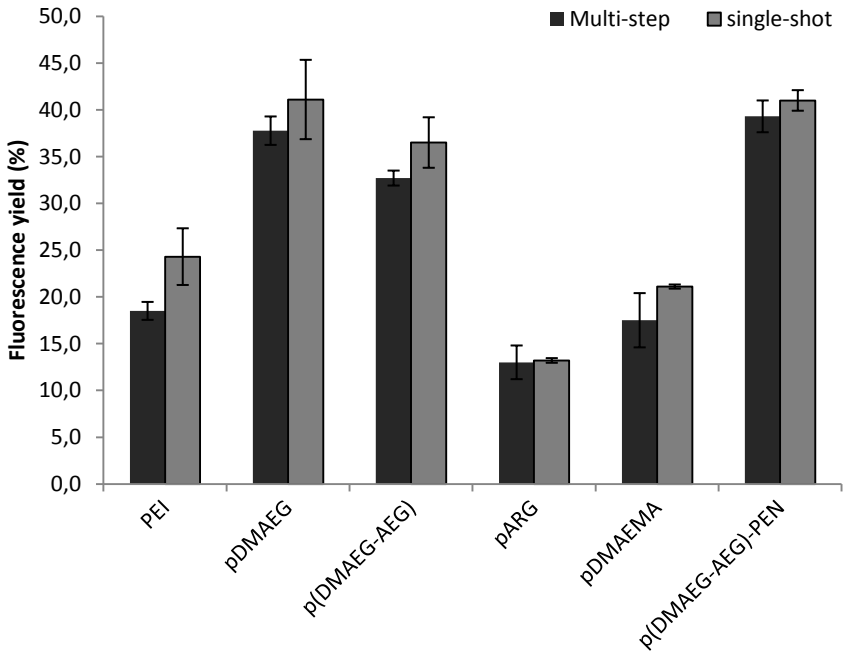


**Figure 4.7 – EtBr Fluorescence data ($Min_F$) in which multi-step and single-shot polyplex formation are compared for different polymers (MW ≈ 10.000 Da, PEI = 25.000 Da).**

### *3.1.2 Polyplex formation: kinetics and stability in time*

Besides the obvious capacity to attract DNA, a polymeric vector needs to preserve this interaction for a sustained time. A simple way to check this feature can be accomplished by measuring the fluorescence intensity of polyplexes for a prolonged time. Additionally, from this experiment, a basic idea on the rate of polyplex formation can be deduced by focusing on the time required to obtain stable polyplexes. This investigation was carried out at a CR of 2/1 so that for all polymers tested, polyplex formation could be reached.

Figure 4.8 demonstrates the EtBr fluorescence yield for several polyplexes as a function of time. In general, polymer-DNA complexes already experience more than 90 % of their total fluorescence decrease 30 seconds past polymer addition (single-shot) after which the value reaches a plateau (Fig. 4.8 – zoomed rectangle). The formation of polyplexes based on PEI deviated considerably from previous conclusion and demands an incubation time of 1 hour to reach a stable value. Initial confirmation of the ability for polymers to condense DNA is already apparent from this experiment but will be discussed further on (section 3.1). Nevertheless, this experiment proved that polyplexes were able to interact with DNA for a prolonged time and were ready to be used after 10 min of incubation (except for PEI). A fully substantiated kinetic approach in understanding polyplexes and polyelectrolyte mediated forces was not within the scope of this doctoral research.

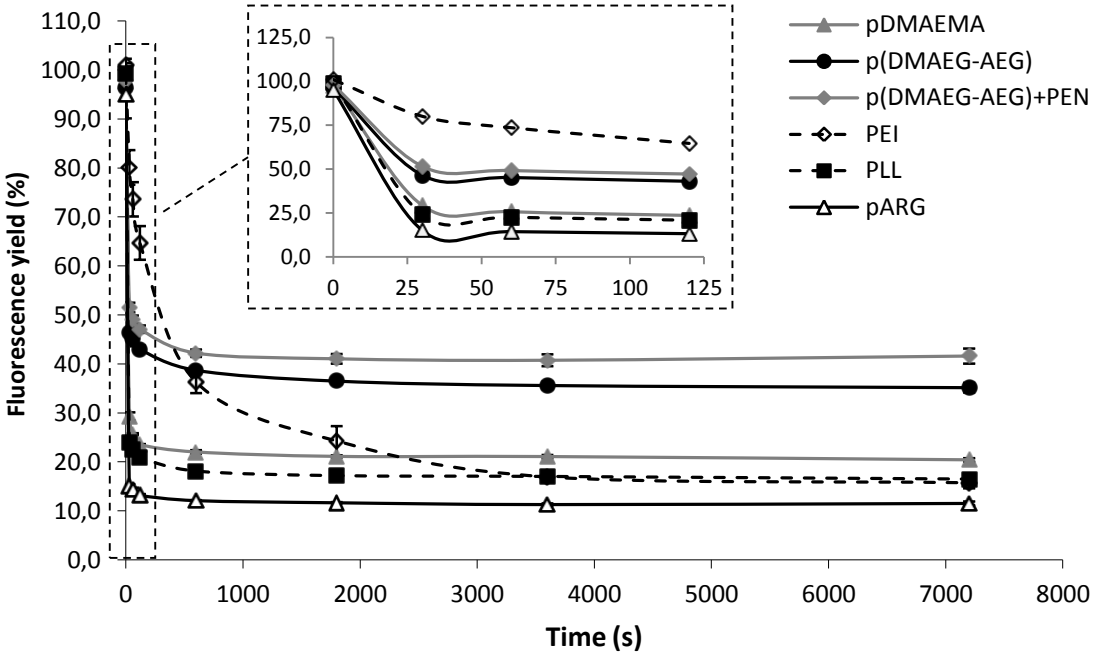


**Figure 4.8 - EtBr fluorescence of different polyplex compositions prepared using single shot addition (CR 2/1): stability as a function of time.**

### *3.1.3 Biodegradable polymers*

In chapter 2, the synthesis of biodegradable poly-α-aminoacids was discussed and several derivatives with potential use as synthetic vectors were produced. As a useful tool EtBr displacement assays were carried out and these results were analysed in a systematic approach including a correlation with structural properties.

#### *3.1.3.1 p(DMAEG)*

At first, the influence of the MW on the condensation ability was verified. This test was carried out on pDMAEG derivatives and is accepted to apply for all poly-L-glutamines. The MW appeared to have a small influence on the DNA-binding capacity and there seems to be a trend that favours the use of short polymer chains since DNA complexation occured at lower CR's (Fig. 4.9). This is advantageous for the *in vitro* viability because the lower the amount of polymer presented inside cells, the lower the toxicity of these delivery systems is expected to be. A lower requirement for cationic polymer to induce a total collapse of DNA into a small particle ($CR_{minF}$) can be ascribed to an optimal polymer rearrangement due to the increased mobility of smaller polymer chains compared to larger ones. Moreover at a CR of 2/1 ($Min_F$), a similar trend was noticed. With decreasing MW, lower fluorescence values were observed which indicated reduced intercalation which corresponds with a tighter DNA interaction. An indication of the $CR_{minF}$ value (= 0.9) and $Min_F$ value (25%) for p(DMAEG) 10 kDa is indicated by dashed lines.

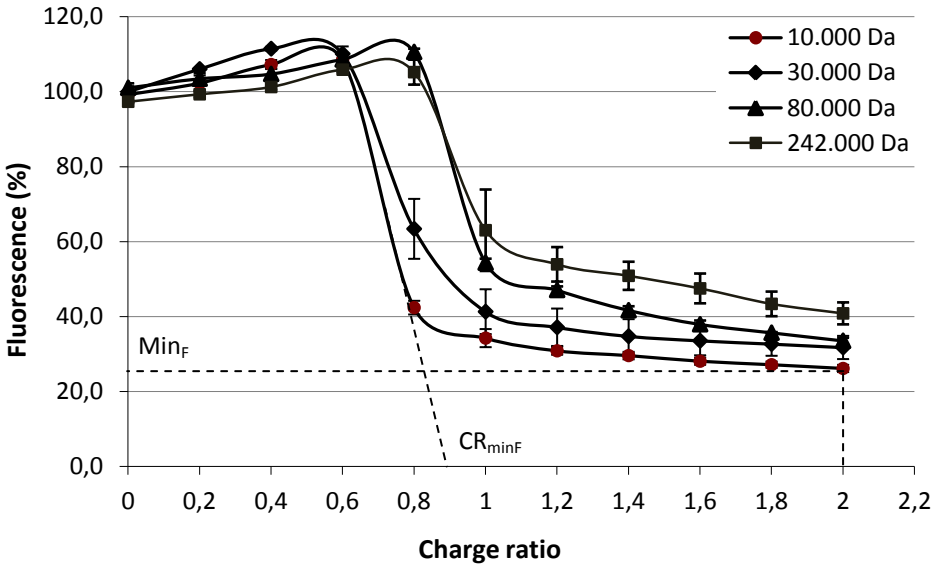


**Figure 4.9 – EtBr fluorescence assay of pDMAEG: Influence of the MW.**

### *3.1.3.2 The main effect of functional group replacement*

The base polymer pDMAEG, which contains tertiary amines, displays intense interaction behaviour with DNA due to its corresponding $pK_a$ and predominantly positive charge when incorporated into a polymer. Because of biological requirements, polymers possessing other functional groups were synthesised and consequently could affect the interaction qualities compared to pDMAEG (MW = 10.000 Da). If a small amount of tertiary amines in the side chain was replaced by primary amines, there appeared to be almost no difference noticeable in complexation behaviour. For p($DMAEG_{90\%}$-$AEG_{10\%}$) with a MW of 6 kDa, the $Min_F$ remained the same and the $CR_{minF}$ increased no more than 5 % (Fig. 4.10). When a non-charged functional group was introduced (-OH) a clear decrease in fluorescence was noticed at a CR of 2/1 (approx. 20%). The importance of the type of cationic group was also here observed, given the fact that the $Min_F$ of p($DMAEG_{61\%}$-$HEG_{39\%}$) is higher than the one of p($DMAEG_{23\%}$-$GuAEG_{27\%}$-$HEG_{50\%}$) while the latter one contains less cationic charges, indicating the stronger attraction force derived from guanidine functional groups.

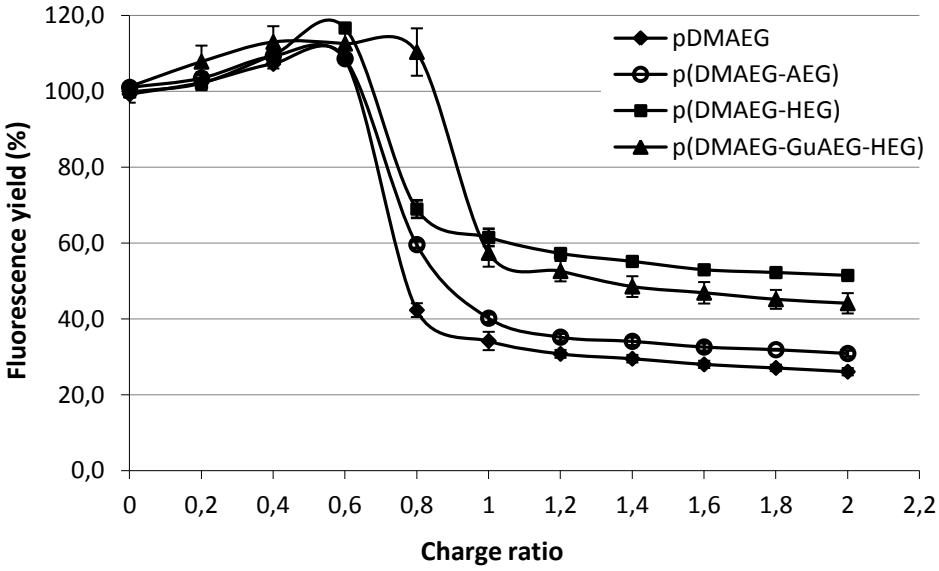


**Figure 4.10 - EtBr fluorescence assay: effect of functional group replacement (MW = 10 kDa): pDMAEG, p($DMAEG_{90\%}$-$AEG_{10\%}$); p($DMAEG_{61\%}$-$HEG_{39\%}$) & p($DMAEG_{23\%}$-$GuAEG_{27\%}$-$HEG_{50\%}$).**

### *3.1.3.3 p(HEG-GuAEG)*

Biologically relevant parameters like the importance of the chemical structure of cell-penetrating peptides and the cytotoxic effects of cationic molecules led to the development of polymers containing a considerable amount of non-charged groups like hydroxyl moieties as well as a certain amount of DNA and cell-interacting charged functional groups like guanidine. Several polymer derivatives with a MW of about 10.000 Da were synthesised with an increasing amount of guanidinium groups in order to determine the essential amount of

charge required for convenient DNA complexation. As can be noticed in figure 4.11, the condensation capacity of the polymers is logically increasing with higher quantities of charge present on the polymer. Optimal condensation is reached when the complexation coincides with a large, sharp drop in fluorescence. This appeared to be the case for the polymer possessing 55 % of guanidine groups while for the derivative containing 35 % (or less) of charges, this drop was smaller in size and smoother. Accordingly, the critical guanidine concentration to induce swift and intense polyplex formation at a low CR is assumed to be between 40 to 50 %.

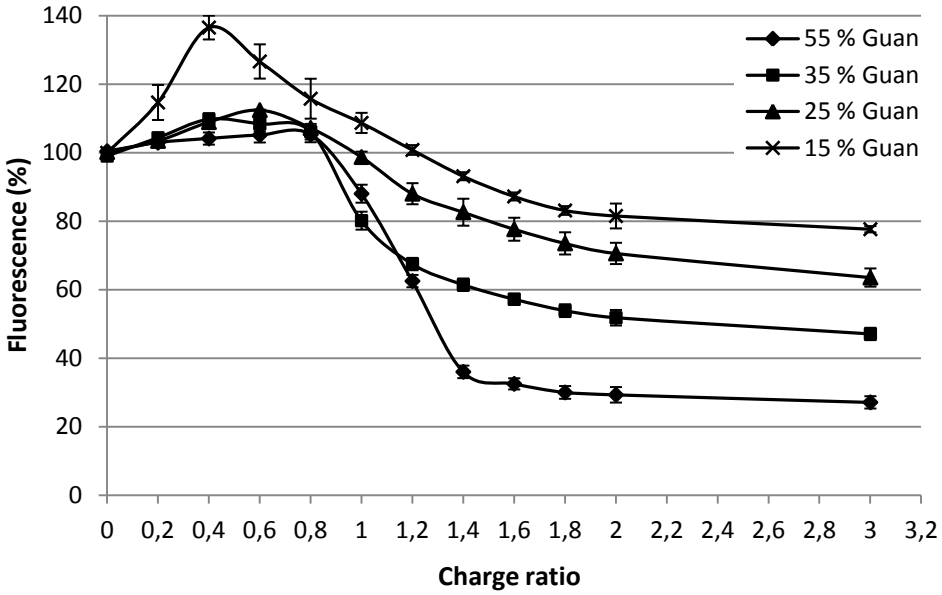


**Figure 4.11 – EtBr fluorescence assay for p($HEG_x$-$GuAEG_y$) 10 kDa: effect of guanidine (% y).**

*3.1.3.4 Imidazole-containing polymers*

In the course of the development of tailor-made polymers, another aspect of major importance for a synthetic vector is the ability to enable endosomal escape (via the proton-sponge theory). It is imperative for polymers to exhibit sufficient buffering capacity. Due to the presence of functional groups that can be protonated and the neighbouring effect typical for macromolecules, most polymers express a certain degree of buffering. To address this need even further, derivatives containing imidazole moieties were developed on account of their $pK_a$ value ($pK_a$ of conjugated acid ≈ 7, partially charged at physiological pH). The fluorescence assay of these derivatives reveals that the contribution of imidazole functional groups in DNA interaction is less than that of the guanidine group. As demonstrated in figure 4.12, a derivative with a substantial higher amount of imidazole (80%) displays a weaker displacement curve than the polymer containing less imidazole but more guanidines (35 %). This confirms that the imidazole molecules are only partially protonated and most likely suitable for enhanced buffering although an augmented hydrophobic effect should be taken

into account when discussing non-charged imidazole groups. Certain hydroxyl-containing variants appear to have lower $CR_{minF}$ values than certain higher charged polymers like p($ImEG_{80\%}$-$GuAEG_{20\%}$)) and comparable $Min_F$ values. This confirms that the DNA interaction based on imidazole is not so intense and suggests that the presence of hydroxyl groups demonstrates a stronger association with DNA than anticipated based on the net charge (for instance by means of H-bonding)[9]. For non-charged imidazole moieties, the quality of H-bridging is much lower than for hydroxyl groups which partially explains the observed effect.

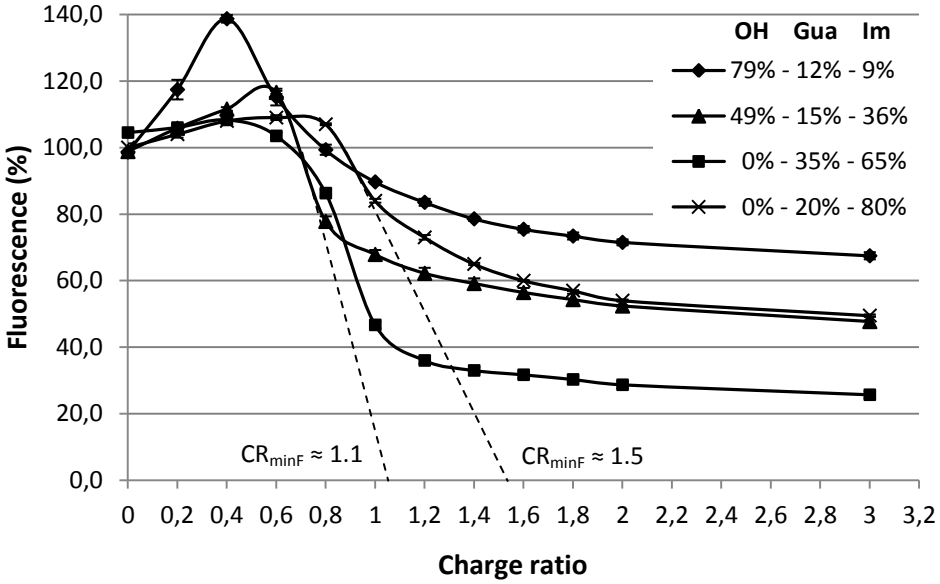


**Figure 4.12 - EtBr fluorescence assay: Imidazole incorporation to enlarge the buffering properties (poly-L-glutamines with a MW of about 10,000 Da).**

*3.1.3.5 The effect of charge on the overall condensation ability*

The aforementioned graphs and conclusions were focussing on specific properties such as presence of functional groups or MW. A less specific trend, considered as a crucial feature, is the extent to which a polymer is charged (in physiological medium). The condensation profile of highly charged and weakly charged polymers shows a clear difference (Fig. 4.13 & 4.14). Not only is the ability to form tightly-complexed particles completely different (visualised through the $Min_F$ value) but also the course of polyplex formation occurs in a dissimilar way. Polymeric vectors containing a high charge density are able to induce a sharp transition in fluorescence upon polyplex formation which indicates that a strong and fast interaction occurs (Fig. 4.13). The strength can be correlated to the $Min_F$ value and is dependent on the charge density as well as the functional groups involved. On the other hand, synthetic vectors that possess only a low charge density (with complementary neutral functionalities) cannot form sudden, firm complexes but demonstrate a rather smooth decrease in fluorescence (Fig. 4.14). In addition to the higher fluorescence values ($Min_F$),

this suggests that the collapse into a small particle is much less intense and happens at a slower pace. Hence, particles of lesser quality (i.e. larger, more weakly bound) are expected although this assumption is not confirmed by DLS measurements (section 4.4). Because all the polymers used for this experiment have an equal MW, the CR at which condensation starts, is similar (ranging from 0.6-1.0). Furthermore, the superior interaction ability of guanidine functional groups as opposed to tertiary amines is apparent when comparing $Min_F$ of p(HEG-GuAEG) and p(HEG-DMAEG) derivatives. On the other hand, the slightly more voluminous guanidinium group (with different charge density) induces a particle formation at a higher $CR_{minF}$ (also confirmed in Fig. 4.10).

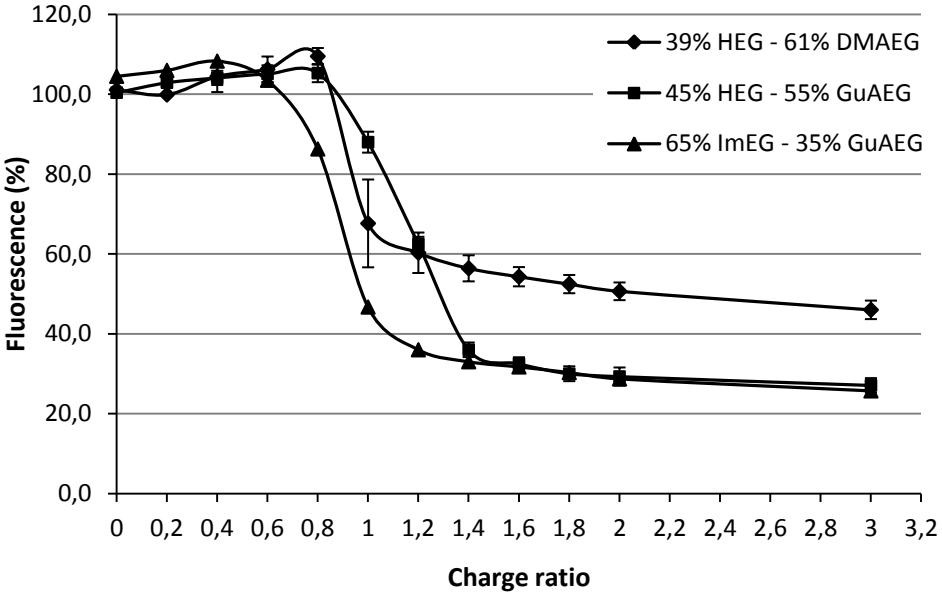


**Figure 4.13 - EtBr fluorescence assay: poly-L-glutamines (MW ≈ 10 kDa), high charge (≈ 60%).**

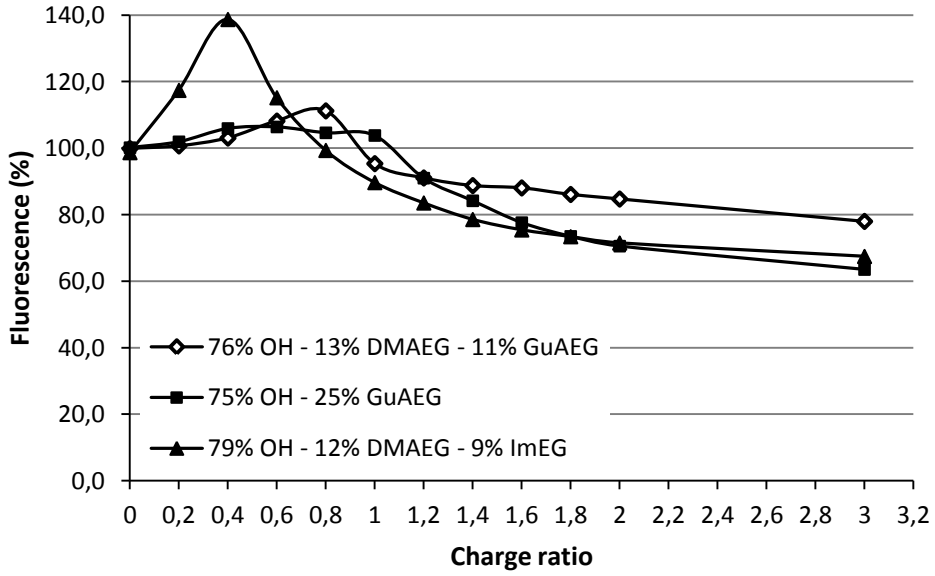


**Figure 4.14 - EtBr fluorescence assay: poly-L-glutamines (MW ≈ 10 kDa), low charge (≈ 25%).**

To finalise, it can be concluded that fully charging a polymer is not required to obtain a fluent and strong complexation between a polymeric vector and DNA. Moreover, the use of guanidine functional groups can induce the most optimal polyplex profile (strong interaction and swift complexation). Imidazole moieties express a lower interaction with DNA (due to partial protonation) than guanidines, yet when present in sufficient quantity (> 40%) or combined with additional charged functional groups, this does not negatively interfere with the complex formation. As a result, they can be involved in the polymer synthesis when considered biologically relevant (e.g. enhanced buffereing). Additionally, neutral hydroxyl functional groups can be used to dissipate charge over the entire polymer and further complete the total composition of the side chain (to influence the desired charge density). Whether a polyplex should be strong and tight or more loose can only be confirmed by biological transfection studies, yet the requirement for intra-cellular polyplex dissociation and the need to protect the therapeutic DNA until the cell nucleus suggests that a little of both approaches is in order.

#### *3.1.3.6 Arginine-based polymers*

Besides poly-L-glutamine based biodegradable vector systems, also poly-L-arginine (pARG) and other L-arginine derivatives were subjected to a physico-chemical characterisation. Considering that the homopolymer, pARG (MW ≈ 80.000 Da) bears solely guanidine functional groups (that represent a $pK_a$ of 12.5 for the conjugated acid), the polymer comprises a high amount of charge as marked in the corresponding EtBr fluorescence assay (Fig. 4.15). Both a low $Min_F$ value (16%) as well as a low $CR_{minF}$ (1.0) are noticed with a very sharp transition upon complex formation. The profile for p($ARG_{82\%}$-$ORN_{18\%}$) of the same MW largely resembles the homopolymer. Hence, the amount of primary amine required for further coupling does not exert a significant influence. A copolymer that contains both a hydroxyetlyglutamine (HEG) and arginine part as backbone, p($HEG_{58\%}$-$ARG_{42\%}$) was likewise prepared and its structure was compared with other arginine derivatives as well as with its glutamine-based counterpart, p(HEG-GuAEG). The small difference in its structure lies in the distance between the charge, located on the side-chain, and the backbone, a parameter which is often not considered and that could have serious biological implications (for instance in receptor communication)[10]. The p($HEG_{58\%}$-$ARG_{42\%}$) vector has a MW of about 56.000 and displays a fluorescence pattern similar to p(HEG-GuAEG) which indicates that there is still sufficient mobility to induce an optimal orientation around DNA despite the shorter side-chain (when compared to GuAEG). When the arginine residues are incorporated in another way, that is by grafting pARG onto an L-glutamine based polymer containing primary amines that can act as an initiator, for instance p($HEG_{87\%}$-$AEG_{13\%}$) with a MW of about 10.000 Da, a very pronounced influence is perceived. More specifically,

condensation occurs at a lower $CR_{minF}$(0.9) and tighter polyplexes are obtained (lower $Min_F$, 22 %) than for p($HEG_{58\%}$-$ARG_{42\%}$) although the effect of the smaller MW should be taken into account as well. The effect of charge position and orientation will be discussed later on.

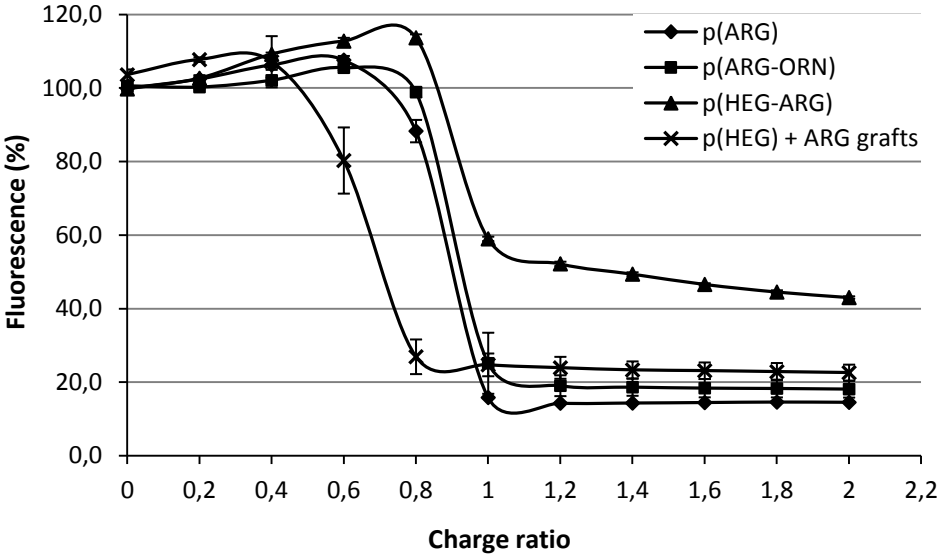


**Figure 4.15 – EtBr fluorescence assay: p(ARG) 80 kDa; p($ARG_{82\%}$-$ORN_{18\%}$) 80 kDa; p($HEG_{58\%}$-$ARG_{42\%}$) 56 kDa; p($HEG_{87\%}$-$AEG_{13\%}$)+p(ARG) grafts (10 + 2 kDa).**

### *3.1.4 Non-biodegradable polymers*

In the framework of developing synthetic vectors that demonstrate a high level of biological activity and to substantiate structure-property relations of polymers applied as gene delivery systems, a group of non-biodegradable polymers based on a methacrylate backbone was likewise evaluated and compared to biodegradable compounds. Since these compounds have a more hydrophobic nature, varying results were expected.

#### *3.1.4.1 p(DMAEMA)*

The basic polymer suitable for comparison to biodegradable counterparts is p(DMAEMA), a polymer containing exclusively tertiary amines. Several compounds with a variable MW were synthesised and their ability to interact with DNA was checked by an EtBr displacement assay. In contrast to glutamine-based polymers, p(DMAEMA) (Fig. 4.16) indicates an optimum existing in the formation of polyplexes. Both high and low MW polymers show complexation at higher CR's ($CR_{minF}$ deviates up to 0.4 CR units) than the intermediate polymer of 121 kDa. The optimal MW also exhibits the strongest interaction with DNA (at $Min_F$) although the difference with other MW's is limited. Seeing that mobility is not the decisive parameter, secondary effects (like the influence of hydrophobic backbone in an aqueous environment) could play a role in explaining the essential function of chain length.

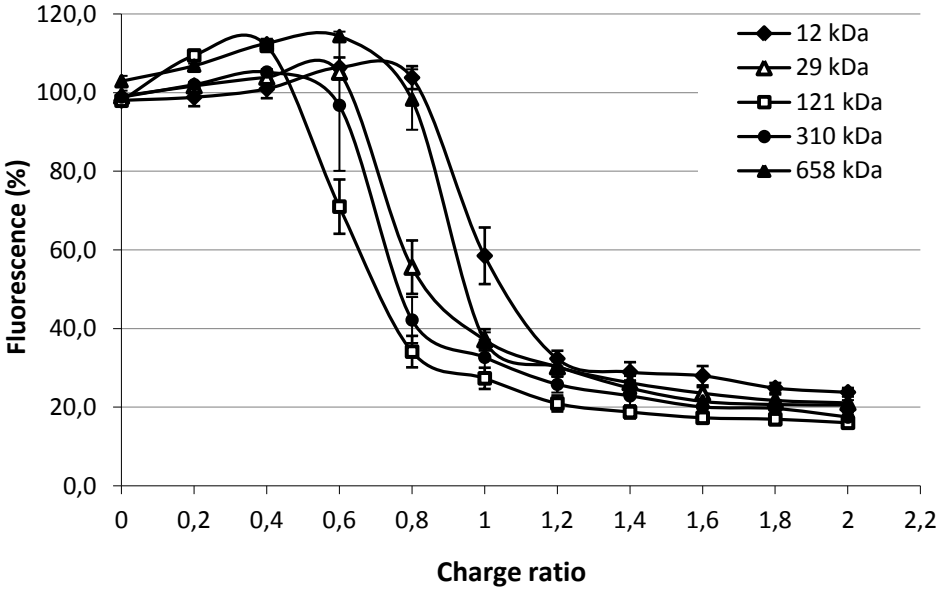


**Figure 4.16 - EtBr fluorescence assay of p(DMAEMA): influence of the MW.**

To facilitate the interpretation of the influence of the MW, the $CR_{minF}$ values of a range of different DMAEMA-polymers with various MW were compared (Fig. 4.17). From these results, the optimal MW appeared to be situated in the range of 100-150 kDa. To validate this assumption, experiments with more polymers having a MW close to the 'optimum' should be carried out. Confirmation of this trend could partially be inferred from previous doctoral research for p(DMAEMA) by Dubruel et al[2].

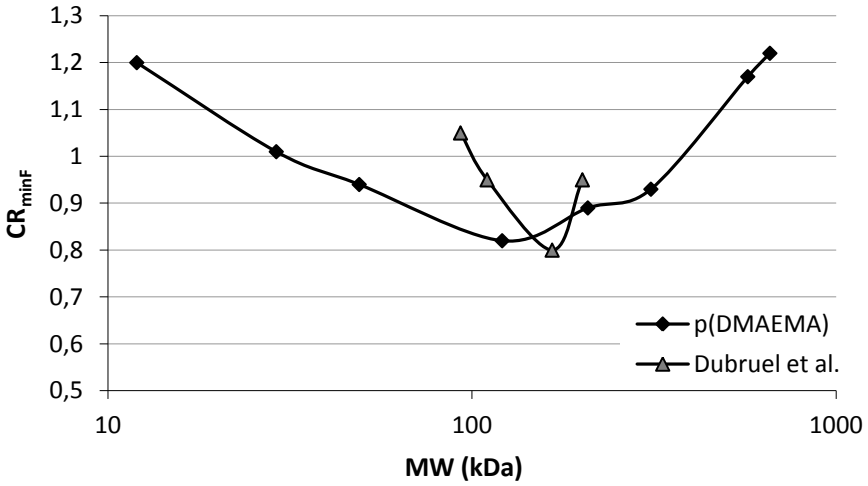


**Figure 4.17 – $CR_{minF}$ of various p(DMAEMA): influence of MW on the condensation ability[2].**

*3.1.4.2 The effect of functional group replacement*

Replacing functional groups in p(DMAEMA) has a more explicit influence than for p(DMAEG). Whereas for glutamine-based polymers only the introduction of a substantial amount of hydroxyl groups provoked a decreased interaction with DNA, for polymethacrylates a minor change of the composition has considerable consequences for

the capacity to prevent EtBr displacement (Fig. 4.18). Even at small concentrations of primary amines present (p(DMAEMA$_{82\%}$-AEMA$_{18\%}$) – 191 kDa), a shift towards a higher $CR_{minF}$ value is required for the start of polyplex formation. This is remarkable because the difference between p(AEMA) 176 kDa and p(DMAEMA) 121 kDa homopolymers is rather small. These unfavourable effects are even more clear when charged groups are replaced by hydroxyl groups (p(DMAEMA$_{80\%}$-HEMA$_{20\%}$) – 187 kDa) causing a $CR_{minF}$ shift of nearly a full CR unit. The interaction strength at full condensation (when a plateau value is reached) is not affected for primary amines but is very pronounced for hydroxyl-based derivatives (loss of about 30 % at $Min_F$) because of the obvious loss of charge. Combining tertiary amine groups and primary functional groups in one polymer confirms the different nature of the methacrylate and amide compounds in polyplex formation ($CR_{minF}$ values). Because the extra opportunity for hydrogen bonding with the backbone is excluded for polymethacrylates, only side-chain/side-chain H-bonding remain possible. The extent to which primary amines are incorporated appears to have a strong effect on the $CR_{minF}$ value and is most likely related to the polymer conformation (e.g. limited intra-molecular interaction for small portions of primary amines). For poly-L-glutamine compounds on the other hand, H-bonding with the backbone compensates the lack of interaction which might be needed to change the polymer conformation in such a way that the spatial rearrangement with DNA is different (expressed by the different $CR_{minF}$). This is also revealed when comparing hydroxyl-based copolymers of both types, specifically the $CR_{minF}$ value is much less shifted in the case of glutamine because backbone H-bonding remains. The MinF value in contrast, is not affect, indicating that the DNA interaction remains mainly driven by the electrostatic forces.

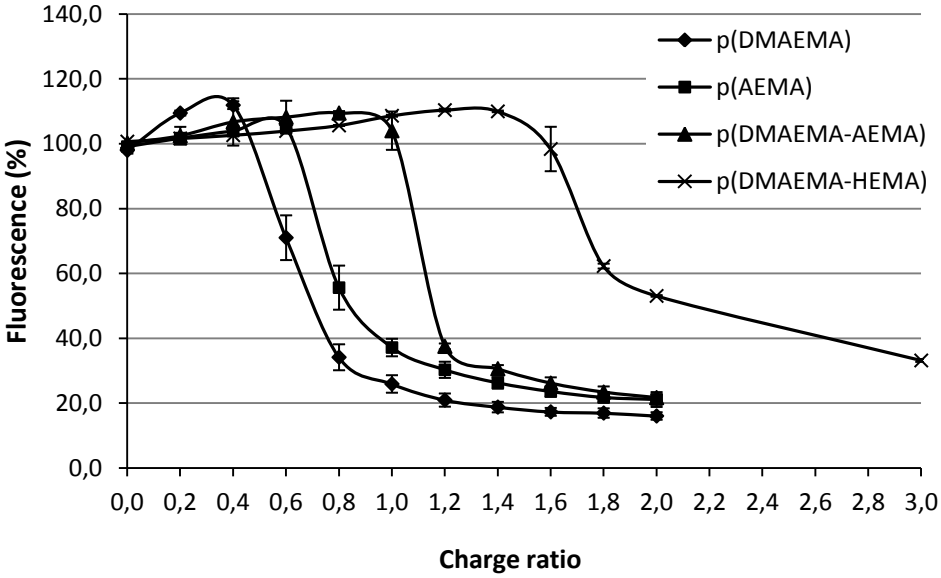


**Figure 4.18 – EtBr fluorescence assay: influence of functional group for p(DMAEMA) 121 kDa, p(AEMA) 176 kDa, p(DMAEMA$_{82\%}$-AEMA$_{18\%}$) 191 kDa & p(DMAEMA$_{80\%}$-HEMA$_{20\%}$) 187 kDa.**

### *3.1.4.3 The impact of type of functional group*

The type of functional group on which the charge is located, was proven to be quite relevant for glutamine based polymers. For methacrylate polymers on the other hand, the difference appeared to be more restricted (Fig. 4.19). The condensation profile of p(DMAEMA) with a MW of 29 kDa and p(GuAEMA) with a MW of 63 kDa turned out to be virtually the same (equal $CR_{minF}$ and a $Min_F$ value differing less than 5 %). For copolymers that also contain neutral functional groups, the effect was more pronounced. The apparent resemblance between p($DMAEMA_{55\%}$-$HEMA_{45\%}$) with a MW of 14 kDa and p($GuAEMA_{40\%}$-$HEMA_{60\%}$) – MW 29 kDa is due to the higher amount of charge present on the former. This discrepancy masks the actual difference of a derivative possessing an equal amount of charges (with a more or less equal $CR_{minF}$ but higher $Min_F$ value in the case of tertiary amines). The effect of the $pK_a$ value is very clear in the case of p($AEMA_{40\%}$-$HEMA_{60\%}$) – 29 kDa and its guanidine modified version that has a weaker ability to attract DNA and a correspondingly higher $Min_F$ value.

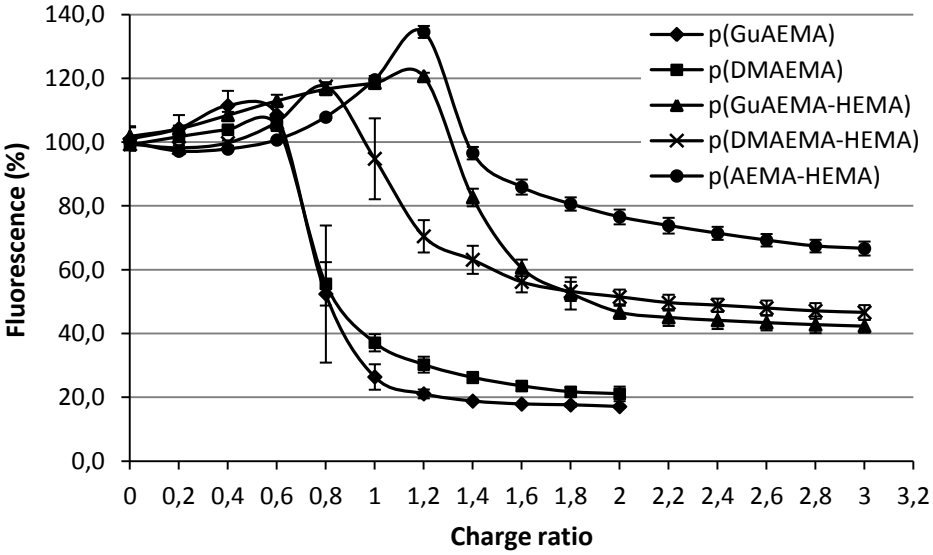


**Figure 4.19 – EtBr fluorescence assay: influence of type of charged functional group on methacrylate based compounds: p(GuAEMA) 63 kDa; p(DMAEMA) 29 kDa; p($GuAEMA_{40\%}$-$HEMA_{60\%}$) 29 kDa; p($DMAEMA_{55\%}$-$HEMA_{45\%}$) 14 kDa & p($AEMA_{40\%}$-$HEMA_{60\%}$) 29 kDa.**

### *3.1.5 PEI & PEI-derivatives*

Throughout this research, the potential of newly developed synthetic vectors was on a permanent basis compared to PEI , a vector that is widely considered as highly active. As a consequence of the negative effect it has cellular viability, several research groups started the investigation of PEI modification during the last years[11,12,13,14,15,16,17]. Based on previous statements, claiming the beneficiary effect of arginine residues on both the DNA interaction and cellular uptake, modified PEI-derivatives were also synthesised and characterised within

this research. Modification was carried out by using similar guanidylation strategies as before and which appeared to be applied as well by others as reported in literature later[18,19]. The interesting potential of grafting onto PEI was likewise evaluated in order to maintain the excellent buffering capacity while enhancing the DNA-interaction and cell toxicity. Therefore, the poly-L-glutamine grafts were modified with both hydroxyl and guanidine functional groups. Fluorescence analysis of PEI, PEI-Guan$_{20\%}$ and PEI-pGLN (HEG$_{63\%}$-GuAEG$_{37\%}$) is shown below in figure 4.20.

According to expectations, PEI displays a swift complexation with DNA ($CR_{minF}$ around 0.8). Converting the primary amines into guanidine functional groups causes a change in $Min_F$ (about 20% lower) but has a similar $CR_{minF}$ value although a a much steeper drop in fluorescence was observed. This contrast is on one hand ascribed to the nature of the guanidinium group (higher $pK_a$ of conjugated acid) but also to the change in charge distribution and corresponding buffering ability. When poly-L-glutamine grafts are introduced, the polyplex profile is largely altered. Due to the nature of the glutamine composition (with a high hydroxyl content), the interaction force is slightly decreased. Additionally, grafting onto a branched molecule, drastically expands the hydrodynamic radius and because of the diminished occurrence of charged groups a more diffuse cationic pattern is observed which leads to higher values of $CR_{minF}$ (1.6). On the other hand, by increasing the charge density on the grafts, the interaction ($Min_F$) can be intensified. The medium $Min_F$ value of PEI could suggest that the success of this compound is attributed to an optimal interaction with DNA, meaning a strong but not inseparable bond with DNA, able to dissociate during endosomal escape.

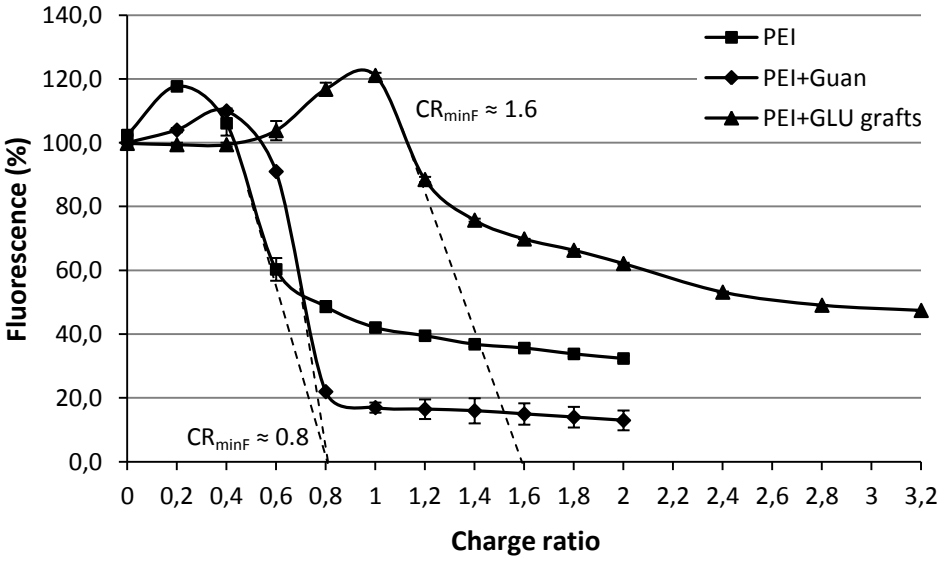


**Figure 4.20 - EtBr fluorescence assay of PEI, guanidylated PEI and L-glutamine grafted PEI.**

### *3.1.6 Conclusion*

EtBr-based fluorescence experiments in which the formation of polyplexes is proportional to the degree of decreased intercalation, proved to be a very suitable characterisation technique that provides global information on the interaction strength of polyplexes and the quality to start forming these complexes. Fully charged polymers, both biodegradable and non-biodegradable readily form polyplexes and do this in strong manner (tight complexes) as indicated by the often low values of $Min_F$. The introduction of other functional groups than tertiary amines, results in different condensation profiles for these two classes of synthetic vectors. If replaced by other charged groups, there was nearly no change observed for poly-$\alpha$-aminoacids whereas a more distinct influence was noticeable for polymethacrylate-derivatives (higher $CR_{minF}$ values). In both cases, the introduction of guanidines appeared to reinforce the interaction, also for PEI. When neutral functional groups where built-in during synthesis, the CR required to induce polyplex formation was increased and the interaction strength lowered (higher $Min_F$ values). For poly-$\alpha$-aminoacids this effect was less pronounced than for polymethacrylates where a small quantity of hydroxyl group causes a clear $CR_{minF}$ increase and $Min_F$ decrease which illustrated the different nature of the polymer backbones. In the case of poly-L-glutamines, imidazole functional groups were deemed appropriate to be assessed as biological enhancers while preserving the physical behaviour. The condensation of DNA was inversely proportional to the MW for biodegradable polymers but for polymethacrylates, an optimum was observed that favours vectors with a MW around 100.000 Da. Grafting onto a polymer via the side-chain generally increases the size and the complexation ability of these compounds. Dependent on the type of grafting (highly charged or rather neutral), the polymers can be rendered highly interacting or considerably less interacting, regardless of the base polymer involved.

Table 4.1 gives an overview of the different $CR_{minF}$ and $Min_F$ values for the tested polymers.

| **Polymer** | **$M_w$ (kDa)** | **$CR_{minF}$** | **$Min_F$** |
|---|---|---|---|
| pDMAEG | 10 | 0.9 | 25 % |
| pDMAEG | 30 | 1.0 | 30 % |
| pDMAEG | 80 | 1.2 | 33 % |
| pDMAEG | 242 | 1.3 | 40 % |
| p($DMAEG_{90\%}$-$AEG_{10\%}$) | 6 | 1.0 | 30 % |
| p($DMAEG_{60\%}$-$HEG_{40\%}$) | 10 | 1.1 | 52 % |
| p($HEG_{85\%}$-$GuAEG_{15\%}$) | 10 | 2.6 | 81 % |

| | | | |
|---|---|---|---|
| p($HEG_{75\%}$-$GuAEG_{25\%}$) | 10 | 2.8 | 70 % |
| p($HEG_{65\%}$-$GuAEG_{35\%}$) | 10 | 1.7 | 48 % |
| p($HEG_{45\%}$-$GuAEG_{565\%}$) | 10 | 1.6 | 26 % |
| p($ImEG_{65\%}$-$GuAEG_{35\%}$) | 10 | 1.2 | 26 % |
| p($ImEG_{80\%}$-$GuAEG_{20\%}$) | 10 | 1.5 | 50 % |
| p($HEG_{49\%}$- $GuAEG_{15\%}$-$ImEG_{36\%}$) | 10 | 1.1 | 47 % |
| p($HEG_{79\%}$- $GuAEG_{12\%}$-$ImEG_{9\%}$) | 10 | 1.5 | 68 % |
| p($HEG_{50\%}$- $GuAEG_{27\%}$-$DMAEG_{23\%}$) | 10 | 1.2 | 43 % |
| p($HEG_{76\%}$- $GuAEG_{11\%}$-$DMAEG_{13\%}$) | 10 | 2.2 | 84 % |
| pARG | 80 | 1.0 | 13 % |
| p($ARG_{82\%}$-$ORN_{18\%}$) | 80 | 1.1 | 19 % |
| p($HEG_{58\%}$-$ARG_{42\%}$) | 56 | 1.2 | 42 % |
| p($HEG_{87\%}$-$AEG_{13\%}$)+pARG grafts | 10 | 0.9 | 22 % |
| PEI | 25 | 0.8 | 33 % |
| PEI+$Guan_{20\%}$ | 25 | 0.8 | 14 % |
| PEI+p(GLN) | 25 | 1.6 | 61 % |
| pDMAEMA | 12 | 1.2 | 23 % |
| pDMAEMA | 29 | 1.0 | 20 % |
| pDMAEMA | 121 | 0.9 | 18 % |
| pDMAEMA | 310 | 1.0 | 19 % |
| pDMAEMA | 658 | 1.1 | 20 % |
| pAEMA | 176 | 1.0 | 21 % |
| pGuAEMA | 63 | 1.0 | 19 % |
| p($DMAEMA_{82\%}$-$AEMA_{18\%}$) | 191 | 1.3 | 21 % |
| p($DMAEMA_{82\%}$-$HEMA_{18\%}$) | 187 | 2.1 | 53 % |
| p($DMAEMA_{55\%}$-$HEMA_{45\%}$) | 14 | 1.8 | 49 % |
| p($GuAEMA_{40\%}$-$HEMA_{60\%}$) | 29 | 1.8 | 42 % |
| p($AEMA_{40\%}$-$HEMA_{60\%}$) | 29 | 1.8 | 77 % |

**Table 4.1 - Summary of $CR_{minF}$ & $Min_F$ values (EtBr fluorescence assay).**

## 3.2 Agarose Gel-electrophoresis

In order to substantiate the results derived from EtBr fluorescence analyses, gel-electrophoresis is applied as a secondary technique in validating polyplex formation. Gel-electrophoresis based on agarose (AGE), the most suitable matrix to separate large nucleic acids, is an easy way to split-up and visualize DNA fragments based on their size, hence its classification as size-exclusion chromatography (SEC). Nevertheless, this method is differently employed in this experiment: vector-associated DNA (polyplex) is prevented from migrating through an agarose gel under the influence of an electric field whereas free DNA is not (Fig. 4.21). In such a way, not the degree of migration is considered important but merely the inhibition of DNA migration towards the positive anode [20]. Complexation of DNA neutralises and shields the negative charge so that migration is prevented. Complete condensation leads to retention in the wells of the gel as is visualised by EtBr staining afterward (no DNA bands visible). The extent of DNA migration will depend on the quality of condensation, determined by the degree of DNA-polymer interaction and in practise, this is noticed by a gradual decrease in staining intensity. When the DNA signal has completely faded, this value is considered as the condensation CR ($CR_{cond}$).

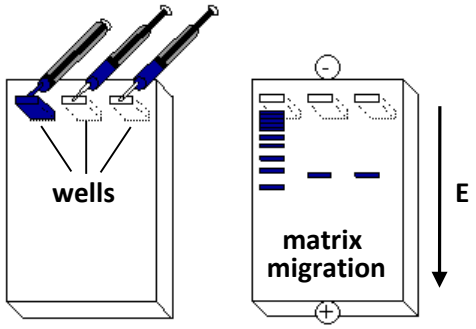


**Figure 4.21 – Schematic impression of gel-electrophoresis with corresponding DNA migration.**

In AGE, mixtures of DNA and polymer with increasing CR (0.2 step) are injected onto an agarose gel (1 %). To prevent diffusion of the compounds into the buffered environment (1x TBE buffer), they were mixed with 10% of loading buffer (50 % glycerol, 0,1 % bromophenol blue). A voltage of 90 V was applied during one hour and subsequent staining of the DNA was carried out by submerging the gel in an EtBr solution (0.5 mg/ml) followed by visualisation on a transilluminator using UV-B light ($\lambda$ = 312 nm). Pure, free DNA was always checked as well to allow comparison. The corresponding results are shown below.

### *3.2.1 DNA-condensation by cationic biodegradable polymers*

The results represented in figure 4.22, confirm the trends derived from EtBr fluorescence measurements. PEI (A) and PEI-$Guan_{20\%}$ (B) display the same CR values as previous established (0.6 / 0.8 units) and in the case of PEI-Guan the DNA band corresponding with a

polyplex of 0.6/1 is stained weaker since complexation is already starting (analogue to Fig. 4.20). For p(DMAEG) and p($DMAEG_{85\%}$-$AEG_{15\%}$) of respectively 80 and 91 kDa, also a consistent result was obtained with both polymers demonstrating polyplex formation at a CR of 1.0 and a sharp transition from stained free DNA (CR 0.8) to non-visible polyplex (CR 1.0). Dependent on experimental irregularities and the fact that AGE is a technique which is based on a different principle (SEC compared to spectrometry for EtBr fluorescence), small deviations of the results obtained by fluorescence are frequently observed (e.g. 0-0.2 CR units). This occurred also for p(ARG) as shown in Fig. 4.22 – E where the inhibition of DNA is only fully achieved at a CR of 1.2 instead of 1.0 for EtBr fluorescence.

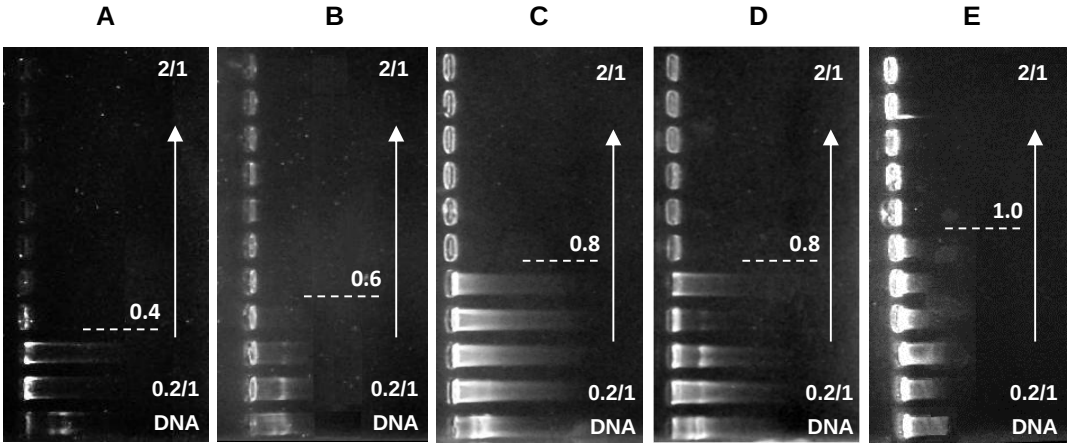


**Figure 4.22 - AGE images of PEI (A), PEI-Guan (B), p(DMAEG) 80 kDa (C), p($DMAEG_{85\%}$-$AEG_{15\%}$) 91 kDa (D) and p(ARG) 79 kDa (E).**

Similar to fluorescence analysis, general trends concerning the composition could be spotted for p(HEG-GuAEG) (Fig. 4.23). With a decreasing amount of charged guanidine functional groups, the ability to enclose DNA becomes less pronounced, visualised by the presence of a DNA smear that is gradually decreasing towards higher CR's (compare to Fig. 4.11). The values obtained here are substantially lower than those measured with fluorimetry and seem to be comparable to the start of the fluorescence drop (starting from the maximum peak value at the beginning, section 3.1) and end when a relative value of 80 % is crossed.

The importance of the nature of the charged group involved as well as the influence of combining two or more types of functional groups could also be verified from electrophoresis (Fig. 4.24). A sufficiently high amount of charged groups in combination with charge separators (hydroxyl groups) is perfectly capable of forming tight complexes at low CR's (0.8), confirmed in image A and B. When smaller amounts of charged groups are applied, the minimal CR for full condensation is accordingly augmented (Fig. 4.24 – C to E). The importance of hydroxyl groups, which are in the first place applied to diminish the overall charge and to induce more charge dispersity, appears from these images. A substantial

amount of imidazole moieties is only efficient in helping attract DNA when hydroxyl groups are present because the polymer containing both hydroxyl and imidazole (C) has a lower complexation point (1.8) despite the lower amount of charged groups on the hydroxyl-containing polymer. This is confirmed by comparing image 4.24 – D ($CR_{cond}$ > 2.0) with figure 4.23 – C/D which have a comparable amount of guanidines.

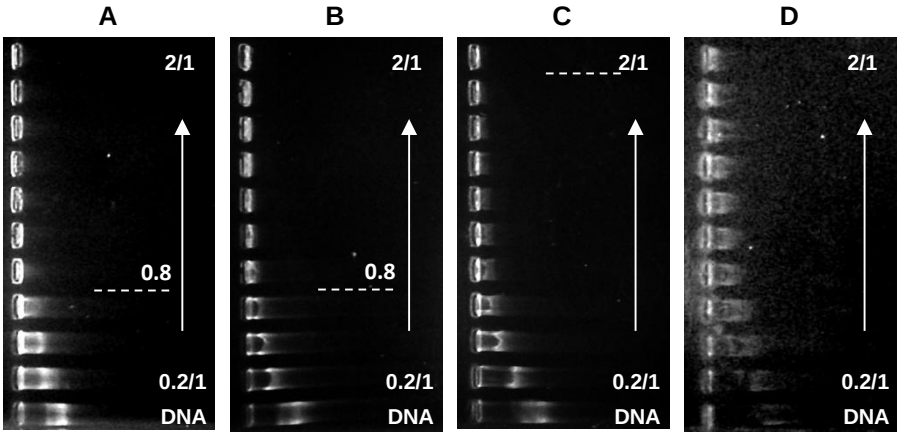


**Figure 4.23 - AGE images of (A) p($HEG_{45\%}$-$GuAEG_{55\%}$), (B) p($HEG_{65\%}$-$GuAEG_{35\%}$), (C) p($HEG_{75\%}$-$GuAEG_{25\%}$) and (D) p($HEG_{85\%}$-$GuAEG_{15\%}$) with a MW of about 10,000 Da.**

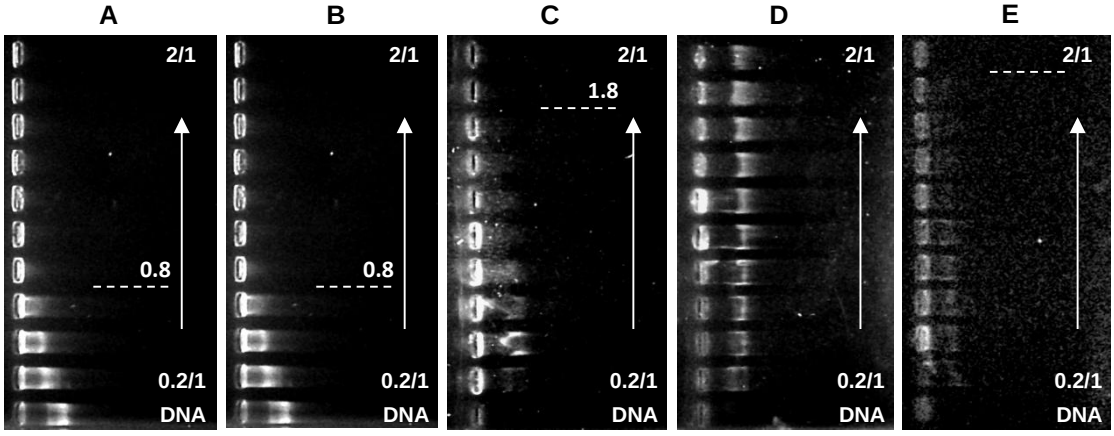


**Figure 4.24 - AGE images of (A) p($HEG_{60\%}$-$DMAEG_{40\%}$), (B) p($HEG_{45\%}$-$GuAEG_{55\%}$), (C) p($HEG_{49\%}$-$GuAEG_{15\%}$-$ImEG_{36\%}$), (D) p($GuAEG_{20\%}$-$ImEG_{80\%}$) and (E) p($GuAEG_{35\%}$-$ImEG_{65\%}$) (MW ≈ 10,000 Da).**

The hypothesis that imidazole functional groups change the way the polymer interacts with DNA is once more proven by mutually comparing imidazole-containing polymers (Fig. 4.25). When drawing a parallel between images B and D, the latter polymer contains more charged groups and more imidazole groups but has no hydroxyl groups ($CR_{cond}$ = 2.0). Nevertheless polymer B, which has about 50% of neutral groups exhibits a more or less equal $CR_{cond}$ (1.6). This leads to believe that a higher ratio of imidazole is required to obtain a polymer that demonstrates swift polyplex formation. But from image C can be concluded that only

weakly associated complexes are formed if the quantity of imidazole groups is raised. Therefore, only if the amount of charged groups is increased, will tighter complexes be formed and a lower $CR_{cond}$ be obtained. The exclusive addition of hydroxyl groups is consequently not sufficient to enhance DNA interaction with imidazole possessing polymers (as noted from image A) and therefore the combination of hydroxyl and charged groups remains advisable in the case of imidazole-containing derivatives.

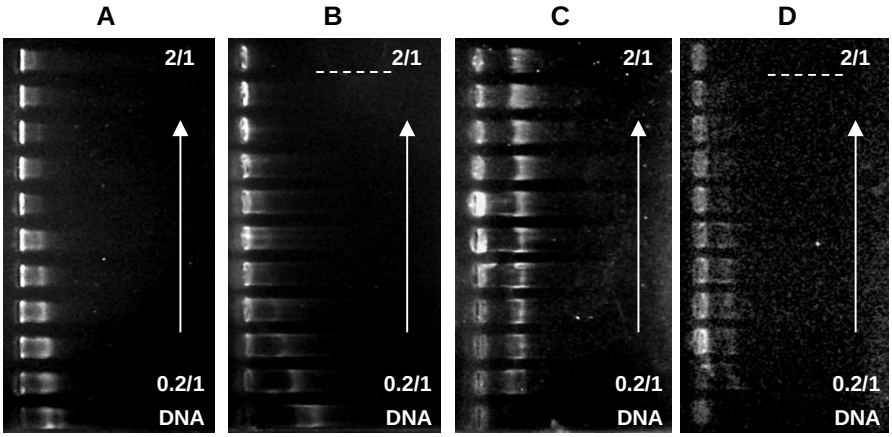


**Figure 4.25 - AGE images of (A) p($HEG_{79\%}$-$GuAEG_{12\%}$-$ImEG_{9\%}$), (B) p($HEG_{49\%}$-$GuAEG_{15\%}$-$ImEG_{36\%}$) (C) p($GuAEG_{20\%}$-$ImEG_{80\%}$) and (D) p($GuAEG_{35\%}$-$ImEG_{65\%}$). MW = 10,000 Da.**

In general, it can be concluded that AGE largely confirms the results given by EtBr fluorescence with a margin for the $CR_{cond}$ that corresponds with full condensation ($CR_{minF}$). When the fluorescence intensity is decreasing, there appears to be a tendency within corresponding AGE experiments to start observing inhibition of DNA. Roughly stated, the CRcond in AGE experiments is reached when the fluorescence intensity of the corresponding EtBr experiments drops below 80%. This indicates that weakly bound complexes can not always be distinguished from tighter ones. On the other hand, in nearly all cases, a graduate decline in fluorescence correlates with a similar decrease in related AGE images, i.e DNA bands that display a shorter run-length and intensity (‘fuzzy smear’). Finally and most importantly, the relative ratio for condensation between the different polymers remains for both techniques.

### *3.2.2 Gel-electrophoresis results of non-biodegradable polymers*

Homopolymers of p(DMAEMA) revealed that the correlation between the MW and the ability to form complexes with DNA was resembling the curve of a parabola with a minimum (in $CR_{minF}$) for polymers with a MW around 100.000-150.000 Da. This trend was equivalent with the one observed from AGE images. Whereas the extreme values display full condensation at the highest CR’s (1.6 for 658 kDa and 1.2 for 11.9 kDa), the derivative of 121 kDa

prevents DNA migration already at a CR of 1.0. The closer the MW is shifted to the optimum, the lower the CR gets (Fig. 4.26).

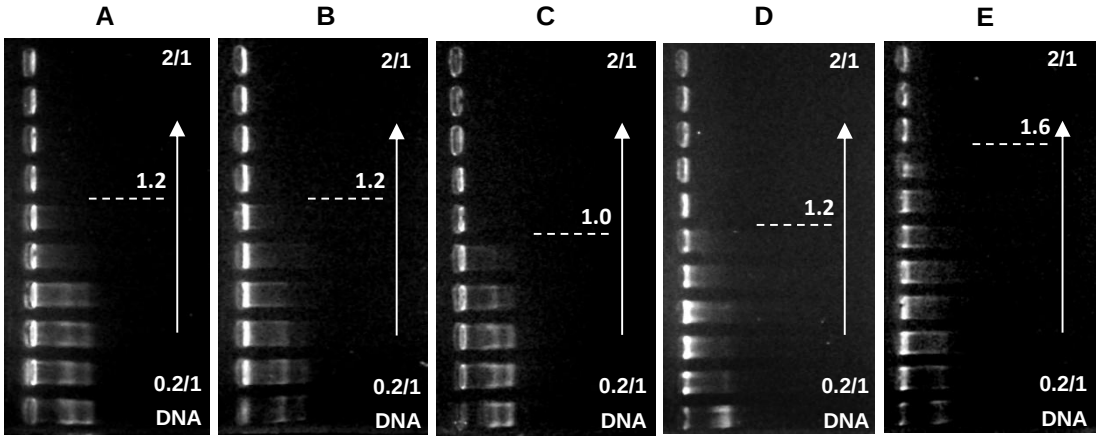


**Figure 4.26 – AGE images of p(DMAEMA): 11.9 kDa (A), 29.2 kDa (B), 121 kDa (C), 310 kDa (D) and 658 kDa (E).**

AGE images of other types of methacrylate polymers are shown below in figure 4.27. For the homopolymer of pAEMA with a MW of 176 kDa (A), a similar result was obtained ($CR_{cond}$ of 1.0 which is similar to pDMAEMA 121 kDa). If copolymers were evaluated, fluorescence analyses pointed out that a high increase in $CR_{minF}$ and/or $M_{inF}$ was readily observed. Nevertheless, the electrophoresis result of p($DMAEMA_{82\%}$-$AEMA_{18\%}$) did not show an increase but rather a decrease in $CR_{cond}$ needed to inhibit DNA migration. Mainly the presence of hydroxyl-containing HEMA in copolymers demonstrated clear deviations, both for $CR_{minF}$ and $Min_F$. Images C – E show a p($DMAEMA_{x\%}$-$HEMA_{y\%}$) derivative with increasing HEMA content (20, 44 and 66 % respectively) and their correspondent augmentation in CR required for the prevention of DNA migration. Despite the analogous trend, lower $CR_{cond}$-values are displayed with gel-electrophoresis (1.2, 1.4 and 1.6) compared to EtBr fluorescence. The incorporation of neutral hydroxyl groups turned out to affect the interaction with DNA differently for methacrylate compounds and poly-$\alpha$-aminoacids, especially for small quantities of hydroxyls. At higher amounts of neutral groups, this reduced attraction was compensated by the lack of cationic charges that induced a general decline in DNA attraction as these forces are evidently of a much higher degree than the inter-molecular forces H-bonding is based on. Briefly, it could be stated that supplying polymethacrylates, which already have a non-polar backbone, with neutral functional groups is disadvantageous since all polarity and charge is ascribed to the presence of protonable side-chains whereas for poly-L-glutamines, sufficient polarity remains provided by the backbone, hence the positive effect of H-bonding neutral groups (in case of charge surplus).

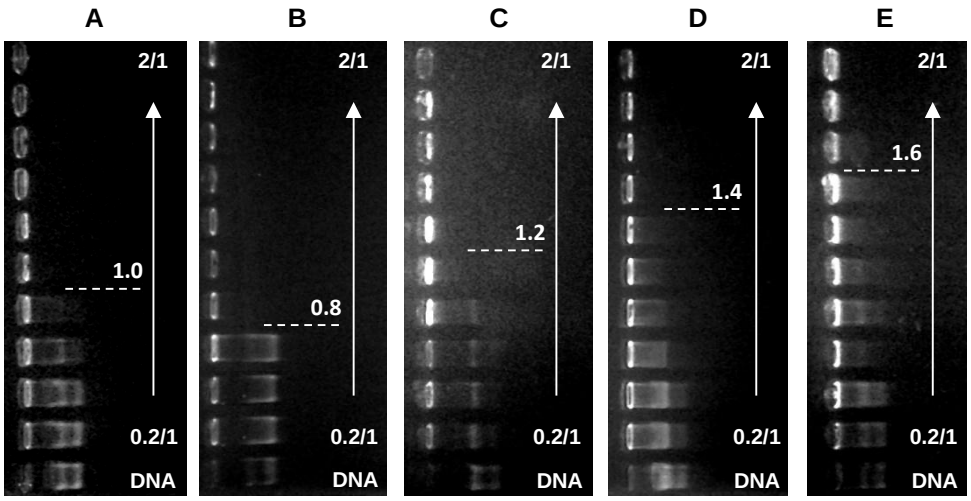


**Figure 4.27 – AGE images: p(AEMA) 176 kDa (A), p(DMAEMA$_{82\%}$-AEMA$_{18\%}$) 191 kDa (B), p(DMAEMA$_{80\%}$-HEMA$_{20\%}$) 187 kDa (C), p(DMAEMA$_{56\%}$-HEMA$_{44\%}$) 218 kDa (D) and p(DMAEMA$_{34\%}$-HEMA$_{66\%}$) 242 kDa (E).**

### *3.2.3 Influence of DNA concentration on polyplex formation*

As the main function of a gene delivery system is to supply DNA to cells of interest, the dose of DNA provided is preferably as large as possible (unless other specific requirements would contradict) to prevent the need for repeated administration. Therefore, the influence of the amount of DNA used for complexation with a cationic polymer was examined for two typical polymers via AGE (Fig. 4.28). In general, when the standard protocol is applied, a dose of 20 µg/ml of DNA is delivered along with the polymer load. With increasing DNA amount, little or no change in complexation behaviour was perceived. Only for doses of 60 µg of DNA, a small decrease in $CR_{cond}$ could be noticed (of about 0.1-0.2 CR units). For PEI (Fig. 4.28 – upper row), this is only visible when focusing on the last DNA band (CR = 0.4) that is appearing as a smear rather than a well-defined line, of which the former is consistent with a higher amount of free DNA. In the case of p(DMAEG) – 80 kDa, the decrease is better identifiable (Fig. 4.28 – lower row) as well as the change in appearance of the DNA-band (vertical line representing a certain MW of DNA rather than a smear). Higher quantities of DNA led to polyplexes that were insoluble or that precipitated shortly after preparation.

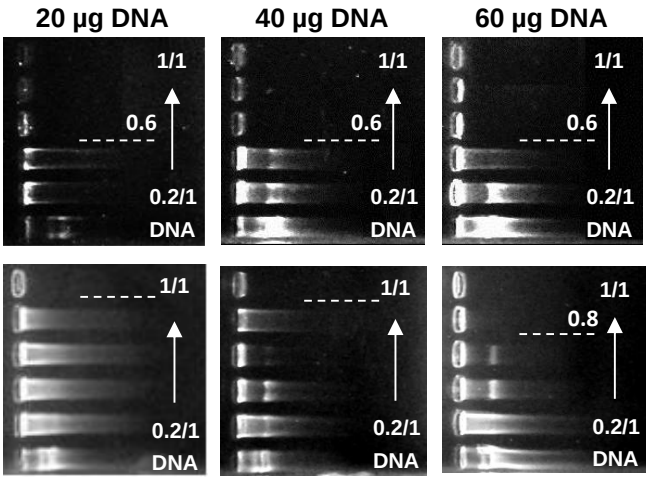


**Figure 4.28 – AGE images of PEI (upper row) and p(DMAEG) (lower row) polyplexes loaded with an increasing amount of DNA.**

Table 4.2 gives an overview of the different $CR_{cond}$ values for the tested polymers.

| Polymer | $M_w$ (kDa) | $CR_{cond}$ | Polymer | $M_w$ (kDa) | $CR_{cond}$ |
|---|---|---|---|---|---|
| PEI | 25 | 0.6 | p($HEG_{40\%}$-$DMAEG_{60\%}$) | 10 | 0.8 |
| PEI-$Guan_{20\%}$ | 25 | 0.8 | pDMAEMA | 12 | 1.2 |
| pDMAEG | 80 | 1.0 | pDMAEMA | 29 | 1.2 |
| p($DMAEG_{85\%}$-$AEG_{15\%}$) | 91 | 1.0 | pDMAEMA | 121 | 1.0 |
| pARG | 79 | 1.2 | pDMAEMA | 310 | 1.2 |
| p($HEG_{85\%}$-$GuAEG_{15\%}$) | 10 | > 2.0 | pDMAEMA | 658 | 1.6 |
| p($HEG_{75\%}$-$GuAEG_{25\%}$) | 10 | 2.0 | pAEMA | 176 | 1.0 |
| p($HEG_{65\%}$-$GuAEG_{35\%}$) | 0.8 | 1.7 | p($DMAEMA_{82\%}$-$AEMA_{18\%}$) | 191 | 0.8 |
| p($HEG_{45\%}$-$GuAEG_{55\%}$) | 0.8 | 1.6 | p($DMAEMA_{80\%}$-$HEMA_{20\%}$) | 187 | 1.2 |
| p($ImEG_{65\%}$-$GuAEG_{35\%}$) | 10 | 2.0 | p($DMAEMA_{56\%}$-$HEMA_{44\%}$) | 218 | 1.4 |
| p($ImEG_{80\%}$-$GuAEG_{20\%}$) | 10 | > 2.0 | p($DMAEMA_{34\%}$-$HEMA_{66\%}$) | 244 | 1.6 |
| p($HEG_{49\%}$- $GuAEG_{15\%}$-$ImEG_{36\%}$) | 10 | 1.8 | p($HEG_{79\%}$- $GuAEG_{12\%}$-$ImEG_{9\%}$) | 10 | > 2.0 |

**Table 2 - overview of $CR_{cond}$ values for various tested polymers.**

# 4 Polyplex size and distribution

## 4.1 Dynamic light scattering (DLS)

Not only the ability of a polyplex to be taken up is dependent on its size but also the mechanism of cell internalisation is highly influenced by the dimensions. Since the formation

of a (tight) complex diminishes the overall spatial occupation of free DNA when collapsing into a nano-sized particle, the presence of tiny complexes is an ideal way to confirm the association between DNA and a cationic polymer. Moreover, an idea on the distribution of the particles can be obtained and the most-likely corresponding cellular uptake mechanism can be derived thereof. Photon correlation spectroscopy (PCS) is an ideal technique to obtain a basic idea of the size and size-distribution of polyplexes in solution[21]. Due to thermal energy and solvent interference, particles in solution move at random (Brownian motion) and the speed at which they do, can be linked to their size. This means that when particles are illuminated with a laser, the monochromatic light that gets scattered is fluctuating in a similar way as the speed of movement of the particles. This constructive and destructive interference of light scattered by moving neighbouring particles gives rise to the intensity fluctuation at the detector plane[22]. Analysis by means of algorithmic correlation of the time dependent intensity fluctuations yields the diffusion coefficient (D) of the particles and allows for the hydrodynamic radius ($r_D$) to be calculated via the Stokes-Einstein equation:

$$r_D = \frac{kT}{6\pi\eta D}$$

$k$ = Boltzmann constant (1.38 x $10^{-23}$ J/K)

$T$ = absolute temperature (K)

$\eta$ = dynamic viscosity of the solvent (cP or centiPoise)

$D$ = diffusion coefficient ($m^2/s$)

This measuring technique enables a fast and sensitive way to detect particles in solution in a theoretical range of 1-5000 nm at low concentrations (up to 0.1 ppm)[23]. The diameter obtained via this method corresponds with that of a sphere possessing an equal diffusion coefficient[24].

The time dependence of the intensity fluctuation is analyzed using a digital correlator which determines the intensity of the autocorrelation function. At short delay times, correlation is high but as particles diffuse, the correlation diminishes to zero. The exponential decay of the correlation function is characteristic for the diffusion coefficient of the particles. A monodisperse sample gives rise to a single exponential decay to which fitting a calculated particle size distribution is relatively straightforward. For polydisperse particles, the autocorrelation function is a sum of contributions from the various particle sizes and diffusional modes, and the interpretation of *D* becomes more complex. Many algorithms exist for fitting autocorrelation functions to particle size distributions.

For DLS experiments, polymer-DNA complexes (20 µg/ml DNA) of various CR (1/1, 2/1 and 4/1) were measured in PS cuvettes (2 ml content) at a scattering angle of 90° using light of 488 nm (Argon laser). All results were integrated using the CONTIN algorithm and measured in triplicate. When measuring the size of a particle via DLS, the algorithm is able to produce a certain value based on the correlation data. Since random (Brownian) motion is at the base of this measurement and the fact that the polymers used for DNA complexation are disperse the outcome of an individual measurement always produces values (peaks) that demonstrate a certain width (distribution). Additionally, more than one distribution is often observed.

## 4.2 PEI and modified PEI derivatives

One of the reasons that PEI is performing exceptionally well as synthetic vector for gene delivery could be explained by the size of the formed polyplexes. As was mentioned earlier, the process by which external particles are taken up by a cell are amongst others related to the size and charge. It appears that PEI shows an uneven distribution (bimodal) that could suggest the requirement for different internalisation mechanisms such as caveolae or clathrin mediated endocytosis[25] (Fig 4.29 – A). At low CR's, polyplexes display an almost identical distribution of which one part (< 200 nm) is within the (theoretical) requirements for receptor-mediated endocytosis. When the CR is increased, the diameter of the particles becomes more uniform and lower in value (table 4.3, size in nm). If PEI is modified with guanidine groups, the size-distribution demonstrates a clear discrepancy with PEI (Fig. 4.29 B), more specifically, unimodal at all CR's and decreasing in size with increasing CR. The decrease in size is attributed to the stronger interaction originating from cationic guanidinium groups. Grafting a copolymer of p($HEG_{63\%}$-$GuAEG_{37\%}$) of about 3.5 kDa onto PEI (= PEI+pGLN), on the other hand results in exclusively monomodal distributions with low values already at a CR of 1.0 even when full condensation had not occurred according to EtBr fluorescence results (Fig. 4.29 – C). It is not fully clear why already small particles are occurring at a CR of 1/1 but two possible hypotheses could explain this: on one hand, there is probably still a significant part of the total amount remaining as free DNA and polymer that causes sufficient fluorescence observed via an EtBr displacement assay. On the other hand, given the non-specific separation of MW during the purificiation process, there's a big chance that some non-coupled PEI and poly-L-glutamine derivative exist that are able to form complexes separately at lower CR's than the CR which corresponds to complexation for the PEI+pGLN graft polymer.

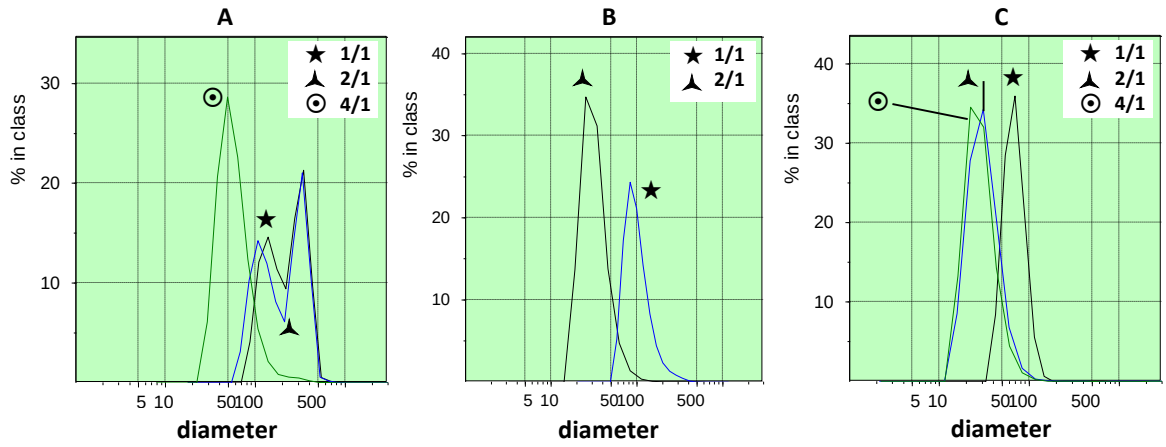


**Figure 4.29 – Size distribution (signal intensity) as a function of complex diameter (nm): (A) PEI 25 kDa, (B) PEI-Guan$_{20\%}$ 25 kDa, (C) PEI+p(HEG$_{63\%}$-GuAEG$_{37\%}$) grafts (25 + 3.5 kDa).**

| Polymer | 1/1 | 2/1 | 4/1 |
|---|---|---|---|
| PEI | 149 (*47%*) / 320 (*53%*) | 128 (*50%*) / 323 (*50%*) | 62 (*98%*) / 295 (*2%*) |
| PEI-Guan$_{20\%}$ | 104 ± 9 | 47 ± 5 | - |
| PEI+GLN grafts | 47 ± 12 | 33 ± 7 | 30 ± 3 |

**Table 4.3 – Size of polyplexes expressed in nm at different CR's. PEI 25 kDa, (B) PEI-Guan$_{20\%}$ 25 kDa, (C) PEI+p(HEG$_{63\%}$-GuAEG$_{37\%}$) grafts (25 + 3.5 kDa).**

## 4.3 Polyplexes based on biodegradable polymers

In a similar way as for PEI, a series of p(DMAEG) with various MW was investigated. It appeared that all particles possessed particles sizes within typical requirements for endocytosis at every CR measured (except 1/1 of the high MW) with values reaching as low as 30 nm. Moreover, there seems to be an influence of the MW on the particle size which is in accordance with the previously performed fluorescence results. High MW compounds display an incomplete formation of complexes because the diameter of the particles decreases with increasing CR. Also, the occurrence of bimodal distributions at a CR of 1/1 is observed. For complexes assembled by low MW polymers, the smallest complexes seem to be formed already at a CR of 1/1 and increasing this ratio negatively affects the complex formation (by creating larger diameters). Additionally, the particles formed using low MW polymers form complexes with a more narrow distribution (Fig. 4.30 & table 4.4).

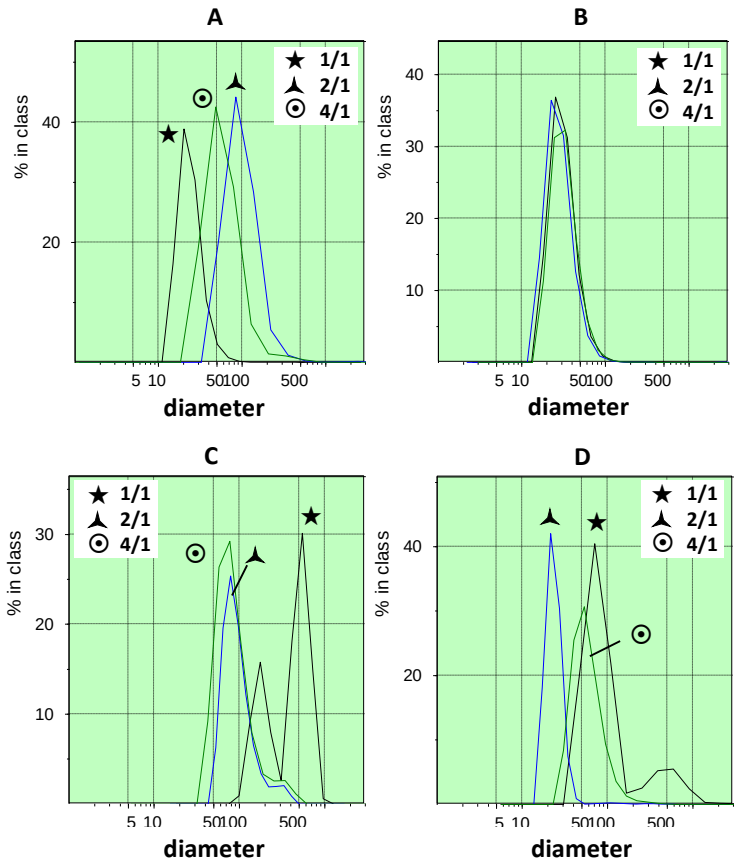


**Figure 4.30 - Size distribution (signal intensity) as a function of particle diameter (nm) for p(DMAEG) compounds: (A) 10 kDA, (B) 30 kDa, (C) 80 kDa and (D) 242 kDa.**

| Polymer | 1/1 | 2/1 | 4/1 |
|---|---|---|---|
| 10.000 Da | 32 ± 5 | 66 ± 12 | 104 ± 8 |
| 30.000 Da | 34 ± 2 | 29 ± 2 | 30 ± 3 |
| 80.000 Da | 543 (*65%* )/ 184 (*35%*) | 94 ± 2 | 87 ± 7 |
| 242.000 Da | 533 (*18%*) / 77 (*82%*) | 24 ± 3 | 62 ± 4 |

**Table 4.4 – Effect of MW on size (in nm) of polymer-DNA complexes using p(DMAEG).**

When different functional groups were introduced, the particle size and distribution was limitedly affected for pDMAEG (table 4.5). Primary amine containing derivatives have polyplex sizes in the same range as the homopolymer and become smaller with increasing CR whereas the hydroxyl-based polyplexes tend to increase slightly with increasing CR, except for the copolymer that contains also guanidine functional groups. Furthermore, the influence of the MW remains clearly visible for all copolymer types and favours low MW compounds for obtaining the smallest polyplexes. For polyplexes with a CR close to the $CR_{cond}$, the presence of (extra) distributions that are marked by a higher value is also

observed since the polyplexes are not yet strongly interacting and are therefore subjected to kinetic phenomena (local increases in electrolyte concentrations can temporarily form denser complexes with higher sizes until thermodynamic stability takes the upper hand).

| Polymer | 1/1 | 2/1 | 4/1 |
|---|---|---|---|
| p($DMAEG_{85\%}$-$AEG_{15\%}$) 91 kDa | 48 ± 4 | 34 ± 4 | 30 ± 2 |
| p($DMAEG_{85\%}$-$AEG_{15\%}$) 242 kDa | 75 ± 9 | 35 ± 13 | 39 ± 1 |
| p($DMAEG_{61\%}$-$HEG_{39\%}$) 11.9 kDa | 31 ± 6 | 30 ± 2 | 39 ± 4 |
| p($DMAEG_{61\%}$-$HEG_{39\%}$) 179 kDa | 47 ± 5 | 61 ± 16 | 68 ± 11 |
| p($HEG_{50\%}$-$DMAEG_{23\%}$-$GuAEG_{27\%}$) 9.3 kDa | 302 (*29%*)/162 (*71%*) | 37 ± 2 | 33 ± 1 |

**Table 4.5 - Size of polyplexes (in nm) of DMAEG-based copolymers.**

In previous sections, the potential of p($HEG_{x\%}$-$GuAEG_{y\%}$) that contain guanidine side-groups in combination with neutral groups for charge separation was cited (table 4.6). These derivatives already form tiny particles at a CR of 1/1, even when condensation appeared to be incomplete (e.g. EtBr fluorescence). At these low CR's, distributions with a large diameter were also detected but disappeared with increasing CR. The polymers that possessed the lowest amount of cationic charges strangely enough yielded the smallest polyplexes and the influence of the MW was not markedly established. A high CR (4/1) the polymers were able to produce small, uniform and monomodal particles in all cases while this was not confirmed at an intermediate CR (2/1).

| Polymer | 1/1 | 2/1 | 4/1 |
|---|---|---|---|
| p($HEG_{45\%}$-$GuAEG_{55\%}$) 12 kDa | 64 ± 6 | 67 ± 3 | 42 ± 5 |
| p($HEG_{65\%}$-$GuAEG_{35\%}$) 10 kDa | 90 (*73%*)/299 (*27%*) | 72 ± 2 | 51 ± 3 |
| p($HEG_{75\%}$-$GuAEG_{25\%}$) 10 kDa | 93 (*92%*)/302 (*8%*) | 70 (*95%*)/284 (*5%*) | 82 ± 11 |
| p($HEG_{85\%}$-$GuAEG_{15\%}$) 11 kDa | 360 ± 23 | 64 (97%)/296 (3%) | 36 ± 2 |
| p($HEG_{87\%}$-$GuAEG_{13\%}$) 27 kDa | 305 *(42%)*/659 (*58%*) | 43 ± 24 | 29 ± 3 |
| p($HEG_{87\%}$-$GuAEG_{13\%}$) 146 kDa | 54 ± 11 | 30 ± 13 | 29 ± 8 |

**Table 4.6 – Size and distribition of polymer-DNA complexes based on p($HEG_{x\%}$-$GuAEG_{y\%}$).**

When extending these trends to other types of guanidine-containing polymers, the results can be largely correlated (table 4.7). The outcome of the particle size is the same but the presence of secondary and larger size-distribution was not perceived. In general, with increasing polymer to DNA ratio, the formed complexes get smaller and the diameter narrower. If imidazole groups were incorporated, a different polyplex formation occurred.

Due to the lack of cationic groups, more diffuse particles were generated at a low CR (1/1) which corresponds with partial condensation and is characterised by secondary distributions. The addition of more polymer eventually created smaller particles but the degree of collapse remained proportional to the amount of charge present on the polymer (limited charge equals limited decrease in diameter).

| Polymer | 1/1 | 2/1 | 4/1 |
|---|---|---|---|
| p(ARG) 187 kDa | 57 ± 5 | 30 ± 1 | 31 ± 2 |
| p($HEG_{58\%}$-$ARG_{42\%}$) 11 kDa | 64 ± 4 | 41 ± 8 | 36 ± 2 |
| p($HEG_{87\%}$-$AEG_{13\%}$) 28 kDa + ARG grafts (1.5 kDa) | 48 ± 3 | 56 ± 2 | 35 ± 1 |
| p($GuAEG_{20\%}$-$ImEG_{80\%}$) 13 kDa | 160 (*46%*)/489 (*54%*) | 67 ± 8 | 42 ± 2 |
| p($GuAEG_{35\%}$-$ImEG_{65\%}$) 13 kDa | 119 (*35%*)/530 (*65%*) | 46 ± 8 | 29 ± 4 |
| p($HEG_{32\%}$-$GuAEG_{11\%}$-$ImEG_{57\%}$) 9.6 kDa | 145 (*19%*)/325 (*81%*) | 92 ± 15 | 52 ± 21 |

**Table 4.7 – Size and distribution of several guanidine containing polymer-DNA complexes.**

## 4.4 Size & distribution of polymethacrylate-DNA complexes

For non-biodegradable compounds like pDMAEMA that have a more hydrophobic backbone, polyplex sizes could possibly be affected by the change in behaviour in a water-based environment when compared to more polar poly-L-glutamines. In excellent accordance with fluorescence results, polyplexes based on p(DMAEMA) are readily formed and undergo nearly no difference in particle dimensions when increasing the CR (table 4.8). For all CR's, starting at 1/1, particles with sizes within endocytotic requirements were obtained. The influence of the MW is due to the limited difference in absolute value not really detectable. Except for high MW pDMAEMA (658 kDa), with a larger particle size close to the $CR_{cond}$, the DLS graphs were virtually identical (Fig. 4.31).

| Polymer | 1/1 | 2/1 | 4/1 |
|---|---|---|---|
| 11.900 Da | 42 ± 5 | 31 ± 4 | 31 ± 2 |
| 29.200 Da | 39 ± 5 | 35 ± 2 | 31 ± 3 |
| 121.000 Da | 30 ± 3 | 20 ± 5 | 27 ± 2 |
| 310.000 Da | 34 ± 8 | 28 ± 3 | 30 ± 7 |
| 658.000 Da | 145 ± 14 | 55 ± 9 | 25 ± 6 |

**Table 4.8 - Size and distribution of DMAEMA-based polyplexes**

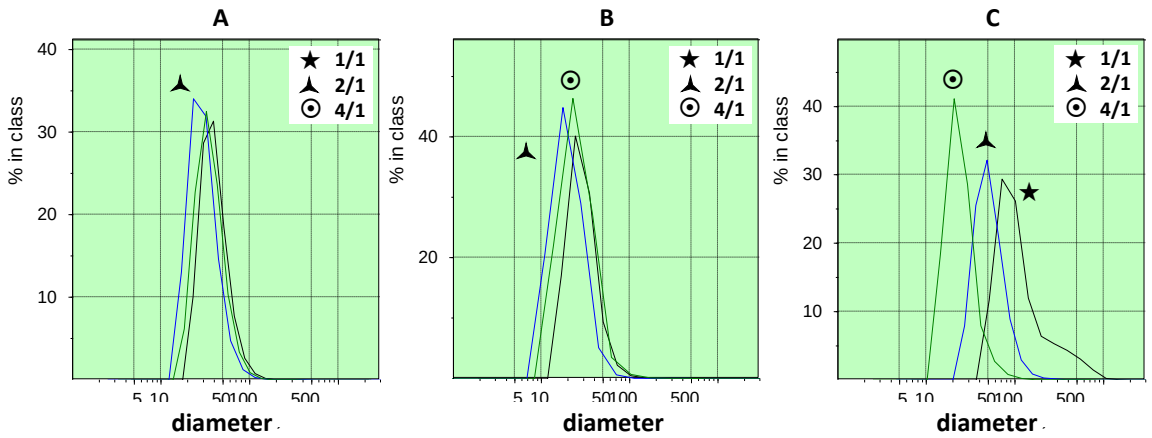


**Figure 4.31 - Size distribution (signal intensity) as a function of particle diameter (nm) for pDMAEMA compounds: (A) 11.9 kDA, (B) 121 kDa and (C) 658 kDa.**

The extent to which copolymerisation influences the interaction with DNA in forming complexes was obvious and considerable from fluorescence and electrophoresis measurements. DLS results of polyplexes formed by methacrylates containing other than tertiary amine functional groups are shown in table 4.9. Similar to pDMAEMA, pAEMA forms small complexes at a low CR but increasing the polymer content yields larger particles (that remain low in absolute value). For copolymers of tertiary and primary amines, a variation in the size of the polyplexes can only be seen at a CR of 1/1 since AEMA slightly increases the complexation point, yet all CR's tested, generated particles with sufficiently low diameters. If hydroxyl groups are built in, the resulting change in complex formation and size is better observed. The appearance of higher size distributions for copolymers with a high amount of hydroxyl groups is detectable and confirms insufficient complexation. When there is less than 50% charged groups remaining, particles with a broader diameter are seen, corresponding with a reduced DNA-interaction.

| Polymer | 1/1 | 2/1 | 4/1 |
|---|---|---|---|
| pAEMA 61 kDa | 29 ± 9 | 34 ± 3 | 43 ± 2 |
| p(DMAEMA$_{82\%}$-AEMA$_{18\%}$) 191 kDa | 64 ± 7 | 39 ± 3 | 31 ± 1 |
| p(DMAEMA$_{54\%}$-AEMA$_{46\%}$) 135 kDa | 54 ± 5 | 32 ± 2 | 27 ± 4 |
| p(DMAEMA$_{23\%}$-AEMA$_{77\%}$) 132 kDa | 36 ± 4 | 34 ± 1 | 31 ± 1 |
| p(DMAEMA$_{80\%}$-HEMA$_{20\%}$) 188 kDa | 88 ± 2 | 31 ± 2 | 25 ± 4 |
| p(DMAEMA$_{56\%}$-HEMA$_{44\%}$) 218 kDa | 51 (*37%*)/258 (*63%*) | 35 ± 2 | 31 ± 1 |
| p(DMAEMA$_{34\%}$-HEMA$_{66\%}$) 242 kDa | 102 (*66%*)/390 (*34%*) | 93 ± 8 | 48 ± 6 |
| p(GuAEMA$_{40\%}$-HEMA$_{60\%}$) 29 kDa | 48 (*58%*)/262 (*42%*) | 27 (*78%*)/189 (*22%*) | 25 ± 1 |

**Table 4.9 – Polyplex sizes of methacrylate copolymers (in nm) at 1/1, 2/1 and 4/1 CR.**

This is not the case when the charges are present as protonated guanidines like in p(GuAEMA-HEMA). The influence of functional group replacement seems generally limited and tends to disappear completely because the size at high CR is comparable for all.

## 4.5 Parameters that influence particle size

### *4.5.1 Time (stability)*

One of the aspects, important for correct interpretation of particle sizes when measuring a polyplex via DLS, is time. Polymer-DNA complexes are constantly in motion (thermal agitation) and realise numerous collisions with other molecules. As a consequence, the integrity of the complex can be affected. Mostly, aggregation and spontaneous dissociation of weakly-interacting species are responsible for the change of particle diameter in time. The impact of this parameter was determined via a DLS measurement at different time-points (table 4.10). In case of multiple distributions, only the presence of the new distributions is noted (the other distribution remains in the same range as for the reference point, 0h). For PEI, measured at 0h, the larger distributions are not shown. As a general trend, it can be concluded that the stability of polyplexes close to the CR at which condensation starts to occur, is limited. More specifically, due to aggregation of inadequately condensed complexes, the total diameter of a particle can increase and even exceed the upper limit boundaries for cellular uptake. It seems that all 3 polymers exhibit this behaviour. Only for pDMAEMA after 24h, a part of the complexes falls out of the specifications for receptor mediated endocytosis. To a certain extent, also pDMAEMA-DNA formed at a 2/1 CR experiences aggregation up to a value that is outside of the endocytotic uptake range. At a high CR, the complexes remain equally small or even produce smaller particles in the case of PEI. Based on these results, polyplex stability is expected to be longlasting when high CR's are applied.

| Polymer | 0h | | | 5h | | | 24h | | |
|---|---|---|---|---|---|---|---|---|---|
| | 1/1 | 2/1 | 4/1 | 1/1 | 2/1 | 4/1 | 1/1 | 2/1 | 4/1 |
| p(DMAEG) | 34 ± 9 | 29 ± 3 | 30 ± 2 | 89 (*42%*) | 33 ± 5 | 35 ± 1 | 113 (*32%*) | 40 ± 7 | 34 ± 4 |
| p(DMAEMA) | 30 ± 7 | 20 ± 3 | 27 ± 1 | 156 (*45%*) | 108 (*9%*) | 25 ± 3 | 307 (*45%*) | 149 (*15%*) | 33 ± 2 |
| PEI | 142 ± 5 | 128 ± 2 | 62 ± 4 | 138 (*37%*) | 75 (*25%*) | 50 ± 4 | 167 (*60%*) | 65 (*98%*) | 41 ± 2 |

**Table 4.10 – Stability of polyplex size in time via DLS measurement: p(DMAEG) 30 kDa, p(DMAEMA) 121 kDa and PEI 25 kDa after 0h, 5h and 24h. Value in nm, partial distribution between brackets.**

### *4.5.2 Temperature*

Another important parameter that appears to exhibit influence on the size of particles is temperature. Because at elevated temperature, molecules posses more energy (and correspondingly an increased mobility), the formation is expected to occur either faster or slower (and also at higher or lower CR). It is noteworthy to mention that a difference exists between stability of polyplexes at 37 °C if the complexes were prepared at 37 °C instead of at 25 °C. Table 4.11 lists DLS values at both temperatures for complexes of selected polymers.

| Polymer | 25 °C | | 37 °C | |
|---|---|---|---|---|
| | 1/1 | 2/1 | 1/1 | 2/1 |
| PEI-Guan$_{20\%}$ | 104 ± 9 | 47 ± 5 | 118 ± 11 | 45 ± 4 |
| p(HEG$_{65\%}$-GuAEG$_{35\%}$) | 90 (*73%*)/299 (*27%*) | 72 ± 2 | 113 (*51%*)/284 (*49%*) | 48 ± 5 |
| p(GuAEG$_{20\%}$-ImEG$_{80\%}$) | 160 (*46%*)/489 (*54%*) | 67 ± 8 | 111 ± 12 | 38 ± 7 |

**Table 4.11 – Polyplex sizes (in nm) of selected polymers at different temperatures (DLS).**

A temperature increase leads to better polyplexes in terms of size. For every example, the resulting size at a 2/1 CR is smaller. For low CR's close to $CR_{cond}$, the influence could alter the dimensions in both a negative (e.g. the hydroxyl variant) and positive way (like for the imidazole-based polymer), especially when an additional time stability is taken into account. Rougly speaking, it could be stated that 37 °C is an environmentally, beneficiary parameter for higher CR's but potentially could destroy the complex (by aggregation or electrolyte dissociation if loosely bound) at CR's corresponding with the start of DNA-condensation (CR-values outside of the $Min_F$ plateau in EtBr fluorescence).

### *4.5.3 Buffer medium*

Up to now, as was standardised by implementation of the universal protocol, polymer-DNA complexes were prepared in ultrapure water in order to maximise the interaction between the polyelectrolytes. If DNA-containing vectors would be administered to the body, the influence of the fluid it resides in during the stay inside the body must be considered. Mainly salts and proteins which contain charges can destabilise the complexes (by electrostatic interaction)[26]. Even more, when polyplex formation is performed in a salt-rich buffer, immediate precipitation is observed. Therefore, polyplexes were to be prepared in ultrapure water prior to buffer mixing. In the test below, polyplexes were combined with cell culture medium, a buffer with a large mixture of salts but without serum[27].

| Polymer | Ultrapure $H_2O$ | | | Cell culture medium | | |
|---|---|---|---|---|---|---|
| | 1/1 | 2/1 | 4/1 | 1/1 | 2/1 | 4/1 |
| p(DMAEG) 30 kDa | 34 ± 9 | 29 ± 3 | 30 ± 2 | 155 (*42%*)/973 (*58%*) | 134 (59%)/328 (*41%*) | 57 ± 4 |
| PEI | 142 ± 5 | 128 ± 2 | 62 ± 4 | 349 ± 22 | 150 (*25%*)/304 (*75%*) | 67 ± 3 |

**Table 4.12 – Polyplex sizes and distributions for PEI & pDMAEG in cell culture medium as measured by DLS (results in nm).**

Similar to the previous section, the presence of an excess of salts has a proven influence on the size of the particles. As they tend to form aggregates, the stability in time will only be sufficient (e.g. within requirements for endocytosis) for high CR's while it leads to precipitation for complexes at lower CR's (table 4.12).

### *4.5.4 DNA concentration*

Because of the elaborate research that is put into the development of synthetic polymers with appropriate functions, the focus on the actual purpose (that is delivery of DNA) is sometimes lost. In order to obtain reproducible, predictable and solid polyplexes, a fixed amount of DNA (20 µg/ml) was implemented for the standardised protocol. As it would be practical to deliver as much DNA as possible in a single dose given the lower exposure to toxic delivery systems and the need for less repeated administrations, delivering higher amounts of DNA seems logic. A comparison in terms of polyplex sizes was made for pDMAEMA 121 kDa and PEI and their corresponding polyplexes containing 20, 40 or 60 µg/ml for typical CR's tested (table 4.13).

| Polymer | 20 µg/ml DNA | | | 40 µg/ml DNA | | | 60 µg/ml DNA | | |
|---|---|---|---|---|---|---|---|---|---|
| | 1/1 | 2/1 | 4/1 | 1/1 | 2/1 | 4/1 | 1/1 | 2/1 | 4/1 |
| p(DMAEMA) | 30 ± 7 | 20 ± 3 | 27 ± 1 | 45 ± 7 | 23 ± 5 | 22 ± 1 | 48 ± 8 | 36 ± 5 | 19 ± 4 |
| PEI | 142 ± 5 | 128 ± 2 | 62 ± 4 | 303 ± 12 | 144 ± 14 | 59 ± 7 | 519 ± 45 | 321 ± 20 | 121 ± 4 |

**Table 4.13 – Influence of DNA concentration (20, 40 , 60 µg/l) on the polyplex distribution of pDMAEMA 121 kDa & PEI 25 kDa: analysis of the size (in nm) via DLS measurements.**

For pDMAEMA, increasing the DNA dose had no clear influence. At a lower CR, the polyplexes experience a slight size-increase but without repercussions towards cellular uptake. In the case of PEI, the effect of an augmented DNA dose was more outspoken with possibly limiting effects for endocytosis, specifically for a low CR and high DNA dose. When preparing polyplexes with higher amounts of DNA incorporated, solutions turned proportionally more turbid although this phenomenon was dependent on the type of base

polymer (hydrophobic polymethacrylates versus hydrophilic polyaminoacids, data of this latter not shown). DNA concentrations higher than 60 µg/ml resulted in precipitation upon mixing with polymer. An similar comparison was also made to study the influence of DNA concentration on the complexation behaviour (see section 3.2.3).

# 5 Polyplex stability

In previous sections, the stability of polymer-DNA complexes was already to some extent discussed but only for specific properties (complexation with DNA) and with respect to the nature of the polyplex (either shape or size). When looking more to the thermodynamic implications of charged particles (polyplexes) in solution, a better and more general understanding of the electronic behaviour and stability can be derived from zeta(ζ)-potential measurements.

## 5.1 Zeta-potential

A relatively unknown but very useful way to study the behaviour of a charged particle in solution is by performing zeta-potential measurements. When charged surfaces such as those from polymer-DNA complexes are brought in an aqueous solution, an electric double layer forms at the particle-liquid interface (Fig. 4.32)[28]. This electric double layer consists of two parts. Firstly a uniform, immobile layer of oppositely charged ions (Stern layer) is formed which are tightly bound to the surface. Secondly, an outer layer rearranges which is diffuse and whose composition is driven by electrostatic balance and random thermal motion[29]. The potential in this region therefore decays with increasing distance from the surface until it reaches the bulk solution value (conventionally fixed at zero). If an electric field is applied to a polyplex solution, each particle and its most closely associated ions move through the solution as one unit. The potential at the surface of shear between this unit and the surrounding medium is called the zeta-potential. In other words, this potential is a measure for the layer of solvent (water) which is moving along with the charged particle and is associated to the polyplex in an electrostatical way.

Parameters that influence the formation of such an electrical double layer are one hand attributed to the particle itself (for instance the ionisation potential of the chemical structures, e.g. $pK_a$ or the morphology) but on the other hand also influenced by the environment for which the type of ions present, the concentration and the temperature appear the most dominant factors. The overall charge of a polyplex particle is not only important for the behaviour related to solution stability (tendancy to form aggregates) but plays an equally

important role in interaction with other (charged) structures of the body (e.g. proteins containing charged residues or the outside of the cellular membrane)[30].

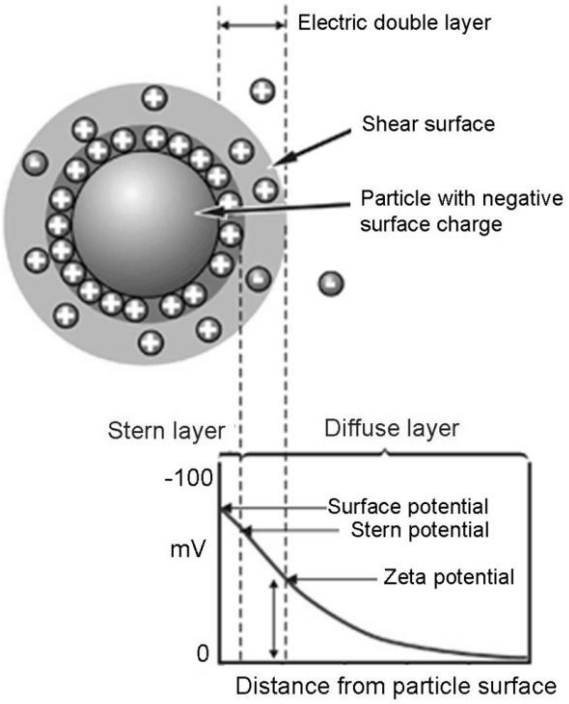


**Figure 4.32 – Schematic representation of the electrical double layer model according to Stern[31].**

The measurement of the zeta-potential is performed by determining the electrophoretic mobility (μ) of a charged particle which is obtained by Laser Doppler Velocimetry. The velocity (v) and electrophoretic mobility (μ) are related by the following equation (with E being the magnitude of the electric field):

$$\mu = \frac{v}{E}$$

By applying the Henry-equation the zeta-potential can be calculated using the following formula:

$$\mu = \frac{\varepsilon . \xi}{6 . \pi . \eta} = \frac{2}{3} \frac{\varepsilon_0 . \varepsilon_r . \xi}{\eta}$$

With $\mu$ = the electrophoretic mobility $\left(\frac{m^2}{V.s}\right)$

$\zeta$ = zeta-potential (V)

$\eta$ = viscosity of the medium (cP)

$\varepsilon$ = (relative) permittivity of the dielectric constant (r = medium, 0 = vacuum)

A practical measurement is in that sense closely related to DLS because accordingly a similar laser set-up is applied to retrieve the electrophoretic mobility. Polymer-DNA complexes at various CR (0.5/1, 1/1, 2/1 and 4/1) and dissolved in (filtered) water are injected into a thermostatic measuring chamber of the zeta-potential device to be measured. The absolute value of the resulting ζ-potential represents the degree of stability according to conventional rules[32]. Typical, sufficiently high values that corresponds with an adequate level of colloidal stability start from 30 mV (sufficient) and can go as high as 60-70 mV for excellent surface potential[23].

## 5.2 Colloidal stability of biodegradable polyplexes

When evaluating the zeta-potential of the polyplexes, a basic idea on the stability (prevention of aggregation) can be derived via the magnitude of this parameter. Also the composition of the surface can, to a certain extent, be deducted from this value. Furthermore, if for measurements with increasing CR, the polarisation is reversed, the corresponding complex formation is additionally proven. This validates the use of zeta-potential as a useful, additional tool for assessing polymers as delivery devices in gene therapy. In general, both the L-glutamine as well as the methacrylate-based polymers yielded polyplexes with a good (> 30 mV) to excellent (> 50 mV) zeta-potential at high CR (4/1).

Fully charged poly-L-glutamines exhibit a high stability with values close to +60 mV (Fig. 4.33 – p(DMAEG)). Moreover, there appears to be hardly any influence of the MW on the zeta-potential value. With increasing CR, a growing number of layers composed of cationic polymers arrange around the preformed complex, proportionally augmenting the surface charge and leading to a continuous rise in zeta-potential. A similar explanation can be given for PEI which demonstrates analogous values despite the lower charge concentration present on the polymer (estimated 25 % at physiological pH). Despite the small or even non-existing difference between the lowest CR tested (1/1) and the CR representing condensation (according to AGE), the zeta-potential values mark the presence of stable polyplexes.

The trends seen for p(DMAEG) can be correlated to copolymers that also possess 100% charged groups (or close to it) like in the case of p(DMAEG-AEG), (Fig. 4.34, A & B). Derivatives that contain non-charged units, like p(DMAEG-HEG) have a considerable lower potential (Fig. 4.34, C & D) at all CR's as could be anticipated[2]. Taking the large standard deviations into account, no real effect of the MW is observed. For the imidazole-containing polyglutamine, the zeta-value was surprisingly higher (Fig. 4.34, E). When comparing results with partially charged p(DMAEG-HEG), an equal, if not higher value is obtained with less charged groups (excluding imidazole groups, not fully charged at physiological pH).

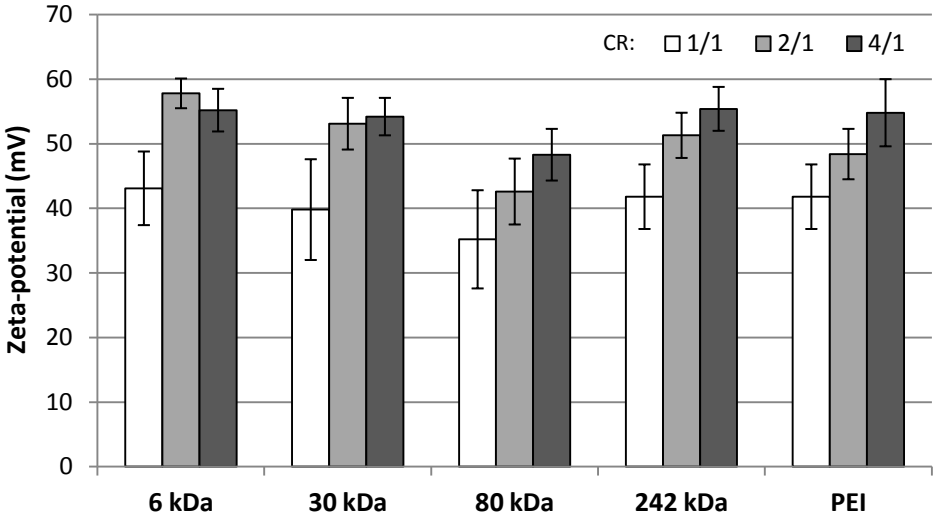


**Figure 4.33 – Zeta-potential of complexes prepared from pDMAEG with variable MW (10, 30, 80 & 242 kDa) and PEI (25 kDa).**

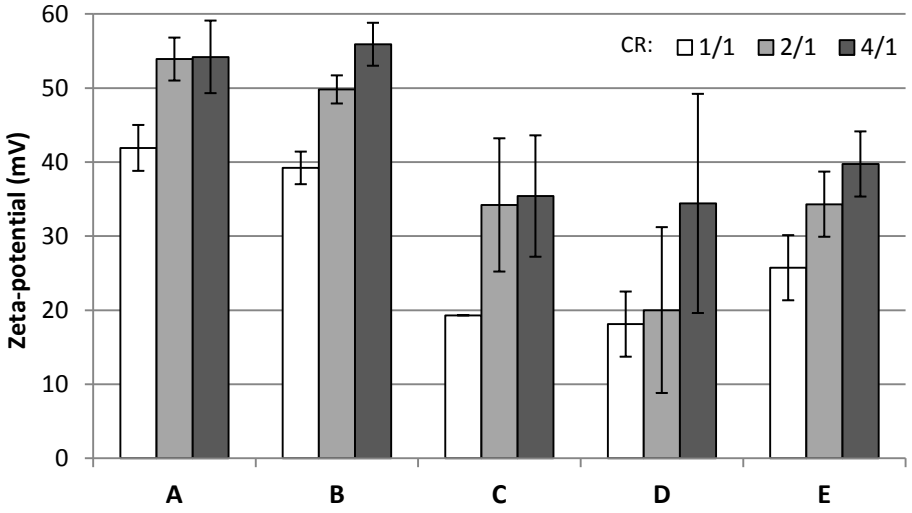


**Figure 4.34 - Zetapotential values corresponding with polyplexes from (A) p(DMAEG$_{85\%}$-AEG$_{15\%}$) 91 kDa, (B) p(DMAEG$_{85\%}$-AEG$_{15\%}$) 242 kDa, (C) p(DMAEG$_{61\%}$-HEG$_{39\%}$) 11.9 kDa, (D) p(DMAEG$_{62\%}$-HEG$_{38\%}$) 179 kDa and (E) p(HEG$_{49\%}$-AEG$_{15\%}$-ImEG$_{36\%}$) 9.9 kDa.**

In cases where the polyplex was not formed at a CR of 1/1 a negative zeta-potential was obtained (Fig. 4.35). The different experiments revealed a sharp transition from a negative to positive potential close to the CR of complexation which indicates that once a polyplex is formed a limited addition of polymer is sufficient to induce adequate particle stabilisation. Remarkably, the potential of pARG (Fig. 4.35 - A) was negative for a 1/1 CR what might be the result of small deviations possible in the production and measurement process since the CR for full complexation is located around 1/1. Other polymers possessing guanidine functional groups in combination with a sizeable amounts of neutral hydroxyl groups (50% or more) resulted in zeta-potential values in the order of 30-40 mV (at CR 4/1) which

represented good to very good stability. Most of the polymers showed, in accordance with fluorescence measurements, a negative potential at a 1/1 CR since condensation did not yet occur (except for E, which has about 50% charged groups). For really low amounts of charged groups (F), the detected, low values were in line with the expectations. Noteworthy is also the diminished stability of the grafted PEI-derivative (grafts = p($HEG_{63\%}$-$GuAEG_{37\%}$)) (D) where the introduction of neutral groups shields the core polymer, transforming the behaviour of the total polymer by adopting the stabilizing properties of its graft.

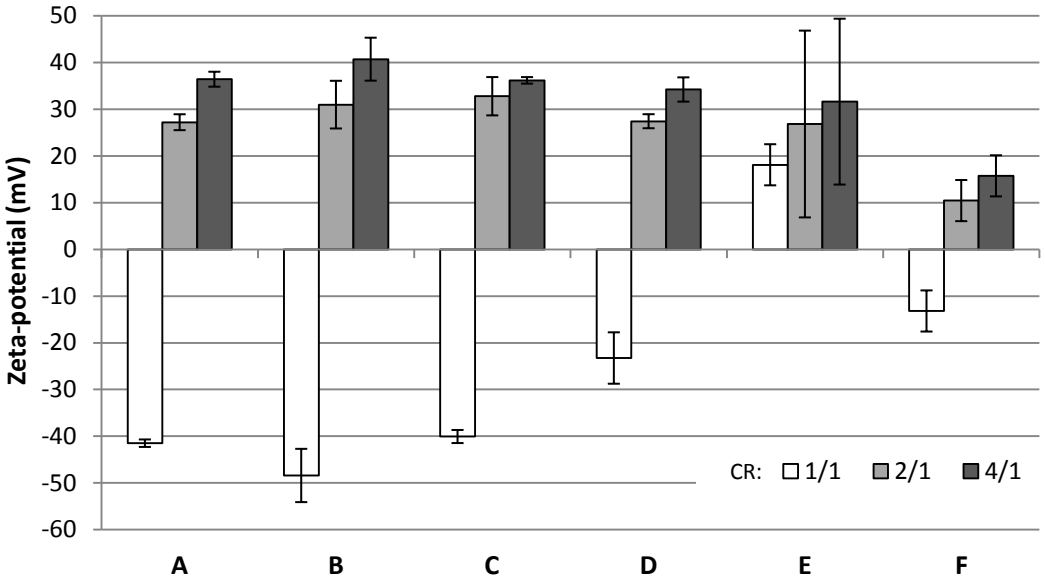


**Figure 4.35 – Zeta-potential values corresponding with polyplexes from (A) p(ARG) 22.8 kDa, (B) p($DMAEG_{23\%}$-$GuAEG_{27\%}$-$HEG_{50\%}$) 9.3 kDa, (C) p($HEG_{58\%}$-$ARG_{42\%}$) 11.2 kDa, (D) pEI + p($HEG_{63\%}$-$GuAEG_{37\%}$), (E) p($HEG_{43\%}$-$GuAEG_{50\%}$-$AEG_{7\%}$) 12 kDa and (F) p($HEG_{85\%}$-$GuAEG_{15\%}$) 11.4 kDa.**

For methacrylate-based polyplexes, the effect of MW was in contrast to previously derived analysis techniques not really detectable in the case of the homopolymer p(DMAEMA) (Fig. 4.36). Although the polyplexes derived from polymers with the highest MW's displayed zeta-values which were considerably higher than the low MW derivatives. The maximum values of these compounds were rather low, especially when comparing with the homopolymers of their biodegradable counterparts (p(DMAEG) > 50 mV). This could be most likely attributed to the difference in polymer backbone structure, which has in this latter case less affinity for polarity (ion-charge).

Copolymers based on p(DMAEMA) exhibited similar values as the homopolymer itself (Fig. 4.37). This is not surprising for copolymers that remain fully protonated as is the case for p(DMAEMA-AEMA) in graphs A & B but is not expected for p(DMAEMA-HEMA) compounds (graph C & D) which have nearly half the amount of charge per polymer chain. Because the

zeta-potential seems to be quite low for fully charged polymers, the nature of the polymer backbone must be a much more important parameter than originally anticipated, hence the small difference observed with non-fully charged polymers. This theory is again confirmed by the values of pGuAEMA, a homopolymer that has a nearly identical zeta-value distribution as pDMAEMA (for different CR's) as shown in graph E.

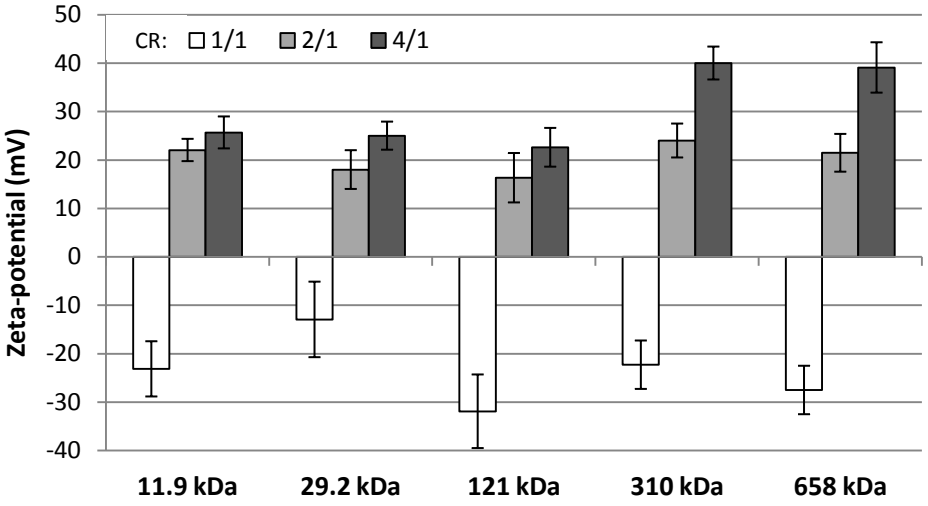


**Figure 4.36 – Zeta-potential values for pDMAEMA with variable MW measured at various CR.**

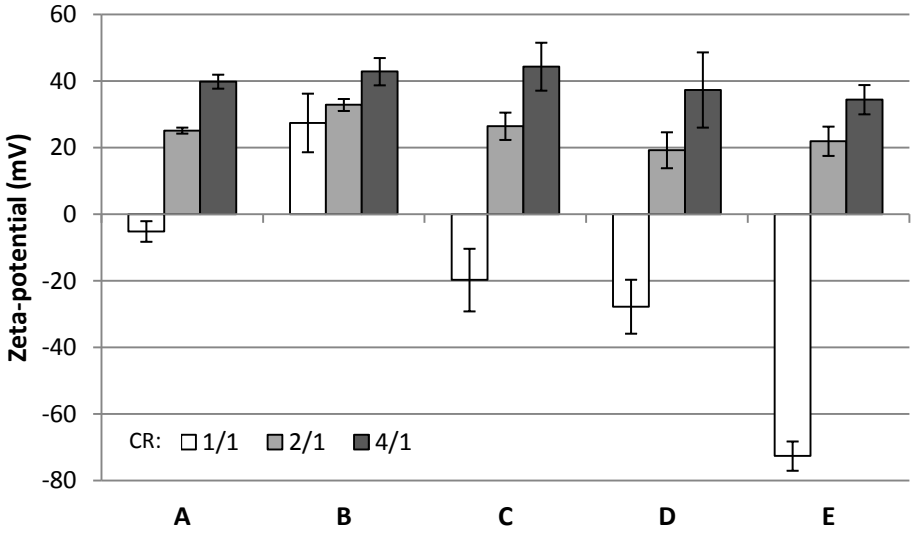


**Figure 4.37 – Zeta-potential values corresponding with polyplexes from (A) p(DMAEMA$_{79\%}$-AEMA$_{21\%}$) 51 kDa, (B) p(DMAEMA$_{82\%}$-AEMA$_{18\%}$) 191 kDa, (C) p(DMAEMA$_{55\%}$-HEMA$_{45\%}$) 10 kDa, (D) p(DMAEMA$_{56\%}$-HEMA$_{44\%}$) 218 kDa and (E) p(GuAEMA) 63 kDa prepared at variable CR.**

## 6 Influence of charge: geometrical orientation on a polymer

Throughout the entire course of polyplex characterisation, the importance of functional group orientation has been several times proposed. To come to a better understanding and to

check the influence of this phenomenon on the formation of polyplexes, EtBr fluorescence data of several guanidine-containing compounds were collected and assembled in the following graph (Fig. 4.38). A curve representing PEI is incorporated to allow comparison and to check the possibility to correlate fluorescence with biological transfection efficiency, based on the fluorescence values obtained by PEI (see also chapter 6).

The composition of each polymer in terms of guanidine groups is described in table 4.14. The number of guanidine functional groups per polymer depends both on composition and MW. To compare these values for polymers with variable MW, the relative ratio of guanidine groups per Da is also calculated. When looking at the series of p(HEG-GuAEG), it is clear that an increasing number of guanidines, proportionally improves the ability to complex DNA (as was described before in section 3.1.1.3) and which is in compliance with the relative ratio. If guanidine-incorporation was carried out by grafting, not only the amount of functional groups can be more easily extended but also the position of the charged groups is altered. Charged groups are now located further away from the backbone and because of that the flexibility to rearrange around opposite charges (e.g. DNA) is optimised. This is especially the case for macromolecules that are limited by their inherent (backbone) stiffness. As a result the fluorescence profile of the grafted equivalent shows a fast and strong condensation ability towards DNA ($CR_{MinF}$ = 0.8 & $Min_F$ = 22%). In comparison to p(ARG), a homopolymer corresponding with a 100% of guanidine functional groups, the profile demonstrates a faster condensation, despite its lower relative molar ratio. This effect is even more expressed in the case of the $Arg_8$-coupled polymer. Not only displays this polymer the highest DNA affinity but it also achieves this at the lowest CR while its relative ratio is substantially lower than the other guanidine-rich components.

| Polymer | MW (Da) | Mol (Gua)/ Mol (pol) | Rel. Ratio (mol/1000 Da) |
|---|---|---|---|
| $p(HEG_{87\%}\text{-}GuAEG_{13\%})$ | 26.950 | 19.3 | 0.71 |
| $p(HEG_{75\%}\text{-}GuAEG_{25\%})$ | 10.200 | 13.4 | 1.31 |
| $p(HEG_{45\%}\text{-}GuAEG_{55\%})$ | 12.000 | 30.8 | 2.56 |
| $p(HEG_{87\%}\text{-}AEG_{13\%})$ + pArg grafts | 27.700 | 152 | 5.48 |
| $p(HEG_{87\%}\text{-}AEG_{13\%})$ + $Arg_8$ 4.5% | 27.700 | 56.5 | 2.04 |
| p(ARG) | 22.800 | 145 | 6.36 |

**Table 4.14 - Guanidine-containing compounds: composition, MW and guanidine/polymer ratio.**

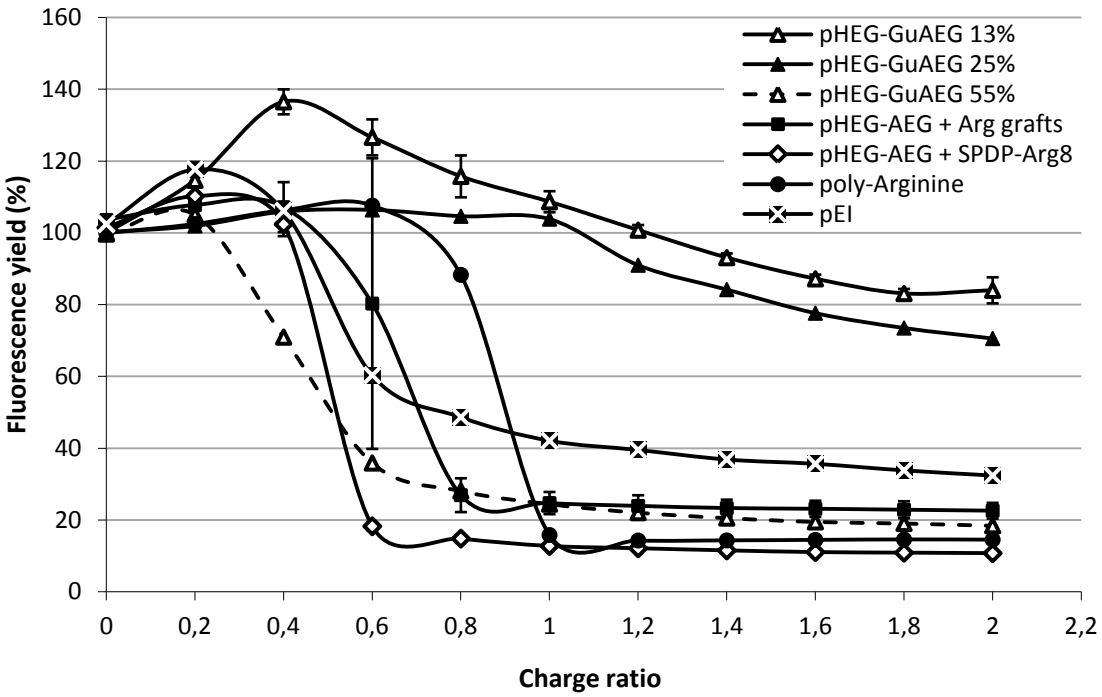


**Figure 4.38 – EtBr Fluorescence yield of several guanidine-containing polymers as a function of increasing CR.**

Another advantage of grafting or coupling of $Arg_8$ (which is a form of grafting but with a fixed amount of guanidine residues) is the larger amount of guanidine that can provided per polymer chain. Since for polymers where the functional groups are located on the side-chain, the maximum guanidine concentration is limited by the number of side-chains (representing 100% occupancy). For the relative ratio of moles of guanidine per MW, this comes down to the MW of a full structure unit. When expressed as mol/1000 Da, the maximum values for p(GuAEG) and p(ARG) is 4,71 and 6.36 respectfully. By extending the grafts on a polymer these values can be readily multiplied (e.g. the relative ratio for p($HEG_{87\%}$-$GuAEG_{13\%}$) + p(ARG) grafts is multiplied by 8 compared to regular p($HEG_{87\%}$-$GuAEG_{13\%}$)).

To conclude, it can be stated that the charge density, present on a polymer, is still a very decisive parameter to interact with DNA but the position and orientation of these charges highly influence the condensation properties. In this way, it is possible to develop synthetic vectors that require a minimum of charge (e.g. relative ratio ≥ 2) to induce sufficient complex formation which is accepted as a mandatory property for minimal toxicity. Consequently, the hypothetical, dual influence of both the amount of charge and its position (distance from backbone) can be visualised in an abstract way by means of a density graph (Fig. 4.39). In this graph, the extent to which a polymer can form a strong polyplex in a fast (at low CR) way is expected to be represented by the intensity of the shades of dark. This means that an

efficient vector composition is situated in the white region and that how darker a region is, the less efficient a vector will be in attracting DNA to eventually form a polyplex.

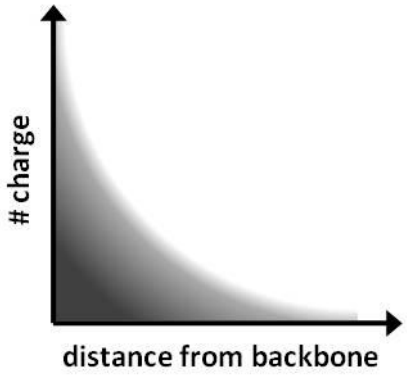


**Figure 4.39 – Hypothetical graphic representation for determining efficient vector compositions in terms of charge and corresponding DNA interaction (dark region = suitable).**

## 7 Summary

In order to decide if a polymer is suitable as a DNA-carrier in terms of physico-chemical qualities, a combination of the aforementioned characterisation techniques is required. From the results that were presented in this chapter, several (groups of) candidates remain in the scope as potential delivery device. Both for poly-L-glutamines as for polymethacrylates, there were several polymers that met all the requirements but they do so at different polyplex compositions. While for polyglutamines, the influence of non-charged or partially charged functional groups seemed efficient (if sufficient charge remained, about 40%), this was not the case for polymethacrylates. Since hydrophobicity (or non-polarity) appeared to be of relevance in polyplex formation, the need for additional non-charged groups for p(DMAEMA) is deemed unfavourable. Moreover, the added value of guanidine functional groups in the case of polyglutamines could not be proven for polymethacrylates. Besides, the optimal MW selection was confirmed different for both classes, indicating the need for low MW polymers in the case of biodegradable compounds whereas for the non-biodegradable ones, an optimal MW was found around 100-150 kDa.

This led to the conclusion that mainly pDMAEMA or primary amine-containing copolymers with small (< 10%) amounts of primary amine and with a MW of around 150 kDa show the most potential as non-biodegradable vectors. For biodegradable vectors, the choice is more complex. Polymers with a MW < 30 kDa and with a partitioned functional group composition (not fully charged) seems the most promising. Although the choice of specific functional group is less relevant, there's a strong preference for guanidines in combination with imidazole moieties. Further feasibility of potential vector systems will be verified by

biologically relevant experiments that address the biocompatibility issue as well as the efficiency/potency in gene therapy applications.

## 8 References


[1] L. Dekie (2001), doctoral research: “Synthese en evaluatie van poly-L-glutaminezuurderivaten als vectoren voor gentherapie”, Ghent University, Ghent.

[2] P. Dubruel (2003), doctoral research: “Studie van synthetische polymeren als vectoren voor gentherapie”, Ghent Universiy, Ghent.

[3] Ulrich, S., M. Seijo, et al. (2006). "The many facets of polyelectrolytes and oppositely charged macroions complex formation." Current Opinion in Colloid & Interface Science **11**(5): 268-272.

[4] Karkas, J. D., R. Rudner, et al. (1968). "SEPARATION OF B SUBTILIS DNA INTO COMPLEMENTARY STRANDS .2. TEMPLATE FUNCTIONS AND COMPOSITION AS DETERMINED BY TRANSCRIPTION WITH RNA POLYMERASE." Proceedings of the National Academy of Sciences of the United States of America **60**(3): 915-&.

[5] Chargaff, E. and H. S. Shapiro (1955). "REMARKS ON DEOXYRIBONUCLEASE." Experimental Cell Research: 64-71.

[6] Tsuboi, M., J. M. Benevides, et al. (2007). "The complex of ethidium bromide with genomic DNA: structure analysis by polarized Raman spectroscopy." Biophysical Journal **92**: 928-934.

[7] Doenecke, D. (1977). "ETHIDIUM-BROMIDE (EB) BINDING TO NUCLEOSOMAL DNA - EFFECTS ON DNA CLEAVAGE PATTERNS." Experimental Cell Research **109**(2): 309-315.

[8] Rodrigues, L., D. Wagner, et al. (2008). "Thioridazine and chlorpromazine inhibition of ethidium bromide efflux in Mycobacterium avium and Mycobacterium smegmatis." Journal of Antimicrobial Chemotherapy **61**(5): 1076-1082.

[9] Liu, Z., Z. Zhang, et al. (2010). "Hydrophobic modifications of cationic polymers for gene delivery." Progress in Polymer Science **35**(9): 1144-1162.

[10] Ramsay, E. and Gumbleton, M. (2002). “Polylysine and polyornithine gene transfer complexes: a study of complex stability and cellular uptake as a basis for their differential in-vitro transfection efficiency.” J Drug Target. **10**(1): 1-9.

[11] Min, S. H., D. C. Lee, et al. (2006). "A composite gene delivery system consisting of polyethylenimine and an amphipathic peptide KALA." Journal of Gene Medicine **8**(12): 1425-1434.

[12] Thomas, M. and A. M. Klibanov (2002). "Enhancing polyethylenimine's delivery of plasmid DNA into mammalian cells." Proceedings of the National Academy of Sciences of the United States of America **99**(23): 14640-14645.

[13] Erbacher, P., T. Bettinger, et al. (2004). "Genuine DNA/polyethylenimine (PEI) complexes improve transfection properties and cell survival." Journal of Drug Targeting **12**(4): 223-236.

[14] Forrest, M. L., G. E. Meister, et al. (2004). "Partial acetylation of polyethylenimine enhances in vitro gene delivery." Pharmaceutical Research **21**(2): 365-371.

[15] Kircheis, R., L. Wightman, et al. (2001). "Design and gene delivery activity of modified polyethylenimines." Advanced Drug Delivery Reviews **53**(3): 341-358.

[16] Sakae, M., T. Ito, et al. (2008). "Highly efficient in vivo gene transfection by plasmid/PEI complexes coated by anionic PEG derivatives bearing carboxyl groups and RGD peptide." Biomedicine & Pharmacotherapy **62**(7): 448-453.

[17] Thomas, M., Q. Ge, et al. (2005). "Cross-linked small polyethylenimines: While still nontoxic, deliver DNA efficiently to mammalian cells in vitro and in vivo." Pharmaceutical Research **22**(3): 373-380.

[18] Lee, Y., M. Y. Cho, et al. (2008). "Enhancement of the transfection efficiency of poly(ethylenimine) by guanidylation." Bulletin of the Korean Chemical Society **29**(3): 666-668.

[19] Nimesh, S. and R. Chandra (2008). "Guanidinium-grafted polyethylenimine: An efficient transfecting agent for mammalian cells." European Journal of Pharmaceutics and Biopharmaceutics **68**(3): 647-655.

[20] Wolfert, M. A., E. H. Schacht, et al. (1996). "Characterization of vectors for gene therapy formed by self-assembly of DNA with synthetic block co-polymers." Human Gene Therapy **7**(17): 2123-2133.

[21] http://www.malvern.com/LabEng/technology/dynamic-light-scattering.html

[22] Murphy, R. M. (1997). "Static and dynamic light scattering of biological macromolecules: what can we learn?" Current Opinion in Biotechnology **8**(1): 25-30.

[23] http://www.atascientific.com.au/

[24] Reschel, T., C. Konak, et al. (2002). "Physical properties and in vitro transfection efficiency of gene delivery vectors based on complexes of DNA with synthetic polycations." Journal of Controlled Release **81**(1-2): 201-217.

[25] Won, Y. Y., R. Sharma, et al. (2009). "Missing pieces in understanding the intracellular trafficking of polycation/DNA complexes." Journal of Controlled Release **139**(2): 88-93.

[26] Grigsby, C. L. and K. W. Leong, (2010), "Balancing protection and release of DNA: tools to address a bottleneck of non-viral gene delivery." Journal of The Royal Society Interface **7**(Suppl 1): S67-S82.

[27] http://www.all-creatures.org/articles/ar-alt-serum.html

[28] Schurz, J., G. Erk, et al. (1990). "ZETA POTENTIAL AS AN ANALYTICAL TOOL FOR GRAFT-COPOLYMERS AND FOR POLYMER SURFACES." Journal of Macromolecular Science-Chemistry **A27**(13-14): 1673-1692.

[29] Elakneswaran, Y., T. Nawa, et al. (2009). "Zeta potential study of paste blends with slag." Cement and Concrete Composites **31**(1): 72-76.

[30] Lin, C. and J. F. J. Engbersen (2008). "Effect of chemical functionalities in poly(amido amine)s for non-viral gene transfection." Journal of Controlled Release **132**: 267-272.

[31] Stern, O. Z. (1924). Electrochem **30**: 508.

[32] "Zeta Potential of Colloids in Water and Waste Water", A. S. D.-., American Society for Testing and Materials, 1985.

# Chapter 5

# Optimisation & modification of multifunctional vectors

# 1 Introduction

When a polymer or polyplex is brought into the body, there's no selective interaction with a designated cell or tissue. The extent to which polyplexes interact with certain components of the body is amongst others dependent on the polyplex charge, size, hydrophobicity and nature of the functional groups present on the polymer. Many studies have aimed to optimise these parameters by performing mechanistic studies in an attempt to fully understand the relation of biological activity and vector structure[1,2,3]. A way to improve the selectivity of polyplexes can be found in the targeting of receptors that are present on cell surfaces. If polymer carriers are modified with ligands or molecules that can interact with the cell, enhanced targeting of specific cells and tissue can be reached. These compounds are often peptides that are referred to as cell-interacting-peptides (CIP) with specific structures that can bind to cell-receptors (e.g. $\alpha_v,\beta_3$-integrins) in order to promote cell adhesion[4,5]. Moreover, certain cell receptor sequences can be used to induce cell-uptake. As described before (chapter 1 – 2.3.3), peptide sequences like TAT or Penetratin are the topic of much recent research and have shown great potential in facilitating cellular entry of DNA when coupled to polymer carriers[6,7,8,9]. Although much controversy exists on their uptake mechanism, the consensus is that a combination of both receptor and non-receptor mediated endocytosis is responsible for CPP-regulated internalisation[10,11] (Fig. 5.1).

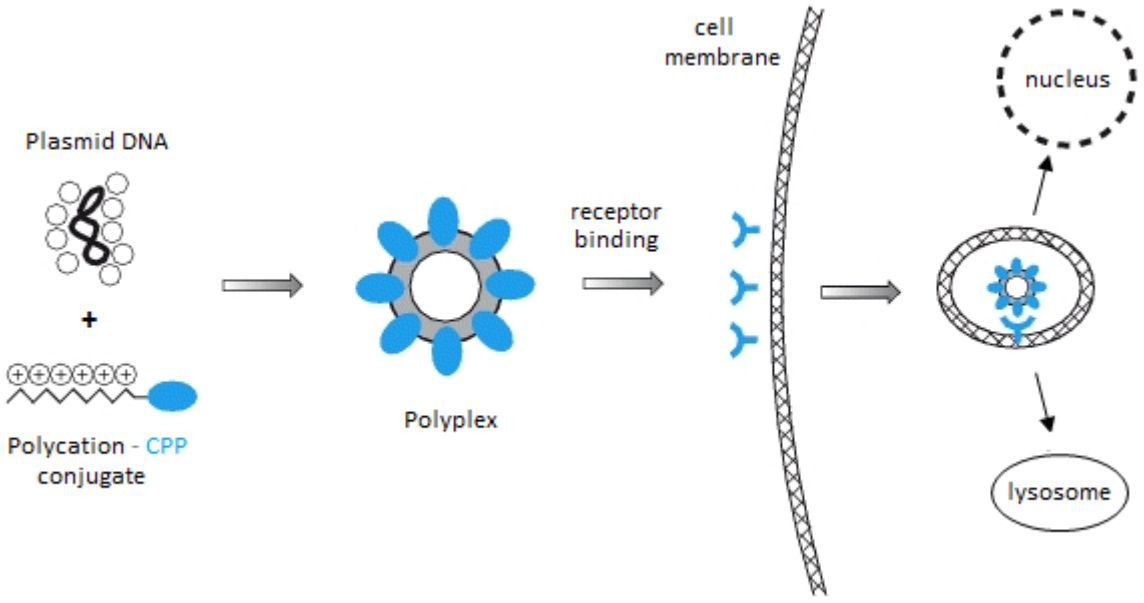


**Figure 5.1 - Internalisation of CPP-containing polyplexes via receptor mediated endocytosis[11].**

So far a large number of CPP-based applications have been reported using either covalent or conjugate CPP-based strategies from *in vitro* to *in vivo* deliveries[12,13,14]. The interest for CPP's is mainly due to their low cytotoxicity and to the fact that there seems to be no limitation for the type of cargo that can be uploaded. Although CPP's were shown to favour

delivery of cargos that vary greatly in size and nature (small molecules, oligonucleotides, plasmid DNA, peptides, proteins, nanoparticles, lipid-based formulations, virus, quantum dots, etc.) most applications describe the delivery of oligopeptides/proteins[15,16] and nucleic acids or analogues[17,18]. At current, a whole series of CPP families are explored (mainstream families shown in table 5.1) with new types still being discovered.

| Organism | Protein | Peptide sequence |
|---|---|---|
| HIV-1 | Transcriptional activator | TAT |
| Herpes simplex virus-1 | Viral protein | VP22 |
| Drosophila | Antennapedia homeodomain | Penetratin |
| Human | calcitonin | hCT (9-32) |
| Maize | γ-Zein | SAP |
| Synthetic | SV40 T-Antigen | MPG |
| Synthetic | Galanin-Mastoparan | Transportan |
| Synthetic | Hydrophobic types | Pep-1, MTS, CADY |

**Table 5.1 - of well-known CPP's and their origin.**

Almost all CPP's are characterised by their amphiphilic nature which is a necessity to induce receptor mediated cell-crossing of the peptide and its cargo since their mechanisms of entry are assumed to occur by both hydrophilic and hydrophobic interactions[19,20,21].

Next to peptides, other compounds can increase the rate of cellular uptake. Amongst these, glycoproteins, insulin, antibodies (fragments) and sugar-based products are well known examples[22,23,24].Other methods of optimising DNA delivery systems are focussed on minimising uncontrollable interaction with wild type substances of the body (proteins in the bloodstream or extra-cellular matrix). Coupling polyethyleneoxide (PEO) by grafting has been investigated with the aim to lower the immunogenic character of substances other than those of the body (such as polymer carriers)[25,26], yet a loss of transfection efficiency was accompanied with the expected gain in viability[27]. Nowadays, the variety of peptides used in gene delivery applications has been further expanded. A recent hot topic is antisense RNA/DNA therapy in which specific peptide nucleic acids are used to block the translation of proteins within a cell[28].

To be able to perform mechanistic studies on a cellular level, it is necessary to visualise polyplexes when present in cells (e.g. via confocal microscopy). This can be achieved by fluorescent staining using polyaromatic compounds like fluoresceine that exhibit high fluorescence yield upon irradiation with visible light. Both DNA as well as the polymer carrier

can be covalently linked to fluorescent labels. Nevertheless, staining of DNA could hamper its function and therefore preference is given to polymer conjugation. Moreover, since polymers already bear cationic charges for DNA interaction, the addition of hydrophobic fluorescent labels can partially mimic the structure and effect of amphiphatic CPP's[29]. Besides the obvious analogy with CPP-structures, the addition of hydrophobic regions to vector systems was presumed beneficiary towards transfection efficiency [30]. The incorporation of these non-polar domains is not only inducing membrane destabilisation during cellular uptake but also during endosomal escape[31].

In this chapter, certain peptides based on penetratin and octa-arginine, which is a TAT-based derivative consisting of eight arginine units and is assumed to be responsible for triggering the actual internalisation of TAT[32], will be coupled to multifunctional polymers. Since these peptides cannot be readily coupled to polymer vectors, thiol and maleimides groups will be introduced along the polymers to allow consequent coupling of the peptides (via a reversible disulfide and stable thioether bond respectively). The influence of spacer types and lengths on the transfection efficiency will also be investigated. Newly developed analysis methods based on impedance measurements will shed further light on the interaction between CPP's and the cell membrane. Besides CPP's also fluorescent tags such as Oregon Green 488 and Alexa Fluor 514 are coupled to allow intra-cellular study of polyplexes (in combination with CPP's). Moreover, fluorescently labelled polymers will assist in better understanding the polyplex formation and its kinetics using fluorescence assisted measurement methods (FRET/FCS). Finally, the possible effect of covalently coupling CPP's to carrier systems in comparison with physical mixing of CPP's (within polyplexes) will be assessed.

All peptides used within this research were developed by the Homeoprotein laboratory of Prof. J. Martinez (CNRS, Montpellier), partner in the PolExGene EU-project (FP6).

## 2 Development of fluorescently labelled polymer carriers

### 2.1 Visualising polyplexes

Trying to unravel the functioning of the body is an essential part of all biomedical based research. For concepts that are to be applied on a cellular level, like for instance in gene therapy, understanding the mechanisms of cellular uptake, trafficking, DNA transcription and protein translation are critical. Since these processes remain subject to considerable doubt, attempting to elucidate them is of huge interest and was therefore also put forward as a goal for the polymers used within this research. A well established technique to study cellular behaviour and the presence of specific compounds in and around cells in a direct,

non-invasive way is confocal microscopy (CM). Laser light of a well defined wavelength is used to pass through the sample to induce fluorescence of specifically labelled compounds (like polymers or DNA). Specific for this method is the use of focal planes that allow to assess a sample in different layers when compared to conventional fluorescent microscopes[33]. The most prominent reason to apply a confocal laser enhanced contrast (by filtering non-focussed light). Consequently, certain polymers were provided with fluorescent tags. A widely spread fluorescent molecule is fluoresceine that shows a high molar extinction-coefficient ($\varepsilon$) for light at a wavelength of 488 nm (and 514 nm). These values correspond perfectly with the spectral lines of an Ar-laser, hence its common use. However, for coupling reactions performed within this research, priority was given to a fluoresceine derivative, namely Oregon Green 488. This fluorinated compound (Fig. 5.2) has several advantages over common fluoresceine:

- No appreciable quenching (even at high labelling degrees)
- Better photostability (allowing an increased acquisition of photons before photodestruction i.e. bleaching)
- Lower $pK_a$ (making the fluorescence essentially pH-insensitive)

Moreover, highly reactive succinimidyl esters of Oregon Green are commercially available and allow swift coupling in buffered environments. Nevertheless, this fluorescent label prevents the analysis of polyplex sizes because DLS also applies Ar-based laserlight which interferes the measurement. To circumvent this problem, Alexa Fluor 546 ($\lambda_{max}$ = 554 nm) was selected as a similar fluorescent dye that still possessed the advantage of Oregon Green over fluoresceine but with a slightly shifted absorbance wavelength that doesn't interfere with DLS measurements (Fig. 5.2).

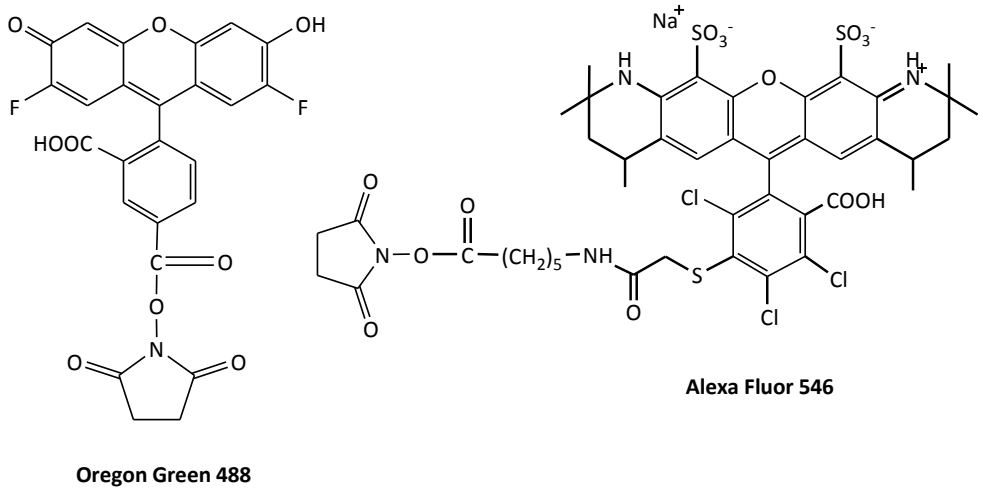


**Figure 5.2 - Chemical structure of succinimidyl ester activated fluorescent tags.**

Noteworthy is the presence of anionic moieties in the structure of the fluorescent labels. Because of this, the interaction with the polymer is possible (which could partially inhibit the interaction between the polymer and DNA). Moreover, the M/C value of the polymer needs to be corrected for the presence of this negative charge.

## 2.2 Covalent coupling of fluorescent tags

Fluorescent groups can only be coupled to polymers containing reactive sites like primary amines. Because of the availability of succinimidyl-activated molecules, coupling can be readily achieved in a one-step reaction. Since the fluorescent probes were selected for their excellent quantum yield (high $\varepsilon$), only small amounts need to be coupled to attain a considerable fluorescent signal. During synthesis, the reagents are shielded from light to limit the loss of activity.

In a typical experiment, a polymer containing free primary amines is dissolved in a 0.1 M $NaHCO_3$ buffer at pH ≈ 8.3 (10 mg/ml). In a separate vial, an amount (0.2 equivalents relative to the amount of primary amines) of staining dye is dissolved in DMSO (10 mg/ml) and added dropwise to the aqueous polymer solution to allow reaction for one hour at room temperature. The reaction is stopped by neutralizing the pH and subsequent purification is performed by dialysis. The degree of coupling can be determined by UV/VIS spectrometry using a calibration curve ($\lambda_{abs}$ = 488 nm) and the following formula:

$$\%\ Labelling = \frac{A.MW_{pol}}{(c.\varepsilon_{mol} - A.MW_{fluor})}$$

With A = absorbance

c = concentration (mol/l)

$\varepsilon_{mol}$ = molar extinction coefficient (l/mol.cm),

$MW_{pol}$ = the molecular weight of a polymer structure unit (g/mol)

$MW_{fluor}$ = the molecular weight of a fluorescent coupled structure unit (g/mol).

Several newly developed polymers where fluorescently labelled as well as certain reference polymers (PEI, PLL) so that the intra-cellular trafficking of polyplexes and polymers could be followed by means of CM and mutually compared (table 5.2). The incorporation of negatively charged (due to the carboxyl/sulphonate functional group) fluorescent tags has an effect on the mass/charge (M/C) of the total polymer. This has to be taken into account when forming polyplexes since higher amounts of polymer (differences up to 40%) are required to obtain equal amounts of positive charge (when compared to the non-labelled polymers). The biological evaluation of the modified polyplexes will be discussed in chapter 6 of this work.

| Polymer | Fluorescent tag | % coupled | M/C |
|---|---|---|---|
| PEI | Oregon Green 488 | 2.7 | 244.7 |
| PLL | Oregon Green 488 | 2.4 | 251.2 |
| PEI-Guan (20 %) | Oregon Green 488 | 1.3 | 297.6 |
| p(DMAEG-AEG) 91 kDa | Oregon Green 488 | 6.1 | 291.3 |
| p(DMAEG-AEG) 242 kDa | Oregon Green 488 | 5.2 | 278.8 |
| P(ORN-ARG) 71 kDa | Oregon Green 488 | 1.3 | 195.7 |
| p(DMAEG-AEG) 91 kDa + PEN (1,9%) | Oregon Green 488 | 3.1 | 264.0 |
| p(DMAEG-AEG) 91 kDa + $Arg_8$ (1,2%) | Oregon Green 488 | 1.3 | 263.0 |
| p(DMAEG-AEG) 91 kDa | Alexa Fluor 546 | 0.6 | 238.5 |

**Table 5.2 - overview of fluorescently labelled polymers.**

### 2.3 Influence of fluorescent tags on the polyplex physico-chemical properties

The requirement of polymer-DNA complexes to be fluorescently active could have implications on the formation of polyplexes. Unless desired (in the case were hydrophobic associations would be regarded as significant), the incorporation of non-polar groups generally lowers the ability for electrostatic interaction with DNA and the formation of (nano-sized) particles. Despite the small quantities that are typically coupled, the effect on the polyplex formation was verified. Employing traditional EtBr fluorescence experiments was not possible since Oregon Green absorbs light of 510 nm ($\lambda_{exc}$ used standard) and therefore the $\lambda_{exc}$ for these experiments was set to 340 nm, a value at which Oregon Green has a low absorption capacity.

The premise that fluorescent coupling should not exert a distinct influence on the capacity of a vector to condense DNA, was readily countered by means of fluorescence measurements. Apparently, the required CR for full condensation was markedly higher in the case of PEI-$OREG_{2.1\%}$ (1.4 instead of 0.6). This effect was less pronounced for p($DMAEG_{85\%}$-$AEG_{15\%}$)+$OREG_{6.1\%}$ ($CR_{minF}$ of 1.3 compared to 1.1 without fluorescent tag) which has a substantially higher amount of cationic charges remaining per polymer for DNA condensation compared to PEI (Fig. 5.3). The hydrophobic effect of the fluorescent groups is one of the main causes for the altered DNA interaction (the potential loss in cationic charges due to coupling is considered only secondary). Hydrophobic interactions between the fluorescent labels could form types of micelles and consequently allow only hydrophobic (weaker) interaction with DNA and possible also shield the DNA from the polymer's cationic charge. This effect, which is already considerable from concentrations as low as 1%, also rendered the fluorescent polyplexes less firm as indicated by the corresponding $Min_F$ value.

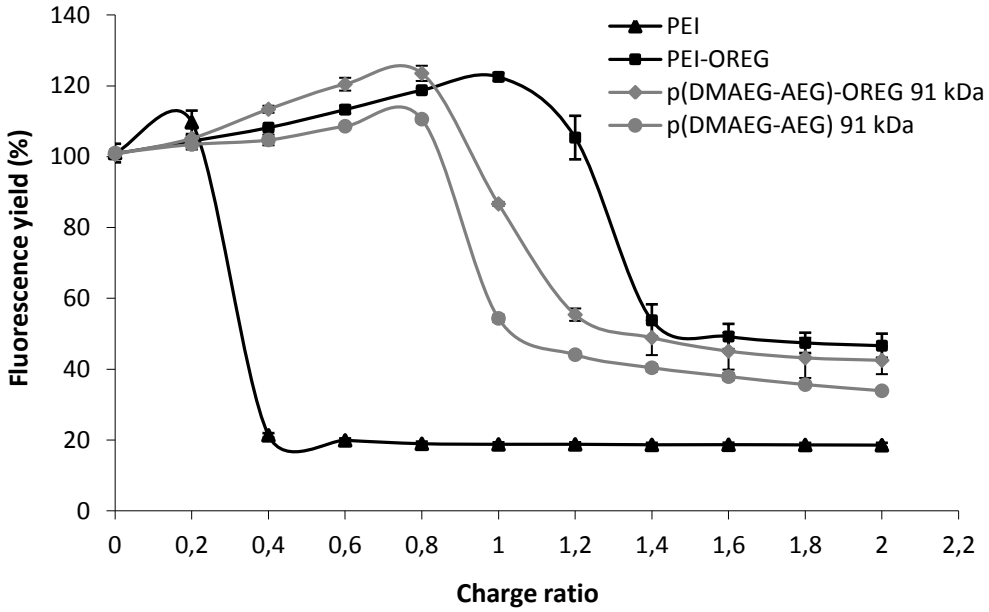


**Figure 5.3 - EtBr fluorescence spectrum: fluorescence yield as a function of added CR for PEI 25 kDa, PEI-OREG$_{2.7\%}$ 25 kDa, p(DMAEG-AEG) 91 kDa and p(DMAEG-AEG)-OREG$_{6.1\%}$ 91 kDa.**

A conclusion of the same kind could be drawn from the agarose gel-electrophoresis experiments although a proportionally smaller effect was noticed (Fig. 5.4). Labelled PEI displays an increase of 0.6 CR units, required for full condensation while the discrepancy for labelled p(DMAEG-AEG) versus the non-coupled polymer is nearly untraceable (weak DNA band at a CR of 1/1 visible). This difference could be ascribed to the utilised analysis method, thermodynamically-based fluorescence spectroscopy versus entropically oriented gel-migration during electrophoresis of which the latter has a much larger sensitivity for detecting small differences.

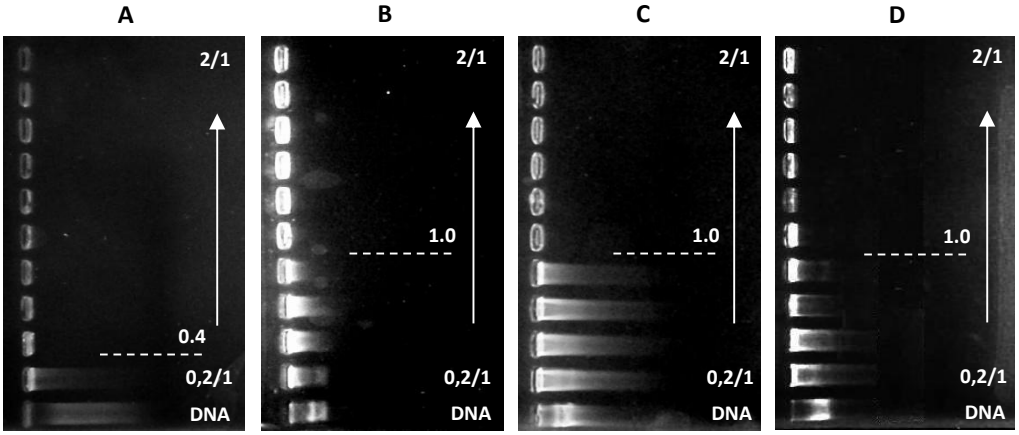


**Figure 5.4 - AGE images: determination of polyplex formation via stepwise addition of polymers: (A) PEI 25 kDa, (B) PEI+OREG$_{2.1\%}$ 25 kDa, (C) p(DMAEG$_{85\%}$-AEG$_{15\%}$) 91 kDa and (D) p(DMAEG$_{85\%}$-AEG$_{8.9\%}$)+OREG$_{6.1\%}$ 91 kDa.**

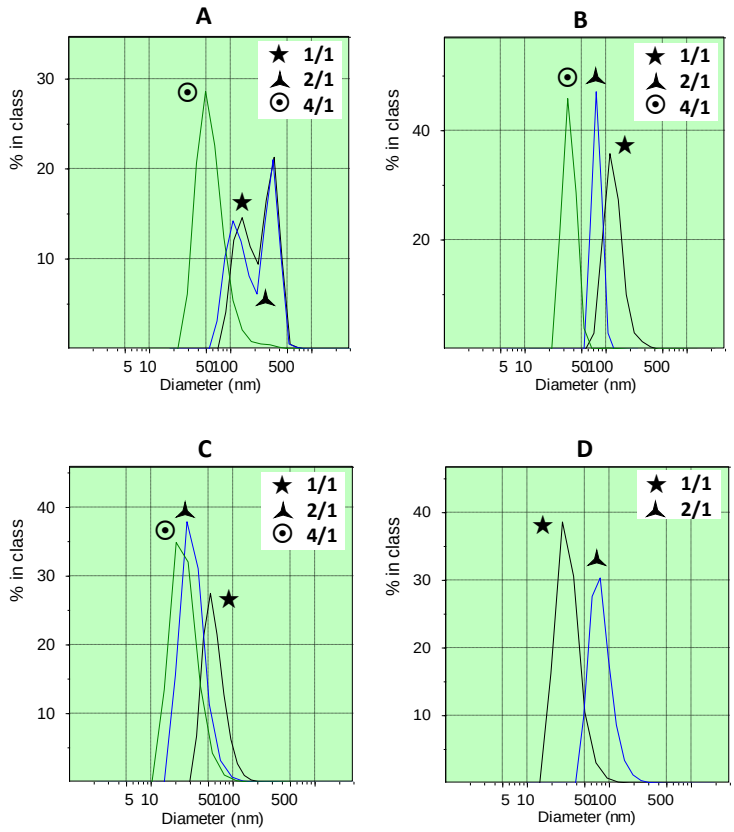


**Figure 5.5 - DLS results of polyplexes (in various CR's) derived from (A) PEI 25 kDa, (B) PEI+OREG$_{2.1\%}$ 25 kDa, (C) p(DMAEG$_{85\%}$-AEG$_{15\%}$) 91 kDa and (D) p(DMAEG$_{85\%}$-AEG$_{8.9\%}$)+OREG$_{6.1\%}$ 91 kDa.**

Concerning the size of polyplexes obtained using fluorescent polymers, various effects could be observed. In contrast to native PEI, labelled PEI does not demonstrate a bimodal distribution (Fig. 5.5 – A & B). Even more, the distributions appear narrower while the dimensions remain more or less of the same order (ranging from 90-35 nm). For labelled, p(DMAEG$_{85\%}$-AEG$_{15\%}$), the observed effect is mainly related to size (Fig. 5.5 – C & D). Already at a CR of 1/1, tiny polyplexes of 30 nm are formed. Additional polymer (i.e. higher CR's) can now only result in increased dimensions because adding extra polycations induces expansion of the particle rather than reinforcing DNA interaction with corresponding collapse of the complex.

In summary, the ideal assumption that the labelling of a polymer exerts no influence on DNA interaction was contested by the results shown above. The effect tends to be proportional to the degree of positively charged functional groups present on the polymer and should as a result be limited.

## 2.4 Formation kinetics of polyplexes

In addition to the unravelling of cellular uptake mechanisms, fluorescently labelled polymers can also be utilised for structural elucidation of the polyplex formation and confirmation of previously stated principles. In collaboration with a project partner (Fraunhofer Institute for Biomedical Engineering, IBMT, St. Inkbert, Germany), fluorescence correlation spectroscopy (FCS) analyses were applied as a feasibility test for retrieving structural and kinetic information on the polyplex formation. Optical microscopy is applied to detect fluorescence intensity fluctuations which can be analysed using temporal autocorrelation and that can provide information of the physics of these fluorescent molecules (mainly through diffusion constants). Typically a single wavelength derived from a corresponding fluorescent label is used for this[34]. The presence of fluorescent tags should ideally have no notable influence on the formation of polyplexes. To verify this latter statement, UV/VIS spectrometry was performed to compare covalently labelled polyplexes with physically mixed labelled polyplexes.

### *2.4.1 FCS analysis*

Oregon Green 488 (for polymer labelling) and rhodamine (for CPP tagging) proved to be suitable for FCS analysis. Two major conclusions with regard to polymer diffusion and polyplex formation could be drawn:

- Diffusion of polymers is detectable and the diffusion times depend on the size of the polymer (Fig. 5.6 – A)
- Polyplex formation (condensation) is detectable and the effect of variable CR and concentration of polyplexes is noticeable (Fig 5.6 – B & C).

The diffusion time of the largest polymers (Fig. 5.6 – A) is not higher than 300 µs and is proportional to the size. The difference in diffusion time between the low (27 µs) and medium (266 µs) MW compound seem to be much larger than that of the medium and high (291 µs) MW polymer. This could indicate that the diffusion time expresses a logarithmic course (with horizontal asymptote or plateau) in function of the MW and that from a certain MW on, the difference in diffusion time will no longer be detectable. In contrast to polymers as such, polyplexes (Fig. 5.6 – B) display a diffusion time which is considerable higher (1500 µs for poyplexes with a CR of 0.6 and 2800 µs for polyplexes prepared at CR 3.0) which is the result of the gain in MW by (electrostatically) coupling to DNA. Dependency of the CR is shown in figure 5.6 (C) and demonstrates that even the smallest differences (0.1 CR) can be detected. Since for this series the concentration of DNA remains constant, this incremental progression is the result of the increase in polymer amount, hence the difference between the various CR's will be influenced by the polymer MW. Also the point of condensation can

be retrieved via FCS, i.e. by the sudden raise in τ (for p(DMAEG) 91 kDa between 0.8 & 1.0 CR).

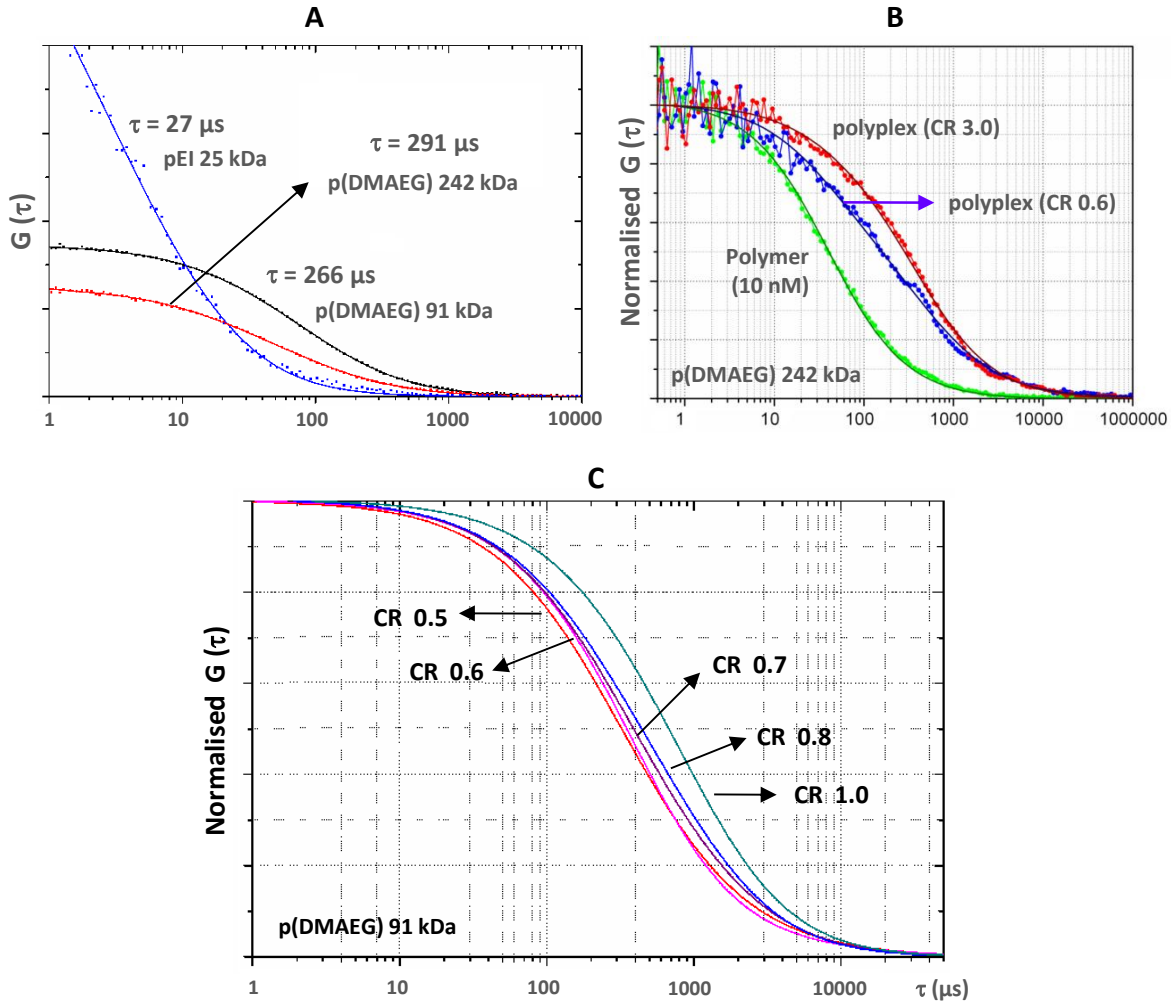


**Figure 5.6 - FCS measurements: auto-correlation fitting of fluorescence (G = autocorrelation function as a function of diffusion time (τ)): (A) polymers, (B) normalized correlation function of polyplex & polymer, (C) normalized correlation function, effect of CR.**

The data acquired confirms that FCS measurements can identify complex formation based on diffusion times and is able to differentiate between polyplexes with a different CR due to the detection ability, both at the level of accuracy and sensitivity (down to a CR difference of 0.1). Nevertheless, FCS measurements can only be validated if the presence of fluorescent molecules do not interfere with the polyplex formation as will be shown below. Moreover, due to the sensitivity of FCS, highly fluorescent peaks of complexes (mulitmolecular complexes, binding of multiple polymers with one DNA molecule or single polymer molecules) are observed and drastically disturbed the analysis of the fluctuation profiles by autocorrelation. Consequently, the analysis has to rely on the presence or absence of highly

fluorescent peaks in the fluctuation profile as representative data for the majority of the polyplexes, namely the baseline (data in between high peaks)[35].

### *2.4.2 UV/VIS absorption tests of fluorescent active polyplexes*

UV/VIS absorbance experiments were carried out to compare the difference between polyplexes with covalently coupled fluorescent groups and polyplexes where the fluorescent group was physically mixed during polyplex formation. The absorption wavelengths selected for labelled polyplexes are 488 nm, which corresponds with the maximum $\lambda_{abs}$ of Oregon Green and 280 nm which corresponds with the $\lambda_{abs}$ of purine and pyrimidine bases of DNA.

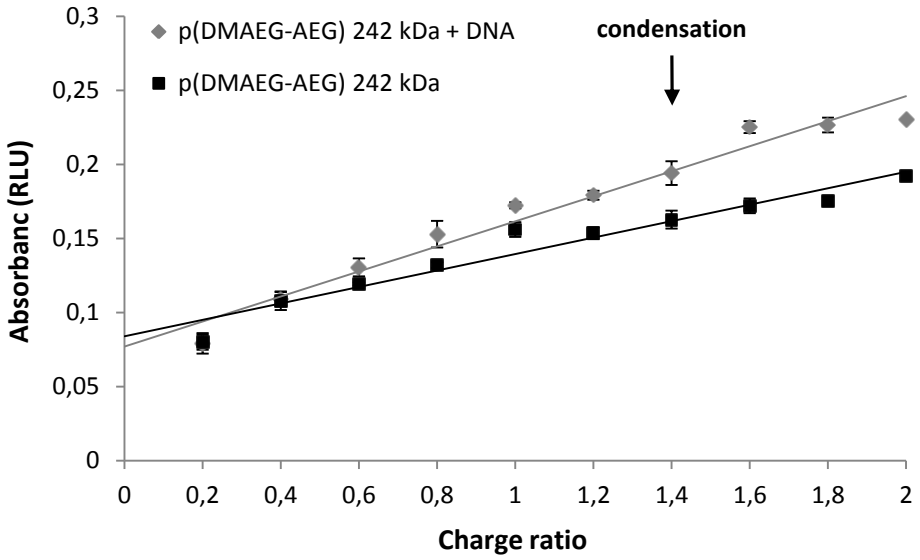


**Figure 5.7 – Absorbance values ($\lambda_{exc}$ = 488 nm) of labeled free polymer as such and upon interacting in proximity or collapsed into a particle with DNA.**

At first, there seems to be only a limited difference in detection of the fluorescent group of a polymer when DNA is present at a wavelength of 488 nm (Fig. 5.7). It appears that with increasing polymer concentration (and CR), the difference becomes clearer and reaches a maximum when condensation into a particle has occurred. Furthermore, no significant difference in condensation ability is observed when comparing covalent and physically mixed fluorescent groups at a wavelength corresponding with DNA detection ($\lambda$ =280 nm), shown in figure 5.8. Since the DNA is now present within the polyplex, a serious decrease in DNA sensitivity is noted. Moreover, when complexation has occurred, both absorption values remain similar and stable.

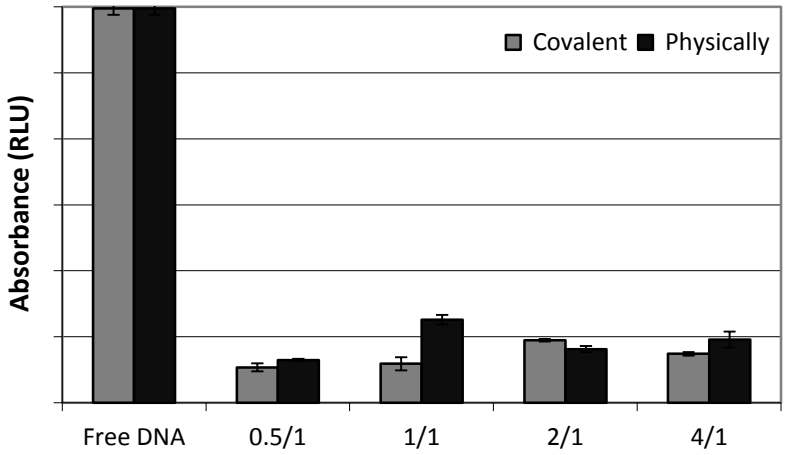


**Figure 5.8 – Absorbance ($\lambda_{ex}$ = 280 nm) of polyplexes preformed by polymers with physically & covalently mixed fluorescent groups of p(DMAEG$_{85\%}$-AEG$_{15\%}$) 242 kDa.**

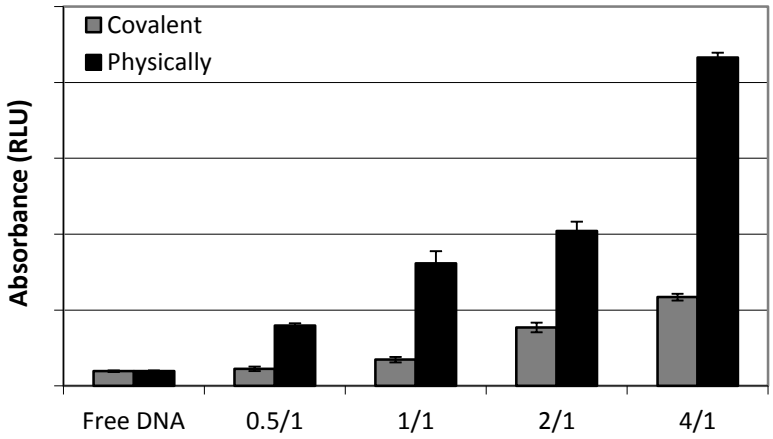


**Figure 5.9 – Absorbance ($\lambda_{exc}$ = 488 nm) of polyplexes preformed by polymers with physically & covalently mixed fluorescent groups of p(DMAEG$_{85\%}$-AEG$_{15\%}$) 242 kDa.**

On the other hand, a distinct difference can be observed when a covalently coupled dye is compared with a dye that is physically mixed during polyplex formation (Fig. 5.9). This allows to safely state that the fluorescent tags are partially located inside the polyplex (due to shielding from the hydrophilic environment). When physically mixing the dye, a more uniform distribution of the fluorescent group can be obtained what is already apparent before full complexation was reached. The measured absorbance increase, once the polyplex is formed (i.e. CRcond = 1.2), is proportional to the additional quantity of polymer added to the solution (and which is electrostatically coupled to the preformed polyplex).

In conclusion, as stated in section 2.3, the presence of fluorescent labels has a small effect on the ability to condense DNA. Moreover, the way of introducing fluorescent groups into a polyplex (either by covalent coupling or by physically mixing) appeared indifferent for the degree of complexation as was measured at a wavelength of 280 nm. Finally, when using

the fluorescent capacity of labelled polyplexes, physical mixing has a clear benefit over covalent coupling due to a more homogeneous fluorophore distribution (also at the surface) as was measured at a wavelength of 488 nm.

# 3 Application of Cell Penetrating Peptides in polymeric gene delivery

## 3.1 Synthesis of polymer-CPP conjugates

### *3.1.1 Coupling strategies*

The ability of cell penetrating peptides to facilitate cellular uptake has been generally accepted and reported extensively in literature[36,37,38]. A wide range of CPP's have been explored and were already used for gene delivery applications as such (without the presence of polymers). Most of these compounds show promising results in cell-internalising applications but nonetheless, they still possess limited cell-specificity and are complex to upscale (time & cost). For that reason, this new class of peptides was examined in combination with polymeric carriers in order to reduce the amount of CPP needed while still preserving the considerable advantage of their cell-internalising effect[39].

The coupling of a peptide to a polymer can be achieved in different ways. On one hand, the peptide can be efficiently incorporated during the aminolysis reaction. Unfortunately, high equivalents of peptide are required to obtain sufficient coupling degrees. Therefore, preference was given to coupling to the final polymers. An elegant tactic for conjugating a macromolecule and a small molecule (e.g. ligand, drug, etc.) is given by thiol-coupling chemistry, a process largely executed in nature[40]. Due to the multi-step production of synthetic peptides, it is possible to incorporate thiol-containing sequences (mainly by means of other amino acids like cysteine) in peptides during the synthesis. Polymers on the other hand can only be functionalised with thiol functions when protected thiolating reagents are used or by thiol-reactive group modification (post polymer synthesis so to prevent inter-molecular crosslinking). Because of commercial availability and costs, the latter option was selected to obtain polymer-CPP conjugates.

### *3.1.2 Coupling protocol*

As was indicated above, thiolated derivatives of poly-L-glutamine and poly-L-arginine could not be obtained during polymer synthesis. Since the direct coupling of a peptide to an amine-containing polymer is not straightforward, the use of a hetero-bifunctional crosslinker was mandatory. Two types of crosslinkers were selected. Both an *N*-(γ-maleimidobutyryloxy)succinimide-ester (GMBS), containing a maleimide functional group as well as an *N*-succinimidyl-3-(2-pyridyldithio)propionic-ester (SPDP), characterised by the

presence of a disfulfide bond, readily enable coupling to the polymer via the formation of an amide-bond[41] (Fig. 5.10). In a subsequent step, a thiolated molecule (e.g. cysteine-modified CPP) can be reacted with the maleimide group (GMBS) to form a stable thio-ether bond[42] or a reversible disulfide bond (SPDP).

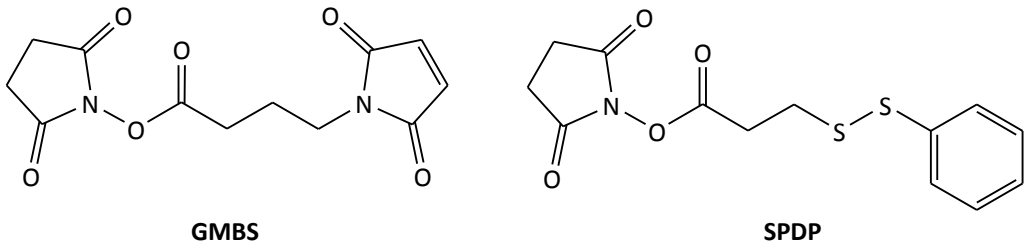


**Figure 5.10 - Structure of GMBS and SPDP.**

The modification with a crosslinker and subsequent peptide coupling is carried out in an aqueous buffer. *N*-hydroxysuccinimide esters are relatively sensitive to hydrolysis and are therefore dissolved just before mixing with the polymer. Also the pH of this reaction is monitored since amine-reactivity is limited to a pH of 7-9. Maleimide functional groups are less prone to hydrolysis but reactivity towards thiols is limited to a pH-range of 6.5-7.5. For the first modification (polymer-crosslinker), a $NaHCO_3$ buffer (0.1 M – pH ≈ 8.3) was used to dissolve the polymer (10 mg/ml). The crosslinker is separately dissolved in DMSO (10 mg/ml) and added to the polymer solution to react for 45 minutes at room temperature. The excess of unreacted crosslinker is removed via size-exclusion chromatography (pd-10 desalting coloumn – General Electric) in a PBS buffer (pH ≈ 7.2). Subsequent coupling of the thiolated CPP is immediately performed by dissolving the CPP in a similar PBS buffer and added to the purified conjugate solution followed by stirring (1h at RT). Because it is common to use higher excesses of crosslinker than thiolated CPP, it is possible that not all functional groups of the conjugated crosslinker are consumed, hence a blocking-reagent (EtSH) is added (only in the case of GMBS). The final product is further purified by dialysis and isolated by freeze-drying (Fig. 5.11).

The degree of coupling can be determined via UV/VIS spectrometry, $^1$H-NMR or a combination (dependent on the availibilty of UV-active groups on the peptide). In the case of Penetratine, UV absorption ($\lambda_{abs}$ = 260 nm) is caused by one tryptophan and two phenylalanine units present in the structure. The amount of coupled $Arg_8$ can only be derived from NMR measurements. When SPDP is used as a crosslinker, confirmation of the degree of coupling can be obtained by measuring the release of thiopyridine, which is a side-product of the coupling reaction and has a specific absorption at 343 nm. The disulfide substitution is a result of the formation of the thermodynamically favoured thiopyridine (pKa ≈ -1)[43].

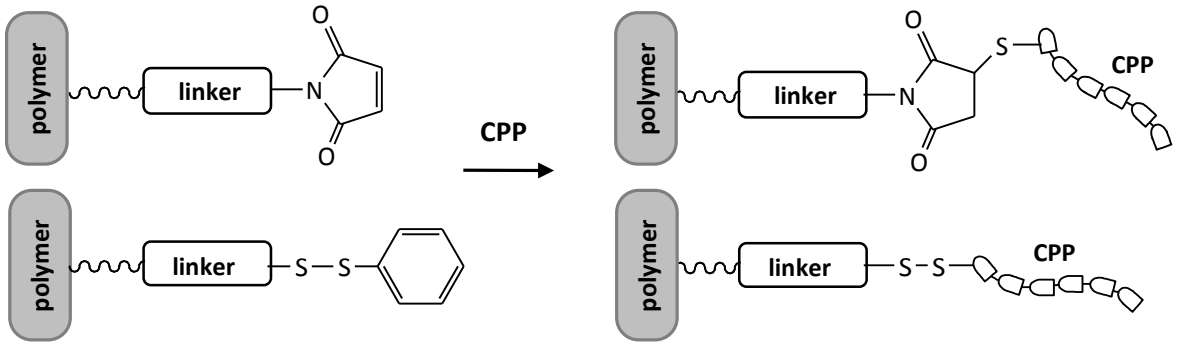


**Figure 5.11 - Coupling of a CPP to a polymer-crosslinker conjugate (via GMBS & SPDP).**

## 3.2 Overview of the developed polymer-CPP conjugates

### *3.2.1 Penetratine (PEN) containing conjugates*

The potential activity increase by coupling Penetratine to biodegradable poly-L-glutamine derivatives synthesised in chapter 2, was investigated by applying the coupling protocol discussed above. The degree of coupling is kept minimal for reasons of cost per gram CPP and to ensure that the polymer properties (e.g. polyplex formation) are not substantially affected (table 5.3). All polymers selected have a comparable percentage of free amines available (10-20%) and were selected, based on differences in functional groups present (guanidine, hydroxyl or tertiary amine) and their corresponding impact on biological properties.

The effect of Penetratin-coupling was investigated by physico-chemical and biological experiments (sections 3.3 & 3.4 of this chapter).

| Base polymer | Type of crosslinker | % coupled | M/C |
|---|---|---|---|
| PEI | GMBS | 1.4 | 210.6 |
| [PEI-Guan] + OREG | GMBS | 2.0 | 323.6 |
| p($DMAEG_{90\%}$-$AEG_{10\%}$) 10 kDa | GMBS | 2.9 | 237.6 |
| p($DMAEG_{85\%}$-$AEG_{15\%}$) 91 kDa | GMBS | 2.8 | 240.0 |
| p($DMAEG_{85\%}$-$AEG_{15\%}$) 242 kDa | GMBS | 1.8 | 234.7 |
| p($ORN_{18\%}$-$ARG_{82\%}$) 71 kDa | GMBS | 4.0 | 209.1 |
| [p($DMAEG_{85\%}$-$AEG_{15\%}$) 91 kDa] + OREG | GMBS | 1.8 | 264.0 |
| p($DMAEG_{85\%}$-$AEG_{15\%}$) 91 kDa | SPDP | 1.8 | 236.0 |
| p($HEG_{87\%}$-$AEG_{13\%}$) 27 kDa | SPDP | 3.5 | 141.8 |

**Table 5.3 – Overview of developed penetratine-coupled polymers.**

### *3.2.2 Octa-Arginine ($Arg_8$)*

Similar to Penetratin, Octa-arginine or $Arg_8$ (the peptide sequence that presumably represents the active sequence of TAT) was selected to be coupled to certain biodegradable polymers. Unlike for Penetratin, the coupling of a higher charged molecule to a cationic polymer appeared to complicate the degree of coupling due to charge repulsion which led to lower coupling degrees. The negative influence of the cationic charge (present on the polymer) on the CPP coupling efficiency could be noticed when equal reaction parameters were applied for polymers containing a substantial amount of neutral groups such as p(HEG-AEG) with a high percentage of hydroxyl groups (85-90 %) resulting in a higher coupling degree (table 5.4).

| Base polymer | Type of crosslinker | % coupled | M/C |
|---|---|---|---|
| PEI | GMBS | 1.0 | 209.8 |
| p($DMAEG_{85\%}$-$AEG_{15\%}$) 91 kDa | GMBS | 1.0 | 232.0 |
| p($DMAEG_{85\%}$-$AEG_{15\%}$) 242 kDa | GMBS | 1.9 | 233.8 |
| [p($DMAEG_{85\%}$-$AEG_{15\%}$) 91 kDa] + OREG | GMBS | 1.2 | 262.7 |
| p($HEG_{87\%}$-$AEG_{13\%}$) 11 kDa | SPDP | 8.0 | 185.0 |
| p($HEG_{87\%}$-$AEG_{13\%}$) 27 kDa | SPDP | 5.0 | 140.8 |

**Table 5.4 – Overview of $Arg_8$-modified polymers.**

### *3.2.3 Influence of spacer on CPP activity*

Providing polymeric vectors with CPP's is expected to be the start of obtaining improved polyplex internalisation and correspondent transfection efficiency. Nonetheless, since polymers form tightly-condensed particles with DNA, the availability of CPP's for cell-surface negotiation can be seriously restricted due to the fact that CPP's are partial (PEN) to fully charged ($Arg_8$) structures that are equally prone to electrostatic forces of oppositely-charged molecules as the polymer. To judge on the importance of this aspect, several $Arg_8$-derivatives with variable spacer lengths were synthesised. Different types of spacer were considered: 1) flexible and rigid ones and 2) short and long ones. Oligo-sized chains of ethyleneoxide (PEO) units were applied as flexible spacers. Moreover, PEO chains are known to limit protein-specific interactions which could be beneficial for the cell-viability. Also regular carbon chains were used with variable length. Specific amino acid sequences were able to give rigidity to the spacer. A repeating sequence of proline and glycine units imparts

rigidity while a repetition of other amino acids such as for arginine-alanine-aspartic acid-alanine (RADA) is known to form fibril-like (helical) structures and believed to act as a lineair version of the RGD-motive (but with non-integrin mediated adhesion)[44]. In this way, each spacer could provide the polymer-CPP conjugate with a specific geometrical property. The spacers were incorporated during peptide synthesis between the active peptide sequence and the cysteine unit (used for covalent coupling) as shown in figure 5.12.

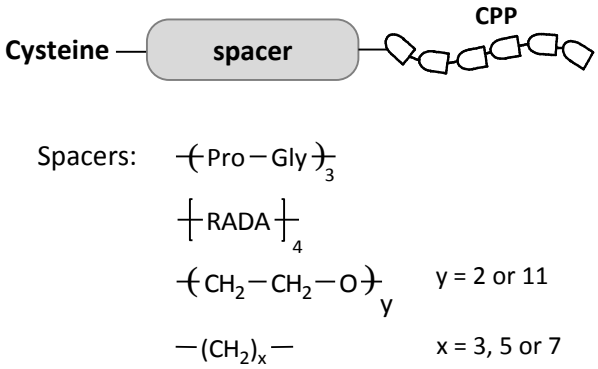


**Figure 5.12 - Different types of spacers coupled to $Arg_8$.**

The effect of the different spacers was tested with $Arg_8$ on p($DMAEG_{85\%}$-$AEG_{15\%}$) (MW = 91.000 Da) using the GMBS crosslinker and the peptide-derivatives by applying the standard protocol. A slight influence of the spacer length and type on the coupling efficiency could be noticed. Long and flexible chains (PEO) allowed a somehow higher amount of coupling while more rigid chains (both -($CH_2$)- and Pro-Gly) proved to be less efficient. Reactions with short spacers or no spacer only reached coupling degrees of about 1 % (table 5.5). Besides p(DMAEG-AEG), an initial coupling reaction was performed on PEI with a spacer-containing PEN-derivative (-$(CH_2)_7$-PEN) which was coupled at a molar concentration of 1%.

| Spacer | % coupled | M/C |
|---|---|---|
| - | 1.0 | 232.0 |
| $(CH_2)_3$ | 0.9 | 231.9 |
| $(CH_2)_5$ | 1.1 | 232.1 |
| $(CH_2)_7$ | 1.8 | 232.8 |
| $(CH_2\text{-}CH_2\text{-}O)_2$ | 2.0 | 233.5 |
| $(CH_2\text{-}CH_2\text{-}O)_{11}$ | 3.7 | 236.1 |
| $(Pro\text{-}Gly)_3$ | 1.8 | 233.4 |
| $(RADA)_4$ | 2.5 | 234.7 |

**Table 5.5 - Overview of $Arg_8$ peptides with variable spacer types and length coupled to p($DMAEG_{85\%}$-$AEG_{15\%}$) 91 kDa.**

## 3.3 Physico-chemical characterisation

It is imperative that cell-penetrating peptides exert a positive influence on synthetic vector systems as they are assumed to act upon this by facilitating cellular entry. On the other hand, incorporating CPP's into the polymer-DNA polyplex should not hamper the ability of a vector system to interact with DNA. Therefore, the focus of CPP-based polymers and polyplexes was, besides biological benefit, also put on improvement (or preservation) of the DNA-interacting properties. The outcome of peptide-coupling is checked in terms of polyplex formation, size and stability using the characterisation methods described in chapter 4.

The influence of CPP coupling is already apparent in the calculation of polyplex composition because the M/C was altered by coupling peptides (responsible for added molecular weight and charge). Dependent on the amount and type of CPP coupled, the M/C can differ up to 10% from the original value (tables 5.3-5.5).

Additionally, in collaboration with the Fraunhofer Institute (IBMT) project partner, newly developed techniques that are based on the measurement of impedance of single cells, were used to help elucidate the mechanism of cell penetration by CPP's on single cells. In this way, the effect of both polyplexes and CPP's on the cell membrane integrity can be assessed.

### *3.3.1 Polyplex formation*

In order to decide if CPP-coupled polymers have a different ability to form small particles with DNA, EtBr fluorescence and agarose gel-electrophoresis experiments were performed to verify the formation of polyplexes and to compare their results with the corresponding non-coupled polymers. Ideally, CPP addition was expected to enhance the attraction towards DNA but in practice, this is only noticeable for systems which don't possess large quantities of cationic charge.

*EtBr Fluorescence*

Via EtBr displacement assays, a rudimentary idea of the complex strength was formed. Both the extent to which EtBr intercalation was prevented and the CR at which polyplex formation started, allowed for information of the polyplex interacting forces to be derived. In figure 5.13, the influence of peptide-coupling to PEI is shown. It appears that the CR for full complexation is slightly shifted (0.2-0.4 CR units) towards a higher CR. This could indicate that peptides interfere (if only little) with the polyplex formation by hindering the optimal orientation of the cationic vector when approaching the polyanion (DNA). All peptide-derivatives show an equal or small improvement in $Min_F$ (lower fluorescence yield) which is in accordance with the precluding claim that additional cationic charges (provided by the

CPP) should enhance the quality of the attraction force displayed by the basic polymer (but due to the limited coupling degree, this effect was rather small).

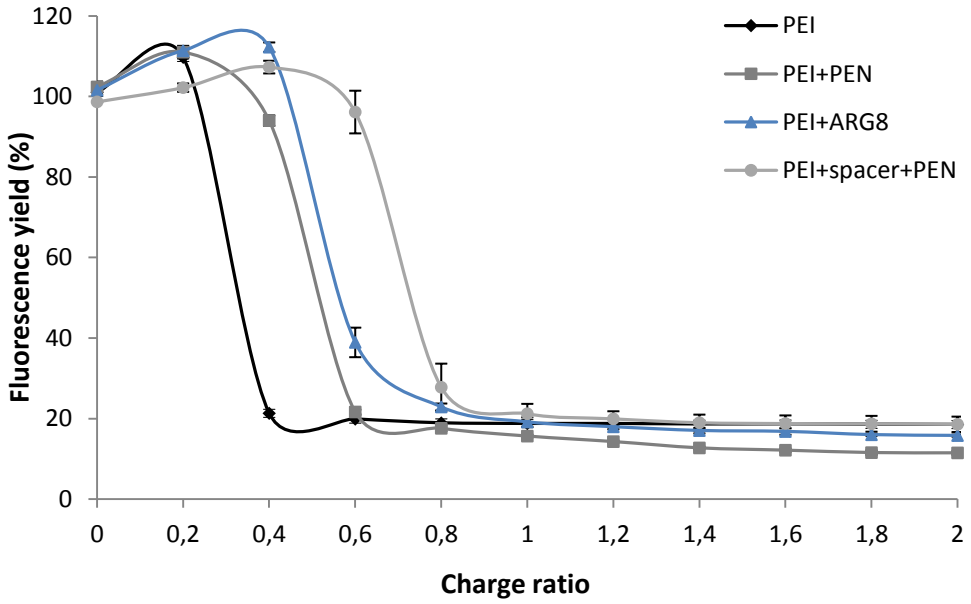


**Figure 5.13 - Fluorescence yield as a function of increasing CR for polyplexes based on PEI, PEI+PEN$_{1\%}$, PEI+ARG$_{1\%}$ & PEI+spacer+PEN$_{1\%}$.**

Providing biodegradable poly-α-amino acids with a CPP gives rise to fluorescence results which differ from the trend noticed for CPP-coupled PEI derivatives. Moreover, they prove to be dependent on the composition of the polymer backbone and functional groups. Similar as for PEI, abundantly protonated, poly-L-glutamines (e.g. p(DMAEG-AEG)) display a shift of the $CR_{cond}$ towards higher values (0.4 units) when a CPP was coupled to it but the interaction forces remain equal (Fig. 5.14 – grey full lines). In the case of a spacer with considerable length (i.e. 11 EO-units), an even bigger shift (0.8 CR units) can be observed as well as a loss in EtBr exclusion ability (20 %) which could be most likely attributed to a shielding effect, induced by the non-charged spacer that possesses sufficient mobility to surround the polymer cationic charges. The effect of shielding the cationic polymer is even more expressed for derivatives which display an optimal DNA interaction (high EtBr exclusion at low CR), observed for p(ORN-ARG). When a substantial amount of PEN is coupled, the $CR_{cond}$ is shifted from 1/1 to 2/1 (Fig. 5.14 – grey dotted lines). As opposed to reduced DNA interaction, the addition of a CPP can also be the origin of (improved) DNA condensation. This is the case for polymers with a low charge density, for instance p($HEG_{87\%}$-$AEG_{13\%}$) to which 5 % of $Arg_8$ was coupled, generates a polymer with excellent condensation properties (strong interaction at low CR) and does not demonstrate a negative shielding effect (Fig. 5.14 – black lines).

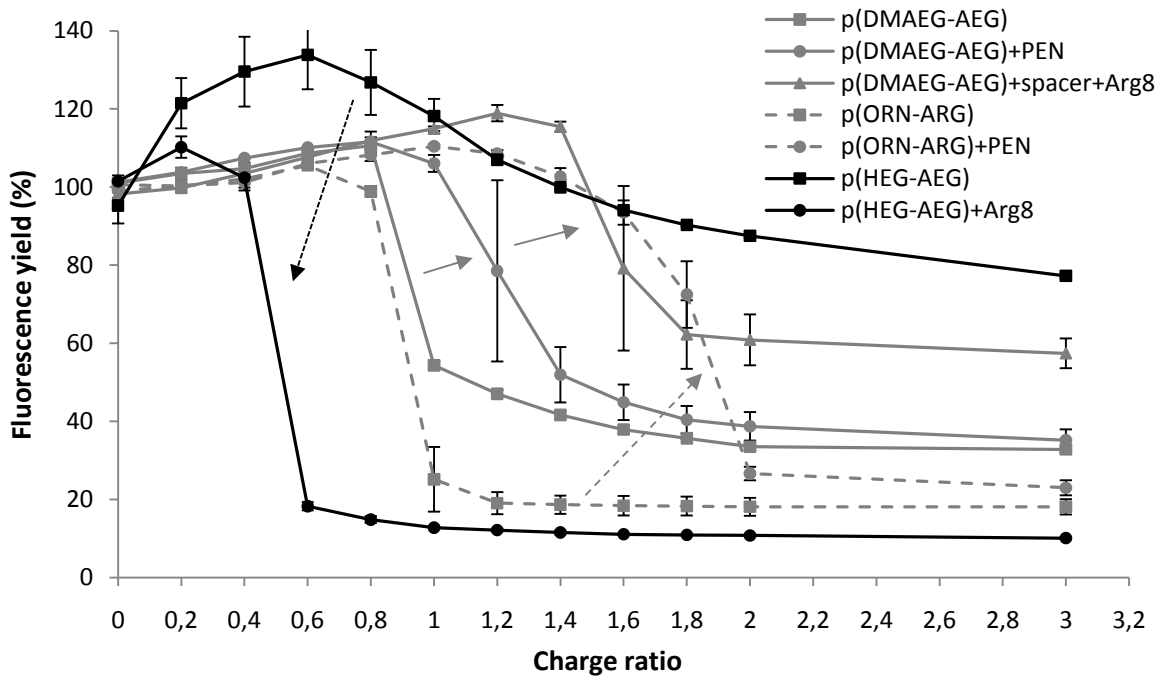


**Figure 5.14 – EtBr displacement assays: influence of CPP addition on DNA condensation by p(DMAEG$_{85\%}$-AEG$_{15\%}$) (grey full), p(ORN$_{18\%}$-ARG$_{82\%}$) (grey dotted) and p(HEG$_{87\%}$-AEG$_{13\%}$) (black full).**

### *3.3.2 Agarose gel-electrophoresis (AGE)*

Complementary to the EtBr displacement test, the effects of peptide coupling on DNA condensation by polymeric vectors could be verified by AGE. Due to the different principle on which both techniques are based (size-exclusion chromatography versus fluorescence spectrometry) slight deviations could be observed when compared to EtBr fluorescence (generally ≤ 0.2 CR units). A similar trend was noticed based on the retardation of DNA when mixed with increasing polymer quantities (steps of 0.2 CR). These results confirm the required increase in CR needed for total DNA complexation when making a comparison between regular and peptide-functionalised derivatives (Fig. 5.15).

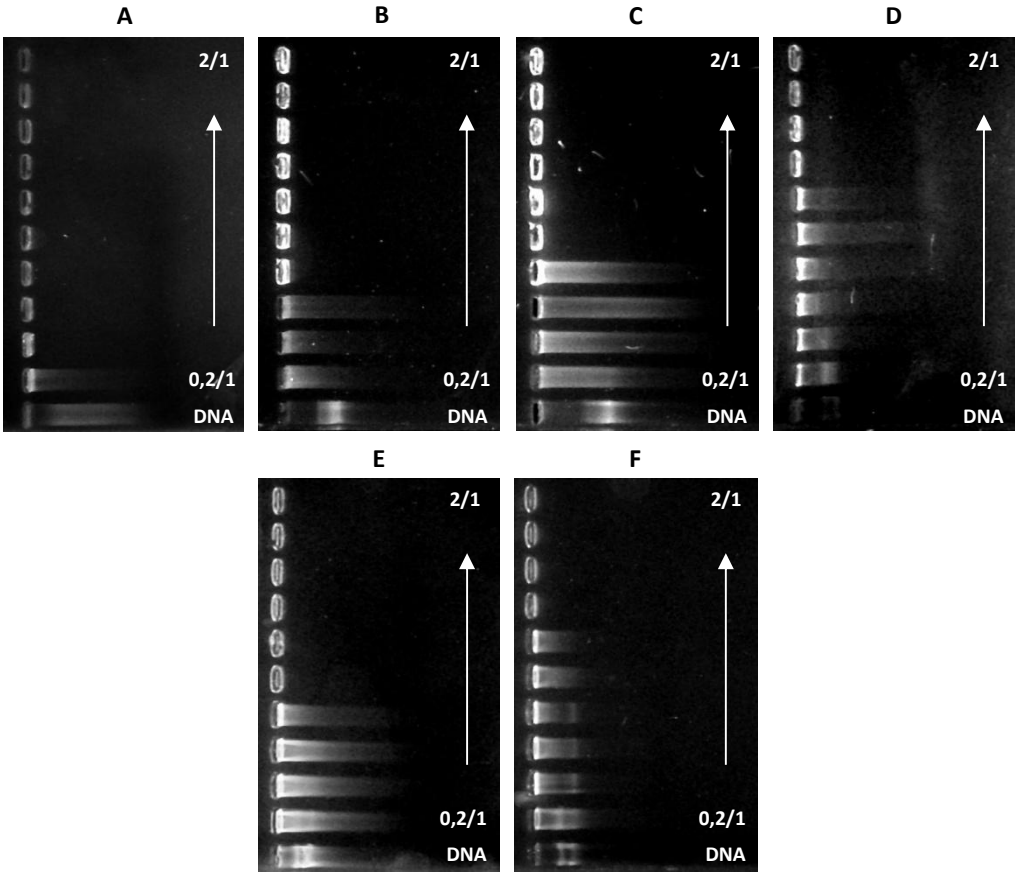


**Figure 5.15 – Agarose gel electrophoresis experiments of DNA condensation by (A) PEI 25 kDa, (B) PEI+PEN, (C) PEI+$ARG_8$, (D) PEI+spacer+PEN, (E) p($DMAEG_{85\%}$-$AEG_{15\%}$) 91 kDa and (E) p($DMAEG_{85\%}$-$AEG_{15\%}$)+PEN.**

### *3.3.3 Polyplex size and distribution*

Despite the lasting doubt about the cellular uptake mechanisms of polyplexes, a great deal of investigations are focussed on obtaining delivery systems with a particular size, compatible with the requirements for the endocytotic pathway. Especially for polymers containing CPP's, the necessity to meet certain size restrictions when receptor mediated endocytosis is considered, should be kept in mind. Therefore, it is imperative that peptide coupling preserves the nano-sized dimensions of vector-DNA particles. With respect to this demand, particle sizes were determined by DLS. From figure 5.16 (A), it can be concluded that native PEI-DNA complexes show an equal bimodal distribution (130 and 320 nm at CR 2/1) of which the smallest distribution predominates at higher CR. Polyplexes based on CPP-coupled PEI remarkably show almost no particle-sizes above 150 nm and appear nearly all as mono-modal peaks. Also, the difference in absolute size between the different CR's is limited. Furthermore, the particles tend to decrease in size with increasing CR and can reach values as low as 30 nm but are characterised by broader distributions.

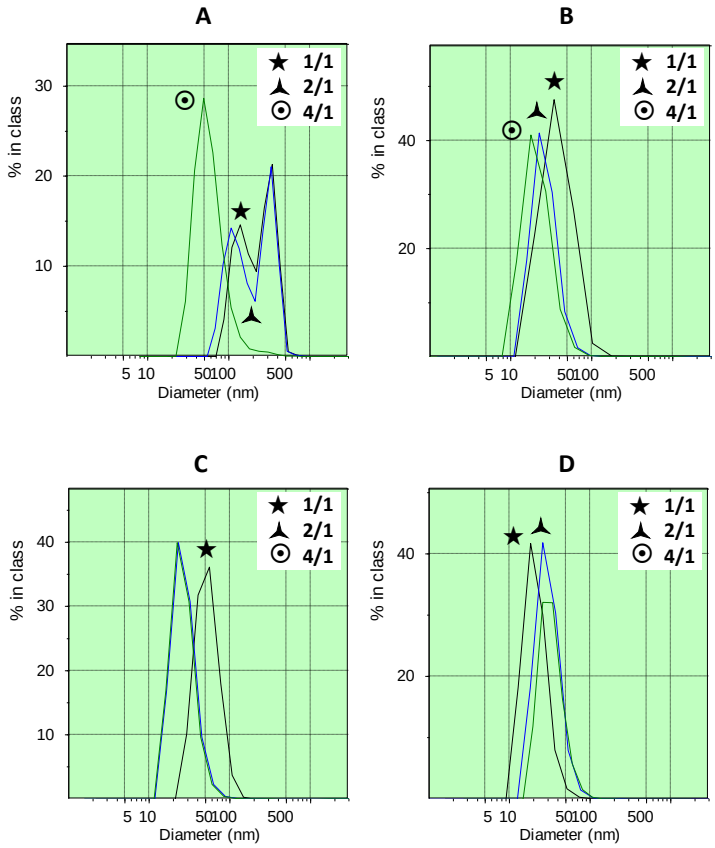


**Figure 5.16 – Overlay graphs of DLS measurements of polyplexes at various CR (1/1, 2/1 and 4/1) based on PEI (A); PEI+PEN (B); PEI+ARG (C) and PEI+spacer+PEN (D).**

For poly-L-glutamine derivatives possessing a high amount of cationic charges (Fig 5.17 - A), small, uniform particles (≈ 60 nm) are already formed at a low CR (1/1) and can reach values as low as approximately 35 nm for a CR of 4/1. It appears that the addition of Penetratine (Fig 5.17 - B) does not influence the polyplex size and distribution. Moreover, in contrast to EtBr displacement and gel-electrophoresis results, condensation of DNA into particles of 30-40 nm appears to occur already at a CR of 1/1. The addition of more polymer (i.e. a higher CR) is in this case disadvantageous given the increased particle size as a consequence of the optimal particle formation that already occurs at a 1/1 CR and which represents a layered expansion of the polyplex particle. In the case of poly-L-glutamines with few cationic charges (Fig 5.17 – C), relatively small particles are apparently formed at a CR of 1/1 (100 & 300 nm) despite the fact that virtually no EtBr was expelled at this CR. This could suggest that the complexation is weaker but sufficient for size reduction (into a particle). When augmenting the CR, smaller particles (up to 35 nm) are formed but a tendency towards larger size distributions remains. The addition of more cationic charge by coupling a CPP ($Arg_8$) proved very successful in fluorescence experiments but the effect on size is less pronounced (Fig. 5.17 – D). With the observed new values only half of the CR is required to obtain similar sizes compared to the reference (uncoupled) polymer. In general,

DLS results are interpreted based on a number-averaged value. If volume or intensity averages are taken into account, extra distributions sometimes arise at higher values (applicable for polyplexes at low CR, close to the $CR_{cond}$).

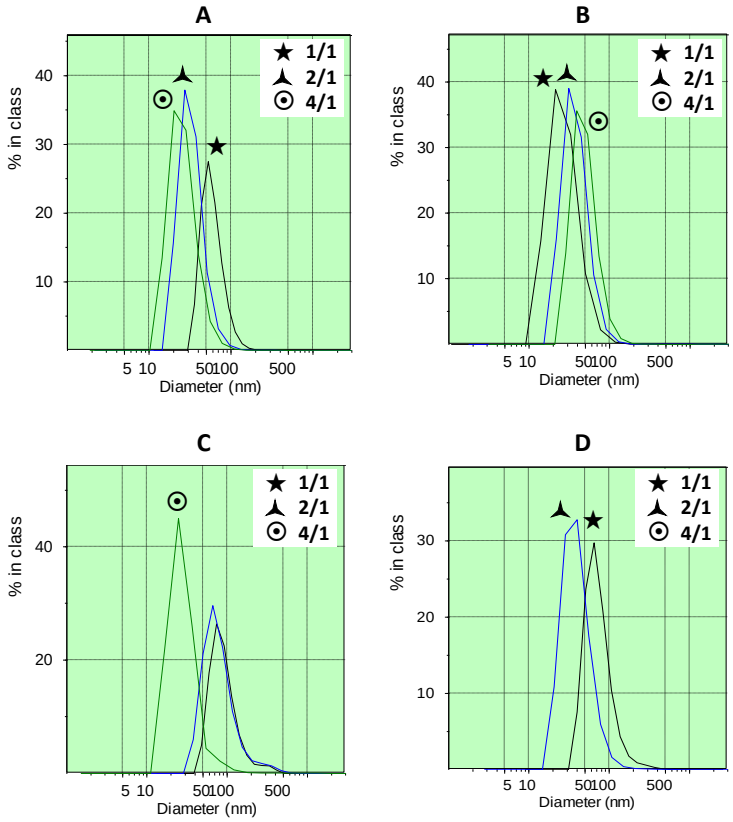


**Figure 5.17 - DLS measurements of polyplexes at various CR (1/1, 2/1 and 4/1) for (A) p(DMAEG$_{85\%}$-AEG$_{15\%}$) 91 kDa, (B) p(DMAEG$_{85\%}$-AEG$_{15\%}$)+PEN, (C) p(HEG$_{87\%}$-AEG$_{13\%}$) and (D) p(HEG$_{87\%}$-AEG$_{13\%}$)+Arg$_8$ based polyplexes.**

### *3.3.4 Stability of polyplexes in aqueous environment*

To what degree, polyplexes, formed in water, remain stable in an aqueous environment is a property that can be revealed by measuring the zeta-potential. The impact of peptide residues which should be present at the surface of the polyplex was investigated and found to be in accordance with preceding results (fluorescence, AGE and DLS). CPP-containing polymers show lower surface charges than their native polymers (or they reach similar values only at higher CR's). Moreover a delay (i.e. higher amount of polymer needed) in polyplex condensation can be noted from the CR corresponding with a value of 0 mV. This is most likely the result of the geometrical conformation of the polyplex which is more diffuse due to CPP extensions which contain also charges and expand the double-layer radius (and correspondingly lower the double layer radius. Still, all polymer-DNA complexes exhibit good stability (> 30 mV) at high CR's (4/1) and are highly, positively charged. This implies an excess of cationic polymer, capable of protecting the DNA and enabling interaction with

anionic cell surfaces. Additionally, when comparing this with fluorescence results, it is clear that polyplex formation and the origination of a positive surface charge are reached at different CR's (zeta-potential: usually higher values).

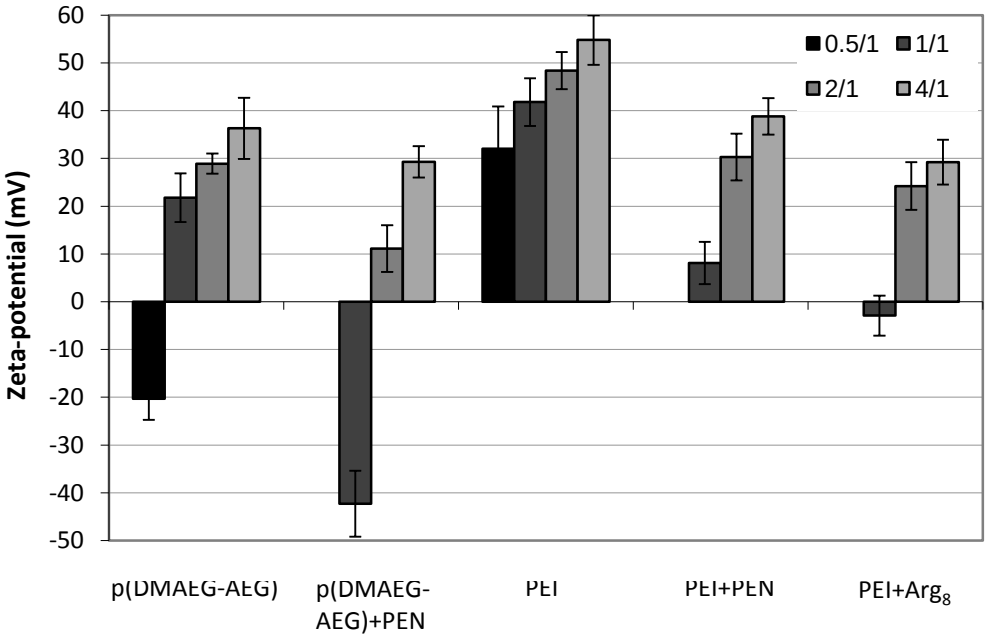


**Figure 5.18 – Results of zeta-potential experiments with polyplexes based on several polymers at various CR's (0.5/1, 1/1, 2/1 and 4/1)**

### *3.3.5 Cell membrane interaction*

An essential, if not the most important, hurdle towards achieving successful gene delivery systems, is crossing of the cell membrane, the most notable boundary between cellular entities and its surrounding. As was mentioned during the introduction, the cell can exploit several processes to take up or excrete substances. Receptor mediated endocytosis can be accounted for as one of the major cellular internalisation processes for peptide-based delivery to cells. With the aim to help clarifying how CPP's mediate internalisation, the interaction of peptides with the cell membrane was investigated. A possible technique to achieve this, is to determine the structural integrity of the cell membrane via impedance measurements[45]. Impedance spectroscopy is a repetitive and non-invasive technique to characterise the frequency dependent electrical characteristics of materials like the double phospho-lipid layer of cell membranes. To avoid electrode polarisation and consequent impedance augmentation (when applying micro-electrodes), a micro-hole based chip was developed to optimise sensitivity and eliminate noise-impedance (caused by the electrodes). Impedance is a concept that extends resistance to AC circuits whereby not only the ratio (Z) of voltage (V) to current (I) is described but also its relative phase-difference ($\theta$). When put in Ohm's law this becomes:

$$Z = |Z| \,.\, e^{j\theta} \quad \text{and} \quad V = I.Z = I.|Z| \,.\, e^{j\theta}$$

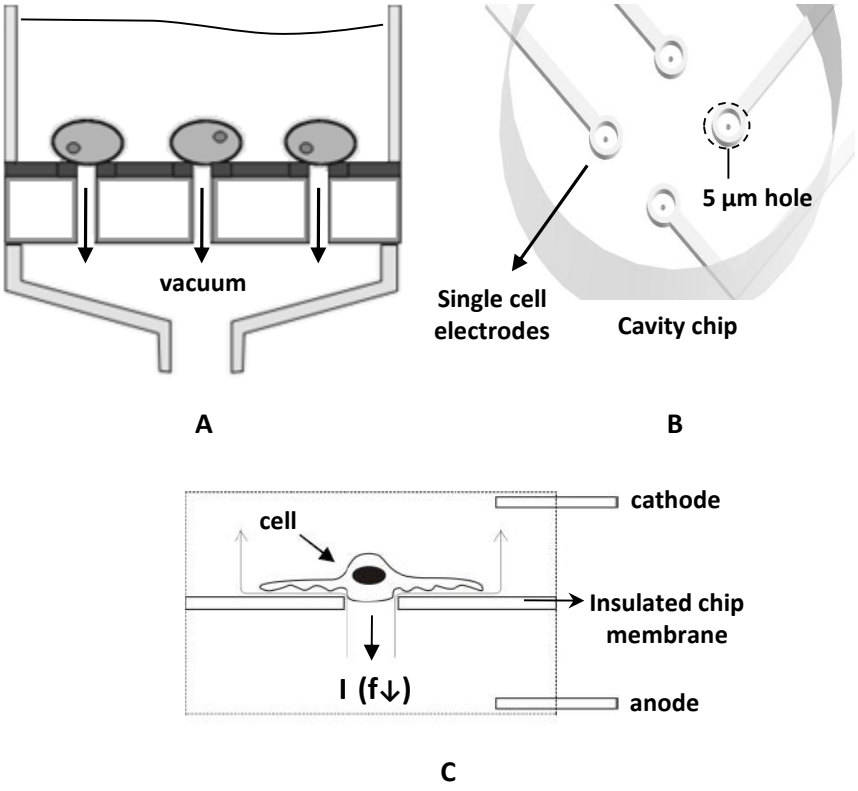


**Figure 5.19 - Impedance measurements of single cells: (A) schematic outline, (B) cavity chip and (C) cell position and impedance manipulation (I = current).**

The schematic outline of the experimental set-up is shown in figure 5.19: single cells are captured onto a gold-coated electrode with a diameter of about 5 µm. By applying a slight vacuum (0,05 mbar), a cell gets positioned into the hole and occupies the complete surface of the electrode (A). Up to 4 individual electrodes are incorporated into a cavity chip that allows for cells to be cultivated in a controlled environment (B). Electrode coatings composed of gold prove additional benefits in coupling CIP's (thiol-gold affinity). The influence of the cell-presence on the electrical signal (impedance, Z) when a voltage is applied between the electrodes, is finally measured and interpreted by plotting the values as a function of time.

An example of such a measurement in shown below for Penetratine and PEI (Fig. 5.20). The addition of Penetratin shows a disturbance in the membrane (of about 5 kΩ) after 15 minutes of incubation. A more severe impact on the membrane is caused by the application of Triton X-100, a non-ionic surfactant, which is used here to give an idea on the degree of membrane disruption. Because membrane instability is related to the origination of pores, microtunnels and other points of entry for extracellular components this confirms interaction of the CPP with the membrane but without specifying the mechanism. A similar effect was observed

when the addition of PEI to a cell (in culture medium) was measured ($\Delta Z \approx 25$ kΩ) although no incubation period was registered here (similar as for Triton X-100) and could be indicative for a difference in internalisation mechanism.

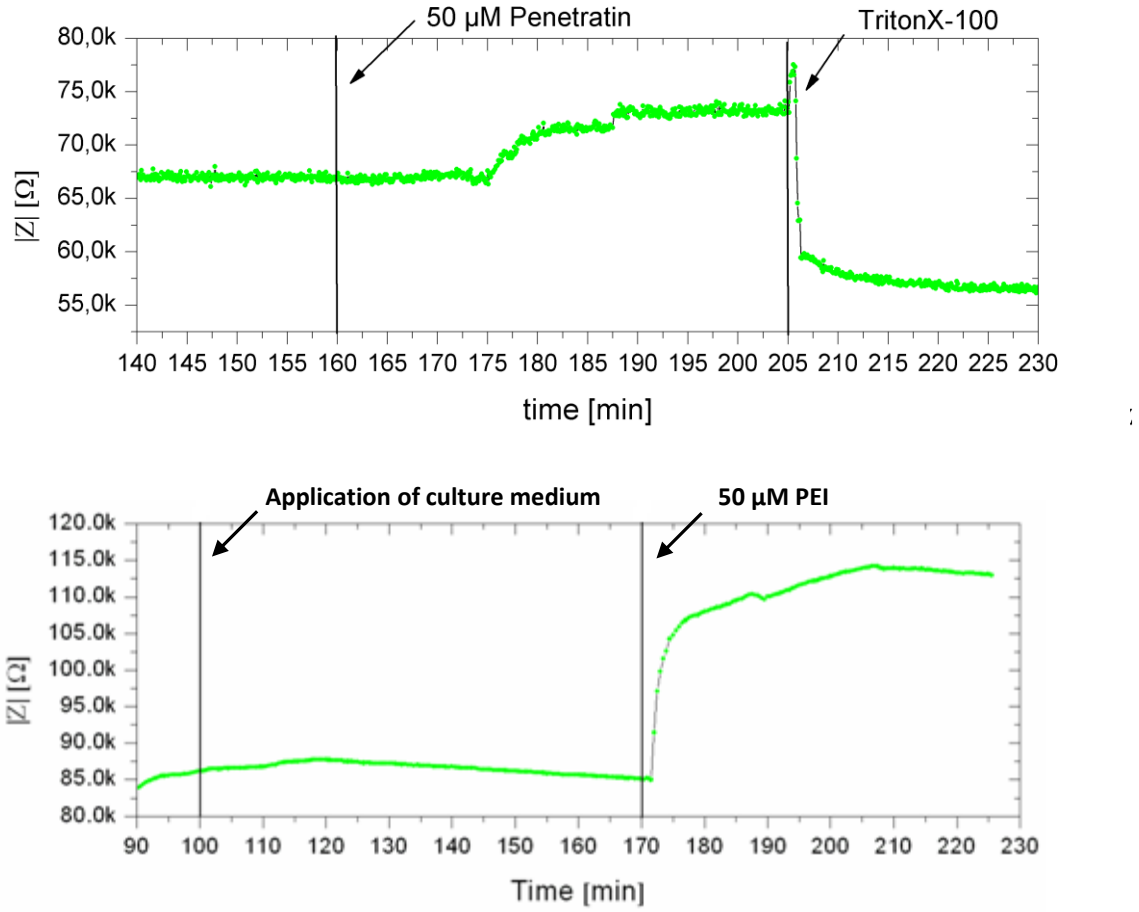


**Figure 5.20 - Impedance experiments on single cells: Influence of the addition of Penetratine (up) and PEI 25 kDa (down) to single cells positioned onto micro-electrodes.**

These experiments were extended to other polymeric carriers and their corresponding polyplexes. The extent to which polyplexes, that are added to the cell medium, can interact with the membrane and engage in certain uptake mechanisms is detectable using this same set-up. From these results important properties could be deducted when comparing (biologically) active with inactive polymers (see also chapter 6). Apparently, the addition of active PEI-Guan$_{20\%}$ polyplexes showed no noticeable change in impedance, hence the conclusion that membrane disruption was not realised (Fig 5.21). This was not the case for inactive polyplexes composed of pDMAEG with a MW of 242 kDa or its Penetratine-containing derivative p(DMAEG$_{85\%}$-AEG$_{15\%}$)-PEN as visualised in figure 5.22. After addition of the polyplexes to the cell medium (marked by the black arrow), a drop in impedance was detected which was even more pronounced for the penetratine derivative. Also, this effect

continued in time for the penetratine compound whereas for the basic polymer, the impedance difference graduately faded in time. Additionally, the increased disruption of the penetratine derivative can only be attributed to the coupling of this CPP. In all cases, there was a short incubation time required before membrane interaction starts. All the measured values (Fig. 5.21-23) were compared with impedance experiments containing only cells (reference) or no cells at all (background signal).

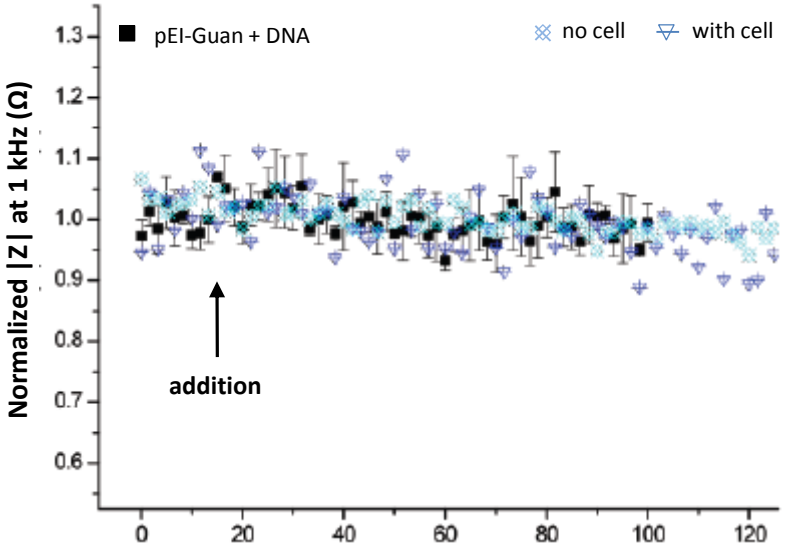


**Figure 5.21 - Impedance values as a function of time: PEI-Guan polyplex and their influence on the membrane destabilisation. Background/noise = signal measured when no cell is present.**

In contrast to polyplexes based on pEI-Guan, which do not seem to interfere with the membrane (based on impedance), the pure polymer affects the membrane stability after an incubation time of 20 min (Fig. 5.23). This leads again to the hypothesis that an excess of cationic charge acts heavily upon the cellular membrane but does not induce membrane crossing as such. The incorporation of DNA and the consequent formation of polyplexes diminishes the excess charge which suggests that polymeric carriers with reduced positive charge (like for neutral or hydrophobic groups) could experience a higher rate of success in transduction processes. Because the presence of peptides (e.g. penetratine) has proven to facilitate internalisation[32] and corresponded with a certain impedance change but this was not readily observed for complexes based on PEI-Guan, impedance measurements alone are not sufficient in validating the uptake of particles. This is probably the result of different internalisation mechanisms used (between pEI derivatives and penetratine) which can't be detected by impedance spectroscopy.

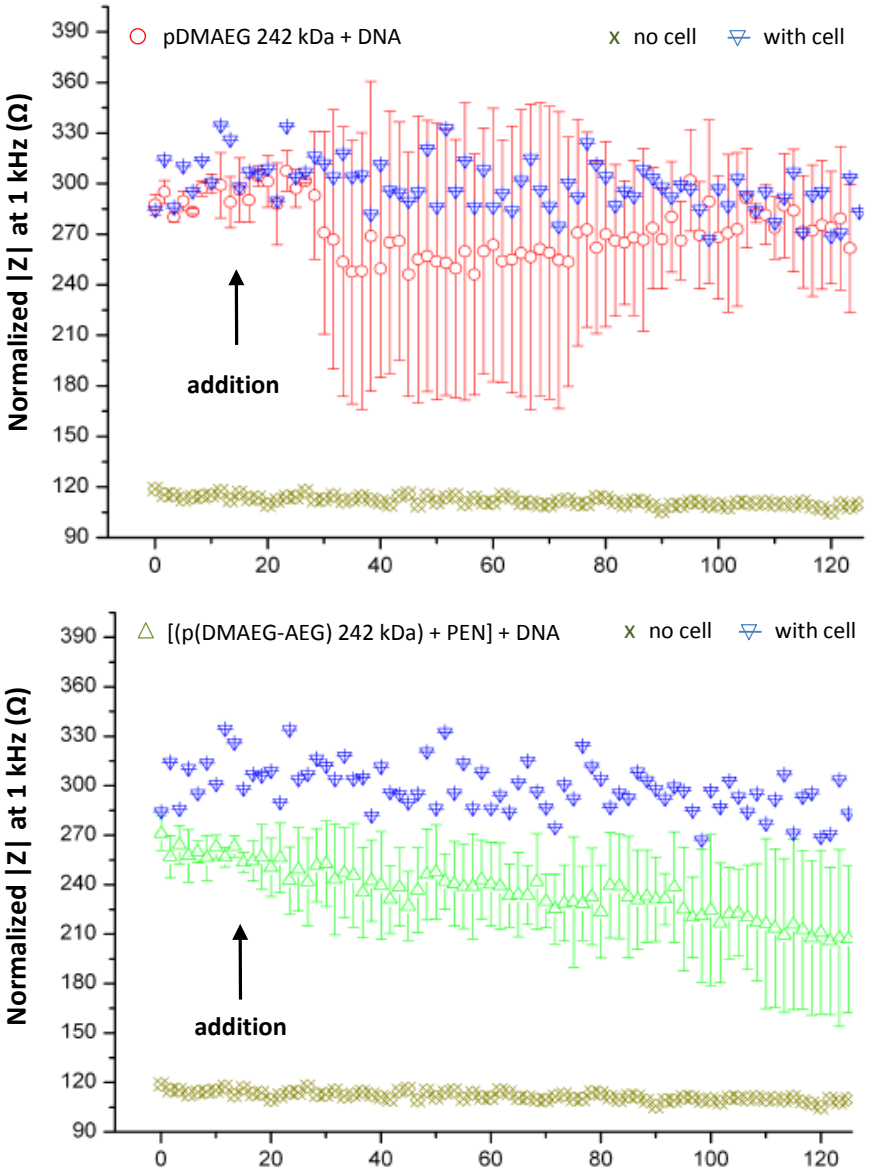


**Figure 5.22 – Impedance values as a function of time: (up) p(DMAEG) 242 kDa polyplex and (down) p(DMAEG-AEG)-PEN 242 kDa polyplex and their influence on the membrane destabilisation. Background/noise = signal measured when no cell is present.**

When correlating these impedance spectroscopy measurements with biological activity (chapter 6), it is unfortunately not possible to confirm the potential use of a polymer as genetic vector by impedance measurements alone. The membrane interaction capacity can be readily validated for polymers but as active complexes (PEI-Guan complexes) do not display a drop in impedance, additional characterisation is required to assess a vector's ability to transfect a cell.

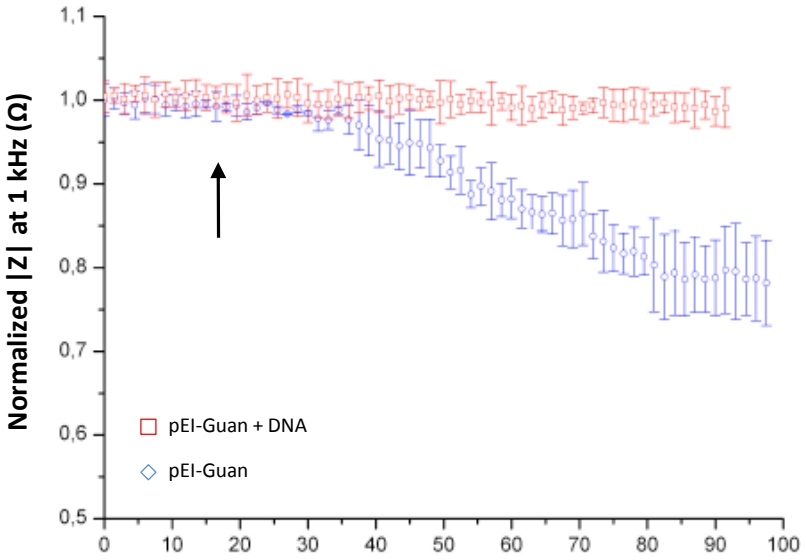


**Figure 5.23 - Impedance values as a function of time: (up) PEI-Guan polyplex and (down) PEI-Guan polyplex and PEI-Guan as such and their influence on the membrane destabilisation. Background/noise = signal measured when no cell is present.**

## 4 Comparison of physical versus chemical CPP mixing

As the interest and the amount of possible applications of cell penetrating peptides is graduately increasing, a growing need for CPP's will originate from this[46]. Considering that the coupling of a CPP onto a macromolecule is a reaction that requires excesses that in most cases are accompanied by a substantial loss of the product (when looking at the final amount coupled), more efficient ways of incorporating CPP's into polyplexes are actively being pursuit. In combination with the laborious (both time and cost) synthesis of these compounds, alternative integration strategies are continuously explored. Since CPP's act as delivery systems as well[47], the use of physically mixing polymer and CPP was put forward in an attempt to avoid coupling steps and to exploit the most efficient delivery system. In this way, the amount of CPP required, can be decreased while still preserving the considerable advantage of cell-internalising benefit[35] whereas the cell-specificity of CPP's can be enhanced by combining with a polymeric vector.

The outcome of this optimised procedure can be assessed on both a physico-chemical and biological level. The latter will be discussed in the next chapter while the consequences related to polyplex formation were interpreted via EtBr fluorescence and gel-electrophoresis shown below (Fig. 5.24-25).

The result of physically mixing a CPP (e.g. penetratine) with a vector rather than coupling it, has a limited significance on the ability to condense DNA. It can be interpreted from figure 5.24 that a small shift in CR (≈ 0.4 units) represents the need for a higher amount of vector (required for full condensation) if the polymer is covalently coupled. The quality of interaction seems nearly unaffected as derived from the fluorescence at full condensation. This implies that the interaction between CPP-coupled polymer and DNA is slightly hampered and can only be the result of changes in orientation or sterical limitation of the cationic charges since both pure penetratine and pure p(DMAEG-AEG) display full condensation at lower CR's.

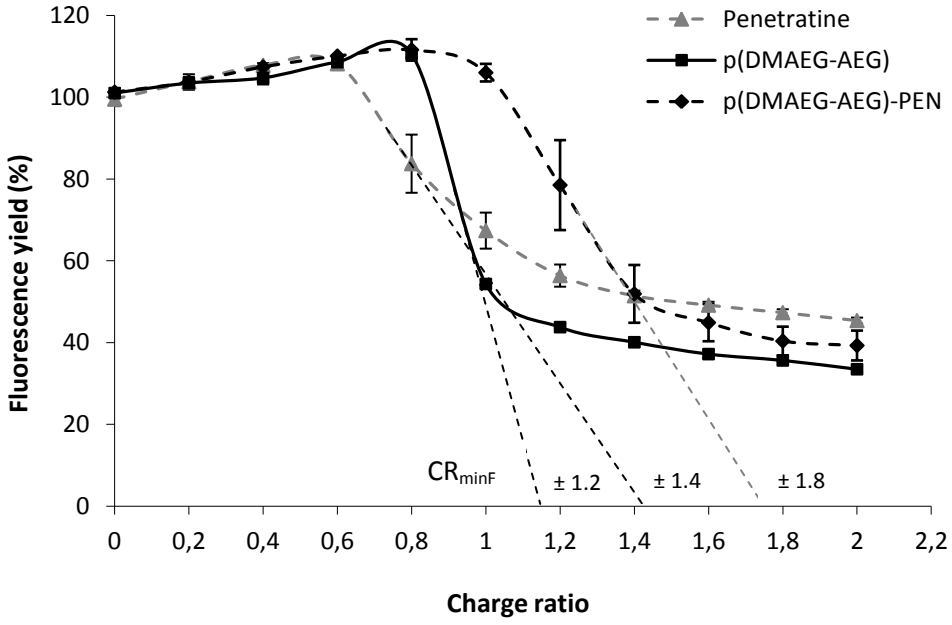


**Figure 5.24 - EtBr Fluorescence yield as a function of increasing CR for polyplexes derived from penetratine, p(DMAEG$_{85\%}$-AEG$_{15\%}$) and penetratine coupled to p(DMAEG$_{85\%}$-AEG$_{15\%}$).**

This assumption was confirmed by means of agarose gel-electrophoresis. Physical mixing of penetratine and p(DMAEG$_{85\%}$-AEG$_{15\%}$) 91 kDa (Fig 5.25 - B) results in similar retardation assays as their individual components (A & D) whereas covalently coupled p(DMAEG-AEG)-PEN (C) requires a higher CR for full condensation (≈ 0.4 CR units). A similar effect is to be expected for polymers coupled with another CPP, i.e. octa-arginine (E).

With respect to the biological data that will be presented in chapter 6, a procedure based on physically mixing of a CPP within a polyplex could lead to a more efficient way of producing gene delivery devices since complexation can occur at lower CR which results in less reagent consumed. Given the limited amount of CPP that can be covalently coupled to polymer carriers, this method enables also the incorporation of relative higher amounts of CPP, a condition that was proven to be more efficient in obtaining stronger polyplexes.

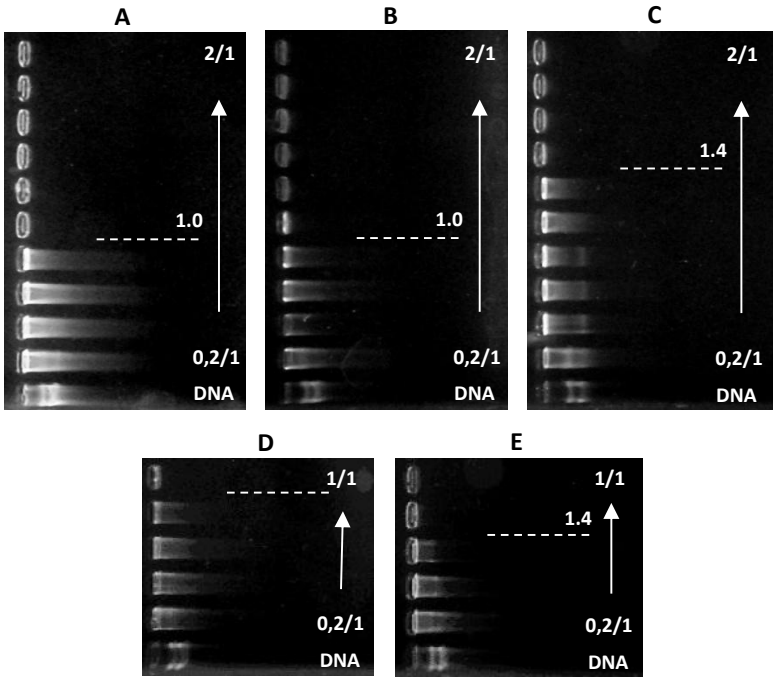


**Figure 5.25 – Gel-electrophoresis images of p(DMAEG$_{85\%}$-AEG$_{15\%}$) (A); physically mixed PEN & p(DMAEG$_{85\%}$-AEG$_{15\%}$) (B); p(DMAEG-AEG)-PEN (C); Penetratine (D) and Arg$_8$ (E).**

## 5 Conclusion

Based on the results of this chapter, it can be concluded that modification of the final polymers with small molecules or peptides can be performed using different coupling strategies. The effect of the coupling can in most cases already be observed at low coupling degrees (e.g. 1-5%) which is a necessity for certain charged peptides as it was proven difficult to reach coupling degrees higher than 5%. The interaction with DNA on the other hand is slightly decreased compared to non-coupled polymers and was the result of charge shielding or the overall increase of the mass/charge ratio. Because of that the CR for full condensation is higher, which is a disadvantage in terms of cell viability. Also the zeta-potential and the size distributions experienced minor changes. Other characterisation techniques were presented in this chapter, on one hand as valid alternative to the standard methods for assessing interaction with DNA (such as FCS) and on the other hand as a useful tool for mapping the interaction of polymers and polyplexes with the cell membrane (impedance), although additional methods are required for confirming the obtained results. Furthermore, physically mixing of CPP's with polyplexes was validated as an improved way of incorporating CPP's into polyplexes without loss of DNA-interaction ability.

# 6 References


[1] Hajitou, A., M. Trepel, et al. (2006). "A Hybrid Vector for Ligand-Directed Tumor Targeting and Molecular Imaging." Cell **125**(2): 385-398.

[2] Vert, M. (2007). "Polymeric biomaterials: Strategies of the past vs. strategies of the future." Progress in Polymer Science **32**(8-9): 755-761

[3] Vert, M. (2006). "Biorelated polymers: biodegradation, bioactivity and biomedical therapeutic applications." Actualite Chimique: 36-39.

[4] Pierschbacher, M. D. and E. Ruoslahti (1984). "CELL ATTACHMENT ACTIVITY OF FIBRONECTIN CAN BE DUPLICATED BY SMALL SYNTHETIC FRAGMENTS OF THE MOLECULE." Nature **309**(5963): 30-33.

[5] Dijkgraaf, I., J. A. W. Kruijtzer, et al. (2007). "Improved targeting of the alpha(v)beta(3) integrin by multimerisation of RGD peptides." European Journal of Nuclear Medicine and Molecular Imaging **34**(2): 267-273.

[6] Wadhwa, M. S., W. T. Collard, et al. (1997). "Peptide-mediated gene delivery: Influence of peptide structure on gene expression." Bioconjugate Chemistry **8**(1): 81-88.

[7] Vaysse, L. and B. Arveiler (2000). "Transfection using synthetic peptides: comparison of three DNA-compacting peptides and effect of centrifugation." Biochimica Et Biophysica Acta-General Subjects **1474**(2): 244-250.

[8] Brasseur, R. and G. Divita. (2010). "Happy birthday cell penetrating peptides: Already 20 years." Biochimica Et Biophysica Acta-Biomembranes **1798**(12): 2177-2181.

[9] Chugh, A., F. Eudes, et al. (2010). "Cell-Penetrating Peptides: Nanocarrier for Macromolecule Delivery in Living Cells." Iubmb Life **62**(3): 183-193.

[10] Brooks, N. A., D. S. Pouniotis, et al. (2010). "Cell-penetrating peptides: Application in vaccine delivery." Biochimica et Biophysica Acta (BBA) - Reviews on Cancer **1805**(1): 25-34.

[11] El-Andaloussi, S., T. Holm, et al. (2005). "Cell-penetrating peptides: Mechanisms and applications." Current Pharmaceutical Design **11**(28): 3597-3611.

[12] Heitz, F., M. C. Morris, et al. (2009). "Twenty years of cell-penetrating peptides: from molecular mechanisms to therapeutics." British Journal of Pharmacology **157**(2): 195-206.

[13] Patel, L. N., J. L. Zaro, et al. (2007). "Cell penetrating peptides: Intracellular pathways and pharmaceutical perspectives." Pharmaceutical Research **24**: 1977-1992.

[14] Foerg, C. and H. P. Merkle (2008). "On the biomedical promise of cell penetrating peptides: Limits versus prospects." Journal of Pharmaceutical Sciences **97**(1): 144-162.

[15] Eguchi, A. and S. F. Dowdy (2009). "siRNA delivery using peptide transduction domains." Trends in Pharmacological Sciences **30**(7): 341-345.

[16] Gros, E., S. Deshayes, et al. (2006). "A non-covalent peptide-based strategy for protein and peptide nucleic acid transduction." Biochimica Et Biophysica Acta-Biomembranes **1758**(3): 384-393.

[17] El-Andaloussi, S., P. Jarver, et al. (2007). "Cargo-dependent cytotoxicity and delivery efficacy of cell-penetrating peptides: a comparative study." Biochemical Journal **407**: 285-292.

[18] Hassane, F. S., A. F. Saleh, et al. (2009). "Cell penetrating peptides: overview and applications to the delivery of oligonucleotides." Cellular and Molecular Life Sciences **67**(5): 715-726.

[19] Joliot, A. and A. Prochiantz (2004). "Transduction peptides: from technology to physiology." Nat Cell Biol **6**(3): 189-196.

[20] Scheller, A., J. Oehlke, et al. (1999). "Structural requirements for cellular uptake of alpha-helical amphipathic peptides." Journal of Peptide Science **5**(4): 185-194.

[21] Min, S. H., D. C. Lee, et al. (2006). "A composite gene delivery system consisting of polyethylenimine and an amphipathic peptide KALA." Journal of Gene Medicine **8**(12): 1425-1434.

[22] Kurz, S. M., S. S. Diebold, et al. (2002). "The impact of c-met/scatter factor receptor on dendritic cell migration." European Journal of Immunology **32**(7): 1832-1838.

[23] Chen, C.-p., J.-s. Kim, et al. (2007). "Synthetic PEGylated Glycoproteins and Their Utility in Gene Delivery." Bioconjugate Chemistry **18**(2): 371-378.

[24] Taniguchi, H., E. Yamato, et al. (2003). "[beta]-cell neogenesis induced by adenovirus-mediated gene delivery of transcription factor pdx-1 into mouse pancreas." Gene Ther **10**(1): 15-23.

[25] Kircheis, R., L. Wightman, et al. (2001). "Design and gene delivery activity of modified polyethylenimines." Advanced Drug Delivery Reviews **53**(3): 341-358.

[26] Vinogradov, S., E. Batrakova, et al. (1999). "Poly(ethylene glycol)-polyethyleneimine NanoGel (TM) particles: novel drug delivery systems for antisense oligonucleotides." Colloids and Surfaces B-Biointerfaces **16**(1-4): 291-304.

[27] Dubruel, P. and E. H. Schacht (2000). "Effect of polyethylene oxide blocks or grafts on the physicochemical properties of poly(2-N-(dimethylaminoethyl) methacrylate) DNA complexes." Journal of Bioactive and Compatible Polymers **15**(4): 279-296.

[28] Nielsen, P. E. (2010). "Gene Targeting and Expression Modulation by Peptide Nucleic Acids (PNA)." Current Pharmaceutical Design **16**(28): 3118-3123.

[29] Lorenz, S., C. P. Hauser, et al. (2010). "The Softer and More Hydrophobic the Better: Influence of the Side Chain of Polymethacrylate Nanoparticles for Cellular Uptake." Macromolecular Bioscience **10**(9): 1034-1042.

[30] Khalil, I. A., S. Futaki, et al. (2004). "Mechanism of improved gene transfer by the N-terminal stearylation of octaarginine: enhanced cellular association by hydrophobic core formation." Gene Therapy **11**(7): 636-644.

[31] Liu, Z., Z. Zhang, et al. (2010). "Hydrophobic modifications of cationic polymers for gene delivery." Progress in Polymer Science **35**(9): 1144-1162.

[32] Futaki, S. (2002). "Arginine-rich peptides: potential for intracellular delivery of macromolecules and the mystery of the translocation mechanisms." International Journal of Pharmaceutics **245**(1-2): 1-7.

[33] Wilson, T. and D. K. Hamilton (1984). "DIFFERENCE CONFOCAL SCANNING MICROSCOPY." Optica Acta **31**(4): 453-465.

[34] Forster, T. (1957). "MOLECULAR ELECTRONIC SPECTROSCOPY." Annual Review of Physical Chemistry **8**: 331-352.

[35] Van Rompaey, E., Y. Engelborghs, et al. (2001). "Interactions Between Oligonucleotides and Cationic Polymers Investigated by fluorescence Correlation Spectroscopy." Pharmaceutical Research **18**(7): 928-936.

[36] Järver, P. and Ü. Langel (2006). "Cell-penetrating peptides--A brief introduction." Biochimica et Biophysica Acta (BBA) - Biomembranes **1758**(3): 260-263.

[37] Torchilin, V. P. (2008). "Tat peptide-mediated intracellular delivery of pharmaceutical nanocarriers." Advanced Drug Delivery Reviews **60**(4-5): 548-558.

[38] Mäe, M. and Ü. Langel (2006). "Cell-penetrating peptides as vectors for peptide, protein and oligonucleotide delivery." Current Opinion in Pharmacology **6**(5): 509-514.

[39] Nori, A. and J. Kopecek (2005). "Intracellular targeting of polymer-bound drugs for cancer chemotherapy." Advanced Drug Delivery Reviews **57**(4): 609-636.

[40] Greg T. Hermanson (2008), Bioconjugate Techniques, Second edition, Elsevier Inc.

[41] Kitagawa, T., T. Shimozono, et al. (1981). "PREPARATION AND CHARACTERIZATION OF HETERO-BIFUNCTIONAL CROSS-LINKING REAGENTS FOR PROTEIN MODIFICATIONS." Chemical & Pharmaceutical Bulletin **29**(4): 1130-1135.

[42] Smyth D. G. (1964). “Reactions of N-ethylmaleimide with peptides and amino acids.” Journal of Biochemistry **91**: 491

[43] Tatsumi, E. and M. Hirose (1997). "Highly ordered molten globule-like state of ovalbumin at acidic pH: Native-like fragmentation by protease and selective modification of Cys367 with dithiodipyridine." Journal of Biochemistry **122**(2): 300-308.

[44] Ye, Z. Y., H. Y. Zhang, et al. (2008). "Temperature and pH effects on biophysical and morphological properties of self-assembling peptide RADA16-1." Journal of Peptide Science **14**(2): 152-162.

[45] Cho, S. B. and H. Thielecke (2007). "Micro hole-based cell chip with impedance spectroscopy." Biosensors & Bioelectronics **22**(8): 1764-1768.

[46] Vives, E. (2005). "Present and future of cell-penetrating peptide mediated delivery systems: "Is the Trojan horse too wild to go only to Troy?"." Journal of Controlled Release **109**(1-3): 77-85.

[47] van Rossenberg, S. M. W., A. C. I. van Keulen, et al. (2004). "Stable polyplexes based on arginine-containing oligopeptides for in vivo gene delivery." Gene Therapy **11**(5): 457-464.

# Chapter 6

# Biological evaluation of polymer-DNA complexes

# 1 Introduction

Since the ultimate goal of gene therapy is the introduction of a gene of interest into cells and enable the subsequent expression of this particular gene inside the cell, the possible effect of the carrier system onto processes that assist in realising the corresponding protein expression needs to be investigated. An ideal way of delivering polyplexes to cells comprises of intravenous administration (*in vivo*) and calls for the evaluation of the interaction between (charged) polyplexes or polymers and blood components. Besides red blood cells (RBC) which is the most abundant substance in the blood, also the presence of enzymes degrading the DNA, the polymer or both should be taken into account when describing the biocompatibility of a polymer. The presence of polyplexes inside the bloodstream can mutually affect each other with complex disruption or alteration of the blood composition (morphology or lysis) as a consequence.

In general, issues that are related to global toxicity on a cellular level are interpreted by measuring specific characteristics like metabolic activity (MTT test) or cell membrane integrity (dye exclusion assays) of healthy cells. Furthermore, it is equally important to check whether a polymer can be removed from the body after its task as a delivery system was executed. With respect to the natural degrading mechanisms of the cell (lysosomes), polymers need to be subjected to a degradation test that simulates the internal composition of lysosomes, the waste disposal entities within cells.

Ultimately, the performance of delivery systems for gene therapy applications is assessed by measuring the result of its genetic function. Despite the numerous genetic effects that are targeted in gene therapy, the mechanism to obtain therapeutic correction of pathologic conditions via DNA is universal, that is the transcription of a genetic sequence and production of a protein. Therefore, standard transfection experiments were developed that make use of a typical reporter gene that encodes for a chemical structure which can easily be detected (e.g. a physical constant like fluorescence yield). In this part of the work, several chemical and biological tests are performed to acquire more information on the biocompatibility of the polymers and their corresponding polyplex. In a first approach, the use of *in-vitro* vectors is screened to check the activity and the possibility to exploit the potential as a delivery device even further, as for instance by in-vivo relevant experiments.

## 2 Efficiency of polyplexes as *in-vitro* gene delivery systems

### 2.1 Principle of cell toxicity - viability

For gene therapy to play a leading role in advanced disease and illness control, the use of it must result in a proper and efficient solution with minimal side-effects for the patient. Because of that, the use of gene carriers that will aid in the delivery of the 'curing agent' (e.g. therapeutic DNA), should not inflict additional discomfort. On a more basic level, this is expressed as cellular damage in which for instance the production of proteins or the capacity to continue to divide is negatively altered. It is therefore possible to examine the influence of polymer carriers and polyplexes on cells by subjecting them to *in-vitro* cell viability tests. Such experiments assess living cells in a sample and this is accomplished by either directly counting the number of living cells (using specialised instruments) or by measuring a corresponding indicator for cellular activity (e.g. an assay). In most cases, decreasing values of cell survival represent the presence of a toxic effect related to the genetic carrier applied. Achieving efficient *in-vitro* transfection is the basis for proceeding with *in-vivo* testing.

Most viability assays are based on one of two characteristic parameters, namely metabolic activity or cell membrane integrity of healthy cells. The metabolic activity is usually measured in cell populations by incubating the cells with a reagent, such as a tetrazolium salt (MTT test – Fig. 6.1), that is converted by metabolic active cells into a compound (insoluble formazan crystals) that is readily detectable by for instance UV/VIS spectroscopy[1]. The second type of assay, also termed dye-exclusion assay, makes use of the ability of healthy cells to exclude dyes (e.g. trypan blue) from penetrating the cellular membrane due to conservation of the structural integrity. As a result, dead cells will be stained with an intensity that is proportional to the mortality rate while healthy cells will remain unstained.

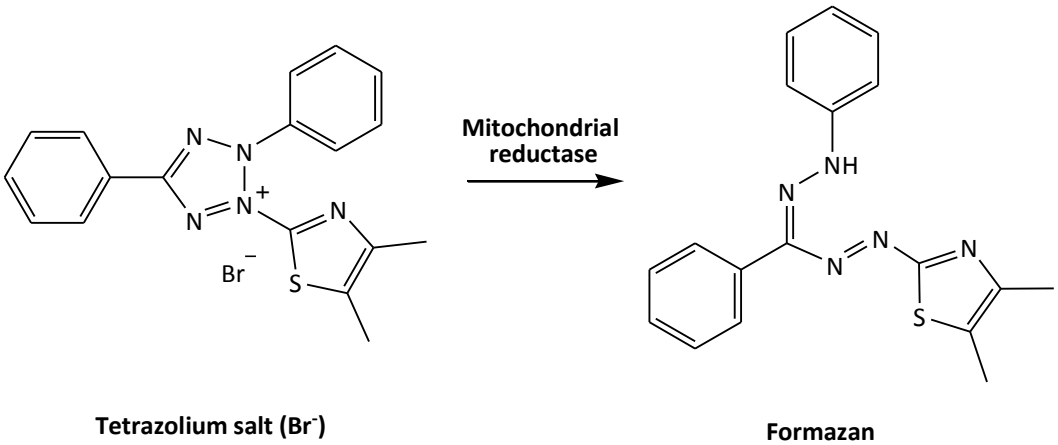


**Figure 6.1 – Reduction process of tetrazolium salt into formazan crystals, catalysed by mitochondrial reductase (MTT test).**

For these *in-vitro* experiments, the UptiBlue assay is performed. UptiBlue (resazurin) consists of a redox indicator that fluoresces and changes color in response to cell growth (Fig. 6.2). As cells under investigation grow, the innate metabolic activity causes a chemical reduction of UptiBlue which causes the indicator to change from an oxidised, non-fluorescent, blue form to a reduced, fluorescent, red state[2]. This indicator was preferred above the classic MTT assay because of several reasons. Firstly, the indicator exhibits both fluorescence and colorimetric behaviour, allowing intra-cellular visualisation before and after substrate conversion by spectrofluorimetry or regular spectroscopy. Also, the required irradiation corresponds with traditional wavelengths. Furthermore, this compound is minimally toxic to living cells, has a long-term stability and is water soluble which eliminates the need for complex extractions (like for formazan crystals).

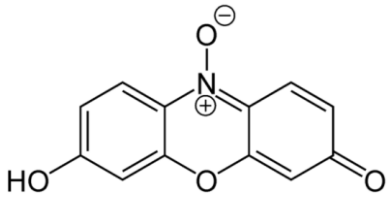


**Figure 6.2 – Chemical structure of resazurin (Uptiblue).**

Practically, cell viability tests are often carried out in combination with transfection experiments. After the cells were conditioned for transfection and incubated with genetic material by means of a vector with a specific CR (see experimental section), the uptiblue product is added (10% v/v) and left for incubation at 37 °C in an atmosphere containing 5 % $CO_2$ for about 2 hours. Following incubation, the excitation/emission can be measured for all the samples including a positive (Triton X-100) and negative (non-transfected cells in buffer, no vector-DNA added) control set to 0 and 100% viability respectively.

## 2.2 Transfection efficiency: protein production of modified DNA

Generally, the ability of genetic vectors to be successful in the elimination of genetic defects with corresponding introduction of specific, therapeutic genes into the core of a cell to cure pathogens or diseases, is assessed by *in-vitro* testing using plasmid models. Most plasmid models use specific cell-lines and standardized protocols in combination with modified DNA that encodes for easy-detectable proteins to produce reliable and reproducible results. The total transfection process or efficiency of a (polymeric) vector comprises of cell incubation (in buffer medium) with polyplexes. The subsequent uptake in the cell and introduction of the genetic material in the cell-core enables it to be used for replication and protein synthesis. Traditional assays applied for these kind of tests normally give an indication of the last step

(protein production) by providing modified DNA that encodes for proteins that can be detected via (VIS light) spectrometry. Unfortunately, when the total process of uptake, cellular trafficking and protein expression is for any reason disturbed, no signal can be measured. To partially resolve this disadvantage, confocal microscopy was adopted as an extra analytical technique that could shed light on the intra-cellular transfection process (section 6).

For the following transfection tests, the activity of polyplexes was measured quantitatively and qualitatively by a Renilla Luciferase based assay. These experiments were carried out in the framework of the PolExGene project by Dr. Alain Joliot and Dr. L. Tibaldi (Laboratory for Homeoprotein Cell Research, Collége De France, Paris, France). Renilla Luciferase (ReLu) is an enzyme (36 kDa) isolated from the marine sea anemone (anthozoa) Renilla Reniformis. The substrate on which ReLu can act, luciferine (coelenterazine), can oxidize into coelenteramide by emitting light and $CO_2$ when doing so (Fig. 6.3). Specific for this type of luciferase, is the close association with a green fluorescent protein (GFP) and a luciferine-bound protein (which is partially protected). The addition of calcium can readily allow decoupling of this protective protein and make the luciferine available for oxidation. Furthermore, the (blue) light that is normally emitted when oxidized is now coupled to the fluorophore of GFP through resonance energy transfer for corresponding release of a photon with a peak value of about 510 nm (green). When no catalyst (luciferase enzyme) is used, this reaction is nearly unexisting. The enzyme does not require post-translational modification for its activity and may perform its function immediately following translation[3].

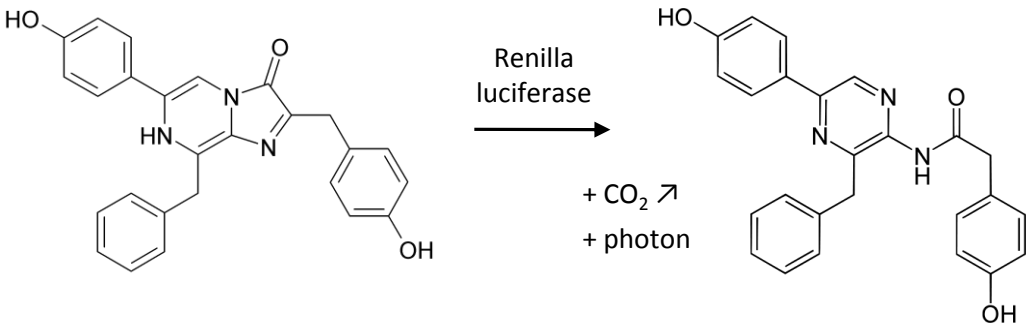


**Figure 6.3 - Renilla Luciferase oxidation process with corresponding emission of light.**

By introducing the PcRUCHA plasmid, encoding for luciferase, into the cells by means of a polymeric vector, the transfection efficiency of these vectors can be obtained quantitatively. Only cells which are able to express luciferase will be capable of converting coelenterazine and yield the corresponding emission of light.

Experimental transfection tests are always combined with viability tests to minimize the laborious cell preparation. The measurement of cell transfection continues with the cells utilized for the uptiblue assay. Firstly the supernatant is removed and passive lysis buffer (PLB – Promega) is added to each well and left on a plate shaker to induce lysis of the cells so that the luciferase is released into the medium. Additionally, the cells are subjected to a freezing (-80 °C)/thawing (37 °C) cycle to ensure complete lysis. The coelenterazine substrate is added automatically inside the luminometer and the resulting luminescence is measured for 10 seconds with a delay of 2 seconds between injection and measurement (maximum photon peak a couple seconds past enzyme-substrate mixture). The transfection efficiency is expressed in relative luciferase units (RLU) and therefore it's necessary to compare the results with a reference compound (PEI). Furthermore, in the case of weak signals a background correction is carried out for the luminescence signal of the cells.

## 2.3 Results

### *2.3.1 PEI & CPP-coupled PEI-derivatives*

The development of new vector-based delivery systems requires a full evaluation and a corresponding classification system in order to decide if its use can be promising for continued research. Since the use of cell lines for *in-vitro* research applications is very extensive and the combinations of cell types and protocols are numerous, most experiments make use of a reference polymer that is widespread and who's properties are well known. Via this reference compound, it is possible to compare different candidates in variable batches mutually and compared to the reference polymer (PEI), even when not always displayed in certain graphs. Therefore it is important to test the transfection and toxicity of the reference compound prior to evaluation of new candidates. Furthermore, modifications of this polymer were also carried out and compared accordingly.

It is important to stress that no values are given for the y-axis because of the relative nature of the experiment. Also, due to considerable variation that exists for the standard testing methods (sensitive behaviour of cells), the obtained results can differ strongly per test, hence the high standard deviations observed. A summary of all active components, reported in the following results and graphs is compiled at the end to allow comparison mutually and with PEI (Fig. 6.20).

The results for PEI, PEI coupled to Oregon Green (PEI-OREG) and PEI coupled to CPP's like penetratine or arginine$_8$ (PEI-PEN & PEI-ARG$_8$) are displayed in figures 6.4-6.5. Since polyplexes composed of PEI give rise to substantial toxicity, these parameters are often not tested at CR's above 2/1. While the viability of PEI steadily decreases with increasing CR,

the effect of coupling a molecule appears to keep cells viable at higher CR. On the other hand, the efficiency of the PEI-derivatives seems not to influence transfection significantly (except for PEI-ARG which can maximally reach half the efficiency of regular PEI). The maximum values that were obtained are nearly equal for the modified compound but they are only reached at higher CR's compared to native PEI. This suggests also the importance of the condensation value and the corresponding impact on molecular structure. The coupled molecules are expected to arrange in a more or less surrounding way around the PEI backbone and accordingly shield the cationic charge. Fortunately, the resulting shielding effect lowers the toxic nature of the polymer, hence the increased viability values.

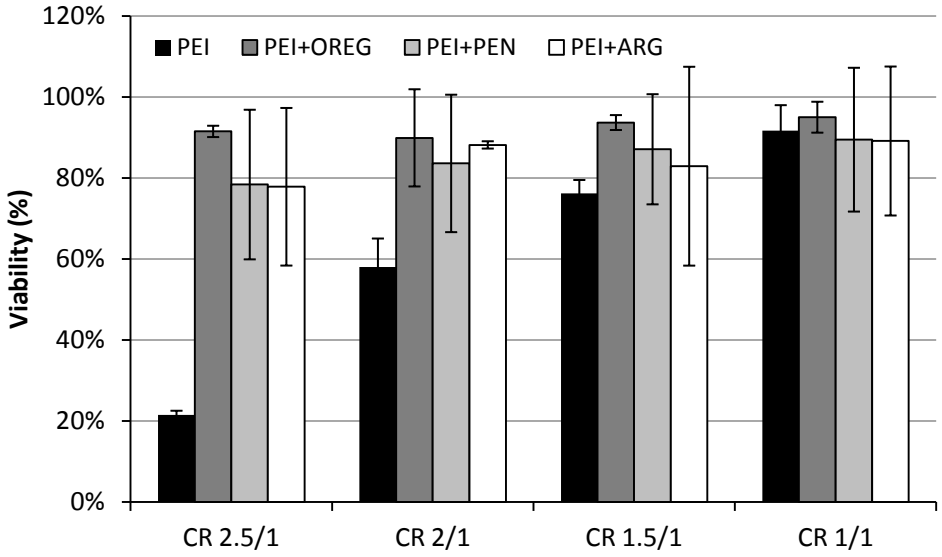


**Figure 6.4 – Toxicity of cells incubated with polyplexes at variable CR.**

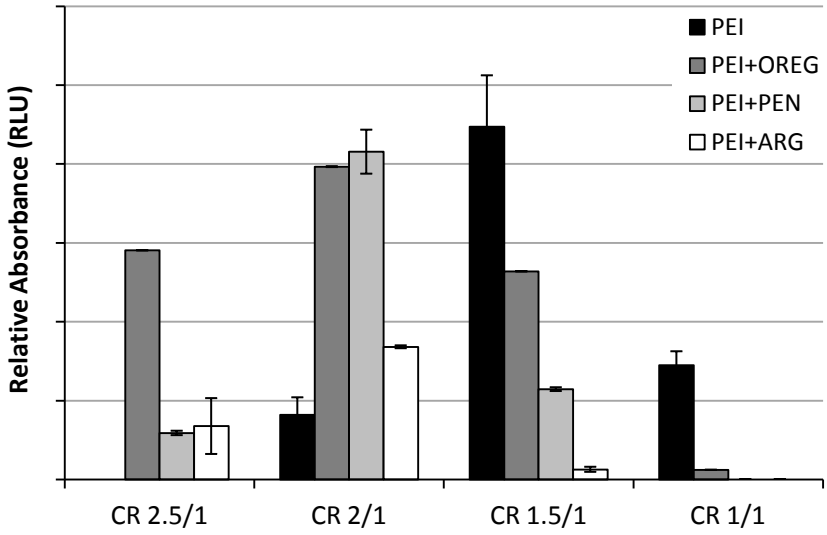


**Figure 6.5 - Transfection efficiency of PEI & PEI-derivatives on ARPE19 cells (24 h).**

### *2.3.2 Vector efficiency of poly-L-glutamines*

Because of the biocompatibility related to using protein-like biodegradable polymers as genetic vectors, the potential of poly-L-glutamine derivatives is high. As was mentioned before, a whole range of compounds with different MW and functional groups was prepared and characterised in terms of physico-chemical properties. Ultimately, these products need to be able to efficiently and safely deliver genetic material to the cell. The first series of polymers tested, were based on pDMAEG. Next to the influence of the MW also the coupling of a cell-penetrating peptide was checked and mutually compared (Fig. 6.6 & 6.7). When looking at toxicity, it is clear that this polymer exhibits a very high biocompatibility with limited to no effect on cell survival when applied as vector. Influence of the MW is hardly visible (the lowest value is reached for the highest MW compound at 4/1 CR) and also the difference in CR has no clear effect on the viability. If a peptide was coupled to the polymer, again limited changes were observed, especially for the peptide penetratine (pDMAEG 80 kDa + PEN = 80k+P, similar for 242k+P). In the case of $Arg_8$ coupling (pDMAEG 242k + $Arg_8$ = 242k+A), the resulting decrease was significant, especially with increasing CR and a corresponding higher amount of $Arg_8$ present in the polyplexes.

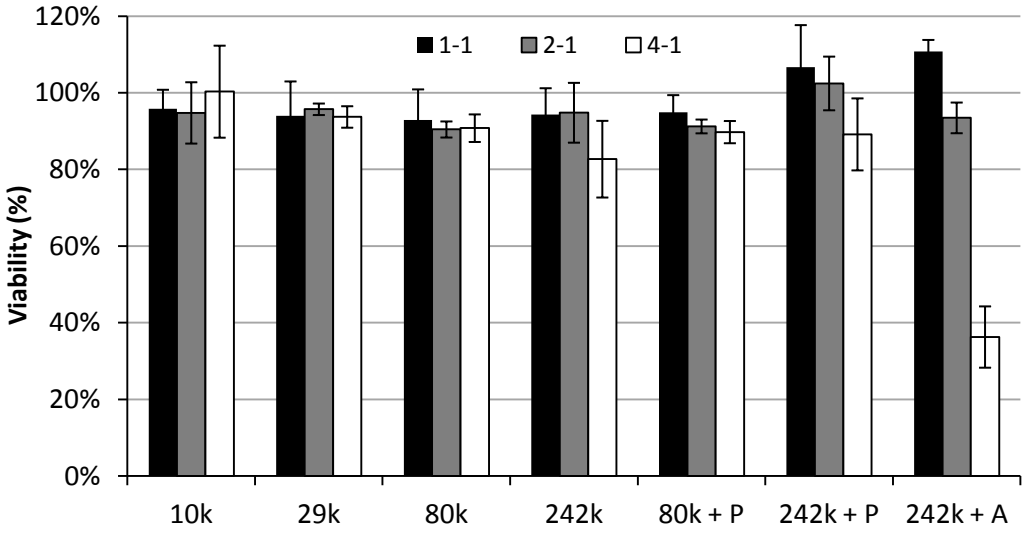


**Figure 6.6 – Toxicity results of cells incubated with polyplexes based on pDMAEG with a variable MW and CPP-coupled pDMAEG 80 kDa & 242 kDa at variable CR (P = PEN, A = $ARG_8$).**

Unfortunately the transfection efficiency of glutamine-containing homopolymers proved to be virtually zero (Fig. 6.7). If focus was put on the different pDMAEG, a higher MW seemed to be responsible for increasing efficiency. Nevertheless, compared to PEI, the efficiency remained < 1% at all times (see Fig. 6.20). Moreover, polyplexes with a higher CR were more active than those composed of a low CR. Strangely, the coupling of penetratine to the

polymer caused a (small) decrease in activity rather than an augmentation. The opposite result was achieved for $Arg_8$ coupled pDMAEG (242+A) where transfection efficiencies were reached that exceeded the pure homopolymer by 10-fold as was anticipated from literature. In contrast, while this compound produces the better efficiency, also the highest degree of toxicity was detected which confirms again the difficult nature of an optimised vector.

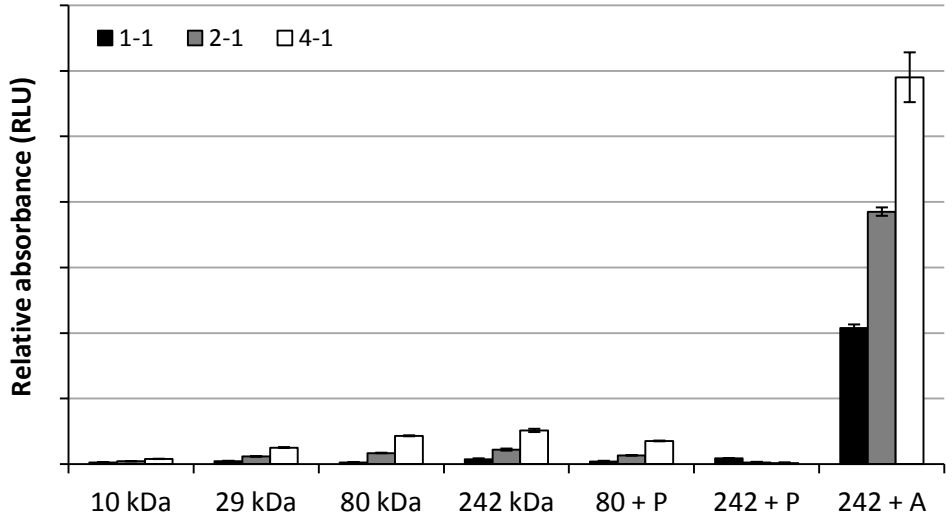


**Figure 6.7 - Transfection efficiency of pDMAEG with a variable MW and CPP-coupled pDMAEG 80 kDa & 242 kDa at variable CR (P = PEN, A = $Arg_8$) on ARPE19 cells (24 h).**

For other polyglutamine derivatives, the toxicity and degree of efficiency was likewise evaluated. In figure 6.8, the cell viability of p(HEG-GuAEG) compounds is shown and compared to PEI. Again, very high survival rates were displayed (nearly 100%). Importantly, the effect of an increasing amount of guanidine did not cause higher toxicity unlike the previous result (pDMAEG+$Arg_8$) where the introduction of arginine (and guanidine) residues had a negative impact on toxicity. Additionally, the variation in polyplex CR appeared as a rather irrelevant factor. Finally also an increase in MW for polymers with similar composition kept the overall viability quite constant.

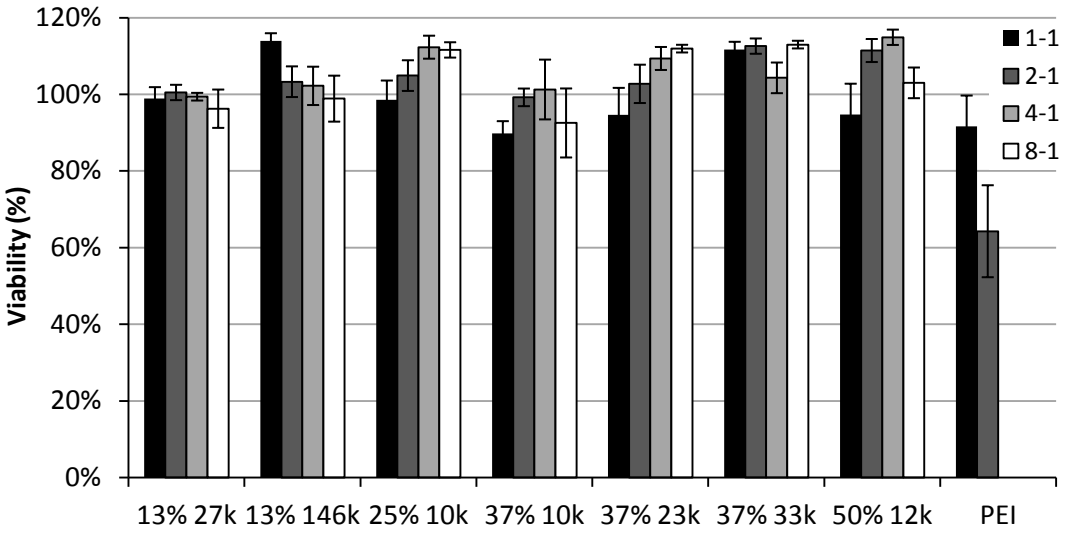


**Figure 6.8 - Toxicity results of cells incubated with polyplexes based on p($HEG_{x\%}$-$GuAEG_{y\%}$) indicated by the % of GuAEG and the MW (in kDa).**

Based on the transfection results (Fig. 6.8), only one p(HEG-GuAEG) composition was revealed as potential vector. It is remarkable that only this specific structure (37% guanidine, 10 kDa) induced a high transfection efficiency outperforming even PEI. Because it was previously demonstrated that the ability to form complexes increased with a higher amount of guanidine functional groups, a continuation of high transfection efficiency was to be expected for compounds with more than 37% guandines but this was not confirmed. The reduced efficiency of p($HEG_{63\%}$-$GuAEG_{37\%}$) with a MW of 23 kDa on the other hand more or less confirms that this specific composition is succesfull in transfection. This suggests on one hand that sufficiently charged functional groups need to be present to obtain well-defined, stable polyplexes with optimal cell interaction but on the other hand reveals that charge density cannot be too high because hampered polyplex dissociation leads to inactivity. Ultimately this resulted in the survival of one optimal structure. Furthermore, activity was only detected at high CR's which in most cases implies an augmented risk of toxicity due to the increased polymer concentration but with limited effect due to the excellent biocompatibility.

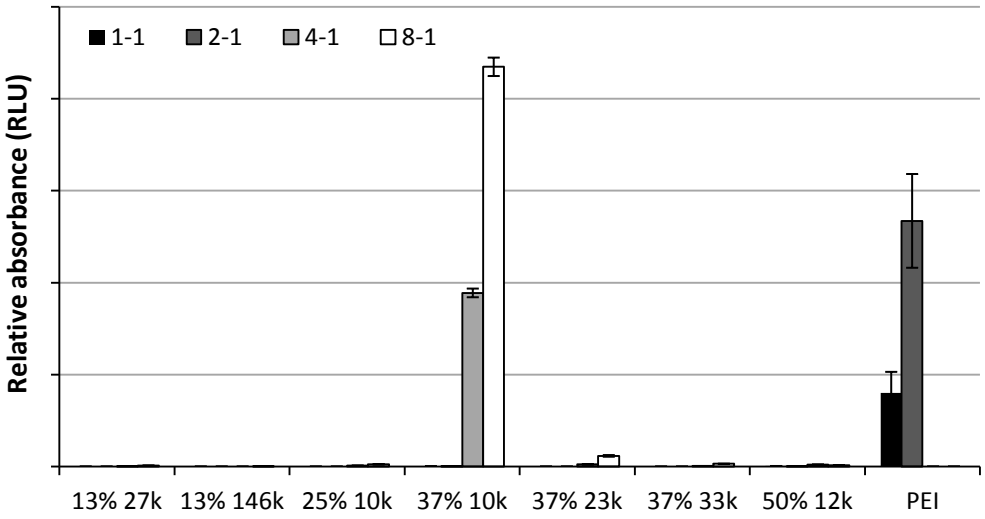


**Figure 6.9 - Transfection efficiency on ARPE19 cells (24 h) of p($HEG_{x\%}$-$GuAEG_{y\%}$) as a function of the % of GuAEG and the MW (in kDa).**

As was explained during the introduction, the conclusions above confirm the potential of guanidine (and to a certain extent, arginine residues) as a powerful modification to enhance transfection activity compared to other cationic functional groups like amines. Because this type of modified polymers not always results in an optimised efficiency (e.g. PEI+$ARG_8$), the introduction of other functional groups was also checked. Besides different functional groups, homopolymers based on guanidines were also als included in these experiments. The observed toxicity for some imidazole and arginine modified polymers is shown in figure 6.10. As a first, clear observation, the large difference in viability between imidazole-containing polymers (A-C) and the derivatives that possessed arginine residues (D-J) was reported. While the increase in CR had only minor effect on imidazole-based polymers, the viability of the arginine-based vectors drastically decreased at higher CR's, often resulting in complete cell-death. Grafted copolymers (H & I) display a strong reduction in viability compared to the non-grafted base polymer (Fig. 6.8), especially for p($DMAEG_{85\%}$-$AEG_{15\%}$) which has grafted p(ARG) units of about 5.000 Da long. Comparable to the grafting onto PEI, the biological properties largely adopt those of the grafted (co)polymer. The copolymer, p($ARG_{82\%}$-$ORN_{18\%}$) (J) that contains a small percentage of primary amines does not provoke a notable change in toxicity compared to the homopolymer (F), although this small structural difference caused a markedly higher efficiency (Fig. 6.11).

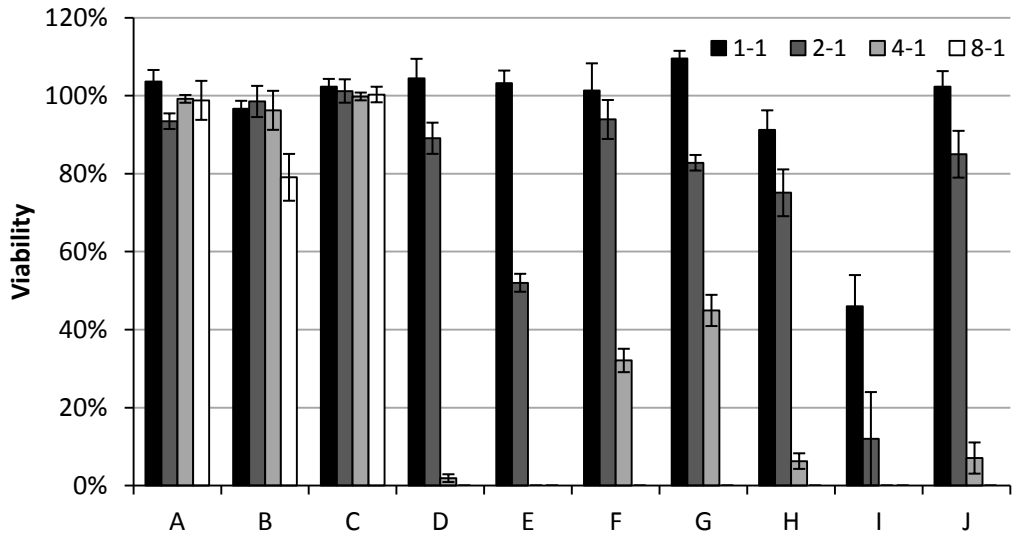


**Figure 6.10 - Toxicity results of cells incubated with polyplexes from various polymers.**

| Code | Polymer | Code | Polymer |
|---|---|---|---|
| A | p($HEG_{49\%}$-$GuAEG_{15\%}$-$ImEG_{36\%}$) 12 kDa | F | p(ARG) 78.8 kDa |
| B | p($GuAEG_{35\%}$-$ImEG_{65\%}$) 13 kDa | G | p(ARG) 187 kDa |
| C | p($HEG_{32\%}$-$GuAEG_{11\%}$-$ImEG_{57\%}$) 9.6 kDa | H | p($HEG_{87\%}$-$AEG_{13\%}$)+pARG 27.7 kDa |
| D | p(ARG) 13 kDa | I | p($DMAEG_{85\%}$-$AEG_{15\%}$)+pARG 91 kDa |
| E | p(ARG) 22.8 kDa | J | p($ARG_{82\%}$-$ORN_{18\%}$) 71.1 kDa |

**Table 6.1 – Corresponding polymer-code for figures 6.10-6.11.**

Similar to p(HEG-GuAEG) derivatives with a high amount of cationic charges, polyarginine does not display considerable transfection activity (Fig. 6.11, D-G). Probably this is the result of an excess of positive charge (100% protonation given the $pK_a$ of guanidine). An enlarged visualization of the transfection efficiency is shown to differentiate between the influence of the different MW's but no conclusion could be derived. In the case of the copolymer p($ARG_{82\%}$-$ORN_{18\%}$) a substantially larger activity was found for a 2/1 CR (compared to p(ARG) with a similar MW). Graft-copolymers, H & I exhibited virtually no efficient transfection behaviour. Synthetic vectors that contain a significant amount of imidazole moieties on the other hand appeared capable of transfecting a many number of cells (also COS cells). Importantly, guanidine functional groups were also present in these polymer structures and the highest activity was again established for the polymer containing about 35% of guanidine functional groups. Since these type of polymers are not fully charged (due to the $pK_a$ of imidazole or the presence of neutral groups), higher ratio's of polymer/DNA are

required to obtain a clear level of transfection. The relative ratio of compounds B and J compared to PEI is shown in figure 6.20.

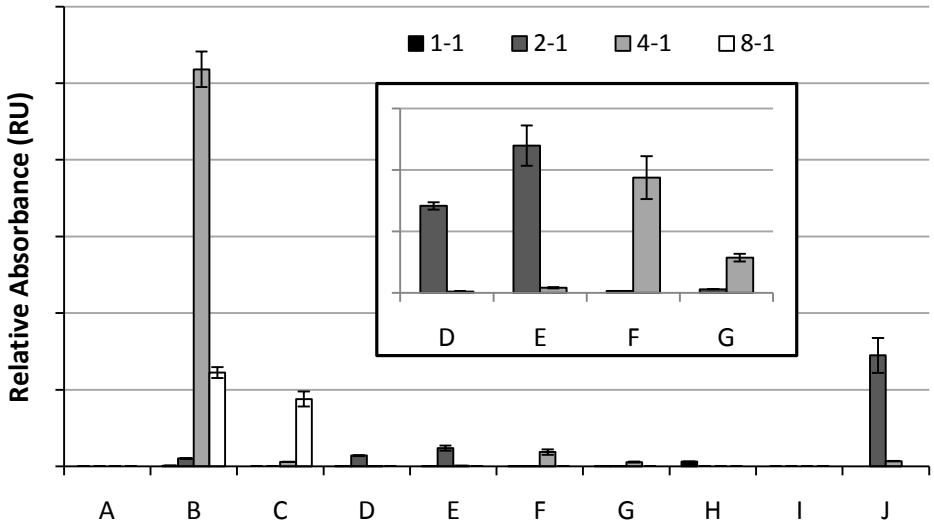


**Figure 6.11 - Transfection efficiency on ARPE19 cells (24 h) of several polymers (table 6.1).**

For certain applications, specific molecules like fluorescent tags or peptides are coupled to polymers. Because the coupling of fluorescent tags brings about an increased level of hydrophobicity within the polymer, the consequent change in transfection activity needs to be examined. Combining polymers with CPP's is generally performed to boost the activity of certain vectors and and figure 6.12 reports on their performance in transfection. The viability tests confirms once more the toxic nature of fully charged guanidine compounds as the PEN labelled p(ARG-ORN) becomes increasingly toxic as the CR rises and the coupling of penetratine even enlarges this negative effect. All other derivatives, mainly p(HEG-AEG) and p(DMAEG-AEG) compounds with small quantities of AEG (< 15%), possess a very high degree of viability at all CR's tested.

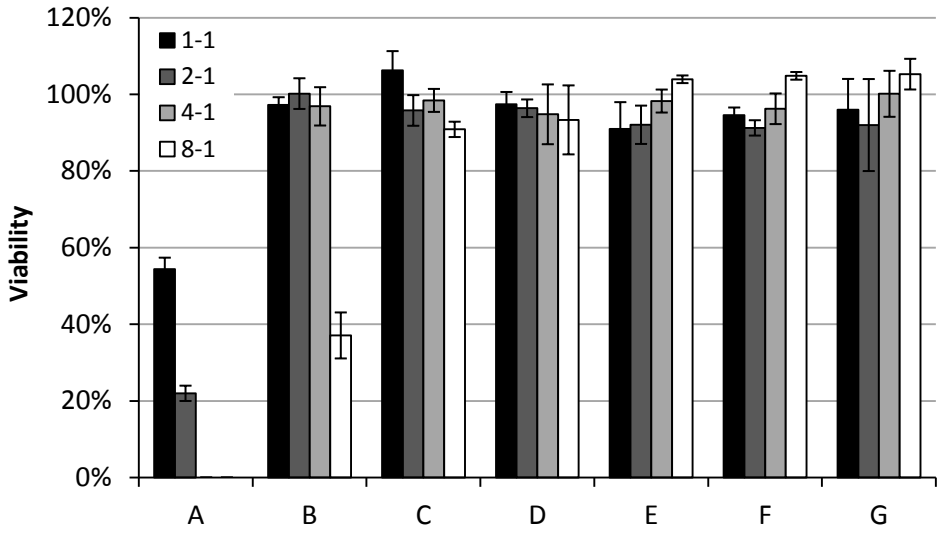


**Figure 6.12 - Toxicity results of cells incubated with polyplexes from various polymers.**

| Code | Polymer | Crosslinker | Coupled agent |
|---|---|---|---|
| A | p(ARG-ORN) 71.1 kDa | GMBS | Penetratine (4 %) |
| B | p(DMAEG-AEG) 91 kDa | SPDP | Penetratine (1.8%) |
| C | p(DMAEG-AEG) 91 kDa + OREG | GMBS | Penetratine (1.9%) |
| D | p(DMAEG-AEG) 91 kDa + OREG | GMBS | $Arginine_8$ (1.2%) |
| E | p(HEG-AEG) 27 kDa | SPDP | Penetratine (3.5%) |
| F | p(DMAEG-AEG) 91 kDa | GMBS | Penetratine (3%) |
| G | p(HEG-AEG) 11 kDa | SPDP | $Arginine_8$ (8 %) |

**Table 6.2 – corresponding polymer-code for figure 6.11-6.12.**

With respect to transfection, the addition of cell penetrating peptides did not provoke the expected transfection enhancement (Fig. 6.13). Penetratine demonstrated no real improvement since only p(ARG-ORN) showed activity but with a reduced intensity compared to the non-coupled polymer. The addition of $Arg_8$ was limitedly successful in the case of p(HEG-AEG) which was best at a high CR. A comparable improvement was seen for the addition of $Arg_8$ to p(DMAEG) with a MW of 242 kDa in figure 6.6. Based on these resultss $Arg_8$ seems to act as the more efficient CPP although its influence was only poor. The comparison between with PEI and p(ARG-ORN) 71.1 kDa is summarized in figure 6.20.

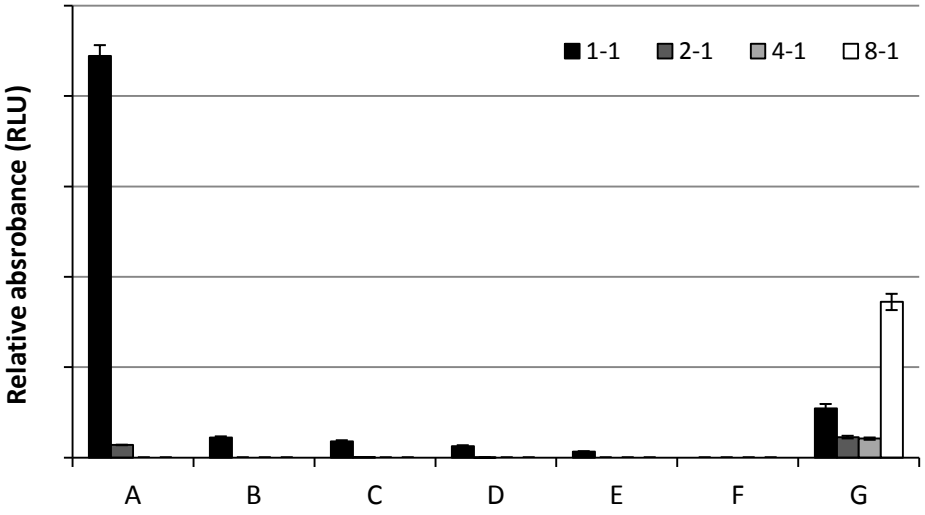


**Figure 6.13 - Transfection efficiency on ARPE19 cells (24 h) of several polymers (table 6.2).**

### *2.3.3 Guanidylated PEI and other reference polymers*

The positive results of certain guanidylated products like p(HEG-GuAEG) and the (partially) beneficiary effect of $Arg_8$ confirmed that the guanidine functional group possesses special, advantageous properties towards biological activity enhancement. This led to the believe that other active polymers could be modified in such a way as to improve their transfection efficiency by introducing guanidine moieties while keeping their toxicity constant. Also the results of other important reference vector systems are shown in this paragraph. The degree of toxicity for guanidylated PEI (B-E) is shown in figure 6.14 (and table 6.3). It is difficult to conclude if modification allows for a statistically improved viability but the conversion reaction definitely did not reduce the toxicity. Only in the case of (PEI-$Guan_{20\%}$)+OREG+PEN, a much lower degree of toxicity was observed.

| Code | Transfection agent | Coupled agent |
|---|---|---|
| A | Lipofectamine 2000 | - |
| B | PEI-$Guanidine_{14\%}$ | - |
| C | PEI-$Guanidine_{20\%}$ | - |
| D | PEI-$Guanidine_{20\%}$ + OREG | Oregon Green 488 (3.7%) |
| E | PEI-$Guanidine_{20\%}$ + OREG + PEN | Oregon Green 488 (3.7%)<br>Penetratine (2 %) |
| F | Poly-L-Lysine 50 kDa | - |

**Table 6.3 – corresponding polymer-code for figure 6.13-6.14.**

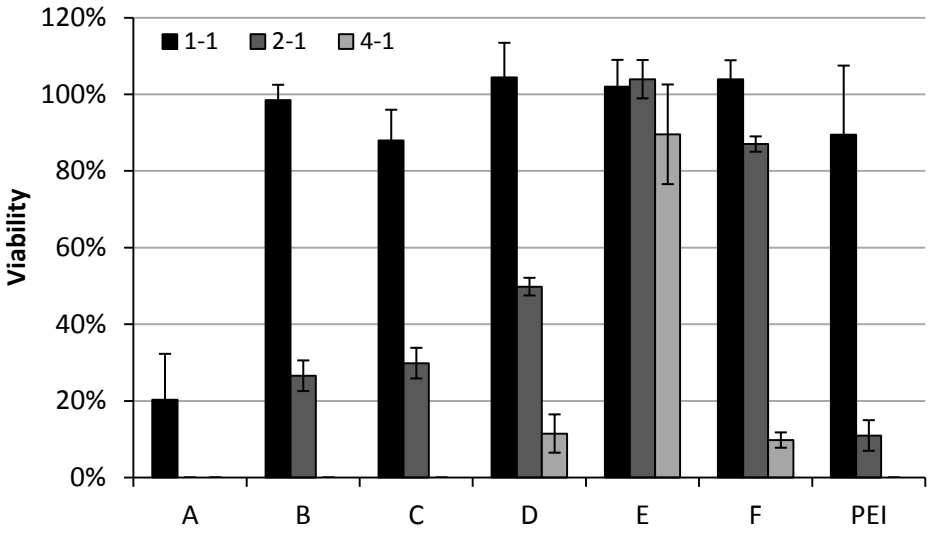


**Figure 6.14 - Toxicity results of cells incubated with various transfection agents (table 6.3).**

Charge ratio's above 2/1 as a result are not advised for PEI-modified compounds. Another widespread polymer that was explored already in the early years of synthetic gene therapy was poly-L-lysine. This homopolymer contains 100% protonable groups (primary amines), hence the limited viability for high CR's. Lipofectamine, another acknowledged transfection agent is a cationic lipid that can achieve extremely high levels of transfection but is linked with strong toxicity as visualised in figure 6.14 – A where one equivalent (1x) of Lipofectamine 2000 was applied and yielded incredible efficiency but with a low survival rate.

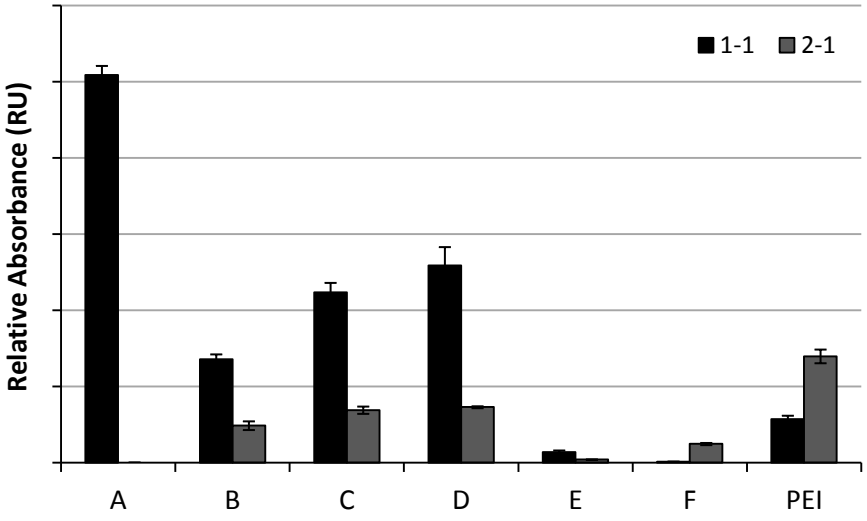


**Figure 6.15 – Transfection efficiency on ARPE19 cells (24 h) of several transfection agents.**

It is clear that lipofectamine achieves the highest transfection levels by far (4x higher than PEI) but also guanidylated PEI seems to enhance the activity (with about 50%) and because of the stronger interaction, this is established at a lower CR than for unmodified PEI. When

Oregon Green was coupled to PEI-Guan$_{20\%}$, the resulting efficiency was even higher and will most-likely be the result of enlarged hydrophobicity, a phenomenon that was already perceived to improve polyplex uptake (and corresponding protein expression). On the other hand, no convincing explanation could be given for the substantial decrease observed for CPP+OREG coupled PEI-Guan$_{20\%}$. The efficiency of PLL confirmed the rather low results shown in literature as well[4].

### *2.3.4 Polymethacrylates*

As alternative strategy to explore synthetic vectors with a high ranking transfection ability that could be applied for direct or non-direct applications in gene therapy, the use of non-biodegradable polymers was assessed and compared to the biodegradable polymers discusses before. Elaborating on previous work by amongst others Hennink et al[5] the use of poly(dimethylaminoethyl)methacrylates (pDMAEMA) and derivatives there-off were selected as delivery systems. By providing these polymers with similar functional groups as for the biodegradable polyglutamines (primary/tertiary amine, hydroxyl and guanidine), it was possible to examine the influence of the type of backbone (hydrophobic versus hydrophilic). The transfection efficiency of all following polyplexes were examined on HEK (Human Endothelial Kidney) 293 cells.

The basic polymer, pDMAEMA, was first analysed as such (homopolymer). The corresponding toxicity results are displayed in figure 6.16 for a series of different MW's. A clear trend in terms of toxicity was observed for high CR's: the viability decreased proportionally with increasing MW. For a low CR (1/1 and to a certain extent also 2/1) this was less the case. The overall viability was lower than for the biodegradable counterpart pDMAEG since a 1/1 CR for pDMAEMA rises in most cases not higher than 80% (except for 11.9 kDa) while for pDMAEG the viability remained above 80% for all CR's and MW tested. The polymer with the largest MW provoked complete cell death at a CR of 8/1 but even this polymer was still able to outperform PEI in terms of viability. Regarding viability, it can be concluded that the lowest MW compounds generate the best results and could to be advised for optimised gene delivery systems.

When looking at the corresponding transfection efficiency (Fig. 6.17), all polymers appear to be active. Moreover, the levels of transfection are similar to PEI. The most active compound is found for the highest MW pDMAEMA because considerable activity is achieved for all CR's whereas for the smaller compounds, transfection efficiency manifests only from high CR's (≥ 4/1) on. Additionally, the viability of this high MW derivative was the lowest, especially for high CR's. As a result, the amount of cells expressing the protein are smaller which means that the polymer should be interpretated as being even more efficient in terms

of activity per viable cell. The highest MW compound also exhibits the highest level of transfection but the difference with smaller compounds (e.g. derivative with a MW of 62.9 kDa at a CR of 4/1) is not that extreme although these results are relative when taking the higher viability into account.

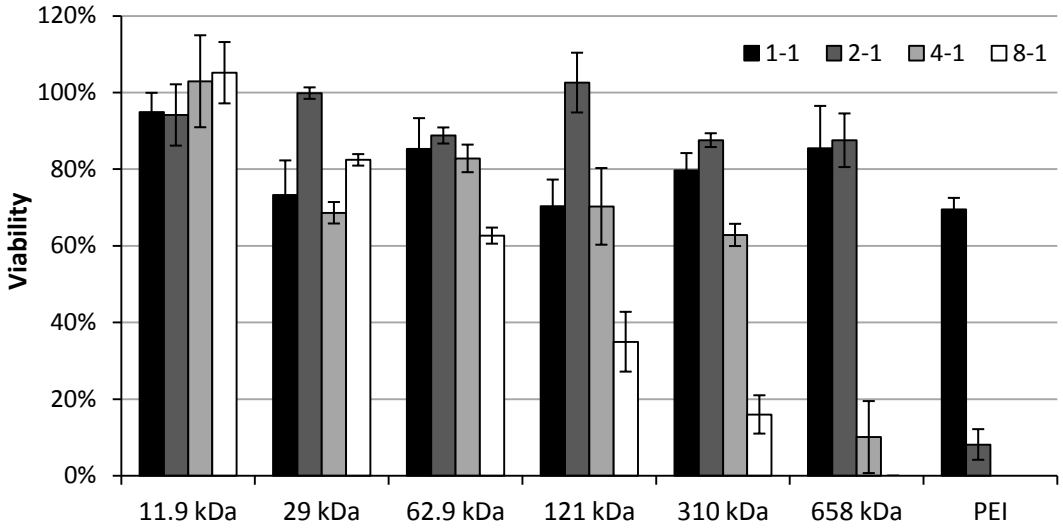


**Figure 6.16 - Toxicity results of cells incubated with polyplexes based on pDMAEMA.**

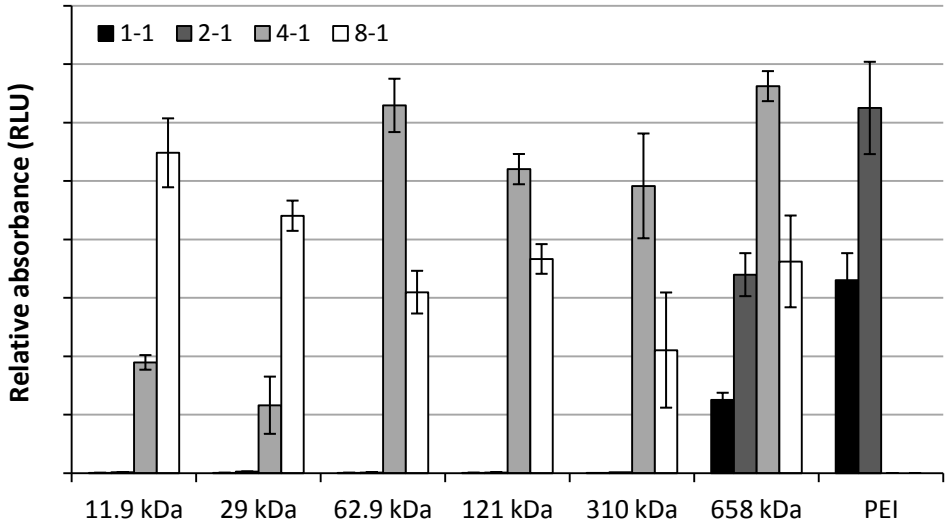


**Figure 6.17 - Transfection efficiency on HEK cells (24 h) of pDMAEMA complexes.**

In the case of methacrylate copolymers (Fig. 6.18), both the HEMA- and AEMA-containing copolymers were analysed. The p(DMAEMA$_{56\%}$-HEMA$_{44\%}$) compound with a MW of 218 kDa (DH218) was tested as was done for a compound with a ratio of 55 % DMAEMA and 45% HEMA and MW of 9.8 kDa (DH9.8). For p(DMAEMA$_{82\%}$-AEMA$_{18\%}$), a derivative of 191 kDa (DA191) together with a compound containing DMAEM$_{54\%}$A/HEMA$_{46\%}$ with a MW of 135 kDa

was examined (DA135). All 4 polymers exhibit a similar degree of toxicity compared to the homopolymer (of comparable MW) indicating a good viability at low CR but severe to complete cell death at high CR.

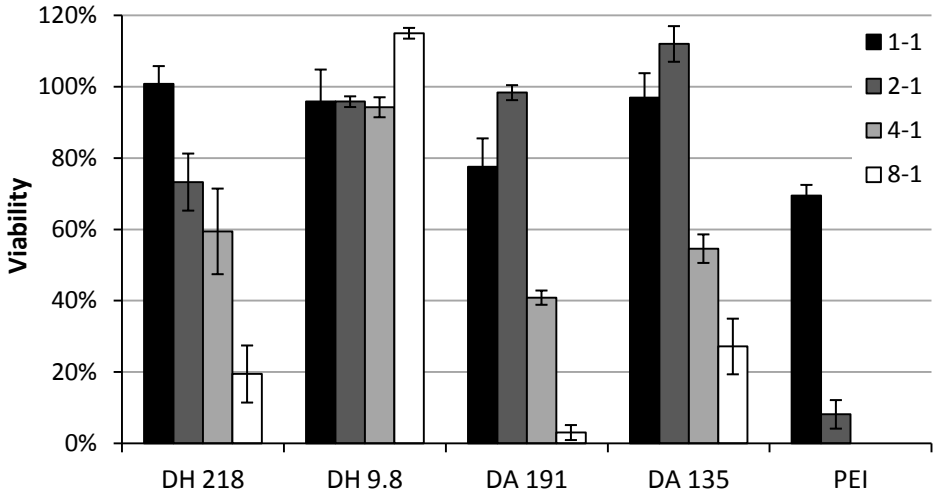


**Figure 6.18 - Toxicity results of cells incubated with polyplexes based on DMAEMA copolymers.**

Unfortunately, if transfection efficiency is considered, the least toxic polymer (DMAEMA/HEMA 9.8 kDa) showed no activity at all (Fig. 6.19). The other HEMA-containing vectors in contrast demonstrated an activity in the range of PEI and were able to achieve a comparable level of transfection but with a much higher degree of viability (> 70%) than for PEI. Copolymerising primary amine-units into with DMAEMA revealed to have a positive effect on the efficiency. Compared to the homopolymer, a small improvement in activity was measured for the DMAEMA/AEMA 191 kDa compound. This effect turned out to be even more outspoken for p($DMAEMA_{54\%}$-$AEMA_{46\%}$) with a MW of 135 kDa where protein expression levels 3 times as high as PEI were achieved although in contrast the viability degree of these polyplexes was not higher than 50%. Nevertheless, there are several methacrylate-based vectors that seem appealing for further exploration. The relative transfection ratio compared to PEI is depicted in figure 6.20.

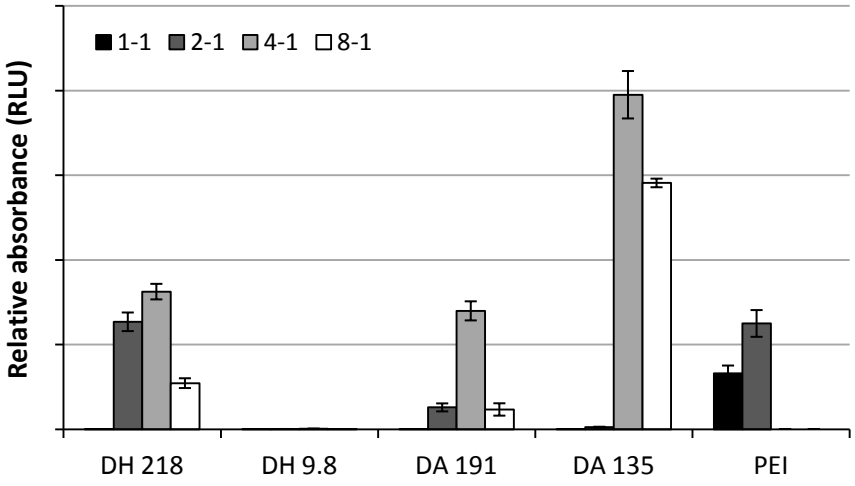


**Figure 6.19 - Transfection efficiency on HEK cells (24 h) of DMAEMA copolymers.**

### *2.3.5 Summary: activity of vectors compared to PEI*

To conclude, the degree of transfection as well as the viability for all active compounds is combined in figure 6.20 & 6.21 (with corresponding codes in table 6.4) to summarise the best performing vectors and to compare with PEI. This reference polymer was analysed as control for every polymer evaluated (but the data was not always depicted on the previous graphs). When focusing on the separate results, reported above, incorrect interpretations could be derived for certain cases (A, D, F) since the activity is lower than 1% of the maximum activity of PEI. From the biodegradable polymers only the copolymers containing about 35 % of guanidine moieties and 65% of less or non-charged units (hydroxyl for B and imidazole for E) display significant activity compared to PEI. In contrast, these values can only be reached at higher CR's but due to their excellent biocompatibility (≥ 90%), excess amounts of polymer have nearly no negative impact on viability. Additionally, the MW's corresponding with the highest degree of transfection are in most cases of low MW (around 10 kDa). Polymethacrylates proved to have an even higher transfection efficiency than polyglutamines and PEI, especially for DMAEMA copolymers containing hydroxyl or primary amines (H & I). The most optimal results were also achieved for polyplexes with a high CR which puts certain restraints on the success of polymethacrylate compounds since maximum 70% of these cells can survive the addition of these polyplexes. Nevertheless, all the formentioned polymers still exhibit significantly better viability than PEI which allows then to be used as an attractive alternative for gene delivery *in-vitro*. The modification of PEI with guanidine functional groups (J) was also able to enhance the transfection efficiency with a comparable level of viability (especially at a CR of 1-1).

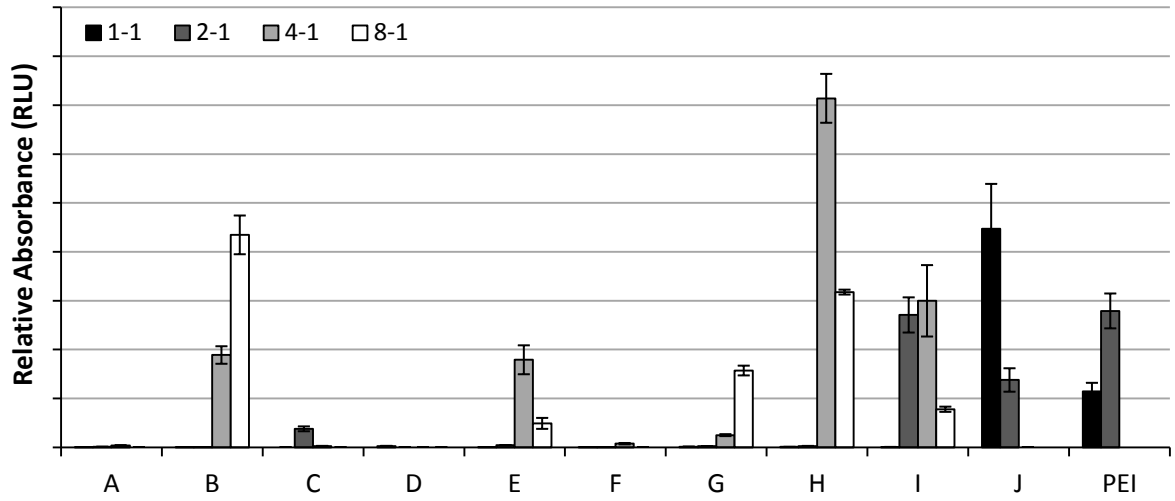


**Figure 6.20 – overview of all active polyplexes compared to PEI (transfection efficiency.**

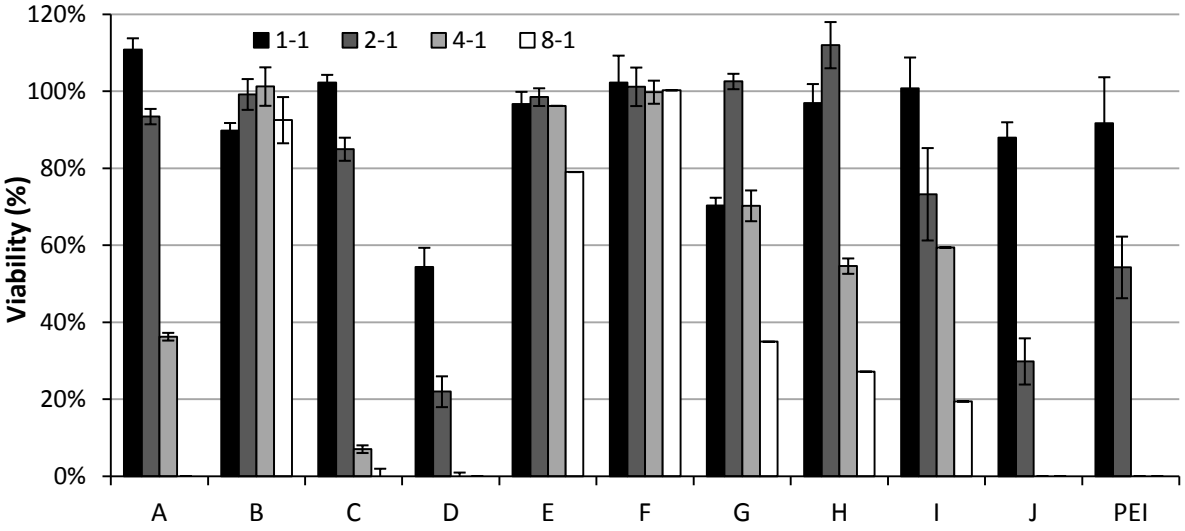


**Figure 6.21 - overview of all active polyplexes compared to PEI (cell-viability).**

| Code | Polymer | Code | Polymer |
|---|---|---|---|
| A | p(DMAEG)+$Arg_8$ 242 kDa | F | p($HEG_{32\%}$-$GuAEG_{11\%}$-$ImEG_{57\%}$) 9.6 |
| B | p($HEG_{63\%}$-$GuAEG_{37\%}$) 9.6 kDa | G | p(DMAEMA) 121 kDa |
| C | p($ARG_{82\%}$-$ORN_{18\%}$) 71.1 kDa | H | p($DMAEMA_{82\%}$-$AEMA_{18\%}$) 135 kDa |
| D | p($ARG_{82\%}$-$ORN_{18\%}$)+PEN 71.1 kDa | I | p($DMAEMA_{56\%}$-$HEMA_{44\%}$) 218 kDa |
| E | p($GuAEG_{35\%}$-$ImEG_{65\%}$) 13 kDa | J | PEI-$Guanidine_{20\%}$ |

**Table 6.4 - corresponding polymer-code for figure 6.20 & 6.21.**

## 2.4 Physical mixing of CPP's with vector systems: sequence of addition

The use of cell penetrating peptides to improve the transfection efficiency has already established a solid reputation as a potent method of gene delivery. As was mentioned, in most cases, these units are coupled in a chemical way to the polymer backbone in order to facilitate the entry of the vector-based delivery system. Because the coupling comprises of additional synthesis steps (with unifying loss of material), it's efficiency was compared to vector systems that make use of physically mixed CPP's as a method to enhance delivery of DNA. Since the combination of different compounds to one single solution can be varied and the sequence of addition has an important effect on the corresponding transfection efficiency, a comparison was made between the addition of CPP's to a preformed polymer-DNA complex (PEI+DNA/PEN) and the combination of adding DNA to a premixed CPP-polymer solution (PEI+PEN/DNA) in order to form a 3-compound 'multiplex' (Fig.6.22).

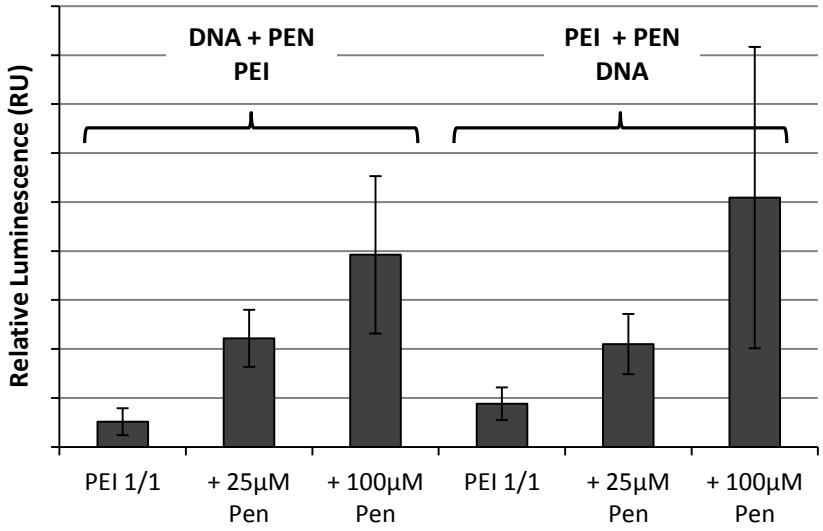


**Figure 6.22 – Transfection efficiency of physically mixed Penetratine (varying concentration).**

It appears that the addition of PEN by means of physical mixing has a huge advantage over covalent coupling (see Fig. 6.4) which yielded comparable results as non-modified PEI. Regardless the higher standard deviation, the addition of PEN in a range of 25 to 100 µM can induce a 2- to 5-fold increase of the efficiency. The most optimal sequence of CPP addition was not clear from these experiments.

An analogue experiment was carried out for a broader range of CPP concentrations for both Penetratine and TAT in combination with a DMAEMA-based polymer (CR = 3/1). In contrast to PEI, the addition of a higher concentration of peptide is not advantageous (Fig. 6.23). Also, the difference in order of addition, is clearer for these tests. Adding a mixture of polymer and peptide to DNA, results in a more efficient multiplex compared to the addition of

CPP to a preformed polymer-DNA complex. Moreover, combining cationic compounds during the multiplex formation results in more stable efficiency which is less influenced by the variation in CPP-concentration. Results derived from TAT-based multiplexes showed higher (if only very slightly) values than multiplexes composed of PEN.

In correspondence with the physico-chemical properties (section 5.5) of covalently coupled CPP's, which caused an elevation in the CR representing full condensation, the physically mixed multiplex achieved a similar value as the non-coupled vector system. This gives preference to the physical combining of peptides and polymer vectors to be selected over covalently-coupled polymer derivatives as vectors. Moreover, the total concentration of peptide present in the multiplex can already induce a significant effect at low values.

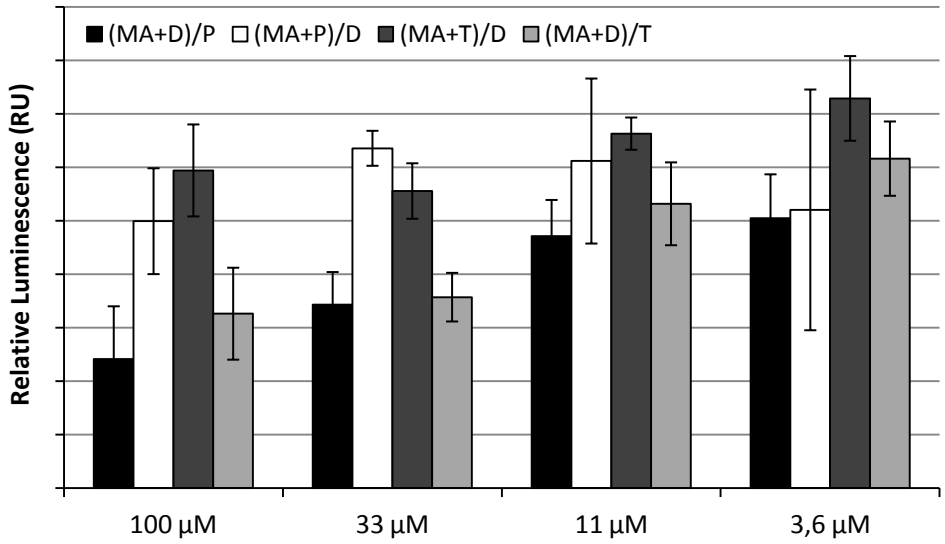


**Figure 6.23 – Relative transfection efficiency of multiplexes (CR 3/1) composed of methacrylate (MA), DNA (D) and a peptide (Penetratine, P or TAT, T) in variable concentrations.**

## 3 DNA-protection ability

### 3.1 Principle of enzymatic DNA degradation

Given the preferred route of systemic polyplex delivery (via the bloodstream), it is imperative that polyplexes survive this first part of the total transfection process, that is by examining if the polymers are capable of adequately protecting the DNA against the hydrolytic activity of nucleases[6]. Nucleases are a class of enzymes that function as regulators of DNA activity and can cleave the phosphodiester bonds between the nucleotide subunits of nucleic acids (DNA, RNA). Processes under the control of nucleases include DNA synthesis, degradation of host cell DNA after viral infections, DNA repair, DNA recombination and protection against foreign DNA[7]. If free DNA is injected in the bloodstream, it is quickly degraded by those

nucleases hence the importance of investigating to what extent the (co)polymer prevents the degradation of DNA, present within polyplexes.

Nucleases are classified as exo- or endo-nucleases based on their specificity. Endo-nucleases cleave the phosphodiester bond within a polynucleotide chain, in contrast to exonucleases, which cleave phosphodiester bonds at the beginning or end of the polynucleotide. Some nucleases, however possess both endo and exo properties. Most nucleases are specialised in either cleavage of single-stranded DNA (ss-DNA) or double-stranded DNA (ds-DNA) but certain are able to act on both DNA types. Furthermore, some exo-nucleases work in a specific direction for phosphodiester cleavage (3' ► 5' or 5' ► 3' direction) while others cleave at random[8]. Additionally, to reach maximum activity, these enzymes require the presence of divalent cations like $Ca^{2+}$ or $Mg^{2+}$ which are consequently added to the buffer or medium.

The method used to determine if DNA degrades when exposed to a solution of nucleases is based on UV-spectroscopy. Free nucleotides absorb more ultraviolet (UV) light than nucleotides stacked in a DNA-helix as was proven by Kunitz[9] (Fig. 6.24). This is the result of both physical limitation whereby the rigid helical structure disturbs optimal exposure to incoming light as well as the occurrence of $\pi$-$\pi$ interactions induced by aromatic stacking that transfers previously absorbed energy. Consequently, the quality of a nuclease that is applied as degrading enzyme is often expressed in Kunitz units. The increase in the absorption of UV light by the degraded DNA can be detected along a wide range of the EM-spectrum (225-300 nm) and is most significant at 260 nm (increase of nearly 30 % relative to undigested DNA)[10].

For complexed DNA (polyplexes), it is possible that DNA is degraded while remaining complexed to the polycation (mainly for high CR's where considerable interaction exists), hence a control using degraded DNA-complexes should be used. Given the complex preparation of this latter, this experiment was not carried out. Moreover, it is believed that the effect of DNA degradation would still be detectable as the degradation would unambiguously result in a conformational change that affects the absorbance values (similar as for free DNA, yet to a smaller extent). An indication to substantiate this hypothesis is shown in the different results, where at modest CR's (just above $CR_{cond}$), there appears to be nearly no degradation occurring.

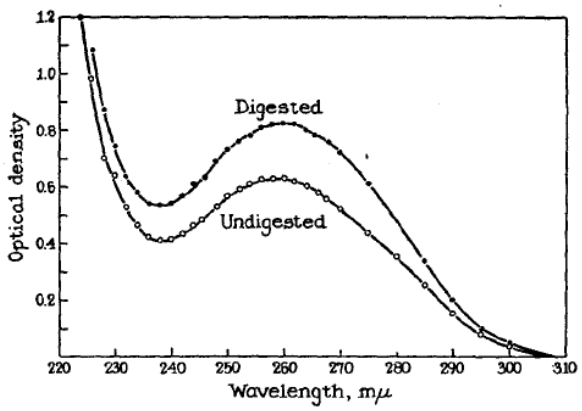


**Figure 6.24 – UV absorption spectrum of nuclease digested and undigested free DNA[9].**

### 3.2 Experimental set-up

For these experiments, the stability of the polyplexes against the endo-nuclease deoxyribonuclease I (DNase I - Bovine) was investigated. DNase I is a nuclease that cleaves DNA preferentially at phosphodiester linkages adjacent to a pyrimidine nucleotide, yielding 5'-phosphate terminated nucleotides. It acts upon ss-DNA, ds-DNA and chromatin. A critical concentration of divalent ions such as $Ca^{2+}$ and $Mg^{2+}$ are necessary to activate DNase I and were accordingly added to the buffer.

Several polymer-DNA complexes were prepared at different CR's in a modified version of the standard protocol (chapter 4, section 2). Since for these experiments, an appropriate buffer is required (40 mM TRIS.HCl, 10 mM NaCl, 6 mM $MgCl_2$, 10 mM $CaCl_2$, pH = 7.9), the formation of polyplexes was accordingly disturbed by precipitation phenomena. Therefore, initial polyplexes were prepared in 1 ml of ultrapure $H_2O$ (concentration DNA = 40 µg/ml) and subsequently diluted with 1 ml of TRIS buffer (at double concentration) to obtain polyplexes in a buffered solution at a final concentration of 20 µg/ml DNA. Prior to utilisation, the buffer was filtered (0.45 µm PTFE membrane) and degassed for 10 minutes. A solution representing 40 Kunitz units of DNase I was added to the polyplex solutions in quartz cuvettes and the total mixture was correspondingly measured (λ = 260 nm) at given time-points while maintaining a constant temperature of 37 °C.

### 3.3 Results

As a first test, the influence of the temperature on the efficiency of nuclease enzymes was examined (Fig. 6.25). These results confirmed the importance of using the appropriate temperature setting (corresponding with the body temperature of 37° C) and its reflection on the kinetics of protein-based reactions. For an equal concentration of DNA and DNAse I, nearly maximum absorbance was detected after 120 seconds at 37 °C while at 25 °C, even

one hour of reaction was not enough to obtain 90% absorbance increase. Full efficiency (100%) was selected to correspond with the absorbance increase after one hour of nuclease degradation with free DNA (at 37 °C) since it counts as an ideal benchmark for correlating shielding ability (whereby 0% equals perfect shielding and 100% indicates no protection towards nucleases).

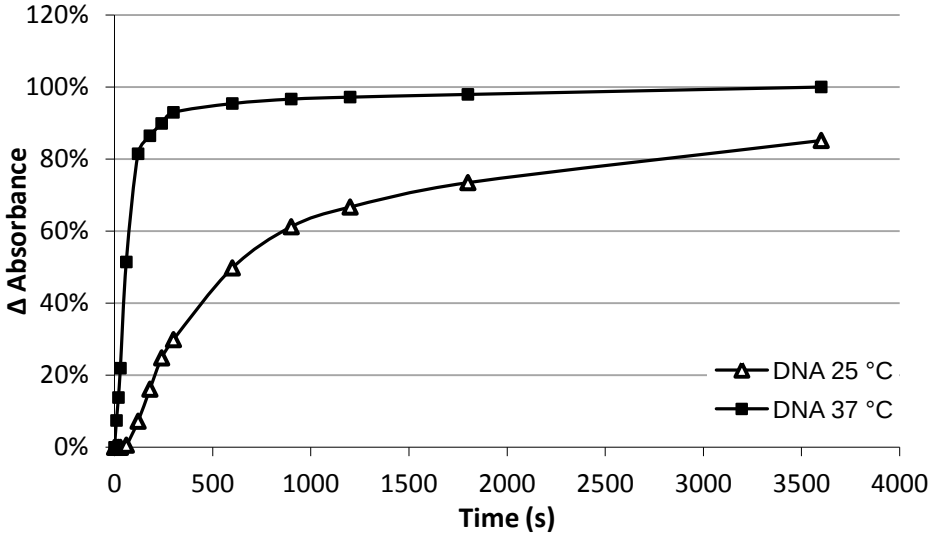


**Figure 6.25 - Influence of temperature on the activity of DNAse I for DNA degradation (% absorbance expressed relative to free DNA).**

Because the activity eventually reaches a plateau value, the sample measurements were reduced in time and carried out between 0 – 1800 seconds to limit experimental analysis. Accordingly, experiments were only tested in 1-fold.

### *3.3.1 PEI*

The individual results for PEI, measured at different CR's (1/1, 2/1 and 4/1) demonstrate nearly perfect protection of DNA (Fig. 6.26). This trend is in line with the data obtained before and explained by its low condensation CR (≈ 0.6/1). Even a relatively low CR can provide adequate protection against enzymatic attack. With increasing time, there seems to be no significant change in absorbance so that excellent stability is to be anticipated.

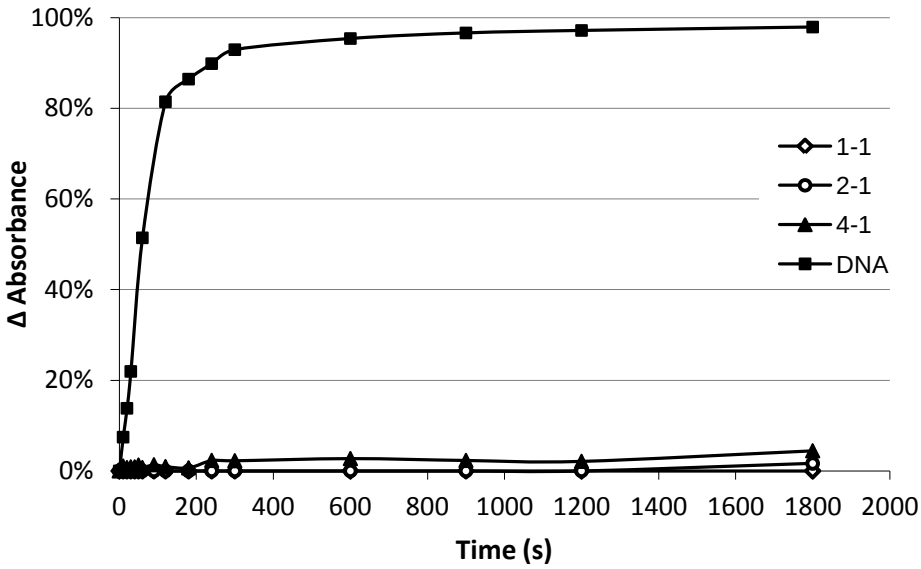


**Figure 6.26 – Nuclease degradation of polyplexes formed with PEI.**

### *3.3.2 Poly-L-glutamine derivatives*

Several selected polyglutamines were subjected to DNA degradation tests. One of the specific compositions examined was pDMAEG with a MW of 29 kDa (Fig. 6.27). The effect of complex formation is clearly visible for this compound. With respect to the CR corresponding with full condensation (≈ 1/1), a polyplex with a low CR demonstrates no protective properties. Moreover, the maximal degradation efficiency appears even higher due to the stabilisation effect of the polymer on the DNA (small conformation changes allow more and better exposed sites for enzymatic attack). Close to the condensation CR, an initial increase in absorbance is noticed. Since particle formation is only partial at this CR (equilibrium between polyplexes and free polyelectrolytes), some of the free DNA remains exposed for degradation and is responsible for the partial increase. When the degraded DNA fragments become increasingly smaller, the non-complexed polymer chains are correspondingly better able to rearrange around the small DNA fragments (kinetic effect), hence the secondary decrease in DNA absorption. When complexes with higher CR's are prepared, complete protection of the DNA is obtained (starting right at the beginning of mixing) without the initial absorption increase noticed (stable value in time).

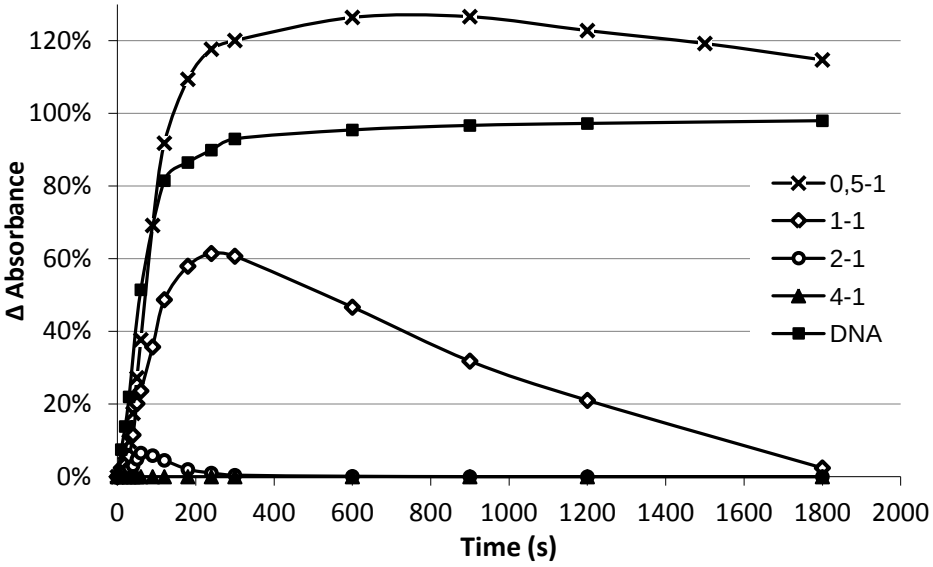


**Figure 6.27 - Nuclease degradation as a function of time for polyplexes formed with pDMAEG (MW = 29 kDa) at various CR's.**

In the case of (co)polymers that possess a partial lower amount of cationic functional groups (Fig. 6.28), the interaction ability and accordingly the level of DNA protection, is highly dependent on the composition. For a weakly charged polymer p($HEG_{87\%}$-$GuAEG_{13\%}$), complete DNA shielding can not be achieved. Burst degradation of DNA is initially noticed in all cases which decreases with increasing CR (ranging from 60% at a CR of 0.5/1 to 10% at 4/1). Only in the case of a 4/1 CR, the secondary complexation effect is capable of preventing further degradation of DNA over a prolonged time-range. Initial burst degradation, even if only small and rapidly decreasing, can be devastating for the therapeutic function of the DNA, RNA or protein sequences can get seriously disturbed by it.

Copolymers with a higher amount of cationic charges on the other hand like p($HEG_{38\%}$-$DMAEG_{62\%}$) demonstrate a much better DNA-shielding ability (Fig. 6.29). Even at a CR of 1/1, which is just above the complexation value, burst degradation is small and subsequent decline in absorbance over time is short. When compared with the homopolymer, p(DMAEG), a better shielding ability is observed for low CR's, a conclusion which rules in favour of the use of hydroxyl groups that act as charge separators. The loss of complexation capability (due to the lower strength of H-bonding relative to electrostatic attraction) is here corrected by the feasibility to sufficiently cover the DNA in a more homogeneous but diffuse way. At higher CR's, the resulting burst degradation of free DNA is more or less equal to that of fully charged p(DMAEG) and can only be avoided at the highest CR (4/1).

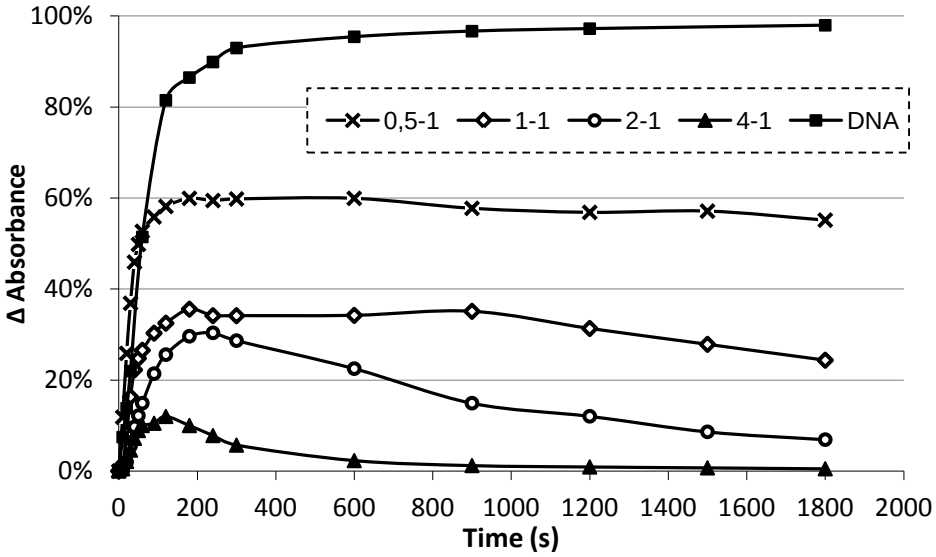


**Figure 6.28 - Nuclease degradation as a function of time for polyplexes formed with p($HEG_{87\%}$-$GuAEG_{13\%}$) (MW = 26.9 kDa) at various CR's.**

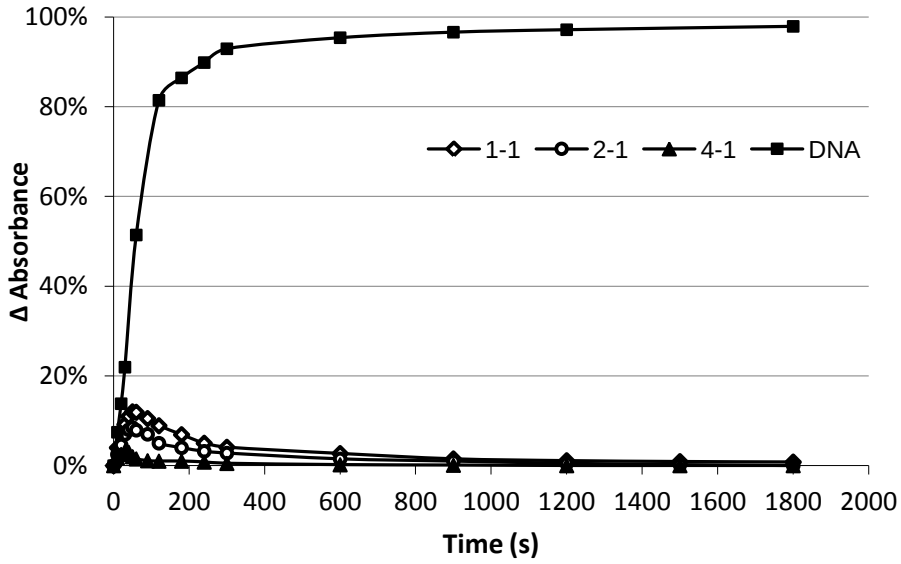


**Figure 6.29 - Nuclease degradation as a function of time for polyplexes formed with p($HEG_{38\%}$-$DMAEG_{62\%}$) (MW = 11.9 kDa) at various CR's.**

As was mentioned above, the properties of vectors are strongly influenced by the composition of their charged entities. For a series of p(HEG-GuAEG) with a MW of 10.000 Da, the decline in degradation rate for a 2/1 CR is shown in figure 6.29. The higher the amount of guanidine groups that are present, the better a copolymer is at preventing enzymatic degradation due to the more intense attraction forces. In combination with the other enzymatic degradation results, it appears again that the minimum amount of charged

side groups, present on a polymer, is estimated to be around 50-60%. Moreover, in the case of DNA-shielding, the importance of the type of functional group seems less relevant.

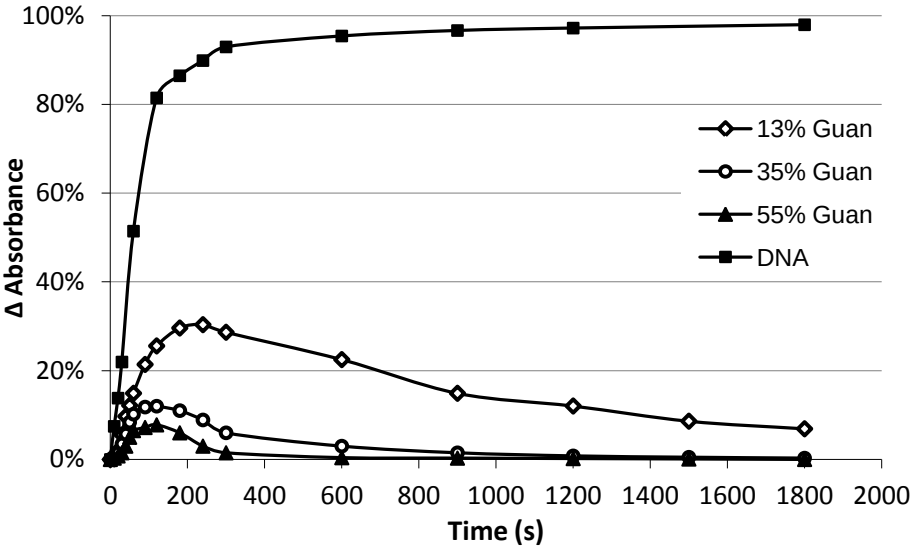


**Figure 6.30 - Nuclease degradation as a function of time for polyplexes formed with different p(HEG-GuAEG) (MW ≈ 10 kDa) at a CR of 2/1 as a function of % GuAEG.**

From figure 6.31, several trends were derived for the protection of DNA (for polyplexes containing an equal CR of 2/1). Firstly, the effect of the MW on shielding ability was only modest (15% burst degradation for a MW of 242 kDa compared to 8% burst degradation of DNA for a MW of 30 kDa). Additionally, if primary amines are present in the copolymer, no significant consequences in terms of shielding effect were observed. Finally, the incorporation of imidazole (e.g. 36%) as a typical functional groups that can promote endosomal escape does not exert a strong, negative influence on DNA shielding. Taking into account that this polymer contains only 15% of guanidine groups, the performance is in line with the result of a p(HEG-GuAEG) derivative of equal charge but is better for a derivative containing the same amount of guanidines. Again this might be attributed to the more diffuse nature of the complexes when less charged groups like imidazole are present in the polymer structure.

Nevertheless, the most important aspects for an acceptable level of protection from enzymatic attack, comprise of a substantial amount of charge (> 50%) and the use of a polyplex with a CR of at least 2/1 (mostly higher if zero burst-degradation is desired). If for other purposes, fully charged polymers are unwanted, the introduction of hydroxyl and imidazole (or a combination thereof) comprehends a good alternative since nearly no shielding difference can be noticed (when provided with sufficient charged groups). In contrast to the effect of chemical composition, the influence of the MW can be neglected.

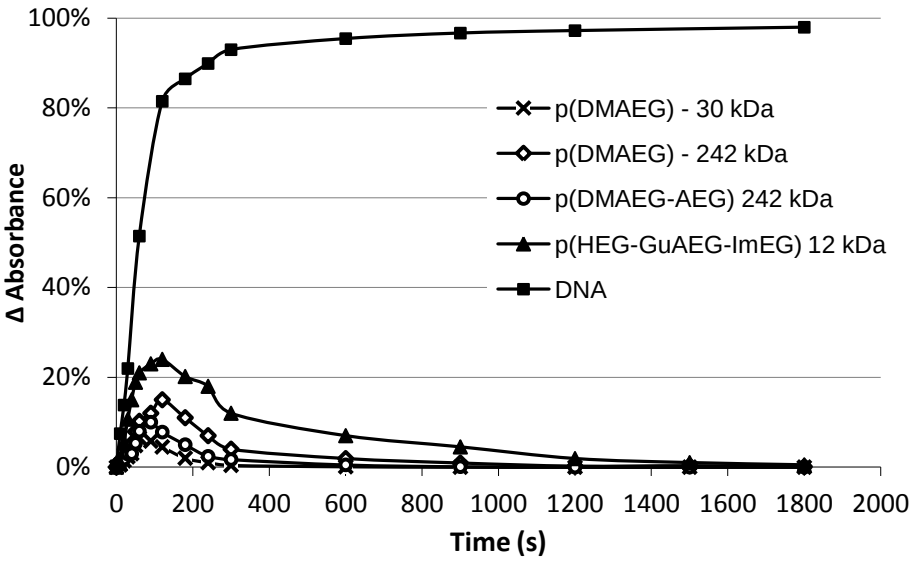


**Figure 6.31 - Nuclease degradation as a function of time for polyplexes formed with different composition and MW at a CR of 2/1: pDMAEG 30 kDa, pDMAEG 242 kDa, p($DMAEG_{85\%}$-$AEG_{15\%}$) 242 kDa and p($HEG_{49\%}$-$GuAEG_{15\%}$-$ImEG_{36\%}$) 12 kDa.**

### *3.3.3 Polymethracylate derivatives*

The extent to which DNA could captured by a polymer and induce shielding from degrading enzymes was also investigated for a selection of polymethacrylate-based complexes. These results were consequent with respect to the conclusions drawn from the EtBr fluorescence tests. It should be mentioned that these experiments were performed prior to optimisation of the degradation test and were therefore executed at 25 °C instead of 37 °C. As can be deduced from figure 6.31, the temperature has a serious effect on the kinetics of an enzyme. Nevertheless, the obtained results remain valid but due to the reduced activity at 25 °C, the discrepancy between individual results is less explicit. Moreover, some sort of induction period (200-300s) was encountered for many samples and as a consequence the interpretation of the start and end of the degradation process was performed differently.

In figure 6.32, the influence of the CR on DNA shielding was studied for p(DMAEMA), a homopolymer with a MW of 12 kDa. At a CR below complexation (0.5/1), the polymer was unable to protect the DNA from degradation and because of the DNA stabilisation, better accessibility for enzymatic attack caused an even higher degradation compared to pure DNA. With an increasing amount of polymer, the DNA is proportionally better protected and close to the complexation point (i.e CR 1/1), nearly no absorbance augmentation was noted. Adding more polymer (CR > 1/1) does not improve the protective ability of the polyplexes.

Also the secondary effect (drop in absorbance due to re-complexation of fragmented DNA) was not observed.

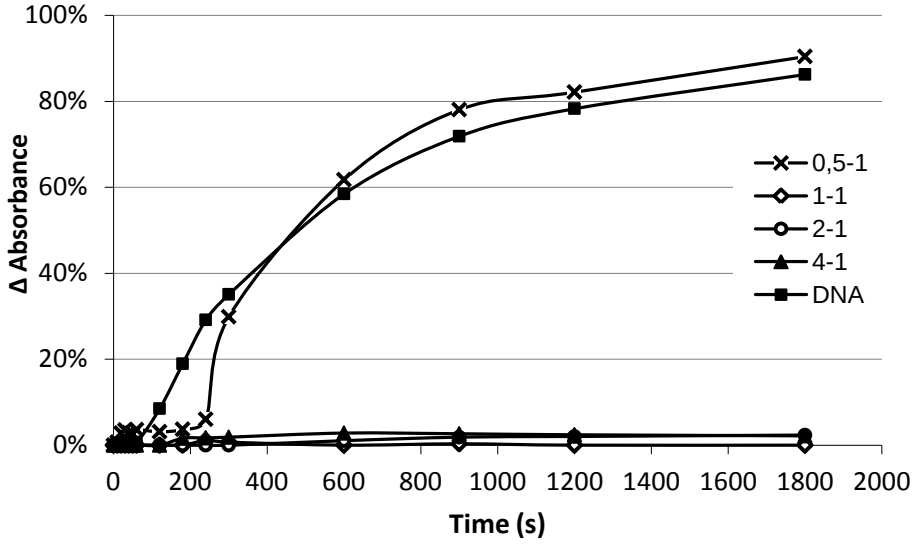


**Figure 6.32 - Nuclease degradation as a function of time for polyplexes formed with pDMAEMA (MW = 12 kDa) at various CR's.**

The effect of the MW was just as for the biodegradable counterparts not traceable at high CR's (2/1) and is shown for different DMAEMA-containing polymers (Fig. 6.33 – full lines). A MW influence can only be noticed if the CR is just below or around the CR representing condensation since this is the most distinguishable parameter in the case of p(DMAEMA) (represented by the dotted lines, CR = 0.5/1, Fig. 6.33). In accordance with fluorescence measurements, the optimal MW which complexes at the lowest CR has a MW of 121 kDa. The (delayed) burst degradation of DNA is very small (6-7 %) and a secondary complexation effect by which uncomplexed, remaining polymer forms polyplexes in a 2$^{nd}$ phase (post-initial polyplex formation) is observed. A similar but reduced trend was displayed by p(DMAEMA) with a MW of 658 kDa. Given the higher value for condensation, a more pronounced DNA burst degradation was measured as was the occurrence of polyplex formation in a second phase. The polymer derivative of 12 kDa showed the lowest ability to shield DNA from nucleases at this low CR which is completely in correspondence with the requirement for full polyplex formation. Furthermore, there was no indication of secondary complexation within the measured time-frame. Degradation (burst or delayed) was not visable for higher CR's since a sufficient amount of polymer was present at the initial polyplex formation (due to the strong basic interaction between excess polymer and DNA).

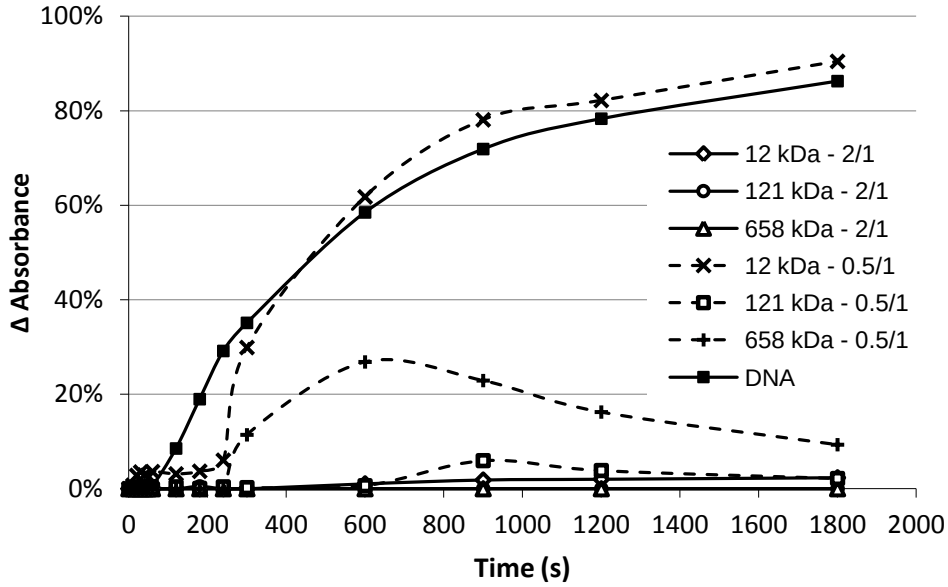


**Figure 6.33 - Nuclease degradation as a function of time for polyplexes formed by p(DMAEMA) with different MW at a CR of 0.5/1 and 2/1.**

The application of DMAEMA-based copolymers in which monomers containing different functional groups are applied, could affect the shielding ability. Therefore, copolymers with a similar MW (≈ 150 kDa), composed of 50% DMAEMA and another functional group were examined (Fig. 6.34). At a CR of 2/1, p(DMAEMA) is able to fully protect the DNA from enzymatic attack but when the tertiary amines are replaced with primary amines (46%), the protective ability is lowered (absorbance increase of about 10%) with no indication of secondary complexation. Remarkably, the introduction of non-charged hydroxyl (43%) moieties retained full protection behaviour as no DNA-absorption increase could be detected. This was not the case for p($GuAEMA_{40\%}$-$HEMA_{60\%}$) given the occurrence of DNA degradation (≈ 15%) although the lower amount of positive charges (40% vs 55%) could partly be responsible for the cause of this aberrant result.

For polymethacrylates, it appeared that comparable trends were derived as for polyglutamines. The MW of the polymer showed little to no influence for polyplexes at higher CR and was only able to differentiate polymers of variable MW at a CR close to the condensation value (where stable polyplexes are not yet formed). Homopolymers of DMAEMA display excellent shielding ability and the introduction of other functional groups seems not to disturb this quality significantly although maximum CR's remain the best option. Analogous to polyglutamines, hydroxyl-containing derivatives demonstrate excellent protection (nearly no DNA burst degradation). Finally, the nature of the polymer (and the polyplex) seems to play a role in the occurrence of secondary complexation processes.

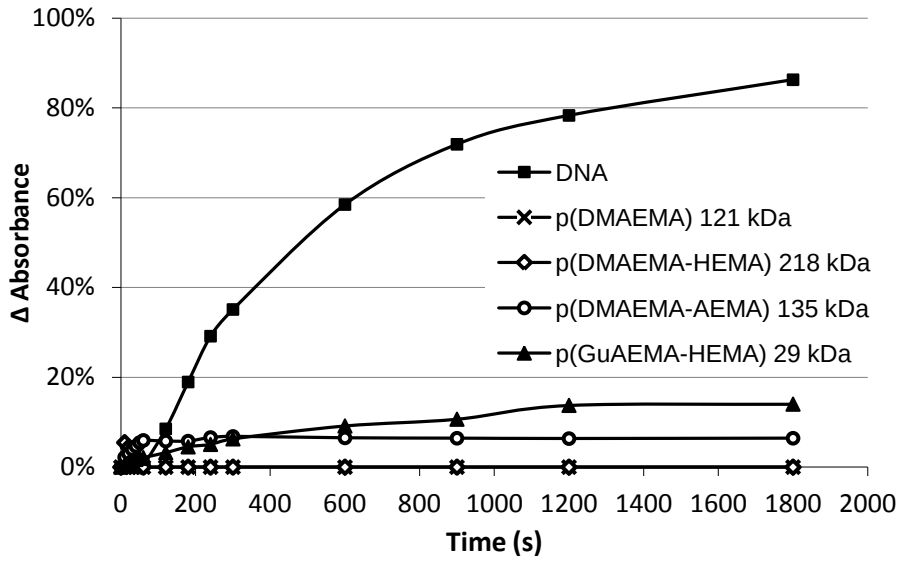


**Figure 6.34 - Nuclease degradation as a function of time for polyplexes formed with methacrylate polymers at a CR of 0.5/1 and 2/1: pDMAEMA 121 kDa, p(DMAEMA$_{56\%}$-HEMA$_{44\%}$) 218 kDa, p(DMAEMA$_{54\%}$-AEMA$_{46\%}$) 135 kDa and p(GuAEMA$_{40\%}$-AEMA$_{60\%}$) 29 kDa.**

# 4 In vitro degradation

## 4.1 Principle of enzymatic polymer degradation

Synthetic poly-α-amino acids like poly-L-glutamine and poly-L-arginine are often considered as suitable candidates for biomedical applications because of their anticipated biocompatible behaviour. Besides the fact that they can be tailor-made, they potentially possess low toxicity for *in vitro* or *in vivo* experiments due to their resemblance with naturally occurring systems like proteins. The backbone of poly-α-amino acids consists of a repetition of amide-bonds that can be degraded by proteolytic enzymes which enables the polymers to act as biodegradable systems (e.g. in gene delivery), an important asset compared to non-biodegradable systems (e.g. polymethacrylates or PEI).

When delivery systems have fulfilled their task (protecting and delivering DNA), they should be removed from the body to reduce the possibility of unwanted side-effects. Initially, it was believed that the administered vectors were filtered out by the renal system but with increasing knowledge of the internalisation pathway, it appeared that a large part of the cationic polymers ended up in the lysosomal compartments after endocytotic uptake. This could eventually lead to lysosomal storage disease (accumulation of the non-degraded polymers)[11,12]. Lysosomes are cell organelles that are responsible for the degradation of nutrients and waste products of the cell. Protein breakdown is carried out within these

vesicles and not by the digestive system. Given its resemblance with protein structures, poly-α-amino acids are expected to be degraded inside these lysosomes by proteolytic enzymes (proteases). One of the best known, high performance proteases is Cathepsin B (Cathepsin family), a lysosomal cysteine-containing enzyme capable of degrading amide-bonds of peptides[13]. The degradation capacity of an enzyme is dependent on several parameters like correct environmental conditions (temperature, pH, concentration, activators/catalysts) but also on the nature of the target substrate. The hydrophobicity, the overall charge, the type of chemical bonds and the macromolecular structure all play a considerable role in this process. Other typical enzymes frequently encountered in degrading processes include pronase and leucine aminopeptidase (LAP)[14]. Each degrading enzyme has a specific range of substrates and properties it aims to address and in combination with others, total breakdown of a entire, large molecule can be achieved down to (single) molecular level (e.g. basic amino acids in the case of proteins). Total degradation of waste products is necessary to ensure complete recycling of the base components but also to allow crossing of the lysosomal membrane that is impermeable for large, polar components[15].

In the framework of this doctoral research, the naturally occurring enzyme papaine was used to assess the degradability of poly-α-amino acids. Papaine is a thiol-based endopeptidase derived from the papaya tree (latex extract) which is a very potent degrading enzyme[16]. It was already proven that papaine is able to degrade poly-L-glutamic acid and derivatives down to oligomer size by a single addition of papaine. Subsequent treatment with other endo- or exopeptidases resulted in complete breakdown of the polymer[10]. To obtain preliminary information on the response of the produced polymers, the experiments were limited to the single use of papaine.

### 4.2 Experimental set-up

A selection of synthesised polymers was subjected to a degradation test by addition of papaine to a buffered polymer-solution to examine the influence of polymer chemical structure and MW on the biodegradability. A simulation of the intra-lysosomal environment is therefore created by applying polymer samples (10 mg/ml) in an appropriate phosphate/citrate buffer (0.2 M, pH = 6) of 2 ml which contains EDTA (4 µM), a highly efficient chelating agent and dithioerythritol (DTT, 4 µM), a reducing protein required to maintain enzyme function. Next, the polymer solution is incubated at 37 °C and afterwards analysed via GPC to determine the MW of the polymer prior to degradation. Degradation

was then initiated by adding 40 µg of papaine (5 mg/ml stock solution) followed by GPC analysis at different times in a 72 h frame (GPC buffer: 5% $NaH_2PO_4$, 3% $CH_3CN$, pH = 4).

### 4.3 Results

To obtain a preliminary idea on the degradation rate of the synthesised and modified polymers, a single dose of papaine was incubated with a buffered polymer solution. After GPC analysis, the MW decrease could be plotted as a function of time. All polymers appeared to be degrading rather fast and reached values as low as 1.500 Da which corresponded to nearly complete degradation (oligomer level). For large MW polymers, no significant difference in degradation result was noticed since the degradation limit reached values of about 2-3 % of the original MW (down to 3000 Da) after 48 h as depicted in figure 6.35. The influence of the overall charge was only slightly detectable. In the case of p($HEG_{38\%}$-$DMAEG_{62\%}$) about 20% of the initial MW was reached after 120 minutes of incubation whereas the MW of the less charged p(HEG-GuAEG) derivatives were reduced to 7-8%. The starting MW seemed not to differentiate in terms of degradability amongst the two guanidine/hydroxyl polymers although minimal MW difference remained between the polymers with charges based on tertiary amines and those based on guanidine functional groups. As a secondary effect, the reduced charge density of the functional group applied (delocalisation in guanidine groups) could have a (minor) influence on this.

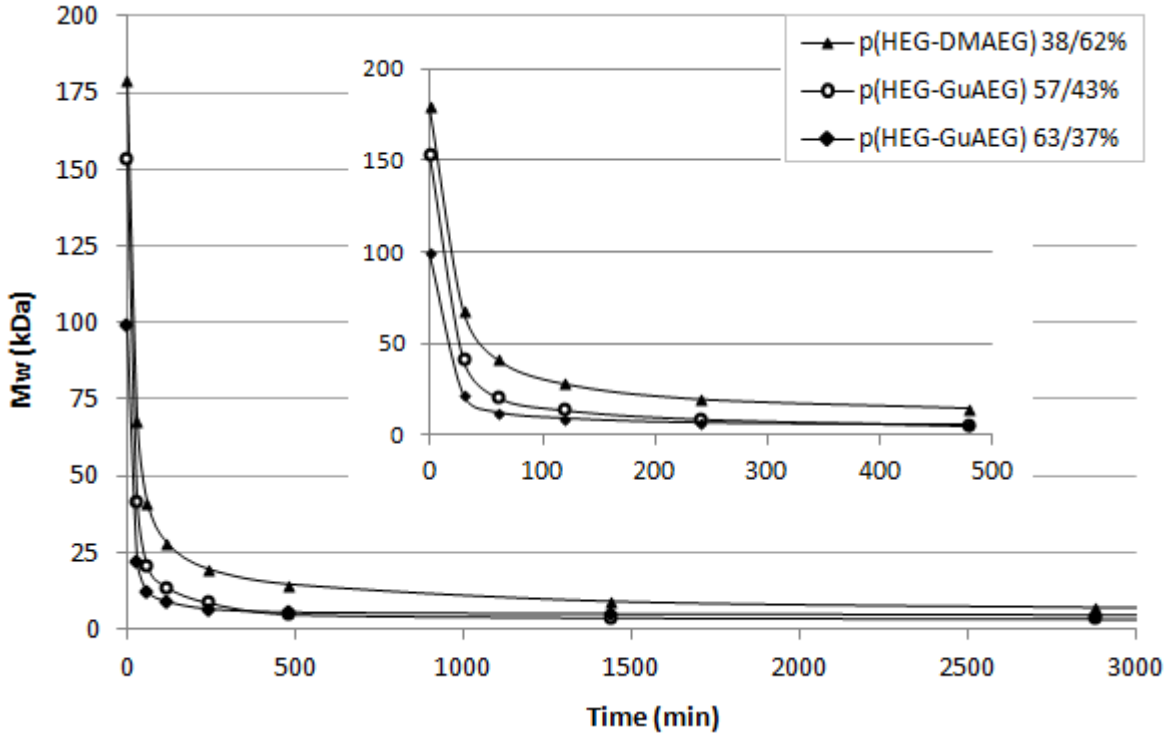


**Figure 6.35 – MW decrease of polymers in the presence of papaine: p($HEG_{38\%}$-co-$DMAEG_{62\%}$) 179 kDa; p($HEG_{57\%}$-co-$GuAEG_{43\%}$) 164 kDa; p($HEG_{63\%}$-co-$GuAEG_{37\%}$) 9.9 kDa.**

When polymer derivatives with a lower MW were tested, similar trends could be interpreted (Fig. 6.36). The denser charged p($HEG_{49\%}$-$GuAEG_{15\%}$-$ImEG_{36\%}$) degraded slower than in the case of p($HEG_{75\%}$-$GuAEG_{25\%}$) which was again slightly slower in degradation rate than the weakly charged p($HEG_{85\%}$-$GuAEG_{15\%}$) although the discrepancy was minimal, especially for the last two. At the end of the experimental time frame, a small but distinct difference in MW remained between the guanidine/hydroxyl derivatives and the one containing a substantial amount of imidazole. Despite the possibility of delocalizing the charge within the aromatic entity, the total amount of charge proved to be of principal interest for the final degree of degradation.

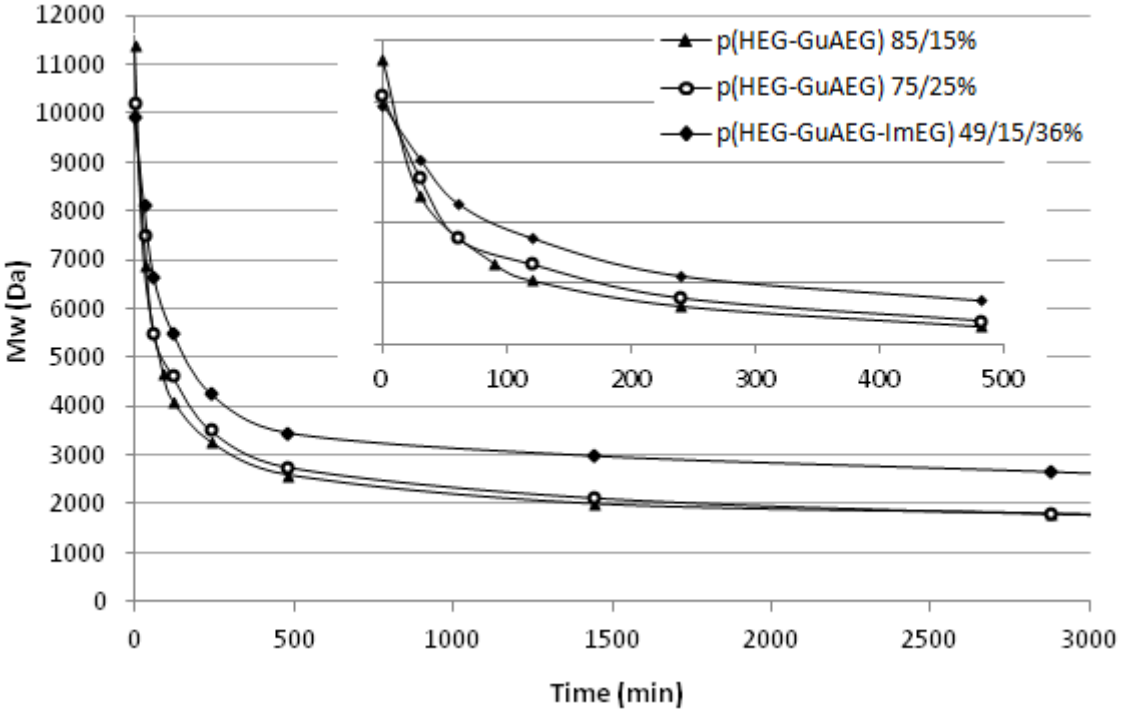


**Figure 6.36 - MW decrease of polymers in the presence of papaine: p($HEG_{85\%}$-co-$GuAEG_{15\%}$) 11.4 kDa; p($HEG_{75\%}$-co-$GuAEG_{25\%}$) 10.2 kDa; p($HEG_{49\%}$-co-$GuAEG_{15\%}$-co-$ImEG_{36\%}$) 9.9 kDa.**

When taking into account the mean molecular weight of the structure units present within the above mentioned polymers, degradation products of oligomeric size could be achieved (4-8 amino residues) which was in accordance with literature findings on poly-L-glutamic acid derivatives[10]. High MW compounds degraded down to about 2-3% of their initial molecular weight while for low MW compounds the relative ratio of initial to final MW was higher (15%) but lower absolute values could be achieved. For all compounds, other types of peptidase enzymes (added post-papaine degradation) are required to ensure complete structural disintegration of the polymer backbone although not feasible for the applied GPC set-up which makes use of SEC columns with a lower limit of 1.000 Da (representing tetrameric degradation compounds). Also, to enable clearer distinction of the influence of total charge

or type of functional group, studies at decreased enzymatic activity are advised (smaller dose of papaine).

## 5 Blood compatibility

To investigate the potential use of the synthesized (co)polymers as gene vectors for systemic administration they must express an acceptable blood compatibility. Common methods to assess this property are the investigation of possible haemolysis (lysis or rupture of red blood cells) and haemagglutination (red blood cell clustering). Because polymer-DNA complexes are charged components, certain compounds from the blood can induce interaction with these polyplexes with potentially harmful implications (for the blood components, the polyplexes or both). The blood is mainly composed of plasma, a water-based liquid in which a wide spectrum of compounds is suspended and of which the most abundant are erythrocytes (red blood cells, RBC), leukocytes (white blood cells, WBC) and platelets (Fig. 6.37). Erythrocytes vastly outnumber the other types of formed elements present in the blood and are shaped like biconcave discs but do not possess a nucleus or organelles. Their main function is to collect $O_2$ in the capillary beds of the lungs and release it to tissue across other capillaries throughout the body and are accordingly equipped with haemoglobin (Hb), a protein molecule that binds respiratory gasses. Since each cell contains about 250 million Hb-molecules and every molecule is provided with a $Fe^{2+}$ ion, it is responsible for the characteristic red colour of blood[17].

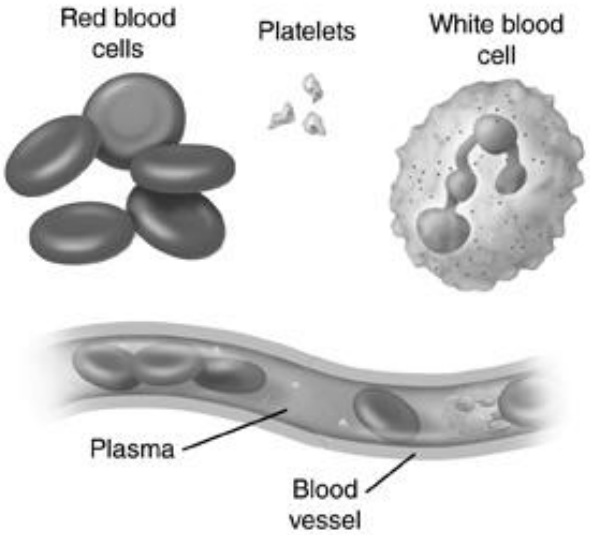


**Figure 6.37 - Main cellular structures of the blood and their relative size.[18]**

The interaction between polyplexes and RBC's is most likely to occur at the membrane of the erythrocyte which is composed of a lipid bilayer (40 % w/w), membrane proteins (52 %

w/w) and carbohydrates (8 % w/w)[19]. The lipid bilayer is made of cholesterol and phospholipids which are asymmetrically distributed, an outer monolayer consisting of choline and uncharged phospholipids and the inner monolayer contains charged phospholipids[20]. For the proteins, distinction is made between integral and peripheral proteins. Peripheral proteins are located on the cytoplasmic surface of the lipid bilayer and are responsible for membrane elasticity and stability while the integral proteins are embedded in the membrane via hydrophobic lipid interactions. As a final class of membrane structures, carbohydrates, of which the main part (90%) is bound to proteins (forming glycoproteins) and the remainder combined with lipids (giving rise to glycolipids). One of the main glycoproteins are the glycophorins that comprise 2 % of the RBC membrane proteins and which are rich in *N*-acetylneuraminic acid (or sialic acid). This imparts a negative charge to the cell membrane and in combination with other membrane proteins, electrostatic interactions with polyplexes may emerge from this (leading amongst other to agglutination or lysis)[21,22].

## 5.1 Haemolysis

### *5.1.1 Description of haemolytic effect*

As previously mentioned, the energetic implications of electrostatic attraction between (oppositely) charged species, like polyplexes and cell membranes can result in a physically altering process with one or many consequences. Whereas the formation of polyplexes is to a certain extent reversible, the rupture of a cell-membrane is mostly detrimental to the cell itself. That is why RBC-rupture or haemolysis forms a good benchmark to check the biological viability of polyplexes when used for *in vitro* or *in vivo* applications. When a RBC lyses, its contents (mainly Hb) is released and can be measured spectroscopically ($\lambda_{abs}$ = 545 nm) and corresponds with the absorption of the $Fe^{2+}$-porphyrine molecule present in the haem group of Hb[23]. Therefore the haemolytic activity can be quantified by applying the following formula:

$$\%haemolysis = \frac{A_{sample} - A_{blank}}{A_{triton} - A_{blank}} \cdot 100$$

With $A_{sample}$ = absorbance of a RBC suspension with polymer or polyplex

$A_{triton}$ = absorbance of a RBC suspension incubated with Triton X-100 (0.2 %)

$A_{blank}$ = absorbance of a RBC suspension in buffer

A Triton X-100 solution, a non-ionic surfactant able to destabilise cell-membranes, is used as a positive control and will be correlated with 100% haemolyis. The negative control is checked by applying RBC's in buffer and calibrating this solution as 0% haemolysis.

### *5.1.2 Experimental part*

Performing experimental tests with RBC's, derived from human blood, requires careful pretreatment in order to achieve pure and well-defined cells. The RBC's applied for haemolysis (and haemagglutination) were extracted from human whole blood (obtained by 'Red Cross' – Belgium) and a concentrate of this suspension was received as such. Further purification and isolation of the proper concentration of RBC was achieved by subjecting the liquid to a series of centrifuge and rinsing steps as described by the following protocol.

In a first step, a portion of the concentrate was centrifuged (3700 rpm for 5 min). Remaining plasma was removed with the supernatant and the suspension of RBC's was gently washed in HBS buffer (HBS = HEPES Buffered Saline, 20 mM HEPES and 150 mM NaCl at pH 7.4) after which another centrifuge step was performed (3700 rpm for 5 min). Again, the contaminated supernatant was removed together with the top layer of the RBC mass. Following rinsing of the solid product, a final centrifuge step was carried out (same conditions) and both the supernatant and the top layer were once more removed to ultimately obtain concentrated, pure, red blood cells. These could subsequently be diluted in HBS buffer to a concentration of 2%.

In order to test the possible lysis effect on RBC's, a selection of polymers were added to a 2% RBC suspension prepared prior to experimental analysis and incubated for 24h at 37 °C under continuous shaking (100 rpm). The polymers as such were added in a concentration range of 1-2000 µg/ml while the polyplexes were tested at a 2/1 CR, sufficient to enable full condensation for all polymers applied. Since the test is carried out in a buffered environment, polyplexes were prepared in slightly adapted way of the standard protocol (as described in section 2.2) which combines a double concentrated RBC-buffer with a double concentrated polyplex solution. After incubation, the degree of haemolysis was measured by separating the liquid from the solids (via centrifugation at 3700 rpm for 2 min) and subjecting the supernatant for a UV/VIS analysis. The values were then compared with the negative (0%) and positive (100%) control and plotted as a function of the concentration (not the case for polyplexes).

### *5.1.3 Results*

#### *5.1.3.1 Vectors based on poly-$\alpha$-aminoacids*

The haemolytic activity of cationic polymers is generally proportional to the amount of charge present. Nonetheless, this trend was not always observed. As an example when comparing highly charged pDMAEG with partially charged PEI (Fig. 6.38). Already at low concentrations

(≈ 100 µg/ml), PEI causes about 40% of haemolytic activity while for the other polymers this effect is below 10%. With increasing amount of polymer, the haemolytic activity gradually rises although at a certain concentration (approx. 1000 µg/ml), nearly no deviation was observed. When a copolymer, consisting of hydroxyl and guanidine groups, was grafted onto PEI, the resulting haemolysis was decreased up to 50% of its initial value and clearly indicates the shielding ability of grafts. Moreover, the PEI-graft-p(HEG-GuAEG) haemolysis was comparable ($\Delta \leq 5\%$) to the graft-copolymer itself which proves that the resulting biocompatibility properties could be largely adopted. Claiming that higher amounts of charge induce higher haemolytic activity was contested by the low value (≈ 10 %) of p(DMAEG), hence the more complex origin of haemolysis-inducing effects.

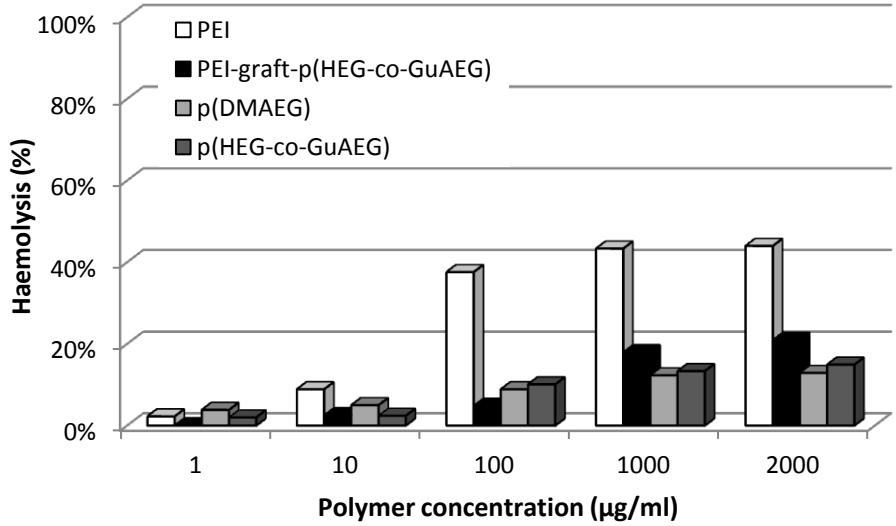


**Figure 6.38 - Haemolysis of RBC's incubated with increasing polymer amount: PEI 25 kDa; PEI-graft-p($HEG_{63\%}$-$GuAEG_{37\%}$) 25 kDa; p(DMAEG) 80 kDa; p($HEG_{63\%}$-$GuAEG_{37\%}$) 9.6 kDa.**

Although haemolytic activity is not unilaterally connected with cationic charges as confirmed for p(DMAEG), a substantial influence of the amount of positive charge is noticed in the case of p(ARG) (Fig. 6.39). Already at a concentration of 1 µg/ml, more than 30% of lysis was detected and complete rupture of cell-membranes was achieved at polymer concentrations relevant for polyplexes (≈ 100 µg/ml). If copolymerization with neutral functional groups (≈ 50%) was carried out, reduced values of lysis were measured (10% or less). This reduction was noticed in case of copolymers containing either guanidine or tertiary amine functional groups with a slight preference towards tertiary amines groups as they exhibited the lowest values. Additionally, from these results, the effect of guanidine presence on haemolysis can be directly correlated (as being negative) but also the influence of the side-chain composition on lysis is clear from the difference between ARG & GLN copolymers. Imidazole-containing polymers displayed a positive effect on haemolysis (in combination with guanidine groups).

Besides cationic charge, secondary effects like hydrophobicity influence haemolysis to a certain extent. This is for instance clear, if only limited, for the different haemolytic effect between p(HEG-GuAEG) and p(HEG-ARG) where the influence of side-chain plays a role.

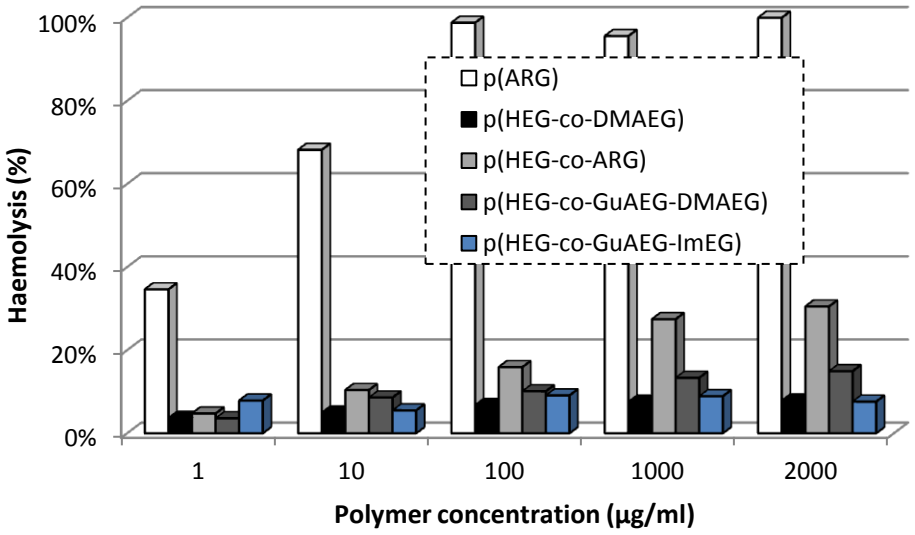


**Figure 6.39 – Haemolysis of RBC's incubated with increasing polymer amount: p($HEG_{39\%}$-$DMAEG_{61\%}$) 11.9 kDa, p(ARG) 22.8 kDa, p($HEG_{58\%}$-$ARG_{42\%}$) 11.2 kDa; p($HEG_{50\%}$-$DMAEG_{27\%}$-$GuAEG_{23\%}$) 9.3 kDa; p($HEG_{49\%}$-$GuAEG_{15\%}$-$ImEG_{36\%}$) 12.2 kDa.**

The MW of the applied polymers seems to have little to no influence on the haemolytic activity (Fig. 6.40), both at high and low concentrations. Furthermore, the copolymers composed of hydroxyl and tertiary amines show again the lowest amount of RBC-rupture over almost the entire concentration range. In all cases, the resulting membrane destabilisation and corresponding lysis for polymer concentrations that are used in typical polyplex compositions remains below 10%.

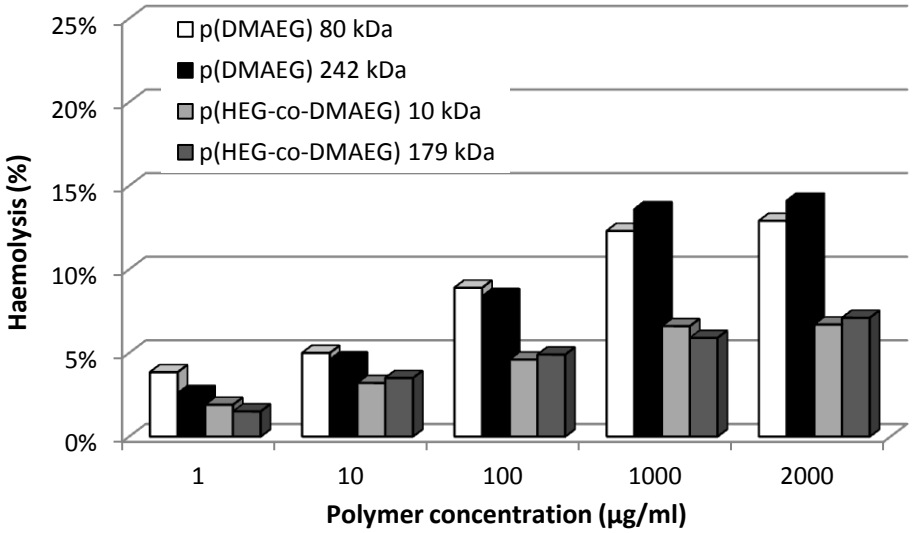


**Figure 6.40 – Haemolytic activity of pDMAEG and p($HEG_{39\%}$-$DMAEG_{61\%}$), high and low MW.**

In the above mentioned graphs, results of RBC's incubated with polymers were shown. When polymers are combined with DNA into complexes, reductions in haemolytic behaviour are to be expected since cationic charge are partially neutralised by the presence of DNA. In contrast to this hypothesis, the measured values appear to be equal or even higher than those corresponding with pure polymer (at equal concentration). Besides PEI, the highest values are obtained for polyplexes on arginine-rich polymers which confirms the intensely charged nature of this functional group compared to p(DMAEG)-based polyplexes. This was confirmed if copolymers were analysed. Whenever guanidine functional groups are present, the resulting haemolytic activity is proportional to the relative amount present in the polymer structure. Polymers that are combined with hydroxyl groups as neutral units exhibit relatively low haemolysis. Finally, the positive effect of grafting in terms of decreased haemolytic activity is again noticeable for PEI, where p(HEG-GuAEG) grafts reduce lysis by almost 50%. The relative ratio of haemolysis for the different type of polymers is reflected in the results for polyplexes (Fig. 6.41).

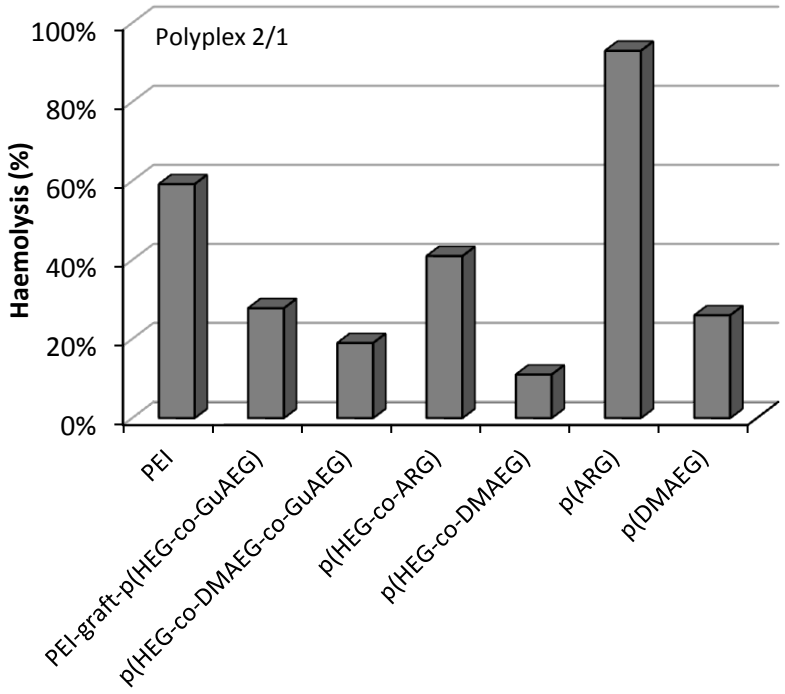


**Figure 6.41 – Amount of RBC-haemolysis provoked by polyplexes at a CR of 2/1.**

*5.1.3.2 Vectors based on polymethacrylates*

Similar to its biodegradable counterparts, the lysis effect of polymethacrylates was assessed and compared to PEI to allow correlation with other polymer classes. As a first analysis, the influence of MW on RBC membrane disruption was established for p(DMAEMA) compounds of different MW (Fig. 6.42). The variation in observed values gives preference to the use of small compounds as the polymer with a MW of 12 kDa gives rise to the lowest increment

when applying higher polymer concentrations. With increasing MW, the corresponding haemolytic values reaches higher peaks. For all p(DMAEMA) compounds, a plateau value is reached at a concentration of about 100 µg/ml and the extent of this value is proportional to the MW. Replacing tertiary amines with hydroxyl groups is also for this class of polymers beneficiary in reducing membrane disruption. Already 40 % of neutral units are sufficient to keep the haemolytic effect below 5% irrelevant of the concentration applied. Guanidine functional groups (40%) caused a negative influence at all tested polymer concentrations even considering the significant presence of neutral groups and relatively low MW (29 kDa).

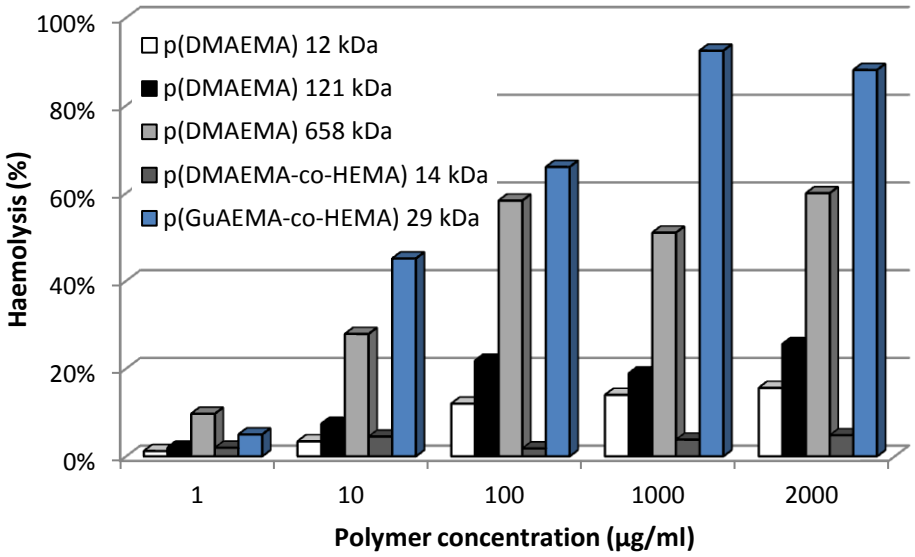


**Figure 6.42 - Haemolysis of RBC's incubated with increasing polymer amount: p(DMAEMA) with variable MW; p(DMAEMA$_{61\%}$-HEMA$_{39\%}$) 14 kDa and p(HEMA$_{60\%}$-GuAEMA$_{40\%}$) 29 kDa.**

When extending the influence of polymers on RBC's to polyplexes, the trends visualised in figure 6.41 were likewise noticed (Fig. 6.43). For DMAEMA-based polymers with different MW, the haemolytic activity displays again a proportional ratio relative to the MW. Also the influence of the CR on haemolysis is in general proportional but the discrepancy between the different applied CR's is more pronounced for polymers that already exhibit a significant activity at low CR (e.g. 1/1). The low effect of the p(DMAEMA-HEMA) combination on haemolysis was again clearly marked in this test with values lower than 10% but this result was not better than p(DMAEMA) with an equal MW. If polyplexes based on p(DMAEMA-AEMA) were used, a rather insignificant increase of lysis was noted. In all cases the effect of the MW was obvious and most significant, more specifically where low MW compounds display the best behaviour towards RBC haemolysis and a rapidly increasing level of membrane disruption is only to be expected for high MW polymers (> 200 kDa). Compared

to the reference value of PEI, polymethacrylate-based complexes perform better in terms of membrane disruption at any given MW, concentration or composition tested.

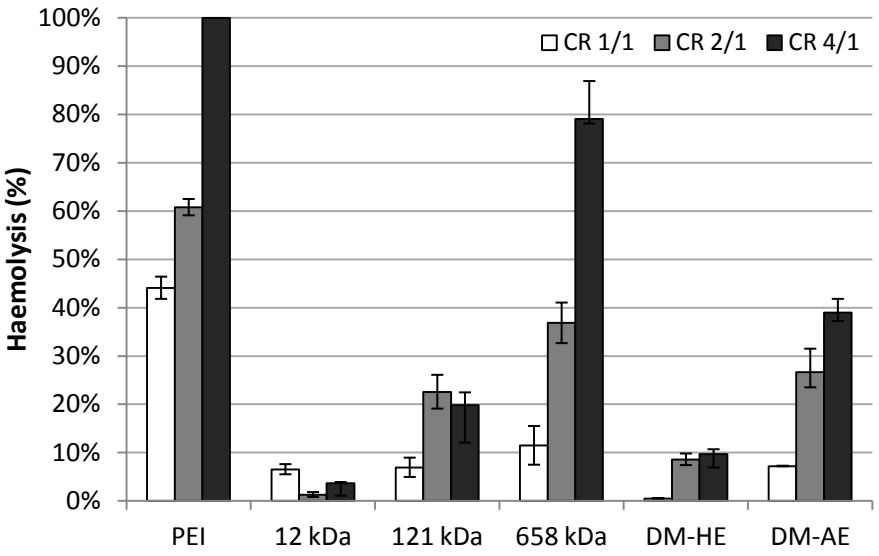


**Figure 6.43 – RBC lysis induced by polyplexes based on p(DMAEMA) 12–121–658 kDa; p(DMAEMA$_{55\%}$-HEMA$_{45\%}$) 9.8 kDa and p(DMAEMA$_{54\%}$-AEMA$_{46\%}$) 135 kDa.**

## 5.2 Haemo-agglutination

### *5.2.1 Description & experimental set-up*

One of the main functions of erythrocytes in the human body, is the delivery of $O_2$ to tissue all over the body. For that, RBC's need to have sufficiently small dimensions so that delivery in narrow spaces and poorly accessible places, like for instance via blood capillaries (d ≈ 10 µm) is achievable. Given the normal size of a RBC (6-8 µm, see also Fig. 6.37), it is clear that not much additional space is available to manoeuvre through those channels. If mutual interaction of RBC's would cause aggregation of individual cells (agglutination), the smallest capillaries would easily get clogged leading to miniaturised versions of thrombosis[24]. This phenomenon should therefore be carefully considered when applying foreign substances like vectors into the body. It has been demonstrated that some polycations induce agglutination RBC's, even at very low concentrations (several µg/ml) while this effect was not observed for cationic monomers hence the cause is most likely of macromolecular origin[25]. Neutral or anionic polymers on the other hand do not affect the agglutination behaviour of RBC's. Structural parameters that are important for agglutination effects are amongst others based on the amount of charge, the functional groups applied (hydrophilicity) and their corresponding conformation.

Since all polyplexes employed for this research exhibit a positive surface at a CR of 2/1, both polymers and polyplexes were subjected to a haemo-agglutination test. For this test, a 2%

RBC suspension in HBS was prepared as described above (section 4.1.2) and combined with either a polyplex solution or with a polymer solution that represents an equal amount of polymer as the amount mixed in a 2/1 CR complex. These solutions were then incubated for 1 hour at 37 °C, followed by optical microscopy for 2D visualisation.

### *5.2.2 Results for poly-α-amino acids*

Using optical microscopy, the effect of the cationic polymers and their polyplexes on RBC's was studied. As a negative control, RBC's were also incubated in pure buffer (HBS) to allow comparison of the level of agglutination. From figure 6.44 (left), an abundant amount of individual cells can be noticed for the negative HBS control without indications of agglutination. Lighter coloured shapes represent RBC's that are oriented orthogonal to the incident light beam and appear to partially escape the focal plane, a limitation of this 2D-visualisation method. When RBC's were exposed to polyplexes containing pDMAEG, again no significant coagulation effect was perceived. The individual cells are clearly distinguishable and appear with a shape and size correspondent with the negative standard while for pure pDMAEG a considerably higher amount of coagulation is detected. Combining the vector with DNA, has in this case a positive effect on the interaction with RBC's. Additionally, small areas in the pictures mark crystallized salt depositions and should not be confused with the occurrence of agglutination phenomena.

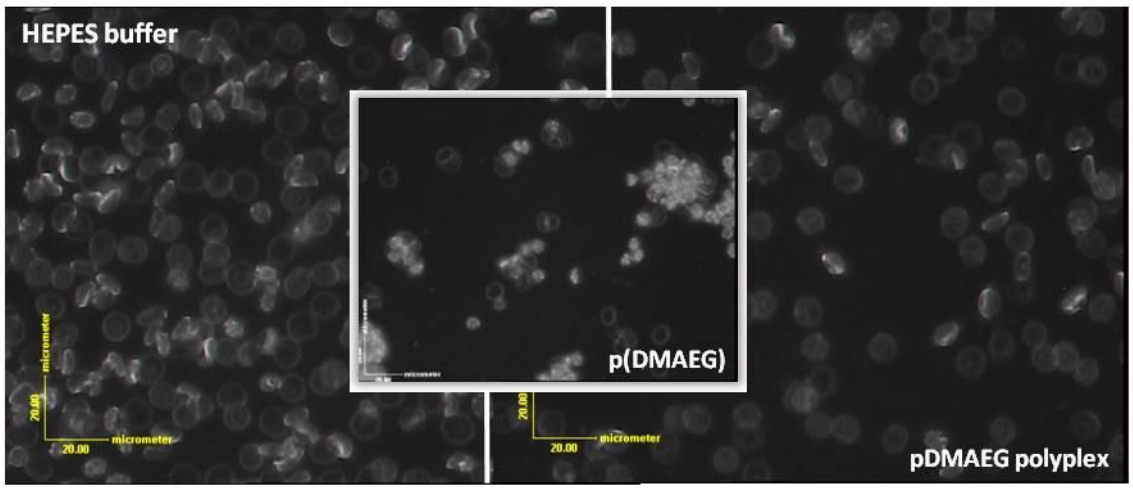


**Figure 6.44 - Agglutination effect of HEPES buffer and pDMAEG - 30 kDa (including polyplex CR 2/1) on RBC's after 1h of incubation (200x).**

In comparison with fully charged polymers, the incorporation of neutral hydroxyl groups (38% HEG) demonstrates no agglutination effect as anticipated (Fig. 6.45). Both for low (11.9 kDa) and high (179 kDa) MW, individually distributed cells could still be detected. If pure p(DMAEG-HEG) was brought into contact with RBC, only the low MW compound showed no

coagulation while for the high MW derivative, rather unexpected, severe agglutination was observed, an effect for which no unambiguous solution is to be found but which should at least find its origin in the different macromolecular size and its inherent kinetics.

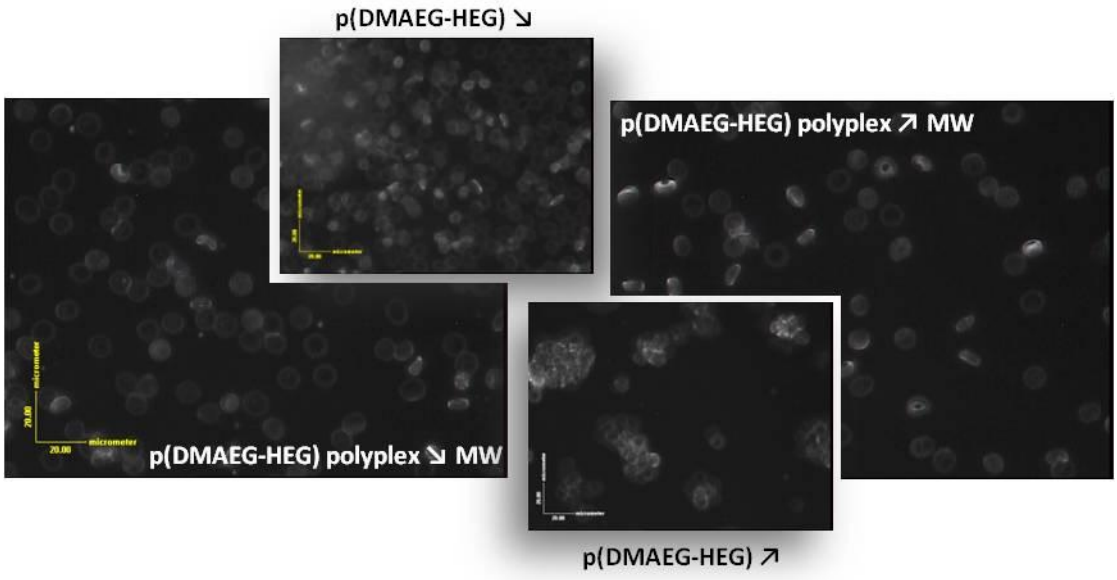


**Figure 6.45 – Haemo-agglutination of p(DMAEG$_{62\%}$-HEG$_{38\%}$) with a high (179 kDa) and low (11.9 kDa) MW and their polyplexes (CR 2/1) at 200x magnification.**

The presence of guanidine functional groups, compared to tertiary amines, exerts a higher influence on membranes which results in an elevated agglutination degree for polyplexes and nearly complete coagulation of the pure p(HEG$_{57\%}$-GuAEG$_{43\%}$) with a MW of 143 kDa (Fig. 6.46). This considerably, negative effect is due to both the high MW and the nature of the functional group itself. When this polymer, composed of a combination of tertiary amine, hydroxyl and guanidine functional groups, p(HEG$_{50\%}$-GuAEG$_{27\%}$-DMAEG$_{23\%}$) – 9.3 kDa, is applied, a substantial improvement is observed for the polyplex as well as for the pure polymer in terms of haemo-agglutination. In accordance with haemolysis tests, tertiary amine-based polyglutamines perform better than guanidine-based ones. On the other hand, when guanidine residues were derived from polyarginine and combined with hydroxyl-based polyglutamines, the resulting p(HEG$_{58\%}$-ARG$_{42\%}$) and its polyplexes performed better, in other words causing almost no agglutination and substantially less than p(HEG$_{57\%}$-GuAEG$_{43\%}$) allthough an effect of the lower MW should be taken into account as well. In addition, the homopolymer p(ARG), was not able to prevent clustering of cells both on the level of polyplexes as well as for free polymers and yielded the largest aggregates of all the tested polymers (d ≈ 20-50 µm). As a preliminary conclusion, the influence of hydroxyl functional groups clearly has a positive effect on haemo-agglutination (and to a larger extent on biologically related processes).

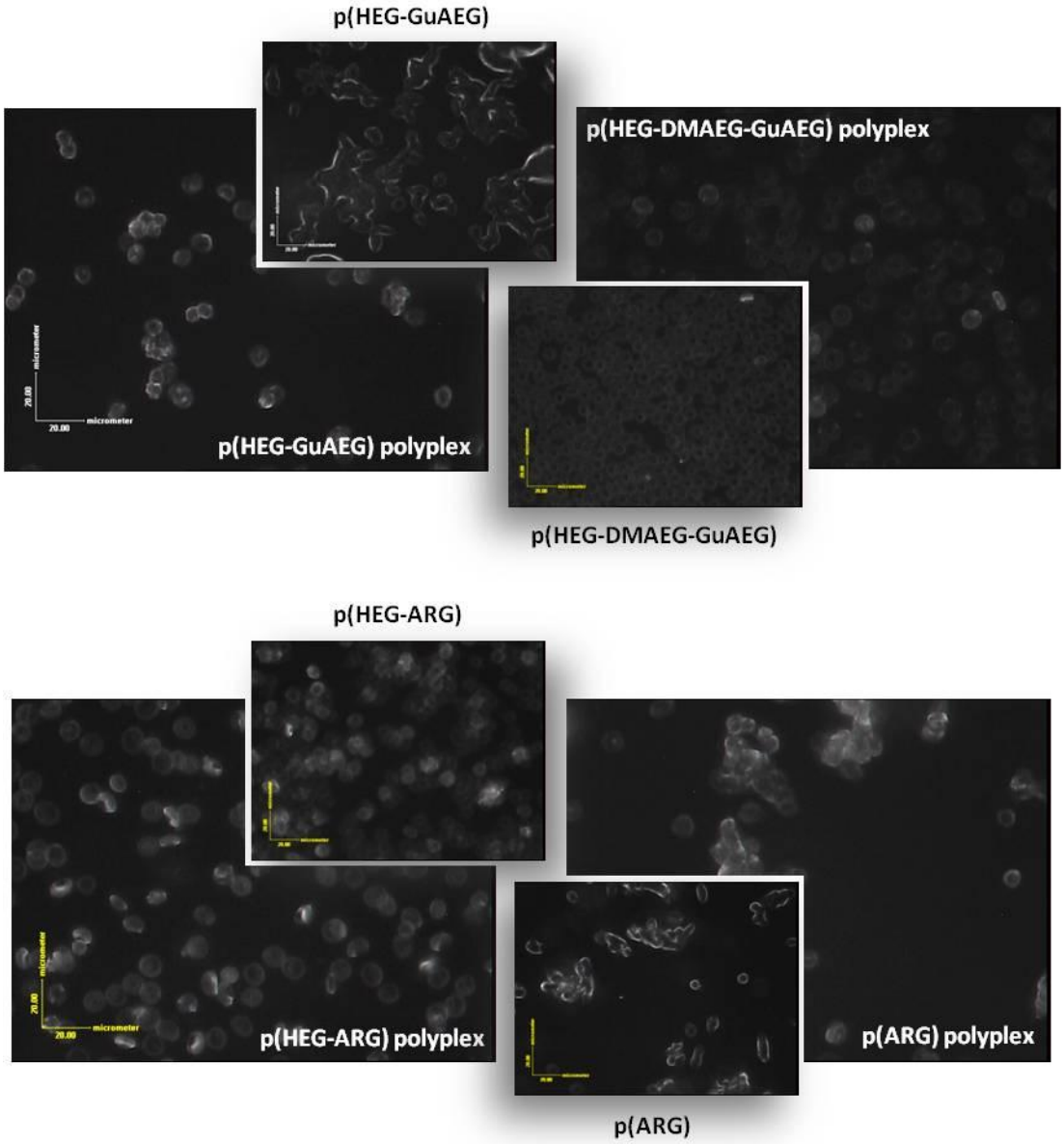


**Figure 6.46 - Haemo-agglutination of p(HEG$_{57\%}$-GuAEG$_{43\%}$) – 143 kDa; p(HEG$_{50\%}$-GuAEG$_{27\%}$-DMAEG$_{23\%}$) – 9.3 kDa; p(HEG$_{58\%}$-ARG$_{42\%}$) – 11.2 kDa and p(ARG) – 22.8 kDa, including their polyplexes (CR 2/1) at 200x magnification.**

Other functional groups (or combinations) like imidazole or a CPP such as penetratine (PEN), were likewise subjected to aggregation tests (Fig. 6.47). The covalent coupling of PEN to p(DMAEG-AEG) for a total of about 2% did not cause extra clustering when compared to pDMAEG as such but the effect remained signifcant. The corresponding polyplexes were able to mask the considerable clustering arising from the pure polymer. Imidazole-containing polymers can be considered as ideal candidates for blood-related applications since both haemolysis and agglutination did not occurr, even in combination

with guanidines. Moreover, the agglutination difference between pure polymer and the polyplex is minimal, confirming the non-toxic behaviour of imidazole containing compounds.

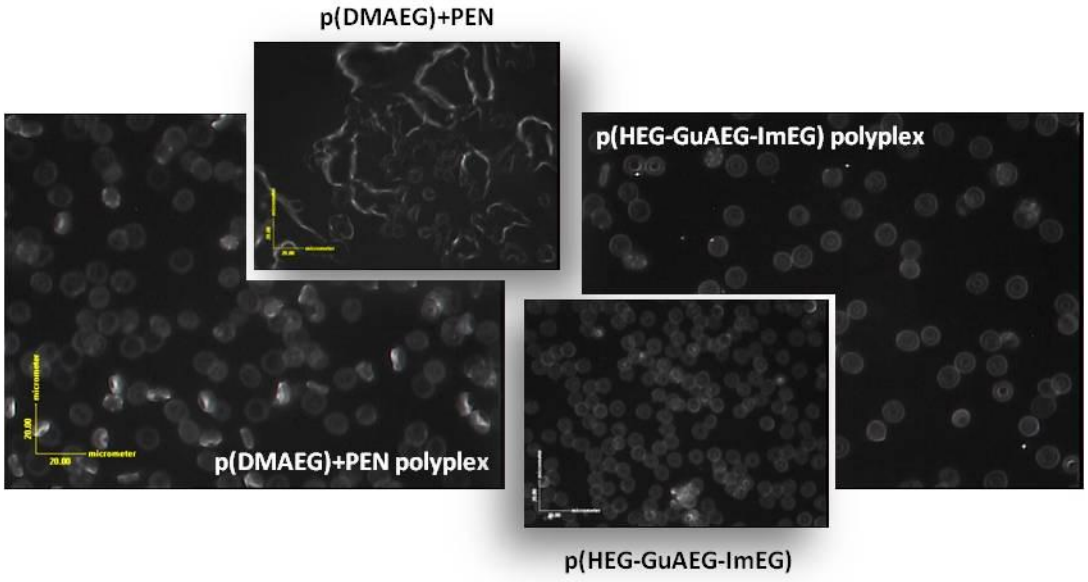


**Figure 6.47 - Haemo-agglutination of p(DMAEG$_{85\%}$-AEG$_{15\%}$)+PEN and p(HEG$_{49\%}$-GuAEG$_{15\%}$-ImEG$_{36\%}$) – 12.2 kDa (including polyplex CR 2/1) at 200x magnification.**

Reference values were based on the agglutination results of PEI (Fig. 6.48), which were in correspondence with previous haemolysis experiments that showed significant, membrane interactions. Few individual cells were left and a notable amount of cells were deformed. The advantage of grafting onto PEI to compensate for the negative impact of native PEI, was established for PEI+p(HEG$_{63\%}$-GuAEG$_{37\%}$). A higher amount of cells as well as a more homogeneous occurrence of naturally shaped RBC's were noticed for the polyplexes. Also for the polymer as such, a slight improvement was identified. Contradictory to the effects of its separate components (PEI & p(HEG$_{63\%}$-GuAEG$_{37\%}$)) for which both demonstrated high levels of haemo-agglutination, the modified conformation and spatial rearrangement of charged groups of the complete polymer provokes lower membrane interactions, even when incorporated in a polyplex, hence the reduced coagulation. This effect is expected to be more outspoken at higher CR's where increased quantities of polymers will be present at the outer boundary of the polyplex particle.

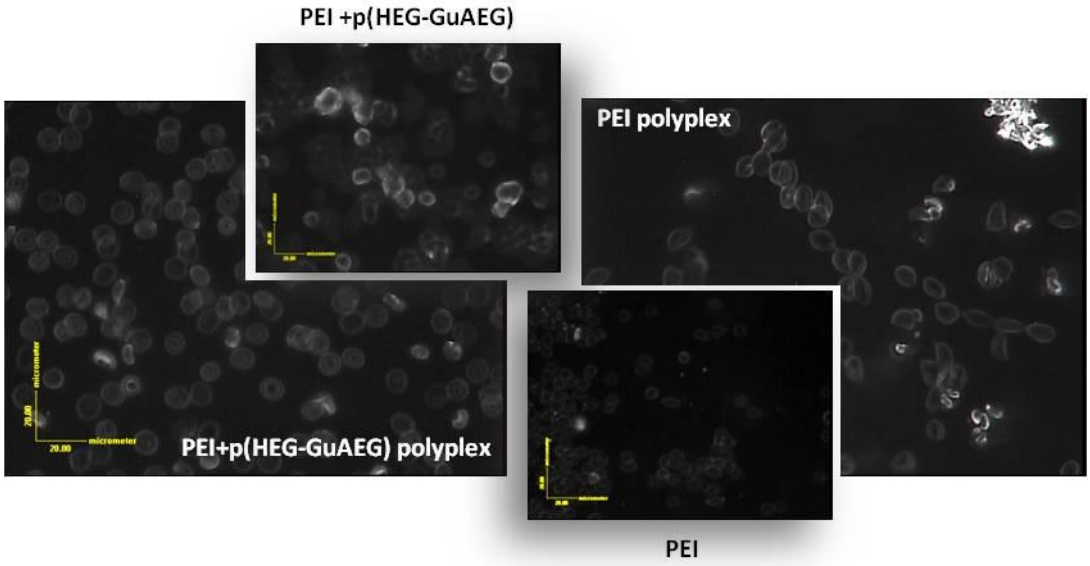


**Figure 6.48 – Haemo-agglutination of PEI & PEI+p(HEG$_{63\%}$-GuAEG$_{37\%}$) (+ polyplexes (CR 2/1)).**

### *5.2.3 Results of polymethacrylates*

In general, polymethacrylates tend to exhibit a higher degree of agglutination when combined with RBC's compared to polyglutamines. A striking observation could be derived from a MW stud that focuses on the increase in agglutination for pDMAEMA with augmenting MW (Fig. 6.49). At the lowest MW (12 kDa), very limited clustering was noticed, yet irregularly shaped cells (non-circular) occurred. For polymers with a medium MW (121 kDa), the degree of clustering was already of such a level that few single cells could be observed and mainly clusters of almost 30 µm in size were seen. The highest MW compound (658 kDa) induced full agglutination leaving no single cells and thereby formed cell-aggregates up to 40 µm. Also for methacrylate-based copolymers, the agglutination effect was dominantly influenced by the MW which is clearly marked by p(DMAEMA-HEMA) with a low MW that displays limited aggregation whereas a similar polymer structure with higher MW (Fig. 6.49) give rise the formation of large cell clusters. The appearance of large clusters starts already at a medium polymer MW (100-150 kDa) and was again confirmed for p(DMAEMA-AEMA) with a MW of 135 & 176 kDa repsectively. It has to be indicated that the best result of the developed polymethacrylate compounds and polyplexes is considerably worse than in the case of polyglutamines (and their polyplexes). The reason for the importance of the MW can not be readily traced back to physico-chemical properties like polyplex size or DNA-interaction as no clear difference amongst them could be derived but must be influenced by kinetic (polymer mobility & hydrodynamic radius of the polymer) and thermodynamic (intra- and intermolecular forces) differences in polyplex formation.

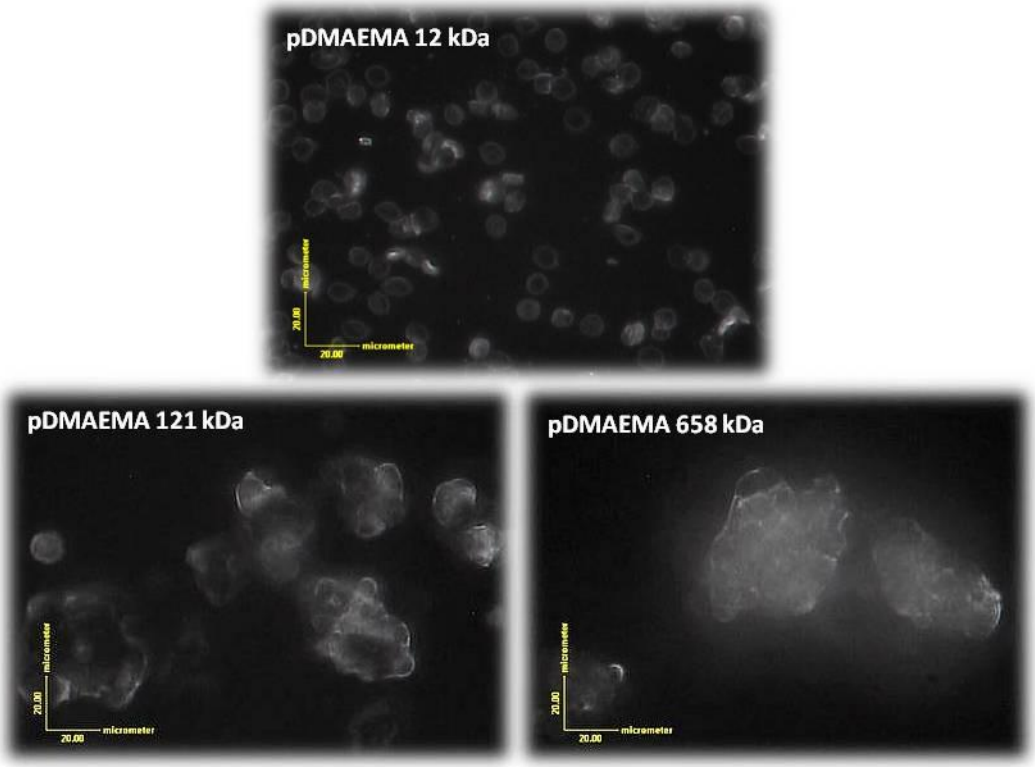


**Figure 6.49 - Haemo-agglutination of pDMAEMA based complexes (CR 2/1) (200x).**

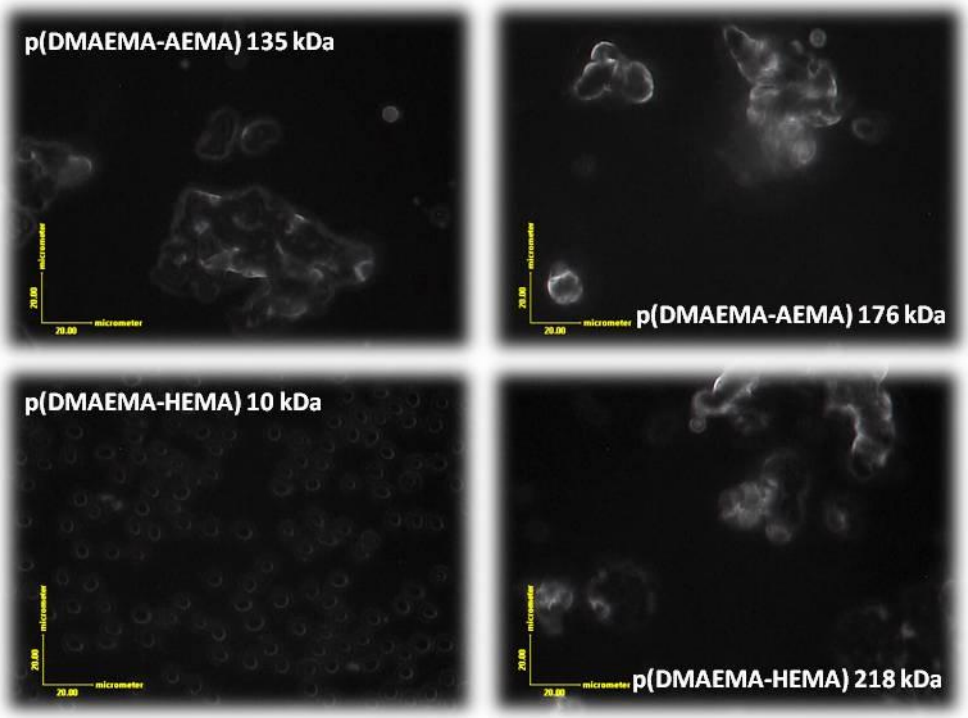


**Figure 6.50 - Haemo-agglutination of polyplexes (CR 2/1) derived from: p(DMAEMA$_{54\%}$-AEMA$_{46\%}$) 135 kDa; p(DMAEMA$_{73\%}$-AEMA$_{27\%}$) 176 kDa; p(DMAEMA$_{55\%}$-HEMA$_{45\%}$) 9.8 kDa and p(DMAEMA$_{56\%}$-HEMA$_{44\%}$) 218 kDa.**

## 5.3 Histologocial data

Because the final application of gene therapy should comprise of *in-vitro* and *in-vivo* techniques, the possible influence of genetic vectors and polyplexes on biological aspects such as cell-cycle, apoptosis or the survival of whole tissues, has to be assessed. Many of these criteria can be investigated by histological experiments that give an basic understanding of cell-toxicity, viability, metabolic activity and stimulation of cellular growth. Within the PolExGene project this investigation was carried out by the institute of microbiology (IMIC, academy of sciences of the Czech republic, Prague). An brief summary of their conclusions is shown below.

To assess if a cell remains healthy after addition of a foreign compound, many assays exist nowadays that aid in the evaluation. One of such methods that is generally applied to determine proliferation of cells and their potential to keep dividing find its origin in $^{3}$H-thymidine incorporation. Tritium-containing thymidine counts as a radioactive label and is provided within the buffer medium. When mitosis occurs, the cells will take up this radio-labelled molecule from its surrounding enabling subsequent detection by a liquid scintillation counter. Repeated cell-division cycles incorporate consequently more tritium and increases sensitivity, hence longer incubation times need to be respected (24-48 h)[26].

The experimental evaluation of polymers and polyplexes in terms of proliferation was performed on mouse spleen cells (BALB/c). The standard protocol for polyplex formation was applied and tissue culture plates (96FB) were provided with 500.000 cells per well. An amount of 600 ng DNA was added to each well and both polymer as well as polyplex representing a CR of 4/1, 2/1 and 1/1 were used for incubation with cells. Two hours after incubation, the cells were washed and fresh medium (RPMI 1640, glutamine, antibiotics, 2-ME 0.005 M and 10 % fetal calf serum) was added. One batch of samples was loaded with a mitogen, pokeweed mitogen (PWM – 1 µg/ml), an enzyme which stimulates the occurrence of mitosis, while the other was left as such. The cells were cultivated after 3 days and the amount of $^{3}$H-thymidine was measured accordingly.

The corresponding results for PEI are displayed below (Fig. 6.51). For polyplexes, the proliferation was higher than for pure polymers and at a low CR, the activity approached the level of the control test which is equal to the distribution of pure DNA among the cells, without the presence of a vector. Again the activity increased with decreasing polymer concentration (amounts representing a 4/1, 2/1 & 1/1 CR). Moreover, the sensitivity was higher for denser populated wells.

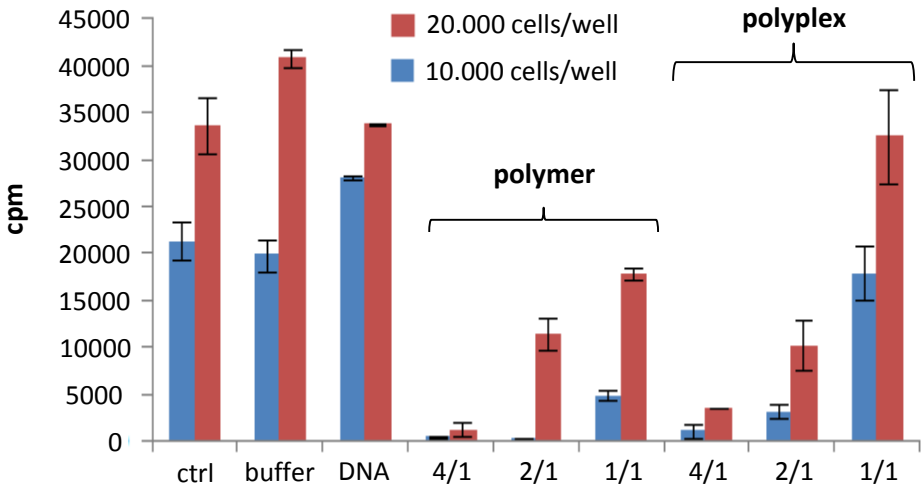


**Figure 6.51 – $^{3}$H-thymidine assay of PEI on BALB/c cells: level of proliferation**

When pDMAEG with a MW of 80.000 was used, the obtained results demonstrated higher biocompatibility (Fig. 6.52). Because at low CR's, the activity of cells incubated with pDMAEG-based complexes was elevated compared to the control, the polyplexes were labeled as (limited) stimulators as their value reached as high as 2.5. The stimulation index of cell proliferation via the $^{3}$H-thymidine assay was determined from the amount of cells present for the control signal and set to 1 for further comparison. Whereas the presence of pokeweed mitogen has no influence on cellular activity in buffer or DNA-containing solutions, the effect on polymer and polyplex incubated cells was positive for all CR's and is the main driver for the increase in stimulation properties rather than the type of polymer used (as derived from the result for PEI and pDMAEG). The use of the polymer alone resulted in a decrease in viability rather than in a stimulation of the cell proliferation.

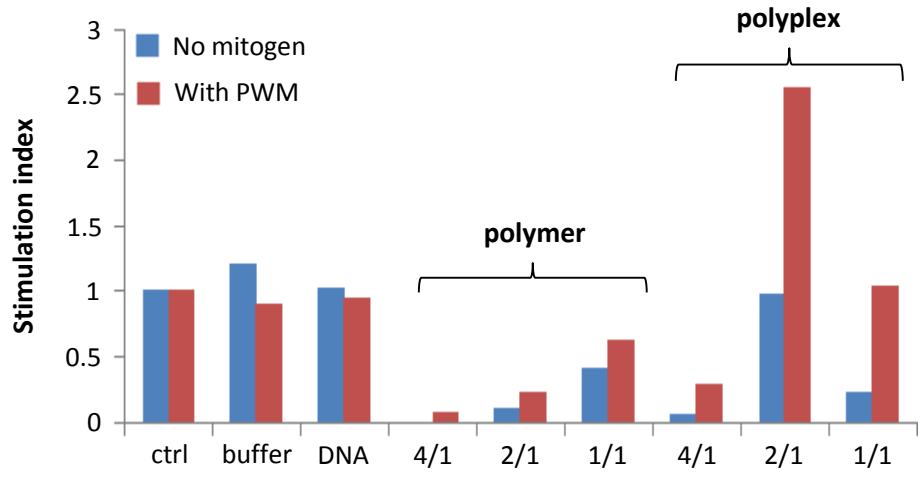


**Figure 6.51 - $^{3}$H-thymidine assay of p(DMAEG) on BALB/c cells: stimulation index (ctrl = 1)**

The compatibility on cell proliferation was also investigated for other polyglutamines and was able to confirm the positive effect of the PWM and the advantageous use of polyplexes rather than polymers in stimulating cell proliferation although this later effect was always very small. The effect of the MW variation is in favour of low MW compounds and the covalent coupling of a CPP did not really influence the proliferation behaviour (in-line with previous viability experiments). The copolymer, composed of 63% hydroxyl groups and 37 % guanidine functional groups and a MW of 9.6 kDa was able to achieve the higher values for cell proliferation/stimulation with respect to the control.

## 6 Confocal microscopy

A huge drawback in fully understanding genetic manipulation is the behaviour of polyplexes once they are internalised within the cell and subsequently move towards the nucleus of the cell for genetic transcription. Because this phenomenon is complex, most hypotheses that are put forward as feasible solutions on how the polyplex could be taken-up and guided through the cytosol focus generally on a specific compound of the polyplex (polymer or DNA). As a result, some polymers and polyplexes were subjected to a confocal microscopy study in order to obtain extra information on intra-cellular properties. This was done by the group of Dr. Alain Joliot as mentioned before. This analysis technique enables the identification of specific molecules within the cell by fluorescent spectroscopy. In this way, the contents of the cell can be visualised without affecting the integrity of the cell. The compounds that will be visualised are to be provided with a fluorescent tag that corresponds with the laser detection[27]. Moreover, only the detection of molecules lying in the focal plane can be detected, which allows for the analysis at specific depths of the cell (dividing it in layers). As previously mentioned (section 6.2), a list of fluorescently labelled (Oregon Green 488) polymers were synthesised for this reason. When combined with DNA (with or without fluorescent tag), the resulting polyplex can be tracked *in-vitro*.

An example of confocal imaging is shown in figure 6.51 where a fluorescently-labelled derivative of PEI is visualised and shown to be localised at the borders of HEK 293 cells. When different polymer-based DNA complexes are added, different morphologies can be detected. PEI-based polyplexes tend to give a more diffuse appearance whereas the p(DMAEG) of 80 kDa yields polyplexes that are present as intensily coloured, smaller dots, characteristic for the stronger interaction with DNA (as was confirmed by EtBr fluorescence exclusion).

If polyplexes are mixed with cells *in-vitro*, the first step towards delivery of therapeutic genes is achieved by crossing the cell membrane. In order to visualise this process, cells incubated

with polyplexes are analysed at different time points to give an idea on the location inside the cell. Since fluorescence signals are only detected in a 2D-plane and a perceived signal can be the result of more than one fluorescently active compound on the same Z-axis, a specific compound is added to the cell medium that enables to distinguish between intra-cellular and extra cellular fluorescence.

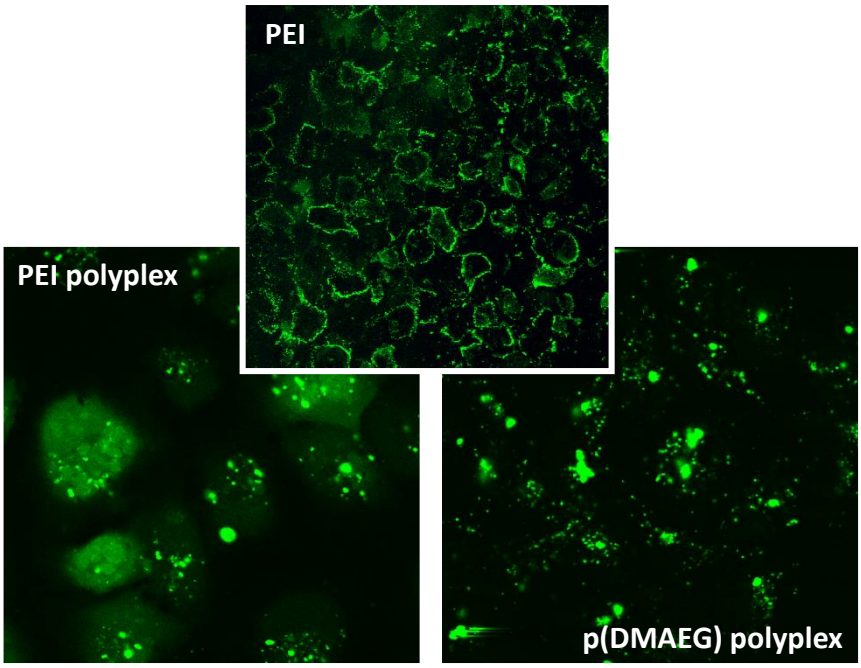


**Figure 6.51 - Confocal images of PEI-OREG, PEI-OREG/DNA and p(DMAEG)-OREG/DNA.**

This product, Tryphan Blue® (TB), is a dye that can not pass the membrane of living cells but is able to traverse the membrane of dead cells and consequently stain them blue. Due to the addition of TB, the ECM is quenched and accordingly the fluorescent signal of non-internalised polyplexes is removed which allows only fluorescence of internalized polyplexes to be detected. In the case of incubation with PEI-based complex for 4h (Fig. 6.52), diffuse polyplex signals are observed as well as small particles (A). When TB is added, the extra-cellular fluorescence is quenched and the remaining fluorescence can be attributed to a considerable amount of internalised polyplexes which appear again in a diffuse state (B). For a prolonged incubation (24h) the fluorescence signal seems to be higher and in a more evenly spread, diffuse pattern (C). Likewise, the addition of TB demonstrated that the polyplexes where taken up by the cells and that they were homogeneously distributed (D) compared to 4h incubation. From previous biological tests, it was established that pDMAEG expressed no transfection behaviour. If these results are linked to the confocal imaging (Fig. 6.53), it could be concluded that not only the lack of internalisation lies at the base of its failure. Because both after 4h and more specifically after 24h of incubation, a certain amount of polyplexes was able to be internalised (B/D), an error or problem in of the intermediate

process steps must still hamper the transfection process. As a result, a substantial group of polyplexes are lost due to the take-up incapacity by the cell as revealed by the discrepancy in fluorescence before (A/C) and after BT staining (B/D). Furthermore, the internalised polyplexes remain visible as small, clearly defined, coloured spots which could be indiciative for the incapacity to escape the endosomes (most likely, due to the limited buffering properties) or the lack of polyplex dissociation inside the cytosol.

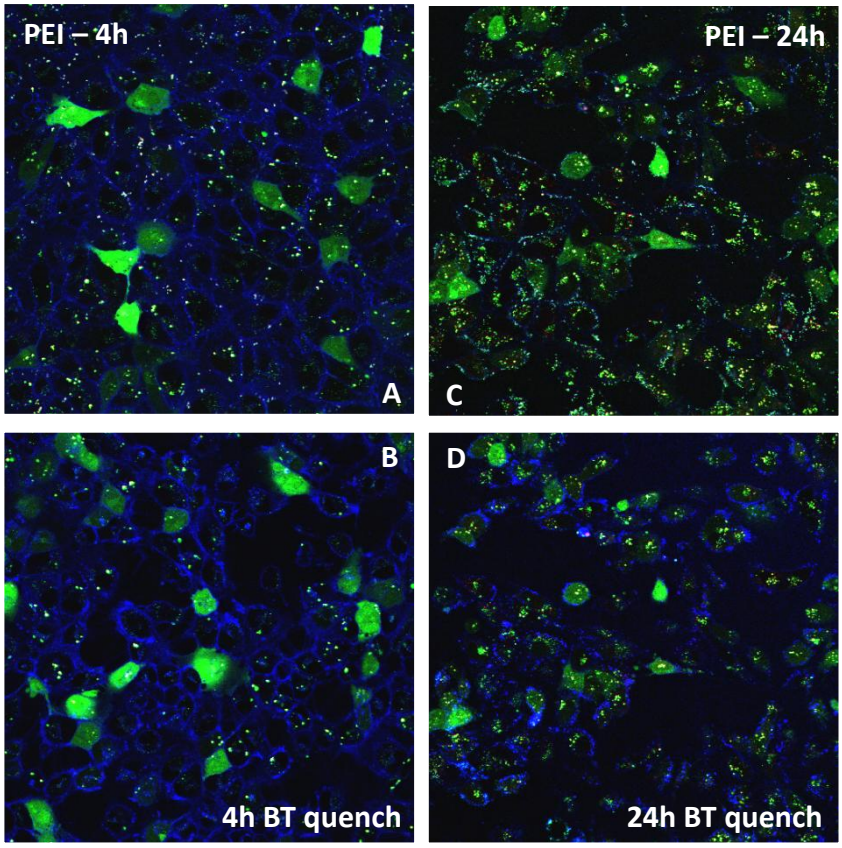


**Figure 6.52 – Confocal images of PEI complexes incubated for 4 & 24h, before & after BT.**

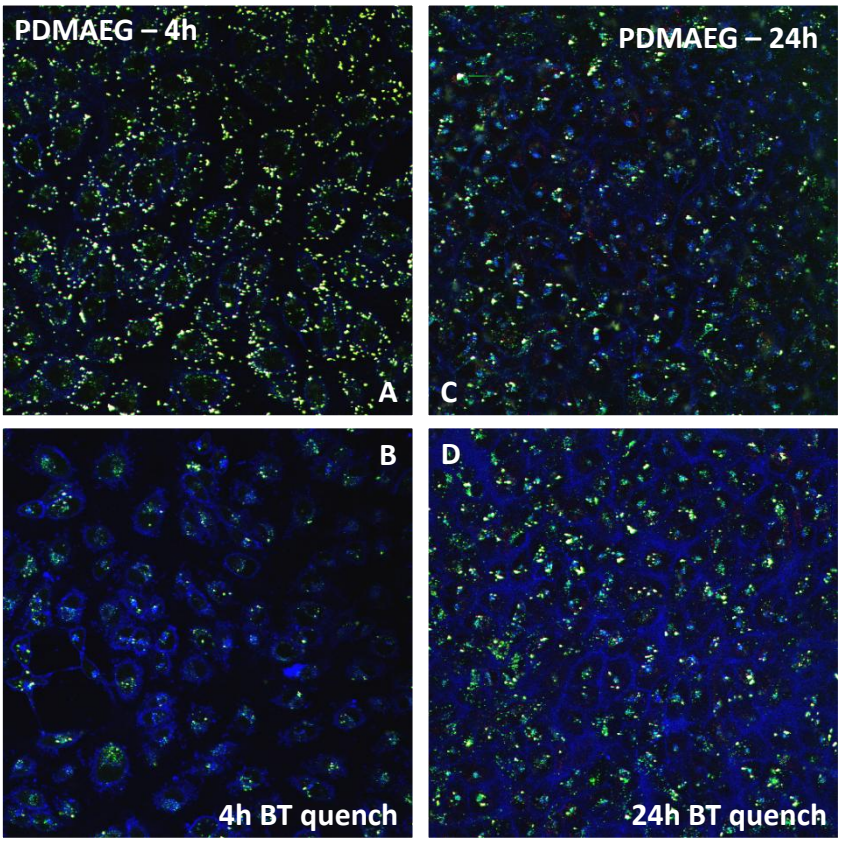


**Figure 6.53 - Confocal image of pDMAEG complexes incubated for 4 & 24h, before & after BT.**

It is possible to use non-labelled polymers in complexes and still be able to detect the resulting polyplexes by using fluorescently tagged DNA. From a therapeutic perspective, this could possible limit or even inhibit the function of the DNA involved leading to non-efficient transfection. In the following confocal images, pDMAEMA was examined without being fluorescently labeled. For DNA, a similar green-fluorescent-protein (GFP) is used to mark the molecule and at the same time provide the ability to translate and expresse a protein, which emits in this case a cherry red light. After 2h of incubation, it seemed that the pDMAEMA 121 kDa polyplexes were not yet internalised but could be retrieved at the borders of the cells (Fig. 6.54). When displaying only the green detection channel, the imaging is limited to visualising the green fluorescent polyplexes. If the cells are treated with wheat germ agglutinin (WGA), the cells are stained blue and it can be observed that the polyplexes collect at the borders of the cells (to be further internalised) as seen in the RGB (red-green-blue) picture from figure 6.54.

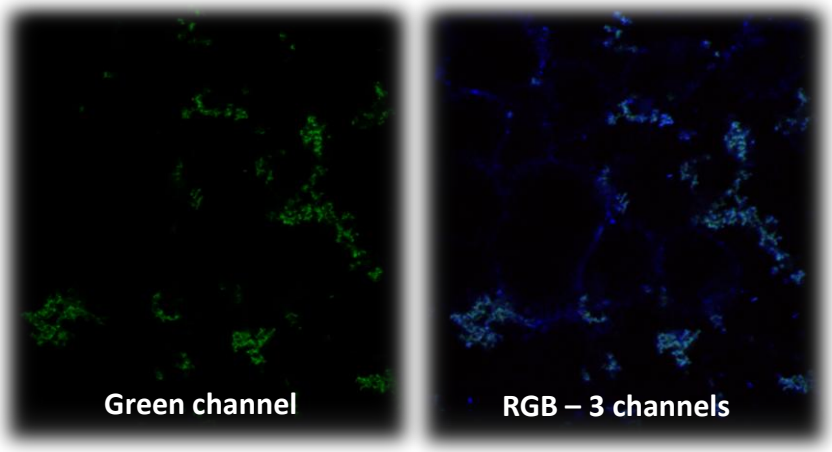


**Figure 6.54 – Confocal imaging of a pDMAEMA complex in Green & RGB detection mode.**

A similar explanation can be given for pDMAEMA 12 kDa based polyplexes. The polyplexes are situated at the border of the cells after 2h of incubation as visualised in figure 6.55 (RGB picture in which the cells are stained by WGA and no internalised fluorescence is detected). In contrast to the intensity derived from a DMAEMA polymer of 121 kDa, the polyplexes derived from 12 kDa pDMAEMA are considerably more intense, an effect that could be due to the higher ability to shield the fluorescently labeled DNA which is entangled by the polymer. This hypothesis is strengthened by the weak detection of polyplexes based on pDMAEMA with a MW of 658 kDa (visible as light blue spots in RGB detection, again at the borders of the cells). Moreover, the high toxicity of this compound is confirmed by the significant TB staining, representative of cell death (Fig. 6.56). In conclusion it is proven that for this family of amine containing polymethacrylates 2h is not sufficient for internalisation.

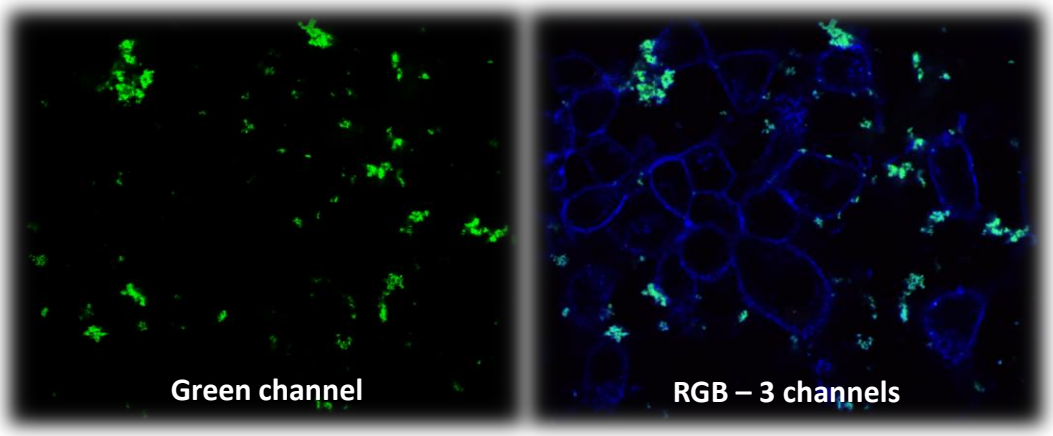


**Figure 6.55 – Confocal image of polyplexes based on pDMAEMA 12 kDa in Green/RGB mode.**

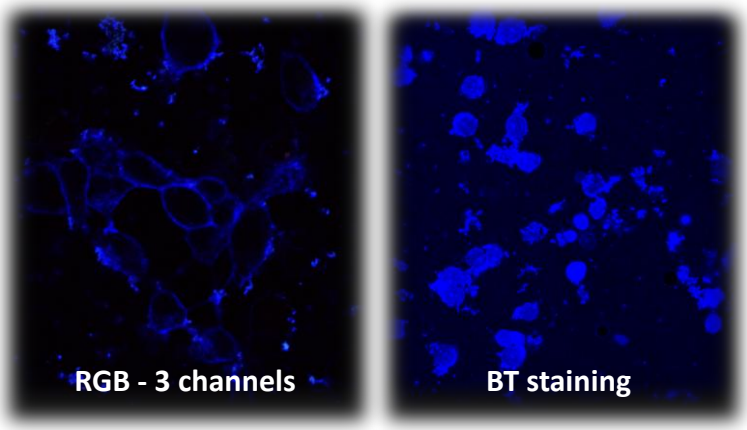


**Figure 6.56 - Confocal image of polyplexes based on p(DMAEMA) 658 kDa in Green/RGB mode.**

Successful transfection of cells is also visualised using confocal microscopy (Fig. 6.57). For PEI, protein expression is seen in image A after 24h of incubation. In this image the RGB detection covers the identification of the cells, marked by WGA (blue), the localization of the diffuse polymer pattern (green, indicative for homogeneous spread throughout the cell, most likely in combination with dissocation) and the emerging red signal originating from the transcribed protein. Once a cell is transfected, strong expression is observed over the entire cell volume. In image B, the non-internalised and better-defined polyplexes do not give rise to red fluorescence. Positive transfection results were likewise obtained for delivery systems that make use of pDMAEMA.

In figure 6.58, polyplexes based on pDMAEMA 658 kDa are visualised (RGB image). Analog to PEI, the protein expression is responsible for the strong discoloration of the cell (red fluorescence) while the borders of the cells are stained in blue and remaining green fluorescent spots confirm that certain polyplexes dit not yet fully dissociate (A). If the red channel detection (B) is isolated, only the signal coming from the produced protein is observed. When focusing specifically on the green fluorescence, randomly scattered polyplexes are visible as well as the diffuse pattern of dissociated polymer within the transfected cells.

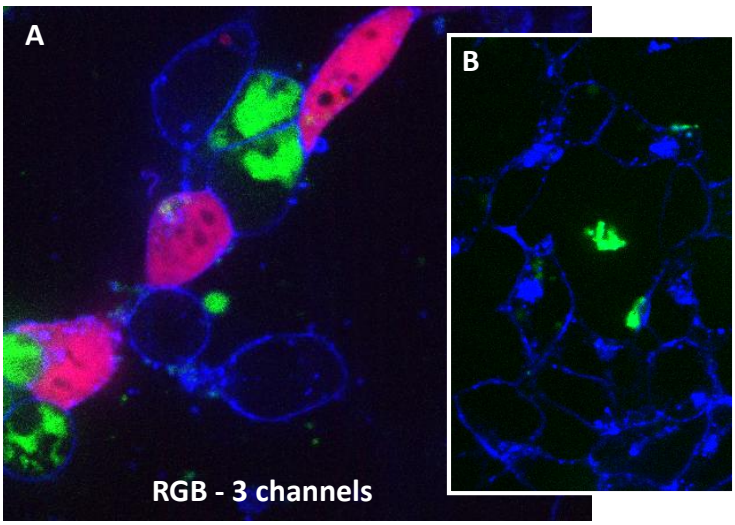


**Figure 6.57 – Confocal images of PEI-complexes: protein transcription with red light emission.**

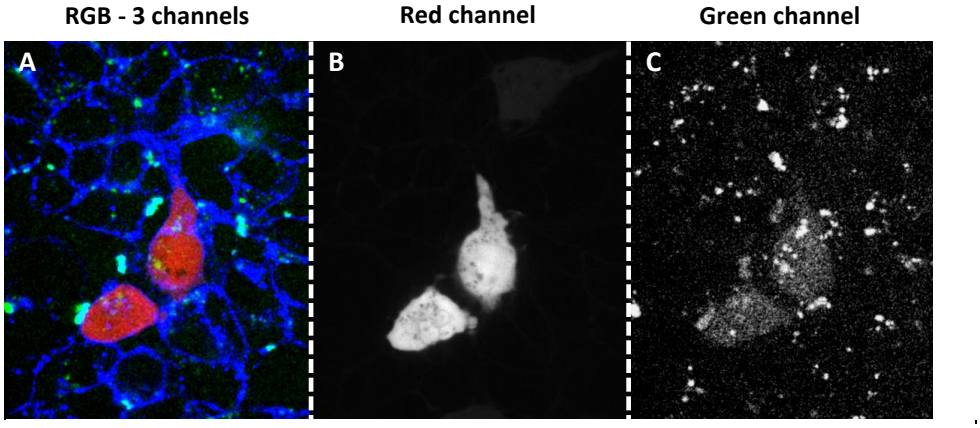


**Figure 6.58 – Confocal images of p(DMAEMA) complexes after 24h incubation: RGB detection (A), exclusive red channel detection (B) and exclusive green channel detection (C).**

## 7 Conclusion

During the extensive biological testing of the polymers and polyplexes developed for this doctoral research, several interesting properties of the applied polymers were exposed. Many different, individual conclusions could be derived from these results but in several cases, it was also possible to draw global conclusions. For instance, it was shown that all polymers can protect DNA from being degraded when the charge ratio is sufficiently high. The MW appeared to have almost no influence and also the composition was not crucial (as long as a minimal amount of charge was present). In the case of poly-L-glutamines, swift degradation of the polymer backbone was demonstrated in the presence of papaine as was the relevancy of catonic charge in delaying the degradation rate. The compatibility of most polymers with red blood cells was largely negative, especially for highly charged polymers where haemolytic and coagulation effects proved to seriously hamper the potential *in vivo* usage. The presence of neutral (hydroxyl/imidazole) functional groups on the other hand demonstrated high compatibility and in general, low MW compounds perform better in terms of biocompatibility compared to high MW polymers. Nearly all polymers that were produced during this research exhibited very low toxicity in *in vitro* cell tests (except high MW polymethacrylates and PEI derivatives). Unfortunately, a lot of vector candidates showed no sign of transfection activity. Nevertheless, positive results were retrieved for polymethacrylate derivatives that proved to be successfully internalised and able to express proteins by gene delivery. Also a few isolated cases of polyglutamines achieved high levels of transfection but no general trend could be detected. Finally, PEI modifications could be carried out that were able to reduce the inherent toxicity of PEI while preserving or even slightly increasing the biological activity.

# 8 References


[1] Sgouras, D. and R. Duncan (1990). "methods for the evaluation of biocompatibility of soluble synthetic-polymers which have potential for bio-medical use. 1. Use of the tetrazoluim-based colorimetric assay (MTT) as a preliminary screen for evaluation invitro cytoxicity." Journal of Materials Science-Materials in Medicine **1**(2): 61-68.

[2] Uptima – Uptiblue: cell viability assay (FT-UP66941) http://www.interchim.com/interchim/bio/produits_uptima/tech_sheet/FT-UP66941(UptiBlue).pdf

[3] Woo, J. and A. G. von Arnim (2008). "Mutational optimization of the coelenterazine-dependent luciferase from Renilla." Plant Methods **4**(23).

[4] Toncheva, V., M. A. Wolfert, et al. (1998). "Novel Vectors for gene delivery formed by self-assembly of DNA with poly(L-lysine) grafted with hydrophilic polymers." Biochimica Et Biophysica Acta-General Subjects **1380**(3): 354-368.

[5] Verbaan, F. J., G. W. Bos, et al. (2004). "A comparative study of different cationic transfection agents for in vivo gene delivery after intravenous administration." Journal of Drug Delivery Science and Technology **14**(2): 105-111.

[6] Wickstrom, E. (1986). "Oligodeoxycucleotide stability in subcellullar extracts and culture media." Journal of Biochemical and Biophysical Methods 13(2): 97-102.

[7] Kachalsky, A., D. Danon, et al. (1959). "Interaction of basic polyelectrolytes with the red blood cell II. Agglutination of red blood cells by polymeric bases." Biochimica et Biophysica Acta **33**(1): 120-138.

[8] N'Soukpoé-Kossi, C. N., S. Diamantoglou, et al. (2008). "DNase I - DNA interaction alters DNA and protein conformations." Biochemistry & Cell Biology **86**(3): 244-250.

[9] Kunitz, M. (1949). "Crystalline desoxyribonuclease (Digestion of thymus nucleid acids. The kinetics of the reaction.)." Journal of General Physiology: 363-377.

[10] Kunitz, M. (1949). "Crystalline Desoxyribonuclease (Isolation and general properties)." Journal of General Physiology: 349-362.

[11] Deduve, C., T. Debarsy, et al. (1974). "Lysosomotropic agents." Biochemical Pharmacology **23**(18): 2495-&

[12] Sedel, F., J. C. Turpin, et al. (2007). "Neurological presentations of lysosomal diseases in adult patients." Revue Neurologique **163**: 919-929.

[13] Hayashi, T., E. Nakanishi, et al. (1995). "PREPARATION AND PROPERTIES OF COPOLY(N-HYDROXYALKYL-D,L-GLUTAMINE) MEMBRANES." European Polymer Journal **31**(5): 453-458.

[14] Barrett, A.J. (1984). Biochemical Society Transcriptions **12**: 899

[15] Pytela, J., R. Kotva, et al. (1998). "Enzymatic degradation of poly[N-5-(2-hydroxyethyl)-L-glutamine] and poly[N-5-(2-hydroxyethyl)-L-glutamine-stat-L-glutamic acid]: Analysis of final degradation products." Journal of Bioactive and Compatible Polymers **13**(3): 198-209.

[16] Lauwers, A. and R. Ruyssen (1963). "DE STANDAARDISATIE VAN PROTEINASEN EN DE VERGELIJKENDE BEPALING VAN PAPAINE." Archives Internationales De Physiologie Et De Biochimie 71(4): 637-&.

[17] Marieb, E. N. and K. Hoehn (2008). "Anatomy and physiology." Pearson Education Inc

[18] http://www.redcross.org/blood/composition/blood-in-blood-vessel.jpg

[19] Mohandas, N. and J. A. Chasis (1993). "Red blood cell deformability, membrane material properties and shape-regulation by transmembrane, skeletal and cytosolic proteins and lipids." Seminars in Hematology 30(3): 171-192.

[20] Mohandas, N. and P. G. Gallagher (2008). "Red cell membrane: past, present, and future." Blood 112(10): 3939-3948.

[21] Agre, P. and J. C. Parker (1989). "Red blood cell membranes." Marcel Dekker Inc.

[22] Jan, K.-M. and S. Chien (1973). "Role of surface electric charge in red blood cell interactions." Journal of General Physiology 61: 638-654.

[23] Zijlstra, W. G. and A. Buursma (1997). "Spectrophotometry of hemoglobin: Absorption spectra of bovine oxyhemoglobin, deoxyhemoglobin, carboxyhemoglobin, and methemoglobin." Comparative Biochemistry and Physiology Part B: Biochemistry and Molecular Biology 118(4): 743-749.

[24] Moreau, É., I. Ferrari, et al. (2000). "Interactions between red blood cells and a lethal, partly quaternized tertiary polyamine." Journal of Controlled Release **64**(1-3): 115-128.

[25] Katchalsky, A., D. Danon, et al. (1959). "INTERACTIONS OF BASIC POLYELECTROLYTES WITH THE RED BLOOD CELL .2. AGGLUTINATION OF RED BLOOD CELLS BY POLYMERIC BASES." Biochimica Et Biophysica Acta **33**(1): 120-138.

[26] Goncharova, E. A., P. Lim, et al. (2007). "Assays for in vitro monitoring of proliferation of human airway smooth muscle (ASM) and human pulmonary arterial vascular smooth muscle (VSM) cells." Nat. Protocols **1**(6): 2905-2908.

[27] Wilson, T. and D. K. Hamilton (1984). "Difference confocal scanning microscopy." Optica Acta **31**(4): 453-465.

# Chapter 7

# Final conclusions

# Final Conclusions

At the beginning of this doctoral research, a concept was proposed that ideally would result in the successful development of one or more efficient, biocompatible, synthetic vectors that could be applied in gene delivery. Based on existing research and literature, a family of poly-α-amino acids and polymethacrylates was selected to form the basis of what should eventually lead to an optimised delivery system. By carrying out a complete & fundamental characterisation of the polymer properties in terms of DNA-interaction and biological efficiency, establishing a relation between the structure of the vector and its physico-chemical and biological behaviour was put forward as one the key targets of this investigation. Finally, the complete focus of these trends and correlations was aimed at obtaining efficient and successful transfection of specific cells (e.g. retinal) to be used in the application of related conditions (e.g. ARMD).

## 1 Synthesis of suitable vectors for gene delivery

Between both polymer classes employed in this research, a clear difference in synthetic pathway exists. Besides the obvious shorter synthetic route, the commercial availability and the different polymerisation mechanism, the inherent, higher hydrophobicity of the methacrylate counts as the most relevant differentiator compared to poly-α-amino acids. Considering the requirements in overcoming the hurdles related to DNA-protection, cellular entry and delivery of the genetic cargo to the nucleus of a cell, specific chemical functional groups were selected to be built into the polymer, either via separate modification reactions or by selecting the appropriate starting monomer.

As a first step in the total development process, an extended library of polymers was synthesised. For poly-α-amino acids, two groups of biodegradable polymers were studied. Both poly-L-glutamines and poly-L-arginines were derived from their corresponding *N*-carboxyanhydride after which one or more modification reactions were carried out. During the polymerisation step, intermediate compounds with a predefined MW were obtained for both polymer groups (pBG or pZO). Low MW polymers were derived from n-butylamine (range: 5.000 – 30.000 kDa) while the higher MW polymer were produced using tributylamine yielding molecules of roughly 50.000 to 250.000 kDa. As the polymerisation mechanism was different for both initiator types, also the polydispersity of low MW compounds was lower (nearly 1) than for high MW compounds (1.2 – 1.8). For poly-γ-benzyl-L-glutamate (pBG), it was possible to set-up a mastercurve that enabled to select any desired molecular weight (MW) based on the monomer-initiator ratio which could theoretically reach infinite MW's but which is in practice limited by the concentration of the

monomer and the proximity requirement between two reacting species. Once an intermediate polymer of desired MW was available, further modification was performed by the aminolysis reaction of pBG with a suitable amine-containing reagent or by deprotection followed by guanidine conversion in the case of poly-N-benzyloxycarbonyl-L-ornithine (pZO). It was found that full control over the aminolysis reaction was difficult to reach, especially when multiple reagents were involved (production of copolymers) because of the number of parameters (concentration, MW of intermediate, reactivity of the reagents, temperature, etc.) that could influence the conversion reaction. The conversion of poly-L-ornithine into poly-L-arginine could be more easily tailored by monitoring the reaction time, the reagent excess and the concentration of KI.

Finally, polyarginine derivatives with a broad MW range were obtained as well as polyglutamines that contained, besides different MW's, also a variable composition in functional groups. There appeared to be limitations to the composition of certain glutamine (co)polymers, dependent on the reactivity of the applied reagent, mainly in the case of trityldiethyleneamine. For that reason, it was difficult to produce aminoethylglutamine (AEG) or guanidinethylglutamine (GuAEG) containing polymers that contained > 50% AEG/GuAEG. Also, full conversion could only be obtained at elevated temperatures (50°C) using excess reagents (10-20x) for an extended time (48-72h). The use of the catalyst (2-hydroxypyridine) was confirmed to be highly efficient since chain-cutting of the backbone was minimal and the corresponding polydispersity only limitedly affected . The purity of the final products was positively verified by $^{1}$H-NMR and the overall yield of the total synthetic pathway sufficient (30-40%) given the multiple steps involved.

The synthesis of polymethacrylates occurred by free-radical polymerisation and proved to be difficult in MW control. Moreover, the success of the polymerisation was highly dependent on the absence of $O_2$ in the reaction mixture. Obtaining the desired MW was to a certain extent possible by varying the M/I concentration and the type of initiator and resulted in polymers with a MW as high as 700.000 Da. The use of a chain transfer agent (2-mercaptoethanol) was successful and enabled the production of methacrylates with MW's of 10.000 – 50.000. A whole range of polydimethylaminoethylmethacrylate (pDMAEMA) and copolymers were prepared from commercially available monomers (e.g. trimethylsillyloxyethylmethacrylate) and also copolymers based on aminoethylmethacrylate and guanidinethylmethacrylate could be synthesised via a protected monomer. The composition of the copolymers was proportional to the monomer composition which indicates that the reactivity of the different monomers was virtually equal. In all cases, the polydispersity of the polymethacrylates was considerably higher (up to 2.5) than for the biodegradable counterparts but on the other

hand, it was possible to reach yields values as high as 60 % (when one-step syntheses were applied).

Besides new classes of polymeric vectors, also certain existing compounds like polyethyleneimine (PEI) and poly-L-lysine (PLL) were modified in an attempt to decrease the inherent toxicity and increase the efficiency. For both vectors, fully guanidine-modified derivatives could be readily synthesised by adopting the guanidine conversion method applied for poly-L-arginine.

## 2 Physico-chemical properties of developed polymers

In order to decide if a polymer is suitable as a DNA-carrier in terms of physico-chemical qualities, they were subjected to a combination of characterisation techniques. From the results that were presented, most polymers exhibit good interaction behaviour with DNA and this mainly depended on the degree of cationic charges present but also on the orientation or position of the cationic charge within the polymer. For poly-$\alpha$-amino acids, the best interaction was achieved for fully charged polymers consisting of guanidine residues followed by tertiary and primary amine-containing polymers. For copolymers, it was concluded that a minimal amount of charged groups must remain in order to keep the ratio of polymer/DNA (charge ratio or CR) for complexation low. In this way, copolymers with hydroxyl and imidazole groups could be synthesised without decreasing DNA-interaction. In contrast, polymethacrylate derivatives containing both neutral and cationic functional groups displayed worse DNA-interaction properties (e.g. higher CR for full complexation) than the homopolymers or copolymers which are fully charged and is believed to be the result of the more hydrophobic nature of the polymer backbone. Moreover, the optimal MW was confirmed different for both polymer types, requiring low MW polymers (≈ 10 kDa) in the case of biodegradable vectors whereas for the non-biodegradable ones, an optimal MW was found around 100-150 kDa. The difference in polyplex formation between regular PEI and guanidine-modified PEI was validated but no remarkable change in complex size or stability was found. Furthermore, the importance of the orientation of the cationic charge onto the polymer was proven by comparing several guanidine-modified compounds and it showed a clear advantage for polymers possessing cationic functional groups, located further away from the backbone.

The dimensions of the polyplexes were for nearly all cases small enough to ensure easy uptake and gradually decreased in size with increasing CR unless the minimal size was already reached at low CR's. In that case, a slight increase was detected. No real influence could be derived from the difference in MW and strikingly, also the composition of the

copolymers (either low or high amounts of cationic charge) appeared not to induce a substantial effect on the size of the complex.

Regarding the stability of formed polyplexes, the rule of thumb demonstrated a better stability (towards coagulation and precipitation) for higher charged vectors which means that homopolymers reached higher values than copolymers (with neutral groups), both for polyglutamines as well as for polymethacrylates. The effect of MW variation was not readily observed. This extensive physico-chemical characterisation led to the conclusion that mainly pDMAEMA or primary amine-containing copolymers with small (< 10%) amounts of primary amine and with a MW of around 150 kDa show the most potential as non-biodegradable vectors. For biodegradable vectors, the selection was more elaborate because several polymers with a MW < 30 kDa and with a subdivided functional group composition (not fully charged) seem promising. Selection of the most optimal functional group was less relevant but a preference towards guanidine groups in combination with imidazole moieties or hydroxyl entities exists, especially when keeping biological implications in mind.

To be able to create the most optimal polyplexes, the best way to combine polymer and DNA was investigated prior to characterisation. From this screening, it was found that the addition of DNA could be achieved stepwise or in a single shot without inducing significant differences in polyplex behaviour. Also the stability in time and kinetics were to a certain extend examined and proved that polyplexes were quickly formed and remained stable (for at least a couple of hours). On the other hand, when using non-flexible macromolecules, the concentration is critical for obtaining homogeneously dispersed, uniform polyplexes, hence the use of diluted solutions is advised.

## 3 Optimising polymeric vectors

Due to the continuous advances in research of gene delivery systems, the use of peptides has gained additional importance, not only as facilitators of cellular recognition, targeting and internalisation but also as a class of compounds fit for DNA delivery and protection. Accordingly, two peptides (penetratine & $Arg_8$) were coupled to a selection of vectors to examine the benefits in biological and DNA-protective properties. Because vector optimisation is not exclusively limited to the structure but also to the mechanism by which polyplexes are being guided to the nucleus of a cell, fluorescent tags were required to allow investigation of the polyplex position.

As a result, certain key polymers were provided with 1-5 % of Oregon Green 488 via a succinimidyl bridge and the effect of incorporating hydrophobic, voluminous molecular

structures on the interaction with DNA was examined. The effect on higly charged vectors revealed to be rather minimal but for PEI (≈ 25% charged at physiological pH) the consequent shielding effect provoked a much higher CR for full condensation, hence the influence of fluorescent coupling should be kept in mind when further exploring fluorescent vectors. Additionally, fluorescently labelled polymers could be used to confirm certain kinetic properties like polyplex formation and mobility based on diffusion experiments (FCS or UV/VIS). These techniques were successfully validated as alternatives for determining the CR for condensation.

Coupling of peptides to the polymer backbone was achieved via two different bifunctional crosslinkers, *N*-succinimidyl-3-(2-pyridyldithio)propionic-ester or *N*-(γ-maleimidobutyryloxy)succinimide-ester. Penetratine was coupled to amine-containing polymers in 1-4 % whereas $Arg_8$ was coupled with a percentage ranging from 1-8. Furthermore, $Arg_8$ was coupled to p(DMAEG) using a variety of spacers which allowed the peptide to be further located from the polymer to assess its influence on transfection enhancement. One part of the improvement was not fulfilled since for polymers that exhibit a clear interaction behaviour with DNA, the coupling of cell-penetrating peptides (CPP) resulted in vectors with decreased condensation properties. In general the presence of CPP's induced a certain retarding effect, requiring higher CR's for condensation to occur but while maintaining the same level of DNA-interaction at full condensation. However, for certain polymers with a weak ability to condense DNA, transformation into a compound with an intense attraction force was feasible if a cationic peptide (like $Arg_8$) was coupled. This negative effect was to some extent confirmed by DLS (with a slightly reduced polyplex size for CPP-coupled polymers) and zetapotential, where a more significant delay and decrease in positive zeta-value was observed when CPP's where present in the polyplex.
The ability of Penetratine, which counts as a model CPP, to interact with the cellular membrane was proven by impedance spectroscopy and compared to PEI. This latter strangely demonstrated a difference in impedance signal (clear membrane disruption for penetratine-compounds but not detectable for PEI polylpexes), hence the believe that multiple ways of cellular uptake are feasible, was again supported. Finally, incorporating CPP's by physically combining them within polyplexes was suggested as more efficient alternative for biological enhancement since the properties of the vector seemed not to be affected compared to coupling through chemical linkage.

## 4 Biological properties of improved vector systems

Because the coupling of additional compounds to vectors, in order to optimise their biological activity, proved to have in most cases a (limited) negative effect on condensation properties with DNA, the better strategy could be found in the development of a successful polymeric vector as such without the need for additional covalent peptide coupling to enhance transfection efficiency. During the elaborate biological testing of the developed polymers and polyplexes, several interesting properties of the applied vectors were exposed. Apart from deductions applicable for each type tested, it was also possible to draw global conclusions. For instance, it was shown that all polymers can protect DNA from being degraded when the charge ratio is sufficiently high, even when only a limited amount of charged groups are present, regardless the MW of the polymer. In the case of poly-L-glutamines, swift degradation of the polymer backbone was demonstrated and this was influenced by the amount of cationic charge present (slower degradation rate with increasing positive charge). The compatibility of most polymers with red blood cells was largely negative, especially for highly charged polymers where hemolytic and coagulation effects proved to seriously hamper the potential *in vivo* usage. The presence of neutral (hydroxyl/imidazole) functional groups on the other hand demonstrated high compatibility and generally, this tendency was more explicit for low MW compounds. Nearly all polymers that were produced during this research exhibited very low toxicity in *in vitro* cell tests (except high MW polymethacrylates and PEI derivatives). The coupling or incorporation of peptides did not provoke a decrease in toxicity but was unfortunately not able to transform a non-active vector into an active version. Improvement of transfection efficiency was noticeable by CPP-addition but only if the base polymer was already active. Nevertheless, positive results were retrieved for several polymers like polymethacrylate derivatives which proved to be successfully internalised and able to express proteins by delivering DNA cargo, irrelevant of the MW. Also a few cases of polyglutamines achieved high levels of transfection (even outperforming PEI) but it was difficult to identify a general trend related to the structure. However, for poly-L-glutamines, it appears that fully charged polymers should be avoided and the incorporation of functional groups with a lower $pK_a$ is advisable, although a minimum amount of positive charges is necessary to keep the DNA-attraction sufficiently high (dependent on the type of cationic group but presumably > 30%). The most active compounds were also low in MW which was not a requirement for polymethacrylates. For those, it was proven that a higher MW corresponded with a higher transfection (but with an equally high toxicity). Therefore the use of polymers with an intermediate MW is preferable to extremely high or low MW's. The composition of polymethacrylates favors the presence of completely charged functional groups (especially a combination of primary and tertiary amines), given the lower activity of

hydroxyl-containing derivatives. Furthermore, PEI modifications were carried out that brought about derivatives with a reduced inherent toxicity while preserving or even slightly increasing the biological activity, for instance by coupling a fluorescent group or CPP

Finally, the internalisation process was explored for both polymer classes as well as the reference polymer PEI by confocal imaging. Already at the stage of polyplex formation, discrepancies were visualised. Whereas polyplexes based on p(DMAEG) formed intensily, coloured dots which represent strongly interaction complexes, the appearance of PEI-based complexes proved to be much more diffuse, presumed to be the result of weaker interactions. Higher success-rates for PEI could be partially attributed to the swift internalisation property (already considerable after 3h of incubation) compared to p(DMAEG) which was only significantly internalised after 24h. Nevertheless, internalisation was no guarantee for positive transfection as the complex still needs to dissociate and move towards the nucleus, an additional need that was probably not met and the result of too tightly bound polyplexes.

## 5 Epilogue

Because the search for the ideal vector is influenced by such a high number of parameters, the questions remains if it will ever be possible to identify a general correlation between *in vitro* or *in vivo* transfection activity and the chemical structure of a synthetic compound. With increasing knowledge on a vastly growing group of explored polymers, additional trends and properties will hopefully enable the detection of the underlying connections that form the key to developing a successful uniform delivery system. With respect to these hypotheses, this research has proven the advantages and flaws of a certain class of synthetic polymers and based on this information, this knowledge should be part of the global information matrix for continued unveiling of the principle that can guarantee success of implementing adequate gene therapy in the long run.

# Chapter 8

# Experimental Work

## 1 Products

L-glutamic acid (Bachem), 2-hydroxypyridine (Avocado), diphosgene (Acros) , dry *N*,*N*-dimethylformamide (Aldrich), poly-L-lysine (MW 30.000 – 70.000, Sigma) polyethyleneimine (PEI, branched, $M_w$ 25.000 – Sigma), trifluoroacetic acid (Acros), aminoethylmethacrylate.HCl (Polysciences), HBr/CH3COOH (33%) (Acros); 3,5-dimethyl-1-guanylpyrrazolenitrate (Sigma), 2-hydroxypyridine 99% (Avocado), histamine (Sigma), diphosgene (Acros), Tris base (Sigma), EDTA (Fischer scientific), boric acid (Acros), Bromophenol blue (Acros), Agarose (Fischer scientific), glycerol (Acros), 2-mercaptoethanol (Sigma) were used as such. Tributylamine (Acros), ethanolamine (Acros), *n*-butylamine (Acros) and 2-dimethylaminoethylamine (Fluka), *N*,*N*-dimethylaminoethylmethacrylate (Sigma), trimethylsilyloxyethylmethacrylate (Sigma), triethylamine (Sigma), acetic anhydride (Sigma) were distilled prior to use. *N*-(γ-maleimidobutyryloxy)sulfosuccinimide-ester (Sulfo-GMBS) and *N*-succinimidyl 3-(2-pyridyldithio) propionate (SPDP) were obtained from Pierce. Oregon Green 488 (5* isomer, succinimidyl ester) was obtained from Invitrogen. Methanol, dicholoromethane, toluene, n-pentane, DMF and diethylether were dried on calciumhydride and distilled. Ethylacetate was dried on $K_2CO_3$ and distilled. Ultrapure water (type III) was obtained through purification on a Synergy UV unit (Millipore).

Sephadex G-25 pd-10 desalting columns were received from GE.

Papaine and DNAse I were provided by Sigma.

## 2 Instruments

$^1$H-NMR spectra were recorded on a Bruker Avance 300, 500 or 700 MHz and chemical shifts are expressed as ppm (δ) relative to TMS. FTIR measurements were measured by means of a Bio-Rad 575C spectrometer in transmission mode (KBr) or in total reflection mode (ATR using a diamant crystal). UV/VIS analysis was performed on a Uvikon 810 spectrometer (Kontron Instruments?). Fluorescence intensity was detected by a Kontron SFM25 fluorimeter (Kontron Instruments). Microscopy images were taken with a light microscope (Axio – Zeiss). MW determination was achieved on an analytic GPC unit (Waters 600 controller) with differential refractometry (Waters R410) detection using an eluens composed of 5 % $NaH_2PO_4$, 3 % $CH_3CN$ at pH 4 (filtered 0.45 µm and degassed with He) and separation coloumns (Waters Ultrahydrogel 1000 and Shodex SB803HQ). Individual Refractive index was measured on a differential refractometer (DRM-1020, Polymer laboratories). Zetapotential values were obtained from a Zetasizer 3000 (Malvern Instruments) whereas dynamic light scattering results were derived from a Malvern Autosizer

4800 (Malvern Instruments). Agarose gel-electrophoresis was performed on a Gibco BRL apparatus (Life Technologies) and a Gibco BRL UV transilluminator TFX-20M (UV-B light).

# 3 Synthesis of biodegradable polymers (Chapter 2)

## 3.1 preparation of γ-benzyl-L-glutamate (BG)

To an ice-cooled suspension of 50 ml $H_2SO_4$ (98%) in 500 ml diethylether, 500 ml of benzylalcohol is added dropwise. Next, the ether fase is reduced through vacuum rotavaporation and 0.5 moles of L-glutamic acid is added to it to let react overnight. Subsequently, 900 ml of distilled water is added and the mixture is cooled to 0 °C and the pH adjusted to 6-6.5 with concentrated LiOH until the resulting product, γ-benzyl-L-glutamate (BG) precipitates. Following filtration and washing with distilled water, ethanol and diethylether, the product is dried *in vacuo*. A final recrystallisation from water/ethanol (9/1) is required. A total yield of around 50% can be achieved via this method.

*$^1$H-NMR* ($D_2O$/DCl; 500 MHz): δ = 7.35 ppm (5H, m, Aromatic-H), δ = 5.19 ppm (2H, s, $C_6H_5$-$\underline{CH_2}$-O-), δ = 4.25 ppm (1H, t, α-$CH_2$), δ = 2.60 ppm (2H, t, γ-$CH_2$); δ = 2.10-2.30 ppm (2H, m, β-$CH_2$)

*FTIR* : 1725 $cm^{-1}$ (ester)

## 3.2 Synthesis of γ-benzyl-L-glutamate-*N*-carboxyanhydride (BG-NCA)

In order to synthesise the *N*-carboxyanhydride (NCA) of L-glutamine the carboxylic group located on the side-chain was protected by means of a benzyl ester. In short, 15 g of BG was suspended in 250 ml of dry ethylacetate (EtOAc) and heated to 60 °C. A solution of diphosgene in EtOAc (15%) is added to the mixture in portions (7x10 ml). With every portion, the mixture is let react for 20 min after which $N_2$ is flushed through for 10 min to eliminate HCl from the mixture. This procedure is repeated until all BG was converted into BG-NCA (solution becomes transparent). Afterwards, the mixture is flushed with $N_2$ (1 hour at 60 °C followed by 1 hour at room temperature). In case suspended product remains, the mixture is filtered off and the filtrate used accordingly. Following partial solvent removal (to a 100 ml total), the product was precipitated in cold pentane and recrystallized from ethylacetate. The product is then filtered off again and dried *in vacuo*. The absence of $Cl^-$ was verified via a precipitation reaction with $AgNO_3$. Therefore, 10 mg of BG-NCA is dissolved in 1 ml $HNO_3$ (2M), heated close to boiling temperature in a Bunsen-flame after which 3 drops of $AgNO_3$ were added. If the product turned out to be less turbid than reference (tap water with $AgNO_3$), the BG-NCA was considered sufficiently $Cl^-$ free. The product was confirmed using

$^1$H-NMR and FTIR (yield = approximately 80-90%, dependent on amount of recrystallisation steps).

*$^1$H-NMR* ($CDCl_3$; 500 MHz): δ = 7.35 ppm (5H, m, Aromatic-H), δ = 6.30 ppm (1H, s, CO-NH), δ = 5.14 ppm (2H, s, $C_6H_5$-$CH_2$-O-), δ = 4.39 ppm (1H, t, α-$CH_2$), δ = 2.60 ppm (2H, t, β-$CH_2$); δ = 2.10-2.30 ppm (2H, m, γ-$CH_2$)

*FTIR* : 1780 $cm^{-1}$ (anhydride peak 1); 1860 $cm^{-1}$ (anhydride peak 2); 1715 $cm^{-1}$ (ester)

### 3.3 Synthesis of δ-carbobenzyloxy-L-ornithine-*N*-carboxyanhydride (ZO-NCA)

Analogue to the synthesis of BG-NCA, the formation of ZO-NCA occurs via a cyclisation reaction with diphosgene. Since a protective derivative is commercially available ($^{\delta}$N-carbobenzyloxy-L-Ornithine or ZO), there's no preceding reaction required.

*$^1$H-NMR* ($CDCl_3$; 500 MHz): δ = 7.35 ppm (5H, m, Aromatic-H), δ = 7.10 ppm (1H, s, CO-NH, side-chain), δ = 5.15 ppm (2H, s, $C_6H_5$-$CH_2$-O-), δ = 5.05 ppm (1H, s, CO-NH, ring), δ = 4.32 ppm (1H, t, α-$CH_2$), δ = 3.25 ppm (2H, t, δ-$CH_2$); δ = 1.80-2.10 ppm (2H, m, β-$CH_2$); δ = 1.60-1.75 ppm (2H, m, γ-$CH_2$)

*FTIR* : 1780 $cm^{-1}$ (anhydride peak 1); 1860 $cm^{-1}$ (anhydride peak 2); 1690 $cm^{-1}$ (carbamate)

### 3.4 Synthesis of poly(γ-benzyl-L-glutamate) – low MW

Poly(γ-benzyl-L-glutamate) (pBG) was synthesised with different initiators, dependent on the desired MW. For low MW compounds, BG-NCA (1g, 3.8 mmol) was dissolved in 10 ml DCM/EtOAc (6/1 v/v) and *n*-butylamine (41.2 µl of a 10% solution in DCM for a MW = 10.000) was added and the reaction was continued for 40h ($N_2$ atmosphere). After 40h, the reaction was terminated by adding a 10-fold excess of acetic anhydride and triethylamine (30 min). Next, the polymer was purified by precipitating in a cold mixture of MeOH/diethylether (1/2). Subsequently, the product was filtered off, washed and vacuum dried. The MW could be calculated from the $^1$H-NMR spectrum (butyl δ-H) and the reaction followed by FTIR. Yield = 80 %.

*$^1$H-NMR* (TFA; 500 MHz): δ = 7.35 ppm (5H, m, Aromatic-H), δ = 5.25 ppm (2H, s, $C_6H_5$-$CH_2$-O-), δ = 4.80 ppm (1H, t, α-$CH_2$), δ = 2.65 ppm (2H, t, β-$CH_2$); δ = 2.10-2.40 ppm (2H, m, γ-$CH_2$); δ = 1.05 ppm (3H, t, butyl δ-H)

*FTIR :* 1730 $cm^{-1}$ (ester); 1650 $cm^{-1}$ (amide)

### 3.5 Synthesis of poly(γ-benzyl-L-glutamate) – high MW

Similar to the synthesis of low MW pBG, 1g of BG-NCA ( was dissolved in 10 ml DCM/EtOAc (6/1 v/v) but now tributylamine (80 µl of a 10% solution in DCM for M/I = 100) was added dropwise to start the reaction for 40h. No termination reaction was required and purification was carried out subsequently in a mixture of MeOH/diethylether (2/1). Finally, the product was filtered off, washed and dried. The molecular weight ($M_v$) was determined by viscosimetry measurements in distilled dichloroacetic acid (a = 0.78 & K = $2.78.10^{-5}$ g/ml). Yield = 80%.

$^1$H-NMR spectrum and FTIR spectrum analogue to pBG low MW (no initiator signal).

### 3.6 Synthesis of poly-($^{\delta}$N-CBZ-L-ornithine)

The polymerisation of ZO-NCA was carried out in the exact same way as for pBG (both low & high MW). Only in the case of low MW pZO, the reaction solvent was composed of pure DCM.

Since deprotection was performed, immediately following polymerisation, no confirmation was researched.

### 3.7 Synthesis of poly-L-ornithine (pORN)

The final product of the polymerisation, pZO (0.5g – $2.10^{-3}$ mol), was dissolved in 5 ml of $CHCl_3$ after which 10 ml of a HBr solution (33%) in $CH_3COOH$ was carefully added. The mixture was stirred for 1h and then precipitated in cold diethylether. The product was filtered off, washed and redissolved in 10 ml of a dilute $NaHCO_3$ solution (4%) after which it was purified by liquid extraction using 50ml of cold diethylether. The water phase was tapped off and collected for dialysis against ultrapure $H_2O$, NaCl (0.1 M) and HCl (0.05 M) to be finally dialysed against ultrapure water. The end product was isolated by freeze-drying. Yield = 70%.

*$^1$H-NMR* ($D_2O$/DCl; 500 MHz): δ = 4.25 ppm (1H, t, α-$CH_2$), δ = 2.90 ppm (2H, t, δ-$CH_2$); δ = 1.60-1.80 ppm (2H, m, β-$CH_2$); δ = 1.65 ppm (2H, t, γ-$CH_2$)

*FTIR* : 1650 $cm^{-1}$ (amide); 3300 $cm^{-1}$ (primary amine)

### 3.8 Synthesis of poly-L-arginine (pARG)

Starting from 0.5g of pORN ($3.3.10^{-3}$ mol) solubilised in 5 ml of ultrapure water, 9.96g of KI is added (to have an end concentration of 6 M). In a separate flask, 16 equivalents of 3,5-dimethyl-1-guanylpyrrazolenitrate (DMGP) are suspended in 4 ml of water. Using

concentrated KOH (4M) the solution is brought to pH 9.5 and added to the pORN solution. The total volume is brought to 10ml while maintaining a pH of 9.5 and let react for 24h at room temperature. Afterwards the mixture is neutralised using concentrated HCl (1 M) and collected in a dialysis membrane (MWCO range $1/5^{th}$-$1/10^{th}$ of the MW of pORN) to be purified against ultrapure water. After 24h, the dialysis solution is acidified via 1 M HCl and again dialysed against ultrapure water, 0.1 M NaCl, 0.05 M HCl and again ultrapure water to end. The final product was then obtained by freeze-drying. Yield = 95%.

*$^1$H-NMR* ($D_2O$/DCl; 500 MHz): δ = 4.25 ppm (1H, t, α-$CH_2$), δ = 3.10 ppm (2H, t, δ-$CH_2$); δ = 1.60-1.75 ppm (2H, m, β-$CH_2$); δ = 1.50-1.60 ppm (2H, m, γ-$CH_2$)

*FTIR* : 1650 $cm^{-1}$ (amide); 3300-3400 $cm^{-1}$ (primary & secondary amine)

### 3.9 Synthesis of poly(dimethylaminoethyl-L-glutamine)

pBG (0.5g – 2.28 mmol) is dissolved in 5ml of dry DMF and 1.08g (11.4 mmol) of 2-hydroxypyridine was added. Next, 4.7 ml (45.6 mmol) of 2-dimethylethylenediamine was added after which the mixture was heated tot 50 °C and stirred for 60h (while followed by FTIR). For high MW pBG, another 1.175 ml of 2-dimethylethylenediamine was added to let react for another 2h. Poly(dimethylaminoethyl)-L-glutamine (pDMAEG) was obtained by precipitation in ice-cooled diethylether, filtered, washed and redissolved in 10 ml of water (pH = 5) to be dialysed (MWCO = $1/10^{th}$ of the MW of pBG) against ultrapure water, 0.05 M HCl and finally again ultrapure water. Isolation of the product was achieved by freeze-drying. Yield = 75 %

*$^1$H-NMR* ($D_2O$; 500 MHz): δ = 4.30 ppm (1H, t, α-$CH_2$); δ = 3.60 ppm (2H, t, -$\underline{CH_2}$-NH-CO-), δ = 3.30 ppm (2H, s, -N-$\underline{CH_2}$-$CH_2$-NH-CO-), δ = 2.90 ppm (6H, s, $CH_3$-N-), δ = 2.35 ppm (2H, t, γ-$CH_2$); δ = 1.90-2.10 ppm (2H, m, β-$CH_2$)

*FTIR:* 1650 $cm^{-1}$ (amide); 3250 $cm^{-1}$ (tertiary amine)

### 3.10 Synthesis of poly(dimethylaminoethyl-co-aminoethyl)-L-glutamine

For a composition of 15% primary amines, pBG (0.5g – 2.28 mmol) is dissolved in 5 ml of dry DMF and 1.08g (11.4 mmol) of 2-hydroxypyridine was added. Next, 3.525 ml (34.2 mmol) of 2-dimethylethylenediamine was added as well as 3.54 g (11.4 mmol) of *N*-trityl-ethylenediamine after which the mixture was heated tot 50 °C and stirred for 60h (while followed by FTIR). For high MW pBG, another 1.175 ml of 2-dimethylethylenediamine was added to let react for another 2h. The product was precipitated using ice-cooled diethylether and filtered off. Trityl removal was obtained through acidolysis in pure TFA during 1h which

was followed by precipitation in cold diethylether. Subsequently, the polymer was filtered, washed and dried to be finally dissolved in water (pH = 5) and collected in a dialysis membrane. p(DMAEG-AEG) was obtained by precipitation in ice-cooled diethylether, filtered, washed and redissolved in 10 ml water (pH = 5) to be dialysed against ultrapure water, 0.05 M HCl and finally again ultrapure water. Isolation of the product was achieved by freeze-drying. Yield = 65%.

*$^1$H-NMR* ($D_2O$; 500 MHz): δ = 4.30 ppm (1H, t, α-$CH_2$); δ = 3.65 ppm (2H, t, -$\underline{CH_2}$-NH-CO-, % $NR_2$), δ = 3.55 ppm (2H, t, -$\underline{CH_2}$-NH-CO-, % $NH_2$), δ = 3.30 ppm (2H, s, $R_2N$-$\underline{CH_2}$-$CH_2$-NH-CO-), δ = 3.20 ppm (2H, s, $H_2N$-$\underline{CH_2}$-$CH_2$-NH-CO-), δ = 2.90 ppm (6H, s, $CH_3$-N-), δ = 2.35 ppm (2H, t, γ-$CH_2$); δ = 1.90-2.10 ppm (2H, m, β-$CH_2$)

*FTIR:* 1650 $cm^{-1}$ (amide); 3200-3300 $cm^{-1}$ (primary & tertiary amine)

### 3.11 Synthesis of poly(dimethylaminoethyl-co-hydroxyethyl)-L-glutamine

Analogue to the synthesis of p(DMAEG), the reaction of p(DMAEG-HEG) was achieved by adding 3.31 ml of 2-dimethylethylenediamine and 1.09 ml of aminoethanol as aminolysis reagents for a 40% hydroxyl composition. Yield = 80%.

*$^1$H-NMR* ($D_2O$; 500 MHz): δ = 4.30 ppm (1H, t, α-$CH_2$); δ = 3.60 ppm (2H, t, -$\underline{CH_2}$-NH-CO-, % OH), δ = 3.55 ppm (2H, t, -$\underline{CH_2}$-NH-CO-, % $NR_2$), δ = 3.25 ppm (2H, s, $R_2N$-$\underline{CH_2}$-$CH_2$-NH-CO-) + (2H, s, HO-$\underline{CH_2}$-$CH_2$-NH-CO-), δ = 2.90 ppm (6H, s, $CH_3$-N-), δ = 2.35 ppm (2H, t, γ-$CH_2$); δ = 1.90-2.10 ppm (2H, m, β-$CH_2$)

*FTIR:* 1650 $cm^{-1}$ (amide); 3250 $cm^{-1}$ (tertiary amine), 3500 (hydroxyl, H-bonded)

### 3.12 Synthesis of poly(dimethylaminoethyl-co-aminoyethyl-co-imidazolethyl)-L-glutamine

Analogue to the synthesis of p(DMAEG-AEG), the reaction of p(AEG-HEG-ImEG) was achieved by adding 2.37 ml of aminoethanol, 0.76 g of histamine and 2.76 g of N-tritylethylenediamine as aminolysis reagents for a 80% hydroxyl, 10% imidazole and 10% amine composition. Yield = 65%.

*$^1$H-NMR* ($D_2O$; 500 MHz): δ = 8.40 ppm (1H, s, -N=$\underline{CH}$-NH-); δ = 7.15 ppm (1H, s, -C=$\underline{CH}$-NH-); δ = 3.65 ppm (2H, t, -$\underline{CH_2}$-NH-CO-, % OH), δ = 3.50 ppm (2H, t, -$\underline{CH_2}$-NH-CO-, % $NH_2$) + (2H, s, , -$\underline{CH_2}$-NH-CO-, % Imidazole), δ = 3.30 ppm (2H, s, HO-$\underline{CH_2}$-$CH_2$-NH-CO-), δ = 3.10 ppm (2H, s, $H_2N$-$\underline{CH_2}$-$CH_2$-NH-CO-), δ = 2.85 ppm (2H, s, Imid-$\underline{CH_2}$-$CH_2$-NH-CO-), δ = 2.35 ppm (2H, t, γ-$CH_2$); δ = 1.90-2.10 ppm (2H, m, β-$CH_2$)

*FTIR:* 1650 $cm^{-1}$ (amide); 3300 $cm^{-1}$ (primary amine), 3500 (hydroxyl, H-bonded)

### 3.13 Synthesis of poly(hydroxyethyl-co-guanidylethyl)-L-glutamine

For a composition of 40 % guanidine functional groups, 0.5 g pBG was dissolved in 5 ml dry DMF and 1.08g (11.4 mmol) of 2-hydroxypyridine was added to start the first subreaction. Next, 10.55 g of N-tritylethylenediamine was added in two portions (spread over 1h) and heated to 50 °C and reacted for 24h followed by the addition of 2.73 ml of aminoethanol. After a total reaction time of 60h, another 8.66 ml of aminoethanol was added. Precipitation was carried out after 72h of reacting by adding the mixture to cold diethylether. The product was filtered off and washed followed by dissolving in pure TFA during 1h. Again the product was precipitated, filtered off and dried *in vacuo*. Subsequently, the dried polymer was dissolved in water (pH = 5) and dialysed again in a sequence of ultrapure, 0.05 M HCl and again ultrapure water. The intermediate p(HEG-AEG) compound was isolated by freeze-drying. In a second sub-reaction, 0.4 g (2.15 mmol) of p(HEG-AEG) was dissolved in 4 ml of water and 7.97 g of KI was added. 34 mmol of DMGP was dissolved in 3 ml of water and adjusted to pH = 9.5 prior to mixing with the dissolved p(HEG-AEG). The total volume of the reaction was brought to 8 ml (pH = 9.5) and let react for 24h. Next, the solution was neutralised and collected to be dialysed against a sequence of ultrapure, 0.05 M and ultrapure water. Product isolation was achieved by freeze-drying. Yield subreation 1 = 65%, subreaction 2 = 95%.

*$^1$H-NMR* ($D_2O$; 500 MHz): δ = 4.30 ppm (1H, t, α-$CH_2$); δ = 3.60 ppm (2H, t, -$\underline{CH_2}$-NH-CO-, % OH), δ = 3.35 ppm (2H, t, -$\underline{CH_2}$-NH-CO-, % GuAEG), δ = 3.30 ppm (2H, s, Gua-$\underline{CH_2}$-$CH_2$-NH-CO-) + (2H, s, HO-$\underline{CH_2}$-$CH_2$-NH-CO-), δ = 2.35 ppm (2H, t, γ-$CH_2$); δ = 1.90-2.10 ppm (2H, m, β-$CH_2$)

*FTIR:* 1650 $cm^{-1}$ (amide); 3300-3400 $cm^{-1}$ (primary & secondary amine), 3500 (hydroxyl, H-bonded)

### 3.14 Synthesis of graft-copolymers

The synthesis of graft-copolymers is preceded by the synthesis of amine-containing units like aminoethyl-Lglutamine or L-ornithine. For p($HEG_{87\%}$-$AEG_{13\%}$), 40 mg (0.029 mmol) is dissolved in 3 ml DMF. To obtain an M/I of 8, 65 mg of ZO-NCA was added to the mixture and the reaction was carried out for 40h. Afterwards, a 10-fold equivalent of TEA & acetic anhydride was mixed in and stirred for an additional 30 min. The solution was then precipitated in ice-cooled diethylether, filtered off and dried. In a next step, the Z-protecion was removed by dissolving the dry product in 5 ml of HBr/$CH_3COOH$ for 45 min. The resulting p(HEG-AEG)+pORN was purified by precipitating the mixture in ice-cooled diethylether. The isolated product was further dissolved in 10 ml $NaHCO_3$ (4%) and purified

by liquid extraction in cold diethylether (25 ml). The water phase was separated and acidified to pH = 5 after which dialysis was performed against pure water, 0.05 M HCl and finally ultrapure water. The resulting p(HEG-AEG)+pORN was isolated by freeze-drying and in a subsequent reaction modified with guanidine functional groups, analoge to section 3.8, yielding eventually p(HEG-AEG)+pARG. The MW of the grafted copolymers could be calculated via $^{1}$H- NMR by assuming initiation of all –$NH_2$ units and comparing the $\delta$-H signal of pARG with the $\alpha$-H of the backbone.

### 3.15 Synthesis of PEI-Guanidine

PEI (60 mg – 1.39 mmol) is dissolved in 1 ml of ultrapure water and 2.99 g of KI is added. 1.12 g of DMGP is dissolved in 1.5 ml of water and adjusted to pH = 9.5 with KOH (4 M) after which it is mixed with the PEI solution. The total volume of the mixture is brought to 3 ml and let react for 24h. Subsequently, the solution is neutralised and dialysed against neutral water. Then the dialysed solution was acidified (pH = 4) and further purified against ultrapure, 0.05 M HCl and ultrapure water. Isolation of the product was done via freeze-drying. The yield of this reaction was around 95 %.

### 3.16 Synthesis of PEI + p(HEG-co-GuAEG) grafts

Prior to modification, the commercially available PEI was purified by dissolving 100 mg in 10ml of acetone and precipitated in ice-cooled pentane, followed by filtration and drying *in vacuo*. To start, 40 mg of PEI was solubilised in 5 ml of DCM (slightly clouded impression) and 350 mg of BG-NCA was added to let react for 40h. A 10-fold excess of TEA and acetic anhydride was added and stirred for 30 min to acetylate the free primary amines. The product was purified by precipitation in a 2/1 mixture of diethylether/methanol and filtered off. In a next step, 290 mg of the intermediate compound was dissolved in 5 ml of DMF and 5 equivalents of 2-hydroxypyridine (560 mg) and 10 equivalents of tritylethylenediamine (3 g) were added and reacted overnight at 50 °C after which 10 equivalents of aminoethanol (1.8 ml) were mixed and continued to be stirred for another 48h. The product was precipitated in cold diethylether, filtered off and washed. The remainder was dissolved in 2 ml DCM and 10 ml of TFA was added and reacted for 1h. Again the product was precipitated in cold diethylether, filtered off and washed. The product was dissolved in water and adjusted to pH = 5 followed by collection in a dialysis membrane and equilibrated against ultrapure water, 0.05 M HCl to end finally with ultrapure water. Isolation of the product was achieved by freeze-drying. In a final step, 130 mg of PEI+p(HEG-AEG) was dissolved in 3 ml water and 4 gr of KI was added. DMGP (700 mg), dissolved in 1 ml of water and adjusted to pH = 9.5 was added to this mixture and reacted for 24h. The final solution was neutralised and

dialysed against ultrapure water, followed by acidification of the dialysis solution (pH = 4) after which dialysis was continued (ultrapure water, 0.05 M HCl and ultrapure water). Isolation of the product was done by freeze-drying. The MW and the composition of the grafts was determined by $^1$H-NMR ($\alpha$-H and -$\underline{CH_2}$-NH-CO-).

# 4 Synthesis of polymethacrylates

## 4.1 Synthesis of poly(dimethylaminoethyl)methacrylate (pDMAEMA)

### *4.1.1 Synthesis via non water-soluble initiators*

#### *4.1.1.1 Synthesis via AIBN*

To start, dimethylaminoethylmethacrylate (DMAEMA) (1,5 ml – 8,9 mmol) was dissolved in 8.5 ml of distilled toluene. The mixture was degassed (*in vacuo*) for 5 minutes while vigorously stirring and an inert gas ($N_2$) was added afterwards. This step was repeated 3 times. Subsequently, an amount of initiator (77 µl – $4{,}67.10^{-6}$ mol) from a 10 mg/ml stock in toluene, correspondent with an intended MW of 100.000 Da was added. Afterwards, the degassing step was repeated and an $N_2$-atmosphere was maintained throughout the total reaction process. The temperature was elevated (70 °C) and the mixture was allowed to react overnight. The final product was retrieved by precipitation in ice-cooled pentane followed by filtration and washing. The product was redissolved in water (brought to pH = 5) and dialysed against ultrapure water, 0.05 M HCl and once more with ultrapure water to end with. Eventually, the product was obtained by freeze-drying and characterised via $^1$H-NMR. Yield = 30%.

*$^1$H-NMR* ($D_2O$, 500 MHz): δ = 4.05 ppm (2H, b, -$\underline{CH_2}$-O-CO-); δ = 3.25 ppm (2H, b, -N-$\underline{CH_2}$-), δ = 2.65 ppm (6H, s, $\underline{CH_3}$-N-), δ = 1,70 ppm (2H, b, -$\underline{CH_2}$-C-); δ = 0.6-0.9 ppm (3H, b, $\underline{CH_3}$-C-).

*FTIR:* 1730 cm$^{-1}$ (ester); 3400 cm$^{-1}$ (tertiary amine)

#### *4.1.1.2 Synthesis via AIBN & CTA*

DMAEMA (1,5 ml – 8,9 mmol) was dissolved in 8.5 ml of distilled toluene and 31 µl 2-mercaptoethanol was added (e.g. M/CTA ratio of 20/1 for a MW of 30.000). The mixture was degassed following the above mentioned procedure (4.1.1.1) and 77 µl of initiator was likewise added. The reaction occurred overnight at elevated temperature and was purified in a similar way as above (4.1.1.1). The product was obtained by freeze-drying and characterised via $^1$H-NMR. Yield = 30%.

### *4.1.2 Synthesis via water-soluble initiator*

Distilled DMAEMA (1.5 ml – 8.9 mmol) is dissolved in 8.5 ml ultrapure water and degassed according to the previously described method. An amount of APS initiator corresponding with the desired MW (1 % for 500.000 kDa or 202.9 µl of a 10 % (w/v) solution) is added and the mixture is degassed once more after which the reaction is carried out overnight at 70 °C. Post reaction, the product is purified by precipitating in ice-cooled acetone. Following filtration and washing, the polymer was dissolved in water (pH = 5) and dialysed against ultrapure water, 0.05 M HCl and ultrapure water. Freeze-drying enabled isolation of the product. Yield = 40%.

## 4.2 Synthesis of poly(dimethylaminoethyl-co-aminoethyl)methacrylate (pDMAEMA-AEMA)

For a composition of 50/50, DMAEMA (1.07 ml – 6.8 mmol) and AEMA.HCl (1.13 g – 6.8 mmol) were dissolved in 6.066 ml of ultrapure water. After thorough degassing, 1.934 ml (2 %) of APS (10 mg/ml stock) was added to the mixture and the pH of the solution was adjusted to pH = 5 (using 1M HCl) followed by a final degassing step while vigorously stirring. The total reaction time was set to 24h at 75 °C after which the mixture was diluted to 50% by ultrapure water. Purification was obtained by precipitation in cooled acetone and continued by extensive dialysis (72h in total in a sequence of ultrapure water, 0.05 M HCl and finalised by ultrapure water). The final product was obtained by freeze-drying and characterised by $^{1}$H-NMR. Yield = 50 %).

*$^{1}$H-NMR* ($D_2O$, 500 MHz): δ = 4.10 ppm (2H, b, -$\underline{CH_2}$-O-CO-, % -$NH_2$); δ = 3.95 ppm (2H, b, -$\underline{CH_2}$-O-CO-, % -$NR_2$); δ = 3.25 ppm (2H, b, $R_2$-N-$\underline{CH_2}$-); δ = 3.05 ppm (2H, b, $NH_2$-$\underline{CH_2}$-) δ = 2.70 ppm (6H, s, $\underline{CH_3}$-N-), δ = 1,70 ppm (2H, b, -$\underline{CH_2}$-C-); δ = 0.6-0.9 ppm (3H, b, $\underline{CH_3}$-C-).

*FTIR:* 1730 $cm^{-1}$ (ester); 3200-3400 $cm^{-1}$ (tertiary + primary amines)

## 4.3 Synthesis of poly(dimethylaminoethyl-co-hydroxyethyl)methacrylate (pDMAEMA-HEMA)

To a solution of 1.07 ml DMAEMA (6.8 mmol) and 1.48 ml TMS-HEMA (6.8 mmol) in 7.5 ml of toluene, that was thoroughly degassed, 148 µl of AIBN (10 mg/ml stock) was added after which it was degassed for a final time to yield a 50/50 % composition and a MW of 100.000 Da. Optionally, for low MW compounds, 2-mercaptoethanol can be added to the mixture before degassing (43 µl for a M/CTA = 10 or a MW of 10.000 Da). The reaction was stirred overnight at elevated temperature (70 °C) and afterwards purified by precipitation in a cold

3/2 solution of pentane/diethylether. The intermediate p(DMAEMA-TMS-HEMA) was filtered off, washed and dried to be finally redissolved in 10 ml of pure TFA and stirred for 45 minutes. The product was separated via precipitation in cold pentane and after decanting and drying again dissolved in water (pH = 5) to undergo dialysis (against ultrapure water, 0,05 M HCl and ultrapure water). The final product was received by freeze-drying. Yield = 25%.

*$^1$H-NMR* ($D_2O$; 500 MHz): δ = 4.20 ppm (2H, b, -$\underline{CH_2}$-O-CO-, % DMAEMA); δ = 3.90 ppm (2H, b, -$\underline{CH_2}$-O-CO-, % HEMA), δ = 3.65 ppm (2H, b, HO-$\underline{CH_2}$-, % HEMA), δ = 3.40 ppm (2H, b, $Me_2$-N-$\underline{CH_2}$-, % DMAEMA), δ = 2.80 ppm (6H, s, $CH_3$-N-), δ = 1,85 ppm (2H, b, backbone $CH_2$); δ = 0.70-0.90 ppm (3H, b, $CH_3$-C-).

*FTIR:* 3200-3600 (hydroxyl + tertiary amine); 1721 (ester)

## 4.4 Synthesis of p(HEMA- GuAEMA)

### *4.4.1 Synthesis of N-(tert-butoxycarbonyl)aminoethylmethacrylate (BOC-AEMA)*

To a suspension of 4 g of aminoethylmethacrylate hydrochloride (24.2 mmol) in 70 ml anhydrous dichloromethane, which is stirred for 10 min in an ice-water bath, 3.68 ml (1.1 eq) of triethylamine is added and stirred for another 20 min. Next a solution of 5.76 g of bis(tert-butyl)dicarbonate in 10 ml DCM is added and the reaction is allowed to reach room temperature and continued for 24h. Afterwards the mixture is washed 2 consecutive times with 50 ml of 0.5 M HCl. This is followed by liquid extraction of the organic phase with 0.5 M NaHCO3 (50 ml) and 0.1 M NaCl. The organic phase is dried over $MgSO_4$ for 20 min and the filtered. Next, the filtrate is concentrated by rotary evaporation until 20 ml remains. This solution is allowed to crystallise in a 2/1 solution of pentane/diethylether. After decantation the product is dried in vacuo and characterised by 1H-NMR. Yield = 80 %.

*$^1$H-NMR* ($D_2O$; 500 MHz): δ = 6.1 & 5.5 ppm (2H, s, $\underline{CH_2}$=C-); δ = 4.70 ppm (1H, b, -NH-), δ = 4.15 ppm (2H, t, -O-$\underline{CH_2}$-$CH_2$-,) δ = 3.40 ppm (2H, t, -$CH_2$-$\underline{CH_2}$-NH-), δ = 1.90 ppm (3H, s, $CH_3$-C-), δ = 1,40 ppm (9H, s, $CH_3$-C-O-).

*FTIR:* 3380 (urethane N-H stretch, sharp); 1710 (urethane)

### *4.4.2 Synthesis of poly(hydroxyethyl-co-guanidylethyl)methacrylate (pHEMA-GuAEMA)*

Polymerisation of TMS-HEMA and BOC-AEMA is carried out analogue to the synthesis of p(DMAEMA-HEMA). After freeze-drying of the p(HEMA-AEMA), the product is guanidylated as performed in section 3.8 to yield p(HEMA-GuAEMA). The final composition is obtained by $^{1}$H-NMR and FTIR. Yield = 25 %.

*$^{1}$H-NMR* ($D_2O$; 500 MHz): δ = 4.15 ppm (2H, b, -$\underline{CH_2}$-O-CO-, % GuAEMA); δ = 3.90 ppm (2H, b, -$\underline{CH_2}$-O-CO-, % HEMA), δ = 3.65 ppm (2H, b, HO-$\underline{CH_2}$-, % HEMA), δ = 3.45 ppm (2H, b, Gua-N-$\underline{CH_2}$-, % GuAEMA), δ = 1,85 ppm (2H, b, backbone $CH_2$); δ = 0.65-0.95 ppm (3H, b, $CH_3$-C-).

*FTIR:* 3200-3600 (hydroxyl & guanidine); 1715 (ester)

# 5 Phycisochemical characterisation

## 5.1 Polyplex formation: protocol

When a polymer is dissolved in water at physiological pH, the charge ratio (dependent on the composition) is calculated based on the mass/charge. This value is derived from the structure assuming protonation of the appropriate functional groups and is expressed as Da/mol of charges. For every polymer-DNA complex, the charge-ratio (positive to negative or polymer to DNA) is defined using the mutual relation of mass/charge between the macro-ions, expressed in the following equation:

$$z . ( \frac{X}{Y} . y ) = x$$

Where *X* = mass/charge of polycation (Da/mol)

*Y* = mass/charge of polyanion (Da/mol)

*y* = amount of polyanion added (g)

*x* = amount of polycation added (g)

*z* = integer multiple of the excess of polycation over polyanion (where z = 1 for an equal charge ratio, 1/1)

Polyplexes are obtained in 2 ml solutions via a specific order of mixing:

16µl of DNA (2,5 mg/ml stock solution) is added to an empty vessel. Next, demineralised water is added. Subsequently, an amount of polymer (*x*), correspondent to the intended charge-ratio, is added from a 1 mg/ml stock solution. This solution is vortexed for 5 seconds at medium speed (≈ 1500 rpm) and is ready for use afterwards. In this way a polyplex

solution with 20 µg/ml DNA can be used for *in vitro/in vivo* experiments. In certain experiments, augmented doses of DNA were tested (like 40 or 60 µg/ml), in that case the polymer dose for a certain CR is proportionally increased.

For specific experiments, the use of buffer solution is in order. Since the formation of IPEC's in the presence of ions is highly contested, the polyplexes are first prepared in ultrapure water at double concentration and subsequently diluted (1/1) using a double concentration of the final required buffer.

### 5.2 One-step versus multi-step addition

For UV detection of multi-step addition, the polyplexes were prepared in triplicate starting from a DNA solution (20 µg/ml) in 2 ml ultrapure water. This solution was initially measured Subsequently an amount of polymer was repeatedly added, corresponding with a CR increase of 0.2 units (e.g. 5.76 µl for p(DMAEG) with a mass/charge of 235 Da/mol), gently vortexed (2 s) and measured. This step was repeated until the desired final CR (in the same test solution). In single-shot addition, 16 µl of DNA was placed into a cuvette and water was added, followed by an amount of polymer solution (1 mg/ml) corresponding with the desired CR, gently vortexed and measured (in triplicate). A new solution was prepared for every CR tested. Polyplexes for fluorescence measurements were prepared in a similar way but using a solution of EtBr (400 ng/ml) in stead of ultrapure water. A solution of 20 µg/ml DNA was used to calibrate the device (100 % fluorescence) at 510 nm excitation and 590 nm emission wavelength.

### 5.3 Polyplex kinetics: stability and formation in time

Fluorescence measurements were performed on polyplex solutions that were measured immediately following preparation (510 nm excitation wavelength and 590 nm for emission). To start, the device was calibrated using a DNA solution of 20 µg/ml (in triplicate) and counts as zero time point. In a single shot, an amount of polymer corresponding with a 2/1 CR was added, immediately vortexed (2 s) and measured at given time intervals (10, 20, 30, 60, 120, 300, 600, 1200, 1800, 3600 & 7200 s).

### 5.4 Polyplex mixing sequence

These tests were performed by IBMT, Fraunhofer, Skt. Ingbert, Germany. Polyplex solutions were prepared in the standard way (2 ml total) or in reversed order, by adding the polymer first (conform the desired CR) to an empty vessel, adding water and finalise by adding 16 µl of DNA (2.5 mg/ml stock).

### 5.5 EtBr Fluorescence measurements for validation of polyplex formation

EtBr based exclusion fluorescence was measured by calibrating a DNA solution (20 µg/ml in 400 µg/ml EtBr solution) using $\lambda_{exc}$ = 510 nm and detecting the fluorescence intensity at $\lambda_{em}$ = 590 nm. This intensity was set to 100 % relative fluorescence. In subsequent steps of 0.2 CR units (corresponding to an amount of polymer calculated as described in section 5.1), polymer was added (from a 1 mg/ml stock) and vortexed (2 s) after which the change in fluorescence intensity was measured. Standard measurements were performed up to a total CR of 2/1 (at which the volume total reached exactly 2 ml). If no sufficient condensation was registered, additional polymer was added, either in similar step or in higher CR's (e.g. 1/1). The tests were performed in triplicate.

### 5.6 Agarose gel electrophoresis

Applied buffers: 10x TBE buffer = 1 M Tris base, 0.9 M anhydrous boric acid, 10 mM $Na_2EDTA.2H_2O$ & ultrapure water type III

10x loading buffer = 50% (v/v) glycerol, 100 mM $Na_2EDTA.2H_2O$, 0.1% bromophenol blue & ultrapure water type III

*Gel-preparation:*

1 g of agarose is suspended in 100 ml 1x TBE buffer and is heated using the 'au bain marie' close to the boiling temperature and maintained until the suspension is completely dissolved. The solution is then removed from the hot water bath and cooled down. The gel is then poured into a cast (Gibco – Horizon) and allowed to cool down for 45 min (gel thickness ≈ 8 mm) while preformed wells are created using a plastic well applicator. Next, the gel is completely submersed in 1x TBE.

*Polyplex preparation:*

The polyplex solutions are prepared using the section 5.1 for a range of CR (0 to 2/1 in steps of 0.2) . For every CR, a separate vessel is made (single-shot addition). 20 µl of every solution is mixed with 2 µl of loading buffer and thoroughly mixed (pipetting up and down) in an eppendorf tube after which it is injected into a designated well in the submerged gel.

*Gel-retardation assay:*

By applying a voltage of 90 V during 1 hour, the condensed DNA is separated from the free DNA. Staining of the gel and visualization is consequently achieved by immersing the gel completely in a 0.5 mg/ml solution of EtBr during 1.5 hours after which a digital still image

was taken upon irradiation of the gel using an UV transilluminator (UV-B) (processed in specific software for EtBr staining).

### 5.7 Dynamic light scatteing (photon correlation spectroscopy)

For DLS measurements, polyplexes were prepared in the standard way with 3 CR's, 1/1, 2/1 and 4/1 unless otherwise specified. Following preparation, the solutions were immediately measured unless the influence of time was taken into account. All measurements were performed at 25 °C or 37 °C and with a scattering angle of 90° in polystyrene cuvettes. One measurement consisted of 3 repeat analyses (10 subruns each) and were fitted using the CONTIN algorithm.

### 5.8 Zeta-potential measurements

Polyplexes for zeta-potential analysis are prepared using the standard protocol in a 0.5/1, 1/1, 2/1 and 4/1 CR. Prior to injection into the measuring compartement, the solution are diluted (50%). Every value is the result of 10 subruns and all measurements were achieved using a celvoltage of 220V and 1000 Hz frequency.

## 6 Optimisation and modification of multifunctional polymers

### 6.1 Coupling of fluorescent tags

Succinimidyl-activated fluorescent labels were coupled to primary amine-containing polymers in a one step reaction. For a coupling degree of 1-5%, 40 mg polymer was dissolved in 4 ml 0.1 M $NaHCO_3$ (pH = 8.3) and shielded from light (using aluminum foil). Separately, 2.5 mg of Oregon Green was dissolved in 250 µl of dry DMF and immediately added to the polymer solution (dropwise) and the mixture was allowed to react for 1h. The reaction was stopped by adding 1 ml of HCl (0.5 M) to lower the pH. The product was purified by extensive dialysis (against 0.1 M NaCl, ultrapure water, 0.05 M HCl and finally ultrapure water) after which it was freeze-dried. Characterisation of the product was achieved by UV/VIS spectroscopy (using the formula in chapter 5 or by preparing a standard curve).

### 6.2 Polyplex kinetics: UV/VIS absorption tests

To compare the detection of polyplexes composed of labeled polyplexes and labeled polymer as such, 2 solutions (2 ml each) were prepared. One solution was provided with DNA (20 µg/ml) and the other plain water. Stepwise, fluorescently labeled polymer was added (in steps corresponding with 0.2 CR units) and the solution was measured until a final

CR of 2/1. Dependent on the information required, analysis was performed at 488 nm (polymer detection) or 280 nm (DNA detection).

## 6.3 Coupling of peptides

### *6.3.1 Coupling of a heterobifunctional crosslinker (Sulfo-GMBS)*

For this reaction, typically 40 mg (26 µmol $-NH_2$ groups) of polymer was dissolved in 4 ml of $NaHCO_3$ (0,1 M - pH 8,5). Then, a 2-fold molar excess of *N*-(γ-maleimidobutyryloxy) sulfosuccinimide, dissolved in 1ml of $NaHCO_3$ (0,1 M) was added dropwise and incubated for 45 minutes at room temperature. Afterwards, the excess of sulfo-GMBS was removed via a pd-10 desalting column (Sephadex G-25, $M_r$ = 5.000 Da) stabilised and eluted with PBS (pH = 7.2). The purified polymer-crosslinker solution (7 ml collected fraction) was immediately freeze-dried and continued for use in the 2nd reaction. Yield = 80 %

### *6.3.2 Coupling of a heterobifunctional crosslinker (SPDP)*

To a solution of 40 mg polymer (26 µmol $-NH_2$ groups) in 4 ml of $NaHCO_3$ (0,1 M - pH 8,5), a solution of 5 mg N-succinimidyl-3-(2-pyridyldithio)propionate (SPDP) in 250 µl of DMSO was added dropwise and stirred for 45 minutes at room temperature. Afterwards, the excess of SPDP was removed via a pd-10 desalting column (Sephadex G-25, $M_r$ = 5.000 Da) stabilised and eluted with PBS (pH = 7.2). The purified polymer-crosslinker solution (7 ml collected fraction) was immediately freeze-dried and continued for use in the 2nd reaction.

### *6.3.3 Coupling of CPP to a polymer-crosslinker conjugate*

Traditionally, to a 3.5 ml solution of polymer-crosslinker (10 mg/ml in PBS – pH 7,2) , 0,5 ml of peptide solution in PBS (5-20 mg/ml) is added an the mixture is reacted for 1,5 hours at room temperature. Afterwards, a stop reagent (EtSH – 100 µl) is added. Finally the solution is dialysed against 0,1 M NaCl, 0,1 M HCl and ultrapure water using a semi-permeable dialysis membrane. The product is isolated by freezedrying and confirmed by $^1$H-NMR. The amount of peptide coupled is determined using NMR or UV/VIS spectroscopy (CPP calibration curve).

*$^1$H-NMR*: comparison of polymer signal (e.g. backbone α-H) to unique signal derived from peptide (e.g. Pen = Tryptophan signal (8.1 ppm) or $Arg_8$ = γ-H) with no polymer signal overlap.

*UV/VIS:* only for Penetratine, $\lambda_{abs}$ = 280 nm

### 6.4 Physical mixing of CPP versus covalently coupled CPP's

Polyplexes with covalently coupled CPP's were prepared using the standard protocol. Physical mixing of CPP's was achieved by mixing the following components (2 ml total):

- 16 µl of DNA (2.5 mg/ml stock)
- Water is added (2 ml – 16 µl – $amount_{polymer}$ – $amount_{CPP}$)
- Polymer is added (1 mg/ml stock) corresponding to the desired CR and vortexed
- CPP is added (10 mg/ml stock) corresponding to the desired CPP concentration
- Vortex the solution (2 s)

## 7 Biological evaluation

### 7.1 Nuclease degradation

The polymer-DNA complexes for nuclease experiments were prepared in several CR's (0.5/1, 1/1, 2/1 & 4/1) and the preparation is carried out as described in section 5.1 of this chapter, but in a total volume of 1 ml of $H_2O$. The prepared polyplex solution is then diluted with 1 ml of TRIS buffer (80 mM TRIS.HCl, 20 mM NaCl, 12 mM $MgCl_2$, 20 mM $CaCl_2$, pH = 7,9). This buffer is previously filtered on a 0,45 µm Millipore filter and degassed for 10 minutes. The UV-spectrometer is auto-zeroed against a solution containing 1 ml of TRIS buffer and 1 ml $H_2O$. After the addition of 40 Kuntzunits of DNase I (Pierce), the different solutions were shortly vortexed (1 s) and measured in quartz cuvettes at a wavelength of 260 nm), at given time-points (0s, 10s, 20s, 30s, 40s, 50s, 60s, 2m, 3m, 4m, 5m, 10m, 15m, 20m, 25m and 30m) at 37 °C.

### 7.2 Haemolysis

At first, a 2 % RBC suspension was prepared from whole blood samples (Red Cross Belgium). Purification was obtained by centrifugation at 3700 rpm for 5 minutes. Subsequently, the top layer was removed and the remaining blood cell suspension washed with HBS buffer (20 mM HEPES, 150 mM NaCl, pH 7,4). This suspension was again centrifuged at 3700 rpm for 5 minutes and the supernatant together with the top layer of cells was removed. At last, the suspension was once more washed with HBS buffer and after centrifugation both the supernatant as well as the top layer of cells were equally removed. The obtained pure RBC's were then used to prepare a diluted concentration of 2 % RBC's in HBS buffer.

Polymer was added to this 2 % RBC suspension in concentrations ranging from 1 till 2000 µg/ml. The polyplexes were added in a 2/1 charge ratio. The polyplexes are prepared as described in section 5.1 but in a total volume of 1 ml of water. The prepared polyplex solution was then diluted with 1 ml of a 2 % RBC suspension prepared in a double concentrated HBS buffer after which they were incubated for 24 h at 37 °C while shaking at 100 rpm (horizontally and submerged in water along the shaking-axis). Also a positive and negative control was prepared, either by adding 0.2 % Triton X-100 (w/v) (positive control) or by appling RBC to a buffer solution (negative control)

After incubation, the solutions are centrifuged at 3700 rpm and the supernatant is used for UV/VIS-measurement. The UV-meter was auto-zeroed against HBS buffer ($\lambda$ = of 545 nm) and the different samples were put into cuvettes and measured. The haemolytic activity is quantified by comparing the values of the samples with a negative control and a positive control, which corresponds to pure HBS buffer (0 % haemolysis) and a Triton-X solution (100 % haemolysis) respectively.

### 7.3 Haemo-agglutination

For these tests, polyplexes were prepared in a 2/1 CR as described in section 5.1 but again in a total volume of 1 ml after which the solution was diluted using 1 ml of HBS. In the agglutination tests of free polymer, the amount added to a 2 % RBC suspension was corresponding to the amount of polymer used in a 2/1 polyplex. The obtained solution containing RBCs and polyplexes (or free polymers) was incubated at 37 °C for 1 h (while shaking). Hereafter, a few drops of the solution are put on a glass plate and the agglutination is visualised by optical microscopy. A 2 % RBC suspension (in HBS buffer) was also incubated as a reference.

### 7.4 Protease (enzyme) degradation of biodegradable polymers

Enzyme degradation of biodegradable poly-a-amino acids is performed using 40 µg of papaine. Polymer solutions of 10 mg polymer in 1,6 ml phosphate/citrate buffer (0.2 M – pH = 6 – containing 0.2 % w/v) were prepared to which 200 µl of EDTA (20 mM in buffer) and 200 µl dithioerythritol (20 mM in buffer) were added. The solution was incubated at 37 °C while shaking (60 rpm) to allow for complete dissolution. Finally, 8 µl of a papaine stock (5 mg/ml) were added and the solution was continued to be incubated. The MW of the polymer was measured as a function of time using GPC (buffer: $NaH_2PO_4$ 5%, $CH_3CN$ 3%, pH =4) at given time-points (30m, 1h, 2h, 4h, 8h, 24h and 48h) by injecting 20 µl of the incubated solution (without adding new buffer).

## 7.5 Transfection

### *7.5.1 Transfection protocol*

#### *7.5.1.1 Cell preparation*

Before transfection experiments can occur, cells are treated to be in the proper (confluent) state for application of gene vectors. Therefore, a transparent, bottom 96 well plate is treated with polyornithine. This protein, facilitates cell attachment, spreading, growth, morphology, differentiation, and motility of the HEK (human embryonic kidney) cells on the 96 well plate. In many cell cultures normal attachment, growth, and development are dependent on attachment factors and extracellular matrix components. In order to speed up this natural process 50 µl of polyornithine (1,5 µg/ml) is added in each well. After 1 h the 96 wells plate is washed 2 times with distilled sterilized water. Here, HEK 293 cells are used as they are extremely easy to bring in culture and to transfect.

When the HEK cells almost reach confluence, they are washed with PBS without Ca and Mg. Subsequently, the cells are trypsinized (trypsin-EDTA 1x in PBS without Ca and Mg) for 5 minutes at 37 °C. Then, the trypsinization is slowed down by adding 10 % of fetal calf serum and hereafter the cell solution is transferred in a centrifugation tube. After 5 min of centrifugation at 800 rpm, the supernatant is removed and the cells are re-suspended in 8 ml (dependent on the initial cell density) of DMEM medium without serum. Thereafter, the cells are counted by means of a counting chamber and diluted in DMEM medium to a final concentration of 400 cells/µl. Then, 50 µl of cells are seeded onto the treated 96 wells black plate with transparent bottom by using a Gilson Distriman. The plate has to be black in order to avoid interfering background during fluorescence measurements. To allow attachment of the cells to the plate, they are left in the incubator for 1 h at 37 °C and 5 % $CO_2$. When the cells are evenly distributed throughout the bottom of the wells, 50 µl of DMEM medium with 20 % fetal calf serum is added (to have a final concentration of 10 % serum in each well). At last, the cells are left overnight in the incubator to allow growing.

#### *7.5.1.2 Cell transfection*

After cell conditioning and preparation overnight, the medium in the wells is replaced by 50 µl of DMEM medium without serum. Then, the pCDNA7RucHA encoding plasmid is diluted in $H_2O$ in order to have a 90 ng/µl solution. The exact concentration of the stock solution of plasmid is determined by a spectrophotometer and subsequently, the polymers are diluted to the correct concentration according to the desired polymer/DNA ratios. Therefore, 2/3 volume (16,7 µl) of 90 ng/µl plasmid is added to 1/3 volume (8,3 µl) of concentrated polymer. This mixture is vortexed for 2 seconds and incubated for 1 h at room temperature.

After 1 h of incubation, the complex solution is diluted in DMEM medium in order to have 10 µl complex solution in 40 µl medium. The mixing must be done carefully by pipetting up and down for a couple of times. Then, 40 µl of this complex-DMEM solution is distributed in each well and incubated at 37 °C and 5 % $CO_2$. After 4 hrs incubation, 10 µl of fetal calf serum and doxycycline (1000-fold dilution) is added to each treated well. The latter is necessary to allow plasmid expression in HEK cells. After this addition the cells are incubated for 20 hrs at 37 °C and 5 % $CO_2$. In case of a 3 h incubation approach, the previously described 4 hrs incubation is reduced to 3 hrs and followed by a washing step by PBS with Mg and Ca, in order to remove those polyplexes which do not adhere to or interact with the membrane after 3 hrs of incubation. After washing, 10 µl fetal calf serum, 40 µl of DMEM medium and doxycycline (1000-fold diluted) is added to the well and incubated for 20 hrs at 37 °C and 5 % $CO_2$. The 24 hrs incubation is performed twice whereas the 3 hrs incubation approach is performed only once.

After 24 hrs of transfection, 10 % UptiBlue is added into the wells. This mixture is again incubated for 2 hrs at 37 °C and 5 % $CO_2$. Hereafter, the fluorescence is measured at an excitation and emission wavelength of 540 nm and 600 nm respectively by means of a fluorimeter. A negative control (0 % viability) is achieved by adding 2 µl of Triton X-100 to a well while 3 wells were left untreated (with no polymer added) and served as the positive control (100 % viability).

After the viability test, the supernatant is removed and 50 µl of passive lysis buffer (PLB) is added to each well. Subsequently, the plate is left on a plate shaker at room temperature for 30 min to ensure complete and even coverage of the cell monolayer with PLB. This procedure is performed to lyse the cells hereby releasing the translated enzyme which is necessary to allow measurement. To ensure complete lyses, a freezing/thawing approach is also performed. Therefore the plate is frozen until -80 °C and rapidly thawed by placing it in a water bath of 37 °C. Hereafter, the plate is placed in the luminometer 96 wells plate reader and 50 µl of coelenterazine is injected by the apparatus into wells containing cell lysates. The luminescence is measured for 10 seconds with a delay of 2 seconds between injection and measurement. Since, it has been demonstrated that RLUC is inactivated in the presence of substrate, resulting in emission of most of the light as a flash of a few seconds after addition. The excitation and emission wavelength used is 540 nm and 600 nm. The transfection efficiency is expressed in relative luciferase units (RLU) and was therefore compared with a reference (e.g. PEI). In most cases, the background created by the reagent in the absence of Renilla luciferase is very small compared to the luciferase signal, thus the luciferase activity is normally directly proportional to the total luminescence. However, when

measuring very small amounts of luciferase it is important to subtract the background signal from the measurement of the total luminescence. Background luminescence is obtained by measuring the luminescence produced by lysed untransfected cells. Tests performed and worked out by the Homeoprotein & cell-biology lab, école de France, Paris.

#### *7.5.1.3 Confocal microscopy*

Prior to visualization, 30 µl MSS with a 500-fold dilution of the stock WGA (5 mg of lyophilized WGA conjugate dissolved in 5 ml of phosphate-buffered saline) is added to the reservoir. After an incubation period of 10 minutes at room temperature the transfected cells are visualized by confocal microscopy. In order to visualize the exact location of the polyplex and to determine the amount of cell death, 30 µl of 0,4 % trypan blue (TB) is added, to have a final concentration of 0,1 % of TB in each channel. Living cells are very selective towards membrane passage and because of that cells with intact cell membranes exclude dyes such as TB. In dead cells, TB traverses the membrane and colors the cells blue. Due to the addition of TB, the ECM is quenched and the polyplexes present in the ECM are colored blue. In this way, internalized polyplexes can be differentiated from complexes outside the cell. Tests performed and worked out by the Homeoprotein & cell-biology lab, école de France, Paris.

# Chapter 9

# Dutch Summary
# (Nederlandse samenvatting)

# Nederlandse samenvatting (Dutch summary)

## 1 Inleiding

Op het vlak van biotechnologie en geneeskunde is gentherapie een relatief nieuwe techniek die alsmaar meer aandacht trekt. Momenteel is er een breed scala aan aandoeningen, zowel erfelijk als besmettelijk, waarvoor geen gepaste behandeling bestaat. Gentherapie werd daarom vooropgesteld als een veelbelovende behandeling voor talrijke ernstige ziektes zoals taaislijmziekte, kankerbestrijding of macula degeneratie. De techniek is gebaseerd op doelgerichte afgifte van DNA aan weefsels waarna het ingebrachte DNA een specifiek, therapeutisch proteïne codeert dat wordt vrijgesteld aan de omgeving om op die manier een bepaalde functie in het lichaam toe te voegen of te verwijderen. Het toedienen van 'vrij' DNA (in oplossing) blijkt slechts beperkt efficiënt door de grote van de molecule, de negatieve lading (ongewenste interactie) en vooral de aanwezigheid van nucleases in de bloedstroom (breken vreemd DNA af). Om deze problemen te vermijden, wordt daarom intens gezocht naar het gebruik van bepaalde dragersystemen (vectoren). Virussen worden reeds geruime tijd succesvol toegepast als afgiftesystemen omwille van hun natuurlijke eigenschappen om gastheercellen te penetreren. Toch bezitten deze systemen een belangrijk beperking, voornamelijk op het gebied van toxiciteit. Dit leidde daarom tot de ontwikkeling van een breed gamma aan synthetische vectoren die als genafgiftesysteem (vectoren) kunnen gebruikt worden. Dankzij de uitstekende controle van het synthese proces kunnen op deze manier structuren verkregen worden die zowel de nodig eigenschappen bezitten om als efficiente drager te fungeren alsook over de juiste kwaliteiten beschikken om een minimale toxiciteit uit te lokken bij gebruik *in vitro* of *in vivo*.

Om tegemoet te komen aan een aantal noden, meer bepaald enkele speciale ziektes zoals macula degeneratie (en bijhorende ouderdomsblindheid) of cardio-vacsulaire aandoeningen, heeft dit project tot doel om via gentherapie, efficiente strategieën te ontwikkelen die een therapeutisch effect kunnen teweegbrengen. Hiervoor wordt een beroep worden gedaan op niet-immunogene, biodegradeerbare polymeervectoren gebaseerd op multifunctionele poly-$\alpha$-aminozuren (lysine, glutamine, arginine) en polymethacrylaten. Deze polymeren zijn o.a. in staat om negatief geladen DNA te condenseren in kleine partikels (nm-orde) door middel van elektrostatische interactie tussen positief geladen functionele groepen, aanwezig op het polymeer en negatief geladen DNA. Deze elektrolytcomplexen kunnen vervolgens door de cellen worden opgenomen via o.a. endocytose waarna ze hun DNA cargo kunnen vrijstellen zodat deze kan getransloceerd worden naar de celkern voor daaropvolgende protein-expressie. Zowel cell-penetrerende peptides als fluorescente labels worden covalent

gekoppeld aan de polymeren om de cell-opname van deze partikels te stimuleren en te bestuderen. Daarnaast zal ook worden gebruikt gemaakt van diverse analyse-technieken zoals agarose gel-electroforese (voor de bepaling van de condensatie capaciteit), dynamische lichtverstrooing (deeltjesgrootte bepaling), zeta-potentiaal metingen (colloid stabiliteit) en fluorescentie metingen om een complete fysico-chemische karakterisatie te bekomen. Verder wordt ook de interactie met bloed en bloed componenten onderzocht via hemolyse en hemo-agglutinatie experimenten alsook d.m.v. bescherming tegen nuclease enzymes. Biodegradeerbare polymeren worden ook getest op hun degradatievermogen via protease afbraak. Uiteindelijk kan ook de *in vitro* transfectie en viabiliteit geregistreerd worden via cell testen.

# 2 Synthese van multifunctionele polymeren

## 2.1 Biodegradeerbare polymeren

Uitgaande van basis bouwstenen voor het lichaam, meer bepaald L-aminozuren, kan door middel van een reeks synthese stappen, een uitermate biocompatibel en biodegradeerbaar polymeer bekomen worden. Naast de samenstelling van deze synthetische molecule wordt ook het moleculair gewicht (MW) gecontroleerd. Hiervoor wordt gebruikt maakt van specifieke initiatoren die in precieze hoeveelheden worden toegevoegd om de polymerisatie op maat te laten doorgaan. Polypeptide analogen, zoals poly-$\alpha$-aminozuren kunnen het eenvoudigst verkregen worden door een ring-openings-polymerisatie (ROP) van hun corresponderende N-carboxyanhydride ('Leuchs' anhydride). Om dit te verkrijgen, dient het basis aminozuur eerst beschermd te worden (R-functionele groep) om vervolgens selectief te reageren met difosgeen (met retentie van het stereocenter).

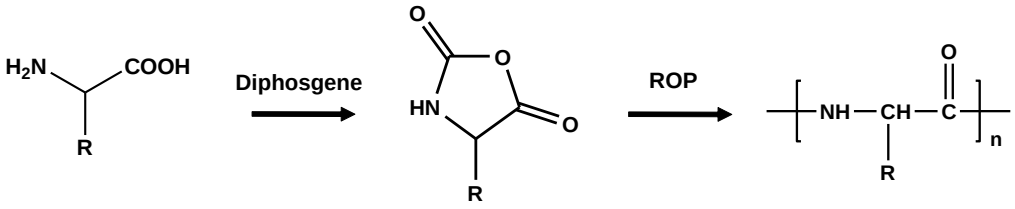


Het MW wordt in deze laatste stap bepaald. Het gebruik van primaire amines als initiatoren laat toe om via nucleofiele aanval (carbamaat mechanisme) polymeren met een laag MW te bekomen (< 40.000 Da) terwijl tertiary amines via proton abstractie polymerisaties initiëren die molecules tot 250.000 Da kunnen genereren (geactiveerd monomeer mechanisme). In een volgende stap kunnen daarna specifieke functionele groepen ingevoegd worden door de vorming van amides met typische eigenschappen in de zijgroep (aminolyse). Tijdens deze reactie wordt ook de beschermgroep verwijdert van de zijketen. Een combinatie van

aminolyse reagentia laat dan ook toe om multifunctionele polymeren te bekomen die een veelvoud aan eigenschappen hebben (gaande van DNA-interactie over ladingsseparatie tot buffering en koppeling van secundaire structuren). Aangezien deze polymeren water-oplosbaar zijn speelt de $pK_a$ van deze functionele groepen een grote rol. Alle gesynthetiseerde producten worden gekarakteriseerd via $^1$H-NMR & FTIR (samenstelling) en GPC (MW bepaling).

In het geval van poly-L-arginine wordt eerst een precursor molecule gesynthetiseerd (poly-L-ornithine) om daaropvolgend een modificatie reactie uit te voeren die alle primaire amines omzet in guanidine functionele groepen.

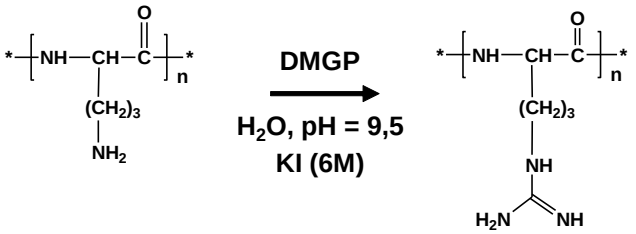


Bij uitbreiding, worden in dit werk poly-$\alpha$-aminozuren uitgaande van een gemengde polymeerbackbone geproduceerd (copolymeren). Bovendien worden combinaties van intermediaire polymeren als initiator voor het ontwikkelen van polymeerstructuren in de zijketen (graft-copolymeren) gevormd, waarbij de invloed van de positionering van functionele groepen op de polymeerketen kan nagegaan worden.

### 2.2 Niet-biodegradeerbare polymeren

Polymethacrylaten worden, in tegenstelling tot polypeptides, gekenmerkt door een hydrofobe, alifatische hoofdketen die niet biodegradeerbaar is en zich daardoor anders gedraagt in waterig milieu (zoals rondom cellen). Deze polymeren komen veelvuldig voor in de literatuur als vector omwille van hun beduidende efficiëntie en de relatief eenvoudige synthese. De meeste methacrylaten zijn commercieel verkrijgbaar en kunnen via een 1-staps procedure reeds kant-en-klare synthetische vectoren opleveren. In dit werk wordt gebruik gemaakt van methacrylaten waarbij de R groep verschillende functionele groepen kan omvatten: tertiare amines (DMAEMA), primaire amines (AEMA), hydroxyl groepen (HEMA) en guanidines, afgeleid van BOC-beschermd AEMA. De polymerisatie van dergelijke monomeren verloopt via een vrij-radicalair mechanisme en het gebruik van een initiator (thermische of redox). Door dit radicalair proces aan te wenden zonder aanwezigheid van radicaal stabilisatoren (zoals gebruikt in ATRP of RAFT) is slechts een beperkte controle van het MW mogelijk met relatief grote polydispersiteit als gevolg. De synthese wordt, afhankelijk van de geselecteerde monomeren, in tolueen of water uitgevoerd en dient steeds stevig

ontgast te worden omdat zuurstof de initiatie inhibeert. Bovendien kan, naargelang het gekozen solvent, een onderscheid gemaakt worden in het gewenste MW bereik (met bijhorende initiator) dat reikt van 50.000 tot 1.000.000 Da. Indien laag-moleculaire (5.000 – 50.000 Da) componenten gewenst zijn, dient gebruik gemaakt te worden van transfer agentia zoals mercaptoethanol. Door combinatie van verschillende monomeren in eenzelfde reactie, kunnen copolymeren gevormd worden met samenstellingen conform de monomeerconcentratie. Naargelang de functionele groep reactiviteit bezit, wordt deze initieel beschermd (BOC-protectie of protonatie in waterig milieu). Ook deze polymeren worden naar samenstelling en MW geverifieerd via $^{1}$H-NMR, FTIR en GPC.

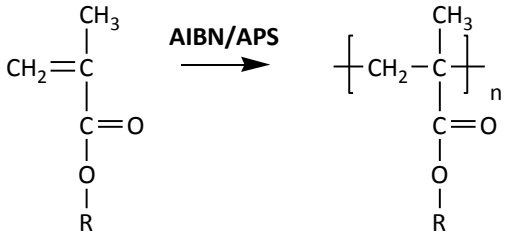


### 2.3 Modificatie van referentie polymeren

Om de potentiële eigenschappen van de ontwikkelde vectoren als gen-afgifte systeem in te schatten, worden deze vergeleken met referentie polymeren zoals polyethyleneimine (PEI) en poly-L-lysine (PLL) waarvan de transfectie efficiëntie alsook de cell-toxiciteit reeds uitvoerig beschreven is in de literatuur. Teneinde deze referentie polymeren, die vaak een hoge efficiëntie en toxiciteit bezitten, te optimaliseren worden guanidine modificaties doorgevoerd zodat een hogere efficiëntie kan bekomen worden met gelijkaardige toxiciteit of een lagere toxiciteit maar met behoud van transfectie potentieel.

## 3 Karakterisatie en verificatie van de vector-eigenschappen

Om te kunnen dienst doen als functioneel dragersysteem in gen-therapie applicaties dient een synthetische vector in staat te zijn om het DNA te beschermen en binnen te dringen in de cel. Aangezien de interactie met DNA voornamelijk op basis van elektrostatische interactie geschiedt is het belangrijk om na te gaan hoe dit gebeurt en als deze inter-polyelektrolyt complexen (polyplex) in staat zijn om door de cel opgenomen te worden. Hiervoor kunnen verschillende analyse technieken aangewend worden.

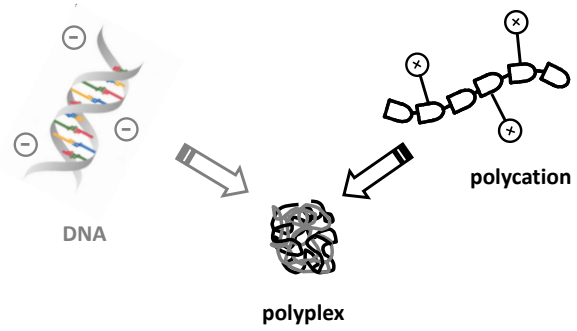


### 3.1 DNA interactie – Complex vorming

De eigenschap van een vector om te kunnen interageren met DNA kan nagegaan worden met 2 aanvullende technieken. Door middel van agarose gel-elektroforese, kan de ideale compositie gevonden worden waarbij polymeer-DNA complexen gevormd worden op basis van retentie in een gel bij het aanleggen van een potentiaalverschil. Niet-gecomplexeerd DNA zal hierbij migreren doorheen de gel terwijl gecomplexeerd DNA geneutraliseerd wordt (door een overmaat aan positief polymeer) en daardoor niet meer aangetrokken wordt tot de positieve anode. Een andere techniek, gebaseerd op fluorescentie van geïntercaleerd DNA (d.m.v. Ethidiumbromide), laat toe om de daling in fluorescentieopbrengst te meten die representatief is voor de vorming van een polyplex waarbij het ethidiumbromide niet langer kan intercaleren met DNA. De mate waarin de fluorescentie daalt en het punt waarop de intensiteit afname maximaal is kan dan verder gebruikt worden om het polyplex te ontleden.

Uit deze testen is gebleken dat vooral de samenstelling van het polymeer een grote rol speelt in het bekomen van complexen met een minimum aan kationisch polymeer (zodat de *in-vitro* toxiciteit kan beperkt worden) en in beperkte mate het MW. Hoe meer positieve ladingen aanwezig zijn op een polymeer hoe sterker de interactie met het DNA. Het implementeren van minder geladen structuren zoals imidazole of hydroxyl liet toe om vectoren te bekomen die nog steeds voldoende sterk interageren met DNA en dit doen zonder substantiële verhoging van de minimum ladingsverhouding nodig voor het induceren van complexatie. Niettegenstaande blijft een minimum hoeveelheid aan positieve lading nodig om voldoende, welgevormde polyplex formatie te verkrijgen (minimaal 25-30 %). Het varieren van het MW blijkt vooral een effect te hebben op de minimale ladingsverhouding (LV) waarbij complexatie optreedt. In het geval van poly-$\alpha$-aminozuren worden minimale LV's gekenmerkt door polymeren met een zo laag mogelijk MW terwijl voor polymethacrylaten een optimum bekomen wordt voor molecules met een gewicht van 100-120 kDa. Voor de meest polymeren ligt de LV voor minimale complexatie tussen 0.8 – 1.6 (zie figuren onder).

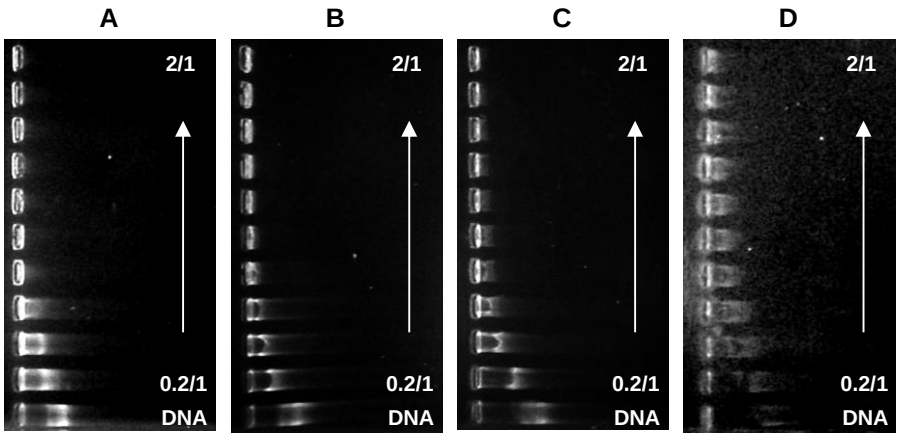


**Agarose gel-elektroforese: p(HEG-GuAEG) with descending percentage of guanidine (A → D)**

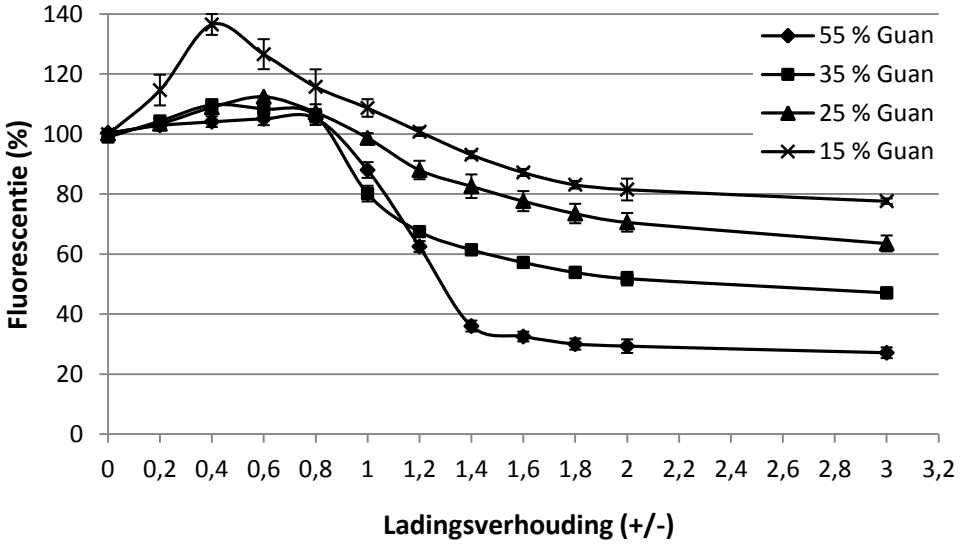


**EtBr Fluorescentie grafiek: polyplex vorming in functie van de ladingsverhouding voor p(HEG-GuAEG)**

## 3.2 Deeltjesgrootte van polyplexen (DLS)

Aan de hand van dynamische lichtverstrooiing is het mogelijk om de gemiddelde grootte van een bepaald type polyplex te meten. Bovendien kan ook de distributie hiervan berekend worden. Via lichtverstrooiing en correlatie van de signaalintensiteit in functie van de uitstervingsfactor (tijdsparameter) wordt de diffusie coëfficiënt afgeleid die op zijn beurt gebruikt wordt in de Stokes-Einstein vergelijking om uiteindelijk een waarde op te leveren voor de hydrodynamische radius ($r_h$) van een idealiter sferisch voorgesteld partikel. Deze waarde heeft belangrijke biologische implicaties, meer bepaald naar opname in de cel toe. Er wordt aangenomen dat het belangrijkste mechanisme voor celopname steunt op receptor gemedieerde endocytose waarbij uitgegaan wordt van de vereiste dat de partikel diameter maximaal 150-200 nm mag zijn. Dit blijkt voor bijna alle polyplexen met een LV van 2/1 of

hoger haalbaar te zijn. Aangezien bij lagere LV'en voor sommige vectoren nog geen stabiele, welomlijnde complexen mogelijk zijn, situeert de diameter zich vaak in de orde van enkele µm (los polymeer en DNA). In het geval van polymeren die condenseren bij lage LV, worden de kleinste polyplexen initieel gevormd waarna het toevoegen van additioneel polymeer (hogere LV'en) stelselmatig (zij het beperkt) de diameter vergroot. Bij zwakker complexerende vectoren, wordt de partikeldiameter alsmaar kleiner met toenemende LV. Wat betreft de deeltjesgrootte is slechts in beperkte mate een invloed zichtbaar van de hoeveelheid lading aanwezig op de vector. Additioneel kon ook de invloed van de tijd, temperatuur en buffermedium gemeten worden. Zo blijkt het overgrote deel van de polymeren voldoende stabiliteit te bezitten in functie van de tijd. In buffermedium daarentegen vertonen de meeste polyplexen snel aggregatie (zeker bij lage LV'en). Verhoogde thermische agitatie (hogere temperatuur) kan dit echter tegengaan.

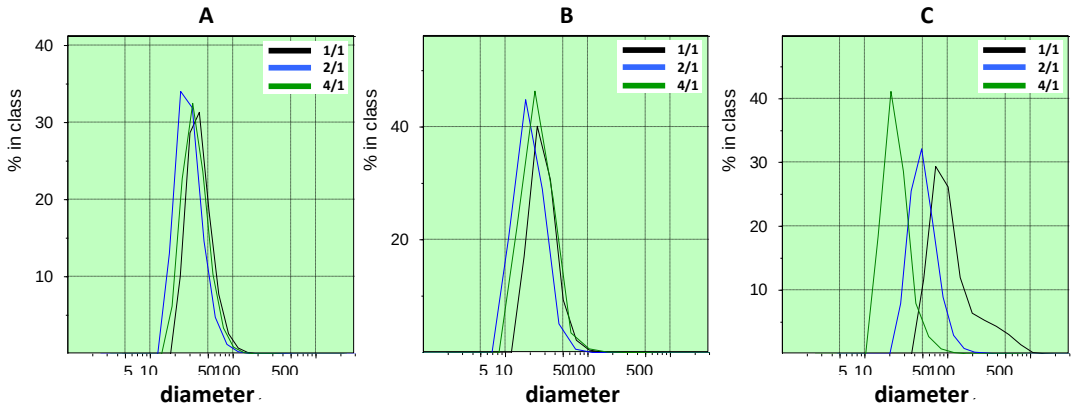


**DLS: deeltjesgrootte en distributie van p(DMAEMA) complexen (11.9 / 121 / 658 kDa)**

## 3.3 Stabiliteit van geladen complexen (Zeta-potentiaal)

Wanneer geladen structuren zoals polyplexen in oplossing gebracht worden, kunnen deze op termijn aggregaten beginnen vormen. Om na te gaan in welke mate complexen hiertegen bestand zijn worden zeta-potentiaal metingen uitgevoerd. Via deze methode, die eveneens steunt op een meting van lichtverstrooiing kan de electroforetische mobiliteit gemeten worden die gerelateerd wordt aan de zeta-potentiaal. Deze laatste geeft een idee van de mogelijkheid van geladen deeltjes om in oplossing te blijven zonder te aggregeren. Hoe hoger de zeta-potentiaal, des te meer zullen equipolaire structuren elkaar afstoten en in oplossing blijven. De algemene trend die wordt waargenomen voor de betreffende vectoren vertoont een correlatie met de ladingsverhouding. Hoe hoger deze laatste, hoe hoger de zeta-potentiaal. Wanneer polyplexen nog niet gevormd zijn, overheerst de negatieve lading van het DNA. Tijdens deze testen is wel gebleken dat de hoeveelheid lading op het polymeer

een rol speelt, met name hoe hoger ladingsdensiteit, hoe hoger de zeta-potentiaal bij eenzelfde LV. Bij een hoge LV (4/1) bedraagt de zeta-potentiaal tussen de 30-60 mV wat overeenkomt met goed tot uitstekende stabiliteit. Dit werd ook bevestigd door metingen met de voorgaande analysetechnieken in functie van de tijd (zie figuur onder: pDMAEMA).

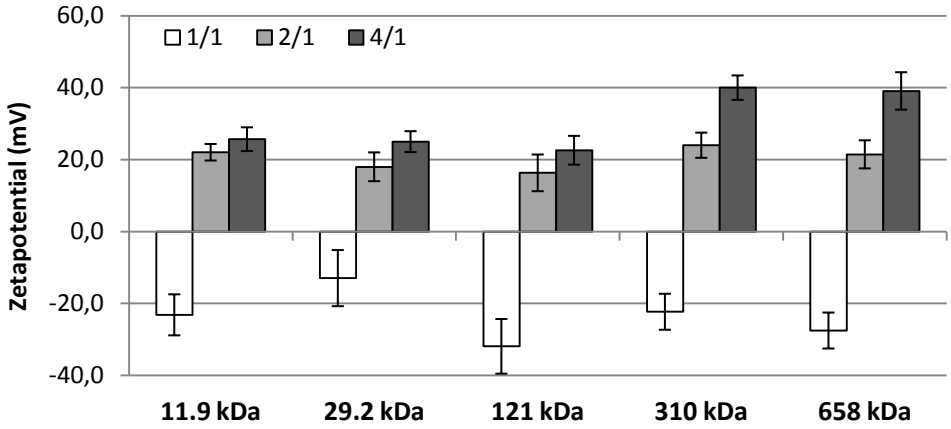


# 4 Optimisatie van vector: koppeling van fluorescente groepen en peptides

## 4.1 Koppelen van fluorescente labels

Een essentieel deel van de karakterisatie van synthetische vectoren bestaat erin om de internalisatie methode van polyplexen te bestuderen. Via confocale microscopie kan een polymeer of polyplex gevolgd worden binnen in de cel om zo de opname van DNA te bevestigen. Hiervoor dient een polyplex visueel waarneembaar te zijn en dit wordt bereikt door een fluorescente molecule toe te voegen. Omdat deze kleine molecules vaak water-onoplosbaar zijn en gemakkelijk uit het complex zouden kunnen diffunderen dienen deze covalent verankerd te worden. Teneinde de werking van het therapeutisch DNA niet te verstoren wordt dit meestal gekoppeld aan het polymeer. In dit werk wordt Oregon Green 488, een fluoresceïne afgeleide gebruikt als model molecule. Via een geactiveerd succinimide derivaat kan koppeling met primaire amines worden bewerkstelligd in een bicarbonaat buffer met typsiche koppelingsgraden van 2-5%. Om na te gaan als de incorporatie van hydrofobe groepen geen impact heeft op de DNA-interactie, worden de hiervan afgeleidde polyplexen aan elektroforese en fluorescentie metingen onderworpen. Hieruit kan worden geconcludeerd dat de koppeling van fluorescente molecules wel degelijk een invloed kan hebben op de minimale LV voor polyplex formatie alsook op de sterkte van de interactie (bv. voor gekoppeld PEI) waardoor minder hechte complexen worden gevormd. Dit blijkt veel minder het geval voor volledige geladen vectoren en heeft te maken met de graad van afscherming die een dergelijke molecule teweegbrengt. Daarom dient de

concentratie aan fluorescente groep zoveel mogelijk beperkt te worden (en toch nog visualisatie toe te laten).

### 4.2 Koppeling van cell-penetrerende peptides

Zoals in de inleiding reeds werd aangehaald, vormt de beperkte transfectie efficiëntie van synthetische vectoren nog steeds een hekelpunt in vergelijking met de potentere virale vectoren. Om dit probleem te counteren wordt recentelijk vaak gebruik gemaakt van peptides die in staat zijn om de cell-internalisatie (één van de prominente barrières in het totale transfectie proces) te vergemakkelijken, vaak door specifieke interactie met receptoren op het celmembraan. Het koppelen van deze structuren kan bovendien een sterkere interactie met DNA uitlokken gezien de overwegend positief geladen structuren waarover de meeste peptides (CPP's) beschikken. Bovendien worden door het koppelen van deze functionele groepen een aantal extra analyse technieken mogelijk die meer informatie kunnen opleveren over polymeer-DNA complexen. Zo kan bv. FRET/FCS analyse toelaten om de LV te bepalen waarop complexatie optreedt en bevestigen UV/VIS analyses dat de fluorescente groepen zich oriënteren naar het midden van het complex toe (zo ver mogelijk verwijderd van het omringende water netwerk). In dit werk, wordt voornamelijk penetratine en arginine$_8$ gekoppeld, 2 CPP's die in de literatuur frequent beschreven worden als internalisatie promotors. Het is mogelijk om deze peptides zowel fysisch in te mengen met de polyplexen als via het covalent verankeren van het peptide op de polymeer backbone. Daarvoor wordt een beroep gedaan op cysteine-gemodificeerde peptides die door middel van een hetero-bifunctionele crosslinker zoals GMBS of SPDP kunnen gelinkt worden aan het polymeer waarbij gemiddeld 1-5 % aan koppeling bereikt wordt. Bovendien wordt ook de invloed van een aantal spacer-bevattende peptides geëvalueerd (met diverse lengte en rigiditeit).

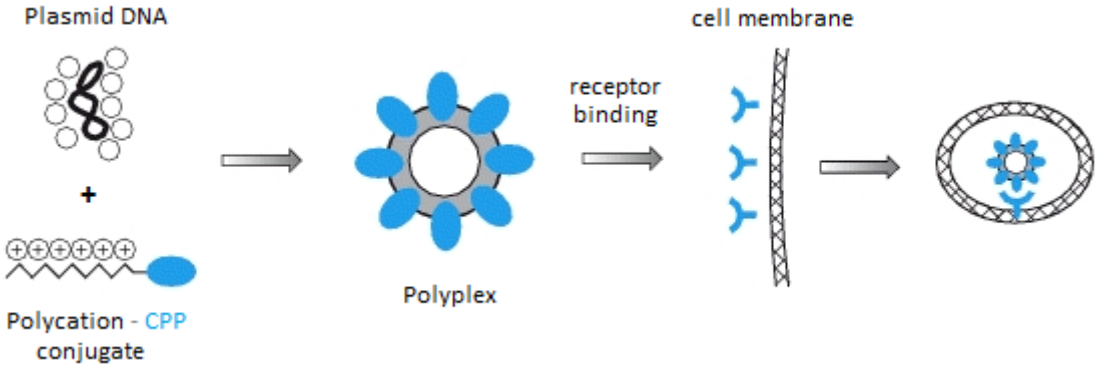


Via elektroforese en EtBr fluorescentie testen is gebleken dat de koppeling van CPP's een wisselende invloed heeft op de complexatie eigenschappen. Voor vectoren die beperkt geladen zijn kan het invoeren van geladen CPP's een gevoelig verbetering opleveren in complexatie gedrag (lagere LV). Indien het basispolymeer reeds voldoende kationische

lading bezit, zorgt de koppeling van CPP's veelal voor een minimale verhoging van de LV waarbij complexatie optreedt maar met behoud van complex sterkte. Wanneer nog eens spacers worden geïncorporeerd, vergroot de toename in minimale LV alsook de DNA interactie capaciteit van het polymeer. Deze trend vertaalt zich ook naar de deeltjesgrootte waar een lichte verhoging in diameter merkbaar is (10-20 nm) maar zonder gevaar voor de cellulair opname. Ook zeta-potentiaal bevindingen bevestigen de verminderde kationische ladingsdichtheid van het polyplex(oppervlak). Door middel van impedantie metingen op alleenstaande cellen wordt de interactie van CPP's met het cellulaire membraan aangetoond. Uit initiele testen met fysisch gemengde complexen wordt verwacht dat CPP's kunnen geïncorporeerd worden zonder de physico-chemische eigenschappen te veranderen.

## 5 Biologische evaluatie van synthetische vectoren

Omdat het uiteindelijke doel van gen therapie gericht is op de toediening van therapeutisch DNA aan levende cellen (systemisch of *in vitro*), is het van vitaal belang dat het gebruik van dragersystemen (vectoren) geen inflammatoire of toxische respons genereert. Om de effecten van polykationen en polyplexen op cellullair niveau na te gaan, kunnen biologisch relevante experimenten (zoals hematologische of transfectie testen) worden uitgevoerd om een initieel idee te krijgen van de bio-compatibiliteit en functionaliteit. Ook de mogelijkheid om via het lichaam gemetaboliseerd te worden behoort tot deze experimenten. Analyses die gebruik maken van cel structuren laten ook toe om het internalisatie proces te onderzoeken, bv. door middel van confocale microscopie.

### 5.1 DNA degradatie bescherming

Wanneer DNA via systemische weg zou worden binnengebracht in het lichaam, kunnen de polyplexen aan heel wat gevaren worden blootgesteld. Een van de meest significante aspecten tijdens dit toedieningsproces is de mogelijkheid van vectoren om DNA af te schermen van nuclease enzymes die abundant teruggevonden worden doorheen het lichaam. Om deze invloed te simuleren worden geselecteerde polyplexen blootgesteld aan DNAse enzymes (type I – 40 Kuntzunits) in een TRIS buffer die Ca en Mg ionen bevat voor de activatie van het enzyme. Op een ideale temperatuur van 37 °C waarbij de fosfodiester binding (zowel endo als exo) wordt verbroken, kan via UV meting (260 nm) de intensiteitstoename van het afgebroken DNA in functie van de tijd gedetecteerd worden. Daarbij is geconstateerd dat de bescherming optimaal is bij LV'en die voldoende boven het punt van complexatie liggen. Wanneer de LV lager dan het complexatie punt ligt is de afscherming vrijwel onbestaande. Ook rond de LV corresponderend met de initiatie van complex vorming, is de bescherming niet afdoend. Indien de graad van bescherming

vergeleken wordt bij een gemiddelde LV (2/1) kan duidelijk de invloed van polymeersamenstelling waargenomen worden. Met name, een toegenomen UV waarde was te zien bij zwak geladen polymeren terwijl exclusief geladen polymeren een nagenoeg vlak verloop vertoonden.

### 5.2 Degradatie van polymeren

Biodegradeerbare poly-$\alpha$-aminozuren werden aan het begin van dit doctoraatswerk o.a. geselecteerd op basis van hun analogie met lichaamseigen peptides die opgebouwd zijn uit amide-bindingen. Aangezien deze vlot door het lichaam kunnen worden gemetaboliseerd, werd dit ook vooropgesteld voor de polymere dragers. Door het lysosomale milieu binnen in het lichaam na te bootsen (papaine enzym 20 µg/ml citraat/fosfaat buffer, pH =6), kan het degradatievermogen van deze polymeren ingeschat worden. Initiële testen hebben uitgewezen dat bij de toegepaste concentratie, zeer vlotte degradatie mogelijk is (t.e.m oligomeren). Tot op zekere hoogte wordt een trend waargenomen in degradatiesnelheid gerelateerd aan de samenstelling (meer positieve lading veroorzaakt tragere degradatie).

### 5.3 Bloed compatibiliteit

Bij in vivo applicaties vormt de compatibiliteit met bloed of componenten van het bloed een zeer belangrijke factor voor o.a. systemisch gebruik. Aangezien erythrocyten, het hoofdaandeel van de bloedcomponenten uitmaken, geven hemolyse en hemoagglutinatie experimenten een goeie indruk van de mogelijke interactie met polyplexen. Hemolyse is een verschijnsel waarbij het celmembraan lyseert onder invloed van cel interactie met externe structuren. Gezien de negatieve oppervlaktelading van membranen en het exces aan positieve lading waarover polymeer-DNA complexen beschikken, vormen deze laatste een gevaar voor de inductie van hemolytische effecten. Daarom worden zowel polyplexen als polymeren op zich geïncubeerd in een HBS buffer met rode bloedcellen (2 %) die vooraf gezuiverd en gefilterd is. Voor alle polymeren is gebleken dat reeds vanaf een kleine concentratie, hemolyse valt waar te nemen en deze blijkt het meest intens voor hoger geladen structuren. Imidazole bevattende polymeren vertonen dan weer de het minste effect. Ook bij polyplexen met een LV van 2/1 hemolyse gedetecteerd worden, al is er een duidelijke verlaging merkbaar door de aanwezigheid van DNA. Bovendien blijkt een stijgend MW een groter hemolytisch effect te veroorzaken.Een ander aspect van het gebruik van polyplexen is de interactie met geladen structuren die leidt tot coagulatie (gevolgd door precipitatie). Hemoagglutinatie (het samenklitten van rode bloedcellen) kan een gevolg zijn hiervan en is makkelijk te verifieren via optische microscopie. Hiervoor worden polyplexen en polymeren geïncubeerd een RBC oplossing gedurende 1uur waarna de agglutinatie voor en

na vergeleken wordt. Opnieuw kan hier het verschil tussen polyplexen en polymeren opgemerkt worden, waarbij de invloed van DNA een gunstig effect veroorzaakt op de agglutinatie. Ook hier blijkt de samenstelling een invloed te hebben met verminderde agglutinatie indien minder geladen groepen aanwezig zijn (zie figuur onder).

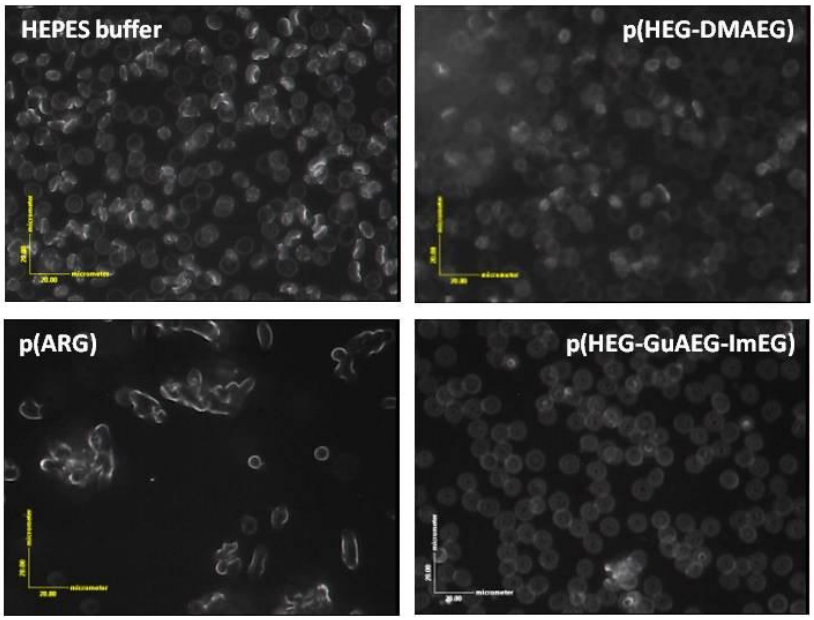


## 5.4 Cel experimenten

De ultieme eigenschap van een afgifte systeem voor gen therapie bestaat erin om DNA tot expressie te laten brengen. Daarom is de meest relevante test voor bepaling van de mate waarin een vector efficiënt kan zijn, het uitvoeren van transfectie experimenten. Zowel de activiteit alsook de toxiciteit kan bepaald worden en vergeleken worden met het referentie polymeer PEI. Cell viabiliteit in functie van de LV wordt voor een selectie aan polyplexen uitgevoerd met behulp van een uptiblue assay die verkleurt in de aanwezigheid van levende, metaboliserende cellen. Voor de transfectie efficiëntie wordt gebruikt gemaakt van een plasmide model (RucHA) dat codeert voor GFP en makkelijk detecteerbaar is via absorptie of fluorescentie spectroscopie. Hiervoor wordt beroep gedaan op specifieke cellijnen (ARPE19, HEK 293 en COS-7) die via een speciaal ontwikkeld protocol uitgetest worden.

De toxiciteit van alle poly-$\alpha$-aminozuren was, afhankelijk van de gebruikte LV, vrij beperkt (tenzij voor LV > 4/1 en voor p(ARG) afgeleides) in vergelijking met PEI dat op zijn beurt substantiële celsterfte induceert, reeds vanaf een 2/1 LV. Modificatie van dit polymeer met o.a. guanidine conversie of fluorescente groepen kon deze toxiciteit wel voor een deel beperken. Polymethacrylaten vertonen een iets lagere viabiliteit, zeker wanneer hoog MW componenten gebruikt worden. Als er neutrale groepen ingebouwd worden, zorgt dit in tegenstelling tot de biodegradeerbare tegenhangers niet tot een verbetering van de viabiliteit.

Meestal vertoont de toxiciteit een stijgend verloop met toenemende LV, al blijken een aantal polyglutamines met o.a. imidazol functionele groepen geen tekenen van afgenomen viabiliteit te vertonen (voor de courant toegepaste LV'en t.e.m. 8-1).

Omdat de graad van efficiente, grotendeels afhankelijk is van de gebruikte cellijn en het aangewende protocol wordt in de meest experimenten gerefereerd naar standaard vectoren. Aangezien in de literatuur PEI als zeer efficiente vector wordt beschreven, is ook in deze testen gebruik gemaakt van dit polymeer. Een heleboel polymeren die zijn getest op hun transfectie efficiëntie vertonen geen significante activiteit. Voor een aantal andere is dit wel het geval, waarbij sommige een betere efficiëntie dan PEI vertoonden (zie figuur onder). Zo blijken polyglutamines met 35% guainidine groepen die partieel geladen zijn (met hydroxyl/imidazole zijgroepen) een vergelijkbare efficiëntie te bezitten bij hogere LV. Enkele polymethacrylaten beschikken zelfs over een dubbele efficiëntie t.o.v. PEI maar dan wel bij hogere LV. Opnieuw corresponderen copolymeren met de hogere waardes in vergelijking met homopolymeren. Ook PEI gemodificeerd met guandine groepen bekomt hogere waardes in transfectie efficiëntie, eveneens bij hogeren LV. Omdat de grootste activiteit is gedetecteerd bij hogere LV dient wel rekening gehouden te worden met de viabiliteit. Hierdoor kunnen polymeren met lager MW beschouwd worden als de meest optimale, vooral bij polyglutamines waar de laagste toxiciteit wordt teruggevonden.

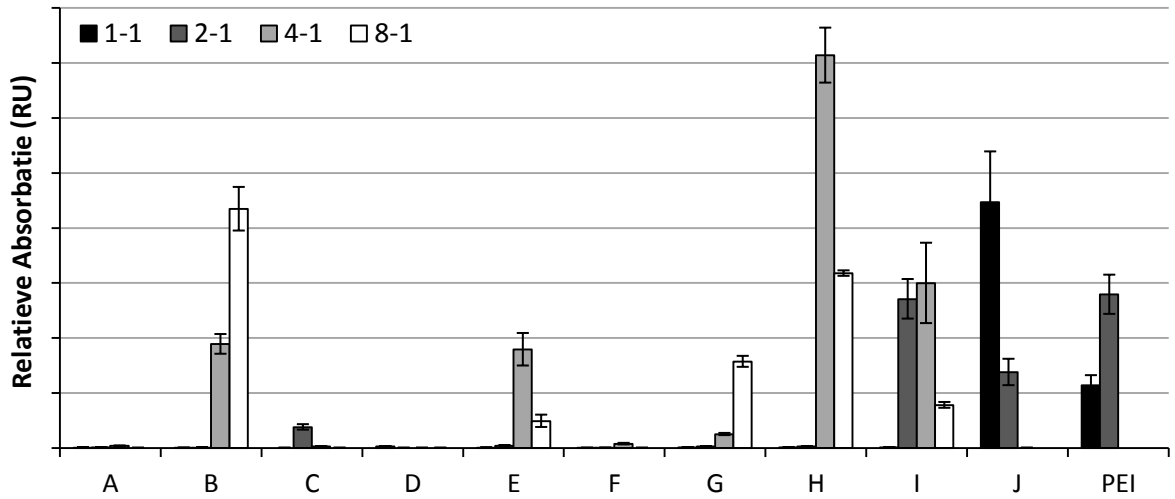

| Code | Polymeer | Code | Polymeer |
|---|---|---|---|
| A | p(DMAEG)+$Arg_8$ 242 kDa | F | p($HEG_{32\%}$-$GuAEG_{11\%}$-$ImEG_{57\%}$) 9.6 |
| B | p($HEG_{63\%}$-$GuAEG_{37\%}$) 9.6 kDa | G | p(DMAEMA) 121 kDa |
| C | p($ARG_{82\%}$-$ORN_{18\%}$) 71.1 kDa | H | p($DMAEMA_{82\%}$-$AEMA_{18\%}$) 135 kDa |
| D | p($ARG_{82\%}$-$ORN_{18\%}$)+PEN 71.1 kDa | I | p($DMAEMA_{56\%}$-$HEMA_{44\%}$) 218 kDa |
| E | p($GuAEG_{35\%}$-$ImEG_{65\%}$) 13 kDa | J | PEI-$Guanidine_{20\%}$ |

## 5.5 Confocale microscopie

Aan de hand van confocale microscopie kan het internalisatie process beter begrepen worden. Deze techniek stelt ook in staat om de morfologie van de polyplexen tot op zekere hoogte te visualiseren. Daardoor kunnen de verschillen in efficiëntie deels verklaard worden. Zo vertonen PEI complexen een heel wat diffusere morfologie in vergelijking met p(DMAEG) complexen die vrijwel geen activiteit vertonen. Door gebruik te maken van bepaalde componenten (Tryphan blue) kunnen de geïnternaliseerde complexen onderscheiden wordt van deze die op het oppervlak blijven. Dit gebrek aan opname zou al een eerste belangrijke oorzaak kunnen zijn voor veel polymeren die niet goed scoren inzake transfectie efficiëntie. Daarnaast moet ook rekening gehouden worden met de sterkte van de complexen, zo blijkt dat een aantal types polymeren wel kunnen geïnternaliseerd worden maar zonder daaropvolgende expressie, een gevolg van enerzijds de samenstelling en anderzijds de vertraging in opname. Wanneer DNA succesvol tot in de celkern kan gebracht worden, is proteïne expressie mogelijk (visualiseerbaar als rode fluorescentie). Voor p(DMAEMA) (zie figuur onder) kan zo een onderscheid gemaakt worden tussen de het geproduceerde proteine, niet-gedissocieerd polyplex alsook overblijfselen van niet-geinternaliseerd polyplex.

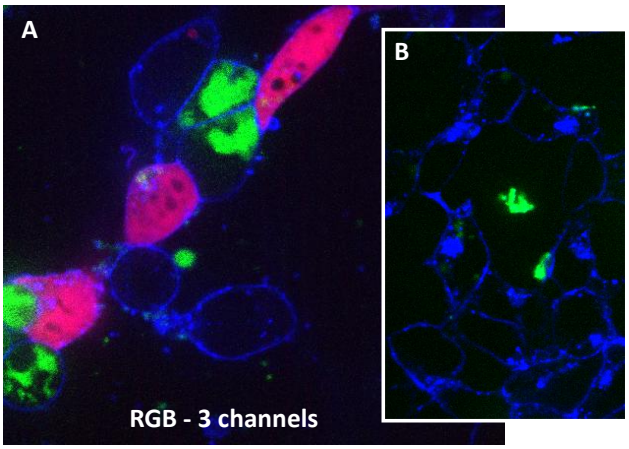

## 6 Conclusie

Tijdens dit doctoraatsonderzoek werden een breed gamma aan polykationische vectoren succesvol gesynthetiseerd met diverse moleculaire gewichten. Naast de vereiste kationische functionele groepen werden ook zijgroepen met neutrale of bufferende eigenschappen geproduceerd, zowel voor poly-$\alpha$-aminozuren als polymethacrylaten. De mogelijkheid om als vector gebruikt te worden werd in bijna alle gevallen positief geëvalueerd door middel van physico-chemische karakterisatie. Wanneer ook biologisch relevante analyses in rekening werden gebracht verkleinde de selectie potentiële vectoren drastisch. Niettegenstaande werden zowel voor polymethacrylaten als polyamides, gunstige kandidaten gevonden die een hogere transfectie efficientie bekwamen terwijl de viabiliteit, hemo-compatibiliteit en nuclease afscherming gelijk of zelfs beter presteerden. Ook de modificatie van referentie polymeren leidde tot verbeterde resultaten op het gebied van biologische evaluatie. Daarenboven kon ook het internalisatie proces met behulp van fluorescente derivaten verder opgehelderd worden om zo tot een optimale polymeersamenstelling te kunnen komen.

# Appendix

# Curriculum Vitae

## Identification


| | |
|---|---|
| Name | Vincent Vermeersch |
| Address | Ten Bosse 50<br>9800 Deinze |
| Telephone | 09/386.88.76 |
| Mobile phone | 0496/25.88.76 |
| Date of birth | 12th of May 1984 |
| Place of birth | Ghent |
| Nationality | Belgian |
| Driver's license | B |


## Education

1996-2002: Higher Secondary Education
Sint-Hendriks- en Zusters Maricoleninstituut
Guido Gezellelaan 105
9800 Deinze
Specialization: Science and mathematics

2002-2006: Master in Chemistry at Ghent University
1e candidacy
2e candidacy
1e master year (cum laude)
2nd master year (suma cum laude)
Master-Thesis: Biodegradable, thermoresponsive hydrogels based on Pluronic® F127

2006-2011: PhD in science, specialization in chemistry at Ghent University
Title: 'Development and characterisation of novel, biodegradable, synthetic vectors as gene delivery systems'
Research team: Polymer Chemistry & Biomaterials Research Group (PBM)
Promotors: Prof. Dr. E. Schacht & Prof. Dr. P. Dubruel

## Scientific accomplishments

Laureate BPG 2006 (Belgian Polymer Group) – laureate for best thesis in polymer research

A1 publications

"Mucosal irritation potential of polyelectrolyte multilayer capsules"
*Liesbeth J. De Cock , Joke Lenoir , Stefaan De Koker , Vincent Vermeersch , Andrei G. Skirtach , Peter Dubruel , Els Adriaens , Chris Vervaet , Jean Paul Remon , Bruno G. De Geest.*

Biomaterials 32 (2011) 1967-1977

"Chip-based impedance measurement on single cells for monitoring sub-toxic effects on cell membranes"
*Kurz, Christian V; Bueth, Heiko; Sossalla, Adam; Vermeersch, Vincent; Toncheva, Veska; Dubruel, Peter; Schacht, Etienne; Thielecke, Hagen.*
BIOSENSORS & BIOELECTRONICS **8**(26) 2011: 3405-3412

"An impaired alveolar-capillary barrier in vitro: effect of proinflammatory cytokines and consequences on nanocarrier interaction"
*Hermanns, Maria Iris; Kasper, Jennifer; Dubruel, Peter; Pohl, Christine; Uboldi, Chiara; Vermeersch, Vincent; Fuchs, Sabine; Unger, Ronald E.; Kirkpatrick, C. James.*
Journal of the royal society interfase **7**(1) 2010: S41-S54

Meeting abstracts (C1)

"Development of non-viral gene delivery systems based on poly-L-glutamic acid and poly-L-arginine derivatives"
*Vermeersch, Vincent; Toncheva, Veska; Van Vlierberghe, Sandra; Tibaldi, Lorenzo; Joliot, Alain; Dubruel, Peter; Schacht, Etienne.*
Human Gene Therapy 10(19) 2008: 1158
16th Annual Congress of the European-Society-of-Gene-and-Cell-Therapy, Brugge 2008 (13-16$^{th}$ of November)

"Poly-alpha-amino acids as improved gene delivery systems"
*V. Vermeersch, V. Toncheva, S. Van Vlierberghe, L. Tibaldi, A. Joliot, P. Dubruel, E. Schacht.*
I-SUP conference 2010, Brugge, Belgium

"Development of new, biodegradable synthetic polymers as non-viral gene delivery systems for the treatment of ARMD"
*V. Vermeersch, V. Toncheva, S. Van Vlierberghe, L. Tibaldi, A. Joliot, P. Dubruel, E. Schacht.*
European Society for Biomaterials congress 2010, Tampere, Finland

"Biodegradable poly-alpha-amino acids as non-viral gene delivery systems"
*V. Vermeersch, V. Toncheva, S. Van Vlierberghe, L. Tibaldi, A. Joliot, P. Dubruel, E. Schacht.*
Belgian Polymer congress 2009, Houffalize, Belgium

Posters (C3)

"Thermo-responsive hydrogels based on Pluronic® F127 as drug delivery systems"
*Swennen I., V. Vermeersch, M. Cornelissen, E. Lippens, E. H. Schacht.*
Frontiers in biomedical polymers congrenss 2007, Ghent, Belgium

"Poly-$\alpha$-amino acid derivatives as novel non-viral gene delivery systems"
*V. Vermeersch, V. Toncheva, S. Van Vlierberghe, L. Tibaldi, A. Joliot, P. Dubruel, E. Schacht.*
European Society for Biomaterials congress 2009, Lausanne, Switzerland

Conference attendances (not with meeting abstract)

Belgian polymer groups yearly conference: 2007 (Houffalize), 2009 (Houffalize), 2010 (Blankenberge)

VJC 2010 (Vlaams jongeren congres, jong KVCV) – Blankenberge

Doctoraatssymposium faculteit Wetenschappen Ugent, 2009

## Professional accomplishments

Training and mentoring bachelor students: laboratory assistance and project assistance
As part of lecturers' and professors' support, providing a set of technical skills during courses of organic chemistry.
Mentoring master students (chemistry and engineering) during their thesis

Member of the intervention team (EIP = Eerste interventie ploeg)
Seminars on internal safety at Ghent University
Fire hazard seminar (Fire fighting centre of Zelzate)
Initiation first aid seminar (Vlaamse Kruis)
Computer responsible within the PBM research team

## Skills

Languages: Dutch – native language
English: excellent knowledge
Frans: basic knowledge
Duits: basic knowledge

Computer skills: Word – excellent knowledge
Excel - excellent knowledge
PowerPoint - excellent knowledge
Internet and networks – excellent knowledge

## Interests

*Sports:* Member of football club FC Poesele since 1990.
Mini-soccer (recreational and University Ghent personnel competition)
Running and biking: competing in amator duathlons and races.

*Film*
*Travelling*
*Computers and internet*